

Development and Application of Chemical Sulfation Methods

By

Jaber Abdullah Alshehri



A Thesis Submitted to the University of Birmingham

For the Degree of DOCTOR OF PHILOSOPHY

School of Pharmacy

College of Medical and Dental Sciences

The University of Birmingham

Submitted: 28th March 2024

Defended: 17th June 2024

UNIVERSITY OF
BIRMINGHAM

University of Birmingham Research Archive

e-theses repository

This unpublished thesis/dissertation is copyright of the author and/or third parties. The intellectual property rights of the author or third parties in respect of this work are as defined by The Copyright Designs and Patents Act 1988 or as modified by any successor legislation.

Any use made of information contained in this thesis/dissertation must be in accordance with that legislation and must be properly acknowledged. Further distribution or reproduction in any format is prohibited without the permission of the copyright holder.

Preface

In 2010, I completed my undergraduate studies from the School of Pharmacy, King Khalid University and then trained as a hospital pharmacist at the Armed Forces Hospital Southern Region. During my studies, I was exposed to a wide range of subjects including pharmaceutical chemistry, pharmacology, pharmacotherapy, and pharmacognosy. My interest in pharmaceutical chemistry was further fuelled by getting exposed to branches of pharmaceutical chemistry such as organic, analytical, medicinal chemistry. After my graduation, I was thinking of getting a job by applying at the Armed Forces Hospital Southern Region and working as a pharmacist. However, a friend of mine who was doing his PhD in the United State of America approached to me and said “Jaber, have you thought about continuing your studies?” at that time, I knew less about postgraduate studies especially a PhD degree and how many years that would take. I was very passionate and enthusiastic person and wanted to learn and explore more. So, I have applied for an academic job at the School of Pharmacy, King Khalid University and I was fortunate enough to be assigned as a demonstrator at the pharmaceutical chemistry department. My interest in teaching and my good conduct earned me a scholarship to travel abroad and improve my English language skills. The Ministry of Higher Education also awarded me a scholarship to pursue my Master degree in one of the esteemed universities around the world. Fortunately, in 2016, I started my Master program in Drug Discovery and Medicinal Chemistry at the University of Birmingham. Throughout my Master program I was learning more about drug discovery, toxicology and metabolism, scientific research, and working with software such as ChemDraw. The last 4 months of my master program were about conducting the dissertation project, which was held in the chemistry lab, Haworth building, School of Chemistry. As I remember I met Dr Alan Jones for the first time in his office discussing one of his offered

projects, but I did not work under his supervision at that time. In 2019, I had a discussion with Dr Alan Jones about applying for PhD position which led me to writing this thesis some four years later. During these years of my postgraduate studies and everything that I have been through more specifically the COVID-19 time and its impact not just on me but the whole world, I have had the support and encouragement of many wonderful people around me and abroad along the way.

First and foremost, I would like to thank my lead academic supervisor, Dr Alan Jones, for his mentoring, guidance, and endless support throughout the years. I would also like to thank my second supervisor, Dr Shan He. I would like to thank my wife (Nawal) and my children (Jehad & Mayam) for their patience, love, sacrifices, and care throughout my studies. I would like to thank my parents and siblings for their endless support and encouragement. I would also like to thank my wife's parents and siblings for their kindness and continuous support. I would also like to thank my sponsor, King Khalid University, Abha, Saudi Arabia and the Saudi Arabia Cultural Bureau in London (SACB) for the scholarship and financial support during these years.

I would like to thank my friends: Anna and Gabriel, Abdulaziz, Aobo, Chloe, Daniel, Fatima, Faisal, Krystal, Maher, Mohammed, Ridho, Tariq, Owayyed, Sameh, Yifei, the people in the 3rd and 4th floor Haworth labs, and the 2nd floor of Denis Howell building, and to all of my friends in the main library for their support and kindness during these years.

Finally, I would also like to thank Dr Allen Bowden, Dr Cecile Le Duff and Ms Bridget Tang, Dr Louise Male, Dr Christopher Williams, and Dr Richard Grainger for their splendid technical support over the years. I also would like to thank Dr Kim Roper and Dr Marie-Christine Jones for their helpful discussion and suggestions.

Abstract

Sulfation is one of the most important modifications that occurs to a wide range of bioactive small molecules including carbohydrates, proteins, flavonoids, and steroids. In turn, these sulfated molecules have significant biological and pharmacological roles in diverse processes including cell signalling, modulation of immune and inflammation response, anti-coagulation, anti-atherosclerosis, and anti-adhesion. However, methods to incorporate sulfate and related sulfur functionality have drawbacks. This thesis is composed of seven individual chapters and contains the collective works of six separate investigations.

Chapter 1 describes the approaches to the sulfation of small molecules: current progress and future directions. This chapter highlights the importance of sulfation in critical biological signalling cascades and a key phase II drug metabolism step. It also summarises the most encountered chemical sulfation approaches of small molecules that have been applied to a wide range of molecules, including carbohydrates, proteins, steroids, amongst many others.

Chapter 2 describes the design and synthesis of novel sulfur trioxide complexes for sulfation chemistry. This includes the synthesis of tertiary amine sulfur trioxide complexes such as tripropylamine and bulky tertiary amines like *triisobutylamine* and *isopropyl-N-methyl-tert-butylamine*. This chapter also provides a general preparation of novel hydrophilic *N*-substituted morpholine sulfur trioxide (4-methylmorpholine SO₃ and 4-ethylmorpholine SO₃) which is suitable for sulfating hydrophilic substrates, including amino acids. These reagents were investigated on a simple benzyl alcohol and benzylamine to test whether they could be used as a sulfation source. The results of this investigation led to the preparation of a series of novel sulfating reagents including tripropylamine sulfur trioxide, *isopropyl-N-methyl-N-*

tert-butylamine sulfur trioxide and 4-methyl and 4-ethylmorpholine sulfur trioxide complexes.

Chapter 3 describes the sulfation of selected amino acids using 4-methylmorpholine SO₃ and 4-ethylmorpholine SO₃. This chapter describes the optimised conditions for the sulfation of selected amino acids using a lower temperature strategy and H₂O/MeCN solvent system without the need for column chromatography techniques.

Chapter 4 describes a novel exchange method to access sulfated molecules using Py•SO₃ and Me₃N•SO₃ complexes. This chapter reports a low-cost *in-situ* version of Bu₃N•SO₃ using Py•SO₃ and Me₃N•SO₃ followed by a lipophilic exchange with tributylamine (Bu₃N). This method provides an alternative sulfation method based on a cheap, molecularly efficient and solubilising cation exchanging method. This method is amenable to a range of differentially substituted benzyl alcohols, benzylamines and aniline and can also be performed at low temperature for sensitive substrates in good to excellent isolated yields.

Chapter 5 provides a convenient chemoselective conversion of the steroidal alcohol and phenol moieties to their corresponding organosulfate using tributylsulfoammonium betaine (TBSAB). This method can be conducted on a millimolar scale and the corresponding steroid sulfates isolated as their biologically relevant sodium salts without the need for ion-exchange chromatography. Furthermore, this chapter reports a convenient method to install an isotopic label, deuterium (²H), combined with estrone sulfation which could be exploited for mass-spectrometric quantification in biological studies. The results of this investigation have demonstrated a suitable method for the preparation of mono- or di-sulfated steroidal skeletons of importance to the fields of biology and spectroscopy. A simplified deuterium labelling-sulfation strategy for estrone is also reported. This isotopically labelled estrone

could be used for the detection of substances of abuse through to cancer diagnosis applications as well as pharmacokinetics studies.

Chapter 6 describes the investigation in to whether the biologically active heparan sulfate-glycomimetic could act as a source of the sulfation pathway in the body. This hypothesis of *in situ* sulfur transfer was tested on a simple benzyl alcohol using a biologically active heparan sulfate-glycomimetic. Unfortunately, this attempt was not successful as confirmed by ^1H NMR spectroscopic data. Additionally, several attempts were made to sulfate other benzyl alcohol analogues using synthesised sulfation sources such as sodium 4-methylbenzyl sulfate and sodium 4-chlorobenzyl sulfate but also there was no robust evidence of the formation of the desired molecule as confirmed by ^1H NMR spectroscopic data. However, for the first time, robust evidence for the stability of benzylic sulfates was found a major anticipated issue with sulfation chemistry more generally.

Chapter 7 discusses the biological role of hydrogen sulfide (H_2S) and the synthesis of cysteine trisulfide (Cys-SSS-Cys). This chapter describes the synthesis of cysteine trisulfide and highlights the proposed reaction mechanism as well as purification and isolation strategies. The gram-scale synthesis of cysteine trisulfide was submitted to our biological collaborator; Dr Madhani (Institute of Cardiovascular Sciences, University of Birmingham, UK) and screened for biological activity. Treatment of HEK293T (Human embryonic kidney) cells with the cysteine trisulfide resulted in high intracellular levels of hydropersulfides and thus, protection from electrophilic stress.

Contents

Chapter 1.	Chemical sulfation of small biomolecules: current and future directions.....	2
1.1.	Sulfation and sulfotransferases	3
1.2.	Chemistry of sulfur.....	5
1.3.	Chemical sulfation approaches of small molecules	8
1.3.1.	Sulfation using sulfuric acid and related reagents	9
1.3.2.	Sulfation using chlorosulfonic acid (ClSO ₃ H) and its derivatives.....	12
1.3.3.	Sulfation using sulfur trioxide amine/amide complexes	14
1.3.3.1.	Trimethylamine sulfur trioxide complex.....	14
1.3.3.2.	Triethylamine sulfur trioxide complex.....	19
1.3.3.3.	Tributylsulfoammonium betaine (TBSAB/Bu ₃ N·SO ₃)	23
1.3.3.4.	Pyridine sulfur trioxide and dimethylformamide sulfur trioxide complexes.....	26
1.3.4.	Sulfation using sulfur (VI) fluoride exchange (SuFEx) strategy	33
1.3.5.	Protection/deprotection approaches	35
1.4.	Conclusion.....	40
1.5.	Aims and Objectives.....	42
Chapter 2.	Design and synthesis of novel sulfur trioxide complexes for sulfation chemistry.....	47
2.1.	Sulfur trioxide complexes	49
2.1.1.	The properties of sulfur trioxide complexes.....	49
2.2.	The preparation of sulfur trioxide complexes	51
2.3.	Results and Discussion	55
2.3.1.	Preparation of novel sulfur trioxide complexes.....	55
2.3.2.	Synthesis of tripropylamine sulfur trioxide complex.....	56
2.3.3.	Synthesis of triisobutylamine sulfur trioxide complex.....	59
2.3.4.	Synthesis of isopropyl- <i>N</i> -methyl- <i>tert</i> -butylamine sulfur trioxide complex	61
2.3.5.	Synthesis of <i>N</i> -substituted morpholine sulfur trioxide complexes.....	63
2.3.6.	Synthesis of cinchonidine sulfur trioxide complex	71
2.4.	Conclusion and future work.....	74
Chapter 3.	Chemical sulfation of selected α-amino acids using 4-methylmorpholine sulfur trioxide and 4-ethylmorpholine sulfur trioxide.....	76
3.1.	Chemistry of α-amino acids	77
3.2.	Chemical modifications of proteins	79
3.3.	Chemical sulfation approaches of proteins	80
3.4.	Results and Discussion	83
3.4.1.	Optimisation and control studies.....	83
3.4.2.	Sulfation of selected α-amino acid using <i>N</i> -substituted morpholine SO ₃	86

3.4.3.	Sulfation of selected α -amino acids using 4-methylmorpholine SO_3 complex.....	88
3.4.4.	Sulfation of selected α -amino acid using 4-ethylmorpholine SO_3 complex.....	93
3.5.	Conclusion and future work.....	97
Chapter 4.	A novel exchange method to access sulfated molecules	100
4.1.	Organosulfates and sulfamates	101
4.2.	Sulfation using a lipophilic cation exchange strategy	101
4.3.	Sulfation using an all-in-one type reagent.....	102
4.4.	Results and Discussion	103
4.4.1.	Optimisation and control studies.....	106
4.4.2.	An analysis of steric and electronic parameters of the sulfation substrate	108
4.4.3.	Sulfation of benzyl alcohols using $\text{Py}\bullet\text{SO}_3$ complex.....	108
4.4.4.	Sulfation of benzylamines using $\text{Me}_3\text{N}\bullet\text{SO}_3$	110
4.5.	Conclusion.....	116
Chapter 5.	A sulfonyl group transfer strategy to selectively prepare sulfated steroids	125
5.1.	Modifications of steroids	128
5.2.	Sulfation pathway of steroids	129
5.3.	Chemical sulfation methods of steroids	130
5.4.	Results and Discussion	132
5.4.1.	Optimisation and control studies.....	132
5.4.2.	Preparation of selected steroid sulfates using TBSAB	132
5.5.	Conclusion.....	147
Chapter 6.	Are sulfated glycomimetics endogenous sulfate source: A control experiment study 155	
6.1.	Glycomimetics.....	156
6.2.	Results and Discussion	161
6.2.1.	Optimisation and control studies.....	161
6.3.	Conclusion.....	168
Chapter 7.	Biological role of hydrogen sulfide and the synthesis and characterisation of cysteine trisulfide 170	
7.1.	Hydrogen sulfide (H_2S)	171
7.2.	Endogenous hydropersulfides (RSSH).....	173
7.2.1.	Cysteine trisulfide (Cys-SSS-Cys)	174
7.3.	Results and Discussion	179
7.3.1.	The synthesis of cysteine trisulfide (Cys-SSS-Cys).....	179
7.4.	Conclusion.....	185
7.5.	Thesis conclusions and future work.....	186

Chapter 8. Experimental and compound characterisation.....	191
8.1. General Methods	192
8.2. General Procedures	193
8.3. Compound characterisation	200
8.4. Preparation of cysteine trisulfide (237) ³⁰⁷	247

List of Figures

Figure 1: Phase I and II metabolism of xenobiotics involving chemical modification and conjugation reactions (Drawn using Biorender-basic version).....	3
Figure 2: Sulfation of phenol (1) (acceptor substrate) mediated by SULTs. The sulfate moiety from PAPS is transferred to the oxygen atom of phenol (2).	4
Figure 3: The resonance structures of sulfur dioxide (SO ₂).	6
Figure 4: The resonance structures of SO ₃	6
Figure 5: Sulfur trioxide adducts with Lewis bases, including trimethylamine, triethylamine, 1,4-dioxane, and pyridine.	7
Figure 6: Examples of FDA-approved drugs with sulfur-containing functional groups.....	8
Figure 7: Sulfated tetrasaccharide examples prepared using the Py•SO ₃ complex.....	27
Figure 8: The structure of pentosan polysulfate sodium (Elmiron®) which is approved for the treatment of interstitial cystitis. ¹²⁹⁻¹³⁰	29
Figure 9: Scope of sulfated biomolecules using SuFEx approach. Yields shown have been calculated based on the isolated molecules after purification. ¹³⁵	35
Figure 10: Sulfate-containing molecules that have different pharmacological applications.	48
Figure 11: Sulfonation, sulfation, and sulfamation reactions using SO ₃	49
Figure 12: The sp ³ orbital hybridisation structure of Me ₃ N.....	50
Figure 13: Crystal structure of TBSAB with ellipsoids drawn at the 50 % probability level. The molecule lies on a 3-fold rotation axis running through N(1) and S(1) such that the butyl groups are all symmetrically equivalent. Symmetry codes used to generate equivalent atoms: \$1, y-x, 1-x, z, \$2, 1-y, 1+x-y, z. ¹⁵⁷	54
Figure 14: The structure of triisobutylamine.....	60
Figure 15: The sp ³ orbital hybridisation structure of isopropyl- <i>N</i> -methyl- <i>tert</i> -butylamine.....	61
Figure 16: The ¹ H NMR (400 MHz, CDCl ₃) spectra of (a) isopropyl- <i>N</i> -methyl- <i>tert</i> -butylamine compared to its SO ₃ complex (b), both dissolved in CDCl ₃	62
Figure 17: The structure of 4-methyl and 4-ethylmorpholine.....	64
Figure 18: The ¹ H NMR (400 MHz, MeOD) spectrum of 4-methylmorpholine SO ₃ complex. Arrows show the cyclic protons in 4-methylmorpholine SO ₃ complex.	65
Figure 19: The stacked ¹ H NMR (400 MHz, MeOD) spectra of (a) 4-methylmorpholine and (b) 4-methylmorpholine SO ₃ complex.	66
Figure 20: The structural isomer of 4-methylmorpholine SO ₃ complex.	66
Figure 21: The ¹ H NMR (400 MHz, MeOD) spectrum of 4-ethylmorpholine SO ₃ complex. Arrows show the cyclic and ethyl group protons in 4-ethylmorpholine SO ₃ complex.	69
Figure 22: The structural isomer of 4-ethylmorpholine SO ₃ complex.	69
Figure 23: The structure of cinchonidine.....	71
Figure 24: The structure of quinoline (a) and quinuclidine (b).....	71
Figure 25: The ¹ H NMR spectra of both (a) cinchonidine and (b) cinchonidine SO ₃ complex.	73
Figure 26: The general structure of an α-amino acid.	77
Figure 27: Zwitterionic form of an α-amino acid at physiological pH.	78
Figure 28: Common α-amino acids which are categorised according to R substituents variations, including aliphatic chain, aromatic, acidic, basic, sulfur-containing, and hydroxylic amino acids.	78
Figure 29: ¹ H NMR (400 MHz, DMSO- <i>d</i> ₆) spectrum for the sulfation test reaction of methanol using 4-methylmorpholine SO ₃ complex, the sample was referenced to DMSO- <i>d</i> ₆ solvent. Black arrows indicate the 4-methylmorpholinium proton signals.....	84
Figure 30: Failed <i>N</i> -sulfamation attempts on glycine, ethyl glycine, alanine, and cysteine.....	88

Figure 31: The sulfation of alcoholic, phenolic, and amine-containing substrates using the Lewis base adducts of SO ₃ . R' = Me ₃ N, Et ₃ N, DMF, Py, and 1,4-dioxane.	101
Figure 32: TBSAB control experiment (300 MHz, CDCl ₃). (a) ¹ H NMR spectrum of Bu ₃ N. (b) ¹ H NMR spectrum of the reaction mixture of Me ₃ N•SO ₃ and Bu ₃ N in MeCN after 30 min. Arrows show the presence of Bu ₃ N peaks in the mixture.	105
Figure 33: Scope of the three-step, one-pot method with benzyl alcohols. (a) use of Me ₃ N•SO ₃ instead of Py•SO ₃ . * The isolated yield using TBSAB methodology for comparison. ¹⁴⁵	109
Figure 34: Scope of the three-step, one-pot method with benzylamine using Me ₃ N•SO ₃ . * Isolated yields using TBSAB methodology for comparison. ⁴⁷	112
Figure 35: Scope of room temperature application of the method to a range of nitrogen-containing scaffolds. Parentheses indicates % conversion as measured by ¹ H NMR spectroscopy (400 MHz, CDCl ₃ and DMSO- <i>d</i> ₆ solvents).	115
Figure 36: The steroidal skeleton structure, a reduced phenanthrene (A, B, and C) and cyclopentane ring (D).	126
Figure 37: The structure of cholesterol with steroidal numbering.	127
Figure 38: Bile acid derivatives, cholic acid (191) and chenodeoxycholic acid (192).	127
Figure 39: Selected steroids with biological functions including the treatment of cardiovascular diseases with digoxin, the treatment of obesity as in 5β-androstane, neuroprotective and immune modulators as in 17β-estradiol, and anti-inflammatory activity as in pregnane. ^{200, 207-210}	128
Figure 40: Chemical modifications of some steroids, including hydroxylation of cortisone (197), sulfation of estrone (198), cholesterol (199), and dehydroepiandrosterone (200). ²¹²⁻²¹³	129
Figure 41: Explanation of hydride ion attack of ketone moiety in pregnenolone from top (Me) and bottom (steroid cyclic frame) sides. The relative stereochemistry of (213) was confirmed by X-ray crystallography as (<i>R</i>).	137
Figure 42: The absolute structure of pregnanediol (213) confirmed by both ¹ H and ¹³ C NMR spectroscopic and the crystal structure of pregnanediol (213), obtained from small molecule single crystal X-Ray diffraction. Ellipsoids drawn at the 50 % probability level. Hydrogen bonding within the asymmetric unit is shown using dotted lines. (Crystal structure solved by Dr L. Male, and CCDC number 2120263).	138
Figure 43: ¹ H NMR spectrum (400 MHz, DMSO- <i>d</i> ₆) of non-deuterated estrone (219). Blue arrows highlight the diastereotopic C16 protons.	143
Figure 44: ¹ H NMR spectrum (400 MHz, DMSO- <i>d</i> ₆) of deuterated estrone(<i>d</i> ₂) (222). Blue arrows highlight the 72% depletion of the diastereotopic C16 protons compared to estrone.	143
Figure 45: Overlay of ¹ H NMR spectra (400 MHz, DMSO- <i>d</i> ₆) of estrone (blue, 219) and estrone- <i>d</i> ₂ (red, 222) shows the diagnostic depletion of the diastereotopic C16 protons.	144
Figure 46: Mass spectrometric theoretical versus observed deuteration levels for sodium estrone- <i>d</i> ₂ and estrone- <i>d</i> ₁ sulfates.	146
Figure 47: Medicines based on glycomimetics, oseltamivir approved as anti-viral, miglitol as an anti-diabetic drug, perindopril approved for the treatment of hypertension, and gemcitabine as an anti-cancer drug.	157
Figure 48: Structure of fondaparinux (229), a carbohydrate-derived medicine which was approved for the treatment of deep vein thrombosis.	158
Figure 49: The mechanism of action of anti-coagulant, fondaparinux (Drawn using Biorender).	158
Figure 50: The synthesised heparan sulfate-glycomimetic (<i>S</i> -10), prepared by Dr Daniel Gill. ¹⁵⁸	161
Figure 51: The ¹ H NMR spectrum (400 MHz, DMSO- <i>d</i> ₆) of the sulfation reaction of benzyl alcohol with <i>S</i> -10 glycomimetic, the blue arrow shows that the benzylic protons (d, 4.49 ppm) of benzyl alcohol did not change and remains as a doublet (d) after 7 days of this control experiment.	163

Figure 52: The stacked ¹ H NMR spectra (400 MHz, DMSO- <i>d</i> ₆) of benzyl alcohol pre-sulfation (1), the benzylic proton signal at 4.49 ppm as a doublet (<i>d</i>) and post-sulfation. The benzylic protons signal as a doublet was also observed post-sulfation (2) indicating that the reaction did not occur.....	164
Figure 53: The stacked ¹ H NMR spectra (400 MHz, DMSO- <i>d</i> ₆) of (a) sodium 4-methylbenzyl sulfate, (b) 4-methylbenzyl alcohol, (c) 4-chlorobenzyl alcohol, (d) control experiment (the sulfation of 4-chlorobenzyl alcohol with sodium 4-methylbenzyl sulfate), and (e) sodium 4-chlorobenzyl sulfate.	166
Figure 54: The stacked ¹ H NMR spectra (400 MHz, DMSO- <i>d</i> ₆) of (a) 4-chlorobenzyl alcohol, (b) sodium 4-chlorobenzyl sulfate, (c) 4-methoxybenzyl alcohol, (d) control experiment (the sulfation of 4-methoxybenzyl alcohol with sodium 4-chlorobenzyl sulfate).....	167
Figure 55: The structure of homocysteine and cysteine amino acids.	172
Figure 56: The structure of cysteine trisulfide (Cys-SSS-Cys).	175
Figure 57: The selected region of the stacked ¹ H NMR spectra of equilibrated samples (post 30 min) of 10 mM 2HED (2-hydroxyethyl disulfide, <i>L</i> -cystine like substrate) with increasing additions of NaHS (0, 5, 10 and 15 mM). the lower spectrum corresponds to 2HED (<i>L</i> -cystine like substrate), with two triplet signals ($\delta = 2.91\text{--}2.95$ and $3.85\text{--}3.90$ ppm). The addition of different concentrations of NaHS (sulfur donor) resulting in the formation of trisulfide substrates (2HET, 2-hydroxyethyl trisulfide). The top three spectra correspond to 2HET (trisulfide like substrate), 2 triplet signals ($\delta = 3.08\text{--}3.11$ and $3.91\text{--}3.94$ ppm). This spectrum was obtained directly from the original source. ³⁰⁶	178
Figure 58: The ¹ H NMR spectrum (400 MHz, D ₂ O) of Cys-SSS-Cys with major detectable impurities, <i>L</i> -cystine (red arrows) and pyridine (blue arrows).	179
Figure 59: The ¹ H NMR spectrum (400 MHz, D ₂ O) of the starting material, <i>L</i> -cystine.....	180
Figure 60: The ¹ H NMR spectrum of Cys-SSS-Cys, (400 MHz, D ₂ O), MeCN was used as an internal reference: C1 (4.45 ppm, stereogenic centres). C2 (3.40 ppm) and C3 (3.25 ppm) are both diastereotopic protons.	182
Figure 61: The ¹ H NMR spectrum of Fukuto's sample, Cys-SSS-Cys (400 MHz, D ₂ O), MeCN was used as an internal reference (Provided by Dr Madhani).	183

List of Tables

Table 1: Selected sulfation approaches of organic molecules using Me ₃ N•SO ₃ complex.....	17
Table 2: Sulfation of organic molecules using Et ₃ N•SO ₃ complex. N.R. not reported.	20
Table 3: Sulfation methods of selected biomolecules using TBSAB.	25
Table 4: Comparison of the reported sulfating reagents: advantages, disadvantages, and applications.	39
Table 5: The orbital hybridisation and pK _a H values of alkylamines and aromatic amines. Obtained from the National Library of Medicine (N.D. not determined).....	51
Table 6: The cLogP values of sp ³ hybridised tertiary amines (These calculated values were derived from ChemDraw 19.1).	53
Table 7: The expected pK _a H values of different bulky and cyclic amines. ¹⁶¹⁻¹⁶²	64
Table 8: The isolated percentage yield of sodium benzyl sulfate 1* and sulfamate 2* using different sulfating agents.	86
Table 9: Optimisation and control studies of benzyl alcohol sulfation–lipophilic exchange–sodium exchange, was converted to the pyridinium salt (164); benzyl sulfate was isolated as sodium salt (105) and analysed by ¹ H NMR spectroscopy, mass spectrometry, and melting point to be in accordance with the literature. ¹⁰⁵	107
Table 10: Optimization of a model tributylammonium benzyl sulfamate reaction. Reaction conversions reported as measured by ¹ H NMR spectroscopy (400 MHz, DMSO- <i>d</i> ₆).	113
Table 11: The ¹ H and ¹³ C NMR spectroscopic data for cysteine trisulfide, Fukuto (original) sample vs this sample. Both are dissolved in D ₂ O, one drop of HCl was added (≈ 0.05 mL), and MeCN was used as internal reference.....	184

List of Schemes

Scheme 1: General reaction scheme for sulfation of ethene using H ₂ SO ₄ .	9
Scheme 2: Double sulfation of betulin with sulfamic acid (H ₂ NSO ₃ H). Conditions: (i) H ₂ NSO ₃ H, urea, and DMF or 1,4-dioxane (60-75 °C, 2-3.5 h); and (ii) work up with 10% H ₂ SO ₄ , or 3–5% KOH, or 3–5% NaOH. ⁶¹	10
Scheme 3: Sulfation reaction of aliphatic alcohol using H ₂ SO ₄ /DCC coupling protocol, where R = Alkyl. Adapted from Hoiberg and Mumma et al. ⁶⁶⁻⁶⁷	11
Scheme 4: The sulfation reaction of agarose polymer (13) using ClSO ₃ H/pyridine. ⁷³	12
Scheme 5: Synthesis of sulfated phenols, benzyl alcohols, anilines, and benzylamines using ClSO ₃ H as a source of sulfation, followed by cation exchange. Conditions: (i) ClSO ₃ H (5.0 mmol, 1 eq.), triethylamine and CH ₂ Cl ₂ , 0 °C to r.t., 1 h; (ii) tetrabutylammonium hydrogensulfate (4.0 mmol), CH ₂ Cl ₂ ; and (iii) B ₂ Pin ₂ (0.25–0.5 mmol), [Ir(COD)OMe] ₂ (1.5–2.5 mol %), dtbpy (3–5 mol %), 1,4-dioxane, 70 °C, up to 16 h. ⁵²	13
Scheme 6: The final two steps of the total synthesis of Avibactam [®] , adapted from Ball et al. ⁵⁰	14
Scheme 7: Site selective sulfation of pyranoside scaffolds using (a) diarylborinic acid. ⁸¹	15
Scheme 8: The sulfation step of TF antigen using Me ₃ N•SO ₃ . Conditions: (i) Bu ₂ SnO, benzene/DMF (5:1, v/v), 125 °C, 24 h, then Me ₃ N•SO ₃ , DMF, r.t., 72 h, then flash chromatography, then Dowex [®] 50WX4 (Na ⁺ form) resin, H ₂ O, r.t., 16 h, 66%. ⁸⁴	16
Scheme 9: Sulfation reaction of tetrahydroisoquinoline derivatives using Me ₃ N•SO ₃ complex. ⁸⁸	16
Scheme 10: Sulfation reaction of resveratrol using Me ₃ N•SO ₃ complex. ⁸⁹	17
Scheme 11: General procedure for sulfation of PCA using Et ₃ N•SO ₃ affording PCA-3-sulfate (36) or PCA-4-sulfate (37). ⁹⁰	19
Scheme 12: The <i>O</i> -sulfation of polyhydroxy organic scaffolds with Et ₃ N•SO ₃ and the addition of TfOH. ¹⁰³⁻¹⁰⁴	22
Scheme 13: The general synthesis of TBSAB (42).	23
Scheme 14: General sulfation synthesis of organic scaffolds using all-in-one type reagent, Bu ₃ N•SO ₃ . Conditions: (i) Bu ₃ N•SO ₃ (2.0 eq.), MeCN, 90 °C, up to 3 h, then sodium 2-ethylhexanoate (NEH) or sodium iodide (NaI) exchange. (ii) Bu ₃ N•SO ₃ (2.0 eq.), MeCN, 30 °C, up to 1 h, then NaI exchange. (iii) Bu ₃ N•SO ₃ (2.0 eq.), MeCN, r.t., up to 18 h, then NaI exchange. (iv) Bu ₃ N•SO ₃ (≥ 2.0 eq.), MeCN, 90 °C, up to 12 h, then NEH or NaI exchange. R = Me, OMe, Cl, CF ₃ , NO ₂ , R ₁ = α-amino acid side chain. ⁴⁷	24
Scheme 15: The regioselective sulfation of trimethylsilyl cellulose (TMSC) using sulfur trioxide complexes (isolated yield not reported). ¹¹⁷	27
Scheme 16: The sulfation reaction of phenolic flavonoids using the Py•SO ₃ complex. ¹²⁷	28
Scheme 17: The sulfation reaction of phenolic acid substrates using the Py•SO ₃ complex. ⁴⁸	29
Scheme 18: The sulfation reaction of xylan derivatives using Py•SO ₃ complex. ¹²⁹	30
Scheme 19: The sulfation reaction of xylobios using DMF•SO ₃ complex affording xylobiose hexasulfate and pentasulfate. ¹²⁹	30
Scheme 20: <i>In situ</i> production of DMF•SO ₃ complex using methyl chlorosulfate (64).	31
Scheme 21: The sulfation reaction of methyl-α-glucoside (66) using methyl chlorosulfate and DMF. Scope of sulfated small molecules with methyl chlorosulfate, sodium Boc- <i>L</i> -serine methyl ester sulfate (68), sodium Fmoc- <i>L</i> -serine methyl ester sulfate (69), sodium Boc- <i>L</i> -tyrosine methyl ester sulfate (70), sodium β-estradiol disulfate (71), and sodium scymnol persulfate (72). ^a Percentage conversion calculated using ¹ H NMR spectroscopy analysis. ¹²⁹	32

Scheme 22: The <i>O</i> -sulfation of a range of molecules, including primary and secondary alcohols, oximes based molecule, carbohydrates, an α -amino acid, and hormone using DMS/DPS and tetrabutylammonium bisulfate (Bu_4NHSO_4). ¹³⁴	33
Scheme 23: General <i>O</i> -sulfation of protected galactopyranose using the SuFEx strategy. Conditions: (i) DBU, MeCN, 2 h, r.t.; (ii) 5 M sodium methoxide, 1 h, r.t.; and (iii) Pd (OH) ₂ /C and H ₂ , buffer solution (MeCN/MeOH/PBS) 2:2:1, 2 h, r.t. ¹³⁵	35
Scheme 24: Scope of selected sulfate monoester using protection/deprotection method. Protection/deprotection method using the protected sulfate neopentyl or <i>isobutyl</i> esters followed by the deprotection reaction with NaN ₃ for the removal of neopentyl (<i>nP</i>) protecting group or sodium iodide (NaI) for the removal of <i>isobutyl</i> (<i>iBu</i>) protecting group affording the final desired sulfates. Yields shown have been calculated based on the isolated molecules after purification.....	36
Scheme 25: The synthesis of $\text{Me}_3\text{N}\cdot\text{SO}_3$	52
Scheme 26: The synthesis of $\text{Et}_3\text{N}\cdot\text{SO}_3$	52
Scheme 27: The synthesis of $\text{Py}\cdot\text{SO}_3$ complex using chlorosulfonic acid.	55
Scheme 28: The synthesis of $\text{Pr}_3\text{N}\cdot\text{SO}_3$	57
Scheme 29: The sulfation control experiment on benzyl alcohol with $\text{Pr}_3\text{N}\cdot\text{SO}_3$. The overall yields were reported over the two steps.....	58
Scheme 30: The <i>N</i> -sulfamation control experiment on benzylamine with $\text{Pr}_3\text{N}\cdot\text{SO}_3$	59
Scheme 31: Attempted synthesis of $\text{TIBA}\cdot\text{SO}_3$ complex.	60
Scheme 32: The synthesis of <i>isopropyl-N-methyl-tert-butylamine</i> SO_3 complex.....	61
Scheme 33: The <i>N</i> -sulfamation of benzylamine with <i>isopropyl-N-methyl-tert-butylamine</i> SO_3 complex.....	63
Scheme 34: The synthesis of 4-methylmorpholine SO_3 complex.	65
Scheme 35: The synthesis of 4-methylmorpholinium benzyl sulfate using 4-methylmorpholine SO_3 complex.....	67
Scheme 36: The <i>N</i> -sulfamation reaction of benzylamine with 4-methylmorpholine SO_3 complex. ...	68
Scheme 37: The synthesis of 4-ethylmorpholine SO_3 complex.....	68
Scheme 38: The <i>O</i> -sulfation reaction test of benzyl alcohol with 4-ethylmorpholine SO_3 complex. ...	70
Scheme 39: The <i>N</i> -sulfamation reaction of benzylamine using 4-ethylmorpholine SO_3 complex.	70
Scheme 40: The synthesis of cinchonidine SO_3 complex.....	72
Scheme 41: The biological sulfation of tyrosine catalysed by tyrosylprotein sulfotransferase (TPST). ¹⁷⁹	80
Scheme 42: Reagents and conditions: i) $\text{DMF}\cdot\text{SO}_3$ complex (4.0 eq.), ii) Bu_4NHSO_4 (2.0 eq.), sat. aqueous NaHCO_3 (50 mL), 0 °C, and iii) 10% citric acid (25 mL, pH 5).....	81
Scheme 43: The <i>N</i> -sulfamation reaction of selected α -amino acids using TBSAB and scope of selected α -amino acids. The isolated yield of glutathione sulfamate (136) was not reported but confirmed by mass spectrometric detection.....	82
Scheme 44: The general sulfation reaction of selected α -amino acids using 4-methylmorpholine SO_3 and 4-ethylmorpholine SO_3 complexes.	87
Scheme 45: The general synthesis of α -amino acid methyl ester substrates.	87
Scheme 46: The <i>N</i> -sulfamation reaction <i>L</i> -phenylalanine methyl ester using 4-methylmorpholine SO_3 complex.....	89
Scheme 47: The <i>N</i> -sulfamation of <i>S</i> -benzyl- <i>L</i> -cysteine methyl ester using 4-methylmorpholine SO_3 complex.....	90
Scheme 48: The unsuccessful sodium salt (NaI) exchange of the intermediate (145) to form <i>S</i> -benzyl- <i>L</i> -cysteine methyl ester sulfamate (146).	90
Scheme 49: The <i>N</i> -sulfamation reaction of <i>O</i> -benzyl- <i>L</i> -serine methyl ester (147) using 4-methylmorpholine SO_3 complex.	91

Scheme 50: Attempted sulfation reaction of Boc-Tyr-OMe (150) using 4-methylmorpholine SO ₃ complex.....	92
Scheme 51: Attempted <i>N</i> -sulfamation reaction of <i>L</i> -tryptophan methyl ester hydrochloride (153) using 4-methylmorpholine SO ₃ complex.	93
Scheme 52: The <i>O</i> -sulfation reaction of 4-chlorobenzyl alcohol (155) with 4-ethylmorpholine SO ₃ complex.....	94
Scheme 53: The <i>N</i> -sulfamation reaction of <i>L</i> -phenylalanine methyl ester hydrochloride using 4-ethylmorpholine SO ₃ complex. Conditions: (i) DIPEA (0.5 mL, 3.0 eq.), MeCN, r.t., 10 min; (ii) 4-ethylmorpholine SO ₃ (2.0 eq.), r.t., 18 h; (iii) Bu ₃ N, r.t., 1 h; and (iv) NaI exchange, MeCN, r.t., 1 h, 79% yield.....	94
Scheme 54: unsuccessful <i>N</i> -sulfamation reaction of <i>S</i> -benzyl- <i>L</i> -cysteine methyl ester (144) using 4-ethylmorpholine SO ₃ complex.	95
Scheme 55: The <i>N</i> -sulfamation reaction of <i>O</i> -benzyl- <i>L</i> -serine methyl ester using 4-ethylmorpholine SO ₃ complex.	95
Scheme 56: The <i>O</i> -sulfation reaction of Boc-Tyr-OMe (150) with 4-ethylmorpholine SO ₃ complex..	96
Scheme 57: Examples of lipophilic cation-exchange strategy used in sulfation reactions.....	102
Scheme 58: General synthesis of adenosine phosphosulfates using an all-in-one-reagent, SO ₄ (Bu ₃ NH) ₂ . Conditions: (i) imidazole, 2,2'-dithiodipyridine, PPh ₃ , (ii) NaClO ₄ , acetone (iii) and SO ₄ (Bu ₃ NH) ₂ , MgCl ₂ , DMF, r.t., 0.5 h, DEAE-Sephadex using triethylammonium bicarbonate (TEAB). ⁵³	103
Scheme 59: The optimised sulfation conditions for benzyl alcohol and its derivatives using Py•SO ₃ in combination with the lipophilic counterion (Bu ₃ N) and sodium exchange method.	108
Scheme 60: The optimised conditions for the benzylamine sulfamation and its derivatives using Me ₃ N•SO ₃ in combination with the lipophilic counterion (Bu ₃ N) and sodium exchange method. ...	111
Scheme 61: <i>In situ</i> synthesis of tributylammonium sulfamate salts using Me ₃ N•SO ₃ complex and importance of order of addition.	114
Scheme 62: Chemical sulfation methods using sulfur trioxide equivalents, including ClSO ₃ H, Et ₃ N•SO ₃ , and Py•SO ₃ , followed by SPE approach to access steroid sulfates. ^{142, 224-225}	130
Scheme 63: The regioselective sulfation of 17 α -methylandrosterone triols. Conditions: (i) PhB(OH) ₂ , DMF, CH ₂ Cl ₂ , 4 Å mol. Sieves; (ii) Py•SO ₃ , DMF; and (iii) H ₂ O ₂ , aq. NaHCO ₃ , THF, MeOH. ²²⁵	131
Scheme 64: The regioselective sulfation of 17 β -estradiol (195) affording the 17 β -estradiol sulfate (207) as the sodium salt using TBSAB analysed by ¹ H NMR spectroscopy (300 MHz, DMSO- <i>d</i> ₆) and mass spectrometry.	133
Scheme 65: The dual sulfation of 17 β -estradiol (195) using TBSAB afforded the disodium-3,17 β -estradiol disulfate (209) in 74% isolated yield.....	134
Scheme 66: Synthesis of sodium-3-pregnenolone sulfate using TBSAB.....	136
Scheme 67: The diastereoselective reduction of pregnenolone using sodium borohydride (NaBH ₄)	137
Scheme 68: Dual sulfation reaction of pregnanediol using TBSAB.....	139
Scheme 69: The regioselective sulfation reaction of cortisol using TBSAB.	140
Scheme 70: Sulfation reaction of estrone using TBSAB.....	141
Scheme 71: The formation of estrone- <i>d</i> ₂ (the procedure was adapted from the literature) ²⁵⁰	142
Scheme 72: The sulfation reaction of estrone- <i>d</i> ₂ (222) with TBSAB to afford sodium estrone- <i>d</i> ₂ sulfate (224).	145
Scheme 73: Sulfation reaction of heparan-like substrates using the optimised TBSAB sulfation methodology affording the desired heparan sulfate-glycomimetics. ^{46-47, 145, 158, 228}	160
Scheme 74: The attempted sulfation reaction of benzyl alcohol with the synthesised heparan sulfate-glycomimetic (S-10).	162

Scheme 75: Attempted control experiment of sulfation of 4-chlorobenzyl alcohol with sodium 4-methylbenzyl sulfate.....	165
Scheme 76: The control experiment of sulfation of 4-methoxybenzyl alcohol with sodium 4-chlorobenzyl sulfate.....	167
Scheme 77: The enzymatic synthesis of hydrogen sulfide (H ₂ S) which is catalysed by pyridoxal-5'-phosphate (PLP)-dependent enzymes, including cystathionine β-synthase (CBS) and cystathionine γ-lyase (CSE).	173
Scheme 78: The reaction of H ₂ S with disulfide (1) and sulfenic acid (2) affording hydropersulfides (RSSH). ³⁰²	174
Scheme 79: The proposed synthesis of cysteine trisulfide (Cys-SSS-Cys).	176
Scheme 80: Synthesis of Cys-SSS-Cys and the proposed mechanism (this scheme was based on the work of Roger and co-workers ³¹¹).	181

List of Abbreviations

ATIII	antithrombin
CBS	cystathionine β -synthase
c-Met	transmembrane tyrosine kinase
CVD	cardiovascular disease
CSE	cystathionine γ -lyase
Cys-SSH	cysteine persulfide
Cys-SSS-Cys	cysteine trisulfide
DEA	<i>N,N</i> -diethylamine
3,4-DHPA	3,4-dihydroxyphenolic acid
3,4-DHPP	3,4-dihydroxyphenyl propionic acid
DIPEA	<i>N,N</i> -diisopropylethylamine
DMF-SO ₃	sulfur trioxide dimethylformamide complex
ED	endothelial dysfunction
EDG	electron-donating group
EWG	electron-withdrawing group
eNOS	endothelial nitric oxide synthase
Et ₃ N·SO ₃	Triethylamine sulfur trioxide
FDA	Food and Drug Administration
GAGs	glycosaminoglycans
GSSH	glutathione persulfide
HGF	hepatocyte growth factor
4-HPA	4-hydroxyphenyl acetic acid
4-HPP	4-hydroxyphenyl propionic acid
HIV	human immunodeficiency virus
IAls	intra-abdominal infections
IL-6	interleukin-6
IPA	isopropyl alcohol

LDL	low-density lipoprotein
LMWH	low molecular weight heparin
NMDA	<i>N</i> -methyl-D-aspartate receptor
NMR	nuclear magnetic resonance
NEH	sodium-2-ethylhexanoate
PAP	3'-phosphoadenosine 5'-phosphate
PAPS	3'-phosphoadenosine 5'-phosphosulfate
PCA	protocatechuic acid
PLP	pyridoxal-5'-phosphate
ppm	parts per million
Py·SO ₃	pyridine sulfur trioxide complex
PI3K/Akt	phosphoinositide 3-kinase/protein kinase B
ROS	reactive oxygen species
RSSH	hydropersulfides
SPE	solid-phase extraction
STS	steroid sulfatase
SULTs	sulfotransferases
TBAOAc	tetrabutylammonium acetate
TBSAB	tributylsulfoammonium betaine
TEA	triethylamine
THF	tetrahydrofuran
Tf	trifluoromethanesulfonyl
TMSC	trimethylsilyl cellulose
TRPM3	transient receptor potential
UTI	urinary tract infection
VCAM-1	vascular cell adhesion molecule-1

Chapter 1. Chemical sulfation of small biomolecules:
current and future directions

Introduction

Biological sulfation was first discovered when phenyl sulfate was extracted from the urine of a patient who had been treated with the antiseptic, phenol.¹ The detoxification of phenol and other related aromatic scaffolds was first discovered in 1876 by Eugen Baumann.²⁻³ Baumann and co-workers also observed sulfated phenols in urine due to the increased polarity/water solubility of sulfated phenols.¹⁻² Generally, the metabolism of xenobiotics is a two-phase process known as phase I and phase II metabolism, involving chemical modifications and conjugation reactions to an original compound leading to detoxification of these molecules, an increase in their polarity which facilitates their excretion from the body (**Figure 1**).⁴

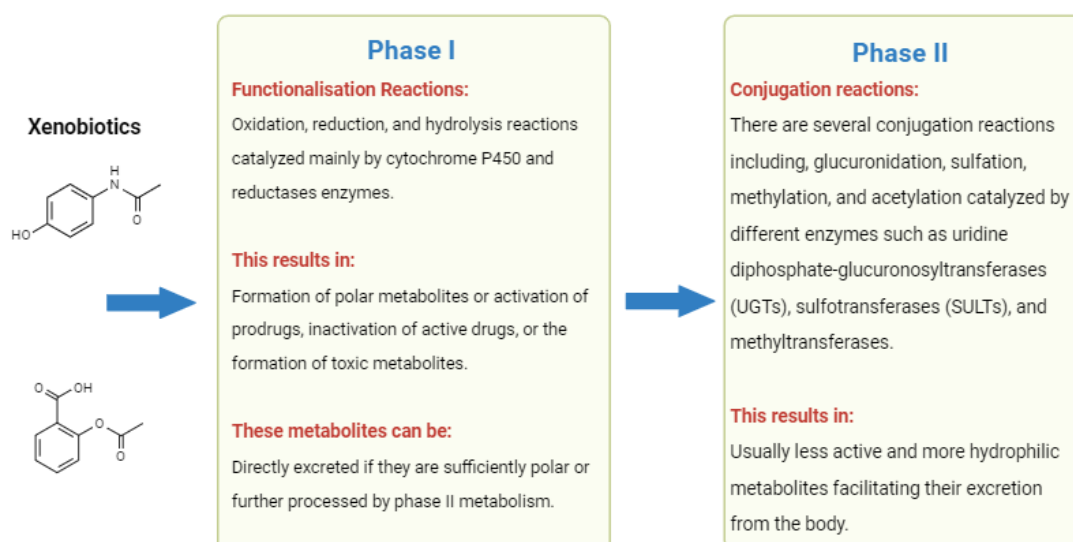


Figure 1: Phase I and II metabolism of xenobiotics involving chemical modification and conjugation reactions (Drawn using Biorender-basic version).

1.1. Sulfation and sulfotransferases

Sulfation is one of the important conjugation reactions of phase II metabolism of xenobiotics and endogenous compounds.⁵⁻⁶ Xenobiotics are substances that are exogenous to the biological system, including medicines and dietary components.³ The sulfation process usually takes place in the liver and other tissues resulting in the increase of the hydrophilicity of

xenobiotic metabolites and therefore facilitating their elimination from the body. The addition of a sulfate group to a molecule introduces a highly polar and negatively charged moiety which increases the overall polarity of the compound and therefore facilitates the elimination process from the body.⁷ Furthermore, sulfate conjugation usually results in decreasing the biological activity of the metabolised molecule.^{6, 8} However, it has also been reported that sulfate conjugation can increase the therapeutic activity of certain drugs, e.g. minoxidil sulfate.⁵ Minoxidil sulfate is the active form of minoxidil which is metabolised by SULT enzymes and approved for the treatment of hypertension and hair loss.⁹⁻¹⁰ The sulfation reaction is catalysed by a group of enzymes called sulfotransferases (SULTs), which facilitate the transfer of the sulfate group from 3'-phosphoadenosine 5'-phosphosulfate (PAPS), the universal sulfate donor, to a nucleophilic site of an acceptor molecule such as phenol (**Figure 2**).^{5, 11-14}

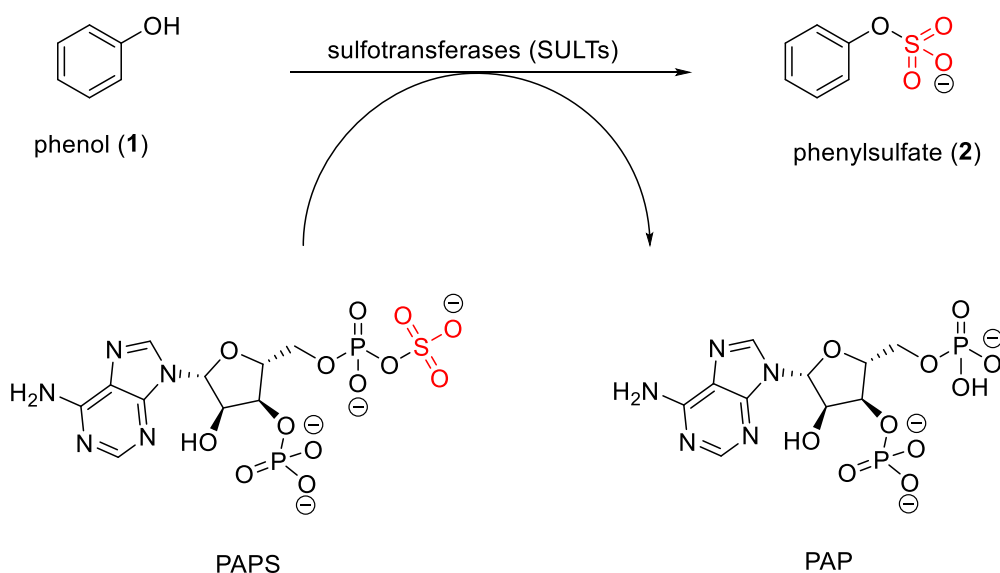


Figure 2: Sulfation of phenol (**1**) (acceptor substrate) mediated by SULTs. The sulfate moiety from PAPS is transferred to the oxygen atom of phenol (**2**).

Sulfotransferase enzymes are generally classified into two main categories; cytosolic and the Golgi membrane-bound sulfotransferases.¹⁵ Cytosolic sulfotransferases are associated with

the phase II metabolism enzymes and involved in the sulfation of low molecular weight molecules.⁸ Like many drug-metabolizing enzymes, cytosolic sulfotransferases are composed of several hundred subtype enzymes.¹⁶ In human, cytosolic sulfotransferases have been classified into several families such as, SULT1, SULT2, and SULT4. SULT1 and SULT2 are the predominant enzymes responsible for the sulfation of xenobiotics and endogenous compounds.¹⁵⁻¹⁸ Recently, Suiko and co-workers discovered a novel sulfotransferase enzyme, SULT7A1 for the C-sulfation reaction on α,β -unsaturated carbonyls, including cyclopentenone prostaglandins.¹⁹ This enzyme exhibits a high degree of specificity and activity towards substrates that contain α,β -unsaturated carbonyl groups such as prostaglandins.¹⁹

On the other hand, Golgi membrane-bound sulfotransferases are responsible for catalysing the sulfation of large molecular weight molecules such as proteins, proteoglycans, and glycolipids.²⁰⁻²¹

1.2. Chemistry of sulfur

Sulfur is the tenth most abundant element in nature accounting \sim 0.03% to 0.06% of the Earth's crust by weight.²² The sulfur atom can exist in multiple oxidation states, ranging from -2 to +6 depending on the chemical compound and its bonding structure.²³ Generally, the oxidation state of an atom in a chemical compound represents the hypothetical charge that atom would have if all bonds to atoms of different elements were 100% ionic. This helps to determine how electrons are distributed in a compound, which is critical for understanding redox reactions.²³ Sulfur is present in anaerobic or volcanic environments and within living cells representing different oxidation states.²³ For instance, sulfur is present predominantly in the +6-oxidation state as the sulfate form of the Earth's atmosphere. While in plants and microorganisms, sulfur exists as the sulfide -2 oxidation state.²³⁻²⁴ With sulfur dioxide (SO_2), the sulfur oxidation state is +4.^{22, 25} Sulfur dioxide is a toxic gas with a pungent odour and has

applications in the industrial sector for producing chemicals such as sulfuric acid (H_2SO_4) and sulfuryl chloride (SO_2Cl_2).²⁵ It has been also used as a preservative agent in the food industry to prevent the growth of bacteria and moulds (**Figure 3**).^{22, 25}

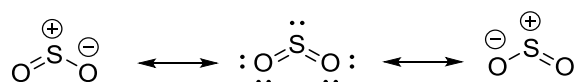


Figure 3: The resonance structures of sulfur dioxide (SO_2).

The oxidation reaction of sulfur dioxide leads to the formation of sulfur trioxide (SO_3). SO_3 is sp^2 hybridized with a trigonal planar structure and a bond angle of 120° .²⁶ SO_3 is available in a liquid form with a density of 1.92 g/mL.²⁷ It can also exist as a gas in fuming sulfuric acid (oleum), a solution of SO_3 25-65 % in sulfuric acid (H_2SO_4). It is also available in a solid form at room temperature (**Figure 4**).²⁶⁻²⁷

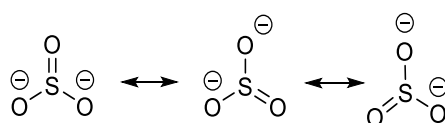


Figure 4: The resonance structures of SO_3 .

SO_3 is a strong Lewis acid, engages in reactions with Lewis bases such as trimethylamine (Me_3N), triethylamine (Et_3N), dioxane, and pyridine (Py). These reactions result in the formation of sulfur trioxide adducts, which can be used in the sulfation of various organic substrates, leading to the formation of organosulfate esters. Furthermore, different interactions with SO_3 occur in polar dioxane, including dipole-dipole interactions due to the electronegativity of oxygen atoms. Thus, there can be dipole-dipole interactions between the lone pairs of electrons on the dioxane oxygen atoms and the electron-deficient sulfur atom in SO_3 , resulting in the stabilisation of the resulting 1,4-dioxane SO_3 complex (**Figure 5**).²⁸

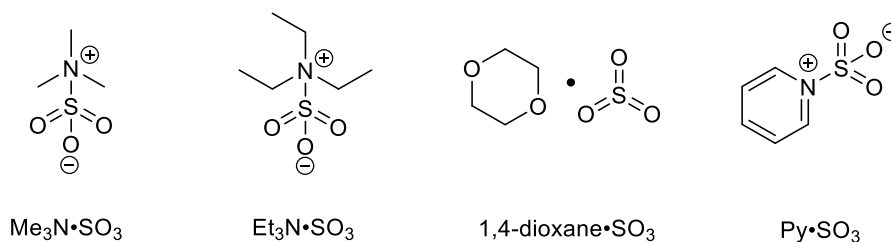


Figure 5: Sulfur trioxide adducts with Lewis bases, including trimethylamine, triethylamine, 1,4-dioxane, and pyridine.

Sulfur has been recognised as one of the earliest known elements for its therapeutic properties by the ancient Greeks dating back over 4000 years.²² It is one of the essential components for all living organisms being found in the α -amino acids: methionine and cysteine, in vitamins: thiamine and biotin, and others.^{22, 29} Approximately, 250 sulfur-containing drugs have been approved by the FDA for the treatment of diabetes mellitus, bacterial infections, migraine, cardiovascular diseases (CVD), neurological disorders, cancer, and human immunodeficiency virus (HIV) as of 2022.^{22, 29-31} These approved drugs have different sulfur-containing functional groups including thioethers, sulfoxides, sulfones, sulfonamides, sulfates, sulfamates, and phenothiazines (**Figure 6**).²⁹

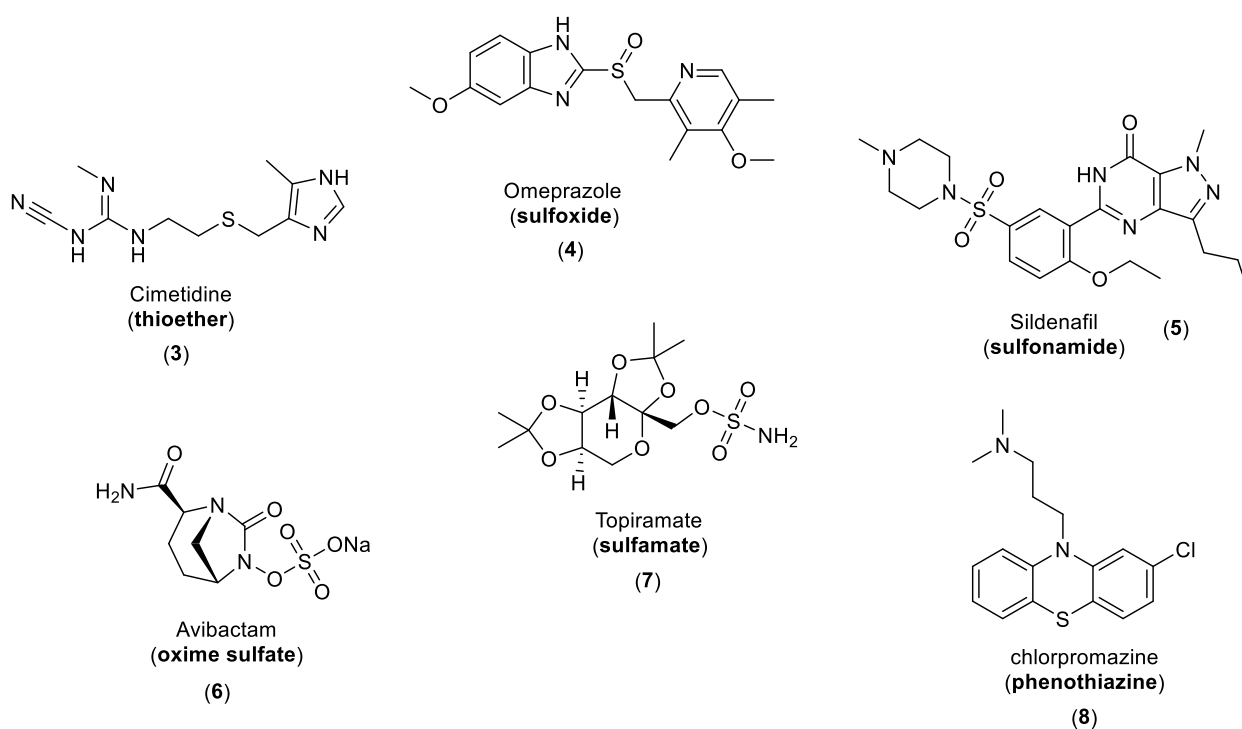


Figure 6: Examples of FDA-approved drugs with sulfur-containing functional groups.

1.3. Chemical sulfation approaches of small molecules

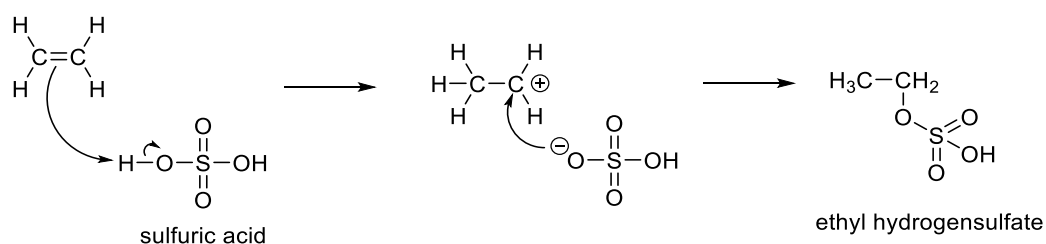
Organosulfates and sulfamates have several biological applications, ranging from the metabolism of xenobiotics to the downstream signalling of steroidal sulfates in pathological conditions.³² Over the past decade, different biological applications, including anti-coagulant, anti-viral, anti-inflammatory, immunomodulatory, and anti-tumour were associated with sulfated polysaccharides, flavonoids, steroids, and proteins.³³⁻³⁷ For instance, heparin and heparan sulfate are examples of glycosaminoglycans (GAGs) that contain sulfate groups which promote molecular interactions with protein and binding at the cell surface.³⁸ The incorporation of a polar hydrophilic sulfate group onto drug-like molecules has facilitated research investigating novel sulfated biomolecules as potential new therapies.³⁹ However, the chemical synthesis and purification of (per)-sulfated compounds are challenging because they have poor solubility in organic solvents.⁴⁰ Moreover, the sensitivity of sulfated

compounds to both acidic and high temperature protocols hampers their widespread use.⁴¹⁻
⁴³ Additionally, some poly alcoholic/phenolic substrates such as carbohydrates and proteins, might not be fully sulfated due to anionic crowding, which results in non-sulfated by-products. Finally, polyfunctional scaffolds suffer from the lack of regioselective sulfation.⁴⁴ As a result, the sulfation reaction is often the last step in a synthetic process, which restricts any potential chemical modifications.⁴⁵ Given the growing interest of sulfation and the significant biological functions of sulfated molecules, several synthetic approaches to sulfate oxygens, nitrogens, oximes, and phosphates have been reported such as the use of sulfuric acid (H₂SO₄), DCC/H₂SO₄, chlorosulfonic acid, sulfur trioxide amine/amide complexes, and miscellaneous methods.^{2, 46-55}

This chapter will report the most common and latest chemical sulfation approaches to a wide range of small molecules. Elements of this chapter have been published in *Essays in Biochemistry* as: Jaber A. Alshehri, Alan M. Jones; Chemical approaches to the sulfation of small molecules: current progress and future directions. *Essays Biochem* 2024; EBC20240001. doi: <https://doi.org/10.1042/EBC20240001>.⁵⁶

1.3.1. Sulfation using sulfuric acid and related reagents

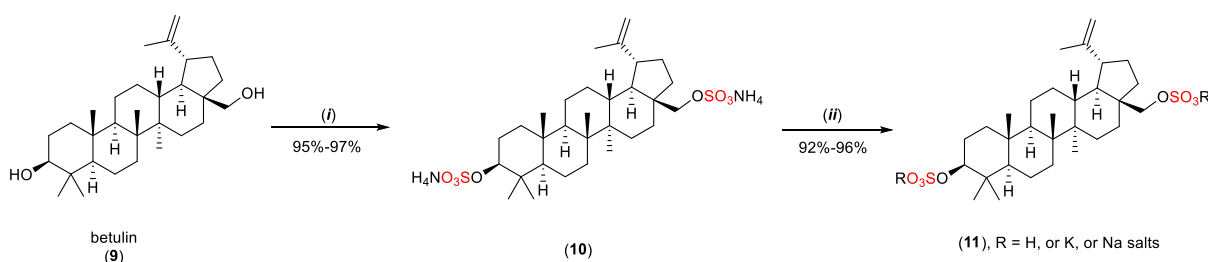
Since the early 20th century, sulfuric acid has been employed for the sulfation of alkenes and cycloalkenes (temperature was not reported) resulting in cycloalkyl sulfates (**Scheme 1**).²⁸



Scheme 1: General reaction scheme for sulfation of ethene using H₂SO₄.

Moreover, sulfuric acid (H_2SO_4) was also a common reagent for the sulfation of polysaccharides and flavonoids.^{37, 57} For instance, the sulfation reaction of a polysaccharide that is derived from the Longan Chinese fruit that has been known for its health benefits such as anti-oxidant, anti-cancer, and immunomodulation activities, was reported using the sulfuric acid method.⁵⁸⁻⁶⁰

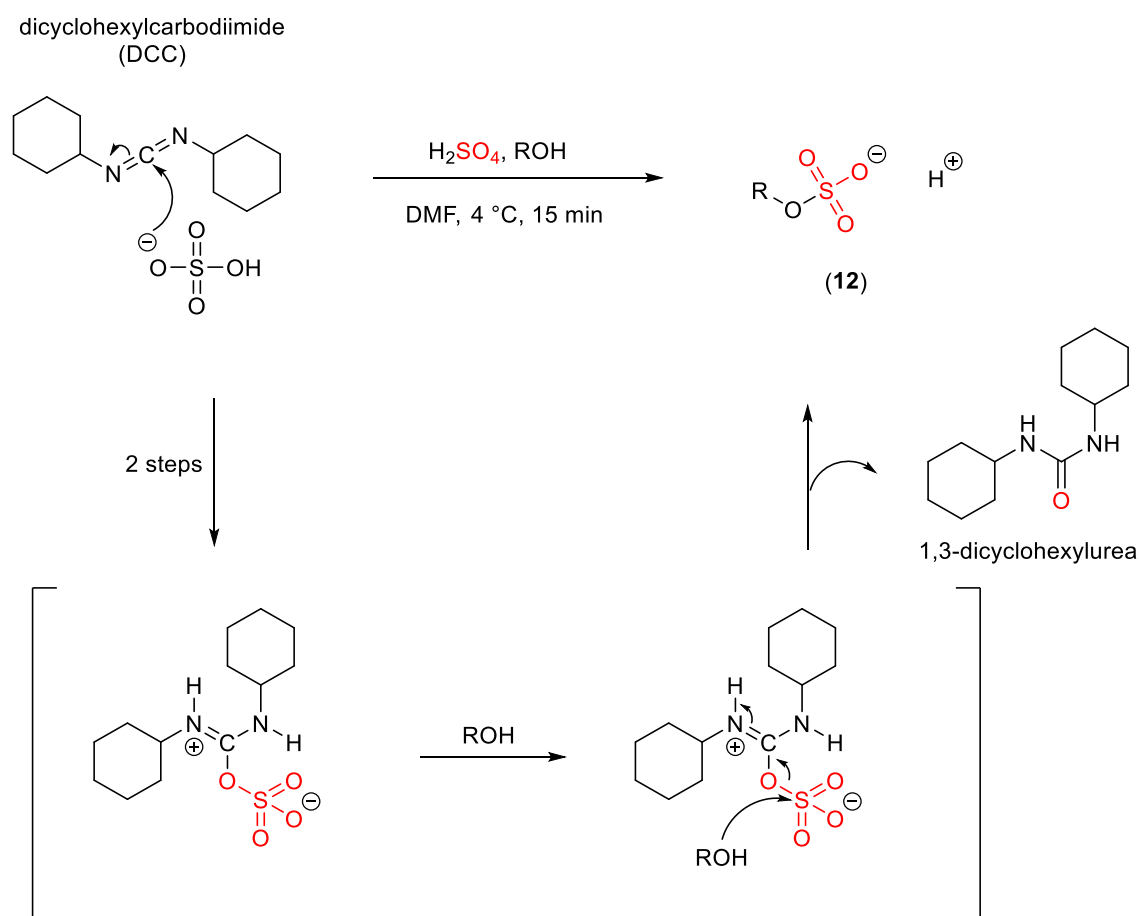
A modified version of the sulfuric acid sulfating method employs sulfamic acid ($\text{H}_2\text{NSO}_3\text{H}$), which has been used for the sulfation of saturated monohydric alcohols, carbohydrates, and flavonoids.⁶¹ A naturally occurring molecule, the triterpenoid, betulin is mainly found in the bark of birch trees.⁶² Studies have shown the biological roles of sulfated betulin, including anti-viral, anti-inflammatory, anti-oxidant, and anti-coagulant activities.⁶¹⁻⁶⁴ Betulin was sulfated using sulfamic acid method in the presence of urea $\text{CO}(\text{NH}_2)_2$ as a catalyst in DMF or 1,4-dioxane solvents.⁶¹ In both cases, double sulfation of betulin occurred and the product was isolated as its ammonium, sodium, and potassium salt (**Scheme 2**).⁶¹



Scheme 2: Double sulfation of betulin with sulfamic acid ($\text{H}_2\text{NSO}_3\text{H}$). **Conditions:** (i) $\text{H}_2\text{NSO}_3\text{H}$, urea, and DMF or 1,4-dioxane (60-75 °C, 2-3.5 h); and (ii) work up with 10% H_2SO_4 , or 3–5% KOH, or 3–5% NaOH.⁶¹

Sulfamic acid sulfation method benefits from the stability and non-hygroscopic nature of sulfamic acid, offering a safer alternative compared to other sulfating reagents including sulfuric acid and chlorosulfonic acid. Despite the effectiveness of both sulfuric acid and sulfamic acid approaches to sulfation, there are issues regarding the use of aggressive reagents, degradation, and nonselective sulfation.⁶⁵ Another modified form of the sulfuric

acid sulfating method employs dicyclohexylcarbodiimide (DCC), for the sulfation of aliphatic/alicyclic alcohols (**Scheme 3**).⁶⁶



Scheme 3: Sulfation reaction of aliphatic alcohol using H_2SO_4 /DCC coupling protocol, where R = Alkyl. Adapted from Hoiberg and Mumma et al.⁶⁶⁻⁶⁷

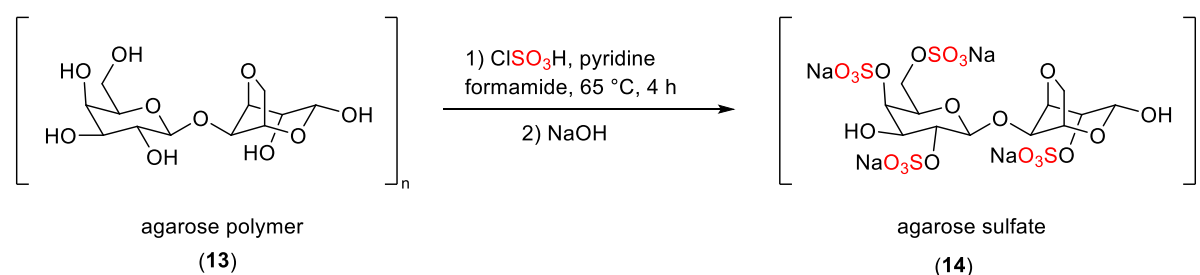
This method provides sulfation under milder conditions compared to the sulfuric acid method, preventing side reactions and decomposition of sensitive substrates. It also offers higher selectivity over other functional groups that may be present in the substrate, such as amines and thiols for the sulfation of alcohols.²

This modified approach was applied to the neuropeptide hormone, cholecystokinin (CCK) which is widely distributed in the central and peripheral nervous system.⁶⁸ The sulfation modification of cholecystokinin has several biological functions including appetite control and

stimulating pancreatic enzyme secretion.⁶⁹ Cholecystokinin was sulfated using the H₂SO₄/DCC method and resulted in a 40% isolated yield but used excess sulfuric acid (4-fold) and DCC (40-fold), highlighting the challenges during its synthesis.⁷⁰

1.3.2. Sulfation using chlorosulfonic acid (ClSO₃H) and its derivatives

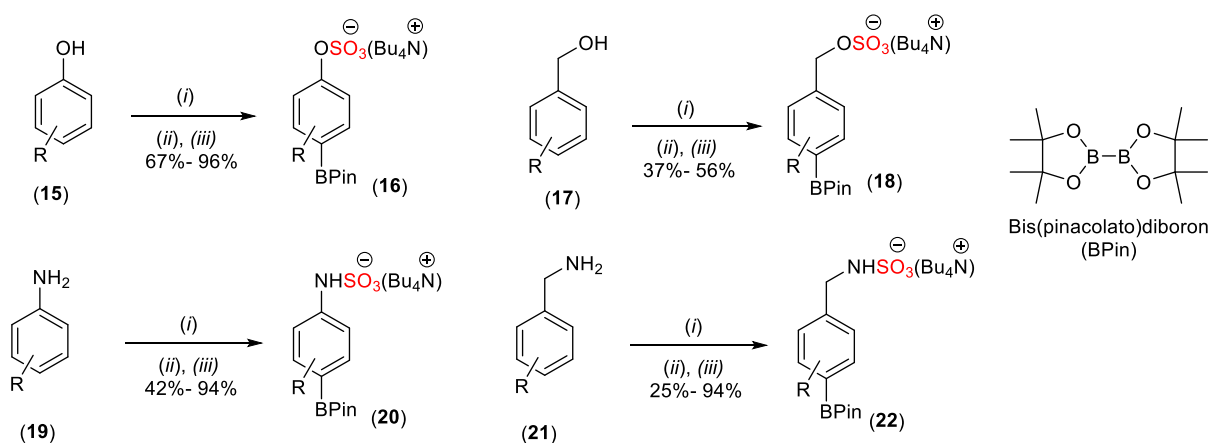
An alternative approach utilises chlorosulfonic acid, which has been applied for the sulfation of polysaccharides, phenolic acids, and flavonoids, amongst others.^{65, 71-72} Agarose sulfate, an example of a sulfated seaweed polysaccharide has been proposed to have anti-coagulant activity comparable to heparin.⁷³ Youping and co-workers reported the formation of agarose sulfate using the chlorosulfonic acid protocol. First, chlorosulfonic acid was added dropwise to the cold pyridine (0 °C) due to the exothermic nature of chlorosulfonic acid. Next, agarose polysaccharide was dissolved in formamide solvent followed by the addition of chlorosulfonic acid solution. The resulting mixture was stirred for 4 h at 65 °C affording agarose sulfate (**14**) (isolated yield was not reported) (**Scheme 4**).⁷³



Scheme 4: The sulfation reaction of agarose polymer (**13**) using ClSO₃H/pyridine.⁷³

Qian and co-workers reported the sulfation of the polysaccharide moiety in *Dendrobium huoshanense* using chlorosulfonic acid-pyridine approach.⁷⁴ *Dendrobium huoshanense* plant is the source of various biomolecules including polysaccharides, flavonoids, and phenols.⁷⁵ Several studies showed that *Dendrobium* plants have various biological applications including anti-cancer, anti-oxidant, hepatoprotective, anti-inflammation, and anti-diabetic activities.⁷⁶⁻

⁷⁸ The sulfation of the polysaccharide moiety of Dendrobium was carried out using chlorosulfonic acid-pyridine employed in a 1:2 ratio at 60 °C for 3 h (yield was not reported).⁷⁴ In 2019, Mihai and co-workers reported the sulfation of phenols, benzyl alcohols, anilines, and benzylamines using chlorosulfonic acid with the addition of tetrabutylammonium hydrogensulfate (Bu_4NHSO_4) as a cation exchange to improve the overall solubility of the intermediate sulfates in organic solvents (**Scheme 5**).⁵²



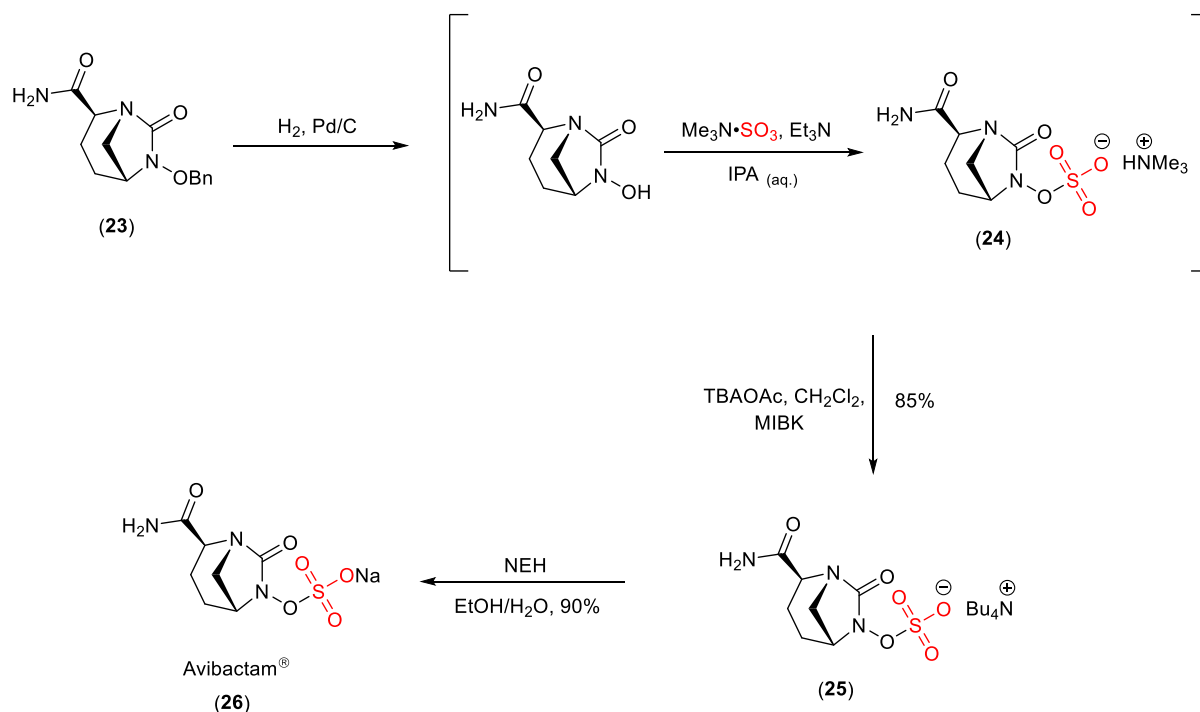
Scheme 5: Synthesis of sulfated phenols, benzyl alcohols, anilines, and benzylamines using ClSO_3H as a source of sulfation, followed by cation exchange. **Conditions:** (i) ClSO_3H (5.0 mmol, 1 eq.), triethylamine and CH_2Cl_2 , 0 °C to r.t., 1 h; (ii) tetrabutylammonium hydrogensulfate (4.0 mmol), CH_2Cl_2 ; and (iii) B_2Pin_2 (0.25–0.5 mmol), $[\text{Ir}(\text{COD})\text{OMe}]_2$ (1.5–2.5 mol %), dtbpy (3–5 mol %), 1,4-dioxane, 70 °C, up to 16 h.⁵²

Furthermore, the resulting tetrabutylammonium sulfate intermediates caused steric hindrance which impacts the regioselectivity of the subsequent Iridium-catalysed borylation reactions using bis(pinacolato)diboron, B_2Pin_2). These steric interactions favour borylation at the *para*-position over the *meta*-position on the aromatic ring.⁵² This protocol introduces new functional groups to the organic molecules changing their reactivity as well as their chemical properties.⁵²

1.3.3. Sulfation using sulfur trioxide amine/amide complexes

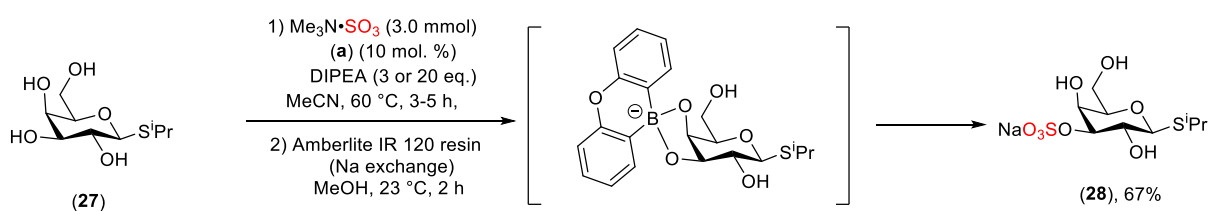
1.3.3.1. Trimethylamine sulfur trioxide complex

The sulfation reaction using sulfur trioxide amine/amide complexes is the most used method for sulfating alcoholic or phenolic groups in carbohydrates, flavonoids, steroids, proteins, and aliphatic or alicyclic scaffolds. For instance, Ball and co-workers have used sulfur trioxide trimethylamine complex ($\text{Me}_3\text{N}\cdot\text{SO}_3$) and a lipophilic cation-exchange to access Avibactam[®], a β -lactamase inhibitor (**Table 1**).^{50, 79-80} They reported a simultaneous one-pot deprotection and sulfation reaction of a hydroxylamine intermediate using $\text{Me}_3\text{N}\cdot\text{SO}_3$ complex. The resulting intermediate was exchanged with tetrabutylammonium acetate (TBAOAc) making it more lipophilic which facilitates extraction of the organosulfate intermediate into CH_2Cl_2 . Finally, a lipophilic sodium salt exchange reagent, sodium-2-ethyl-hexanoate (NEH) was added affording Avibactam[®] in 90% yield as sodium salt (**Scheme 6**).⁵⁰



Scheme 6: The final two steps of the total synthesis of Avibactam[®], adapted from Ball et al.⁵⁰

Due to the importance of the biological functions of sulfated polysaccharides, polysaccharides have been sulfated using different sulfating reagents including sulfur trioxide amine/amide complexes and chlorosulfonic acid despite the structural complexity of polysaccharides, poor solubility in organic solvents, lack of selectivity, and purification and isolation difficulties.⁸¹ In 2019, the $\text{Me}_3\text{N}\cdot\text{SO}_3$ complex was reported for the site-selective sulfation of polysaccharides including pyranoside scaffolds (**Table 1**).⁸¹ The site-selective sulfation of pyranoside scaffolds was carried out under catalytic conditions using a diarylborinic acid.⁸²⁻⁸³ This method led to the site-selective sulfation at the equatorial position of cis-1,2-diol groups in pyranoside derivatives which provides less steric hindrance compared to axial positions.⁸¹ As a result, the diarylborinic acid favourably coordinates to the cis-1,2-diol groups, forming a tetracoordinate borinic ester intermediate with the diol groups of the carbohydrate enhancing the site selectivity at these positions. β -Thioglycoside pyranoside was selected as a model for the site-selective sulfation using $\text{Me}_3\text{N}\cdot\text{SO}_3$ and diarylborinic acid with the addition of DIPEA as a base which improves selectivity and the overall yield (**Scheme 7**).⁸¹

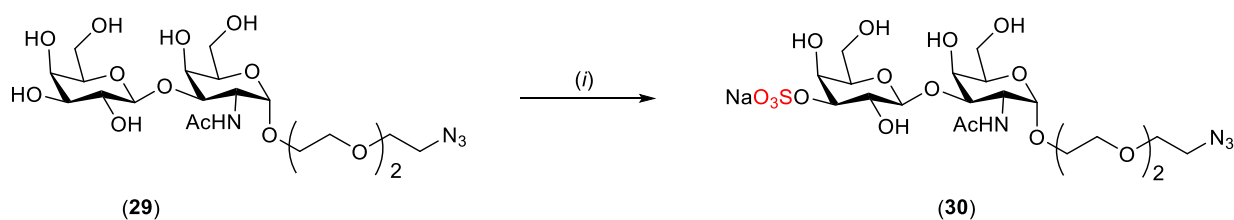


Scheme 7: Site selective sulfation of pyranoside scaffolds using (a) diarylborinic acid.⁸¹

More recently, $\text{Me}_3\text{N}\cdot\text{SO}_3$ complex was also used for the preparation of the 3'-O-sulfated analogue of Thomsen–Friedenreich (TF) antigen (**Table 1**).⁸⁴ The TF antigen is a disaccharide which is found on the surface of the most common types of human cancer cells.⁸⁵ It interacts with galectins, polysaccharide-binding proteins, resulting in tumour growth as well as cancer metastasis.⁸⁶ The sulfated analogue of TF antigen has been recognised to bind to galectin and

other polysaccharide-binding proteins, but its biological functions are not well understood.⁸⁷

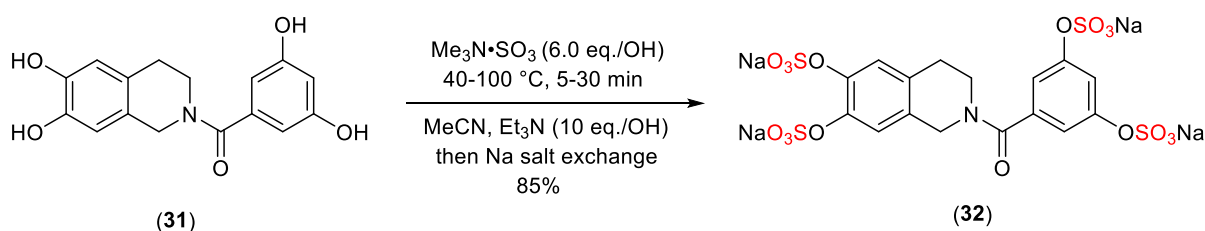
The sulfation of a TF antigen analogue with $\text{Me}_3\text{N}\cdot\text{SO}_3$ complex resulted in the formation of 3'-*O*-sulfated TF antigen in 66% isolated yield (**Scheme 8**).⁸⁴



Scheme 8: The sulfation step of TF antigen using $\text{Me}_3\text{N}\cdot\text{SO}_3$. Conditions: (i) Bu_2SnO , benzene/DMF (5:1, v/v), 125 °C, 24 h, then $\text{Me}_3\text{N}\cdot\text{SO}_3$, DMF, r.t., 72 h, then flash chromatography, then Dowex[®] 50WX4 (Na^+ form) resin, H_2O , r.t., 16 h, 66%.⁸⁴

Desai and co-workers reported the use of $\text{Me}_3\text{N}\cdot\text{SO}_3$ complex for the sulfation of tetrahydroisoquinoline derivatives and other polyhydroxylated small molecules (**Table 1**).⁵⁷

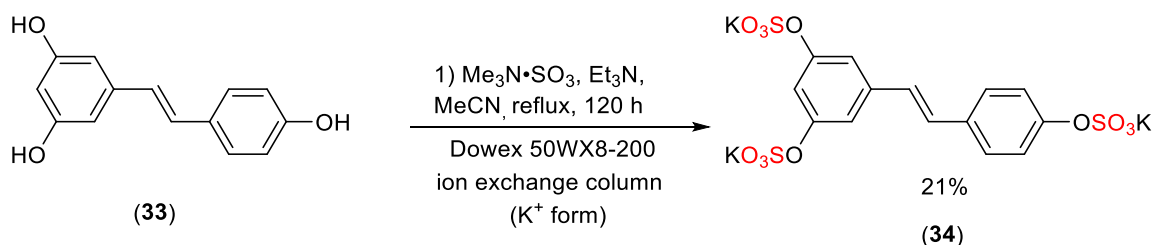
The sulfation of tetrahydroisoquinoline derivative (**31**) has been carried out using $\text{Me}_3\text{N}\cdot\text{SO}_3$ complex in excess (6.0 eq./OH group) at 100 °C and in the presence of base (Et_3N), affording the tetrasulfated isoquinoline (**32**) in 85% isolated yield (**Scheme 9**).⁸⁸



Scheme 9: Sulfation reaction of tetrahydroisoquinoline derivatives using $\text{Me}_3\text{N}\cdot\text{SO}_3$ complex.⁸⁸

The use of $\text{Me}_3\text{N}\cdot\text{SO}_3$ complex was also reported in the sulfation of resveratrol, a naturally occurring polyphenol that is found in many plants, such as peanuts, grapes, and berries.⁸⁹ Resveratrol has gained interest due its important biological applications such as anti-

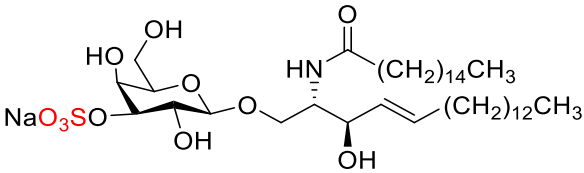
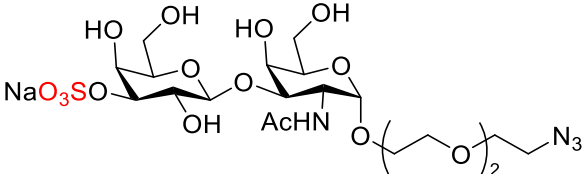
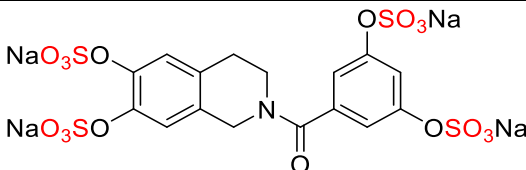
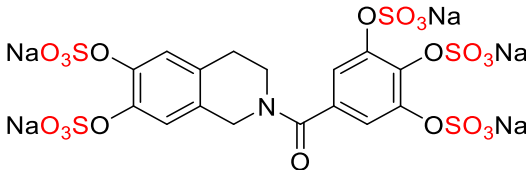
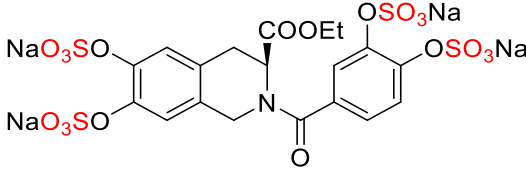
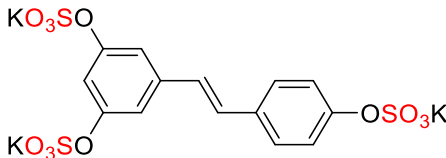
inflammatory, anti-cancer, and anti-oxidant activity.⁸⁹ The sulfation of resveratrol has been carried out using $\text{Me}_3\text{N}\cdot\text{SO}_3$ complex in the presence of base (Et_3N) at reflux (MeCN , b.p. = 82 °C) affording the potassium salt of sulfated resveratrol (**Scheme 10**).⁸⁹



Scheme 10: Sulfation reaction of resveratrol using $\text{Me}_3\text{N}\cdot\text{SO}_3$ complex.⁸⁹

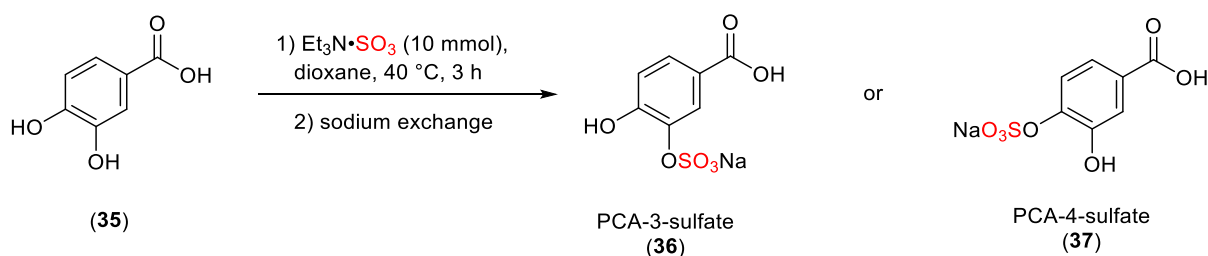
Table 1: Selected sulfation approaches of organic molecules using $\text{Me}_3\text{N}\cdot\text{SO}_3$ complex.

Entry	Sulfated substrate	Isolated yield	Reference
1	<p>Avibactam</p>	90%	50
2	<p>Pyranoside derivatives</p>	64-97%	81
3	<p>Sulfated Lactose-derived β-thioglycoside</p>	66%	81

4	 <p>Sulfated β-galactosylceramide</p>	66%	81
5	 <p>3'-O-Sulfated TF antigen</p>	66%	84
7	 <p>Polysulfated tetrahydroisoquinoline</p>	85%	88
8	 <p>Polysulfated tetrahydroisoquinoline</p>	54%	88
9	 <p>Polysulfated tetrahydroisoquinoline</p>	74%	88
10	 <p>Potassium resveratrol sulfate</p>	21%	89

1.3.3.2. Triethylamine sulfur trioxide complex

Another sulfur trioxide amine complex example is triethylamine SO_3 complex ($\text{Et}_3\text{N}\cdot\text{SO}_3$), which has also been utilised for the sulfation of a wide range of small organic molecules such as flavonoids, polysaccharides, proteins, and steroids.⁹⁰⁻⁹¹ For instance, the sulfation of polyphenolic flavonoids such as protocatechuic acid (PCA), quercetin, and catechin was reported using $\text{Et}_3\text{N}\cdot\text{SO}_3$ complex.⁹⁰⁻⁹¹ Several studies showed the associations of PCA with biological and pharmacological activities such as, anti-oxidant, anti-microbial, anti-cancer, anti-diabetic, anti-inflammatory activities, as well as cardiovascular, hepatic, and neurological effects.⁹²⁻⁹³ Other studies reported that PCA sulfates lower the production of interleukin-6 (IL-6), a pro-inflammatory cytokine, and vascular cell adhesion molecule-1 (VCAM-1), an adhesion protein. Both are linked to cardiovascular diseases.⁹⁴ Gutierrez and co-workers described the monosulfation reaction of protocatechuic acid (PCA) using an excess of $\text{Et}_3\text{N}\cdot\text{SO}_3$ (10-fold) at 40 °C for 3 h affording PCA-3-sulfate or PCA-4-sulfate (**Scheme 11**).^{90, 95}

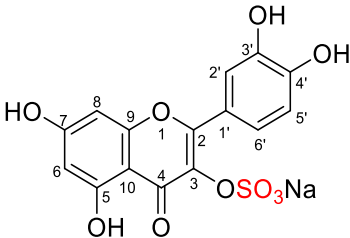
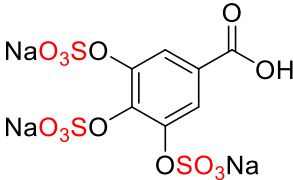


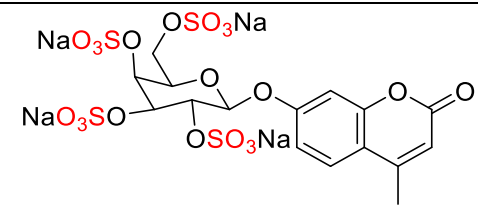
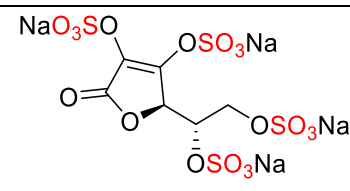
Scheme 11: General procedure for sulfation of PCA using $\text{Et}_3\text{N}\cdot\text{SO}_3$ affording PCA-3-sulfate (**36**) or PCA-4-sulfate (**37**).⁹⁰

Quercetin, and related catechin flavonoids have important biological roles and potential health benefits. Quercetin has been known to inhibit xanthine oxidase and lipoxygenase enzymes which are associated in processes including inflammation, atherosclerosis, cancer, and cardiovascular health.⁹⁶⁻⁹⁷ Catechins have demonstrated the ability to reduce platelet aggregation and inhibit the proliferation of human cancer cell lines.⁹⁸ The monosulfate

analogues of quercetin and catechin were prepared following the procedure of the monosulfation reaction of protocatechuic acid (PCA) using $\text{Et}_3\text{N}\cdot\text{SO}_3$ as a source of sulfation.⁹¹ In 2011, Correia-da-Silva and co-workers investigated the synthesis of new persulfated compounds which can be used as anti-coagulant and anti-platelet agents for the treatment of thrombosis.⁹⁹⁻¹⁰⁰ Sulfation of different polyphenolic molecules such as gallic acid, 4-methyl 7-hydroxycoumarin 7- β -D-glucopyranoside, and ascorbic acid was afforded using $\text{Et}_3\text{N}\cdot\text{SO}_3$ (2-8 eq./OH group) in dimethylacetamide (DMA) at 65 °C for 24 h.⁹⁹

Table 2: Sulfation of organic molecules using $\text{Et}_3\text{N}\cdot\text{SO}_3$ complex. N.R. not reported.

Entry	Sulfated substrate	Isolated yield	Reference
1	 <p>PCA-3-sulfate</p>	N.R.	90
2	 <p>Quercetin 3-sulfate</p>	N.R.	91
3	 <p>Sulfated gallic acid</p>	36%	99-100

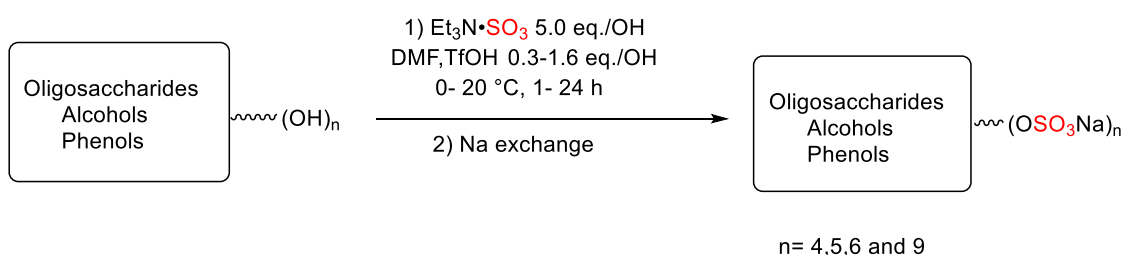
4	 <p>Sulfated 4-methyl 7-hydroxycoumarin</p>	47%	99-100
5	 <p>Sulfated ascorbic acid</p>	7%	99-100

The microwave-assisted sulfation approach using sulfur trioxide complexes such as $\text{Et}_3\text{N}\cdot\text{SO}_3$ has been widely applied due to its efficiency in reducing reaction times, improving yields, and simplifying the purification using straightforward aqueous isolation techniques without the need for extensive chromatographic methods. However, there are several issues and challenges associated with this method that must be addressed to ensure successful outcomes,⁸⁸ for example, the requirement of specialised equipment such as a microwave reactor, which needs precise control of temperature, pressure, and microwave power. Furthermore, this instrument is expensive and may not be available in all laboratories. Another issue is the risk of over-sulfation due to the excessive heat leading to the formation of unwanted side products.

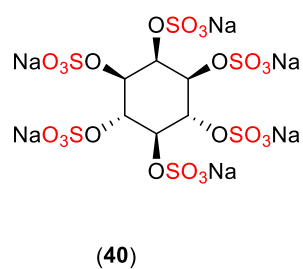
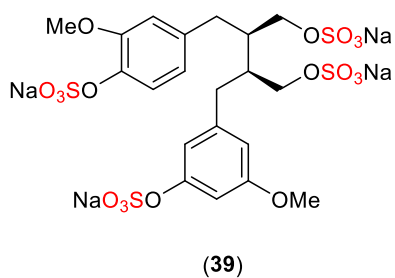
Desai and co-workers studied this approach on a small number of polyhydroxylated molecules, including tetrahydroisoquinoline derivatives using different sulfur trioxide amine complexes including $\text{Et}_3\text{N}\cdot\text{SO}_3$.^{88, 101-102} An improved version of the microwave-assisted sulfation method was employed using sulfur trioxide amine complexes including $\text{Et}_3\text{N}\cdot\text{SO}_3$ with the addition of a strong acid, triflic acid (TfOH) permitted acceleration of this reaction.¹⁰³

Krylov and co-workers investigated the practicality of this method on polyhydroxy organic scaffolds such as lignans, flavonoids, cyclitols, and oligosaccharides.¹⁰³⁻¹⁰⁴ The *O*-sulfation has been carried out using Et₃N•SO₃ complex in the presence of DMF solvent between 0 °C and 20 °C. TfOH was added to the reaction to protonate the Et₃N in the Et₃N•SO₃ complex and generate the highly reactive SO₃ *in situ* that reacts readily with the hydroxyl groups on polyhydroxy substrates. The resulting intermediate was exchanged with sodium hydroxide affording the sodium salt of sulfated polyhydroxy molecules.¹⁰³

Despite the effectiveness of this method, some limitations were reported including the use of a strong acid (TfOH), which might not be compatible with acid-sensitive substrates and the excess of sulfating reagent used (up to 5.0 eq./OH) (**Scheme 12**).¹⁰³⁻¹⁰⁴



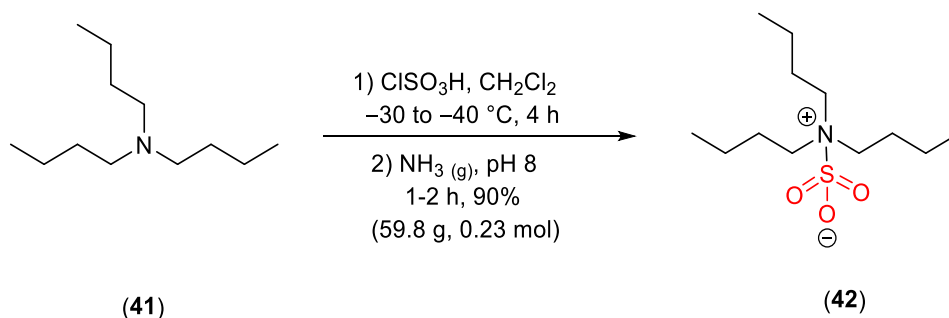
Examples:



Scheme 12: The *O*-sulfation of polyhydroxy organic scaffolds with Et₃N•SO₃ and the addition of TfOH.¹⁰³⁻¹⁰⁴

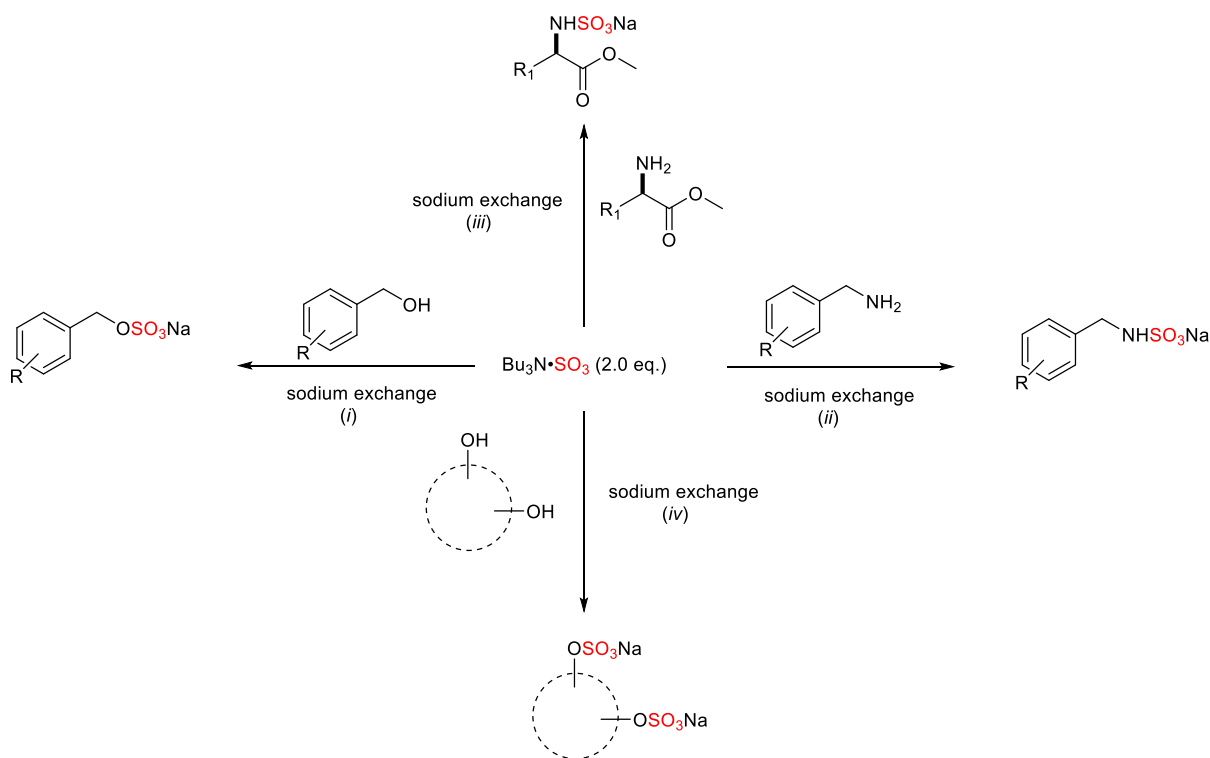
1.3.3.3. Tributylsulfoammonium betaine (TBSAB/ $\text{Bu}_3\text{N}\cdot\text{SO}_3$)

A sulfating reagent was recently developed by our research group, tributylsulfoammonium betaine (TBSAB, $\text{Bu}_3\text{N}\cdot\text{SO}_3$) (**Scheme 13**).



Scheme 13: The general synthesis of TBSAB (**42**).

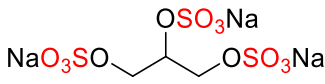
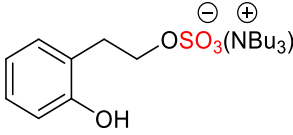
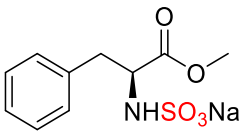
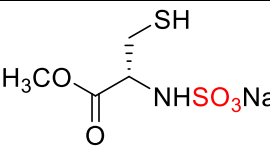
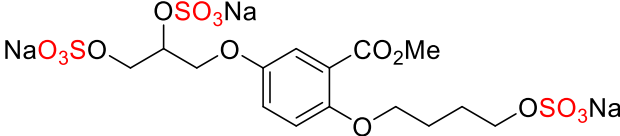
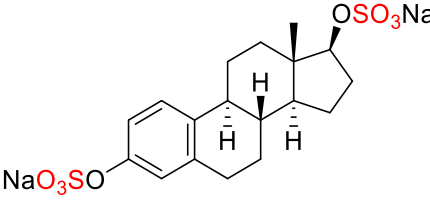
TBSAB was applied to a wide range of small molecules including benzyl alcohols, benzylamines, steroids, carbohydrates, and proteins. TBSAB also provides a simplified purification and isolation of sulfated molecules due to the greater lipophilicity profile of TBSAB ($\text{cLogP} = 4.51$). The increased lipophilicity permits efficient extraction into organic solvents such as dichloromethane or hexane. This makes the isolation of the desired sulfated products straightforward (**Scheme 14**).



Scheme 14: General sulfation synthesis of organic scaffolds using all-in-one type reagent, $\text{Bu}_3\text{N}\cdot\text{SO}_3$. **Conditions:** (i) $\text{Bu}_3\text{N}\cdot\text{SO}_3$ (2.0 eq.), MeCN, 90 °C, up to 3 h, then sodium 2-ethylhexanoate (NEH) or sodium iodide (NaI) exchange. (ii) $\text{Bu}_3\text{N}\cdot\text{SO}_3$ (2.0 eq.), MeCN, 30 °C, up to 1 h, then NaI exchange. (iii) $\text{Bu}_3\text{N}\cdot\text{SO}_3$ (2.0 eq.), MeCN, r.t., up to 18 h, then NaI exchange. (iv) $\text{Bu}_3\text{N}\cdot\text{SO}_3$ (≥ 2.0 eq.), MeCN, 90 °C, up to 12 h, then NEH or NaI exchange. R = Me, OMe, Cl, CF_3 , NO_2 , R_1 = α -amino acid side chain.⁴⁷

Benedetti and co-workers have reported the use of TBSAB for the sulfation and sulfamation of a wide range of benzyl alcohols, benzylamines, amino acids, and carbohydrates that have biological applications including protein-protein interactions, cell signalling, and anti-inflammation activity (**Table 3**).^{47, 54}

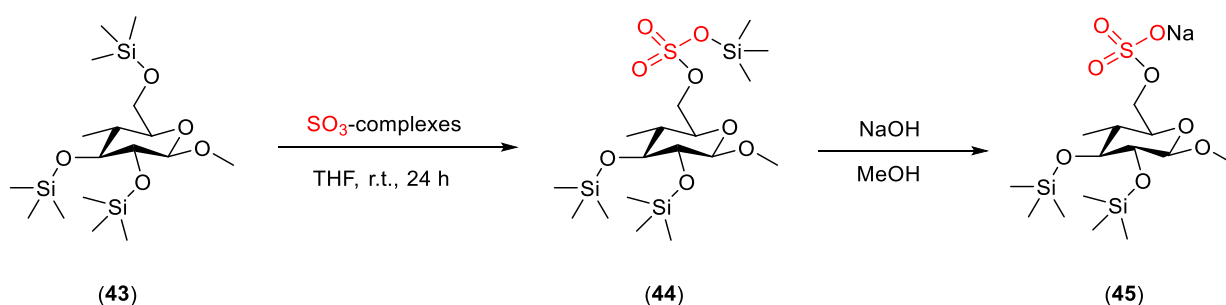
Table 3: Sulfation methods of selected biomolecules using TBSAB.

Entry	Sulfated substrate	Isolated yield	Reference
1	 <p>Sulfated glycerol</p>	92%	
2	 <p>Sulfated 2-hydroxyphenyl ethanol</p>	74%	
3	 <p><i>L</i>-Phenylalanine methyl ester sulfamate</p>	60%	47
4	 <p><i>L</i>-Cysteine methyl ester sulfamate</p>	50%	47
5	 <p>Sulfated glycomimetics C3</p>	76%	54, 105
6	 <p>Estradiol sulfates</p>	84%	

1.3.3.4. Pyridine sulfur trioxide and dimethylformamide sulfur trioxide complexes

Alternative sulfur trioxide complexes involving $\text{Py}\cdot\text{SO}_3$ and $\text{DMF}\cdot\text{SO}_3$ have been used for the sulfation of polysaccharides and polyphenolic flavonoids.¹⁰⁶ For instance, Li and co-workers have reported the sulfation of polysaccharides which were isolated from pumpkin (*Cucurbita maxima*) using a $\text{Py}\cdot\text{SO}_3$ complex.^{102, 107} Several reports have revealed the nutritional and health roles in hypoglycaemic and anti-oxidant activities of these pumpkin polysaccharides.¹⁰⁸⁻¹¹¹ In this method, the pumpkin polysaccharide in *N,N*-dimethylformamide (DMF) was added to the $\text{Py}\cdot\text{SO}_3$ complex resulting in the formation of sulfated pumpkin polysaccharide.¹⁰⁷ Cellulose sulfate is another example of a sulfated polysaccharide which has been studied for its potential biological and pharmaceutical applications such as an anti-coagulant, anti-microbial, anti-oxidant agent, and used in drug delivery systems.¹¹¹⁻¹¹³ Zhu and co-workers reported the preparation of sulfated cellulose using different sulfating reagents including $\text{Py}\cdot\text{SO}_3$, $\text{DMF}\cdot\text{SO}_3$, and H_2SO_4 .¹¹⁴⁻¹¹⁶ Richter and co-workers described the regioselective sulfation of the trimethylsilyl cellulose (TMSC) using sulfur trioxide complexes including $\text{Py}\cdot\text{SO}_3$, $\text{DMF}\cdot\text{SO}_3$, and $\text{Et}_3\text{N}\cdot\text{SO}_3$.¹¹⁷ $\text{Py}\cdot\text{SO}_3$ and $\text{Et}_3\text{N}\cdot\text{SO}_3$ are less reactive reagents compared to $\text{DMF}\cdot\text{SO}_3$ complex.¹¹⁷ In this reaction, SO_3 attacks the trimethylsilyl ether protecting group, breaking the Si-O bond, forming TMS SO_3 , and liberating the hydroxyl group. Subsequently, the OH nucleophile attacks TMS SO_3 resulting in the formation of the intermediate (**44**). This is followed by the formation of sodium sulfate cellulose under sodium hydroxide work-up conditions. Alternatively, SO_3 could attack the Si-O bond of the trimethylsilyl ether initiating a potential insertion mechanism resulting in the formation of an O- SO_3 -Si intermediate. In this pathway, the sulfur atom in SO_3 would form a new bond with oxygen atom, resulting in the formation of $(\text{R-O-SO}_3\text{-Si}(\text{CH}_3)_3)$ intermediate.

Subsequent hydrolysis and sodium exchange affords sodium cellulose sulfate (45) (Scheme 15).¹¹⁷



Scheme 15: The regioselective sulfation of trimethylsilyl cellulose (TMSC) using sulfur trioxide complexes (isolated yield not reported).¹¹⁷

Sun and co-workers reported the successful installation of sulfates and sulfamate moieties into protected heparan sulfate oligosaccharide derivatives using $\text{Py}\cdot\text{SO}_3$ complex.¹¹⁸ The preparation of sulfated and sulfamated tetrasaccharide substrate was achieved despite multiple reaction steps and the use of several protecting groups which add complexity to the sulfation process (Figure 7).¹¹⁸

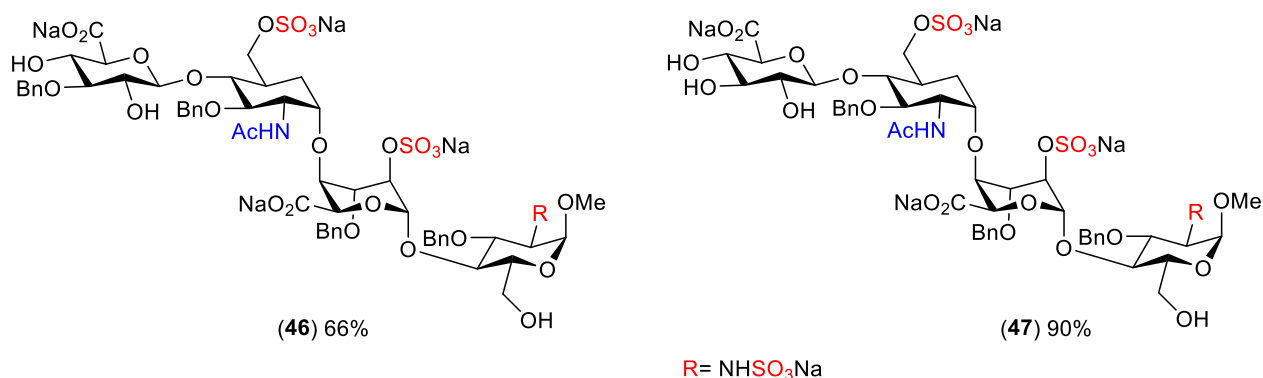
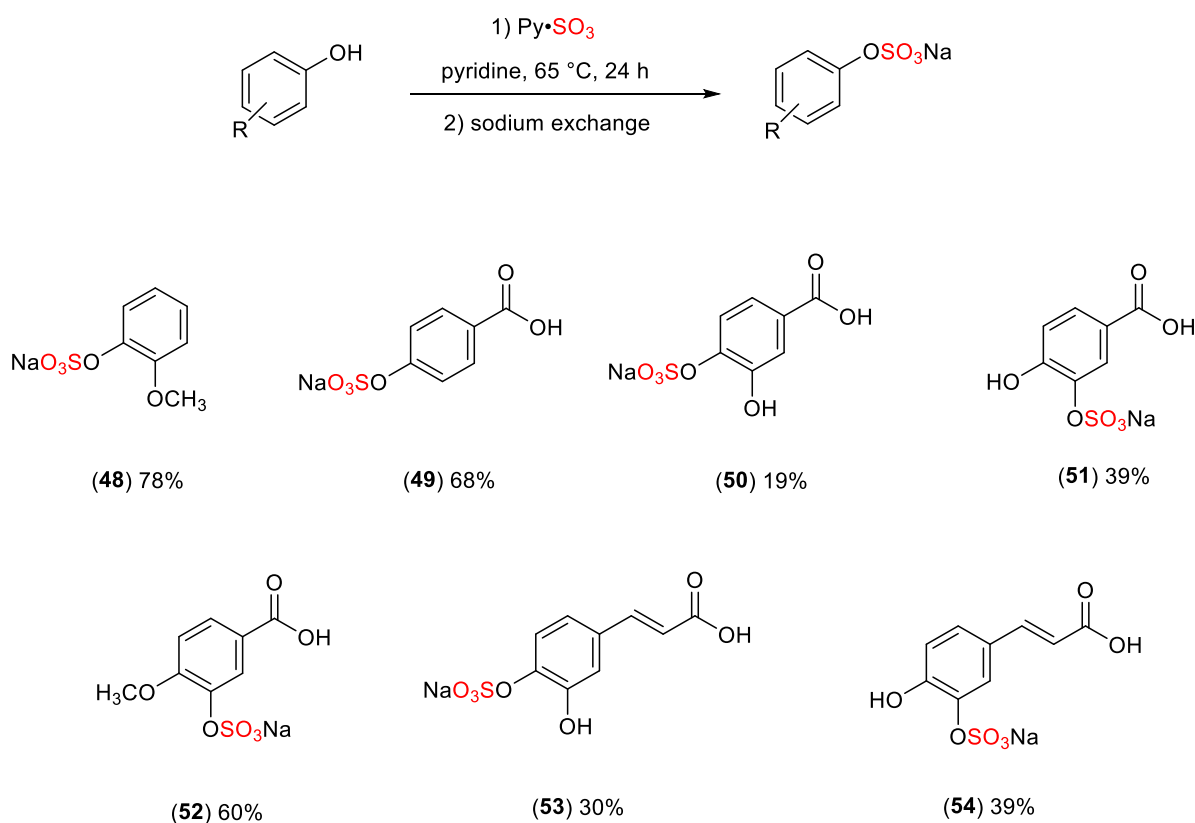


Figure 7: Sulfated tetrasaccharide examples prepared using the $\text{Py}\cdot\text{SO}_3$ complex.

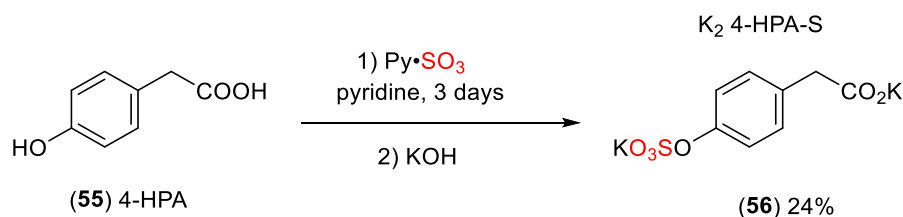
Flavonoids are another example of naturally occurring polyphenolic scaffolds which exist in human dietary sources.¹⁰⁶ Several studies have reported that flavonoids display anti-oxidant, vasodilator, or anti-coagulant activity, resulting in reducing blood pressure and therefore

minimise the risk of death from cardiovascular complications.¹¹⁹⁻¹²⁴ During phase II metabolism, flavonoids are transformed into different metabolites such as sulfated, glucuronidated, and methylated forms.¹²⁵⁻¹²⁶ Almeida and co-workers reported the sulfation of dietary phenolic scaffolds such as guaiacol, 4-hydroxybenzoic acid, and isovanillic acid with Py•SO₃ complex.¹²⁷ The sulfation reaction of phenolic substrates with Py•SO₃ was carried out in a presence of pyridine as a solvent at 65 °C for 24 h, followed by sodium exchange affording the corresponding sulfate sodium salt derivatives (**Scheme 16**).¹²⁷



Scheme 16: The sulfation reaction of phenolic flavonoids using the Py•SO₃ complex.¹²⁷

In 2022, Viola *et al.* reported the sulfation of various mono- and di-hydroxyphenolic acid flavonoids including 4-hydroxyphenylacetic acid (4-HPA), 3-hydroxyphenylacetic acid (3-HPA), 2-hydroxyphenylacetic acid (2-HPA), and 4-hydroxyphenylpropionic acid (4-HPP) using different sulfating reagents including Py•SO₃, DMF•SO₃, and TBSAB (**Scheme 17**).^{48, 128}



Scheme 17: The sulfation reaction of phenolic acid substrates using the Py•SO₃ complex.⁴⁸

In 2021, Malins *et al.* reported the use of Py•SO₃ and DMF•SO₃ complexes for the preparation of sulfated xylooligosaccharides that could be promising therapeutic agents like pentosan polysulfate (PPS).¹²⁹ PPS is a semi-synthetic polysulfated xylan that is related to glycosaminoglycans (GAGs) containing β-1→4-linked xylooligosaccharides and was approved for the treatment of interstitial cystitis (inflammation of bladder) (**Figure 8**).¹²⁹⁻¹³⁰

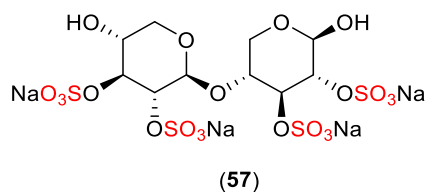
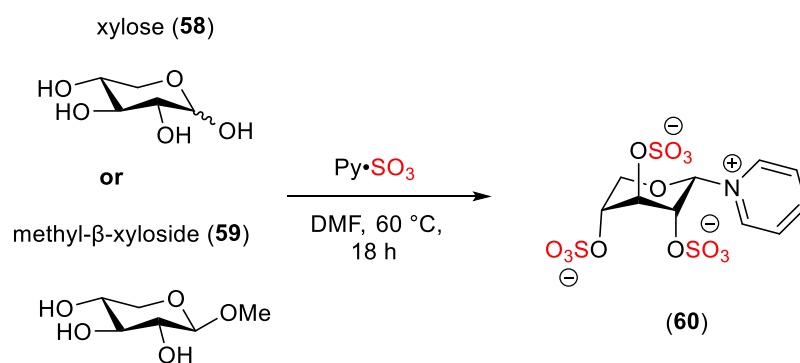


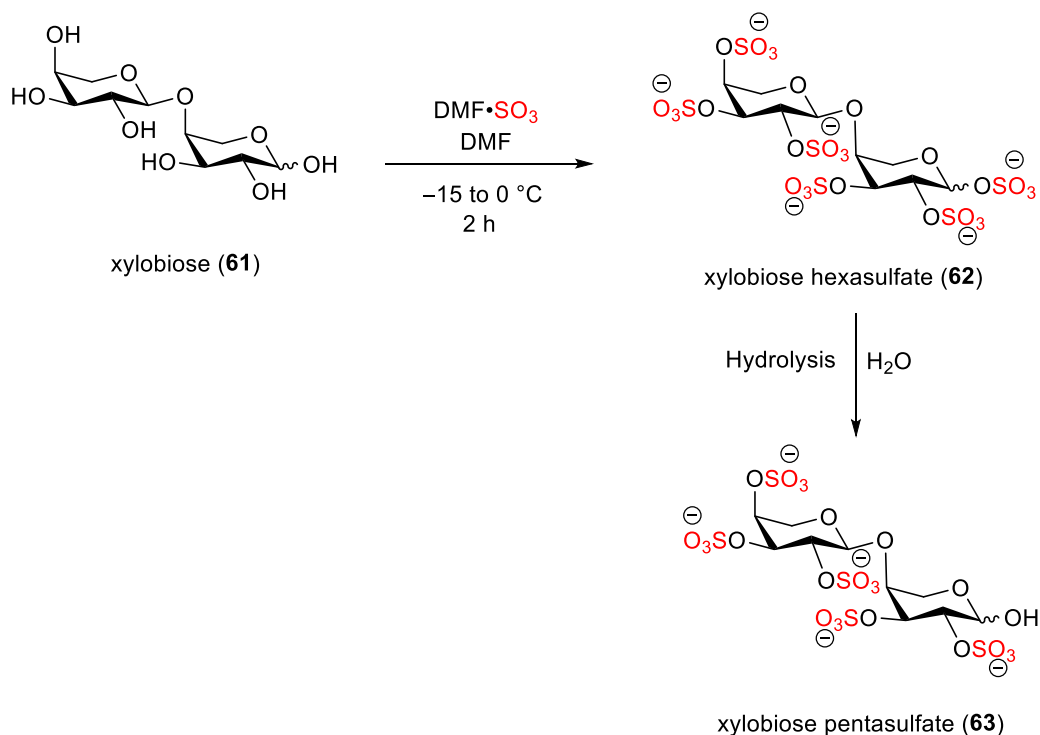
Figure 8: The structure of pentosan polysulfate sodium (Elmiron®) which is approved for the treatment of interstitial cystitis.¹²⁹⁻¹³⁰

An initial attempt for the sulfation of xylooligosaccharides was examined on different substrates including xylose, methyl-β-xyloside, and xylobiose using Py•SO₃ complex at 60 °C for 18 h.¹²⁹ Unfortunately, the β-1→4 linkage of xylan derivatives was cleaved by the addition of pyridine and led to pyridinium contamination e.g. (60) (**Scheme 18**).¹³¹



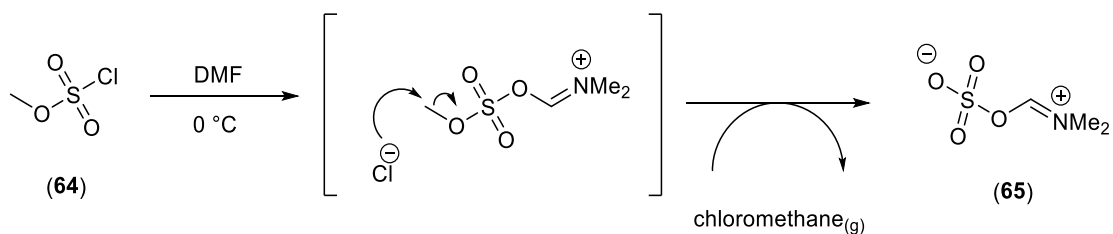
Scheme 18: The sulfation reaction of xylan derivatives using $\text{Py}\cdot\text{SO}_3$ complex.¹²⁹

Due to this previous unsuccessful attempt with $\text{Py}\cdot\text{SO}_3$, the $\text{DMF}\cdot\text{SO}_3$ complex was used for the sulfation of xylobios.¹²⁹ The sulfation of xylobios (**61**) with $\text{DMF}\cdot\text{SO}_3$ complex was carried out between -15 to 0 °C for 2 h affording xylobiose hexasulfate (**62**) and the hydrolysed form of xylobiose hexasulfate, xylobiose pentasulfate (**63**) (**Scheme 19**).¹²⁹



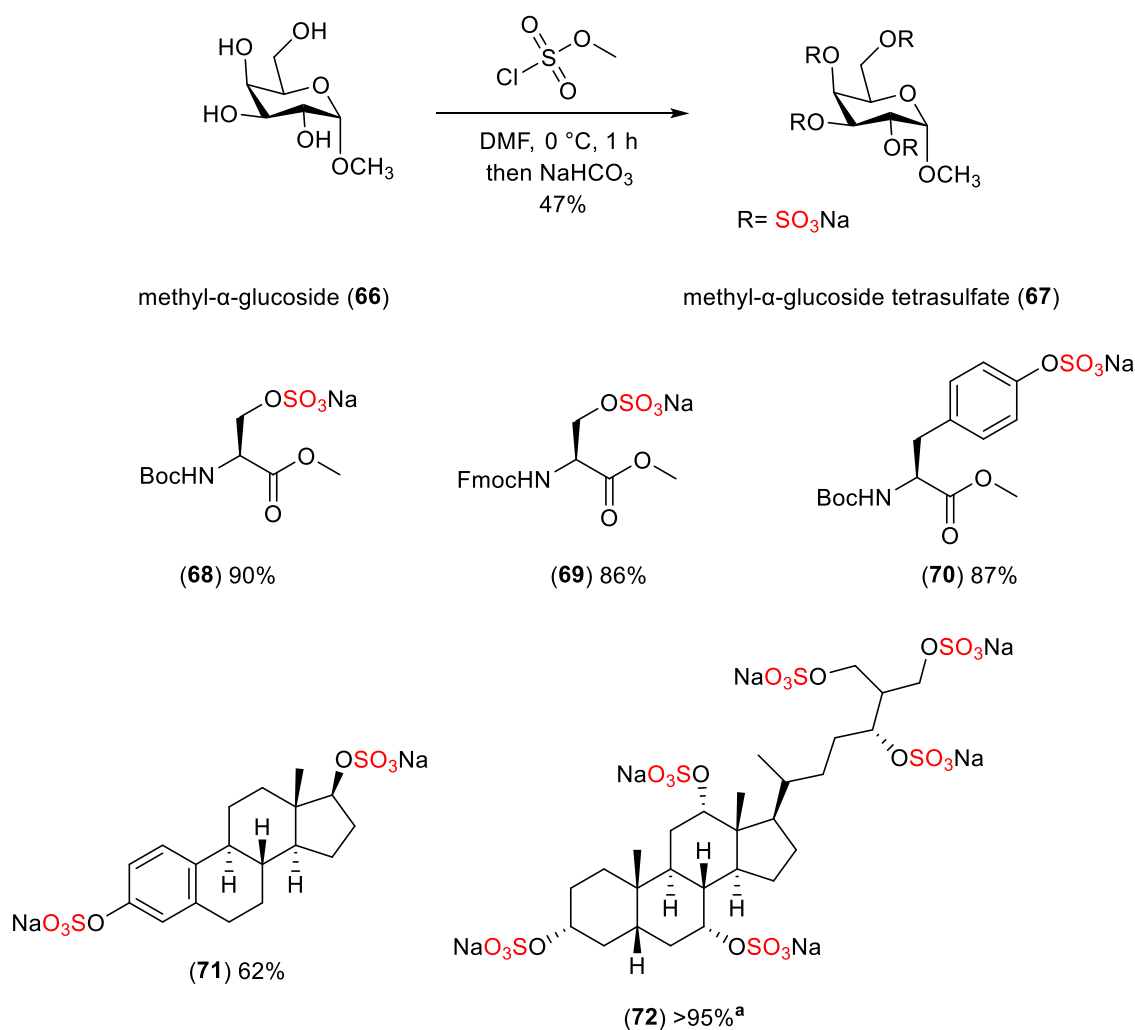
Scheme 19: The sulfation reaction of xylobios using $\text{DMF}\cdot\text{SO}_3$ complex affording xylobios hexasulfate and pentasulfate.¹²⁹

Malins *et al.* reported the *in situ* synthesis of DMF•SO₃ complex using the addition of methyl chlorosulfate to DMF solvent at 0 °C.¹³²⁻¹³³ This reaction is exothermic leading to the formation of chloromethane_(g) as a by-product (**Scheme 20**).¹²⁹



Scheme 20: *In situ* production of DMF•SO₃ complex using methyl chlorosulfate (**64**).

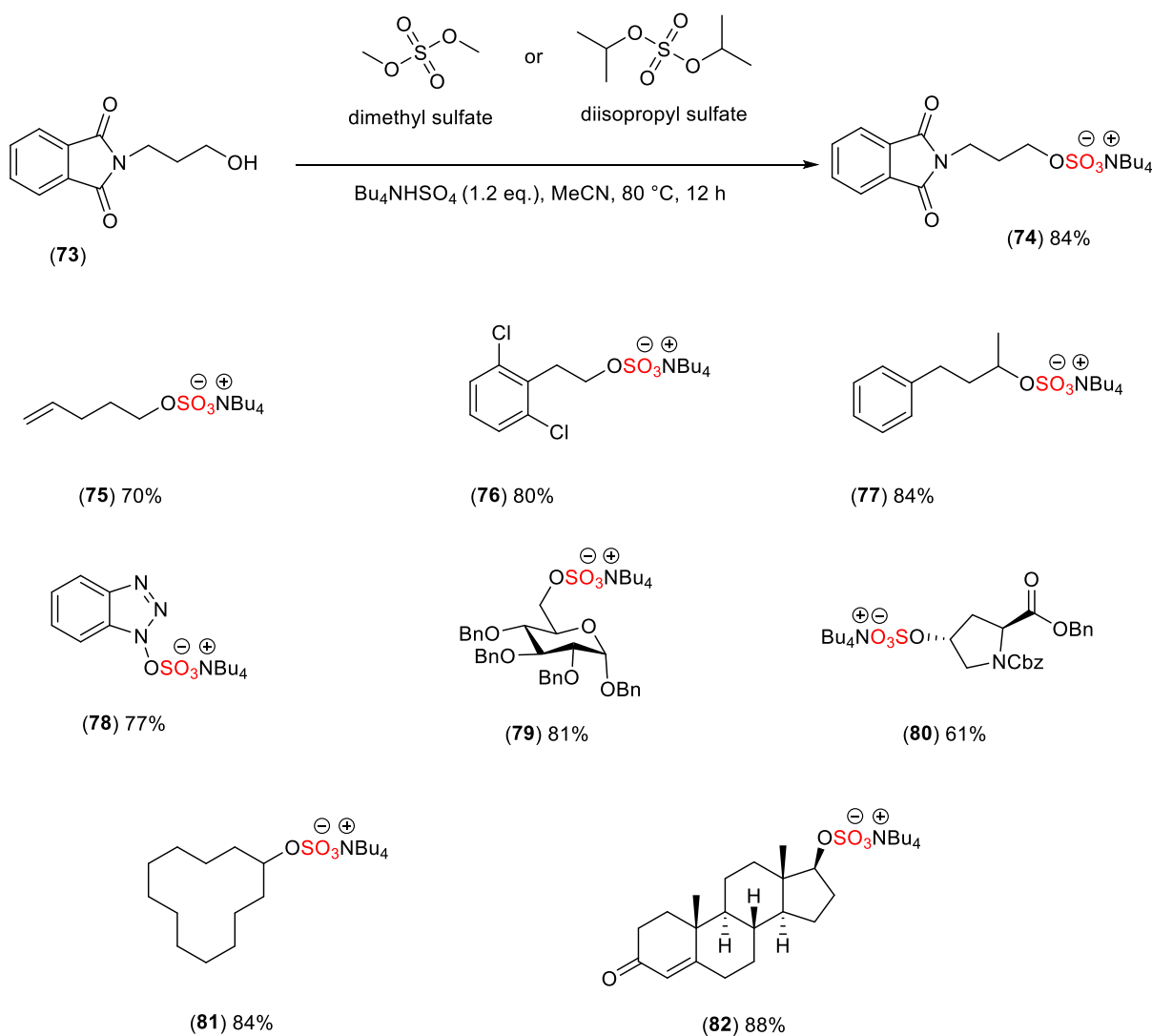
This protocol was initially investigated on methyl- α -glucoside following the optimised conditions; methyl chlorosulfate (1.1 eq./OH) at 0 °C for 1 h affording the methyl- α -glucoside tetrasulfate in 47% isolated yield.¹²⁹ This protocol was further explored on a wide range of small molecules including amino acids, disaccharides, steroids, and acid-sensitive substrates (**Scheme 21**).¹²⁹



Scheme 21: The sulfation reaction of methyl- α -glucoside (**66**) using methyl chlorosulfate and DMF. Scope of sulfated small molecules with methyl chlorosulfate, sodium Boc-*L*-serine methyl ester sulfate (**68**), sodium Fmoc-*L*-serine methyl ester sulfate (**69**), sodium Boc-*L*-tyrosine methyl ester sulfate (**70**), sodium β -estradiol disulfate (**71**), and sodium scymnol persulfate (**72**). ^a Percentage conversion calculated using ^1H NMR spectroscopy analysis.¹²⁹

More recently, Li and co-workers reported an innovative strategy for the *O*-sulfation of various substrates using dimethyl sulfate (DMS) and diisopropyl sulfate (DPS).¹³⁴ This strategy requires tetrabutylammonium bisulfate (Bu_4NHSO_4) to activate the dialkyl sulfates, which facilitates the sulfation of a wide range of functional groups, including alcohols, phenols, and oximes based substrates.¹³⁴ Furthermore, tetrabutylammonium bisulfate improves the solubility of the sulfate substrates in organic solvent.^{53, 134} This investigation was initiated with

the reaction of 3-phthalimido-1-propanol and DMS under mildly acidic conditions (Bu_4NHSO_4) dissolved in MeCN and the reaction mixture was stirred at 80 °C for 12 h affording the tetrabutylammonium 3-phthalimido-1-propanol sulfate in 84% isolated yield (**Scheme 22**).¹³⁴

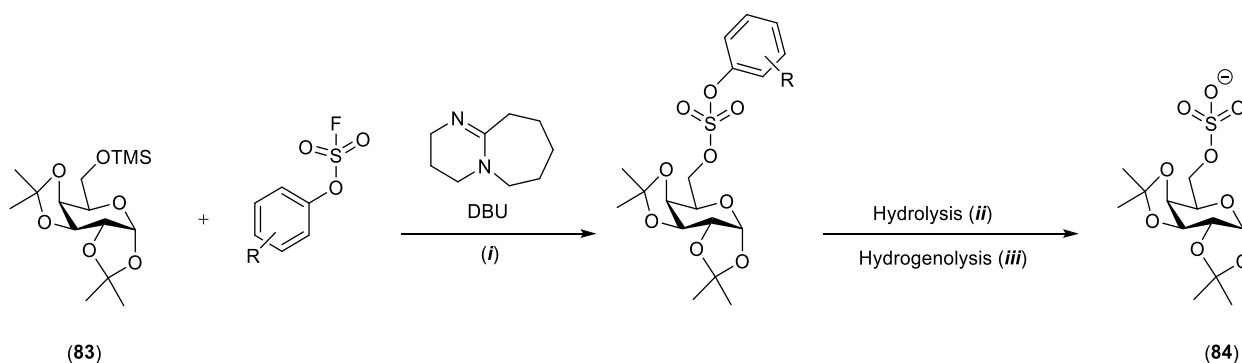


Scheme 22: The *O*-sulfation of a range of molecules, including primary and secondary alcohols, oximes based molecule, carbohydrates, an α -amino acid, and hormone using DMS/DPS and tetrabutylammonium bisulfate (Bu_4NHSO_4).¹³⁴

1.3.4. Sulfation using sulfur (VI) fluoride exchange (SuFEx) strategy

More recently, the early-stage *O*-sulfation reaction between aryl fluorosulfates and silyl ethers was reported leading to the formation of sulfuric acid diesters, which are subsequently reduced to the target sulfates in a hydrogenolysis step.¹³⁵ This strategy was applied to a wide

range of small molecules including monosaccharides, disaccharides, an amino acid, and a steroid.¹³⁵ This method was inspired by the work of Penny and Perlin in which phenyl sulfate diester was reported as a precursor of *O*-sulfation, despite the harsh conditions, stability issues, and lengthy reaction time.¹³⁶ Additionally, in 2014, Sharpless and co-workers reported the use of SuFEx strategy for the preparation of polysulfated molecules by the reaction between aromatic bis-(silyl ethers) and bis-(fluorosulfates) in the presence of 8-diazabicyclo-[5.4.0] undec-7-ene (DBU) as a nucleophilic catalyst.¹³⁷⁻¹³⁸ In 2020, Liu and co-workers explored the SuFEx reaction between silyl ethers and aryl fluorosulfates to introduce sulfate diesters on carbohydrate and non-carbohydrate scaffolds. This was followed by a deprotection step of the aryl sulfate monoester that results in the formation of *O*-sulfate molecules.¹³⁵ The *O*-sulfated galactose was achieved by the reaction of protected galactopyranose and substituted aryl fluorosulfates in the presence of DBU followed by hydrolysis and hydrogenolysis steps. In this reaction, the protected galactopyranose serves as a nucleophile attacking the sulfur atom of the substituted aryl fluorosulfates and displacing the fluoride ion leading to the formation of the sulfate diester. This was followed with a deprotection step of either hydrolysis or hydrogenolysis affording the final *O*-sulfate product **(84)** (**Scheme 23**).^{135, 139}



Scheme 23: General *O*-sulfation of protected galactopyranose using the SuFEx strategy. **Conditions:** (i) DBU, MeCN, 2 h, r.t.; (ii) 5 M sodium methoxide, 1 h, r.t.; and (iii) Pd (OH)₂/C and H₂, buffer solution (MeCN/MeOH/PBS) 2:2:1, 2 h, r.t.¹³⁵

This optimised method was applied to different small molecules including monosaccharides, disaccharides, an amino acid, and a steroid (**Figure 9**).¹³⁵

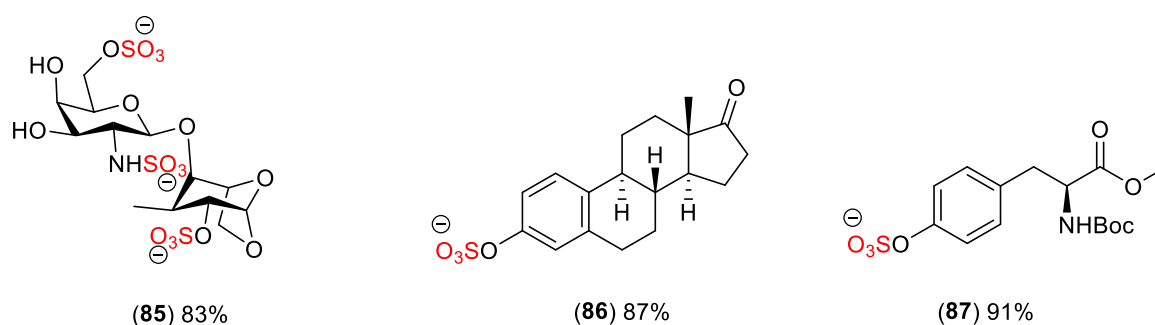
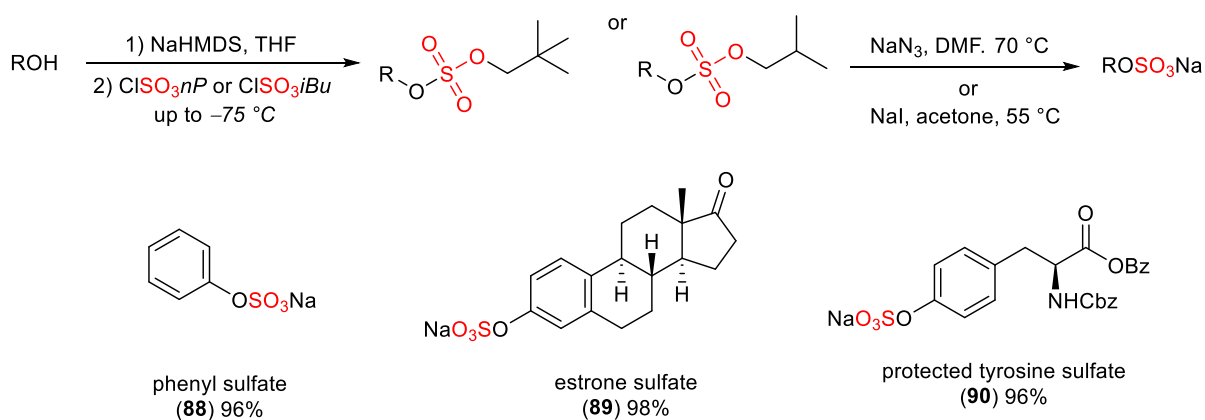


Figure 9: Scope of sulfated biomolecules using SuFEx approach. Yields shown have been calculated based on the isolated molecules after purification.¹³⁵

1.3.5. Protection/deprotection approaches

Despite the effectiveness of direct sulfation methods, the formation of complex sulfated molecules may be hampered by the poor solubility of sulfated molecules in organic solvents, stability issues, and purification challenges of sulfated molecules.² As a result, there has been a growing interest in developing a protection/deprotection strategy for the sulfation reactions, including phenyl and its derivatives, *isobutyl* (*iBu*), *neopentyl* (*nP*), 2,2,2-

trichloroethyl (TCE), trifluoroethylene (TFE) groups.¹⁴⁰⁻¹⁴² These have been employed in the synthesis of sulfate esters due to their unique stability and reactivity profiles. For instance, the neopentyl group is stable under harsh acidic, basic, and nucleophilic conditions, whereas the *isobutyl* protecting group is more labile, making it stable under acidic conditions but degrades under basic or nucleophilic conditions. Simpson and co-workers studied the use of *isobutyl* (*iBu*) and neopentyl (*nP*) protecting groups for the preparation of several sulfate monoesters. In this method, phenolic or alcoholic substrates were initially treated with a strong base such as sodium hydride (NaH) or sodium hexamethyldisilazide (NaHMDS) in THF solvent followed by the addition of *isobutyl* or neopentyl chlorosulfate affording the desired protected sulfate monoesters. A subsequent deprotection step using sodium azide or sodium iodide afforded the desired sulfates (**Scheme 24**).



Scheme 24: Scope of selected sulfate monoester using protection/deprotection method. Protection/deprotection method using the protected sulfate neopentyl or *isobutyl* esters followed by the deprotection reaction with NaN_3 for the removal of neopentyl (*nP*) protecting group or sodium iodide (NaI) for the removal of *isobutyl* (*iBu*) protecting group affording the final desired sulfates. Yields shown have been calculated based on the isolated molecules after purification.

Overall, each method has advantages and disadvantages, and the choice of the reagent depends on the substrates and the desired product of the sulfation process. Sulfuric acid and its derivatives have been used for the sulfation of cycloalkenes, polysaccharides, saturated

alcohols and flavonoids. This method is highly reactive and suitable for large-scale synthesis however some issues have been reported using this method including the need for an excess of the reagents, multiple purification steps, incompatibility with acid-sensitive substrates, and degradation issues. Chlorosulfonic acid has been reported for the sulfation of polysaccharides, phenolic acids, and flavonoids. This method is effective for a wide range of substrates despite its toxicity, handling difficulties, and exothermic nature which requires extra care. Sulfur trioxide amine complexes including $\text{Me}_3\text{N}\cdot\text{SO}_3$ and $\text{Et}_3\text{N}\cdot\text{SO}_3$ are commonly used for the sulfation of alcoholic/phenolic groups in carbohydrates, flavonoids, steroids, and proteins. These reagents can be employed in one-pot sulfation reactions despite the purification challenges, multi-step reactions including protection/deprotection steps, and stoichiometric excess of the reagents which increases the reaction cost. TBSAB is the most recent sulfation reagent developed for a wide range of organic molecules including benzyl alcohols, benzylamines, carbohydrates, protected α -amino acids, and steroids. TBSAB offers a simpler purification and isolation due its greater lipophilicity nature however it is limited to substrates which benefit from its lipophilic features. Another issue is the high cost of TBSAB compared to other sulfating reagents such as $\text{Me}_3\text{N}\cdot\text{SO}_3$ and $\text{Et}_3\text{N}\cdot\text{SO}_3$ resulting from the requirement of specific methods and equipment to prepare TBSAB (See **Chapter 4** for prices comparison). $\text{Py}\cdot\text{SO}_3$ and $\text{DMF}\cdot\text{SO}_3$ complexes are versatile reagents for the sulfation of hydroxyl/phenolic groups in carbohydrates, flavonoids, steroids, amino acids and peptides. These reagents offer high regioselectivity particularly in substrates like carbohydrates and flavonoids. These complexes are efficient sulfation reagents that can be employed under relatively mild conditions. Despite the effectiveness of these complexes, some issues have been reported including, purification challenges due to the presence of pyridine and DMF that are difficult to remove. Another issue is toxicity of both pyridine and DMF which needs

considerable handling and care. Furthermore, these are multi-step reactions which increases the cost and the time of the sulfation process. Finally, a sulfur (VI) fluoride exchange (SuFEx) strategy has been used for the *O*-sulfation of carbohydrates, amino acids, and steroids. This method provides regioselective sulfation of specific hydroxyl groups in carbohydrates and steroids. It is also suitable for a large-scale synthesis, making it practical for industrial applications. This method offers a simplified purification resulting in the desired *O*-sulfate compounds with high purity. More importantly, this strategy permits a one-pot procedure that combines *in situ* hydroxyl silylation and subsequently SuFEx reaction. Despite the success of this method, some issues have been reported including, multi-step synthesis which includes prior preparation of aryl fluorosulfates from phenols, which involves additional synthetic steps and purification which increases the cost of this synthesis (**Table 4**).

Table 4: Comparison of the reported sulfating reagents: advantages, disadvantages, and applications.

Sulfating reagent	Advantages	Disadvantages
H ₂ SO ₄	Highly reactive: Efficient for a wide range of substrates, especially cycloalkenes and polysaccharides. Low cost: Easily available and inexpensive.	Harsh conditions: Can cause degradation of sensitive substrates. Side reactions: High reactivity can lead to over-sulfation and side products. Purification challenges due to the formation of by-products.
ClSO ₃ H	Highly reactive: Suitable for polysaccharides and flavonoids. Selective sulfation for polysaccharides like agarose sulfate. Fast reaction times and low cost.	Highly corrosive and exothermic, requiring specialized handling and equipment. Toxic reagents. Can lead to side products.
Me ₃ N•SO ₃	Moderate reactivity: Useful for alcohols and phenols in carbohydrates and steroids. Regioselective for hydroxyl groups. Stable and easy to handle. Simple purification by ion exchange methods.	Excess reagent often required. Stability issues with the reagent and products.
Et ₃ N•SO ₃	Moderate reactivity and selectivity. Works well with polyphenolic compounds (e.g., quercetin, PCA). Stable and easy to handle.	Requires stoichiometric excess of reagent.
TBSAB	Simple purification and isolation due to its greater lipophilicity. High yields and selectivity. Good for <i>O</i> - and <i>N</i> -sulfation of a wide variety of substrates, including α -amino acids and carbohydrates.	Expensive reagent. Requires specialised equipment for its preparation. Not as widely tested in all reaction types.

Py•SO ₃	Moderate reactivity: Suitable for sulfation of polysaccharides and oligosaccharides. Mild conditions and less harsh compared to H ₂ SO ₄ and ClSO ₃ H.	Toxicity: Pyridine is toxic and can contaminate the product. Poor stability of the complex over time.
DMF•SO ₃	High reactivity: Provides high degrees of sulfation, especially for polysaccharides. Regioselective and efficient sulfation.	Requires careful handling: DMF is toxic. Stability issues. Over-sulfation risk if conditions are not controlled. Longer reaction times.
SuFEx	Early stage of sulfation. High selectivity: suitable for sulfation of complex scaffolds including steroids, polysaccharides, and α-amino acids. Short reaction times.	Requires specialized reagents and equipment (e.g., silyl ethers, fluorosulfates). Still developing and less commonly available.
Protection/deprotection	Improved Selectivity: protection of sensitive or unwanted sites allows for site-selective sulfation. Suitable for a wide range of molecules including steroids, α-amino acids, and natural products.	Additional Synthetic Steps. Risk for the formation of by-products that complicate purification. High cost.

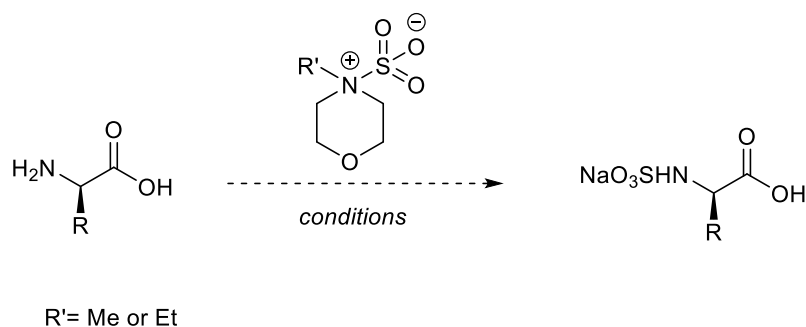
1.4. Conclusion

Sulfation is one of the most important modifications that occur to a wide range of small biomolecules including polysaccharides, proteins, flavonoids, and steroids. Generally, the incorporation of a sulfate moiety to a substrate result in an increase in the substrate's hydrophilicity which therefore facilitates its elimination from the body. The sulfation pathway is catalysed by a group of enzymes called sulfotransferases (SULTs). These enzymes are

generally classified into two main categories; cytosolic and Golgi membrane-bound sulfotransferase. Cytosolic sulfotransferases are associated with the phase II metabolism enzymes and involved in the sulfation of low molecular weight molecules, whereas Golgi membrane-bound sulfotransferase is responsible for catalysing the sulfation of large molecular weight molecules such as proteins, proteoglycans, and glycolipids. Several sulfated scaffolds such as polysaccharides, proteins, flavonoids, and steroids have significant biological and pharmacological roles such as cell signalling, modulation of immune and inflammation response, anti-coagulation, anti-atherosclerosis, and anti-adhesive.

This chapter has reviewed the most common chemical sulfation methods of small molecules which have biological and pharmacological applications. The sulfation reaction using sulfur trioxide amine/amide complexes is the most used method for alcoholic or phenolic groups in carbohydrates, steroids, proteins, and aliphatic or alicyclic scaffolds. Other traditional sulfation reactions were presented using different reagents and protocols such as ClSO_3H , H_2SO_4 , $\text{H}_2\text{SO}_4/\text{DCC}$, SuFEx , and protection/deprotection methods. Despite the effectiveness of these methods, they suffer from issues including multi-step reactions, toxicity issues, purification challenges, use of excess of reagents which leads to increase of a reaction cost, and stability issues.

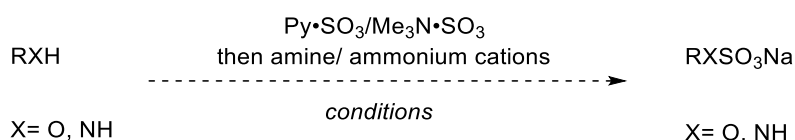
More recently, TBSAB, a sulfating reagent developed by our group was applied to a wide range of small molecules including benzyl alcohols, benzylamines, carbohydrates, and proteins. Furthermore, TBSAB offers a simplified purification and isolation systems for the sulfated molecules due to the high lipophilicity profile of the corresponding tributylammonium intermediates.



Scheme II: Sulfation reaction of amino acids using 4-alkylmorpholine SO₃ complexes.

This method will be explored on selected amino acids including aliphatic and protected aromatic amino acids.

The aim of chapter 4 is to develop a novel sulfation strategy using low-cost and commercially available sulfating reagents (SO₃-R, R = Py or Me₃N). Furthermore, amines and ammonium cations will be explored to increase the lipophilicity of the resulting intermediates and therefore increase the solubility of the resulting sulfates/sulfamates in organic solvents to aid purification cascades (**Scheme III**).

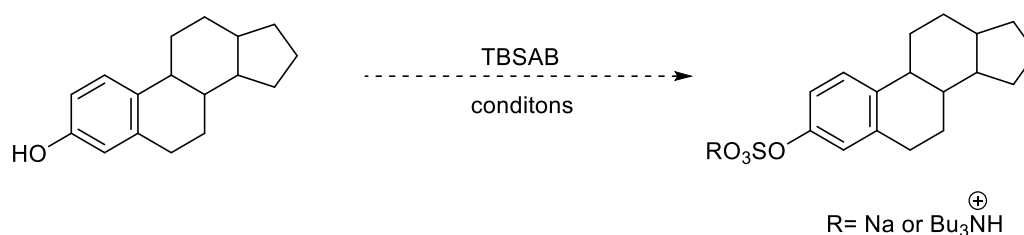


Scheme III: The novel sulfation exchange method to access sulfated/sulfamated substrates.

This strategy will be applied to a wide range of alcohols and amines substrates to explore the scope and limitations of this new approach.

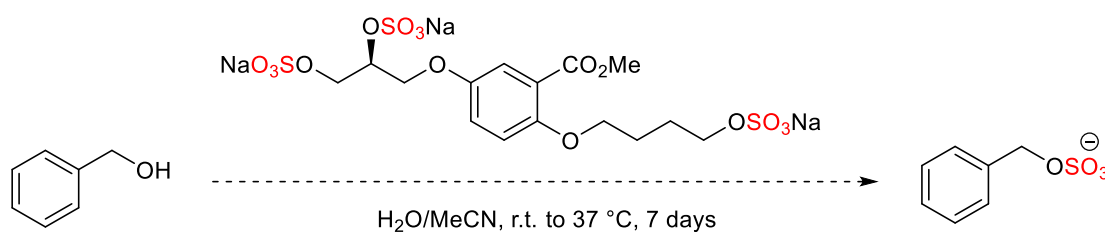
The aim of chapter 5 is to investigate the application of the TBSAB reagent for the sulfation of steroids. The objective of this investigation is to explore whether TBSAB can be used as a general, scalable, and regioselective sulfating reagent in this class of complex bioactive

molecule. Furthermore, the application of TBSAB alongside isotopic labelling for steroidal-organosulfate reference standards will also be investigated (**Scheme iv**).



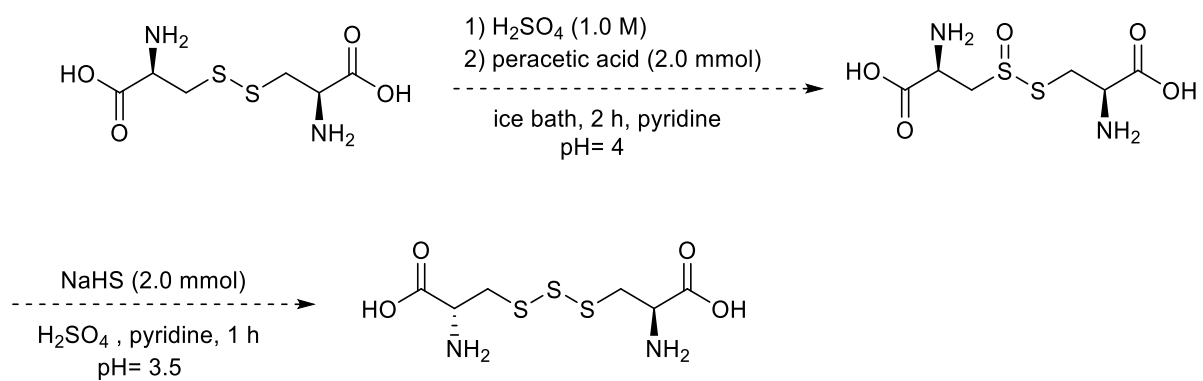
Scheme iv: The proposed sulfation scheme for steroids using TBSAB.

The aim of chapter 6 is to study whether a synthesised heparan sulfate-glycomimetic acts as a source of sulfate *in vivo* rather than solely via HGF/c-MET modulation. This hypothesis of the *in situ* sulfonyl transfer will be tested on simple benzyl alcohols using a sulfated glycomimetic under conditions that mimics the biological system (37 °C, H₂O/MeCN). This investigation will also examine the stability of the benzylic sulfates using ¹H NMR spectroscopic analysis (**Scheme v**).



Scheme v: The proposed sulfation of benzyl alcohol using the synthesised heparan sulfate-glycomimetic.

The aim of chapter 7 is to synthesise cysteine trisulfide. Cysteine trisulfide is an exogenous cysteine persulfide donor known for its biological applications including reduction of lipid peroxidation and enhanced the cardiac functions via cysteine trisulfide supplements but there are issues with the reported synthesis and its characterisation in the literature that require a resolution (**Scheme vi**).



Scheme vi: The proposed synthesis of cysteine trisulfide (Cys-SSS-Cys).

Chapter 2. Design and synthesis of novel sulfur trioxide complexes for sulfation chemistry

Introduction

Sulfur-containing compounds exhibit diverse pharmacological applications including anti-biotics, anti-malarial, anti-viral, and anti-psychotic activities.¹⁴³⁻¹⁴⁴ Sulfate-containing molecules are found in a broad range of pharmaceutical drugs, natural products, and metabolites such as paracetamol sulfate, estrone sulfate, and glycomimetic C3 (**Figure 10**).¹⁴⁴

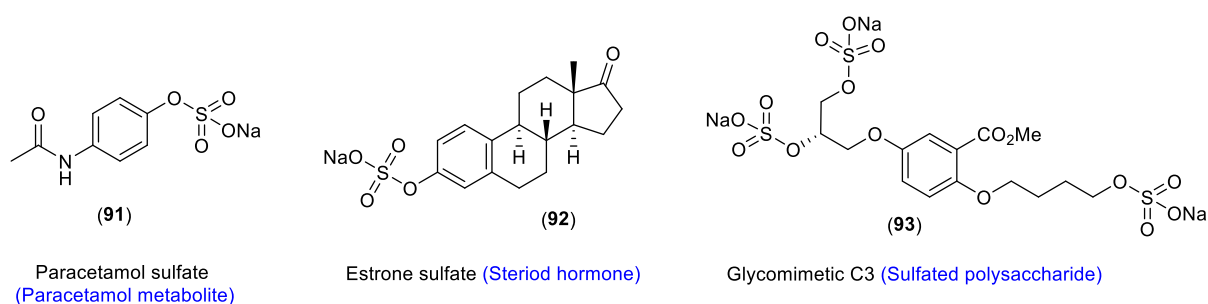


Figure 10: Sulfate-containing molecules that have different pharmacological applications.

Raman and co-workers reported the development of stabilised liquid forms of SO₃, making it more convenient for use in various applications. These liquid formulations of SO₃, which help overcome the challenges of handling the highly reactive gaseous form, are now commercially available and marketed by several companies for use in sulfation reactions and other chemical processes.¹⁴⁵ Additionally, SO₃ can be used for the sulfation and sulfonation of organic compounds.¹⁴⁶ The conventional reactions of SO₃ involves the formation of a sulfur-carbon bond (sulfonation), the formation of a sulfur-oxygen bond (sulfation), and the formation of a sulfur-nitrogen bond (sulfamation) (**Figure 11**).¹⁴⁶⁻¹⁴⁷



Figure 11: Sulfonation, sulfation, and sulfamation reactions using SO₃.

SO₃ is a strong Lewis acid (electron acceptor) which reacts with Lewis bases (electron donors) such as trimethylamine (Me₃N), triethylamine (Et₃N), dioxane and pyridine (Py). These reactions result in the formation of sulfur trioxide complexes, which are used for the sulfation of organic alcohols, leading to the formation of organosulfate esters.²⁸

2.1. Sulfur trioxide complexes

Several attempts for the preparation of sulfur trioxide complexes were made throughout the history of sulfating reagents development from the synthesis of stabilised liquid SO₃ to the production of chlorosulfonic acid (ClSO₃H) and the preparation of sulfur trioxide amine/amide complexes.¹⁴⁸ For a comprehensive review of the preparation of sulfur trioxide complexes and their reactions, see Gilbert *et al.*²⁸ Herein, several commercially available sulfur trioxide complexes were discussed that react with a suitable organic compound to give their corresponding organosulfate or sulfamate ester (**Figure 5, Chapter 1**).²⁸ These sulfur trioxide complexes have been widely used for *O*, *N*, and *S*-sulfation of different substrates, including polysaccharides, amino acids, steroids, flavonoids, amongst others.^{2, 28, 47, 149}

2.1.1. The properties of sulfur trioxide complexes

The reactivity of sulfur trioxide complexes varies depending on the basicity strength of the base and stability of the complex.¹⁴⁸ It was reported that the reactivity of SO₃-amine complexes is highly correlated to the basicity strength of the amine. For instance, Me₃N, Et₃N,

and Bu_3N are Lewis bases which have greater $\text{p}K_{\text{aH}}$ values of their conjugated acids compared to pyridine. This is attributed to the orbital hybridisation of the nitrogen atom and the inductive effect of those amines. In tertiary amines such as Me_3N , the lone pair of electrons is localized in an sp^3 orbital, making it more available for protonation and increasing the basicity of the amine ($\text{p}K_{\text{aH}}= 9.8$). Furthermore, the presence of three methyl donating groups generates an inductive effect which increases the electron density on the nitrogen atom making the nitrogen more nucleophilic and basic (**Figure 12**).

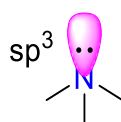
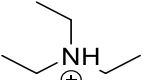
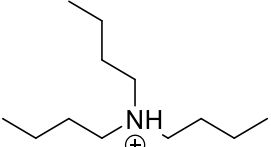


Figure 12: The sp^3 orbital hybridisation structure of Me_3N .

Aromatic heterocyclic amines such as pyridine (Py) are considerably weaker bases compared to tertiary alkyl amines such as Me_3N due to several factors including the orbital hybridisation state and the electron density around the nitrogen atom.²⁸ The lone pair on the nitrogen atom in pyridine is in an sp^2 orbital which is orthogonal to the π -system of the aromatic ring meaning that this lone pair is not delocalized into the π -system but rather stabilized by the aromatic ring. The lone pair on the sp^2 hybridised nitrogen is less available for protonation compared to the lone pair on the sp^3 hybridised nitrogen in tertiary alkyl amines due to the low basicity profile of pyridine ($\text{p}K_{\text{aH}}= 5.23$) (**Table 5**).²⁸

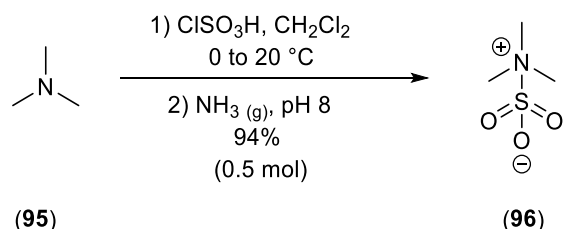
Table 5: The orbital hybridisation and pK_aH values of alkylamines and aromatic amines. Obtained from the National Library of Medicine (N.D. not determined).

Entry	Amine	Structure	Conjugate acid	Orbital hybridisation of nitrogen lone pair	pK_aH (H ₂ O)
1	Me ₃ N			sp ³	9.8
2	Et ₃ N			sp ³	10.9
3	Bu ₃ N			sp ³	10.89
4	Py			sp ²	5.23
5	DMF		-----	sp ²	N.D.

2.2. The preparation of sulfur trioxide complexes

The general preparation and the reaction of sulfur trioxide complexes including Me₃N•SO₃, Et₃N•SO₃, Py•SO₃, amongst others, were reviewed and summarised by Gilbert.²⁸ Herein, the most common approaches will be briefly mentioned. Trimethylamine sulfur trioxide (Me₃N•SO₃) has been prepared by several methods including in a liquid and gaseous phase without using a solvent and in other conditions with compatible organic solvents.¹⁵⁰ The Me₃N•SO₃ has been prepared in the gaseous phase by the reaction of SO₃ and trimethylamine without a solvent. The use of chloroform or sulfur dioxide solvents has also been reported.¹⁵⁰

Other methods have also been employed including the reaction of trimethylamine with chlorosulfonic acid (ClSO₃H) in dichloromethane solvent affording Me₃N•SO₃ reagent (**Scheme 25**).¹⁵¹



Scheme 25: The synthesis of Me₃N•SO₃.

Et₃N•SO₃ complex (recently recharacterized as a betaine)¹⁵² is prepared by different methods including the addition of liquid sulfur trioxide to a solution of triethylamine in carbon tetrachloride solvent or more commonly by the reaction of triethylamine with ClSO₃H in CH₂Cl₂ at 5 °C (**Scheme 26**).¹⁵³⁻¹⁵⁴



Scheme 26: The synthesis of Et₃N•SO₃.

Tributylsulfoammonium betaine (Bu₃N•SO₃, TBSAB) is the most recently developed sulfating reagent among the other commercially available tertiary amine sulfur trioxide complexes which was synthesised by our group.¹⁴⁹ TBSAB is more lipophilic than Me₃N•SO₃ and Et₃N•SO₃ due to the greater cLogP value of its corresponding tributylammonium cations (**Table 6**). Consequently, simplified liquid extraction of sulfated tributylammonium cation intermediates and isolation by column chromatography (SiO₂) were possible.^{47, 149}

Table 6: The cLogP values of sp³ hybridised tertiary amines (These calculated values were derived from ChemDraw 19.1).

Entry	Amine	Conjugate acid	cLogP
1	Trimethylamine	[HNMe ₃] ⁺	0.22
2	Triethylamine	[HNEt ₃] ⁺	1.28
3	Tripropylamine	[HNPr ₃] ⁺	2.65
4	Tributylamine	[HNBu ₃] ⁺	4.51

The first reported preparation of sulfur trioxide tributylamine complex was in 1949, which was characterised solely by melting point (94 °C).¹⁵⁵ In 1976, sulfation of simple aliphatic alcohols was reported using Bu₃N•SO₃ by Parshikov and co-workers but without characterisation data.¹⁵⁶ In 2019, Gill and co-workers reported the preparation of TBSAB and the structure was confirmed by ¹H and ¹³C NMR spectroscopy, mass spectrometry, and IR spectroscopy (**Scheme 12, Chapter 1**).¹⁴⁹ The structure of TBSAB was also confirmed by X-ray crystallography demonstrating that in the solid state, TBSAB adopts a gauche conformation within an asymmetric unit cell. This was due to hydrogen bonding between the α-methylene hydrogen (C1-H₂) to the nitrogen atom and the oxygen atoms of SO₃.¹⁵⁷ Gill and co-workers reported the N–S bond length, 1.88 (±0.003) Å, which falls just outside the range typical for a single covalent bond between nitrogen and sulfur (1.73 – 1.83 Å) compared to 2.06 Å for a donor–acceptor system.¹⁵⁷ Additionally, X-ray analysis demonstrates that the bond angle between oxygen atoms is 115.69 (±0.004)° showing that the tetra-coordinate sulfur adopts a

more tetrahedral like geometry to accommodate the addition of an electron pair into the LUMO of SO_3 (**Figure 13**).¹⁵⁷

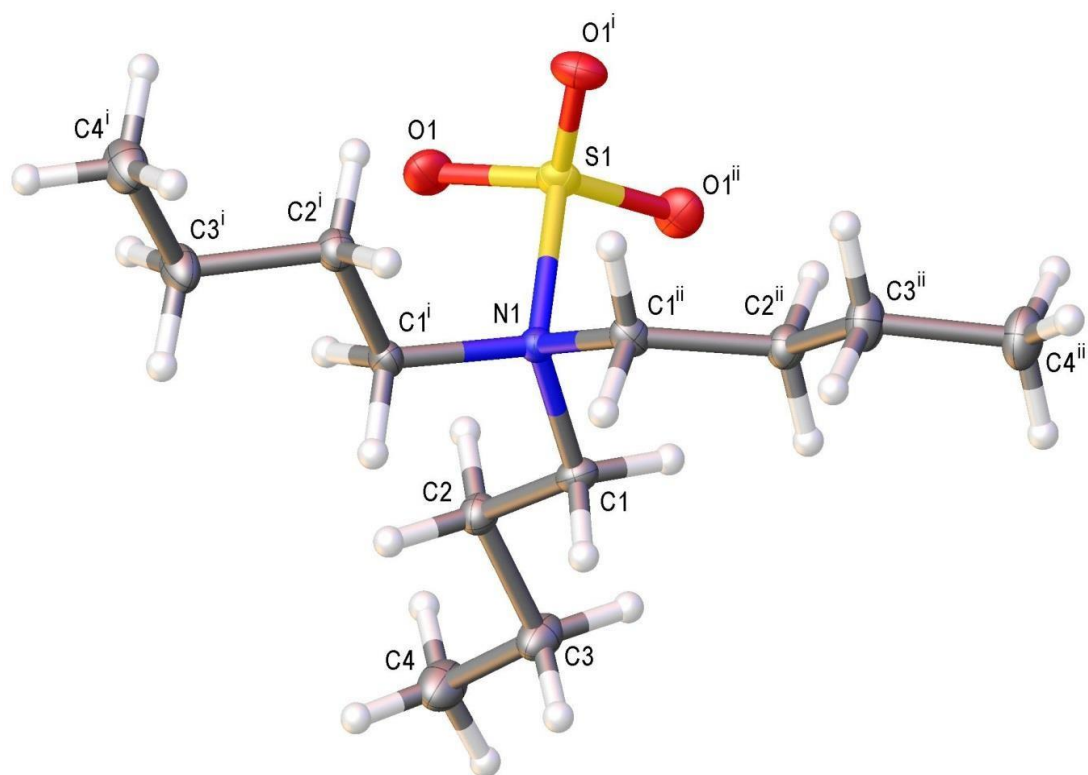
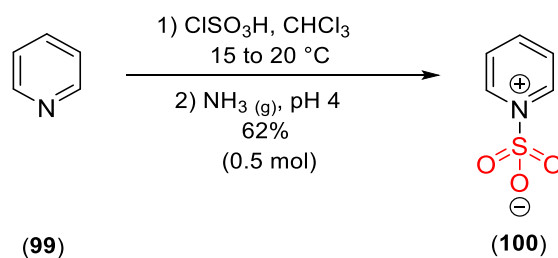


Figure 13: Crystal structure of TBSAB with ellipsoids drawn at the 50 % probability level. The molecule lies on a 3-fold rotation axis running through N(1) and S(1) such that the butyl groups are all symmetrically equivalent. Symmetry codes used to generate equivalent atoms: \$1, y-x, 1-x, z, \$2, 1-y, 1+x-y, z.¹⁵⁷

$\text{Py}\cdot\text{SO}_3$ complex has been prepared by various methods including the reaction of sulfur trioxide with pyridine in carbon tetrachloride as solvent, which gives the desired complex in 90% isolated yield.²⁸ Also, the reaction of pyridine and chlorosulfonic acid (ClSO_3H) in the presence of chloroform as solvent gives $\text{Py}\cdot\text{SO}_3$ complex in 62% isolated yield (**Scheme 27**).²⁸



Scheme 27: The synthesis of Py•SO₃ complex using chlorosulfonic acid.

DMF•SO₃ complex has been prepared using different conditions including the direct reaction of SO₃ and DMF at a temperature between 0-5 °C for 5 h. More recently, Malins and co-workers reported an *in situ* synthesis of DMF•SO₃ complex by the addition of methyl chlorosulfate to DMF at 0 °C (**Scheme 19, Chapter 1**).¹²⁹ The preparation of 1,4-dioxane SO₃ complex involves the reaction of liquid SO₃ and 1,4-dioxane in 1,2-dichloroethane which is utilised immediately due to the stability issues with 1,4-dioxane SO₃ complex.²⁸

This chapter will explore the development of novel sulfur trioxide complexes and further investigation on their use in sulfation chemistry.

2.3. Results and Discussion

2.3.1. Preparation of novel sulfur trioxide complexes

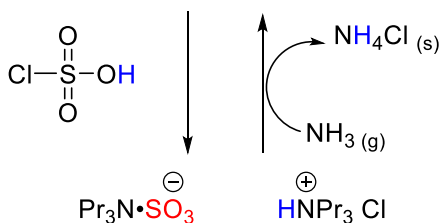
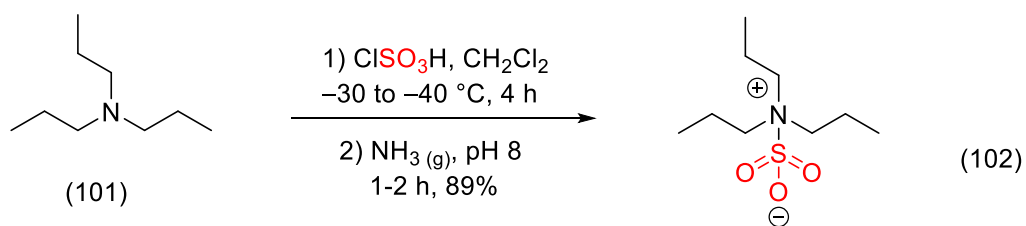
This investigation proposed the general synthesis of novel sulfating reagents which would be exploited for the sulfation of a range of organic scaffolds such as alcoholic and phenolic compounds, polysaccharides, steroids, amines and amino acids. The direct reaction of sulfur trioxide with tertiary alkyl amines affords the corresponding sulfur trioxide amine complexes.^{47, 149, 158} Tripropylamine (known as tri-*n*-propylamine) was chosen for several factors. First, tripropylamine had not been reported as its SO₃ amine complex. Second, tripropylamine is a Lewis base like other tertiary alkyl amines and has a sp³ hybridised nitrogen atom which donates its lone pair of electrons to form a new N-S bond. Furthermore,

the cLogP value of tripropylamine indicates that tripropylamine sulfur trioxide complex ($\text{Pr}_3\text{N}\cdot\text{SO}_3$) would be a lipophilic sulfating agent similar to TBSAB (**Table 6, Entry 3**). $\text{Pr}_3\text{N}\cdot\text{SO}_3$ complex has a lower molecular weight than TBSAB, and is generally more environmentally friendly due to its shorter alkyl chains. Generally, shorter alkyl chains (such as the propyl groups in $\text{Pr}_3\text{N}\cdot\text{SO}_3$) tend to break down more easily and rapidly via natural processes like microbial action, which leads to faster biodegradation. The longer butyl chains in TBSAB are more resistant to degradation due to their larger size and greater hydrophobicity. This means TBSAB is more likely to persist in the environment, increasing the risk of bioaccumulation and long-term environmental effects.¹⁵⁹

2.3.2. Synthesis of tripropylamine sulfur trioxide complex

The synthesis of $\text{Pr}_3\text{N}\cdot\text{SO}_3$ complex was attempted following the optimised conditions of TBSAB preparation.¹⁴⁹ $\text{Pr}_3\text{N}\cdot\text{SO}_3$ complex was synthesised via the nucleophilic addition-elimination reaction mechanism where the nucleophile nitrogen atom of tripropylamine attacks the sulfur atom of chlorosulfonic acid resulting in the formation of $\text{Pr}_3\text{N}\cdot\text{SO}_3$ and HCl.

The reaction of tripropylamine (**101**) and chlorosulfonic acid gave the desired complex (**102**) in 89% isolated yield on a 14 g scale (0.0625 moles). During this preparation, ammonia gas was bubbled into the reaction mixture by heating a mixture of sodium hydroxide (NaOH) and ammonium carbonate ($(\text{NH}_4)_2\text{CO}_3$) in a ratio of 2:1 respectively. This was important to achieve pH 8 and to improve the overall yield by converting any $[\text{Pr}_3\text{NH}] \text{Cl}$ by-product back to Pr_3N for further reaction with chlorosulfonic acid, liberating ammonium chloride (NH_4Cl) as a white precipitate (the yield was not reported prior the ammonia addition). This reaction was exothermic, so the reaction temperature was kept between (-30 to -40 °C) by using a cooling system of acetonitrile and dry ice (CO_2) (**Scheme 28**).

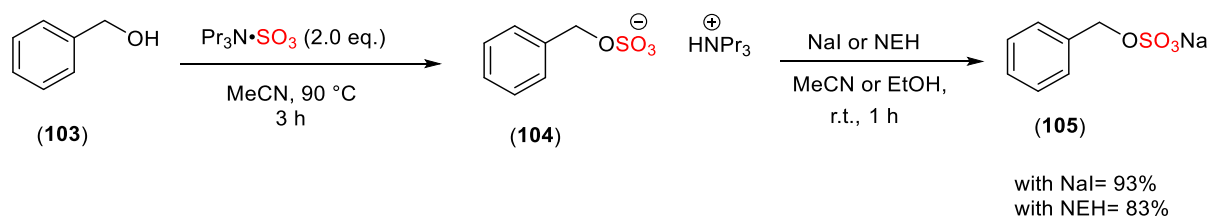


Scheme 28: The synthesis of Pr₃N•SO₃.

The structure of Pr₃N•SO₃ was confirmed by both ¹H and ¹³C NMR spectroscopic as well as mass spectrometric data. The significant feature that confirmed the structure of Pr₃N•SO₃ is the chemical shift of N(CH₂)₃ signal post sulfation (3.29 – 3.18 ppm) compared to its signal pre sulfation (2.37–2.27 ppm). Based on the structural data of TBSAB, Pr₃N•SO₃ was proposed to exist as a betaine in the solid state assuming a similar structure in solution.

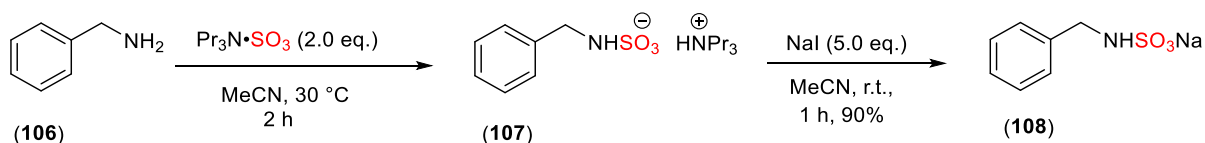
To validate this investigation, control experiments were attempted using benzyl alcohol and benzylamine as model system. First, benzyl alcohol was selected due to the down-field shift of the benzylic protons' signal after sulfation (+0.49 ppm) measured by ¹H NMR spectroscopy.¹⁴⁹ The sulfation reaction of benzyl alcohol was carried out by the reaction of benzyl alcohol and Pr₃N•SO₃ in 1:2 stoichiometric ratio. Acetonitrile was also selected due to its low boiling point (82 °C) which makes it simply removed under reduced pressure. The reaction was carried out at reflux and monitored by thin layer chromatography (TLC) until the reaction was complete. The tripropylammonium benzyl sulfate intermediate (**104**) is soluble in organic solvents such as acetonitrile and ethanol due to its lipophilicity. Then, the intermediate can be exchanged with a sodium source such as sodium iodide (NaI) or sodium-2-ethylhexanoate (NEH). Attempts were made using both sodium salts following the

optimised conditions for the *O*-sulfation reaction of benzyl alcohol using TBSAB.¹⁴⁹ With NaI, the sodium benzyl sulfate (**105**) was afforded in 93% isolated yield whereas NEH gave (**105**) in 83% yield over the two steps (**Scheme 29**).



Scheme 29: The sulfation control experiment on benzyl alcohol with $\text{Pr}_3\text{N}\cdot\text{SO}_3$. The overall yields were reported over the two steps.

The results of this investigation were compared with the TBSAB test reaction results. With TBSAB, sodium benzyl sulfate was afforded in 95% yield whereas with $\text{Pr}_3\text{N}\cdot\text{SO}_3$, sodium benzyl sulfate (**105**) in 93% isolated yield. The difference between the two yields is insignificant, indicating that both organosulfate intermediates exchanged efficiently with the sodium salt. Next, the *N*-sulfamation reaction of benzylamine was also attempted using $\text{Pr}_3\text{N}\cdot\text{SO}_3$. Benzylamine was also chosen due to the slight change of the chemical shift (+0.34 ppm) of the benzylic signal after sulfation as measured by ^1H NMR spectroscopy. The *N*-sulfamation reaction of benzylamine (**106**) was carried out by the reaction of benzylamine and $\text{Pr}_3\text{N}\cdot\text{SO}_3$ in a 1:2 stoichiometric ratio. The reaction temperature was reduced to 30 °C due to the greater *N*-nucleophilicity compared to alcoholic substrates. The resulting tripropylammonium benzyl sulfamate (**107**) was treated with a mixture of sodium iodide (5.0 eq.) and acetonitrile affording sodium benzyl sulfamate (**108**) in 90% isolated yield over the two steps. This result was also compared to the TBSAB test reaction with benzylamine. The sodium benzyl sulfamate (**108**) was afforded in 90% yield using $\text{Pr}_3\text{N}\cdot\text{SO}_3$ whereas with TBSAB, the sodium benzyl sulfamate was afforded in 98% isolated yield (**Scheme 30**).



Scheme 30: The *N*-sulfamation control experiment on benzylamine with $\text{Pr}_3\text{N}\cdot\text{SO}_3$

The overall result of this investigation was the first ever preparation of $\text{Pr}_3\text{N}\cdot\text{SO}_3$ and the sulfation control experiments with benzyl alcohol (**103**) and benzylamine (**106**). $\text{Pr}_3\text{N}\cdot\text{SO}_3$ enhances the solubility of organosulfates intermediates in organic solvents and enables their efficient isolation as $[\text{Pr}_3\text{NH}]^+$ and Na^+ salts. $\text{Pr}_3\text{N}\cdot\text{SO}_3$ is a suitable reagent for a wide range of organic molecules such as alcoholic and phenolic substrates, carbohydrates, sterols, and amines like TBSAB reagent with advantage of lower molecular weight compared to TBSAB, 223.33 Da vs 265.41 Da, respectively.

2.3.3. Synthesis of triisobutylamine sulfur trioxide complex

Triisobutylamine (TIBA) is an organic compound that belongs to the family of tertiary alkyl amines with a high $\text{p}K_{\text{a}}\text{H}$ value (**Table 7, entry 1**). The nitrogen atom of triisobutylamine is also sp^3 hybridised which donates the lone pair of electrons to form a N-S bond surrounding by bulky triisobutyl groups. Triisobutylamine has a bulkier structure than tributylamine, which makes the preparation of $\text{TIBA}\cdot\text{SO}_3$ complex challenging due to the branched *isobutyl* groups. Triisobutylamine has slightly larger C-N-C bond angles than triethylamine and tributylamine, which has bond angles of about 108° and 109.5° , respectively. The branched *isobutyl* groups increase the steric repulsion near the nitrogen atom, increasing the bond angles above the ideal tetrahedral angle of 109.5° (**Figure 14**).¹⁶⁰

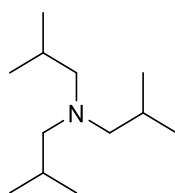
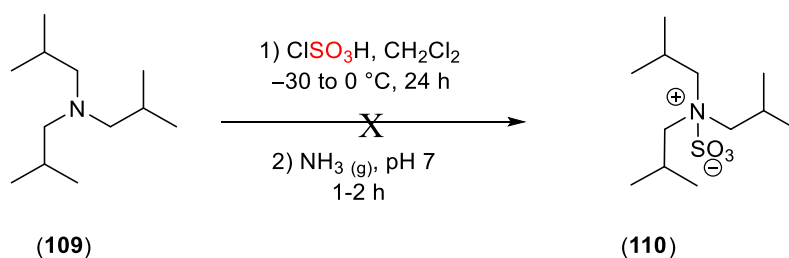


Figure 14: The structure of triisobutylamine.

The first ever preparation of TIBA•SO₃ complex was attempted on a small-scale reaction (0.016 moles) following the TBSAB optimised preparation conditions. This reaction was carried out by the reaction of TIBA with ClSO₃H in a 2:1 ratio. The reaction mixture was stirred and kept between (–30 to 0 °C). The addition of ammonia gas was critical to neutralise the reaction mixture to achieve pH 7. Unfortunately, the reaction was not successful as the desired product (**110**) was not afforded. Furthermore, another attempt was made with an extended reaction time to 24 h however the reaction was also unsuccessful and the desired TIBA•SO₃ complex was not afforded (**Scheme 31**). This was attributed to several factors, including steric hindrance and slow reaction kinetics. The branched bulky *isobutyl* groups create significant steric hindrance around the nitrogen atom, making it more difficult for SO₃ to approach and react with the nitrogen atom to form the desired complex. Furthermore, the low reaction temperature may slow down the reaction rate, particularly given the steric hindrance already present. This could prevent the SO₃ from efficiently reacting with the nitrogen atom, hampering complex formation.



Scheme 31: Attempted synthesis of TIBA•SO₃ complex.

2.3.4. Synthesis of *isopropyl-N-methyl-tert-butylamine* sulfur trioxide complex

Isopropyl-N-methyl-tert-butylamine is a chiral tertiary amine displaying three different alkyl groups (*isopropyl*, *methyl*, and *tert-butyl*) attached to the nitrogen atom (**Figure 15**). The nitrogen atom of *isopropyl-N-methyl-tert-butylamine* is sp^3 hybridised and can donate its lone pair of electrons to form a new bond. The presence of these distinct alkyl groups makes the amine sterically hindered, which affects its reactivity and solubility.

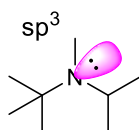
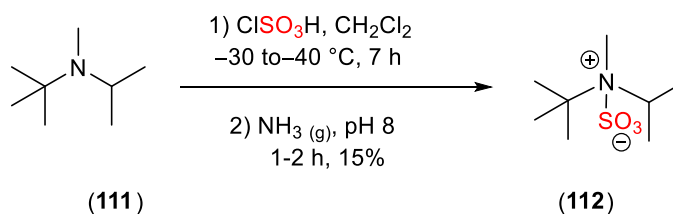


Figure 15: The sp^3 orbital hybridisation structure of *isopropyl-N-methyl-tert-butylamine*.

The *isopropyl-N-methyl-tert-butylamine* sulfur trioxide complex was also prepared by applying similar optimised conditions for the preparation of $Pr_3N \cdot SO_3$ affording this novel complex (**112**) in 15% yield (**Scheme 32**).



Scheme 32: The synthesis of *isopropyl-N-methyl-tert-butylamine* SO_3 complex.

The significant drop of the isolated yield was expected due to the steric effect of the bulky structure of *isopropyl-N-methyl-tert-butylamine* compared to other SO_3 -amine complexes such as $Pr_3N \cdot SO_3$ (**102**). The 1H NMR spectroscopic data confirmed the structure of this complex (**112**) (**Figure 16**) as follows: 1H NMR (300 MHz, $CDCl_3$) δ 3.92 – 3.77 (m, 1H), 2.60 (s, 3H), 1.49 (s, 9H), 1.40 – 1.34 (m, 6H). A downfield shift of the compound signals compared to those for the starting material was observed, indicating the formation of the desired complex

(**112**) as confirmed by ^1H NMR spectroscopic data. Additionally, the ^{13}C NMR spectroscopic data were reported as follows: ^{13}C NMR (101 MHz, CDCl_3) δ 64.0, 57.9, 56.8, 52.3, 48.4, 47.3, 29.6, 28.70, 26.8, 25.6, 23.1, 22.3. Additional signals (56.8, 47.3, 26.8, 25.6, 22.3) were observed suggesting on the formation diastereomeric betaine due to the potential stereogenic axis of (**112**) (See **Chapter 8** for the full data).

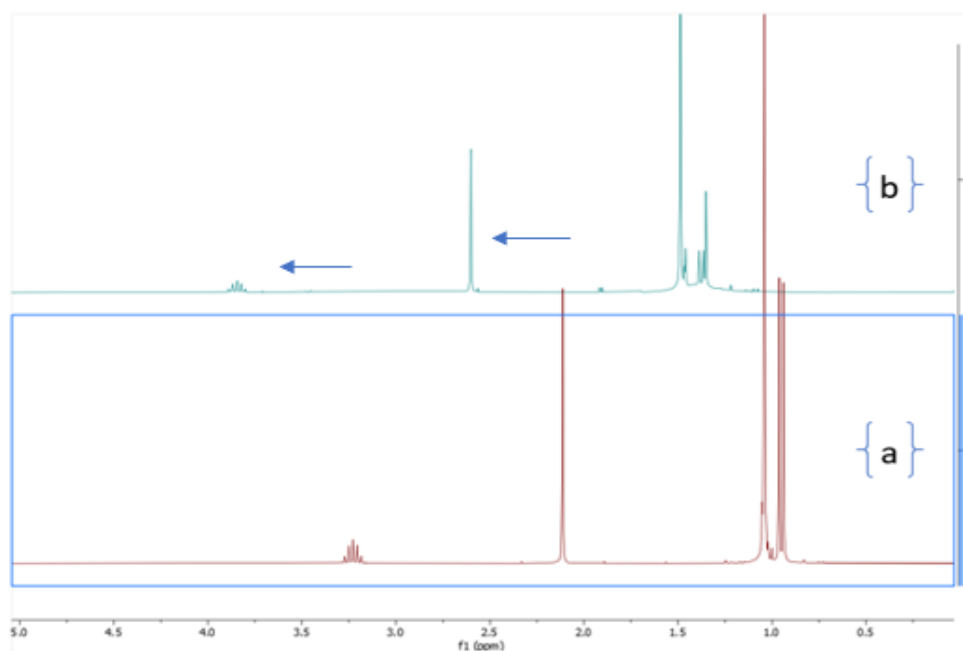
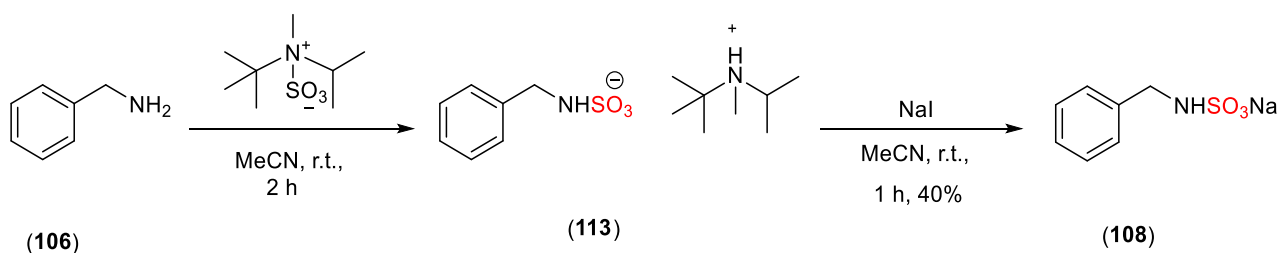


Figure 16: The ^1H NMR (400 MHz, CDCl_3) spectra of (a) isopropyl-*N*-methyl-*tert*-butylamine compared to its SO_3 complex (b), both dissolved in CDCl_3 .

Next, the *N*-sulfamation reaction of benzylamine (**106**) was investigated using isopropyl-*N*-methyl-*tert*-butylamine SO_3 complex (**112**) following the optimised conditions for the *N*-sulfamation reaction using TBSAB.^{47, 149} The desired sodium benzyl sulfamate (**108**) was isolated in 40% yield after the two steps (**Scheme 33**).



Scheme 33: The *N*-sulfamation of benzylamine with *isopropyl-N-methyl-tert-butylamine* SO₃ complex.

The results of this investigation showed that this complex (**112**) was possible to prepare, despite the steric hindrance of *isopropyl-N-methyl-tert-butylamine* which slows the reaction rate and the low isolated yield (15%). The *N*-sulfamation reaction of benzylamine was successful, despite the modest yield of sodium benzyl sulfamate (**108**) (40%) compared to other amine-SO₃ complexes such as Pr₃N•SO₃ and TBSAB, which had yields of 90% and 98%, respectively. This novel complex (**112**) offers a potential chiral sulfation protocol as the nitrogen atom is now a stereogenic centre. This chirality can be exploited in future asymmetric synthesis, where this complex introduces chirality in the sulfated product. The steric hindrance of this complex can also be useful for the regioselective sulfation, which benefits the field of medicinal chemistry and drug development.

2.3.5. Synthesis of *N*-substituted morpholine sulfur trioxide complexes

The current investigation proposed the design and synthesis of hydrophilic sulfation reagents which could be utilised for the sulfation of hydrophilic substrates including amino acids and peptide substrates. 4-Methylmorpholine and 4-ethylmorpholine are significantly less lipophilic molecules compared to other tertiary alkylamines, including tripropylamine (cLogP of 4-methylmorpholine and 4-ethylmorpholine are 0.16 and 0.69 compared to 3.19 for tripropylamine). 4-Methylmorpholine and 4-ethylmorpholine are cyclic tertiary amine-containing alkyl groups attached to the nitrogen atom (**Figure 17**).



Figure 17: The structure of 4-methyl and 4-ethylmorpholine.

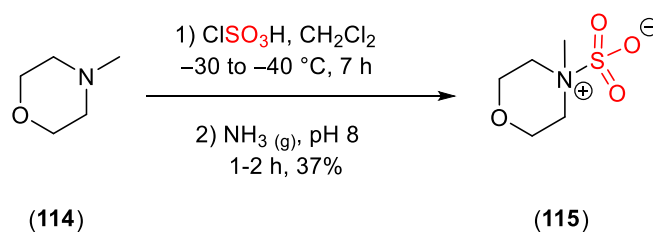
4-Methylmorpholine and 4-ethylmorpholine are weaker bases with the pK_aH value of ~ 8 compared to Me_3N , Et_3N , and Pr_3N (**Table 7**).

Table 7: The expected pK_aH values of different bulky and cyclic amines.¹⁶¹⁻¹⁶²

Entry	Amine	Conjugate Acid	pK_aH (H_2O)
1			10.32
2			10.36
3			7.38
4			7.67

The only report that describes the preparation of 4-methylmorpholine SO_3 and 4-ethylmorpholine SO_3 complexes was in 1946 by Baptist, where 4-methylmorpholine or 4-ethylmorpholine was reacted with sulfur trioxide in organic solvent such as chloroform and ethylene chloride.¹⁶³ However, no isolated yield nor characterisation data were documented except the melting point of 4-methylmorpholine SO_3 between 148-150 °C. It was postulated that the reaction of 4-alkylmorpholine and $ClSO_3H$ would provide 4-methyl and 4-ethylmorpholine SO_3 complexes following the optimised methodology used for $Pr_3N \bullet SO_3$ and TBSAB preparation. The synthesis of 4-methylmorpholine SO_3 started with the reaction of 4-

methylmorpholine and ClSO_3H , affording the desired complex in 37% isolated yield (**Scheme 34**).



Scheme 34: The synthesis of 4-methylmorpholine SO_3 complex.

^1H and ^{13}C NMR spectroscopy analysis and the mass spectrometry data confirmed the formation of 4-methylmorpholine SO_3 complex (**Figure 18**).

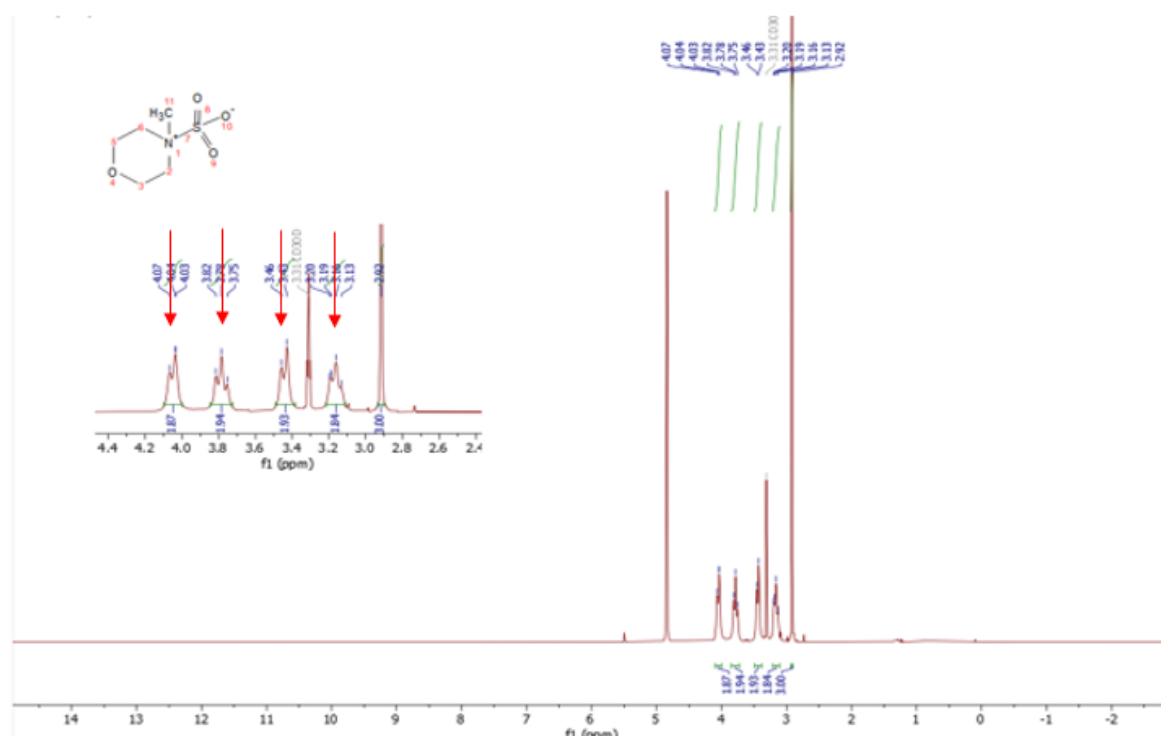


Figure 18: The ^1H NMR (400 MHz, MeOD) spectrum of 4-methylmorpholine SO_3 complex. Arrows show the cyclic protons in 4-methylmorpholine SO_3 complex.

In Figure 18, ^1H NMR spectroscopic data of 4-methylmorpholine SO_3 (**115**) have five different peaks representing; the methyl group as a singlet (s) and the other four peaks which

correspond to the morpholine ring as dd, t, m, and m, respectively. These data were compared to 4-methylmorpholine (**114**) ^1H NMR spectroscopic data using the same solvent (400 MHz, MeOD) showing the splitting peak pattern differences and the number of peaks in each spectrum. The ^1H NMR spectroscopic data of 4-methylmorpholine (**114**) has two triplets representing the cyclic protons and a singlet peak for the methyl group (**Figure 19**).

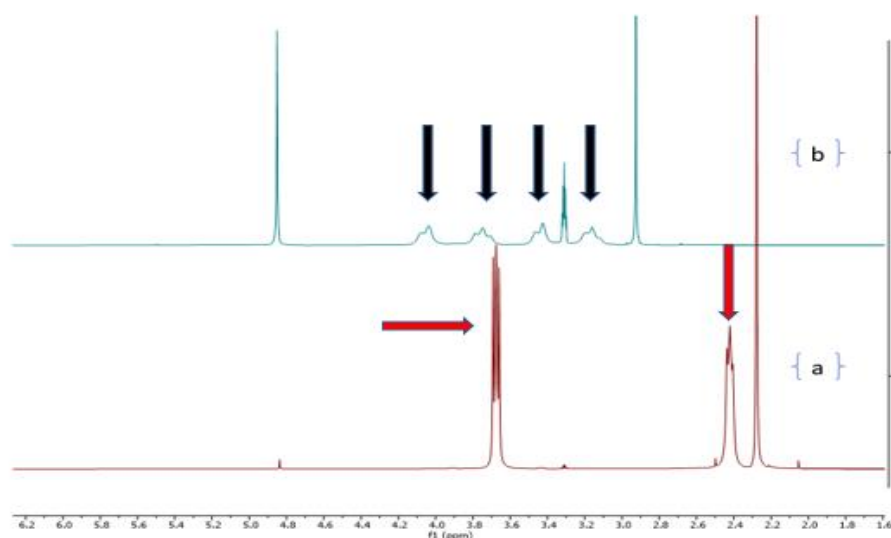


Figure 19: The stacked ^1H NMR (400 MHz, MeOD) spectra of (a) 4-methylmorpholine and (b) 4-methylmorpholine SO_3 complex.

This hypothesis was due to the installation of the SO_3 molecule onto 4-methylmorpholine which changes the electronic environment and causes changes in the 4-methylmorpholine ring conformation. This is due to both the electron-withdrawing effects of SO_3 and its steric impact on the overall structure of the 4-methylmorpholine ring (**Figure 20**).

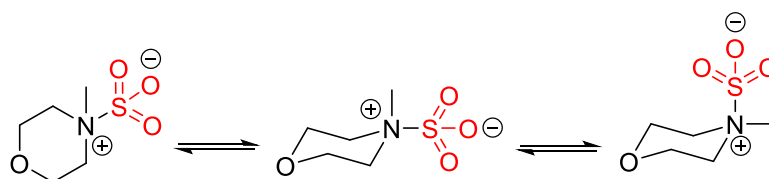
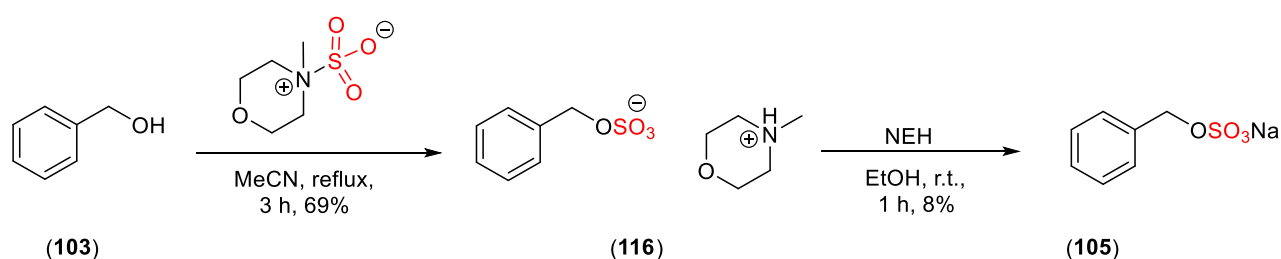


Figure 20: The structural isomer of 4-methylmorpholine SO_3 complex.

Next, 4-methylmorpholine SO_3 complex (**115**) was further investigated for its sulfation reaction on benzyl alcohol (**103**) and benzylamine (**106**). It was anticipated that the resulting organosulfate and sulfamate intermediates would be less lipophilic due to the hydrophilic nature of the 4-methylmorpholinium cation. Therefore, a lipophilic solubilising partner such as tributylamine was hypothesized to improve the lipophilicity of the corresponding intermediate. This was based on our novel work that demonstrated that tributylamine exchanges effectively with $\text{Me}_3\text{N}\cdot\text{SO}_3$ and $\text{Py}\cdot\text{SO}_3$ (see Chapter 4).

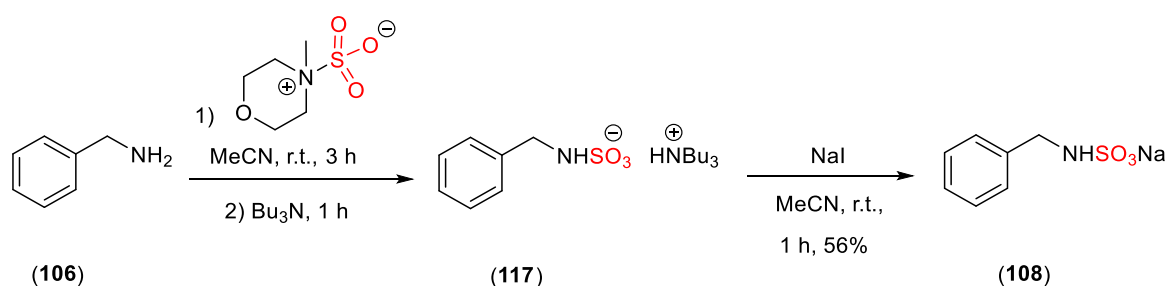
The *O*-sulfation reaction of benzyl alcohol (**103**) with 4-methylmorpholine SO_3 complex (**115**) was carried out in 1:2 ratio, adapting the optimised conditions for the sulfation of alcohols using TBSAB. The 4-methylmorpholinium benzyl sulfate cation (**116**) was purified by column chromatography affording the desired molecule (**116**) in 69% yield (Scheme 35).



Scheme 35: The synthesis of 4-methylmorpholinium benzyl sulfate using 4-methylmorpholine SO_3 complex.

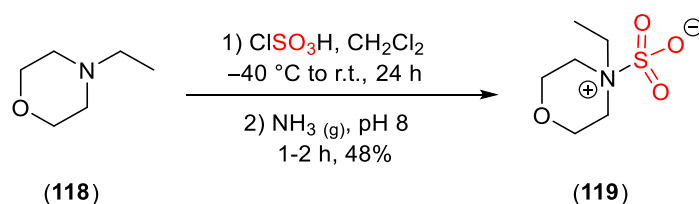
4-Methylmorpholinium benzyl sulfate (**116**) was exchanged with NEH affording sodium benzyl sulfate (**105**) in 8% isolated yield. The substantial drop of the final yield could be associated with lipophilic NEH, which did not exchange efficiently with the 4-methylmorpholinium benzyl sulfate cation (**116**). So, another sodium salt, sodium iodide (NaI), was considered for the following reaction. The *N*-sulfamation reaction of benzylamine (**106**) and 4-methylmorpholine SO_3 (**115**) was also carried out in 1:2 ratio, adapting the optimised conditions for the *N*-sulfamation reaction using TBSAB with the difference of adding tributylamine (Bu_3N) as a

lipophilic partner. This addition was considered to improve the solubility of organosulfamate cation intermediates into organic solvents. This was followed by sodium salt exchange affording the desired sodium benzyl sulfamate (**108**) in 56% isolated yield over the two steps (**Scheme 36**).



Scheme 36: The *N*-sulfamation reaction of benzylamine with 4-methylmorpholine SO₃ complex.

4-Ethylmorpholine SO₃ complex was synthesised by the reaction of 4-ethylmorpholine and ClSO₃H, affording the complex in 48% isolated yield on a 10 g scale (**Scheme 37**).



Scheme 37: The synthesis of 4-ethylmorpholine SO₃ complex.

Both ¹H and ¹³C NMR spectroscopy analysis and mass spectrometry data confirmed the structure of 4-ethylmorpholine SO₃ complex (**Figure 21**).

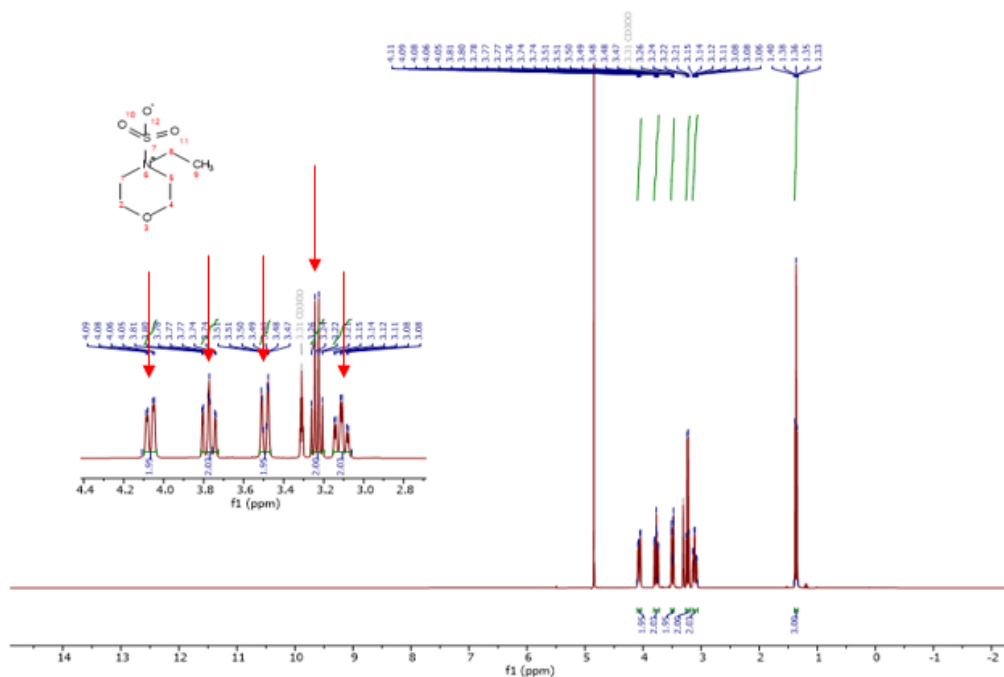


Figure 21: The ^1H NMR (400 MHz, MeOD) spectrum of 4-ethylmorpholine SO_3 complex. Arrows show the cyclic and ethyl group protons in 4-ethylmorpholine SO_3 complex.

Similar to 4-methylmorpholine SO_3 complex (**115**), the ^1H NMR spectroscopic data of 4-ethylmorpholine SO_3 complex (**119**) shows six peaks, two peaks represent the ethyl group (q and t) and the other four peaks correspond to morpholine protons. This hypothesis was also due to the rotamer isomer structure of 4-ethylmorpholine SO_3 complex, adopting a chair conformation form caused by the installation of electrophile SO_3 group into the final complex similar to 4-methylmorpholine SO_3 complex (**Figure 22**).

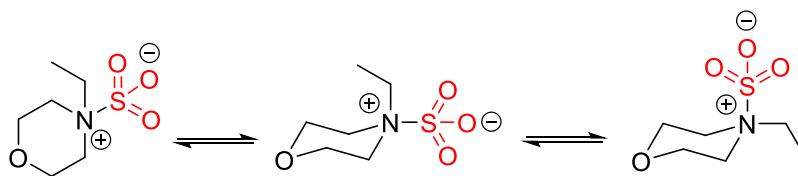
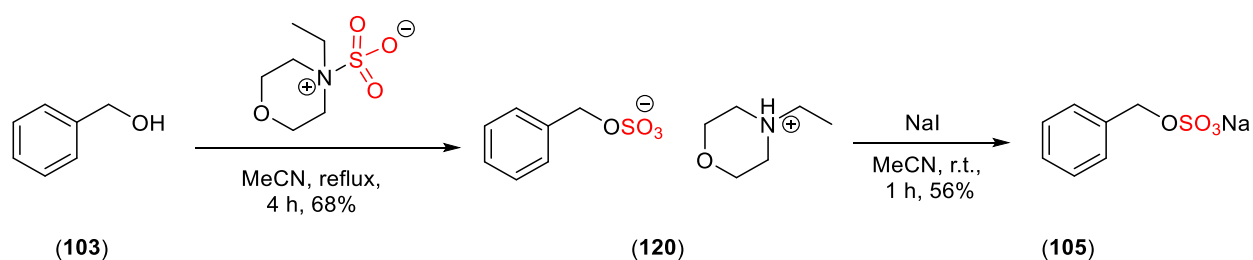


Figure 22: The structural isomer of 4-ethylmorpholine SO_3 complex.

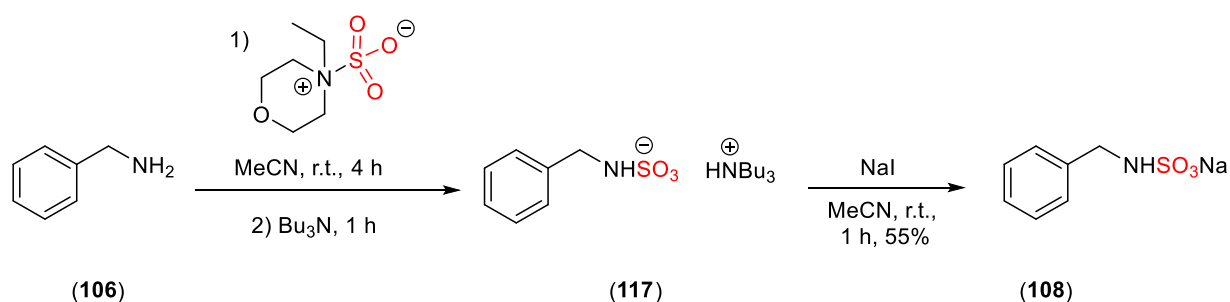
Sulfation test reactions were investigated on benzyl alcohol and benzylamine using 4-ethylmorpholine SO_3 complex. First, the *O*-sulfation reaction was carried out by reacting benzyl alcohol (**103**) and 4-ethylmorpholine SO_3 complex (**119**) in a 1:2 ratio. The reaction

mixture was purified by column chromatography to give 4-ethylmorpholinium intermediate (**120**) in 68% isolated yield. The desired sodium benzyl sulfate (**105**) was also afforded when the pure 4-ethylmorpholinium cation was exchanged with NaI affording the desired compound (**105**) in 56% isolated yield (**Scheme 38**).



Scheme 38: The *O*-sulfation reaction test of benzyl alcohol with 4-ethylmorpholine SO₃ complex.

The *N*-sulfamation reaction of benzylamine (**106**) and 4-ethylmorpholine SO₃ (**119**) was carried out in a 1:2 ratio, adapting the optimised method for the *N*-sulfamation reaction using TBSAB except for the addition of tributylamine. This addition was needed due to the poor solubility of the mixture of benzylamine and 4-ethylmorpholine SO₃ complex in MeCN. Next, the 4-ethylmorpholinium benzyl sulfamate intermediate was exchanged with NaI affording the desired sodium benzyl sulfamate (**108**) in 55% yield over the two steps (**Scheme 39**).



Scheme 39: The *N*-sulfamation reaction of benzylamine using 4-ethylmorpholine SO₃ complex.

The results of this investigation have proved the successful preparation of these novel complexes, despite the extended reaction time for their synthesis and low isolated yield compared for instance to Pr₃N•SO₃ and TBSAB. The successful *O*-sulfation and *N*-sulfamation

test reactions suggest that different substrates such as amino acids and polysaccharides could be sulfated using these novel more hydrophilic sulfating reagents.

2.3.6. Synthesis of cinchonidine sulfur trioxide complex

Cinchonidine is a natural alkaloid compound found in the bark of certain species of trees, which belong to the Cinchona genus.¹⁶⁴ It is chemically related to another alkaloid called quinine, which is also found in Cinchona bark.¹⁶⁴ Cinchonidine have various pharmacological applications such as anti-malarial and anti-arrhythmic activity.¹⁶⁴ Chemically, cinchonidine has been involved in many chemical reactions, including asymmetric reactions due to its unique chiral nature, contain several stereocentres (**Figure 23**).¹⁶⁴⁻¹⁶⁶

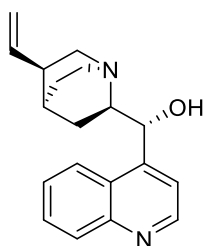


Figure 23: The structure of cinchonidine.

The cinchonidine structure has two nitrogen atoms which have different orbital hybridisation states. The quinoline ring is sp^2 hybridised whereas the nitrogen atom in quinuclidine, is sp^3 hybridised (**Figure 24**).

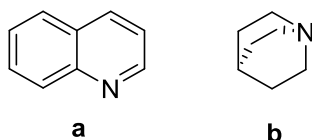
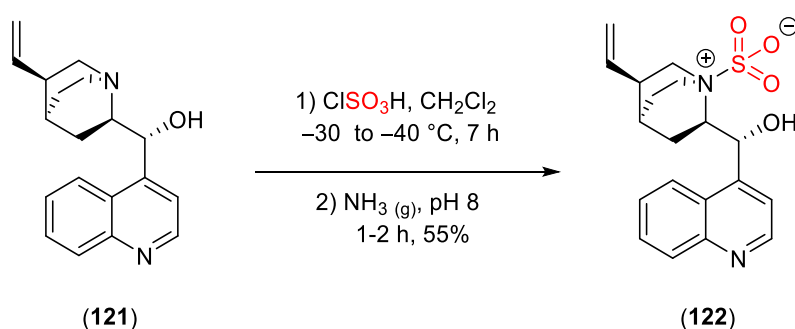


Figure 24: The structure of quinoline (a) and quinuclidine (b).

It was anticipated that the quinuclidine is more likely to form adducts with various Lewis acids than the quinoline ring. This was because of the orbital hybridisation which has an impact on

the reactivity of a reagent.¹⁶⁴ The quinuclidine is a stronger Lewis base with a pK_aH value of 11.0, compared to the pK_aH value of 4.85 for quinoline.¹⁶⁴

The synthesis of cinchonidine sulfur trioxide complex is challenging due to the structural complexity of cinchonidine and different sites for sulfation; the nitrogen atoms and the hydroxyl group. To explore this novel synthesis, the preparation of this complex was attempted by the reaction of cinchonidine (**121**) and $ClSO_3H$, adapting the optimised conditions for TBSAB preparation. This reaction was carried out in a 1:2 stoichiometric ratio and ammonia gas was added to adjust the pH to 8. The desired cinchonidine SO_3 complex (**122**) was afforded in 55% isolated yield (**Scheme 40**).



Scheme 40: The synthesis of cinchonidine SO_3 complex.

Both 1H and ^{13}C NMR spectroscopic and the mass spectrometric data confirmed the structure of the cinchonidine SO_3 complex (See Appendix for the full data).

Based on the stacked 1H NMR spectroscopic data, the quinoline proton peaks that are between 7.6-9.0 ppm in both cinchonidine and cinchonidine SO_3 complex have not shifted significantly indicating that the quinoline nitrogen atom was not affected by the sulfation reactions (**Figure 25**).

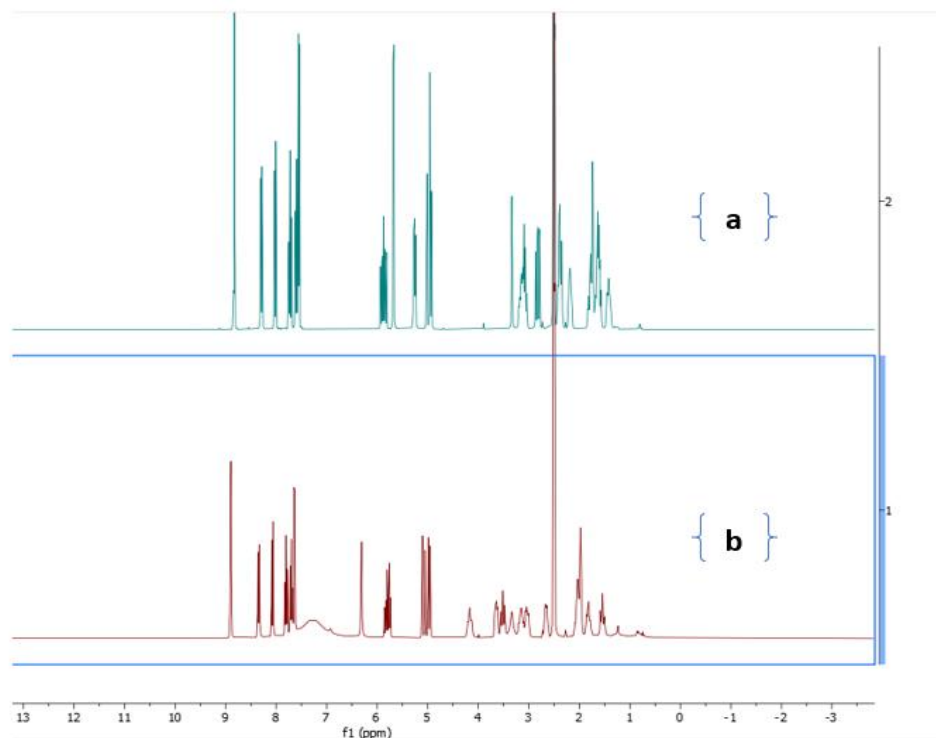


Figure 25: The ¹H NMR spectra of both (a) cinchonidine and (b) cinchonidine SO₃ complex.

Next, the nitrogen atom (quinuclidine ring) and the hydroxyl group were investigated for the possible sulfation site. After the preparation of this complex, ¹H NMR spectroscopy data showed no change in the chemical shift of the quinoline ring suggesting that the nitrogen atom in the quinoline ring was not sulfated. By contrast, the C-H adjacent to the nitrogen atom of the quinuclidine ring has a greater chemical shift (+0.4 and +0.39 ppm). The increased chemical shift suggests that the nitrogen atom in the quinuclidine ring had undergone sulfation, likely making it more electron-withdrawing and causing the shift. The hydroxyl group was also examined as a possible site for sulfation, but the data did not provide robust evidence supporting sulfation at this position. Therefore, further investigations are necessary to determine whether sulfation could occur at the hydroxyl group.

2.4. Conclusion and future work

In conclusion, the results of this investigation have reported the preparation of a series of novel sulfating reagents including the sulfur trioxide-amine complexes of tripropylamine, and 4-methyl and 4-ethylmorpholine. It was also reported the preparation of potential chiral sulfating reagents; *isopropyl-N-methyl-tert-butylamine* and cinchonidine SO_3 complexes. These reagents were applied to test *O*- and *N*-sulfation of benzyl alcohol and benzylamine following the optimised methodology which afforded the organosulfate and sulfamate ester, subsequently exchanged to the sodium salts.

For the future development of this work, additional investigations and further studies would be considered for the following points:

- Confirmation of the $\text{Pr}_3\text{N}\cdot\text{SO}_3$ structure by X-ray crystallography and comparison with similar tertiary amine SO_3 such as $\text{Et}_3\text{N}\cdot\text{SO}_3$ and TBSAB.
- Further studies on the use of $\text{Pr}_3\text{N}\cdot\text{SO}_3$ as the missing tertiary alkylamine compared to Me_3N , Et_3N , and Bu_3N on a range of small molecules, including alcoholic, phenolic-containing substrates, carbohydrates, α -amino acids, and steroids.
- Further optimisation studies on the preparation of the novel stereogenic sulfating agent, *isopropyl-N-methyl-tert-butylamine* SO_3 complex and explore its reactivity on a range of functional groups such as alcoholic and phenolic substrate. This potential chiral reagent will be useful for synthesising chiral sulfate esters.
- Further investigations on cinchonidine SO_3 complex preparation and its reactivity as a potential chiral sulfating agent which could be used in asymmetric synthesis or resolution of racemic mixture.

Chapter 3. Chemical sulfation of selected α -amino acids using 4-methylmorpholine sulfur trioxide and 4-ethylmorpholine sulfur trioxide

Background

Proteins are important biomolecules which are involved in several biological processes within living organisms.¹⁶⁷⁻¹⁶⁸ Proteins such as enzymes, hormones, receptors and antibodies have various biological functions, including contraction of muscles, regulation of glucose metabolism, transporting O₂ to cells, and replicating and repairing DNA.¹⁶⁹⁻¹⁷¹ Furthermore, enzymes act as catalysts to accelerate chemical reactions within living organisms.¹⁶⁹ As hormones, they control the activity of genes and regulate signalling pathways.¹⁷² Proteins are composed of long chains of smaller α -amino acid units.¹⁶⁷ There are more than 300 naturally occurring amino acids, of which 20 α -amino acids form the monomer units of proteins.¹⁶⁷⁻¹⁶⁸ Amino acids are chemically connected via peptide bonds, which are formed between the carboxylic acid group (CO₂H) of one amino acid and the amino group (NH₂) of another amino acid, resulting in liberation of a water molecule.¹⁶⁷ The physicochemical properties of a protein, including its structure, stability, and interaction with another molecule are usually determined by its amino acid side-chain composition.^{167, 169}

3.1. Chemistry of α -amino acids

α -amino acids are small monomers that combine to form proteins. The structure of α -amino acids consists of a central carbon atom (α -carbon) bonded to an amino group (NH₂), a carboxylic acid group (COOH), a hydrogen atom, and a variable side chain (R group) (**Figure 26**).



Figure 26: The general structure of an α -amino acid.

Generally, amino acids are existing as zwitterionic form at physiological pH, where the amino group is protonated and carries a positive charge (H_3N^+) and the carboxylic acid is deprotonated carrying a negative charge (COO^-) (**Figure 27**).

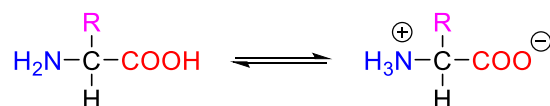
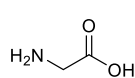


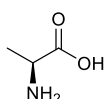
Figure 27: Zwitterionic form of an α -amino acid at physiological pH.

Glycine, is the simplest and smallest α -amino acid where the **R** group is a hydrogen atom. Other amino acids have different side-chains (**R** group), including alkyl, aryl, indole, and thiol groups. The properties of a specific amino acid vary from acidic to basic and from hydrophilic to hydrophobic according to the **R**-group substituent (**Figure 28**).

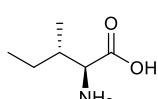
Aliphatic



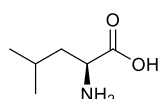
glycine



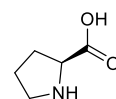
alanine



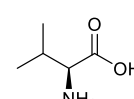
isoleucine



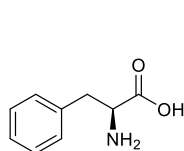
leucine



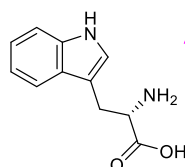
proline



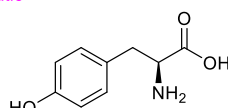
valine



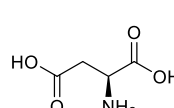
phenylalanine



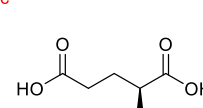
tryptophan



tyrosine



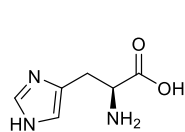
aspartic acid



glutamic acid

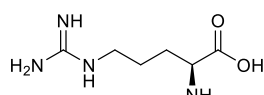
Aromatic

Acidic

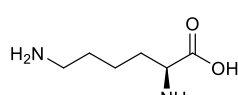


histidine

Basic

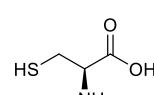


arginine

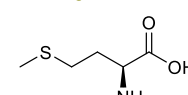


lysine

Sulfur-containing

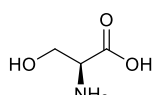


cysteine

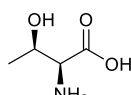


methionine

Hydroxylic

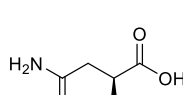


serine

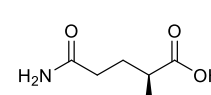


threonine

Amide-containing



asparagine



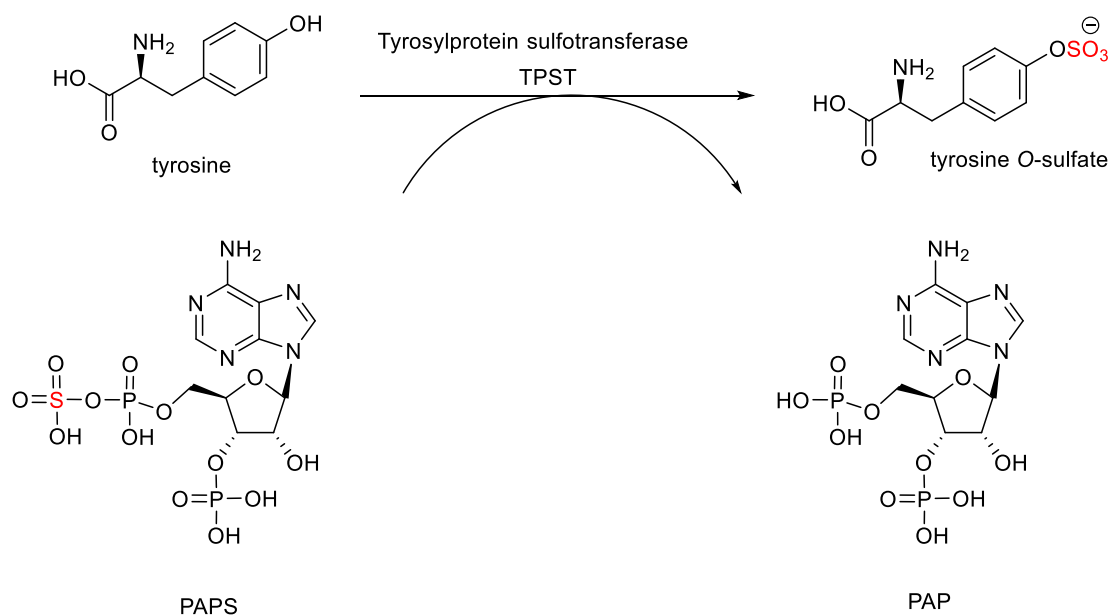
glutamine

Figure 28: Common α -amino acids which are categorised according to R substituents variations, including aliphatic chain, aromatic, acidic, basic, sulfur-containing, and hydroxylic amino acids.

3.2. Chemical modifications of proteins

Proteins undergo a wide range of post-translational chemical modifications including methylation, phosphorylation, and sulfation which affect protein functions, stability, and interaction with other molecules.¹⁷³

The sulfation of proteins is the most abundant post-translational modification (PTM) of tyrosine residues and occurs in approximately 1% of all tyrosine residues of different proteins.¹⁷⁴⁻¹⁷⁵ Bettelheim and co-workers discovered tyrosine *O*-sulfation from bovine fibrinopeptide in 1954.¹⁷⁶ In the early 1980s, Huttner and Lee reported and studied several other tyrosine-sulfated proteins, isolated from different tissues and cells.¹⁷⁷⁻¹⁷⁸ They reported that this post-translational modification takes place in the trans-Golgi network and is mediated by a membrane-bound protein.¹⁷⁸ The tyrosine-*O*-sulfation reaction is catalysed by tyrosylprotein sulfotransferase 1 and 2 (TPST-1 and TPST-2).¹⁷⁹ Tyrosylprotein sulfotransferases are responsible for the transfer of an activated sulfate donor from 3-phospho adenosine 5-phosphosulfate (PAPS) to the hydroxyl group of tyrosine resulting in tyrosine *O*-sulfate ester and adenosine-3'-5'-diphosphate (PAP) (**Scheme 41**).¹⁷⁹

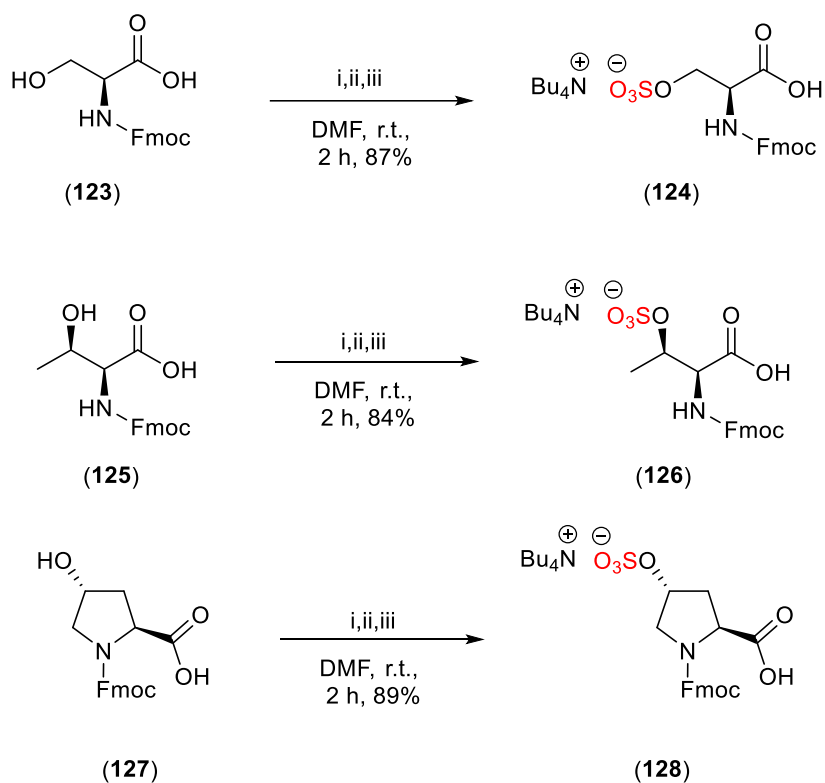


Scheme 41: The biological sulfation of tyrosine catalysed by tyrosylprotein sulfotransferase (TPST).¹⁷⁹

3.3. Chemical sulfation approaches of proteins

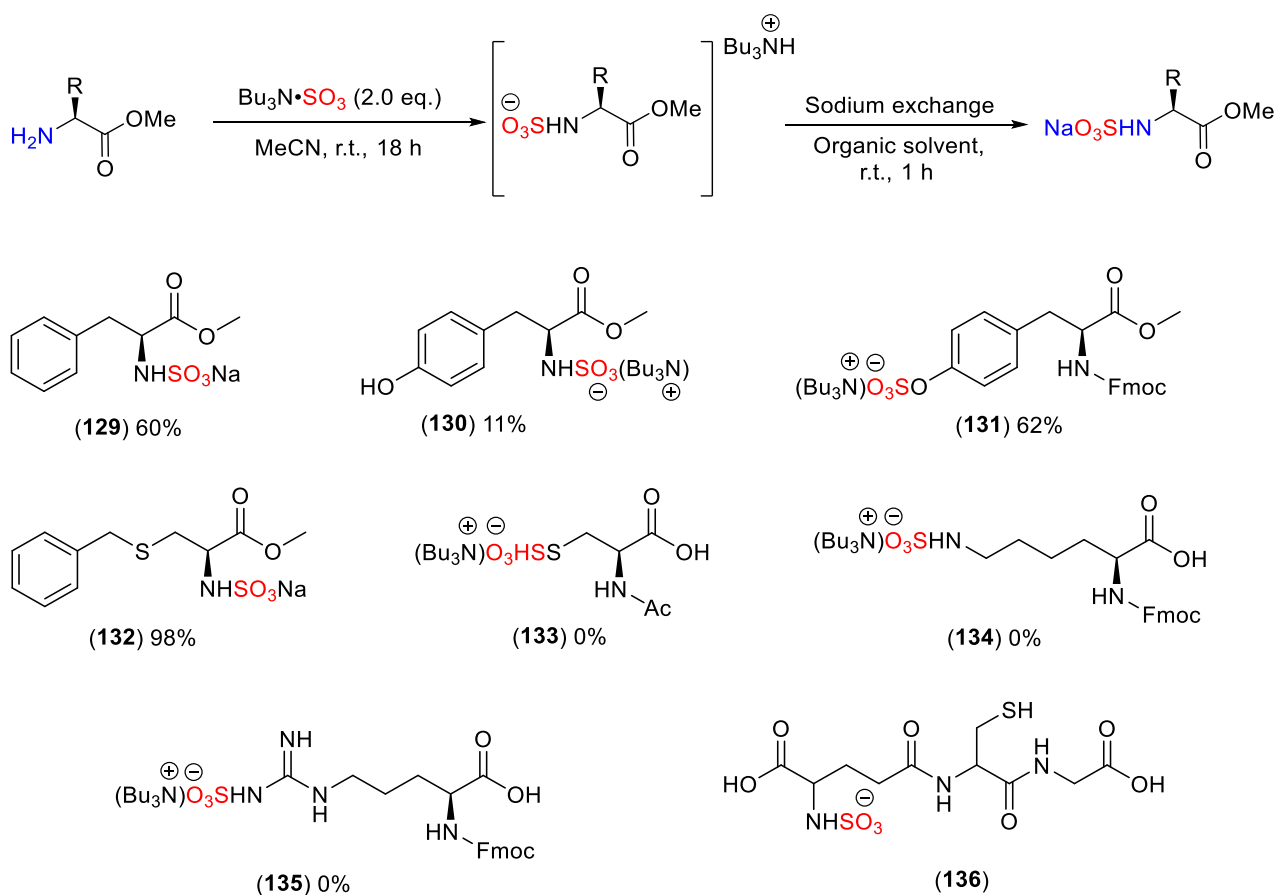
There are a limited number of chemical sulfation approaches to access sulfated proteins due to the structure complexity of proteins, incompatibility in organic solvents, and purification and isolation challenges of sulfated proteins.¹⁸⁰ In nature, the biological sulfation of proteins has been limited to the phenolic tyrosine residues which are catalysed by sulfotransferase (SULT) enzymes.⁴⁷ Other reports have investigated the *O*-sulfation, *N*-sulfamation and *S*-sulfurothiolation of proteins.^{47, 174} For instance, the preparation of sulfated proteins has used the *Fmoc*-based solid-phase peptide synthesis (SPP).¹⁸¹ The *N*-sulfamation reaction of proteins has employed sulfating reagents, including sulfur trioxide amine complexes (Me₃N•SO₃, Et₃N•SO₃, Py•SO₃), H₂SO₄/DDC, and chlorosulfonic acid.^{47, 182} Vázquez and co-workers reported a method for installation of sulfate groups onto *L*-serine, *L*-threonine, and *L*-hydroxyproline using the DMF•SO₃ complex.¹⁸¹ In this method, an excess of DMF•SO₃ complex was added to the *Fmoc*-protected amino acid of *L*-serine, *L*-threonine, and *L*-

hydroxyproline in the presence of anhydrous DMF. This was followed by the addition of a tetrabutylammonium salt (Bu_4NHSO_4) which was needed for the sulfated amino acids to improve the lipophilicity of the desired molecules (**Scheme 42**).¹⁸¹



Scheme 42: Reagents and conditions: i) $\text{DMF}\cdot\text{SO}_3$ complex (4.0 eq.), ii) Bu_4NHSO_4 (2.0 eq.), sat. aqueous NaHCO_3 (50 mL), 0°C , and iii) 10% citric acid (25 mL, pH 5).

In 2020, Benedetti and co-workers reported the *N*-sulfamation and *O*-sulfation reactions of selected α -amino acids and peptides using the TBSAB reagent (**Scheme 43**).^{47, 149}



Scheme 43: The *N*-sulfamation reaction of selected α -amino acids using TBSAB and scope of selected α -amino acids. The isolated yield of glutathione sulfamate (**136**) was not reported but confirmed by mass spectrometric detection.

Despite the effectiveness of existing methods, there are issues which hamper their use including the excess amount of the sulfating reagents used, protection and deprotection steps, various purification techniques such as chromatography, extraction, and ion exchange. Furthermore, incompatibility with acid-sensitive substrates and solubility challenge of α -amino acids in organic solvents is an ongoing issue^{47, 181} Thus, there is a need to develop novel hydrophilic sulfating reagents that are compatible with α -amino acids.

The aim of this chapter is to investigate the use of hydrophilic sulfating reagents; 4-methylmorpholine SO_3 and 4-ethylmorpholine SO_3 complexes for the sulfation of selected α -amino acids under mild reaction conditions using polar solvent systems ($\text{H}_2\text{O}/\text{MeCN}$). This

method will be explored on some selected α -amino acids including aliphatic and protected aromatic α -amino acids.

3.4. Results and Discussion

3.4.1. Optimisation and control studies

This investigation proposed the use of 4-methylmorpholine SO_3 and 4-ethylmorpholine SO_3 complexes for the sulfation of selected amino acids. It was anticipated that 4-methylmorpholine SO_3 and 4-ethylmorpholine SO_3 could be used under milder conditions compared to other sulfation approaches such as sulfuric acid and chlorosulfonic acid protocols. The preparation of 4-methylmorpholine SO_3 (**115**) and 4-ethylmorpholine SO_3 (**119**) was successfully achieved, affording the desired complexes in 37% and 48% isolated yield, respectively (See **Chapter 2, Scheme 34 and 37**).

Next, the sulfation reaction conditions were adapted from the TBSAB optimised conditions for the *O*-sulfation and *N*-sulfamation reactions of alcohol and amine-containing substrates. Due to the hydrophilicity of both sulfating reagents and the α -amino acid, the chosen solvent should be compatible with those reactants. As a result, a polar protic solvent such as methanol was chosen. However, there were concerns that the hydroxyl group in methanol might act as a competitive nucleophile affording methyl sulfate instead of *N*-sulfamation or *O*-sulfation of the amino acids. Consequently, a test reaction was carried out involving the reaction of methanol and 4-methylmorpholine SO_3 complex at room temperature. After 4 h, a sample was submitted for analysis by ^1H NMR spectroscopy. Four distinctive peaks were observed which correspond to the 4-methylmorpholinium ion and methyl sulfate (MeOSO_2OH) as confirmed using ^1H NMR spectroscopy analysis. Furthermore, the disappearance of 4-methylmorpholine SO_3 peaks (as shown in **Chapter 2, Figure 18**) was also

observed suggesting that methanol was sulfated and hence should not be considered as a solvent for the sulfation reaction of selected amino acids (**Figure 29**).

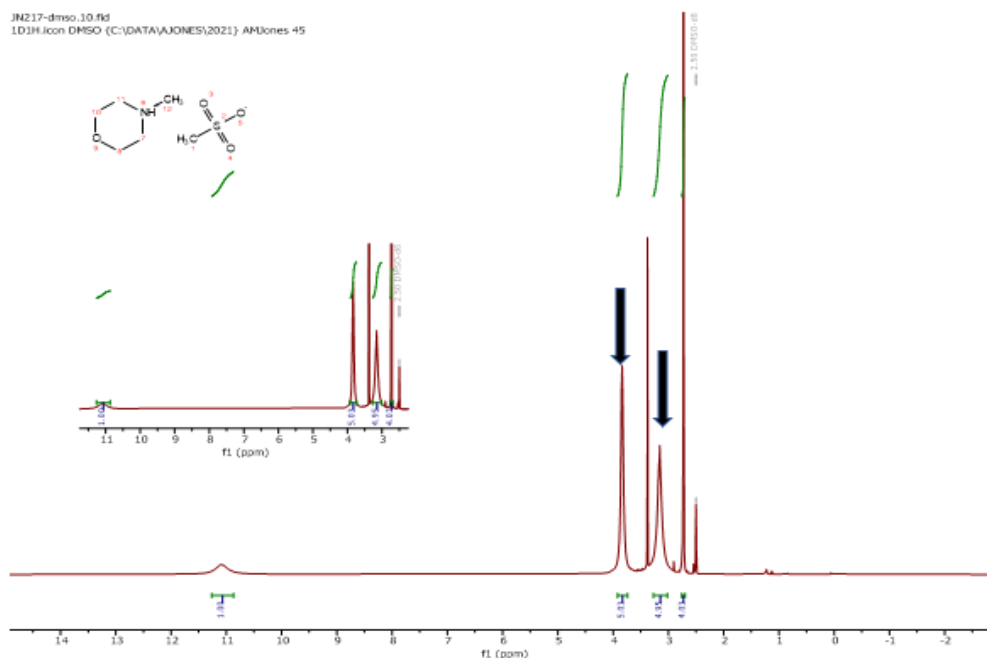


Figure 29: ^1H NMR (400 MHz, $\text{DMSO-}d_6$) spectrum for the sulfation test reaction of methanol using 4-methylmorpholine SO_3 complex, the sample was referenced to $\text{DMSO-}d_6$ solvent. Black arrows indicate the 4-methylmorpholinium proton signals.

Next, the use of a mixture $\text{H}_2\text{O}/\text{MeCN}$ solvents was considered for the sulfation of amino acids. First, the reactivity of both complexes was examined on benzyl alcohol (**103**) and benzylamine (**106**) (See **Chapter 2, Scheme 35, 36, 38, and 39**). Due to the lipophilic nature of benzyl alcohol and benzylamine, both solvent systems were used; MeCN alone and a mixture of MeCN/ H_2O .

The *N*-sulfamation reaction of benzylamine (**106**) and 4-methylmorpholine SO_3 complex was carried out following the adapted TBSAB *N*-sulfamation conditions. Additionally, tributylamine as a lipophilic partner and sodium iodide (NaI) were added. The addition of tributylamine was needed due to the poor solubility of the mixture of benzylamine and 4-methylmorpholine SO_3 complex and the resulting tributylammonium cation would be more

soluble in the 50% organic solvent (MeCN) and subsequently exchange with sodium iodide to afford the desired sulfamate salt.

4-Ethylmorpholine SO₃ complex was also used for the *O*-sulfation reaction of benzyl alcohol (**103**) adapting the TBSAB *O*-sulfation conditions to afford the desired sodium benzyl sulfate (**105**) in 56% isolated yield (See **Chapter 2, Scheme 38**).

The *N*-sulfamation reaction of benzylamine (**106**) and 4-ethylmorpholine SO₃ complex was also attempted affording the desired sodium benzyl sulfamate (**108**) in 55% isolated yield (See **Chapter 2, Scheme 39**). These results were compared to the same substrates using different sulfating reagents, including Pr₃N•SO₃ and TBSAB (**Table 8**). The overall results indicated that 4-methylmorpholine SO₃ and 4-ethylmorpholine SO₃ complexes were feasible for sulfation reactions despite the substantial drop in the final yield of both sodium benzyl sulfates and sulfamates. This was anticipated due to some factors, the polar nature of 4-methylmorpholine SO₃ and 4-ethylmorpholine SO₃ which resulted in poor solubility in organic solvent and therefore partial anion exchange with the sodium salt, NaI and NEH. Besides, the presence of methyl, ethyl and the installed SO₃ groups increases the steric bulk around the nitrogen atom, making it more difficult for 4-methylmorpholine and 4-ethylmorpholine SO₃ complexes to interact with nucleophiles and therefore minimising their reactivity compared to other sulfating reagents. The steric hindrance usually refers to the spatial interference caused by substituents around the reactive centre, which can affect the accessibility of the nitrogen atom to electrophiles or other reactants. For instance, in trimethylamine, the nitrogen atom is bonded to three methyl groups, which are relatively small compared to other alkyl groups like in triethylamine and tributylamine. Whereas, cyclic amines such as 4-methylmorpholine and 4-ethylmorpholine have the nitrogen embedded in a ring structure, which can cause

additional steric hindrance.^{105, 183} The steric effect is further increased by the presence of the alkyl substituents (methyl or ethyl group) on the ring making the nitrogen atom less accessible for reaction.

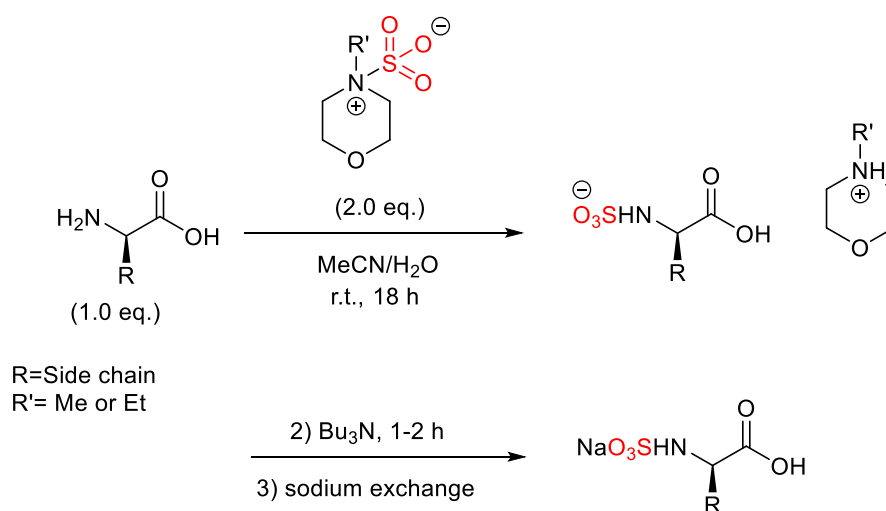
Table 8: The isolated percentage yield of sodium benzyl sulfate **1*** and sulfamate **2*** using different sulfating agents.

Entry	4-methylmorpholine SO ₃	4-ethylmorpholine SO ₃	Pr ₃ N•SO ₃	TBSAB
1* (105)	8%	56%	93%	95%
2* (108)	56%	55%	90%	98%

1*= Na benzyl sulfate (**105**), **2***= Na benzylsulfamate (**108**), % isolated yield.

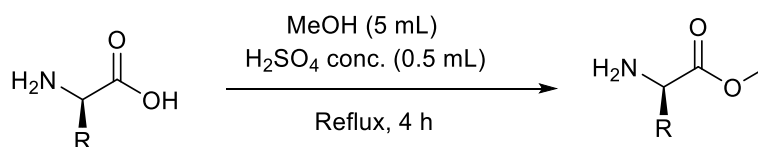
3.4.2. Sulfation of selected α -amino acid using *N*-substituted morpholine SO₃

Following on the success of the previous test reactions, the optimised sulfation conditions were applied to a selection of α -amino acids. The optimised conditions were inspired by the work of Benedetti and co-workers 'chemical methods for *N*- and *O*-sulfation of small molecules, amino acids and peptides'.⁴⁷ The *N*- and *O*-sulfation methodology was used as described with the exception of using a mixture of H₂O/MeCN solvent system, an extended reaction time, and the addition of tributylamine as a lipophilic partner (**Scheme 44**).



Scheme 44: The general sulfation reaction of selected α -amino acids using 4-methylmorpholine SO₃ and 4-ethylmorpholine SO₃ complexes.

Before starting this investigation, the selected α -amino acids were transformed to their corresponding methyl esters, including *L*-phenylalanine, *S*-benzyl-*L*-cysteine, and *O*-benzyl-*L*-serine. This step was required for carboxylic acid protection and the amino group becomes a nucleophilic site for the sulfation reaction. These selected amino acids were reacted with hydrophilic sulfating reagents, including 4-methylmorpholine SO₃ complex using a polar solvent system (H₂O/MeCN) due to the hydrophilic nature of these amino acids followed by a lipophilic counterion exchange using tributylamine. The latter addition improves the lipophilicity of an amino acid substrate facilitating its purification and isolation in organic solvents (**Scheme 45**).



Scheme 45: The general synthesis of α -amino acid methyl ester substrates.

3.4.3. Sulfation of selected α -amino acids using 4-methylmorpholine SO_3 complex

The *N*-sulfamation reaction using 4-methylmorpholine SO_3 complex was investigated on selected aliphatic α -amino acids, including glycine, ethyl glycine, alanine, and cysteine. The reaction conditions were adapted from the TBSAB *N*-sulfamation reactions of amino acids involving 4-methylmorpholine SO_3 complex (2.0 eq.), a mixture of MeCN/ H_2O solvent system, room temperature for 18 h, the addition of tributylamine as a lipophilic partner, followed by sodium exchange using NaI (**Scheme 44**).⁴⁷ Unfortunately, all attempts failed to form the desired amino acid sulfamates as 4-methylmorpholine SO_3 peaks were observed and peaks which corresponded to the starting α -amino acids analysed by ^1H NMR spectroscopy. This was attributed to the poor reactivity of α -amino acids and structural complexity of 4-methylmorpholine SO_3 (**See Chapter 2, Section 2.3.5.**) (**Figure 30**).

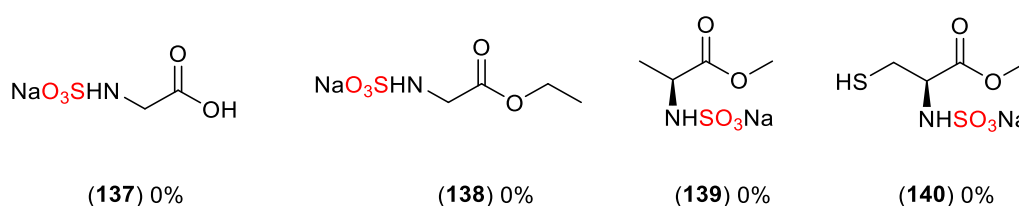
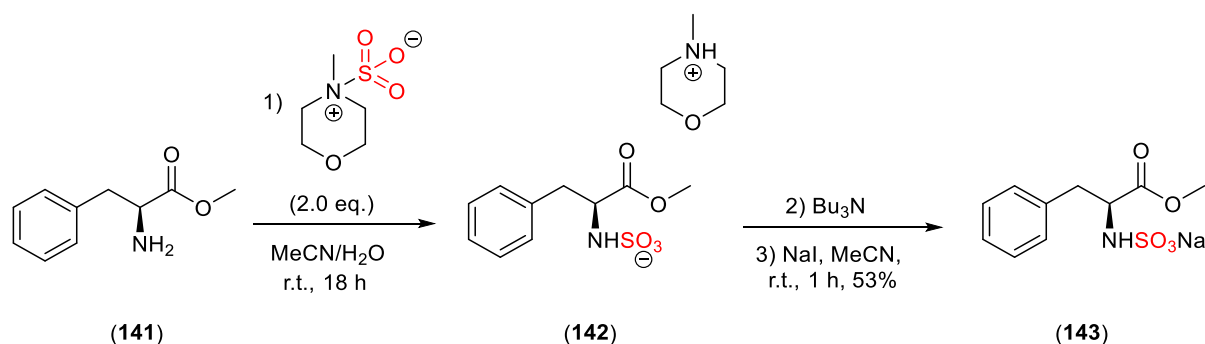


Figure 30: Failed *N*-sulfamation attempts on glycine, ethyl glycine, alanine, and cysteine.

Following the above *N*-sulfamation failed attempts, several aromatic amino acids including *L*-phenylalanine, *S*-benzyl-*L*-cysteine, and *O*-benzyl-*L*-serine were attempted adapting the optimised conditions for the TBSAB *O*-sulfation and *N*-sulfamation reactions of amino acids.⁴⁷ First, *L*-phenylalanine was transformed to its methyl ester form in 98% isolated yield following the general preparation of amino acid methyl esters (**Scheme 45**).

Next, the *N*-sulfamation reaction of *L*-phenylalanine methyl ester (**141**) was carried out using 4-methylmorpholine SO_3 complex (1.0 mmol) and dissolved in 50:50 mixture of MeCN/ H_2O . The presumed (not characterised) 4-methylmorpholinium sulfate intermediate (**142**) was

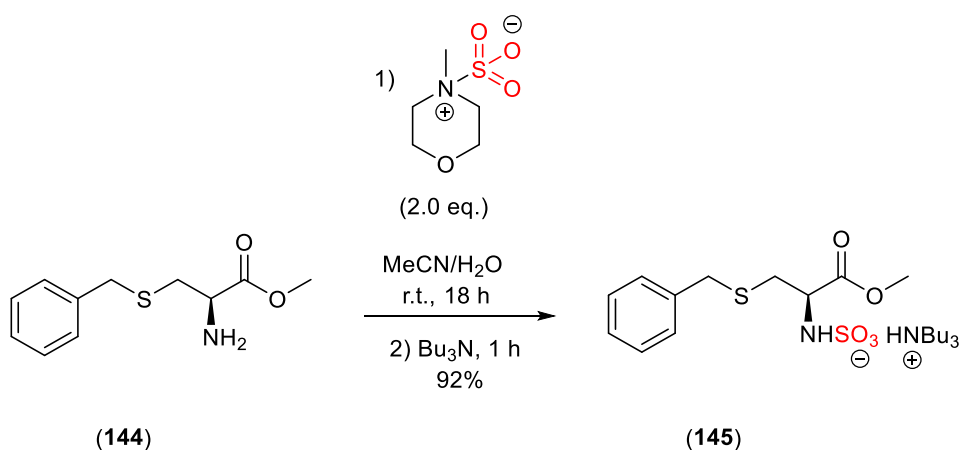
exchanged with tributylamine (Bu_3N) (1.0 mmol) and stirred for 1 h. This was followed by anionic exchange using NaI, affording sodium *L*-phenylalanine methyl ester sulfamate (**143**) in 53% isolated yield (**Scheme 46**).



Scheme 46: The *N*-sulfamation reaction *L*-phenylalanine methyl ester using 4-methylmorpholine SO_3 complex.

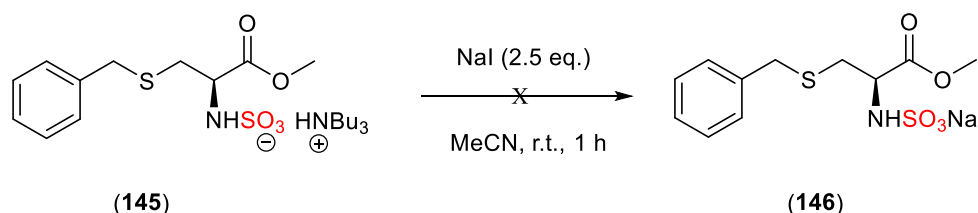
Next, the aromatic cysteine analogue, *S*-benzyl-*L*-cysteine was investigated for the *N*-sulfamation reaction. Although, the protected thiol group in *S*-benzyl-*L*-cysteine is a nucleophile suggesting that *S*-sulfurothiolation might occur over *N*-sulfamation. However, under these mild conditions, no *S*-sulfurothiolation was observed in (**145**), demonstrating the *N*-selectivity profile with 4-methylmorpholine SO_3 complex under these conditions.

S-Benzyl-*L*-cysteine was first transformed to its methyl ester (**144**) in 79% isolated yield. Next, the *N*-sulfamation reaction of *S*-benzyl-*L*-cysteine methyl ester (**144**) with 4-methylmorpholine SO_3 complex gave the corresponding intermediate salt (**145**) as its $[\text{Bu}_3\text{NH}]^+$ salt in 92% isolated yield (**Scheme 47**).



Scheme 47: The *N*-sulfamation of *S*-benzyl-*L*-cysteine methyl ester using 4-methylmorpholine SO₃ complex.

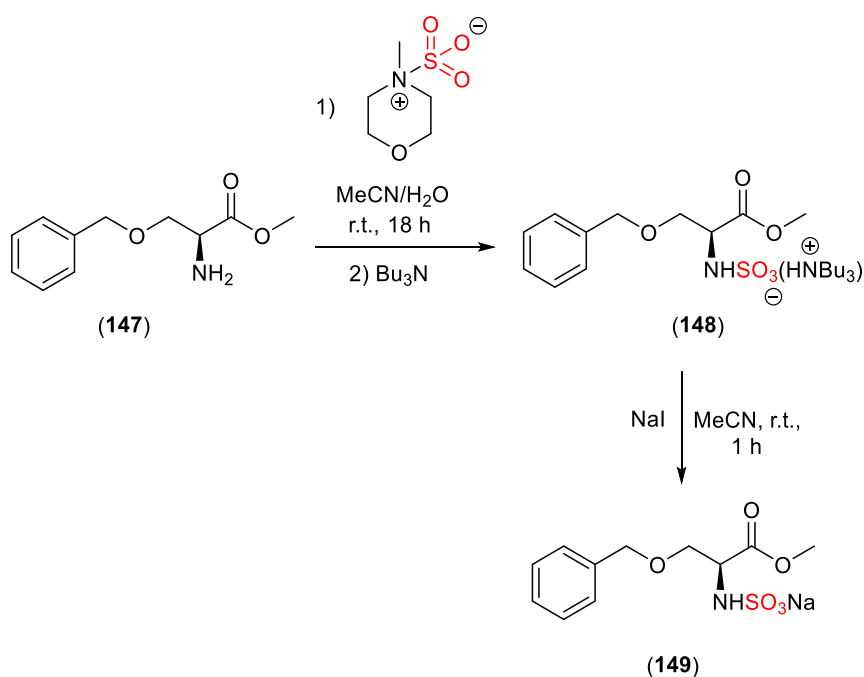
The tributylammonium intermediate (**145**) was subjected to cationic exchange using NaI to afford the desired *S*-benzyl-*L*-cysteine methyl ester sulfamate (**146**). However, this attempt was not successful as the corresponding intermediate (**145**) did not precipitate due to the poor Na exchange. Furthermore, the [Bu₃NH]⁺ peaks were also observed suggesting the [Bu₃NH]⁺ did not fully exchange with NaI as confirmed by ¹H NMR spectroscopy analysis (**Scheme 48**).



Scheme 48: The unsuccessful sodium salt (NaI) exchange of the intermediate (**145**) to form *S*-benzyl-*L*-cysteine methyl ester sulfamate (**146**).

The aromatic *L*-serine derivative, *O*-benzyl-*L*-serine was next considered for sulfation. The *O*-benzyl-*L*-serine was first transformed into its methyl ester analogue in 86% isolated yield. Next, the *N*-sulfamation reaction of *O*-benzyl-*L*-serine methyl ester (**147**) with 4-methylmorpholine SO₃ complex gave the corresponding tributylammonium sulfate intermediate (**148**) in 89% isolated yield. This was followed by sodium salt exchange (NaI)

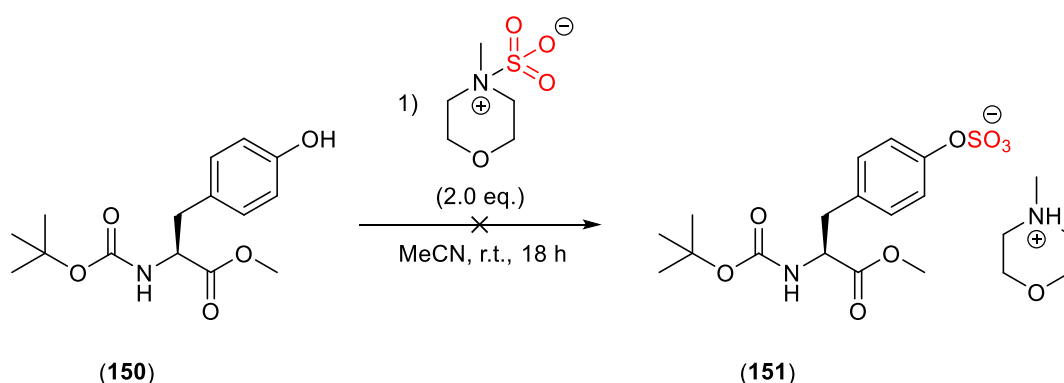
resulting in the formation of sodium *O*-benzyl-*L*-serine methyl ester sulfamate (**149**) in 81% isolated yield. Unlike the *S*-benzyl-*L*-cysteine methyl ester (**144**), *O*-benzyl-*L*-serine methyl ester (**147**) was afforded as the corresponding Na salt. The aromatic *L*-serine derivative (**149**) was afforded as the corresponding Na salt in 81% isolated yield (**Scheme 49**).



Scheme 49: The *N*-sulfamation reaction of *O*-benzyl-*L*-serine methyl ester (**147**) using 4-methylmorpholine SO₃ complex.

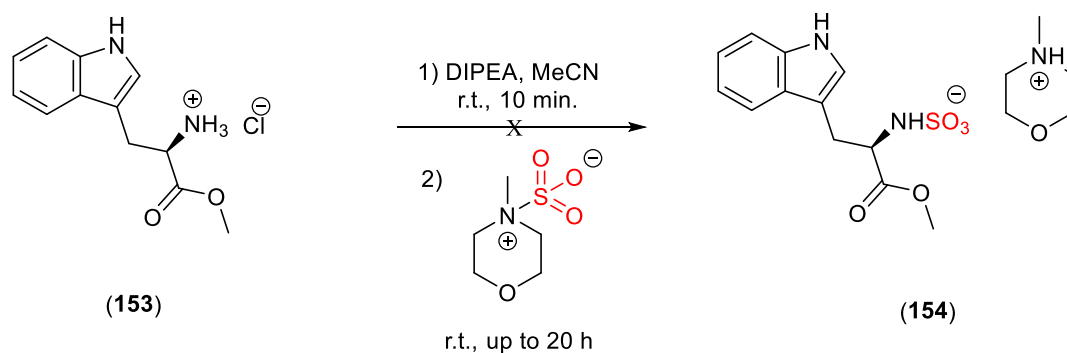
Boc-*L*-Tyrosine methyl ester (Boc-Tyr-OMe) was also explored for the *O*-sulfation reaction. Considering the lipophilic nature of Boc-Tyr-OMe (cLogP= 2.13), MeCN was used as a single solvent for this reaction. The reaction of Boc-*L*-tyrosine methyl ester (**150**) and 4-methylmorpholine SO₃ complex was carried out in 1:2 stoichiometric ratio and stirred for 18 h at room temperature. The corresponding intermediate (**151**) was not observed by ¹H NMR spectroscopy analysis. We hypothesise that this was due to the poor reactivity of the phenolic hydroxyl group compared to the amino group. The phenolic hydroxyl group is less nucleophilic than amino group affecting their reactivity in the sulfation reaction. This was attributed to the lone pair on the oxygen atom being more delocalized into the aromatic ring. This

delocalization reduces the electron density on the oxygen, making phenols less nucleophilic toward 4-methylmorpholine SO₃ complex (**Scheme 50**).



Scheme 50: Attempted sulfation reaction of Boc-Tyr-OMe (**150**) using 4-methylmorpholine SO₃ complex.

The *N*-sulfamation reaction of *L*-tryptophan methyl ester hydrochloride was also investigated. First, the addition of *N,N*-diisopropylethylamine (DIPEA) (0.5 mL, 3.0 eq.) was needed to deprotonate *L*-tryptophan methyl ester hydrochloride (**153**). This was followed by the addition of 4-methylmorpholine SO₃ complex and the reaction mixture was dissolved in MeCN and left to stir for 20 h. The crude intermediate (**154**) was washed multiple times with CH₂Cl₂ to remove DIPEA·HCl from the crude compound. However, this attempt failed as confirmed by ¹H NMR spectroscopy analysis indicating on the presence of DIPEA·HCl in the crude intermediate. Furthermore, another attempt was made to purify the crude intermediate using liquid-liquid extraction with a mixture of CH₂Cl₂/H₂O but unfortunately, this attempt was also not successful as DIPEA·HCl was still present in the crude compound as confirmed by ¹H NMR spectroscopy analysis (**Scheme 51**).

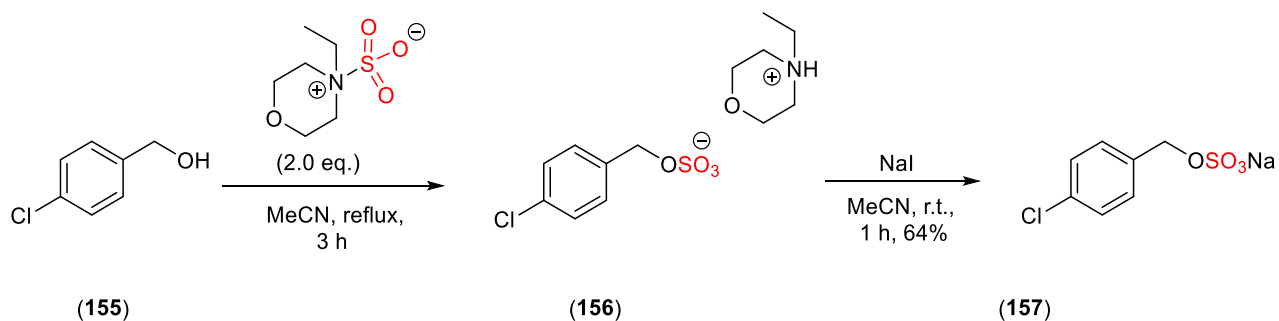


Scheme 51: Attempted *N*-sulfamation reaction of *L*-tryptophan methyl ester hydrochloride (**153**) using 4-methylmorpholine SO₃ complex.

3.4.4. Sulfation of selected α -amino acid using 4-ethylmorpholine SO₃ complex

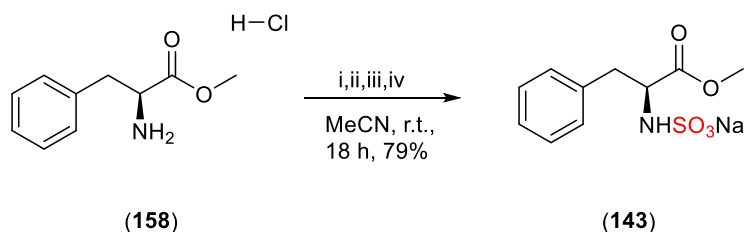
The use of 4-ethylmorpholine SO₃ complex was considered for *N*-sulfamation and *O*-sulfation of selected amino acids. This reagent is slightly less hydrophilic (cLogP= 0.38) than 4-methylmorpholine SO₃ complex (cLogP= -0.13) (these predicted cLogP values were obtained from ChemDraw 19.1). Furthermore, 4-ethylmorpholine SO₃ complex is bulkier due to the ethyl groups which increase its pK_aH value, making the nitrogen more basic, resulting in the complex being less reactive compared to 4-methylmorpholine SO₃ complex (see **Chapter 2, Table 7**).

In addition to the successful *N*-sulfamation and *O*-sulfation reaction tests, the electron-withdrawing (Cl) group in 4-chlorobenzyl alcohol was attempted following the optimised conditions for the TBSAB *O*-sulfation reaction affording the desired Na⁺ salt in 64% isolated yield (**Scheme 52**).



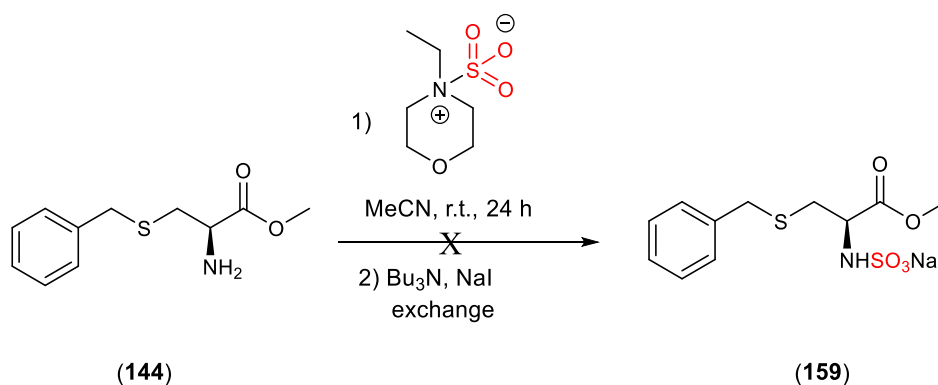
Scheme 52: The *O*-sulfation reaction of 4-chlorobenzyl alcohol (**155**) with 4-ethylmorpholine SO_3 complex.

The *N*-sulfamation reaction of *L*-phenylalanine methyl ester hydrochloride (**158**) and 4-ethylmorpholine SO_3 complex was attempted. The corresponding tributylammonium intermediate was purified by liquid-liquid extraction with $\text{CH}_2\text{Cl}_2/\text{H}_2\text{O}$ solvent system and subsequently exchanged with NaI to afford the desired *L*-phenylalanine methyl ester sulfamate (**143**) in 79% isolated yield compared to 53% with 4-methylmorpholine SO_3 complex. This was attributed to the nature of both 4-methylmorpholine and 4-ethylmorpholine SO_3 complexes which affect the solubility and partitioning of their intermediates during the liquid-liquid extraction step. 4-Ethylmorpholine- SO_3 complex has greater compatibility with $\text{CH}_2\text{Cl}_2/\text{H}_2\text{O}$ solvent system ($c\text{LogP} = 0.38$ vs -0.13 for the 4-methylmorpholine SO_3), resulting in more efficient extraction of the desired product (**143**) and higher isolated yield (**Scheme 53**).



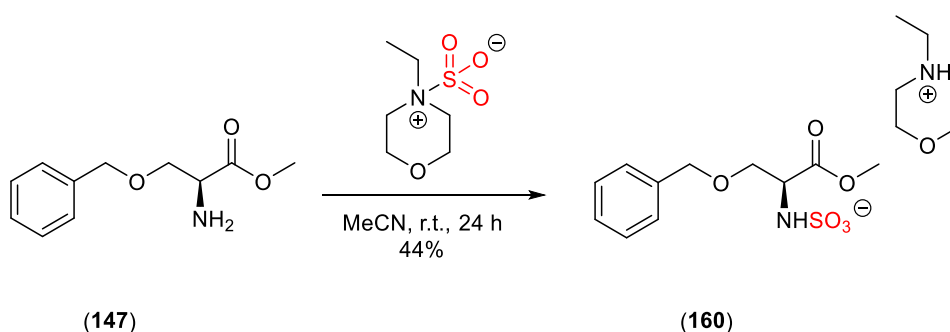
Scheme 53: The *N*-sulfamation reaction of *L*-phenylalanine methyl ester hydrochloride using 4-ethylmorpholine SO_3 complex. **Conditions:** (i) DIPEA (0.5 mL, 3.0 eq.), MeCN, r.t., 10 min; (ii) 4-ethylmorpholine SO_3 (2.0 eq.), r.t., 18 h; (iii) Bu_3N , r.t., 1 h; and (iv) NaI exchange, MeCN, r.t., 1 h, 79% yield.

The *N*-sulfamation of *S*-benzyl-*L*-cysteine methyl ester (**144**) and 4-ethylmorpholine SO_3 complex was carried out following the optimised adapted methodology to successfully afford the desired *S*-benzyl-*L*-cysteine methyl ester sulfamate (**159**). Unfortunately, this attempt failed as the 4-ethylmorpholinium sulfate intermediate (**159**) did not exchange with NaI indicating that this reaction did not occur (**Scheme 54**).



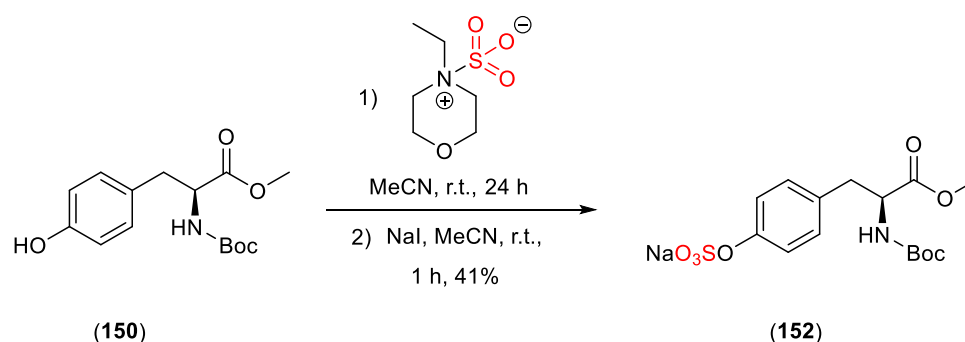
Scheme 54: unsuccessful *N*-sulfamation reaction of *S*-benzyl-*L*-cysteine methyl ester (**144**) using 4-ethylmorpholine SO_3 complex.

The *N*-sulfamation reaction of the protected *L*-serine analogue, *O*-benzyl-*L*-serine methyl ester was investigated using 4-ethylmorpholine SO_3 complex. 4-Ethylmorpholinium sulfate intermediate (**160**) was purified by column chromatography affording the desired molecule (**160**) in 44% isolated yield (**Scheme 55**).



Scheme 55: The *N*-sulfamation reaction of *O*-benzyl-*L*-serine methyl ester using 4-ethylmorpholine SO_3 complex.

The *O*-sulfation reaction of the protected Boc-*L*-tyrosine methyl ester (Boc-Tyr-OMe) was also explored. This reaction was carried out by reacting Boc-Tyr-OMe (**150**) and 4-ethylmorpholine SO₃ complex. The corresponding intermediate was exchanged with NaI to afford the pure sodium salt *O*-sulfate (**152**) in 41% isolated yield (**Scheme 56**).



Scheme 56: The *O*-sulfation reaction of Boc-Tyr-OMe (**150**) with 4-ethylmorpholine SO₃ complex.

Overall, the use of these novel hydrophilic sulfating reagents was well suited for *N*-sulfamation and *O*-sulfation of some selected amino acids. The optimised methodology was appropriate mainly for the protected aromatic amino acids using mild reaction conditions compared to other sulfating reagents that require harsh conditions such as with ClSO₃H and H₂SO₄ protocol or caused pyridine contamination using Py·SO₃ complex. The results of the isolated yields for the selected amino acids sulfates or sulfamates were compared using 4-methylmorpholine SO₃ and 4-ethylmorpholine SO₃ complexes. *L*-Phenylalanine methyl ester sulfamate was afforded in 53% yield using 4-methylmorpholine SO₃ whereas using 4-ethylmorpholine SO₃, afforded the sulfamate product in 79% isolated yield. The *O*-Benzyl-*L*-serine methyl ester sulfamate was isolated in 81% yield using 4-methylmorpholine SO₃ and in 44% isolated yield using 4-ethylmorpholine SO₃. The *S*-benzyl-*L*-cysteine methyl ester [Bu₃NH]⁺ salt was afforded in 92% yield using 4-methylmorpholine SO₃ while with the use of 4-ethylmorpholine SO₃, the reaction was not successful. Finally, the Boc-tyrosine methyl ester

sulfate was not afforded using 4-methylmorpholine SO₃ whereas using 4-ethylmorpholine SO₃ complex, Boc-tyrosine methyl ester sulfate was afforded in 41% isolated yield. In some cases, the higher yield with 4-ethylmorpholine SO₃ complex was attributed to several factors, including better accessibility of 4-ethylmorpholine SO₃ due to the presence of the more flexible ethyl group and better compatibility in the organic solvent. The ethyl group in 4-ethylmorpholine SO₃ complex is bulkier and more flexible than the methyl group in 4-methylmorpholine SO₃ which might allow better access to the nitrogen atom for the *N*-sulfamation reaction compared to the more rigid methyl group in 4-methylmorpholine SO₃ complex. The nature of 4-ethylmorpholine SO₃ is less hydrophilic than 4-methylmorpholine SO₃ resulting in efficient solubility and extraction of the desired sulfate or sulfamate. Finally, some of these sulfated compounds were made using only TBSAB as a source of sulfation, including *L*-phenylalanine methyl ester and *S*-benzyl-*L*-cysteine methyl ester and the results were compared to the ones using hydrophilic sulfating reagents, 4-methylmorpholine SO₃ and 4-ethylmorpholine SO₃. *L*-Phenylalanine methyl ester sulfamate was afforded in 60% yield using TBSAB, whereas with 4-ethylmorpholine SO₃ gave 79%. *S*-Benzyl-*L*-cysteine methyl ester sulfamate was afforded in 98% isolated yield, while with 4-methylmorpholine SO₃ gave 92% yield. Overall, the application of these novel hydrophilic sulfating reagents proved to be highly effective for both *N*-sulfamation and *O*-sulfation of selected amino acids. The optimized methodology demonstrated particular efficacy for protected aromatic amino acids, operating under mild reaction conditions, which enhanced its suitability for such substrates.

3.5. Conclusion and future work

In summary, the *N*- and *O*-sulfation of selected amino acids using the novel hydrophilic sulfating reagents; 4-methylmorpholine SO₃ and 4-ethylmorpholine SO₃ complexes was explored. The addition of tributylamine was critical to improve the lipophilicity of the

corresponding intermediates and therefore dissolve better in organic solvents such as MeCN and EtOH. Despite some failures and difficulties encountered through this investigation, number of α -amino acids were sulfated and afforded either as pure sodium salt or intermediate $[\text{HNBu}_3]^+$ cations in modest to good isolated yields. Furthermore, the reaction conditions were suited for the sulfation of selected protected aromatic α -amino acids, including *L*-phenylalanine methyl ester, *S*-benzyl-*L*-cysteine methyl ester, *O*-benzyl-*L*-serine methyl ester, and Boc-*L*-tyrosine methyl ester affording the corresponding intermediates cations or sodium salts in a modest to good isolated yield.

For the future work:

- Further X-ray crystallography experiments and analysis should be considered for both 4-methylmorpholine SO_3 and 4-ethylmorpholine SO_3 complexes to provide the full data for both molecular structures whether these sulfating reagents are betaines or SO_3 complexes.
- Additional optimisation studies should be also considered, including extending the reaction time and considering reversed-phase column chromatography for purifying the crude mixture especially with more hydrophilic aliphatic amino acids, including *L*-serine, *L*-cysteine, and *L*-threonine and applying the reaction conditions to a wide range of small molecules e.g. peptides.

Chapter 4. A novel exchange method to access sulfated molecules

Background

4.1. Organosulfates and sulfamates

It was reported that the sulfation of alcoholic, phenolic, and amine-containing substrates can be achieved using the Lewis adducts of sulfur trioxide (SO_3) with trimethylamine (Me_3N), triethylamine (Et_3N), dimethylformamide (DMF), pyridine (Py), and 1,4-dioxane.^{149, 184-186} These commercially available reagents react with alcoholic, phenolic, and amine-containing substrates to give their corresponding organosulfates or sulfamates compounds (**Figure 31**).

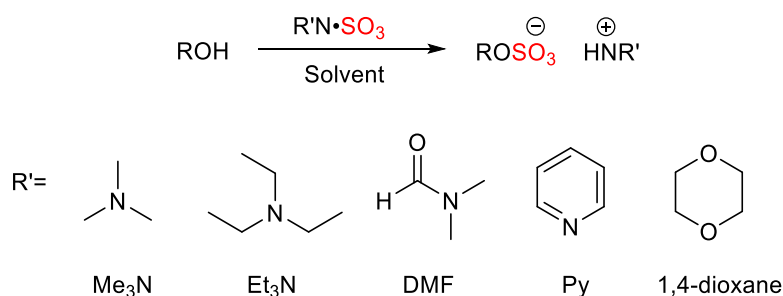


Figure 31: The sulfation of alcoholic, phenolic, and amine-containing substrates using the Lewis base adducts of SO_3 . R' = Me₃N, Et₃N, DMF, Py, and 1,4-dioxane.

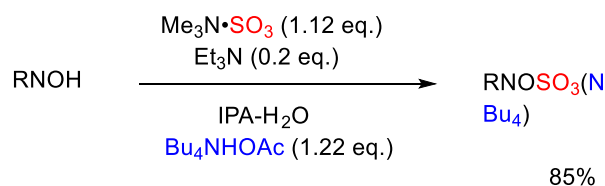
More recently, several methods were reported to access *O*-sulfated and *N*-sulfamated molecules including the cation exchange protocol and all-in-one-type reagents.^{47, 50, 80, 149, 158,}

187

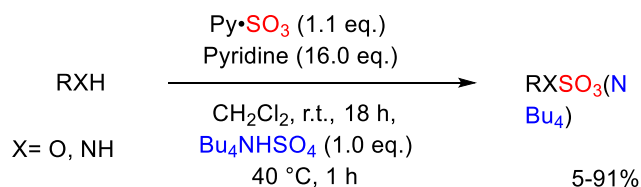
4.2. Sulfation using a lipophilic cation exchange strategy

This strategy demonstrated that increasing the alkyl chain length of the corresponding ammonium cation improves the lipophilicity of organosulfates and therefore facilitates their extraction into non-polar organic solvents.^{50, 80} Additionally, the resulting organosulfates can be exchanged to their corresponding sodium salts without the need for ion exchange columns (**Scheme 57**).¹⁸⁷

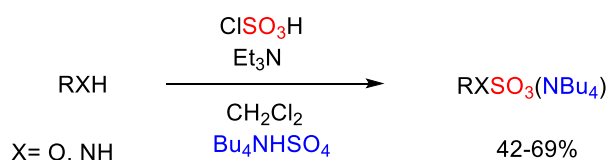
Ball (2016)



Montero Bastidas (2019)



Mihai (2019)

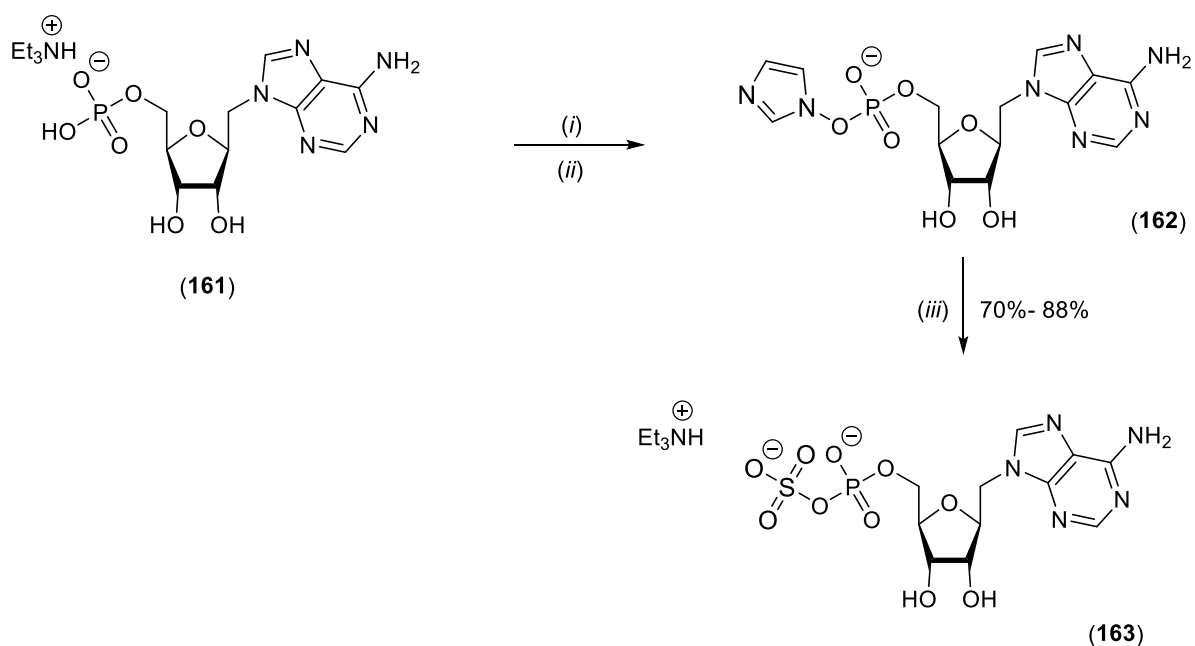


Scheme 57: Examples of lipophilic cation-exchange strategy used in sulfation reactions.

4.3. Sulfation using an all-in-one type reagent

Another sulfation strategy used an all-in-one type reagent which combines a sulfating reagent with a lipophilic counterion such as tributylsulfoammonium betaine, TBSAB.^{47, 149} Gill, Benedetti and co-workers reported the use of TBSAB as an all-in-one reagent for the sulfation of a range of benzyl alcohols, benzylamines, amino acids, and carbohydrates (**See Chapter 1, Scheme 14**).^{47, 149, 158}

Kowalska and co-workers have used bis(tributylammonium) sulfate $\text{SO}_4(\text{Bu}_3\text{NH})_2$ as an all-in-one reagent for the preparation of 2',3'-cyclic 3'-phosphoadenosine 5'-phosphosulfate (2',3'-cPAPS) (**Scheme 58**).⁵³



Scheme 58: General synthesis of adenosine phosphosulfates using an all-in-one-reagent, $\text{SO}_4(\text{Bu}_3\text{NH})_2$.

Conditions: (i) imidazole, 2,2'-dithiodipyridine, PPh_3 , (ii) NaClO_4 , acetone (iii) and $\text{SO}_4(\text{Bu}_3\text{NH})_2$, MgCl_2 , DMF, r.t., 0.5 h, DEAE-Sephadex using triethylammonium bicarbonate (TEAB).⁵³

Despite the effectiveness and success of these approaches, there remain issues including multi-step reaction synthesis and additional purification cascades. As a result, there is a need to develop an alternative, low-cost technology for the sulfation of small compounds that does not require additional purification techniques.

4.4. Results and Discussion

Elements of this chapter have been published in Scientific Reports as: Alshehri, J.A., Benedetti, A.M. & Jones, A.M. A novel exchange method to access sulfated molecules. *Sci Rep* 10, 16559 (2020). <https://doi.org/10.1038/s41598-020-72500-x>.⁴⁶

This study proposed for the first time the development of a novel sulfation method using low-cost and commercially available sulfating reagents ($\text{SO}_3\text{-R}$, R = Py or Me_3N) ($\text{Me}_3\text{N}\cdot\text{SO}_3$, £0.66/mmol, $\text{Et}_3\text{N}\cdot\text{SO}_3$, £1.49/mmol, TBSAB, £82.27/mmol, $\text{DMF}\cdot\text{SO}_3$, £1.83/mmol, and $\text{Py}\cdot\text{SO}_3$, £0.24/mmol, prices per mmol. The prices were taken from Sigma Aldrich on

17/10/2024. Furthermore, tributylamine (Bu_3N) was added as the lipophilic partner to increase the lipophilicity of the resulting intermediates and therefore facilitate their solubility in organic solvents. This idea was also inspired by the preparation of an all-in-one sulfating reagent, $\text{Bu}_3\text{N}\cdot\text{SO}_3$ (TBSAB).^{47, 149} Herein, this novel sulfation strategy was applied to a wide range of alcohol and amine scaffolds by applying the commercially available sulfating reagents ($\text{SO}_3\text{-R}$, $\text{R}=\text{Py}$, or Me_3N). Adding tributylamine was critical to examining whether TBSAB can be prepared from commercial sulfating reagents such as $\text{Py}\cdot\text{SO}_3$ or $\text{Me}_3\text{N}\cdot\text{SO}_3$ and subsequent ion exchange with tributylamine. A control experiment was conducted by Anna Benedetti aimed to determine whether tributylsulfoammonium betaine (TBSAB) could be prepared *in situ* from commercially available sulfating reagents such as $\text{Me}_3\text{N}\cdot\text{SO}_3$ complex via cation exchange with Bu_3N . The control experiment specifically involved the reaction between Bu_3N and $\text{Me}_3\text{N}\cdot\text{SO}_3$ complex in the presence of MeCN, and the results were analysed using ^1H NMR spectroscopy. This experiment revealed the absence of TBSAB signals as the expected chemical shifts corresponding to TBSAB were not observed in the ^1H NMR spectrum indicating that no exchange between Me_3N and Bu_3N had occurred suggesting that TBSAB cannot be formed *in situ* (**Figure 32**).

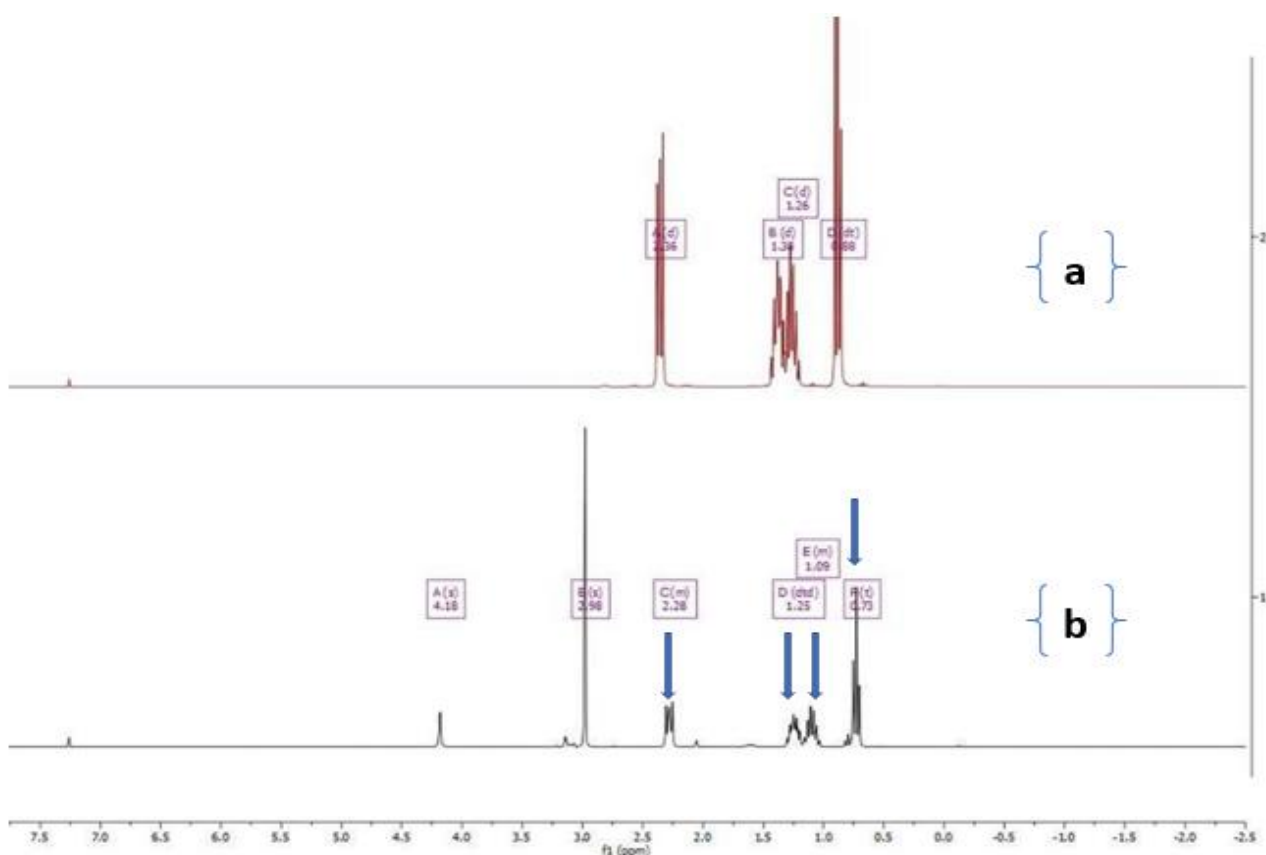


Figure 32: TBSAB control experiment (300 MHz, CDCl_3). (a) ^1H NMR spectrum of Bu_3N . (b) ^1H NMR spectrum of the reaction mixture of $\text{Me}_3\text{N}\cdot\text{SO}_3$ and Bu_3N in MeCN after 30 min. Arrows show the presence of Bu_3N peaks in the mixture.

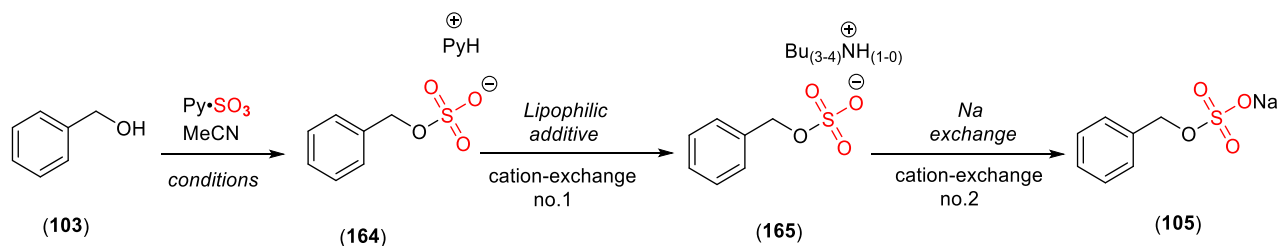
Alternatively, tributylamine could be used to exchange the polar ammonium sulfation product $[\text{PyH}]^+ / [\text{Me}_3\text{NH}]^+$ to a lipophilic tributylammonium cation $[\text{Bu}_3\text{NH}]^+$. To validate this hypothesis, benzyl alcohol was selected due to the down-field shift (+0.49 ppm) of the benzylic protons' signal after sulfation as measured by ^1H NMR spectroscopy (300 MHz, CDCl_3). The chosen solvent was acetonitrile (MeCN) due to its lower boiling point (82 °C) which makes it possible to be removed under reduced pressure compared to the other polar aprotic solvents such as DMF (b.p. 153 °C). The resulting intermediate organosulfate/sulfamate $[\text{PyH}]^+ / [\text{Me}_3\text{NH}]^+$ would be subjected to lipophilic ion-exchange by the addition of Bu_3N and

the lipophilic tributylammonium intermediates subjected to sodium ion-exchange using NEH or NaI following the adapted procedure.¹⁴⁹

4.4.1. Optimisation and control studies

Initially, the sulfation reaction of benzyl alcohol with pyridine sulfur trioxide complex was investigated using different stoichiometric ratios and temperatures (**Table 9**). It was found that increasing the number of equivalents of pyridine sulfur trioxide complex gave a superior conversion to the benzyl sulfate ester pyridinium salt (**164**) (**Table 9, Entries 1-4**). 2.0 equivalents of Py•SO₃ complex gave 85% conversion as measured by ¹H NMR spectroscopy (**Table 9, Entry 4**). Increasing the reaction temperature to 90 °C (heating under reflux), resulted in a greater conversion in 3 h (**Table 9, Entry 5**). Using these optimised conversion conditions (**Table 9, Entry 5**), a wide range of lipophilic cation exchanging additives were studied to compare the tetrabutylammonium salts against tributylamine. This was followed by a sodium salt exchange using sodium 2-ethylhexanoate (NEH) (**Table 9, Entries 6–10**). It was found that tributylamine afforded the greatest isolated yield (**Table 9, Entry 7**) compared to a range of tetrabutylammonium salts of iodide, acetate or bromide. Moreover, NaI was also used in a combination with tributylamine or other tetrabutylammonium salts (**Table 9, Entries 11-15**). The overall results of using different sodium salts were relatively similar with the exception of (**Table 9, Entry 7**), which gave the desired sodium salt sulfate (**105**) in 93% isolated yield. Whereas in **Table 9 (Entry 12)**, sodium benzyl sulfate (**105**) was afforded in 79% isolated yield using NaI instead of NEH. This was attributed to the solubility variations of both organosulfate intermediates and the sodium source in organic solvents.

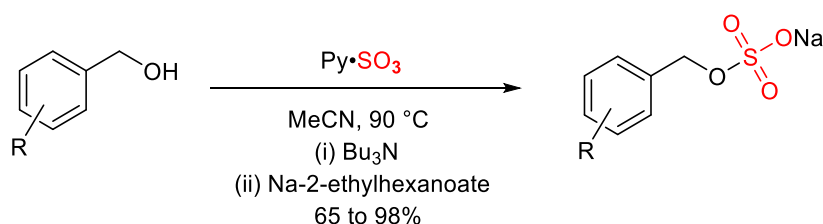
Table 9: Optimisation and control studies of benzyl alcohol sulfation–lipophilic exchange–sodium exchange, was converted to the pyridinium salt (**164**); benzyl sulfate was isolated as sodium salt (**105**) and analysed by ^1H NMR spectroscopy, mass spectrometry, and melting point to be in accordance with the literature.¹⁰⁵



Entry	Py·SO ₃ (eq.)	T (°C)	t (h)	Lipophilic additive	Eq.	Sodium exchange	Eq.	Conversion to 164 (%)	Conversion to 105 (%)
1	1	70	7.0	-	-	-	-	33	-
2	1.2	70	7.0	-	-	-	-	61	-
3	1.5	70	7.0	-	-	-	-	66	-
4	2	70	7.0	-	-	-	-	85	-
5	2	90	3.0	-	-	-	-	99	-
6	2	90	3.0	Bu ₃ N	2.0	NEH	2.5	-	57
7	2	90	3.0	Bu ₃ N	2.0	NEH	5.0	-	93
8	2	90	3.0	Bu ₄ NI	2.0	NEH	5.0	-	73
9	2	90	3.0	Bu ₄ NOAc	2.0	NEH	5.0	-	87
10	2	90	3.0	Bu ₄ NBr	2.0	NEH	5.0	-	52
11	2	90	3.0	Bu ₃ N	2.0	NaI	2.5	-	66
12	2	90	3.0	Bu ₃ N	2.0	NaI	5.0	-	79
13	2	90	3.0	Bu ₄ NI	2.0	NaI	5.0	-	83
14	2	90	3.0	Bu ₄ NOAc	2.0	NaI	5.0	-	80
15	2	90	3.0	Bu ₄ NBr	2.0	NaI	5.0	-	82

4.4.2. An analysis of steric and electronic parameters of the sulfation substrate

The optimised conditions were applied to a wide range of substituted benzyl alcohols exploring different steric and electronic effects using $\text{Py}\cdot\text{SO}_3$ complex as the sulfating agent. Having the optimised conditions in hand, the generality of this one-pot, three-step procedure was explored (**Scheme 59**).



Scheme 59: The optimised sulfation conditions for benzyl alcohol and its derivatives using $\text{Py}\cdot\text{SO}_3$ in combination with the lipophilic counterion (Bu_3N) and sodium exchange method.

4.4.3. Sulfation of benzyl alcohols using $\text{Py}\cdot\text{SO}_3$ complex

This novel method was tolerant to a wide range of substituted benzyl alcohols with isolated yields ranging from 65 to 98% (**Figure 33**). In the comparison with the previous results, using an all-in-one TBSAB methodology¹⁴⁹, the resulting isolated yields using this novel strategy were acceptable but generally lower. For instance, sodium benzyl sulfate (**105**) was afforded in 93% isolated yield following the novel exchange strategy while the TBSAB method gave a 95% isolated yield (**105**) (**Figure 33**).

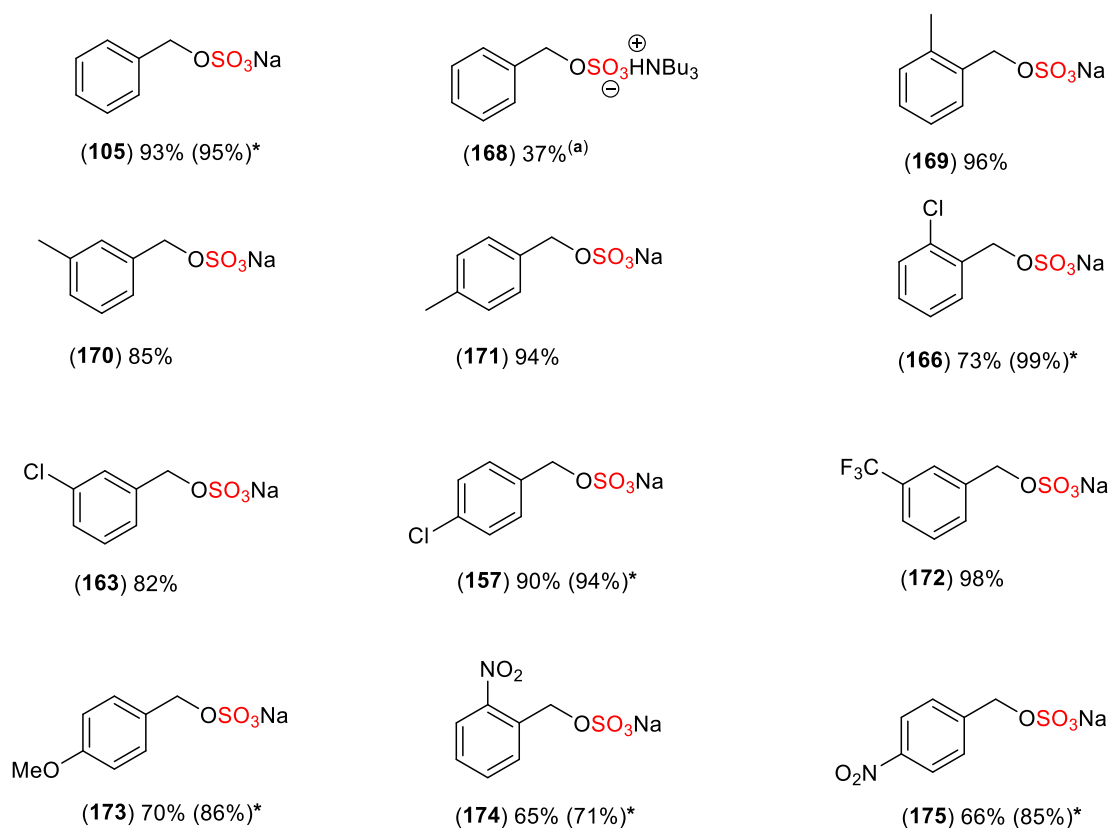


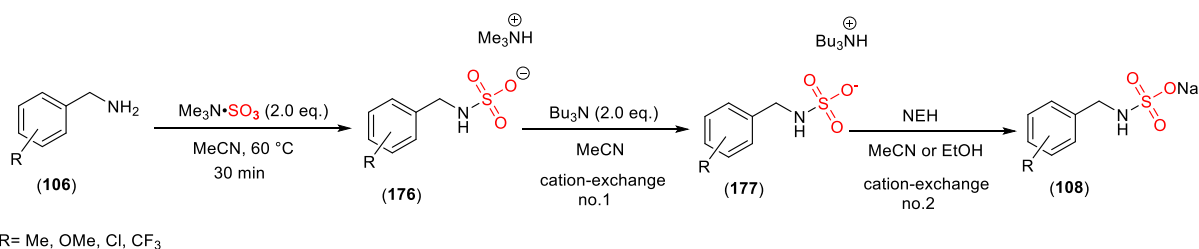
Figure 33: Scope of the three-step, one-pot method with benzyl alcohols. ^(a) use of $\text{Me}_3\text{N}\cdot\text{SO}_3$ instead of $\text{Py}\cdot\text{SO}_3$.
 * The isolated yield using TBSAB methodology for comparison.¹⁴⁹

The differences in isolated yields were observed due to various factors, including the steric and electronic effects of the substituents and unsuccessful ion-exchange. For instance, the analogues incorporating electron-withdrawing chloro substituents (**157**, **163**, and **166**), have different isolated yields due to the steric and electronic effects of the chlorine substituents. It was expected that sodium 2-chlorobenzyl sulfate (**166**) would have a lower isolated yield (73%) compared to the other meta- or para- chlorine positions (**163**, 82% and **157**, 90%). This was due to the ortho-position of chlorine in (**166**) that generates steric hindrance to the hydroxyl group, making the molecular structure more crowded and therefore affects the reaction and lowers the reactivity of the OH group which were presumably responsible for the lower yield. Furthermore, sodium 4-methoxybenzyl sulfate (**173**), containing a π -donating methoxy group which was afforded in a modest isolated yield (70%). Attempts were made to

sulfate the alcohol group in the 2 and 3 positions of methoxybenzyl alcohol. However, sodium 2-methoxybenzyl sulfate was not afforded under the *in situ* ion-exchange conditions. Furthermore, another attempt was made using an alternative sodium salt (NaI) but was also unsuccessful. Notably, the tributylammonium benzyl sulfate (**168**) was afforded in a low isolated yield using Me₃N•SO₃ complex. This was attributed to the Lewis basicity of the amine-SO₃ complex, Py•SO₃ (pK_a = 5.23); Me₃N•SO₃ (pK_a = 10.63). The sp³ hybridised Lewis base of Me₃N donates electrons more strongly into the LUMO of SO₃ forming a hard-hard Lewis adduct with increased stability and decreased reactivity compared to sp² hybridised Lewis base seen in Py•SO₃.¹⁸⁸ Furthermore, the electron-withdrawing nitro analogues (**174** and **175**) showed no substantial variations in isolated yields, with values of 65% and 66%, respectively.

4.4.4. Sulfation of benzylamines using Me₃N•SO₃

The optimised conditions for the preparation of sulfate esters and the previous work on sulfamates⁴⁷ were further explored to identify suitable conditions for benzylamine sulfamation. The optimised conditions were similar to the previous work (*O*-sulfation using Py•SO₃) with the exception of using Me₃N•SO₃ complex and a lower reaction temperature. This was due to the increased nucleophilicity of the sp³ nitrogen atom of Me₃N•SO₃ complex, resulted in a quantitative conversion for both the formation of the sulfamate trimethylammonium (**176**) species and the cation exchanged sulfamate tributylammonium (**177**) species. This was followed by ion exchange with NEH (1.5 eq.) affording the desired pure Na⁺ sulfamate in good to excellent isolated yields (76%-99%) (**Scheme 60**).



Scheme 60: The optimised conditions for the benzylamine sulfamation and its derivatives using Me₃N•SO₃ in combination with the lipophilic partner (Bu₃N) and sodium exchange method.

Benzylamine was selected due to the down-field shift (+0.34 ppm) of the benzylic protons' signal (post-sulfation) as measured by ¹H NMR spectroscopy (CDCl₃). The optimised *N*-sulfamation conditions were explored on a range of substituted benzylamines. In all examples, good to excellent isolated yields were observed (76%-99%) in this three-step procedure and with the presence of different functional groups (EDG and EWG). The results of this investigation were compared to the previous methodology using TBSAB, the following observations were identified: **108** (99% vs 98%*), **180** (90% vs 97%*), **181** (98% vs 61%*), **182** (93% vs 87%*), **183** (99% vs 85%*), and **184** (76% vs 65%*). In the majority of cases, the isolated yields for this new route were equivalent or improved for the benzylamines compared to the TBSAB methodology (**Figure 34**).

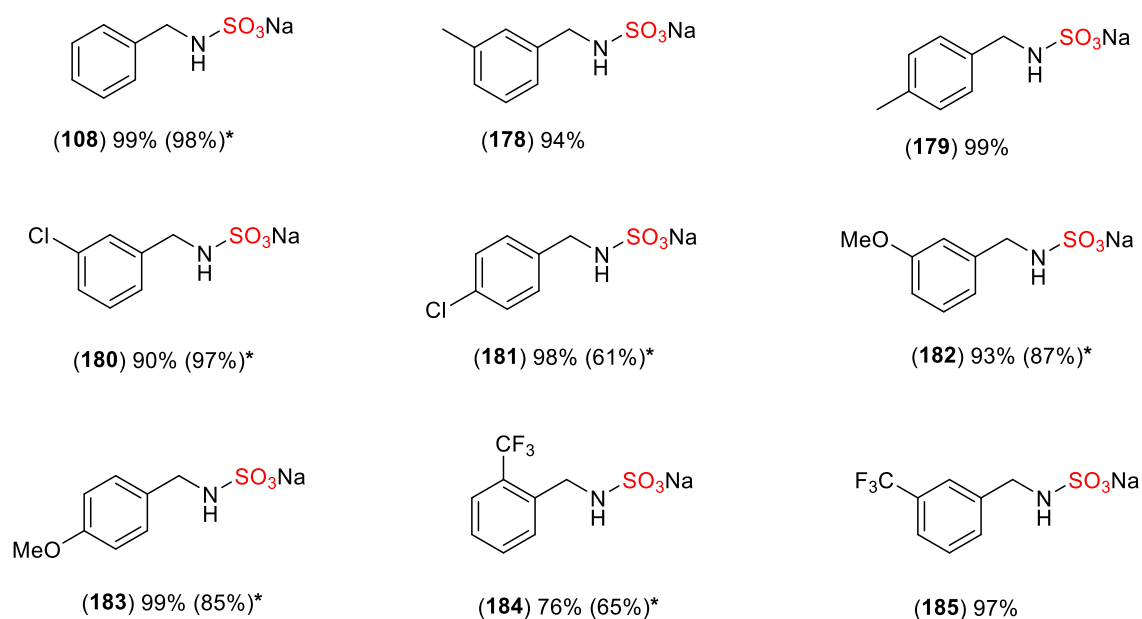
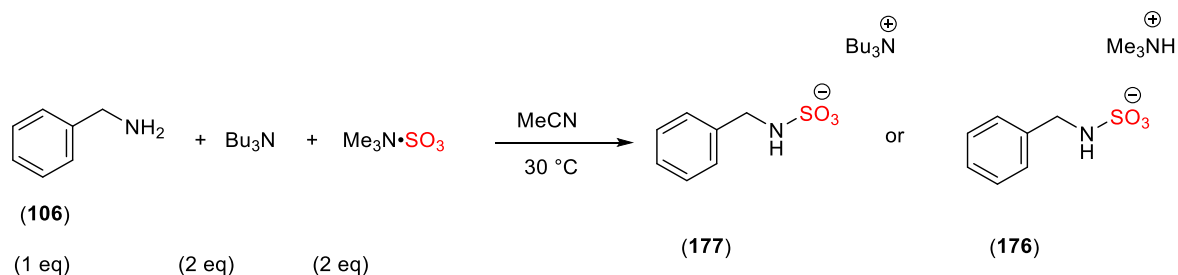


Figure 34: Scope of the three-step, one-pot method with benzylamine using $\text{Me}_3\text{N}\cdot\text{SO}_3$. * Isolated yields using TBSAB methodology for comparison.⁴⁷

Despite the success of this novel three-step methodology, the higher reaction temperature (60 °C) is not compatible with temperature-sensitive molecules e.g. α -amino acid. To examine this, a lower reaction temperature variant of the new method was considered. The reaction of $\text{Me}_3\text{N}\cdot\text{SO}_3$ complex and amines is rapid, especially involving nucleophilic amines with an sp^3 hybridized nitrogen. This fast reaction rate can lead to incomplete conversion to the desired tributylammonium salt if the conditions are not carefully controlled. Lowering the reaction temperature to 30 °C helps to control the reaction kinetics and therefore improves selectivity and conversion. In this method, addition order of tributylamine was investigated to see whether the order of addition was critical for this investigation performed by Anna Benedetti (**Table 10**).

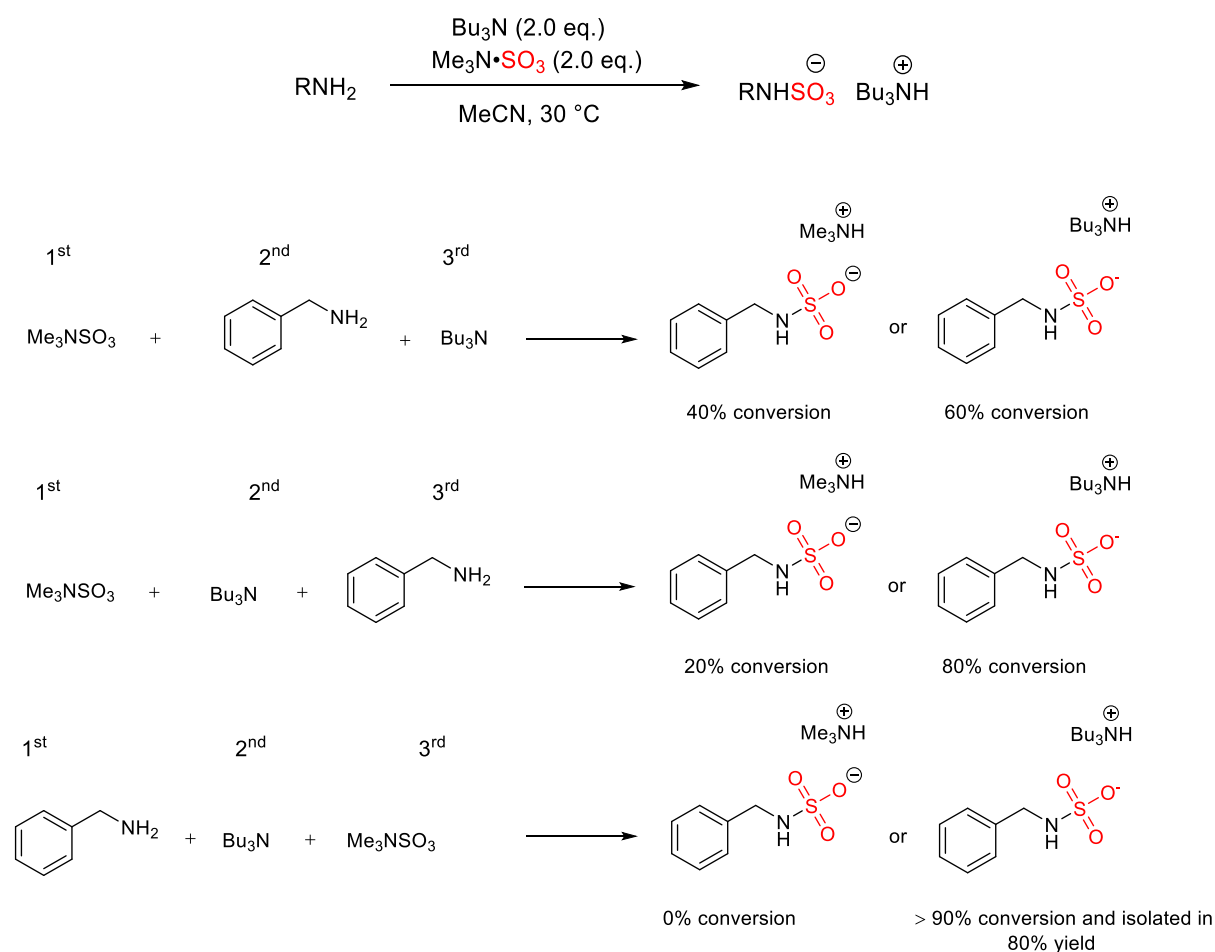
Table 10: Optimization of a model tributylammonium benzyl sulfamate reaction. Reaction conversions reported as measured by ^1H NMR spectroscopy (400 MHz, $\text{DMSO-}d_6$).



Order (The time interval was 1 minute) (400 MHz, $\text{DMSO-}d_6$)						
Entry	1 st	2 nd	3 rd	% conversion to 177	% conversion to 176	% isolation as 177
1	$\text{Me}_3\text{N}^+\text{SO}_3^-$		Bu_3N	60	40	n.a.
2	$\text{Me}_3\text{N}^+\text{SO}_3^-$	Bu_3N		80	20	n.a.
3		Bu_3N	$\text{Me}_3\text{N}^+\text{SO}_3^-$	> 99	0	80

Following this methodology (**30 °C, Entry 1**) confirmed that complete conversion occurs but only 60% results as the tributylammonium cation (**177**). Whereas, the trimethylammonium cation (**176**) was converted in 40%. It was considered whether the tributylamine should be added before the addition of benzylamine (**106**) or after the addition of benzylamine (**Entries 2 and 3**). As a result, the tributylammonium cation was observed with a quantitative conversion to 80% (**Entry 2**). Notably, the optimal conversion was observed when tributylamine was added after the addition of benzylamine and the tributylammonium cation (**177**) was isolated in 80% isolated yield suggesting that the hypothesis of order of addition for rapid and low temperature reaction was relevant with the rapid kinetics of the reaction between the sp^3 hybridised nitrogen of benzylamine and $\text{Me}_3\text{N}^+\text{SO}_3^-$. Next, the room

temperature (30 °C) optimised method was applied to a range of primary, secondary amines and aniline (**Scheme 61**).



Scheme 61: *In situ* synthesis of tributylammonium sulfamate salts using Me₃N•SO₃ complex and importance of order of addition.

This strategy was applicable to different nitrogen-based substrates observing a conversion rate greater than 99%. Nevertheless, the tributylammonium salt (**177**) was obtained in a reduced yield of 50–94% after purification through extraction. The electron-donating (methoxy) group (**186**), was efficiently transformed into its corresponding tributylammonium salt with a conversion rate of (>99%) followed by purification to afford the title molecule (**186**) in a modest isolated yield (50%). The analogue incorporating an electron-withdrawing chlorine substituent (**187**) was afforded with a high yield of 93%. The yield differences can be

explained by the influence of inductive and mesomeric effects on the reactivity of these molecules. For instance, the methoxy group in **(186)**, has both inductive and mesomeric effects in which the lone pair on the oxygen atom can delocalize into the aromatic ring, increasing the electron density at the reaction site. Furthermore, the inductive effect of the methoxy group slightly pulls electron density away and donates electron density via the mesomeric effect, increasing the nucleophilicity of the nitrogen atom. Whereas, substrates with an electron-withdrawing chlorine substituent (**(187)**), stabilise reaction intermediates via inductive effects, pulling electron density away from the aromatic ring.

It was also reported that the trimethylammonium salt (**(176)**) was afforded as a clear oil compound after purification in 50% isolated yield. This strategy was also applied to some primary amines such as 1-phenyl-ethyl amine (**(188)**) and aniline (**(189)**). In both cases, a conversion rate greater than 99% was observed to their corresponding tributylammonium salts and the isolated yields of 94% and 57% were reported after purification, respectively (**Figure 35**).

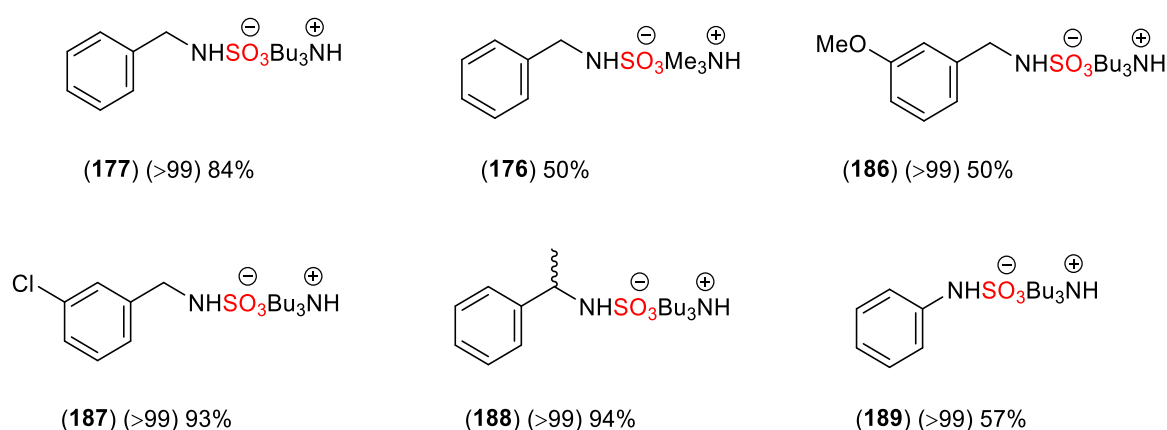


Figure 35: Scope of room temperature application of the method to a range of nitrogen-containing scaffolds. Parentheses indicates % conversion as measured by ^1H NMR spectroscopy (400 MHz, CDCl_3 and $\text{DMSO}-d_6$ solvents).

4.5. Conclusion

An alternative, operationally simple, one-pot, three-step strategy for synthesising small molecular weight organosulfates and sulfamates has been developed. This innovative strategy uses affordable and readily available reagents, resulting in good to excellent isolated yields of the desired compounds. This approach requires an additional operational step, unlike the all-in-one TBSAB reagent which can achieve the same or similar transformations in higher yield. But for laboratories without access to the methods and equipment to prepare expensive TBSAB, including inert atmosphere techniques, solvent purifier system, high-purity reagents to avoid contamination and ensure a high yield, this provides a user-friendly, off-the-shelf approach to preparing sulfated molecules. This novel sulfation strategy also improved the molecular efficiency of lipophilic cation exchange and avoids the formation of acidic tetrabutylammonium salts when using TBSAB as a source of sulfation. These acidic tetrabutylammonium salts are formed when TBSAB is used due to the release of tributylammonium ions.

**OPEN** A novel exchange method to access sulfated moleculesJaber A. Alshehri, Anna Mary Benedetti & Alan M. Jones[✉]

Organosulfates and sulfamates are important classes of bioactive molecules but due to their polar nature, they are both difficult to prepare and purify. We report an operationally simple, double ion-exchange method to access organosulfates and sulfamates. Inspired by the novel sulfating reagent, TriButylSulfoAmmonium Betaine (TBSAB), we developed a 3-step procedure using tributylamine as the novel solubilising partner coupled to commercially available sulfating agents. Hence, in response to an increasing demand for complementary methods to synthesise organosulfates, we developed an alternative sulfation route based on an inexpensive, molecularly efficient and solubilising cation exchanging method using off-the-shelf reagents. The disclosed method is amenable to a range of differentially substituted benzyl alcohols, benzylamines and aniline and can also be performed at low temperature for sensitive substrates in good to excellent isolated yield.

Organosulfates and sulfamates contain polar functional groups that are important for the study of molecular interactions in the life sciences, such as: neurodegeneration¹; plant biology²; neural stem cells³; heparan binding⁴; and viral infection⁵. Recent total syntheses including 11-saxitoxinethanoic acid⁶, various saccharide assemblies^{7–10}, and seminolipid¹¹ have all relied on the incorporation of a highly polar organosulfate motif. Importantly, the first in class organosulfate containing antibiotic, Avibactam¹², has led to the discovery of other novel β -lactamase inhibitors^{13,14}. Despite the importance of the sulfate group, there remain difficulties with the ease of their synthesis to enable further biological study.

Our own interest in developing sulfated molecules resulted from a medicinal chemistry challenge to reliably synthesise sulfated glycomimetics^{15–18}. We recently reported the development of an all-in-one sulfating reagent, Bu₃NSO₃ (TBSAB)^{19,20}.

To accelerate the development of complementary methods to prepare organosulfates for biological applications, and inspired by the use of a lipophilic solubilising cation, we sought to develop an alternative sulfation protocol using low-cost, commercially available reagents.

To the best of our knowledge, methods to sulfate oxygen, nitrogen, oximes and phosphates that include an organic solubilising cation step remain limited (Fig. 1).

Methods to accomplish a lipophilic cation-exchange of highly polar sulfated molecules include the process route to Avibactam reported by Ball et al.¹². Recent work by Montero Bastidas et al.²¹, and Mihai et al.²² have shown the importance of routes to sulfated molecules with a sterically bulky tetrabutylammonium cation for iridium catalysed *para*-selective C–H borylations. An alternate approach is to design an all-in-one reagent with a sulfating agent combined with a lipophilic counterion, such as our own work^{19,20} and the work of Kowalska et al.²³.

Herein we explored an alternative method to access organosulfates and sulfamates on a range of alcohols and amines using the inexpensive bulk commodity sulfating chemicals (SO₃–R, R=Py or NMe₃) and tributylamine as the lipophilic counterion exchange for the first time.

Results and discussion

Due to the current need to prepare an all-in-one reagent such as TBSAB (Bu₃NSO₃) prior to sulfating an alcohol or amine, we initially investigated whether TBSAB could be prepared from commercial sulfating reagents such as Py-SO₃ or Me₃N-SO₃ and tributylamine. Although ¹H NMR spectroscopy ruled out the formation of TBSAB in situ (See supporting Information Figure S5), this result led us to consider whether tributylamine could be used to exchange the polar amine sulfation product to a lipophilic tributylammonium cation (*c.f.* the TBSAB reaction product). Therefore, benzyl alcohol was selected as the model scaffold to optimise the formation of a sulfate ester using a one-pot, three-step procedure due to its diagnostic shift in the ¹H NMR spectrum (Table 1).

Entries 1–4 in Table 1 show that conversion to the benzyl sulfate ester pyridinium salt (2) was improved with super-stoichiometric equivalents of the pyridine sulfur trioxide complex. Increasing the reaction temperature

School of Pharmacy, University of Birmingham, Edgbaston B15 2TT, UK. ✉email: a.m.jones.2@bham.ac.uk

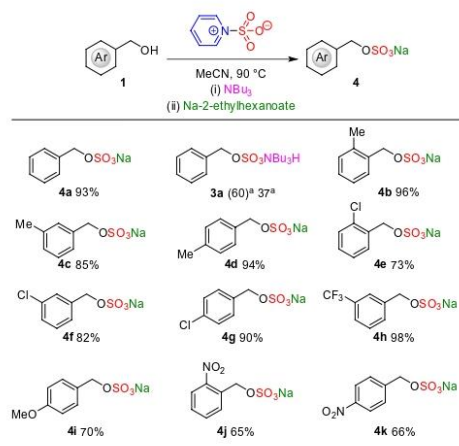
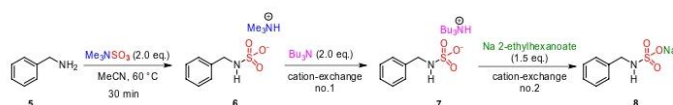


Figure 2. Reaction scope of the 3-step, 1-pot method with benzyl alcohols. Parentheses indicate percentage conversion as measured by ^1H NMR spectroscopy. *use of Me_3NSO_3 instead of PySO_3 .



Scheme 1. Optimised benzylamine sulfamation conditions.

(entry 5 vs entry 4) resulted in quantitative conversion to the pyridinium salt (2). Using the optimal conversion conditions (entry 5) a variety of lipophilic cation exchanging additives were tested to compare tetrabutylammonium salts with tributylamine (entries 6–10). In combination with a sodium salt exchange using sodium 2-ethylhexanoate, it was found that tributylamine afforded the highest isolated yield (94%, entry 7) compared to the tetrabutylammonium salts of iodide, acetate or bromide. The use of an alternative sodium exchange method (NaI, entries 11–15) in tandem with tributylamine or tetrabutylammonium salts was also effective but lower yielding compared to entry 7. With the optimal conditions in hand, we explored the generality of the one-pot, three-step method (Fig. 2).

A variety of benzyl alcohols containing a range of steric and electronic effects were explored (Fig. 2). The method proved tolerant of a wide variety of functionality with isolated yields ranging from 65 to 98%. In comparison with our previously reported all-in-one TBSAB methodology¹⁹ isolated yields were good but generally lower: **4a** (93% vs 95%), **4e** (73% vs 99%), **4g** (90% vs 94%), **4i** (70% vs 78%), and **4k** (66% vs 85%).

The rationale for using PySO_3 over Me_3NSO_3 can be seen from the poor conversion observed with **3a** (using Me_3NSO_3) versus **4a**. An explanation for this relates to the Lewis basicity of the amine- SO_3 complex (Py-SO_3 ($pK_a = 5.23$); $\text{Me}_3\text{N-SO}_3$ ($pK_a = 10.63$)). The sp^3 hybridised Lewis base of Me_3N donates electrons more strongly into the LUMO of SO_3 , forming a hard-hard Lewis adduct with increased stability and decreased reactivity compared to sp^2 hybridised Lewis base seen in Py-SO_3 ²⁴.

Next, using the knowledge obtained from the sulfate ester optimisation and our prior work on sulfamates²⁰, initial conditions of switching to Me_3NSO_3 resulted in quantitative conversion of the benzyl sulfamate (Scheme 1). Slightly lowering the reaction temperature due to the increased nucleophilicity of the sp^3 nitrogen atom, resulted in a quantitative conversion for both the formation of the sulfamate trimethylammonium species and the cation exchanged sulfamate tributylammonium species. It was found that the use of 1.5 eq of sodium 2-ethylhexanoate resulted in a near-quantitative isolated yield (99%).

With the optimal conditions in hand, we explored the methodology on a selection of benzylamines (Fig. 3). In all cases, an excellent isolated yield, considering the three steps involved, was observed (90–99%) independent of functional group effects. In comparison to our previous methodology, using TBSAB, the following observations were identified: **8a** (99% vs 98%), **8d** (90% vs 97%), **8e** (98% vs 61%), **8f** (93% vs 87%), and **8g** (99% vs 85%). In nearly all cases, the isolated yield for this new route was equivalent or improved for the benzylamines. However, one pertinent disadvantage of the three-step method was the higher reaction temperature, which may not be compatible with more complex molecules. To address this, we next studied a low temperature variant of the new method (Table 2 and Fig. 4).

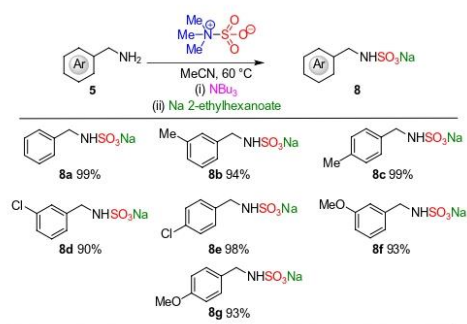
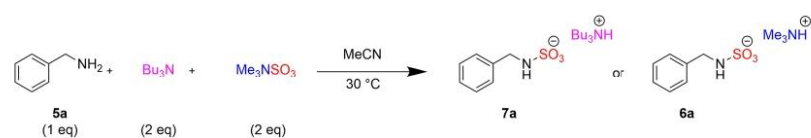


Figure 3. Benzylamine sulfamation reaction scope.



Entry	Order			% conversion to 7a	% conversion to 6a	% Isolation as a 7a
	1 st	2 nd	3 rd			
1	Me ₃ NSO ₃		Bu ₃ N	60	40	n.a.
2	Me ₃ NSO ₃	Bu ₃ N		80	20	n.a.
3		Bu ₃ N	Me ₃ NSO ₃	> 99	0	80

Table 2. Optimization of a model tributylammonium benzyl sulfamate reaction. Reaction conversions reported as measured by ¹H NMR spectroscopy.

Due to the rapid kinetics of the reaction between an *sp*³ hybridised nitrogen and Me₃NSO₃, we explored whether the order of addition at a lower reaction temperature was important with a series of control experiments.

At low temperature (30 °C, entry 1) demonstrated that complete conversion occurs but only 60% results as the tributylammonium cation. Entries 2 and 3 considered whether Bu₃N should be introduced prior to addition of benzylamine or after addition of benzylamine. The order of addition for rapid, low temperature reaction, became apparent, with a quantitative conversion to the tributylammonium salt (**7a**) with entry 3 and high isolated yield.

With this insight, a series of representative primary, secondary amines and aniline were screened using a low temperature method (Fig. 4). In all cases a high conversion (>99%) was obtained (Fig. 4) but a lower 50–94% isolated yield of the tributylammonium cation after purification. The intermediacy of the trimethylammonium species, **6a** was confirmed via isolation in a 50% yield.

Conclusion

In summary, we have developed an alternative operationally straightforward, one-pot, three-step procedure to prepare small molecular weight organosulfates and sulfamates using only low-cost commodity chemicals in generally good to excellent isolated yields. In comparison to the all-in-one TBSAB reagent which can achieve the same or similar transformations in higher yield, the disclosed method does require an additional operational step, but for laboratories without access to methods and equipment to prepare TBSAB, this provides a user-friendly,

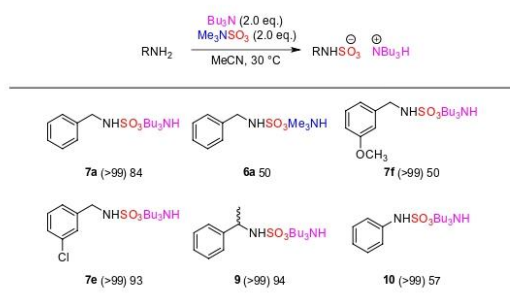


Figure 4. Low-temperature application of the method to a range of nitrogen containing scaffolds. Parentheses indicates % conversion as measured by ^1H NMR spectroscopy.

off-the-shelf approach to preparing sulfated molecules. Improvements in molecular efficiency of lipophilic cation exchange and the avoidance of acidic tetrabutylammonium salts was possible with the new sulfation method.

Methods

All reactions involving moisture sensitive reagents were carried out using standard Schlenk techniques, in a dry reaction vessel under argon. All solvents used under anhydrous conditions were decanted directly from an SPS dispensary or were stored over 4 Å molecular sieves 24 h prior to use.

Solvents used for workup procedures were of technical grade from Sigma-Aldrich, Honeywell, VWR or Fisher Scientific. Unless stated otherwise, solvents were removed by rotary evaporation under reduced pressure between 30–50 °C. All chemical reagents were used as received unless stated otherwise. Reactions were monitored by TLC analysis on Merck silica gel 60 F254 using UV light (254 nm) and/or potassium permanganate.

^1H , ^{13}C and ^{19}F NMR spectra were recorded either on a Bruker AVIII operating at 300 MHz for ^1H and fitted with a 5 mm BBFO probe or on a Bruker AVANCE NEO operating at 400 MHz for ^1H fitted with a 5 mm “smart” BBFO probe, respectively²⁵. Chemical shift data are reported in parts per million (ppm, δ scale) downfield from tetramethylsilane (TMS; δ 0.0) and referenced internally to the residual proton in the solvent²⁶. The deuterated solvents used for NMR analysis were: chloroform (CDCl_3 ; δH 7.26, δC 77.2), dimethyl sulfoxide (d_6 -DMSO; δH 2.50, δC 39.5), and deuterium oxide (D_2O ; δH 4.79). Coupling constants are given in Hertz (Hz)²⁷. All individual signals were assigned using 2D NMR spectroscopy (^1H - ^1H -COSY, ^1H - ^{13}C -HSQC, and ^1H - ^{13}C -HMBC). The data are presented as follows: chemical shift multiplicity (s = singlet, d = doublet, t = triplet, q = quartet, p = pentet, m = multiple, br = broad and combinations thereof), coupling constant, integration, and assignment²⁸. Mass spectra were recorded on a Waters Xevo G2-XS ToF or Synap G2-S mass spectrometer using Zspray, Electro-spray ionization in negative (ESI-) mode. Infrared spectra were recorded on a Perkin Elmer Spectrum 100 FT-IR and a Varian 660-IR FTIR spectrometer using Agilent Resolution Pro, with absorption maxima (vmax) reported in cm^{-1} . Optical rotations were measured using a Bellingham and Stanley ADP450 Series Peltier polarimeter at 25 °C using the D line of sodium (589.3 nm) in the indicated concentration and solvent.

General experimental procedure. *General procedure 1* Synthetic procedure for the preparation of sodium benzyl sulfate ester using sulfur trioxide pyridine complex and tributylamine. A flame dried 100 mL round bottom flask was charged with the appropriate alcohol (1.0 mmol) and pyridine.sulfur trioxide complex (PST) (2.0 mmol) under argon. Anhydrous MeCN (2.0 mL) was added and the reaction mixture heated at 90 °C (monitored by TLC). After 3 h, tributylamine (2.0 mmol) was added to the reaction mixture and stirred for 30 min at 90 °C. The flask was cooled to room temperature and the solvent removed under reduced pressure to afford the desired sulfate ester as its tributylammonium salt.

Work-up procedure A The flask containing the tributylammonium salt was charged with EtOH (30 mL) and sodium 2-ethylhexanoate (5.0 eq. per sulfate group). The reaction mixture was stirred vigorously for 1 h at room temperature. The precipitate was collected by filtration, washed with EtOH (3×20 mL) and dried to a constant weight to afford the desired sulfate ester as its sodium salt.

Work-up procedure B The flask containing the tributylammonium salt was charged with ethyl acetate (30 mL) and sodium 2-ethylhexanoate (5.0 eq. per sulfate group). The reaction mixture was stirred vigorously for 1 h at room temperature. The precipitate was collected by filtration, washed with ethyl acetate (3×20 mL) and dried to a constant weight to afford the desired sulfate ester as its sodium salt.

Work-up procedure C The flask containing the tributylammonium salt was charged with MeCN (25 mL) and sodium iodide (5.0 eq. per sulfate group). The reaction mixture was stirred vigorously for 1 h at room temperature. The precipitate was removed by filtration, washed with MeCN (3×20 mL) and dried to a constant weight to afford the desired sulfate ester as its sodium salt.

General procedure 2 Synthetic procedure for the preparation of sodium benzylsulfamates using sulfur trioxide trimethylamine complex and tributylamine. A flame dried 100 mL round bottom flask was charged with the appropriate amine (1.0 mmol) and trimethylamine.sulfur trioxide complex (TMST) (2.0 mmol) under argon.

Anhydrous MeCN (2.0 mL) was added and the reaction mixture heated at 60 °C (monitored by TLC). After 30 min, tributylamine (2.0 mmol) was added to the reaction mixture and stirred for 30 min at 60 °C. The flask was cooled to room temperature and the solvent removed under reduced pressure to afford the desired sulfate ester as its tributylammonium salt.

Work-up procedure A The flask containing the tributylammonium salt was charged with EtOH (30 mL) and sodium 2-ethylhexanoate (1.5 eq. per sulfate group). The reaction mixture was stirred vigorously for 1 h at room temperature. The precipitate was removed by filtration, washed with EtOH (3 × 20 mL) and dried to a constant weight to afford the desired sulfate ester as its sodium salt.

Work-up procedure B The flask containing the tributylammonium salt was charged with MeCN (25 mL) and sodium iodide (1.5 eq. per sulfate group). The reaction mixture was stirred vigorously for 1 h at room temperature. The precipitate was removed by filtration, washed with MeCN (3 × 20 mL) and dried to a constant weight to afford the desired sulfate ester as its sodium salt.

General procedure 3 Low-temperature preparation of trimethylammonium sulfamate salts using sulfur trioxide trimethylamine complex (Me₃NSO₃, TMST). A 25 mL flask was charged with the appropriate amine (1.0 mmol) and TMST (2.0 eq) under argon. Anhydrous MeCN was added (giving a concentration of 0.50 mol dm⁻³ to the limiting reagent), the reaction mixture was heated at 30 °C and monitored by TLC. After reaction completion the flask was cooled to room temperature and the solvent removed under reduced pressure. The reaction was quenched with EtOH (10 mL) and filtered. The solution was evaporated and extracted with H₂O (10 mL) and ethyl acetate (4 × 40 mL). The organic layer was dried (MgSO₄), filtered, and the solvent was removed *in vacuo* giving the desired trimethylammonium salt as an oil.

General procedure 4 In situ preparation of tributylammonium sulfamate salts using sulfur trioxide trimethylamine complex (Me₃NSO₃, TMST).

A 25 mL flask was charged with the appropriate amine (1.0 mmol) and tributylamine (2.0 eq) dissolved in anhydrous MeCN (giving a concentration of 0.50 mol dm⁻³ to the limiting reagent) under argon. After addition of TMST (2.0 eq), the reaction mixture was heated at 30 °C and monitored by TLC. After reaction completion the flask was cooled to room temperature and the solvent removed under reduced pressure. The reaction was quenched with EtOH (10 mL) and filtered. The solution was evaporated and extracted with H₂O (10 mL) and ethyl acetate (4 × 40 mL). The organic layer was dried (MgSO₄), filtered, and the solvent was removed *in vacuo* giving the desired tributylammonium salt as an oil.

Example compound characterization. *Tributylammonium benzyl sulfate (3a)*. Following general procedure 4: benzyl alcohol (0.10 mL, 1.0 mmol) and tributylamine (0.47 mL, 2.0 mmol) were dissolved in anhydrous MeCN (2.0 mL). After addition of TMST (278 mg, 2.0 mmol) the reaction mixture was heated at 30 °C for 3 h. The crude product was purified with silica gel chromatography (DCM-MeOH; 1:9) to yield the title compound as a yellow oil (138 mg, 37%). ν_{max} cm⁻¹ 3455 br w, 2960 s, 2933 s, 2874 s, 1455 s, 1258 s, 1198 s; ¹H NMR (400 MHz, CDCl₃) δ_{H} 9.57 (s, 1H), 7.35 (dt, $J = 6.0, 1.6$ Hz, 2H), 7.29–7.18 (m, 3H), 5.03 (s, 2H), 3.06–2.80 (m, 6H), 1.82–1.49 (m, 6H), 1.28 (h, $J = 7.4$ Hz, 6H), 0.87 (t, $J = 7.4$ Hz, 9H); ¹³C NMR (101 MHz, CDCl₃) δ_{C} 136.8, 128.4, 128.3, 128.0, 69.7, 52.7, 29.7, 25.3, 20.0, 13.6; LRMS m/z (ESI⁺) 559.45 (100%, [M + Bu₃NH]⁺); HRMS m/z (ESI⁺) C₃₁H₆₃N₂O₄S requires 559.4504, found 559.4503 ([M + Bu₃NH]⁺). Data were consistent with the literature¹⁹.

Sodium benzyl sulfate (4a). Following the general procedure 1: benzyl alcohol (0.1 mL, 1.0 mmol) and sulfur trioxide pyridine complex (318 mg, 2.0 mmol) were dissolved in anhydrous MeCN (2.0 mL) and heated under reflux at 90 °C for 3 h. Tributylamine (0.4 mL, 2.0 mmol) was added to the mixture and stirred for 30 min. After the completion of reaction, the flask was cooled to room temperature and the solvent removed under reduced pressure. The crude product was purified by work up procedure A to yield the title compound as a bright white solid (196 mg, 93%). M.P. 208–210 °C; ¹H NMR (300 MHz, D₂O) δ 7.57–7.33 (m, 5H), 5.09 (s, 2H); ¹³C NMR (101 MHz, D₂O) δ 135.1, 128.7 (CH and C), 128.4, 70.7; LRMS. m/z (ESI⁻) 187.0 ([M¹³C – Na]⁻), 100%, 188.1 ([M¹³C – Na]⁻), 10%; Data were consistent with the literature¹⁹.

Received: 2 May 2020; Accepted: 2 September 2020

Published online: 06 October 2020

References

- Yamada, M. & Hamaguchi, T. The sulfation code for propagation of neurodegeneration. *J. Biol. Chem.* **293**, 10841–10842 (2018).
- Wasternack, C. Sulfation switch in the shade. *Nat. Plants* **6**, 186–187 (2020).
- Chopra, P. *et al.* Fully synthetic heparan sulfate-based neural tissue construct that maintains the undifferentiated state of neural stem cells. *ACS Chem. Biol.* **14**, 1921–1929 (2019).
- Debarnota, C. *et al.* Substrate binding mode and catalytic mechanism of human heparan sulfate D-glucuronyl C5 epimerase. *Proc. Natl. Acad. Sci. USA* **116**, 6760–6765 (2019).
- Earley, D. F. *et al.* Efficient blocking of enterovirus 71 infection by heparan sulfate analogues acting as decoy receptors. *ACS Infect. Dis.* **5**, 1708–1717 (2019).
- Walker, J. R., Merit, J. E., Thomas-Tran, R., Tang, D. T. Y. & Du Bois, J. Divergent synthesis of natural derivatives of (+)-saxitoxin including 11-saxitoxinethanoic acid. *Angew. Chem. Int. Ed.* **58**, 1689–1693 (2019).
- Pawar, N. J. *et al.* Expedient synthesis of core disaccharide building blocks from natural polysaccharides for heparan sulfate oligosaccharide assembly. *Angew. Chem. Int. Ed.* **58**, 18577–18583 (2019).

8. Argunov, D. A., Trostianetskaia, A. S., Krylov, V., Kurbatova, E. A. & Nifantiev, N. E. Convergent synthesis of oligosaccharides structurally related to galactan I and galactan II of *Klebsiella Pneumoniae* and their use in screening of antibody specificity. *Eur. J. Org. Chem.* **2019**, 4226–4232 (2019).
9. Dimakos, V. & Taylor, M. S. Site-selective functionalization of hydroxyl groups in carbohydrate derivatives. *Chem. Rev.* **118**, 11457–11517 (2018).
10. Gao, T. *et al.* Chemoenzymatic synthesis of O-mannose glycans containing sulfated or nonsulfated HNK-1 epitope. *J. Am. Chem. Soc.* **141**, 19351–19359 (2019).
11. Shimada, N., Fukuhara, K., Urata, S. & Makino, K. Total syntheses of seminolipid and its analogues by using 2,6-bis(trifluoromethyl)phenylboronic acid as protective reagent Makino. *Org. Biomol. Chem.* **17**, 7325–7329 (2019).
12. Ball, M. *et al.* Development of a manufacturing route to avibactam, a β -lactamase inhibitor. *Org. Process Res. Dev.* **20**, 1799–1805 (2016).
13. Levy, N. Structural basis for *E. coli* penicillin binding protein (PBP) 2 inhibition, a platform for drug design. *J. Med. Chem.* **62**, 4742–4754 (2019).
14. Reck, F. *et al.* ID572: A new potentially best-in-class β -lactamase inhibitor. *ACS Infect. Dis.* **5**, 1045–1051 (2019).
15. Mahmoud, A. M. *et al.* A novel role for small molecule glycomimetics in the protection against lipid-induced endothelial dysfunction: involvement of Akt/eNOS and Nr2f1/ARE signalling. *Biochimica et Biophysica Acta Gen. Subj.* **1861**, 3311–3322 (2017).
16. Gill, D. M., Male, L. & Jones, A. M. A structure-reactivity relationship of the tandem asymmetric dihydroxylation on a biologically relevant diene: influence of remote stereocenters on diastereofacial selectivity. *Eur. J. Org. Chem.* **2019**, 7568–7577 (2019).
17. Mahmoud, A. M. *et al.* Small molecule glycomimetics inhibit vascular calcification via c-Met/Notch3/HES1 signalling. *Cell. Physiol. Biochem.* **53**, 323–336 (2019).
18. Langford-Smith, A. W. W. *et al.* Diabetic endothelial colony forming cells have the potential for restoration with glycomimetics. *Sci. Rep.* **9**, 2309 (2019).
19. Gill, D. M., Male, L. & Jones, A. M. Sulfation made simple: a strategy for synthesising sulfated molecules. *Chem. Commun.* **55**, 4319–4322 (2019).
20. Benedetti, A. M., Gill, D. M., Tsang, C. W. & Jones, A. M. Chemical methods for N- and O-sulfation of small molecules amino acids and peptides. *ChemBioChem* **21**, 938–942 (2020).
21. Montero Bastidas, J. R., Oleskey, T. J., Miller, S. L., Smith, M. R. III & Maleczka, R. E. Jr. Para-selective, iridium-catalyzed C–H borylations of sulfated phenols, benzyl alcohols, and anilines directed by ion-pair electrostatic interactions. *J. Am. Chem. Soc.* **141**, 15483–15487 (2019).
22. Mihai, M. T., Williams, B. D. & Phipps, R. J. Para-selective C–H borylation of common arene building blocks enabled by ion-pairing with a bulky counteranion. *J. Am. Chem. Soc.* **141**, 15477–15482 (2019).
23. Kowalska, J., Osowniak, A., Zuberek, J. & Jemielity, J. Synthesis of nucleoside phosphosulfates. *Bioorg. Med. Chem. Lett.* **22**, 3661–3664 (2012).
24. Reitz, H. C., Ferrel, R. E., Olcott, H. S. & Fraenkel-Conrat, H. Action of sulfating agents on proteins and model substances. II. Pyridine-chlorosulfonic acid. *J. Am. Chem. Soc.* **68**, 1031–1035 (1946).
25. Zazeri, G. *et al.* Synthesis and spectroscopic analysis of piperine and piperlongumine-inspired natural product scaffolds and their molecular docking with IL-1 β and NF- κ B proteins. *Molecules* **25**, 2841 (2020).
26. Wetzal, A. & Jones, A. M. Electrically-driven N(sp²)-C(sp²/3) bond cleavage of sulphonamides. *ACS Sustain. Chem. Eng.* **8**, 3487–3493 (2020).
27. Barone, M. R. & Jones, A. M. Selective C–H bond electro-oxidation of benzylic acetates and alcohols to benzaldehydes. *Org. Biomol. Chem.* **15**, 10010–10015 (2017).
28. Green, M. T. *et al.* Total synthesis and structural revision of a mangrove alkaloid. *RSC Adv.* **7**, 48754–48758 (2017).

Acknowledgements

The authors thank King Khalid University, Saudi Arabia (JAA) and the Erasmus+ UniPharma programme (AMB) for supporting their studies. Dr D. M. Gill is thanked for helpful discussions.

Author contributions

A.M.J. conceived and directed the project; J.A.A., A.M.B. performed the synthesis and standard characterisation; A.M.J. and J.A.A. wrote the main manuscript; all authors discussed the results and reviewed the manuscript.

Competing interests

The authors declare no competing interests.

Additional information

Supplementary information is available for this paper at <https://doi.org/10.1038/s41598-020-72500-x>.

Correspondence and requests for materials should be addressed to A.M.J.

Reprints and permissions information is available at www.nature.com/reprints.

Publisher's note Springer Nature remains neutral with regard to jurisdictional claims in published maps and institutional affiliations.

 **Open Access** This article is licensed under a Creative Commons Attribution 4.0 International License, which permits use, sharing, adaptation, distribution and reproduction in any medium or format, as long as you give appropriate credit to the original author(s) and the source, provide a link to the Creative Commons licence, and indicate if changes were made. The images or other third party material in this article are included in the article's Creative Commons licence, unless indicated otherwise in a credit line to the material. If material is not included in the article's Creative Commons licence and your intended use is not permitted by statutory regulation or exceeds the permitted use, you will need to obtain permission directly from the copyright holder. To view a copy of this licence, visit <http://creativecommons.org/licenses/by/4.0/>.

© The Author(s) 2020

Chapter 5. A sulfonyl group transfer strategy to selectively prepare sulfated steroids

Background

Steroids are biologically active organic molecules (hormones) that are widely distributed in different living organisms in the animal and plant kingdoms as well as in yeasts and fungi. Approximately 250 steroid-based compounds have been found in plants such as (phytosterols), insects (ecdysteroids), animals (cholesterol, androgens, and neurosteroids), and fungi (ergosterol).¹⁸⁹⁻¹⁹⁰ In 1905, Ernest Starling defined 'hormones' as "the chemical messengers which speed from cell to cell along the blood stream, may coordinate the activities and growth of different parts of the body".¹⁹¹ Butenandt was awarded the Nobel Prizes for his discovery and characterization of steroid hormones including, oestrogen, testosterone and progesterone during the 1920s and 1930s.¹⁹² Interest in steroid hormones has been growing due to the important biological roles of steroids and their correlation in diseases.¹⁹³⁻¹⁹⁵ The steroidal skeleton structure is composed of a tetracyclic hydrocarbon, a reduced tricyclic phenanthrene ring (A, B, and C) and a cyclopentane ring (D) (**Figure 36**).

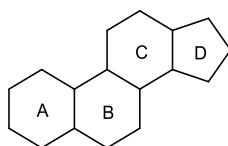
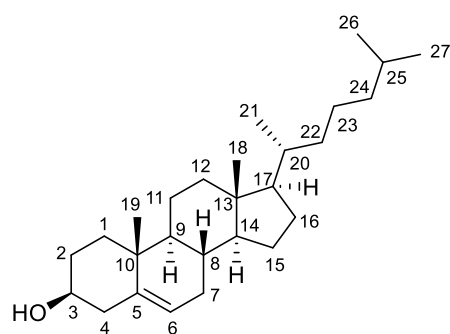


Figure 36: The steroidal skeleton structure, a reduced phenanthrene (A, B, and C) and cyclopentane ring (D).

Cholesterol, an exemplar steroid, is an essential component of mammalian cell membranes and crucial for cell stability and development (**Figure 37**).¹⁹⁶



(190)

Figure 37: The structure of cholesterol with steroidal numbering.

Hundreds of steroids have been isolated from natural sources and others have been chemically synthesised to investigate their biological roles in the body.¹⁹⁷ The biological roles of steroid compounds are diverse and can be edited by, for instance the position of the functional group attached to the steroid skeleton and the oxidation state of the rings.¹⁹⁸ The presence of oxygen at C11 is important for inflammatory activity, whereas in position C17, it controls androgen properties.¹⁹⁹ Aromatization of ring-A leads to estrogenic effects.²⁰⁰⁻²⁰¹

For instance, androstane and pregnane steroids have hormonal activity²⁰¹⁻²⁰³ while bile acids such as, cholic and chenodeoxycholic acids are involved in other biological functions including, the digestive process and absorption of fats, as well as in the metabolic regulation process

(**Figure 38**).²⁰⁴⁻²⁰⁵

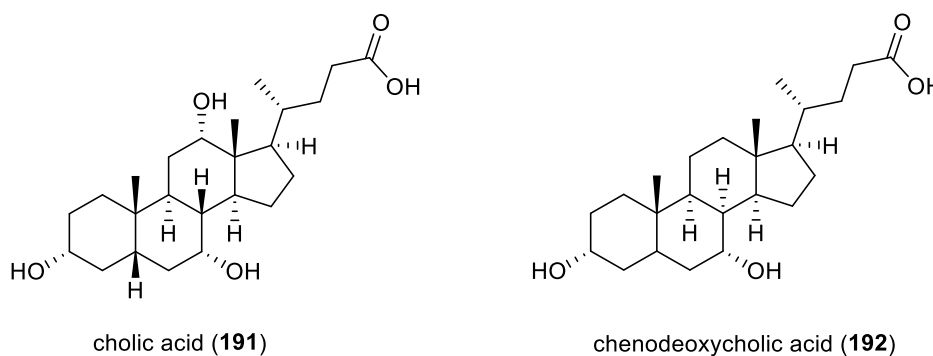


Figure 38: Bile acid derivatives, cholic acid (191) and chenodeoxycholic acid (192).

Digoxin is another steroid-based structure which is a cardiac glycoside compound found in foxgloves, and is approved for the treatment of atrial fibrillation (**Figure 39**).²⁰⁶ Moreover, ~300 steroid-based drugs have been approved and used as anti-inflammatory, anti-cancer, anti-viral, anti-fungal agents, immunosuppressants, diuretics, and for the treatment of obesity.^{200, 207-210}

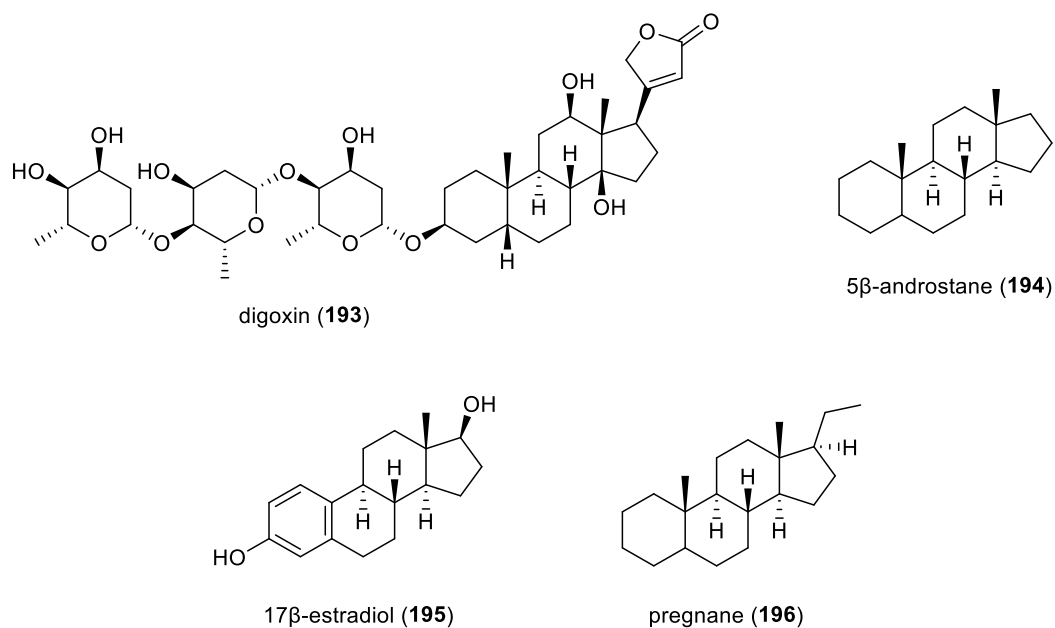


Figure 39: Selected steroids with biological functions including the treatment of cardiovascular diseases with digoxin, the treatment of obesity as in 5β-androstane, neuroprotective and immune modulators as in 17β-estradiol, and anti-inflammatory activity as in pregnane.^{200, 207-210}

5.1. Modifications of steroids

Studies have shown that steroids undergo a range of chemical reactions such as oxidation, reduction, sulfation, esterification, glucuronidation and condensation reactions *in vivo*.²¹¹

These reactions are essential in both biology (e.g. the metabolism of hormones) and in synthetic chemistry (e.g. pharmaceutical development).²¹¹ These reactions are generally carried out in different positions of the steroidal skeleton either on the cyclic site such as the C3, C11, and C17 positions or on the side-chain of a steroid molecule.²¹¹ For instance, the oxidation reaction of a steroid usually happens at different positions including the side-chain

leading to the formation of aldehydes, ketones, or carboxylic acids. Sulfation usually takes place at hydroxyl groups, mostly at the C3 and C17 positions, resulting in the formation of steroid metabolites (**Figure 40**).²¹²⁻²¹³

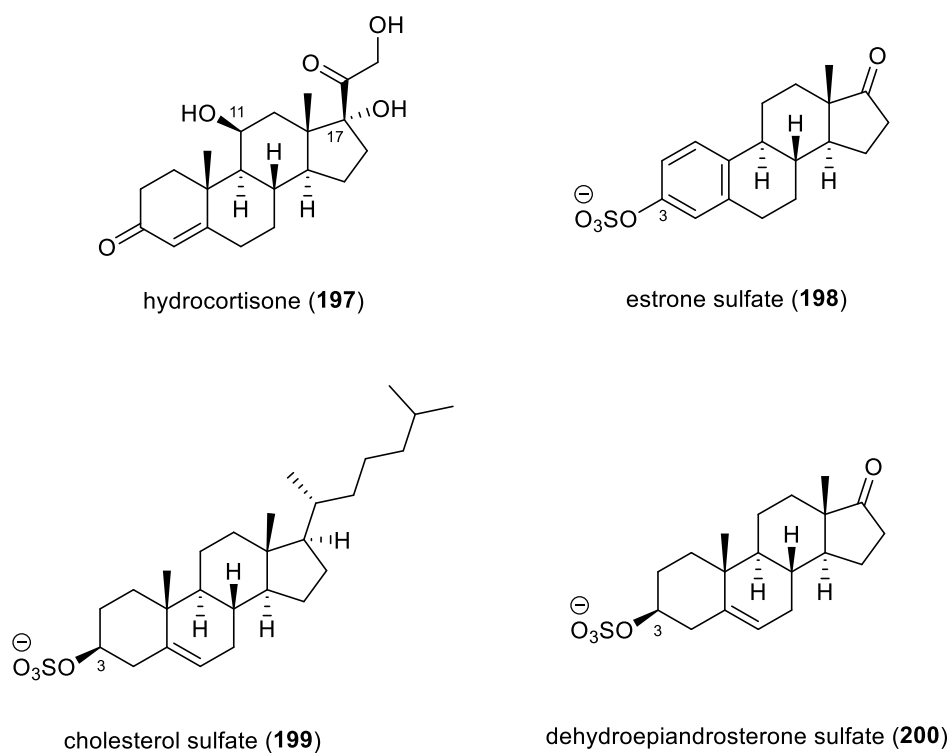


Figure 40: Chemical modifications of some steroids, including hydroxylation of cortisone (**197**), sulfation of estrone (**198**), cholesterol (**199**), and dehydroepiandrosterone (**200**).²¹²⁻²¹³

5.2. Sulfation pathway of steroids

Sulfation of steroids is one of the most well-known conjugation reactions in the liver. Sulfation increases the hydrophilicity of steroids and therefore facilitates their excretion from the body.^{32, 214-215} Many studies have described the association of sulfated steroids with a wide range of diseases and biological applications.²¹⁶ For example, cholesterol-3-sulfate has been connected to a number of biological functions such as regulation of cholesterol synthesis, plasmin and thrombin activities, and activation of protein kinase C.²¹⁶⁻²¹⁷ Furthermore,

marine-derived sulfated steroids have different applications, including as anti-microbial, anti-cancer, and anti-hypertensive agents.²¹⁸⁻²¹⁹

5.3. Chemical sulfation methods of steroids

Due to the growing interest of sulfated biomolecules and their important biological roles in the body, there is a need to find applicable methods to prepare sulfated steroids.^{142, 215, 220-222}

Generally, the sulfation reaction of steroids takes place at the hydroxyl groups of the steroidal skeleton. The chemical sulfation reaction is challenging due to the incorporation of highly polar sulfate group into a steroid making the synthesis and the purification even more difficult.²²³ Therefore, several studies suggested that the *O*-sulfation step should be carried out as the final step of a synthesis.^{46-47, 149, 223} Current methods to access sulfated steroids are classified into two main categories. First, the use of a sulfur trioxide equivalent such as chlorosulfonic acid (ClSO₃H) or sulfur trioxide amine complexes e.g. Et₃N•SO₃ and Py•SO₃, followed by a solid-phase extraction (SPE) approach for purification (**Scheme 62**).²²⁴⁻²²⁵

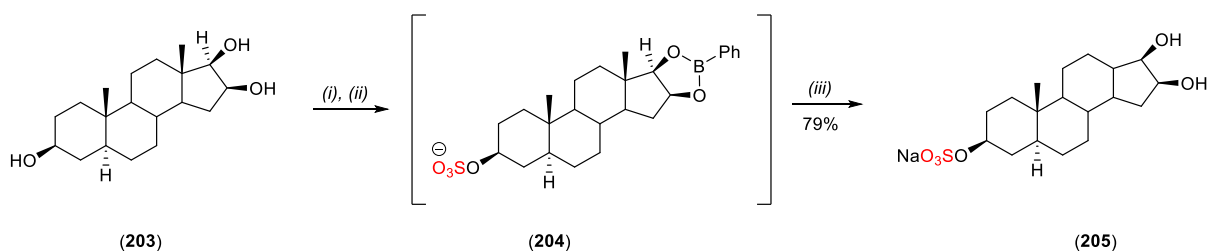


Scheme 62: Chemical sulfation methods using sulfur trioxide equivalents, including ClSO₃H, Et₃N•SO₃, and Py•SO₃, followed by SPE approach to access steroid sulfates.^{142, 224-225}

A second method involves the use of protected sulfate groups such as neopentyl- and isobutyl-protected sulfate esters followed by a deprotection step (See **Chapter 1, Scheme 24**).

Hungerford and co-workers reported the regioselective sulfation of 17 α -methylandrostanetriols using Py•SO₃ applying phenylboronic acid protection strategy.²²⁵⁻²²⁶ This approach was

initiated with the protection reaction of 16,17-diol (**203**) using phenylboronic acid followed by the selective sulfation reaction of 3 β -hydroxy steroid substrate using Py•SO₃ complex. Next, the oxidative phenylboronate deprotection with hydrogen peroxide (H₂O₂) resulted in the formation of the desired sodium-3-sulfate 17 α -methylandrostande (**205**) in 79% yield (**Scheme 63**).²²⁵



Scheme 63: The regioselective sulfation of 17 α -methylandrostande triols. **Conditions:** (i) PhB(OH)₂, DMF, CH₂Cl₂, 4 Å mol. Sieves; (ii) Py•SO₃, DMF; and (iii) H₂O₂, aq. NaHCO₃, THF, MeOH.²²⁵

Despite the success of existing sulfation methods, there remain issues, including the additional steps of protection, deprotection, solubility issues, and/or extensive SPE ion-exchange purification cascades.²²⁴

Our interest in the sulfation area stemmed from the development of tributylsulfoammonium betaine (TBSAB) and its application as a convenient one-pot method for the sulfation of heteroatom-containing molecules.^{46-47, 149, 227} This approach was introduced due to the challenges encountered with the purification of sulfated small-molecule heparin sulfate glycomimetics using conventional, sulfation methods.^{158, 228-231} TBSAB has a significant advantage over similar amine-sulfur trioxide complexes (e.g., Me₃N•SO₃) in that the counterion is lipophilic, making the sulfated scaffolds more suitable for isolation and purification using non-aqueous methods and avoiding the need for ion-exchange chromatography.

In this chapter, the use of TBSAB as a general, scalable and regioselective sulfating reagent was investigated for the sulfation of selected steroids. Furthermore, the application of TBSAB alongside isotopic labelling for steroidal-organosulfate reference standards was investigated.

5.4. Results and Discussion

5.4.1. Optimisation and control studies

Elements of this chapter have been published in *Frontiers in Molecular Biosciences* as: Alshehri JA, Gill DM, Jones AM. A Sulfuryl Group Transfer Strategy to Selectively Prepare Sulfated Steroids and Isotopically Labelled Derivatives. *Front Mol Biosci.* 2021 Dec 24; 8:776900. doi: 10.3389/fmolb.2021.776900.⁵⁵

The use of TBSAB was effective on a range of small organic molecules such as benzyl alcohol, benzylamine, α -amino acid, and glycomimetics.^{46-47, 149, 158} This study was initiated based on an early screening result of TBSAB, including a single example on β -estradiol by Dr Daniel Gill (PhD, University of Birmingham, 2020).^{149, 157} It was decided to further explore this methodology and prepare a diverse range of sulfated steroid scaffolds using TBSAB.

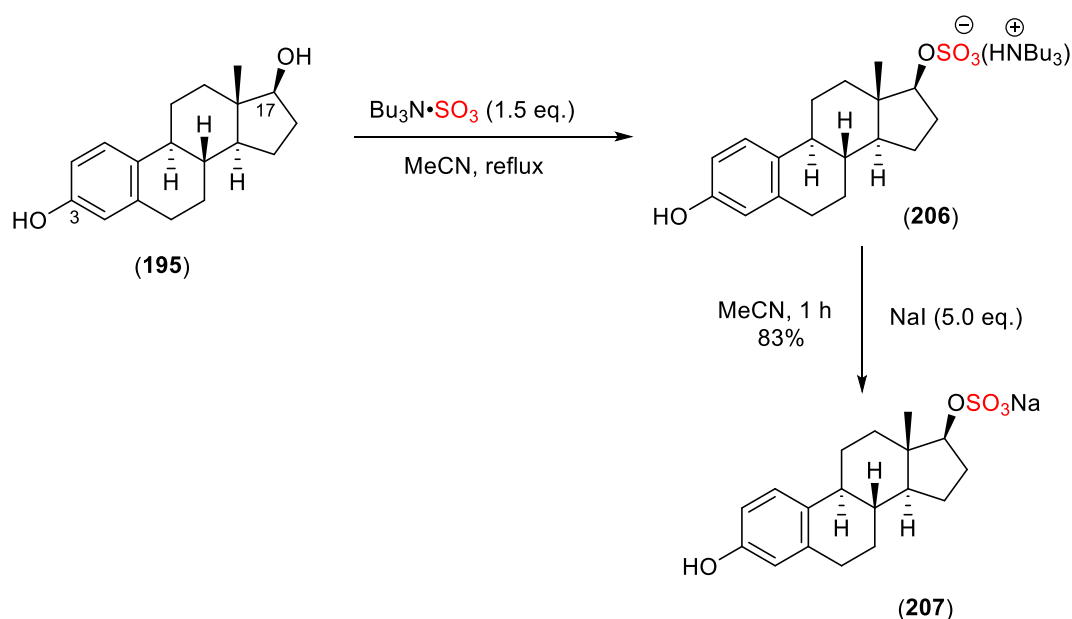
The sulfation reaction of a steroid was optimised using different stoichiometric ratios of the steroid substrates as well as TBSAB. It was also proposed to investigate whether isolating the resulting intermediate as its Na^+ salt was possible. Therefore, the organosulfate $[\text{Bu}_3\text{NH}]^+$ species would be subjected to ion-exchange with sodium salts, NaI or NEH, to afford the desired sodium steroid sulfate molecules.¹⁴⁹

5.4.2. Preparation of selected steroid sulfates using TBSAB

The reaction conditions were optimised on a 1.0 mmol of an appropriate steroid with TBSAB (1.2-5.0 eq.) under inert conditions. The reaction was carried out under reflux for a period

ranging between 2-7 h. After the completion of the reaction, the tributylammonium intermediate was subjected to sodium exchange using NaI or NEH (2.5-5.0 eq.) affording the desired steroid sulfates.

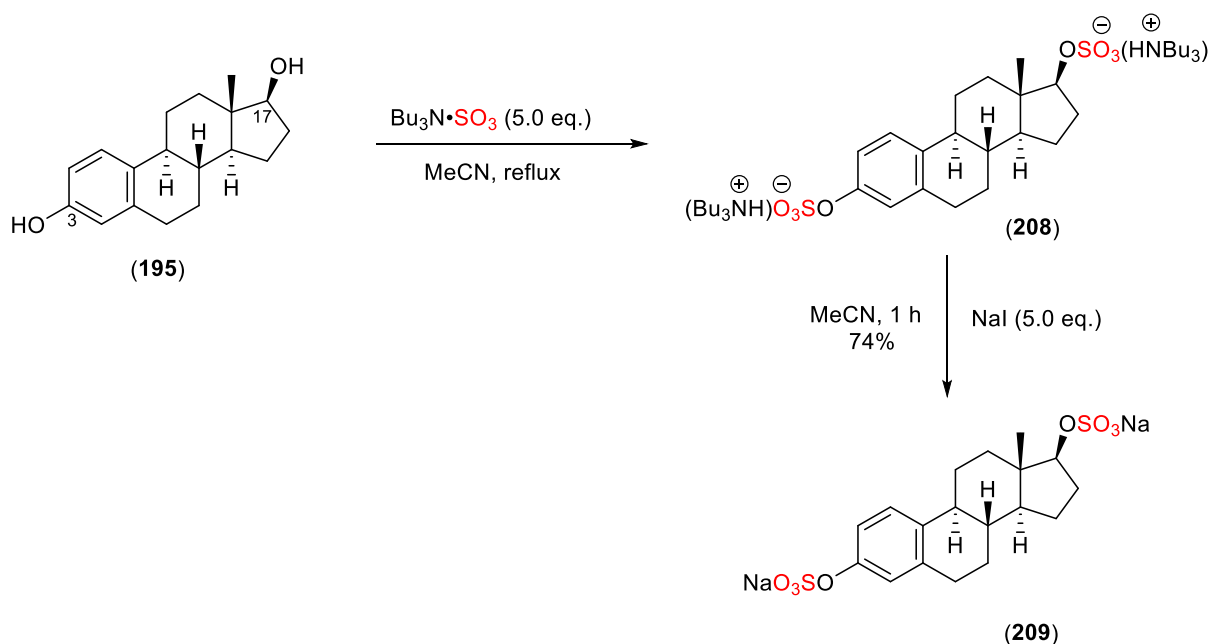
The reproducibility of this method on a 1.0 mmol scale was explored with the commercially available 17 β -estradiol (**195**). The regioselective sulfation of this steroid gave selective sulfation on C17, affording the tributylammonium sulfate intermediate (**206**). This was followed with sodium salt exchange using NaI to give 17 β -estradiol sulfate (**207**) over the more common metabolite 3 β -estradiol in 83% isolated yield as the Na⁺ salt over the two steps. Compound (**207**) was confirmed by ¹H NMR spectroscopy due to the presence of phenolic OH (C3) signal at (9.01 ppm) and C17 signal was found at (4.77 ppm) (**Scheme 64**).



Scheme 64: The regioselective sulfation of 17 β -estradiol (**195**) affording the 17 β -estradiol sulfate (**207**) as the sodium salt using TBSAB analysed by ¹H NMR spectroscopy (300 MHz, DMSO-*d*₆) and mass spectrometry.

Using a super stoichiometric equivalence of TBSAB (5.0 eq.) resulting in the double sulfation of 17 β -estradiol at both C17 and C3 positions (**208**) which presumably happens via a step-wise initial C17 alcohol sulfation followed by C3 sulfation. The resulting intermediate (**208**)

was treated with NaI to give the desired disodium-3,17 β -estradiol disulfate (**209**) in 74% isolated yield over the two steps (**Scheme 65**).

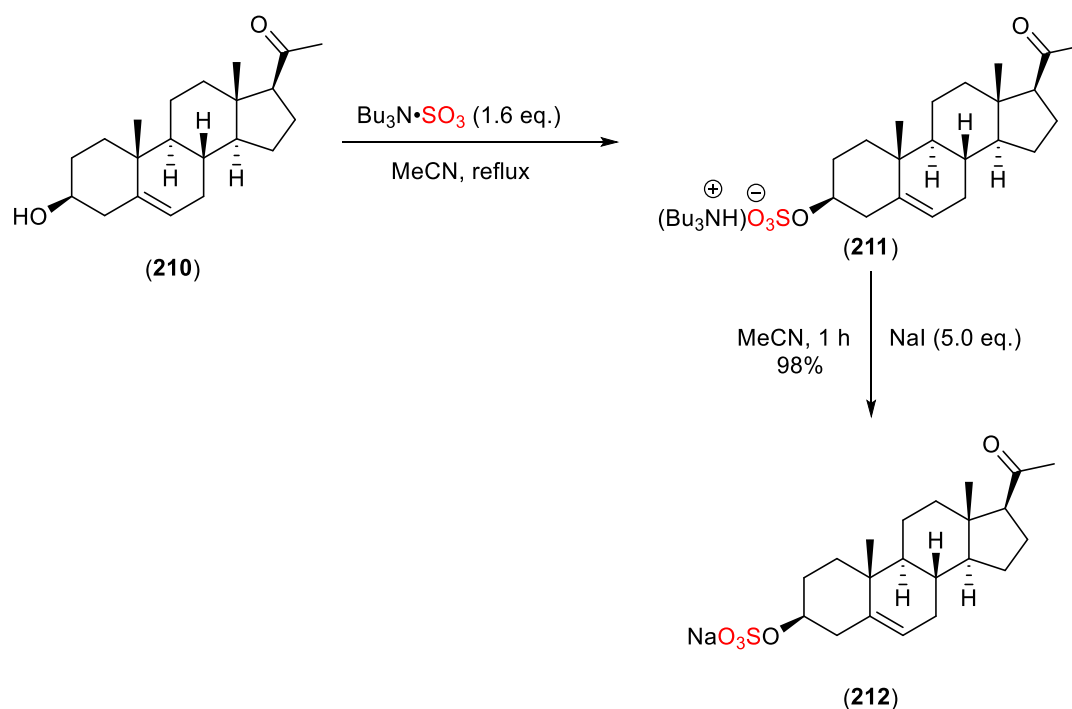


Scheme 65: The dual sulfation of 17 β -estradiol (**195**) using TBSAB afforded the disodium-3,17 β -estradiol disulfate (**209**) in 74% isolated yield.

Several studies have demonstrated that steroid sulfates such as 17 β -estradiol sulfate derivatives are less biologically active due to the incorporation of sulfate group.²³² However, 17 β -estradiol sulfate has biological functions including as a neuroprotective and immune modulator agent and as an important precursor for the biologically active 17 β -estradiol.²³³⁻²³⁵ Wang and co-workers reported the physiological importance of 17 β -estradiol sulfate (**207**) in preventing pre-eclampsia, a disease that affects some women during pregnancy, characterised by elevated blood pressure, proteinuria, severe headache, and swelling of the feet, ankles, face and hands.²³⁶⁻²³⁷ Other studies have reported the high concentrations of estrogen sulfates such as estradiol-3-sulfate in breast tissue and their role in the development of breast cancer.²³⁸⁻²⁴⁰ Estradiol-3-sulfate can be desulfated by sulfatase enzymes into the biologically active estradiol, which also plays a role in breast cancer.²⁴⁰

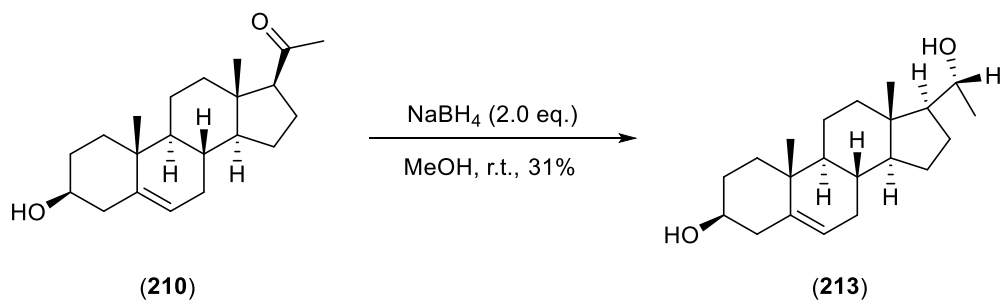
Next, the sulfation of a biologically active steroid, pregnenolone was explored. Pregnenolone is a neurosteroid that can modulate and activate ion channels, transporters, and some neurotransmitter receptors such as *N*-methyl-*D*-aspartate receptor (NMDA), a glutamate-gated cation channel found in the central nervous system.²⁴¹⁻²⁴² Pregnenolone and its metabolites such as pregnenolone sulfate are associated with learning and memory processes, depression relief, and are important modulators for the cognitive functions of the brain.²⁴³ They also have a neuroprotective role in different conditions for instance, Alzheimer's disease, multiple sclerosis, schizophrenia, depression, and autism.²⁴³⁻²⁴⁶ More recently, it was discovered that pregnenolone sulfate activates the transient receptor potential (TRPM3) channel which is associated with rapid calcium influx and enhanced insulin secretion from pancreatic islets.^{241, 247}

An initial attempt to sulfate pregnenolone (**210**) was explored on a 0.3 mmol scale following the optimised conditions for the sulfation of β -estradiol. Pregnenolone (**210**) was reacted with TBSAB, affording the tributylammonium ion intermediate (**211**), which was subsequently exchanged with sodium iodide affording sodium-3-pregnenolone sulfate (**212**) in an excellent 98% isolated yield over the two steps (**Scheme 66**).



Scheme 66: Synthesis of sodium-3-pregnenolone sulfate using TBSAB.

Next, pregnenolone (**210**) was reduced using sodium borohydride (NaBH_4) which afforded the pregnanediol (**213**) in 31% isolated yield. The diastereoselective reduction of the ketone group of (**210**) involves the transfer of hydride ion (H^-) from sodium borohydride (NaBH_4) to the ketone moiety affording the formation of the secondary alcohol (**Scheme 67**). Diastereoselectivity in the reduction of ketones with NaBH_4 depends on the steric and electronic environment around the carbonyl group. This reaction shows a degree of diastereoselectivity, depending on whether the hydride attacks from the top side or bottom side of the steroidal backbone. However, the observed 31% isolated yield suggested that the reaction is not completely diastereoselective, as a mixture of diastereomers may form, but only one diastereomer was isolated as confirmed by ^1H NMR spectroscopy. X-ray crystallography confirmed a single diastereomer of (*R*)-pregnanediol (**213**).



Scheme 67: The diastereoselective reduction of pregnenolone using sodium borohydride (NaBH₄)

This hydride attack can occur from both sides, the less hindered top side (methyl group) or more hindered bottom side (steroidal skeleton) of pregnenolone (**Figure 41**).

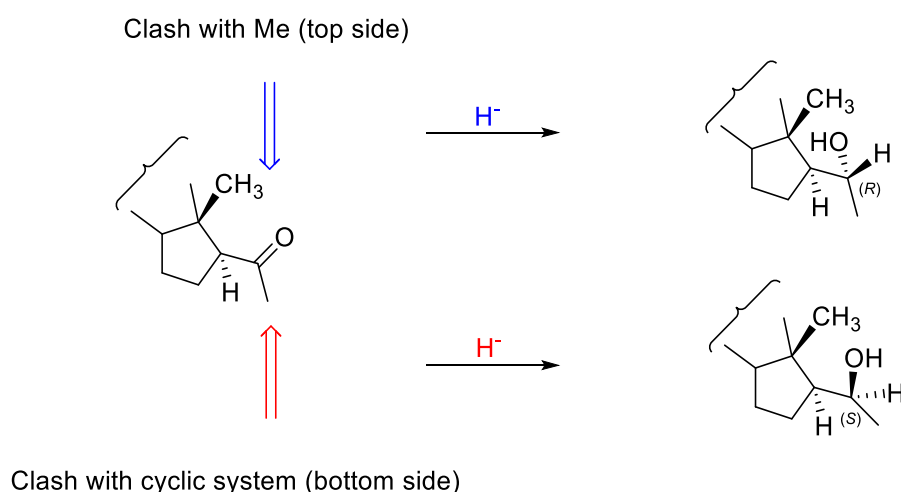


Figure 41: Explanation of hydride ion attack of ketone moiety in pregnenolone from top (Me) and bottom (steroid cyclic frame) sides. The relative stereochemistry of (213) was confirmed by X-ray crystallography as (*R*).

The absolute structure of pregnanediol was confirmed by both ¹H and ¹³C NMR spectroscopic data, mass spectrometric data and the X-ray crystallographic data of the bulk material from d₆-DMSO crystallisation supports the assignment of the major diastereomer as (*R*) at the newly set stereocentre. Furthermore, a patent matches our stereochemical assignment of pregnanediol (213) as the (*R*) isomer at the newly set stereocentre (This patent was filed by China Agricultural University (CN112939732) in 2021) (**Figure 42**, see Appendix for full data).

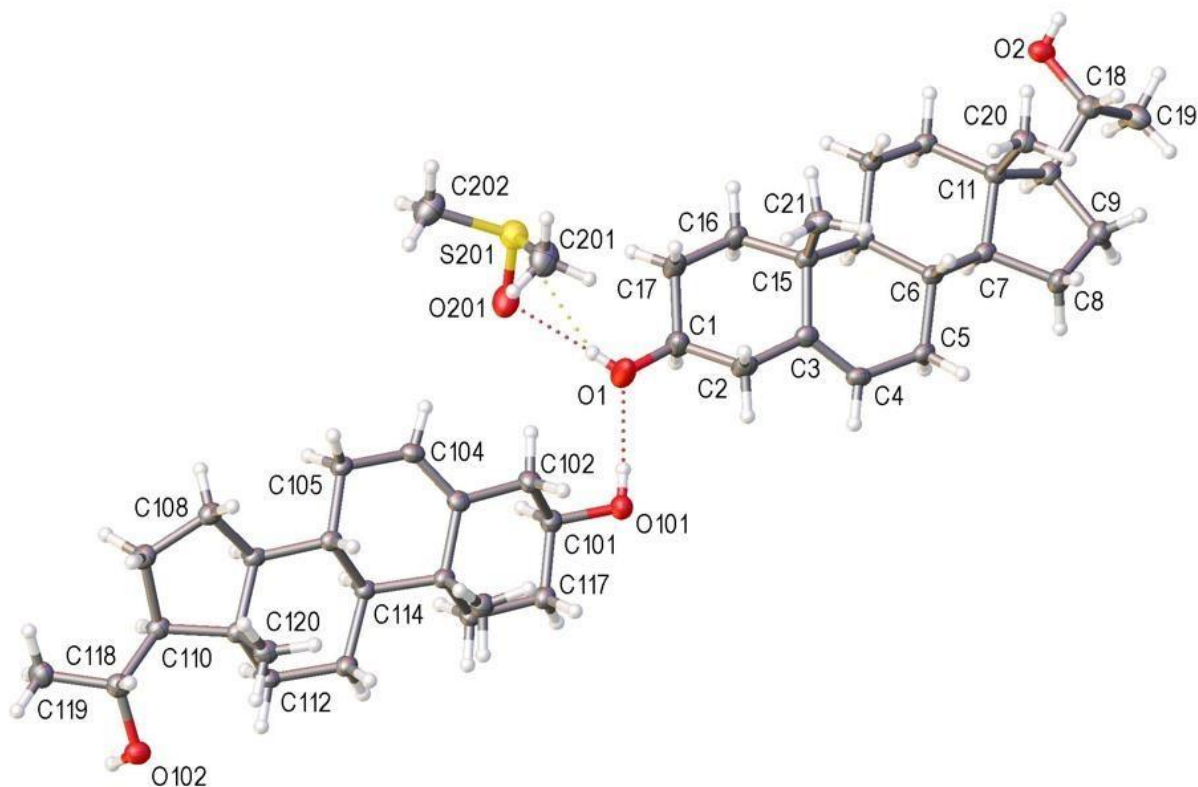
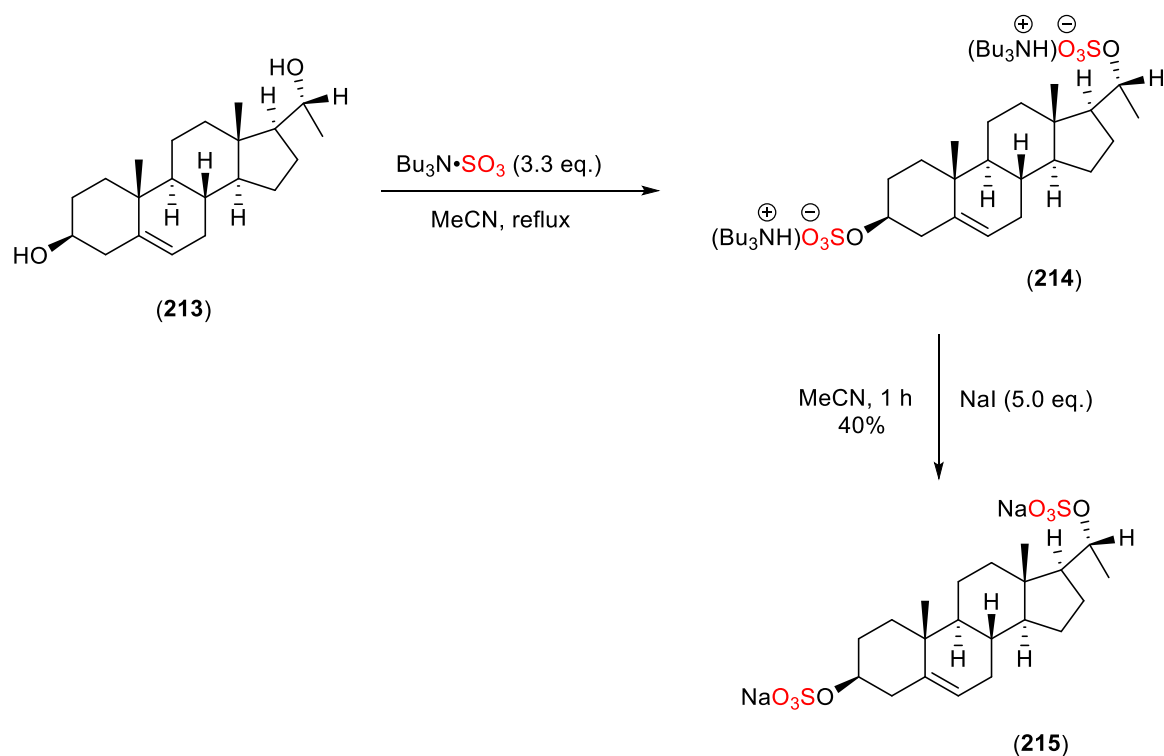


Figure 42: The absolute structure of pregnanediol (**213**) confirmed by both ^1H and ^{13}C NMR spectroscopic and the crystal structure of pregnanediol (**213**), obtained from small molecule single crystal X-Ray diffraction. Ellipsoids drawn at the 50 % probability level. Hydrogen bonding within the asymmetric unit is shown using dotted lines. (Crystal structure solved by Dr L. Male, and CCDC number 2120263).

Next, pregnanediol (**213**) was sulfated using TBSAB following the optimised condition of 17β -estradiol. It was assumed that the sulfation occurs in a step-wise process, initially at C17 hydroxyl group followed by C3 sulfation, affording the intermediate (**214**). The resulting intermediate (**214**) was subjected to sodium salt exchange using NaI (5.0 eq.) affording the disodium-3,17-pregnanediol disulfate (**215**) in a modest 40% isolated yield over the two steps (**Scheme 68**).

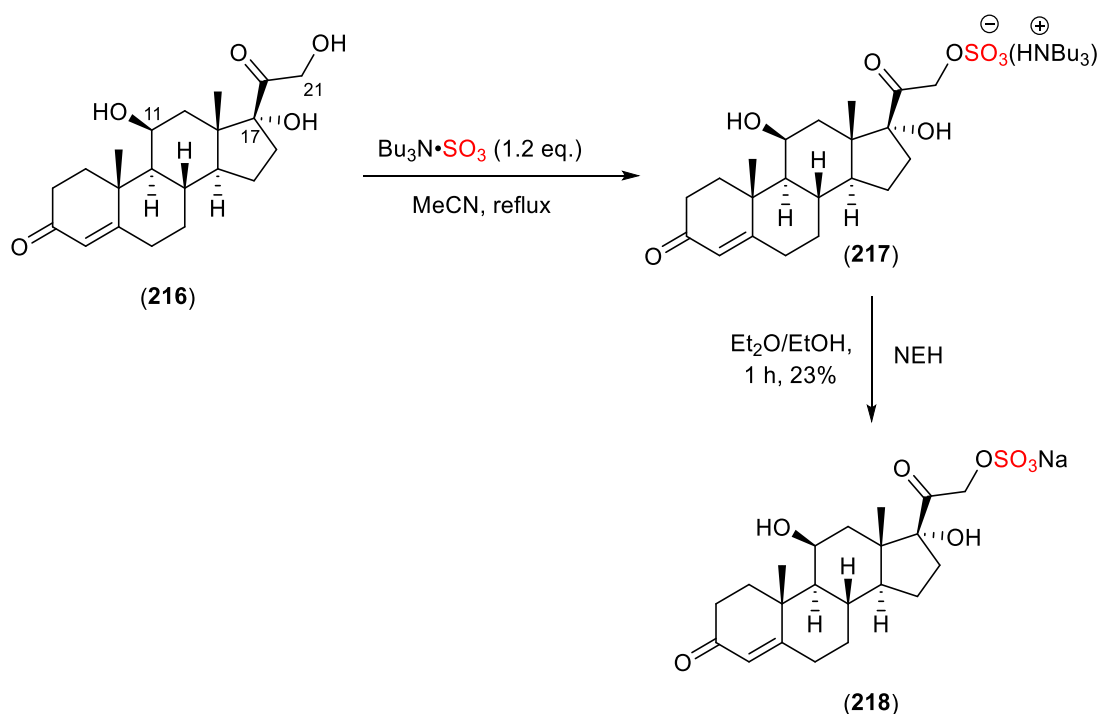


Scheme 68: Dual sulfation reaction of pregnanediol using TBSAB.

Next, the optimised method was investigated on a more complex steroid example, cortisol, which was synthesised by Dr Daniel Gill.¹⁵⁷ Cortisol (**216**) has three potentially reactive hydroxyl groups at C11, C17 and C21 positions. Among these three hydroxyl groups, the primary alcohol at C21 position would be the most favourable site for sulfation as it is less sterically hindered compared to the secondary alcohol group at C11 and the tertiary alcohol group at C17 and therefore more accessible for the sulfation reaction. Furthermore, the presence of the ketone in cortisol may have an electronic effect on the proximal alcohols at C17 and C21. This would decrease the electron density at the C21 oxygen atom resulting in decrease of its nucleophilicity, making it less reactive towards the sulfating reagent, TBSAB.

The sulfation reaction of cortisol (**216**) and TBSAB was carried out on a small scale (0.1 mmol), affording C21 organosulfate intermediate (**217**). The resulting intermediate was exchanged with NEH to give the desired sodium-21-cortisol sulfate in a low 23% overall yield as the

sodium salt (**218**) over the two steps. The low yielding of sodium-21-cortisol sulfate was attributed to the presence of unreacted cortisol (40%) and suspected intermediate (**217**) (not characterised). The crude mixture was purified by chromatography (SiO_2) which might lower the overall yield of the desired molecule. Notably, C11 or indeed C17 sulfate ester formation was not observed confirmed by ^1H NMR spectroscopy and mass spectrometry analysis as the chemical shift of both C11 and C17 remained at (4.26 ppm) and (5.31 ppm), respectively (**Scheme 69**).

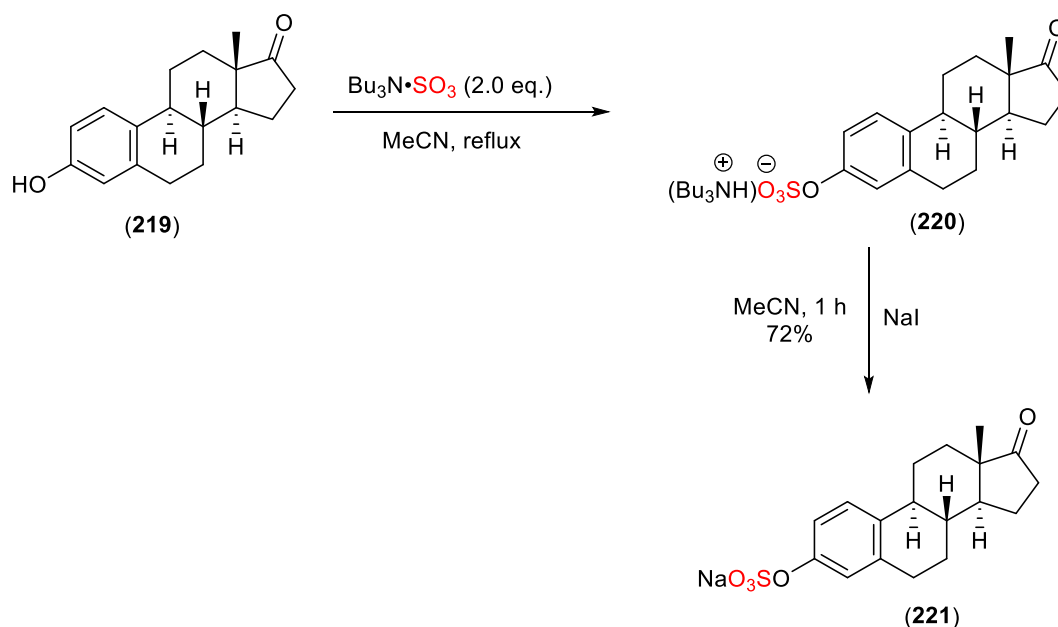


Scheme 69: The regioselective sulfation reaction of cortisol using TBSAB.

Finally, an isotopically labelled, chemoselective sulfation strategy for estrone was investigated as a proof of concept due to estrone's main skeleton structure being present in many biologically active steroids such as estrogen hormones. Generally, isotopic labelling of steroids involves the incorporation of stable non-radioactive isotopes such as deuterium (^2H) into the structure of steroid molecules.²⁴⁸ This labelling technique has been a valuable tool for a variety of research and analytical applications, including metabolic studies,

pharmacokinetics, and anti-doping testing.²⁴⁸ Furthermore, isotopically labelled steroids are used as internal standards for mass spectrometry studies where the labelled and unlabelled steroids are structurally identical with an exception of the presence of heavier isotope label like (²H).²⁴⁸ So, the isotopically labelled steroid will have different mass compared to the original steroid when added to a biological sample.²⁴⁸ Also, the isotopic labelling of steroids could also be a beneficial tool for detecting steroid abuse especially in athletes.^{225, 248}

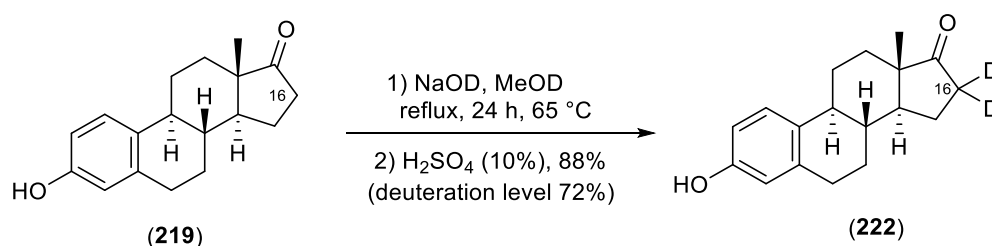
Before the installation of a deuterium (²H) label into the structure of estrone at the C16 methylene position, the sulfation of estrone (**219**) was carried out using TBSAB. The sulfation reaction of estrone with TBSAB was carried out in a 1:2 stoichiometric ratio and the organosulfate intermediate (**220**) was afforded followed by the reaction with sodium iodide to give sodium-3-β-estrone sulfate (**221**) in 72% isolated yield over the two steps (**Scheme 70**).



Scheme 70: Sulfation reaction of estrone using TBSAB.

The formation of estrone-d₂ was adapted from the method of Rudqvist for C19 steroid monosulfates at either hydroxylated carbons or the methylene position.²⁴⁹ Estrone (**219**) was

treated with sodium deuterioxide (NaOD) and deuterated methanol (CD₃OD) resulting in the formation of estrone-d₂ (**222**). The C(16)-H₂ protons were selectively deuterated by enolate formation with sodium deuterioxide and resultant deuterium incorporation by quenching the enolate with MeOD.²⁵⁰ Next, sulfuric acid (H₂SO₄) was added to neutralise the reaction mixture after the completion of deuteration process however the use of D₂SO₄ was avoided due to prevent unwanted deuteration of the phenolic OH group at C3 position (**Scheme 71**).²⁵⁰



Scheme 71: The formation of estrone-d₂ (the procedure was adapted from the literature)²⁵⁰

The deuteration site was confirmed by ¹H and ¹³C NMR spectroscopic analysis. After the deuteration of estrone, a 72% level of ²H₂ deuterium incorporation was validated by ¹H NMR spectroscopy analysis due to the partial disappearance of C(16) signals at 2.48–2.37 (m, 1H, C16-H) and 2.04 (dd, *J* = 18.8, 8.9 Hz, 1H, C16-H) indicating that ²H₂ was present at this location. Also, the comparative 2D COSY ¹H-¹H NMR data of estrone and estrone-d₂ confirmed the disappearance of diastereotopic C16 signals (**Figure 43 & 44**).

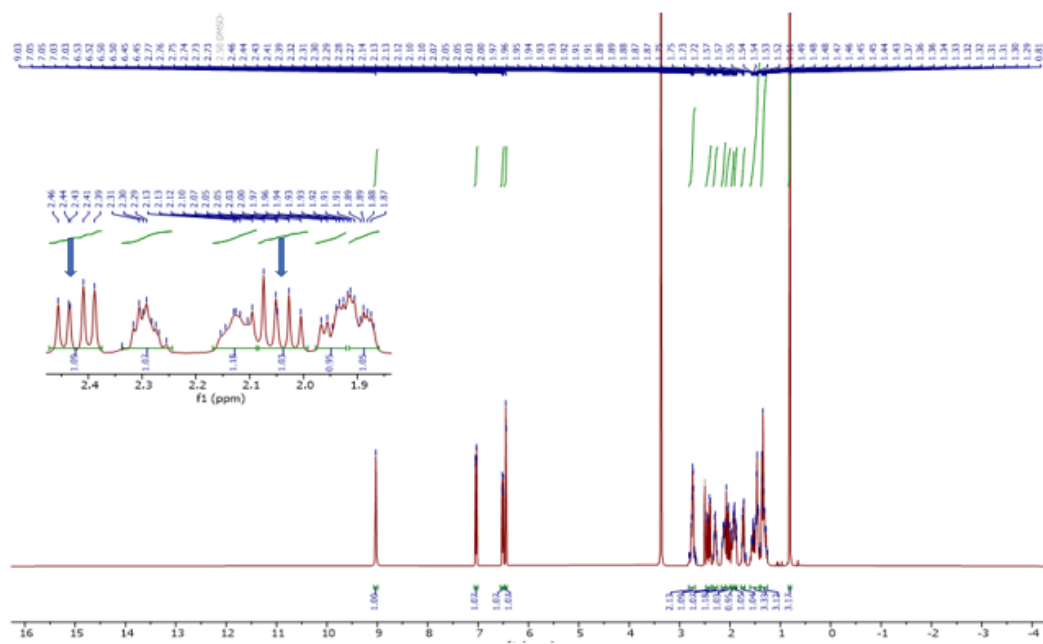


Figure 43: ^1H NMR spectrum (400 MHz, $\text{DMSO-}d_6$) of non-deuterated estrone (**219**). Blue arrows highlight the diastereotopic C16 protons.

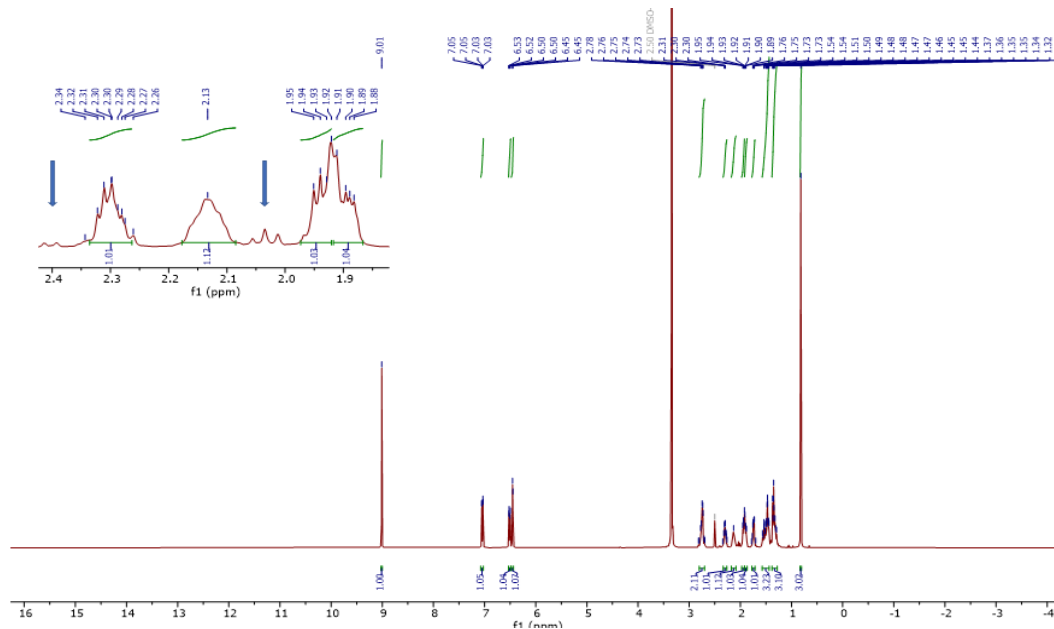


Figure 44: ^1H NMR spectrum (400 MHz, $\text{DMSO-}d_6$) of deuterated estrone(d_2) (**222**). Blue arrows highlight the 72% depletion of the diastereotopic C16 protons compared to estrone.

The disappearance of the key diastereotopic C16 protons can be clearly observed in the ^1H -NMR spectral overlay (**Figure 45**).

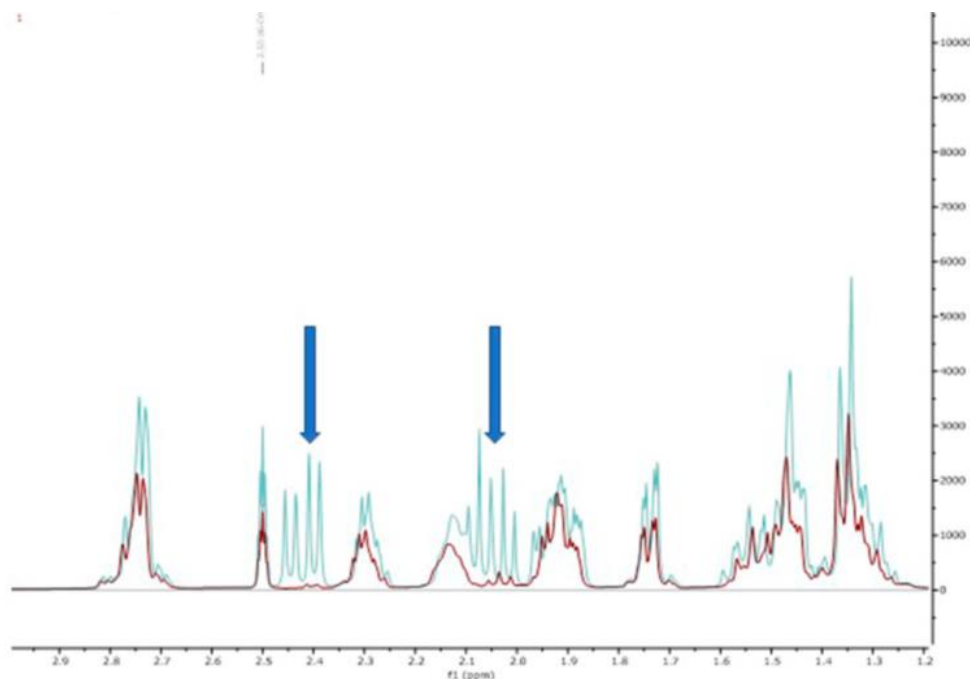
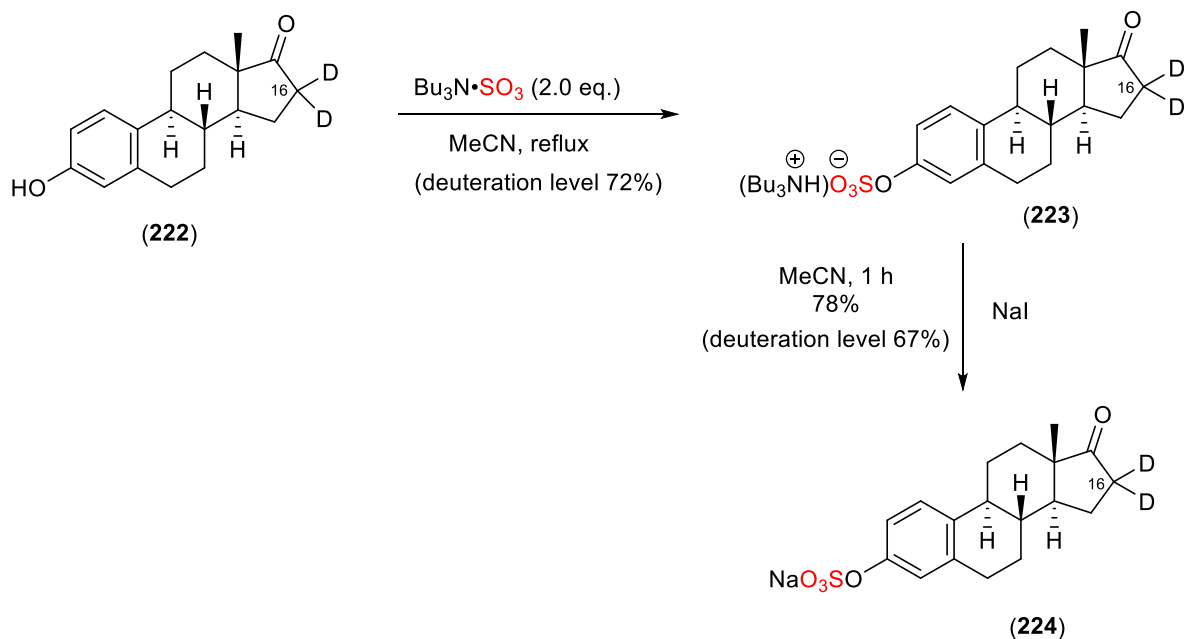


Figure 45: Overlay of ^1H NMR spectra (400 MHz, $\text{DMSO-}d_6$) of estrone (blue, **219**) and estrone- d_2 (red, **222**) shows the diagnostic depletion of the diastereotopic C16 protons.

The mass spectrometric data for the isotopically labelled estrone (estrone- d_2) demonstrated the mass differences between unlabelled estrone (**219**) and estrone- d_2 (**222**) due to the incorporation of a heavier isotope (^2H). However, the deuteration site next to the carbonyl group is not usually recommended for applied quantification studies as the deuterium label can readily back exchange through a keto-enol tautomerisation leading to loss of the label.²⁵¹ In our system this was observed, a decrease of the deuterium label in solution-based mass-spectrometry studies was noted with a 72% deuteration.

Finally, estrone- d_2 (**222**) was sulfated using TBSAB which resulted in the organosulfate intermediate (**223**) which was then subjected to sodium exchange using NaI affording the desired sodium estrone- d_2 sulfate (**224**) in 78% isolated yield over the two steps with a 67% deuteration level (**Scheme 72**).



Scheme 72: The sulfation reaction of estrone-d₂ (**222**) with TBSAB to afford sodium estrone-d₂ sulfate (**224**).

The observed mass spectrometric data showed different peaks of sodium estrone-d₂ sulfate compared to undeuterated estrone-d₂ sulfate indicating that the mass of 351.1243 corresponds to sodium estrone-d₂ sulfate (100%) compared to undeuterated sodium estrone sulfate, 349.1107 (10%) amongst other components (**Figure 46**).

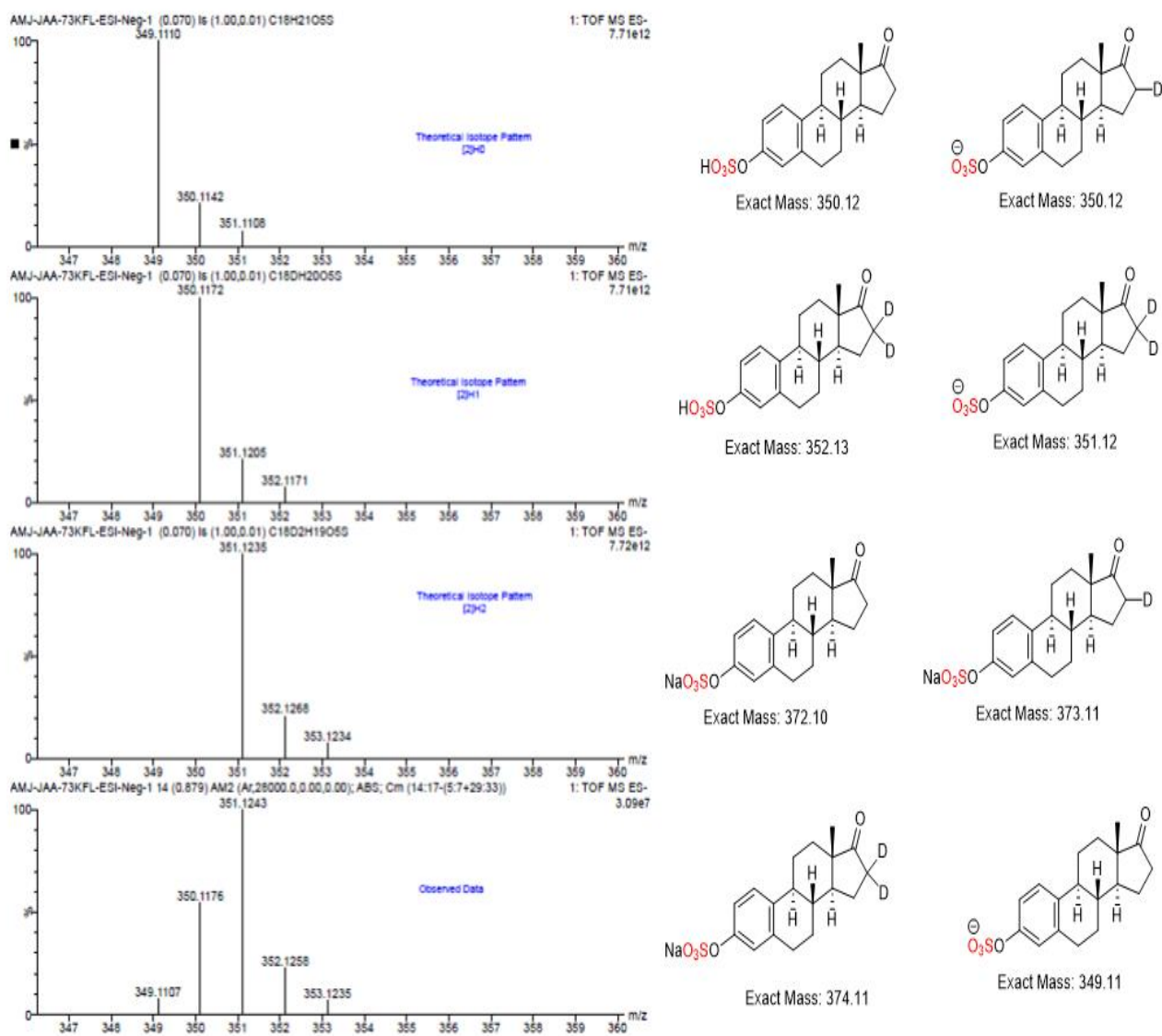


Figure 46: Mass spectrometric theoretical versus observed deuteration levels for sodium estrone-d₂ and estrone-d₁ sulfates.

5.5. Conclusion

In summary, this study presents a robust and scalable methodology for the selective sulfation of steroids, employing TBSAB as a sulfating reagent. This method was effective for the chemoselective sulfation of the selected steroids. A suitable method for the preparation of mono- and di-sulfated steroidal skeletons of importance to the fields of biology and spectrometric analysis was achieved. This approach was successfully applied to estrone, estradiol, cortisol, and pregnenolone, yielding biologically relevant sodium steroid sulfates without the need for complex ion-exchange chromatography. The developed strategy also extends to isotopically labelled derivatives, specifically the sulfation of deuterated estrone (estrone-d₂). The incorporation of the deuterium label would facilitate mass spectrometric quantification for biological studies. Despite the challenges associated with deuterium loss through keto-enol tautomerization, the study achieved substantial retention of the isotopic label (67%), enabling a proof of concept approach.



A Sulfuryl Group Transfer Strategy to Selectively Prepare Sulfated Steroids and Isotopically Labelled Derivatives

Jaber A. Alshehri, Daniel M. Gill and Alan M. Jones*

Molecular Synthesis Laboratory, School of Pharmacy, Institute of Clinical Sciences, University of Birmingham, Edgbaston, United Kingdom

The treatment of common steroids: estrone, estradiol, cortisol, and pregnenolone with tributylsulfoammonium betaine (TBSAB) provides a convenient chemoselective conversion of the steroids alcohol/phenol moiety to the corresponding steroidal organosulfate. An important feature of the disclosed methodology is the millimolar scale of the reaction, and the isolation of the corresponding steroid sulfates as their biologically relevant sodium salts without the need for ion-exchange chromatography. The scope of the method was further explored in the estradiol and pregnanediol steroid systems with the bis-sulfated derivatives. Ultimately, a method to install an isotopic label, deuterium (^2H) combined with estrone sulfation is a valuable tool for its mass-spectrometric quantification in biological studies.

Keywords: sulfation, selectivity, isotopic labelling, sulfuryl transfer, TBSAB

INTRODUCTION

The preparation of authentic reference samples of sulfated steroids with either regioselective mono or disulfation patterns, (Lightning et al., 2021) combined with methods to isotopically label the resulting sulfated steroids is an ongoing challenge to their biological study. The resulting authentic sulfated steroids are key reference standards of paramount importance to the understanding of sulfatases (Mueller et al., 2015), (Günel et al., 2019), (Foster and Mueller, 2018), the role of steroid sulfation in diseases (Mueller et al., 2021) and the fields of detection of steroids, whether in abuse (Waller and McLeod, 2014) or in the environment, (Petrie et al., 2013) using spectroscopic techniques (Hill et al., 2019). Furthermore, the development of improved sulfation methods can be applied to both sulfated steroid containing natural products synthesis and structural elucidation studies (Hoye et al., 2007).

Current methods to sulfate steroids fall into two main categories (**Chart 1**). The use of a protected sulfate group (e.g., isobutyl protected sulfate esters) with subsequent deprotection (Simpson and Widlanski, 2006), or the use of a sulfur trioxide equivalent (e.g., chlorosulfonic acid or pyridine-sulfur trioxide complex) (Waller and McLeod, 2014), (Hungerford et al., 2006). Although these methods are effective, they suffer from the additional steps of deprotection and/or purification cascades. Issues with toxicity regarding pyridine contamination from the use of pyridine-sulfur trioxide complex in related carbohydrate scaffolds (Gabriel et al., 2020), (Vo et al., 2021) requires either an exceptionally vigilant isolation and analysis; or an improved overall method for steroid sulfation.

Our own current interest in the sulfation field derives from the development of tributylsulfoammonium betaine (TBSAB) (Gill et al., 2019a), (Jones, 2021) as a convenient one-pot method for the sulfation of heteroatom containing bioactive molecules. (Benedetti et al., 2020), (Alshehri et al., 2020) This was initiated due to challenges encountered with the purification of sulfated small molecule heparin sulfate glycomimetics (Gill et al., 2021), (Gill et al., 2019b),

OPEN ACCESS

Edited by:

Tarsis G. Ferreira,
University of Houston, United States

Reviewed by:

Jozef Stec,
Marshall B. Ketchum University,
United States
Malcolm McLeod,
Australian National University,
Australia
Fernando Ogata,
Federal University of São Paulo, Brazil

*Correspondence:

Alan M. Jones
a.m.jones.2@bham.ac.uk

Specialty section:

This article was submitted to
Cellular Biochemistry,
a section of the journal
Frontiers in Molecular Biosciences

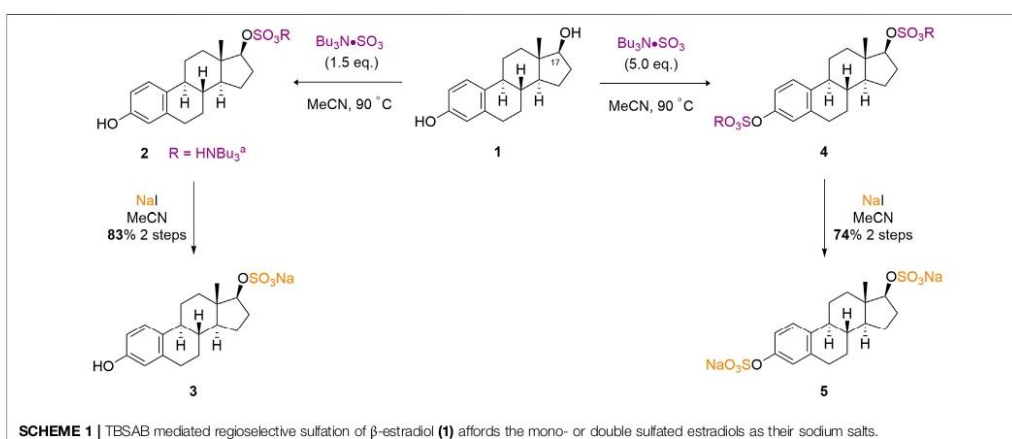
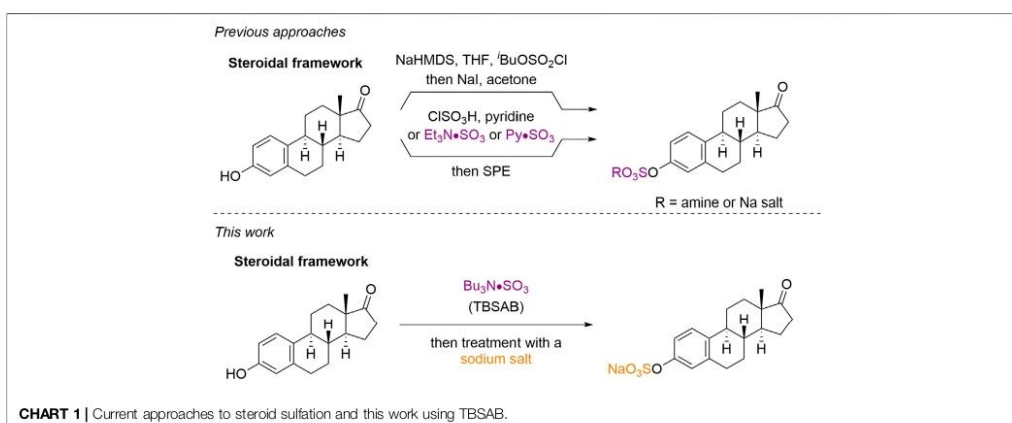
Received: 14 September 2021

Accepted: 15 November 2021

Published: 24 December 2021

Citation:

Alshehri JA, Gill DM and Jones AM
(2021) A Sulfuryl Group Transfer
Strategy to Selectively Prepare
Sulfated Steroids and Isotopically
Labelled Derivatives.
Front. Mol. Biosci. 8:776900.
doi: 10.3389/fmolb.2021.776900



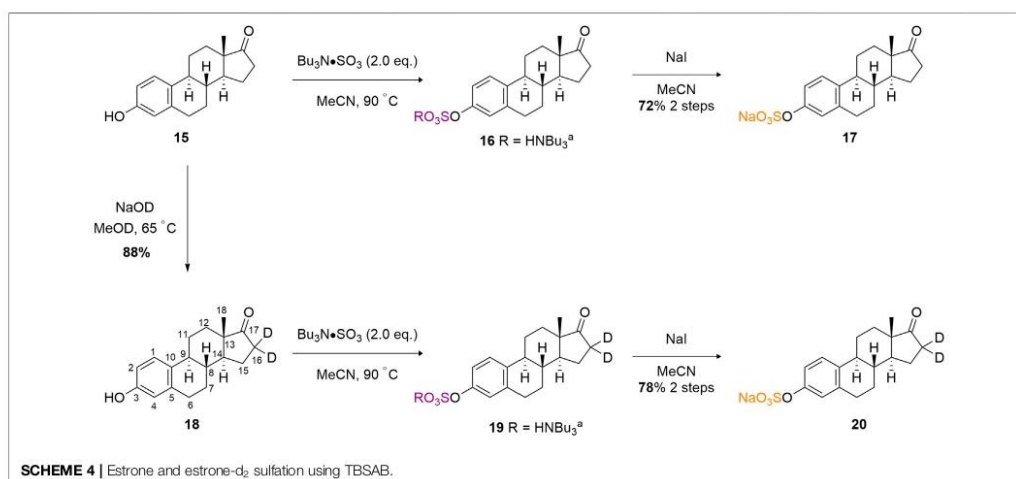
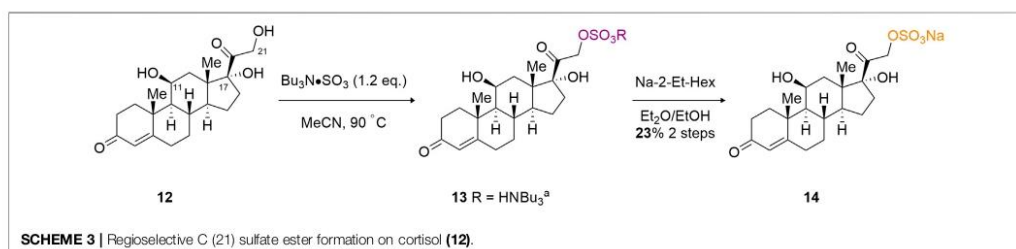
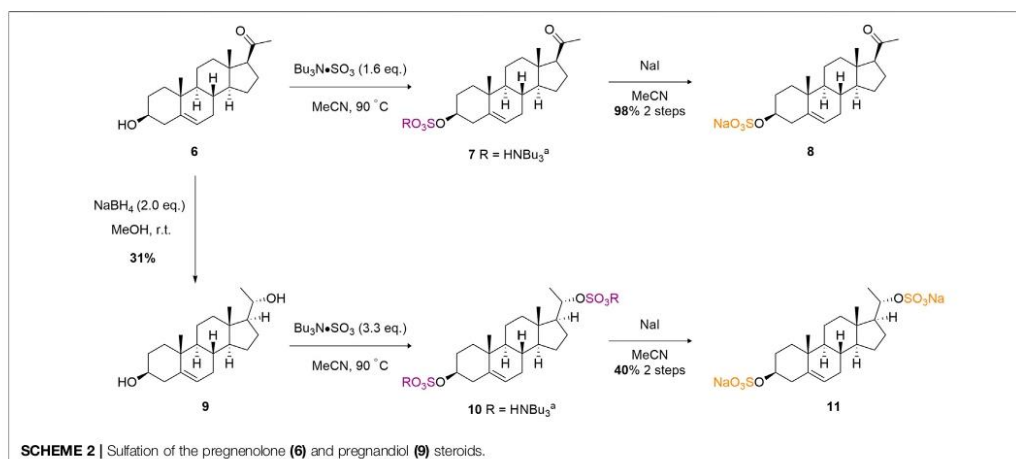
(Mahmoud et al., 2019), (Langford-Smith et al., 2019), (Mahmoud et al., 2017) with conventional, pre-existing sulfation methods. A key advantage of TBSAB over similar amine containing-sulfur trioxide complexes (e.g., triethylamine-sulfur trioxide) is the lipophilic nature of the counterion avoiding the need for ion-exchange chromatography. Herein we report our findings on the use of TBSAB as a general, scalable and regioselective sulfating reagent for steroids, and the application of TBSAB in conjugation with isotopic labelling for steroidal-organosulfate reference standards.

RESULTS AND DISCUSSION

Our initial exploration of the method builds upon early screening results of TBSAB, including a single example on β -estradiol (**1**) (Gill

et al., 2019a). We firstly sought to demonstrate the reproducibility of this method on a 1.0 mmol scale, thus taking commercially available β -estradiol (**1**) and treating it with TBSAB resulted in exclusive C (17), secondary alcohol, sulfation (**2**). Furthermore the same conditions using an excess of TBSAB resulted in both C (17) sulfation and C (3), phenol, sulfation of (**4**) presumably occurs via initial C (17) alcohol sulfation in a stepwise installation. In both cases, a work-up using sodium iodide isolated the mono (**3**) and double (**5**) sulfated steroids as their sodium salts, in good yields without the risk of pyridinium ion contamination (**Scheme 1**).

Next, we considered sulfation of a more challenging biologically active substrate, pregnenolone (**6**). (Harteneck, 2013). Under analogous conditions to the β -estradiol examples, and on a 0.3 mmol scale, steroidal sulfate **8** was afforded after sodium exchange in an excellent 98% isolated yield (**Scheme 2**). Diastereoselective reduction of the ketone



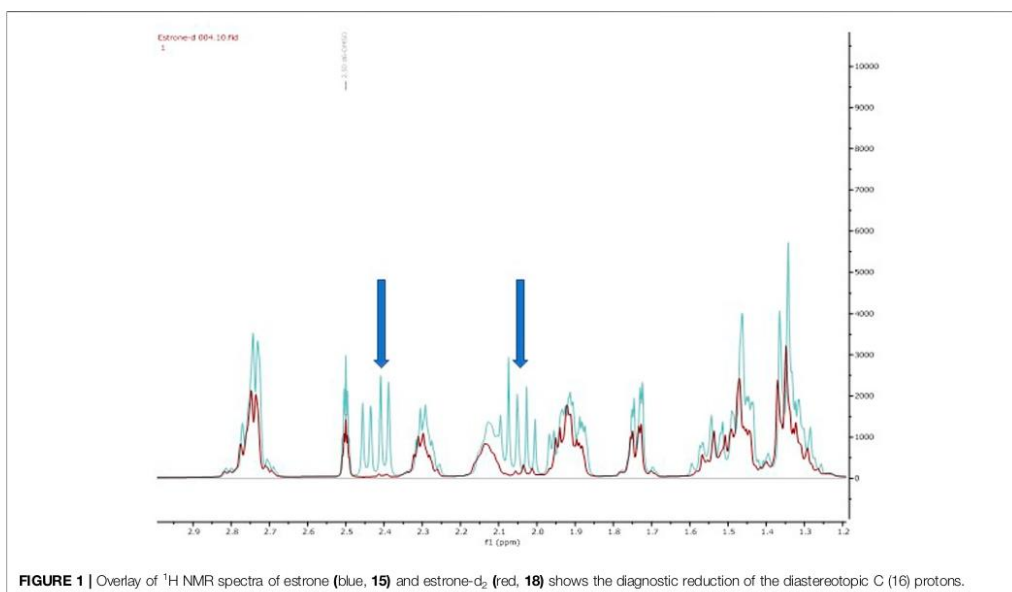


FIGURE 1 | Overlay of ^1H NMR spectra of estrone (blue, **15**) and estrone- d_2 (red, **18**) shows the diagnostic reduction of the diastereotopic C (16) protons.

moiety of pregnenolone using sodium borohydride afforded pregnanediol in 31% yield (**9**). Crystallographic data of the bulk material from d_6 -DMSO crystallisation supports the assignment of the major diastereomer as *R* at the newly set stereocentre (**Supplementary Figure S3**) (2120263 contain, 2120). As **9** contains two secondary alcohol motifs, treatment with TBSAB afforded the double sulfated pregnanediol (**11**) in a modest 40% isolated yield on a 0.6 mmol scale.

The ultimate test of the TBSAB method, in relation to regioselective sulfation, is the complex triol, cortisol (**12**) (**Scheme 3**). Cortisol contains three potentially reactive hydroxyl motifs at the C (11), C (17) and C (21) positions. It was anticipated that a regioselective sulfation of the primary C (21) alcohol would result over the C (11), secondary, or C (17), tertiary, alcohol moieties, despite the presence of the α -ketone affecting the reactivity of the C (21)-OH. To our delight, a microscale (8 mg) treatment of cortisol with TBSAB afforded the C (21) organosulfate in a modest 17% overall yield (23% based on recovered starting material) as the sodium salt (**14**). Furthermore, no unwanted C (11) or indeed C (17) sulfate ester formation was observed.

Finally, we sought to develop a proof-of-concept isotopic labelling-chemoselective sulfation method for the estrone scaffold (**15**) (**Scheme 4**). Prior to developing a deuterium labelling method at the C (16) methylene position, a model non-deuterated estrone was sulfated at the C (3) phenolic position in good 72% isolated yield as the sodium salt (**17**). A higher equivalence of TBSAB (2.0 eq) was used to ensure complete sulfation at the sole reactive C (3) phenolic centre. This provided confidence that sulfation should occur readily at

the C (3) position using TBSAB on the deuterium labeled substrate.

Firstly, we adapted the method of Rudqvist for C (19) deuteration (Rudqvist, 1983). Treatment of the estrone with NaOD in MeOD resulted in estrone- d_2 formation (**18**). The C (16)- H_2 protons were selectively deuterated by enolate formation with sodium deuteroxide and resultant deuterium incorporation by quenching the enolate with methanol- D (CH_3OD). This was confirmed via comparative 2D-NMR spectroscopic studies (see Supporting Information) but the key disappearance of the C (16) protons can be clearly observed in the ^1H -NMR spectral overlay (**Figure 1**). It should be noted that deuteration next to a carbonyl group is not usually recommended for applied quantification studies as the deuterium label could readily back exchange through a keto-enol tautomerisation leading to a loss of the label (Wudy, 1990). In our system we observed, a decline of deuterium label in solution based mass-spectrometry studies (**Supplementary Figures S1, S2**).

Finally, the treatment of estrone- d_2 with TBSAB afforded the sulfated and isotopically labelled estrone- d_2 sulfate in 78% isolated yield and 67% incorporation of the deuterium label (**20**).

CONCLUSION

In summary, we have demonstrated a general method for the synthesis of mono- or di-sulfated steroidal skeletons of importance to the fields of biology and spectroscopic detection. We have

showcased chemo-selective sulfation within a variety of complex structures, such as cortisol, and developed a simplified deuterium labeling-sulfation strategy for estrone. Overall, these approaches provide tractable routes on preparative scales to multiple sulfated steroid classes as reference compounds for detection of substances of abuse through to cancer diagnosis applications.

DATA AVAILABILITY STATEMENT

The original contributions presented in the study are included in the article/**Supplementary Materials**, further inquiries can be directed to the corresponding author. All data files can be found at the following doi: <https://doi.org/10.25500/edata.bham.00000720>.

AUTHOR CONTRIBUTIONS

Conducted experiments, spectral analysis, and revised manuscript (JA and DG); provided materials and supervision,

REFERENCES

- Alshehri, J. A., Benedetti, A. M., and Jones, A. M. (2020). A Novel Exchange Method to Access Sulfated Molecules. *Sci. Rep.* 10, 16559. doi:10.1038/s41598-020-72500-x
- Benedetti, A. M., Gill, D. M., Tsang, C. W., and Jones, A. M. (2020). Chemical Methods for N- and O-Sulfation of Small Molecules, Amino Acids and Peptides. *ChemBioChem* 21, 938–942. doi:10.1002/cbic.201900673
- CCDC 2120263 Contains the Supplementary Crystallographic Data for This Paper. These Data Can Be Obtained Free of Charge from the Cambridge Crystallographic Data Centre. Available at: www.ccdc.cam.ac.uk/data_request/cif.
- Foster, P. A., and Mueller, J. W. (2018). SULFATION PATHWAYS: Insights into Steroid Sulfation and Desulfation Pathways. *J. Mol. Endocrinol.* 61, T271–T283. doi:10.1530/JME-18-0086
- Gabriel, L., Günther, W., Pielenz, F., and Heinze, T. (2020). Determination of the Binding Situation of Pyridine in Xylan Sulfates by Means of Detailed NMR Studies. *Macromol. Chem. Phys.* 221, 1900327. doi:10.1002/macp.201900327
- Gill, D. M., Male, L., and Jones, A. M. (2019). A Structure-Reactivity Relationship of the Tandem Asymmetric Dihydroxylation on a Biologically Relevant Diene: Influence of Remote Stereocenters on Diastereofacial Selectivity. *Eur. J. Org. Chem.* 2019, 7568–7577. doi:10.1002/ejoc.201901474
- Gill, D. M., Male, L., and Jones, A. M. (2019). Sulfation Made Simple: a Strategy for Synthesising Sulfated Molecules. *Chem. Commun.* 55, 4319–4322. doi:10.1039/C9CC01057B
- Gill, D. M., R. Pavinelli, A. P., Zazeri, G., Shamir, S. A., Mahmoud, A. M., Wilkinson, F. L., et al. (2021). The Modulatory Role of Sulfated and Non-sulfated Small Molecule Heparan Sulfate-Glycomimetics in Endothelial Dysfunction: Absolute Structural Clarification, Molecular Docking and Simulated Dynamics, SAR Analyses and ADMET Studies. *RSC Med. Chem.* 12, 779–790. doi:10.1039/D0MD00366B
- Günal, S., Hardman, R., Kopriva, S., and Mueller, J. W. (2019). Sulfation Pathways from Red to green. *J. Biol. Chem.* 294, 12293–12312. doi:10.1074/jbc.REV119.007422
- Harteneck, C. (2013). Pregnenolone Sulfate: From Steroid Metabolite to TRP Channel Ligand. *Molecules* 18, 12012–12028. doi:10.3390/molecules181012012
- Hill, M., Hana, V., Veliková, M., Pařízek, A., Kolátorová, L., Vitkú, J., et al. (2019). A Method for Determination of One Hundred Endogenous Steroids in Human Serum by Gas Chromatography-Tandem Mass Spectrometry. *Physiol. Res.* 68, 179–207. doi:10.33549/physiolres.934124
- Hoye, T. R., Dvornikovs, V., Fine, J. M., Anderson, K. R., Jeffrey, C. S., Muddiman, D. C., et al. (2007). Details of the Structure Determination of the Sulfated

analysed results, drafted and revised manuscript (AJ). All authors agree to be accountable for the content of the work.

ACKNOWLEDGMENTS

The authors thank the above funding bodies for supporting our research programme. The authors thank Louise Male for X-ray crystallography, Allen Bowden for HPLC analysis, Chris Williams for mass-spectroscopic studies, and Cecile Le Duff for NMR assistance. Requests for milligram samples will be considered by the authors until samples are exhausted.

SUPPLEMENTARY MATERIAL

The Supplementary Material for this article can be found online at: <https://www.frontiersin.org/articles/10.3389/fmolb.2021.776900/full#supplementary-material>

- Steroids PSDS and PADS: New Components of the Sea Lamprey (*Petromyzon marinus*) Migratory Pheromone. *J. Org. Chem.* 72, 7544–7550. doi:10.1021/jo0709571
- Hungerford, N. L., McKinney, A. R., Stenhouse, A. M., and McLeod, M. D. (2006). Selective Manipulation of Steroid Hydroxyl Groups with Boronate Esters: Efficient Access to Antigenic C-3 Linked Steroid-Protein Conjugates and Steroid Sulfate Standards for Drug Detection. *Org. Biomol. Chem.* 4, 3951–3959. doi:10.1039/b610499a
- Jones, A. M. (2021). Tributylsulfonium Betaine. *Encyclopaedia Reagents Org. Synth.*, 1–3. doi:10.1002/047084289X.rn02393
- Langford-Smith, A. W. W., Hasan, A., Weston, R., Edwards, N., Jones, A. M., Boulton, A. J. M., et al. (2019). Diabetic Endothelial Colony Forming Cells Have the Potential for Restoration with Glycomimetics. *Sci. Rep.* 9, 2309. doi:10.1038/s41598-019-38921-z
- Lightning, T. A., Gesteira, T. F., and Mueller, J. W. (2021). Steroid Disulfates - Sulfation Double Trouble. *Mol. Cell Endocrinol.* 524, 111161. doi:10.1016/j.mce.2021.111161
- Mahmoud, A. M., Jones, A. M., Sidgwick, G., Arafat, A. M., Wilkinson, F. L., and Alexander, M. Y. (2019). Small Molecule Glycomimetics Inhibit Vascular Calcification via C-Met/Notch3/HES1 Signaling. *Cell Physiol Biochem* 53, 323–336. doi:10.33594/000000141
- Mahmoud, A. M., Wilkinson, F. L., Jones, A. M., Wilkinson, J. A., Romero, M., Duarte, J., et al. (2017). A Novel Role for Small Molecule Glycomimetics in the protection against Lipid-Induced Endothelial Dysfunction: Involvement of Akt/eNOS and Nr2f2/ARE Signaling. *Biochim. Biophys. Acta (Bba) - Gen. Subjects* 1861, 3311–3322. doi:10.1016/j.bbagen.2016.08.013
- Mueller, J. W., Gilligan, L. C., Idkowiak, J., Arlt, W., and Foster, P. A. (2015). The Regulation of Steroid Action by Sulfation and Desulfation. *Endocr. Rev.* 36, 526–563. doi:10.1210/er.2015-1036
- Mueller, J. W., Vogg, N., Lightning, T. A., Weigand, I., Ronchi, C. L., Foster, P. A., et al. (2021). Steroid Sulfation in Adrenal Tumors. *J. Clin. Endocrinol. Metab.* 106, Dgab182. doi:10.1210/clinem/dgab182
- Petrie, B., McAdam, E. J., Richards, K. H., Lester, J. N., and Cartmell, E. (2013). Application of Ultra-performance Liquid Chromatography-Tandem Mass Spectrometry for the Determination of Steroid Oestrogens in Wastewaters. *Int. J. Environ. Anal. Chem.* 93 (13), 1343–1355. doi:10.1080/03067319.2012.717272
- Rudqvist, U. (1983). Synthesis of C19 Steroid Monosulphates Labelled with Deuterium at Specific Positions. *J. Label Compd. Radiopharm.* 20, 1159–1170. doi:10.1002/jlcr.2580201005
- Simpson, L. S., and Widlanski, T. S. (2006). A Comprehensive Approach to the Synthesis of Sulfate Esters. *J. Am. Chem. Soc.* 128, 1605–1610. doi:10.1021/ja056086j
- Vo, Y., Schwartz, B. D., Onagi, H., Ward, J. S., Gardiner, M. G., Banwell, M. G., et al. (2021). A Rapid and Mild Sulfation Strategy Reveals Conformational

- Preferences in Therapeutically Relevant Sulfated Xylooligosaccharides. *Chem. Eur. J.* 27, 9830–9838. doi:10.1002/chem.202100527
- Waller, C. C., and McLeod, M. D. (2014). A Simple Method for the Small Scale Synthesis and Solid-phase Extraction Purification of Steroid Sulfates. *Steroids* 92, 74–80. doi:10.1016/j.steroids.2014.09.006
- Wudy, S. A. (1990). Synthetic Procedures for the Preparation of Deuterium-Labeled Analogs of Naturally Occurring Steroids. *Steroids* 55, 463–471. doi:10.1016/0039-128X(90)90015-4

Conflict of Interest: The authors declare that the research was conducted in the absence of any commercial or financial relationships that could be construed as a potential conflict of interest.

Publisher's Note: All claims expressed in this article are solely those of the authors and do not necessarily represent those of their affiliated organizations, or those of the publisher, the editors, and the reviewers. Any product that may be evaluated in this article, or claim that may be made by its manufacturer, is not guaranteed or endorsed by the publisher.

Copyright © 2021 Alshehri, Gill and Jones. This is an open-access article distributed under the terms of the Creative Commons Attribution License (CC BY). The use, distribution or reproduction in other forums is permitted, provided the original author(s) and the copyright owner(s) are credited and that the original publication in this journal is cited, in accordance with accepted academic practice. No use, distribution or reproduction is permitted which does not comply with these terms.

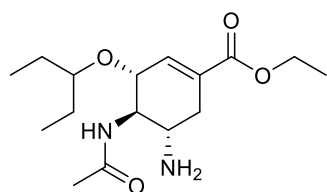
Chapter 6. Are sulfated glycomimetics an endogenous sulfate source: A control experiment study

Background

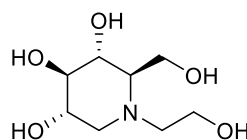
6.1. Glycomimetics

Glycomimetics are synthetic compounds which mimic carbohydrates and therefore have similar biological applications including in cell signalling, adhesion, the immune response, as a metabolic energy source, anti-inflammatory, anti-cancer, and anti-coagulant properties.²⁵²⁻

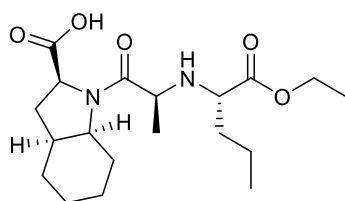
²⁵⁴ The use of carbohydrates directly as medications is limited due to the low binding affinities with their biological targets and poor pharmacokinetics profiles.²⁵⁵ Polysaccharides are complex structures with high molecular weight containing multiple functional groups. Several hydroxyl groups and the phospholipid bilayer affecting the pharmacokinetic profiles,²⁵⁵ although this structural complexity and diversity might reduce the binding affinity with other biological targets and improve the selectivity within the biological system.²⁵⁵ Structural modifications of carbohydrates may improve the pharmacokinetics characteristics as well as binding affinity such as by attaching carbohydrates to lipophilic functional groups which can promote cell membrane permeability.²⁵⁵ Other chemical modifications have been employed such as endocyclic oxygen replacement with carbon as in oseltamivir or nitrogen as in miglitol and perindopril and installation of fluorine as shown in gemcitabine.²⁵³ These modifications improved the interaction with its biological target and balanced drug-like properties within the biological system (**Figure 47**).²⁵⁵⁻²⁶²



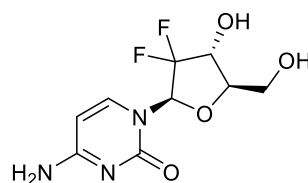
oseltamivir (225)



miglitol (226)



perindopril (227)



gemcitabine (228)

Figure 47: Medicines based on glycomimetics, oseltamivir approved as anti-viral, miglitol as an anti-diabetic drug, perindopril approved for the treatment of hypertension, and gemcitabine as an anti-cancer drug.

Notably, 131 carbohydrate-based drugs have been documented in various pharmacopoeias such as European and Japanese Pharmacopoeias (at the time of writing on 28/03/2024).^{257,}

²⁶³ For instance, approximately 33% of all commercially available carbohydrate-based drugs are used as clinical anti-tumour adjuvants due to their immunomodulatory properties and low cytotoxicity.²⁵⁷ Whilst, about 22% of the marketed carbohydrate-based medicines are associated with the treatment of cardiovascular diseases. For instance, Fondaparinux (**229**) is a carbohydrate-based drug and chemically related to low molecular weight heparin (LMWH), and was approved by the FDA in 2001 as an anti-coagulant for the treatment of deep vein thrombosis (DVT) (**Figure 48**).^{257, 264}

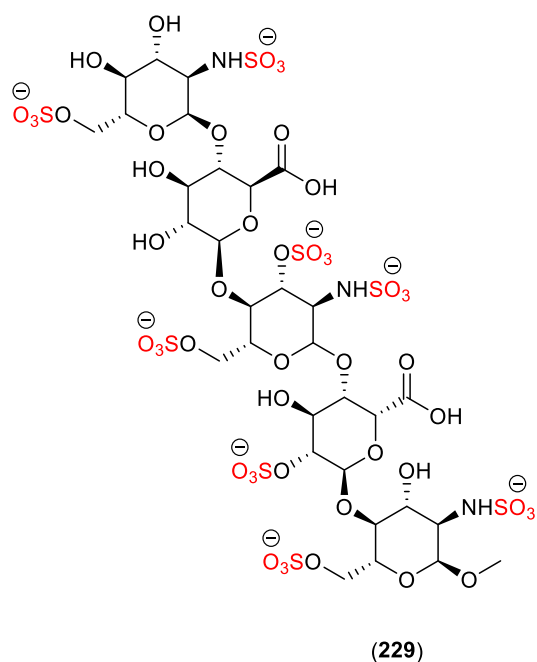


Figure 48: Structure of fondaparinux (229), a carbohydrate-derived medicine which was approved for the treatment of deep vein thrombosis.

Fondaparinux binds selectively to antithrombin III (ATIII) resulting in conformational changes that increase the ability of antithrombin III to inhibit factor Xa.²⁵⁷ This inhibition leads to the reduction of thrombin formation and therefore disruption of the blood coagulation cascade (Figure 49).²⁶⁴

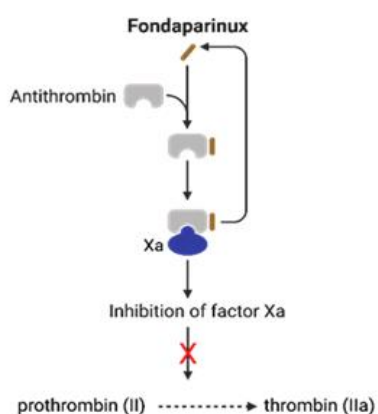
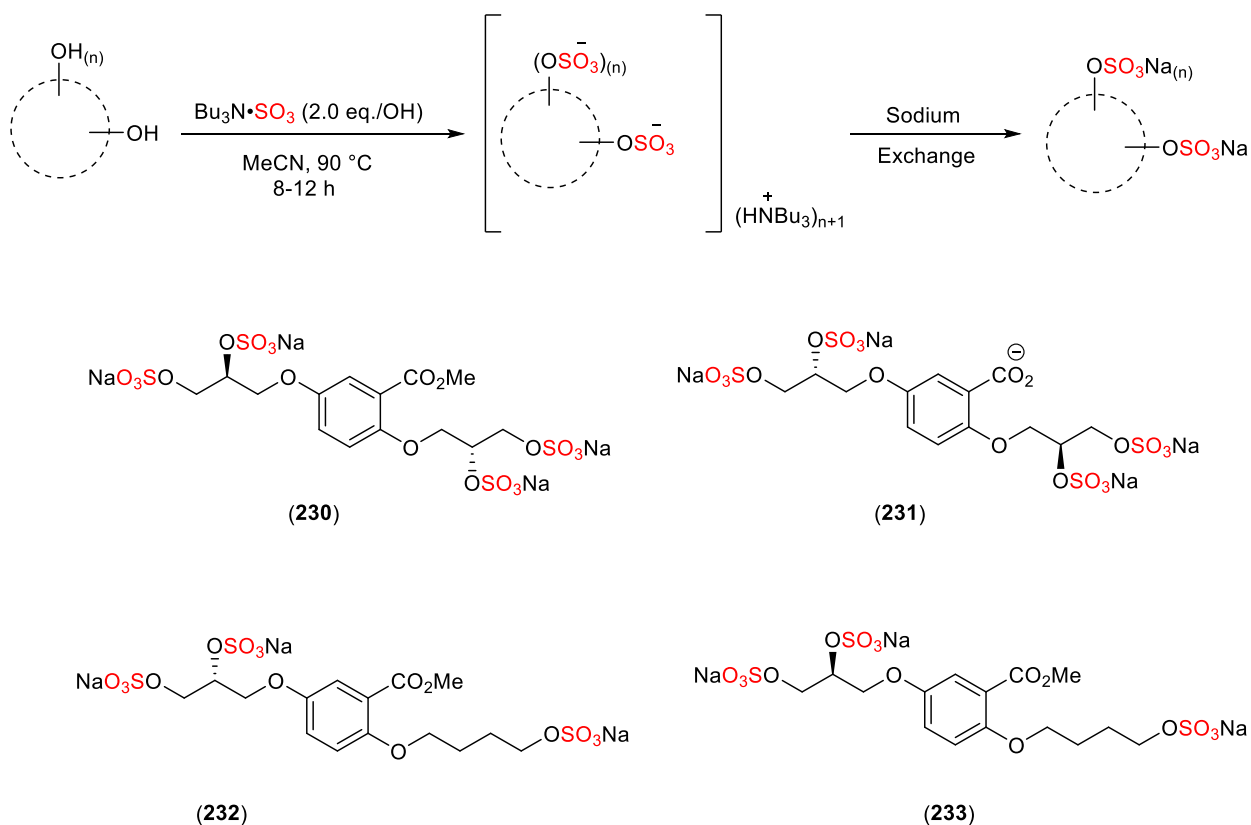


Figure 49: The mechanism of action of anti-coagulant, fondaparinux (Drawn using Biorender).

Several studies have reported the correlation between polysaccharide-based glycomimetics and the endothelium layer.²⁶⁵⁻²⁶⁶ The endothelium layer plays a critical role in maintaining vascular health, homeostasis, thrombosis, angiogenesis, and regulating blood flow.²⁶⁵ Recent studies have reported that endothelial dysfunction (ED) reduces the production and bioavailability of nitric oxide, as a vasodilator, and increases the level of reactive oxygen species (ROS) which results in oxidative stress that damages the endothelium as well as the endothelial functions.²⁶⁶⁻²⁶⁷ Moreover, ED causes the disruption of endothelium permeability and increased vasoconstrictor production.²⁶⁶⁻²⁶⁷ For instance, endothelin-1 and thromboxane A₂ production increases the risk of cardiovascular disease.²⁶⁶⁻²⁶⁸ There are ED modulators that regulate and restore the biological functions of the endothelium including heparin and heparin derivatives (polysaccharide-based glycomimetic), and Iloprost (an analogue of prostacyclin).^{158, 269-270}

More recently, polysaccharide-templated glycomimetics have been synthesised and developed by Dr Daniel Gill (PhD, University of Birmingham, 2020).^{149, 157-158} These sulfated glycomimetics were prepared following the optimised TBSAB sulfation methodology affording the desired compounds in good to excellent isolated yields (**Scheme 73**).^{46-47, 149, 158}

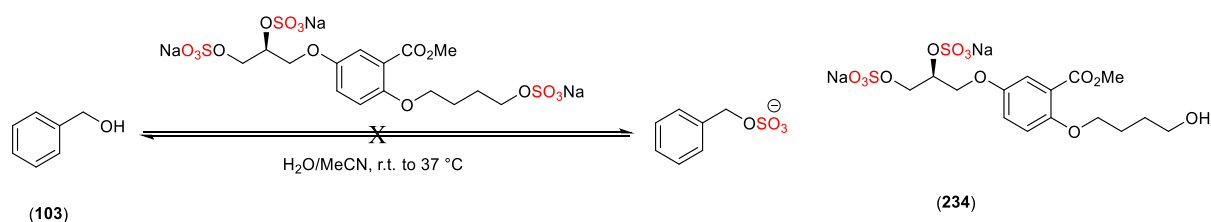


Scheme 73: Sulfation reaction of heparan-like substrates using the optimised TBSAB sulfation methodology affording the desired heparan sulfate-glycomimetics.^{46-47, 149, 158, 228}

These synthesised glycomimetics were initially designed to mimic the functions of polysaccharide-based biomolecules and used as a new therapeutic strategy for various diseases.^{255, 258} The sulfated glycomimetics were originally considered for the inhibition of the hepatocyte growth factor (HGF), induced hepatocyte growth factor receptor (c-Met) activation, affecting tumour cell growth and angiogenesis.^{158, 271}

Hepatocyte growth factor HGF/c-Met is a cellular signalling pathway that plays a critical role in many cellular processes, including cell growth.²⁷² This signalling pathway has been linked to vascular calcification which is a key characteristic of atherosclerosis.²⁷² Heparan sulfate serves as a ligand for the activation of the HGF/c-Met signalling pathway and therefore reduces vascular calcification and the risk of CVD.²³¹ It was hypothesised that the synthesised heparan sulfate-glycomimetics which mimic the structure and the function of heparan sulfate

Benzyl alcohol was selected due to the down-field shift of the benzylic protons' signal post-sulfation (+0.49 ppm) as measured by ^1H NMR spectroscopy (CDCl_3). The reaction conditions were chosen to mimic the biological system and the reaction temperature was adjusted between r.t. and $37\text{ }^\circ\text{C}$. The solvent of choice was a (50:50) mixture of $\text{H}_2\text{O}/\text{MeCN}$ to balance the hydrophilicity of the glycomimetic (*S-10*) and the solubility of the substrates which was needed for effective sulfation. The sulfation reaction was carried out by the reaction of benzyl alcohol and the heparan sulfate-glycomimetic (*S-10*) in a 1:1 stoichiometric ratio. Then, A 50:50 mixture of water/MeCN was added and the mixture was stirred at r.t. to $37\text{ }^\circ\text{C}$. However, this reaction may be reversible leading back to the starting material but there was no evidence of hydrolysis during this reaction which was carried out for 7 days as confirmed by ^1H NMR spectroscopy analysis (**Scheme 74**).



Scheme 74: The attempted sulfation reaction of benzyl alcohol with the synthesised heparan sulfate-glycomimetic (*S-10*).

The control experiment was reacted for up to 7 days and monitored by ^1H NMR spectroscopy analysis (**Figure 51**).

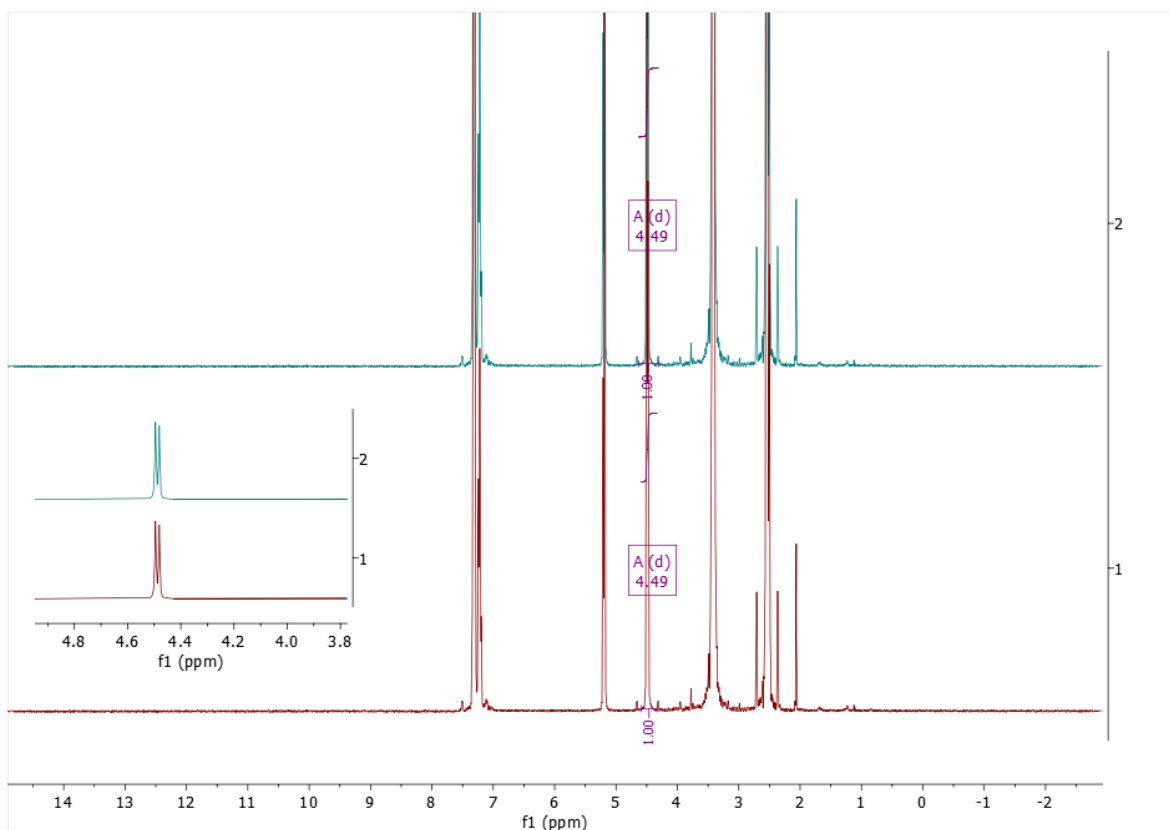
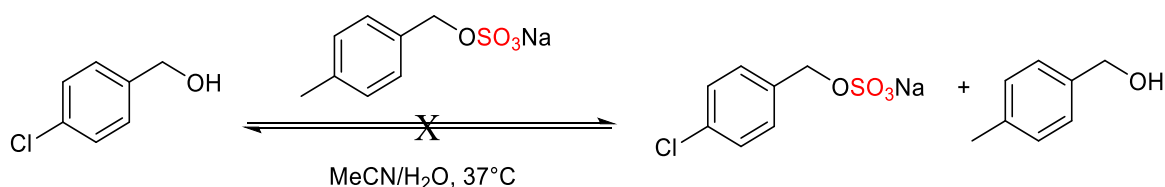


Figure 52: The stacked ^1H NMR spectra (400 MHz, $\text{DMSO-}d_6$) of benzyl alcohol pre-sulfation (**1**), the benzylic proton signal at 4.49 ppm as a doublet (*d*) and post-sulfation. The benzylic protons signal as a doublet was also observed post-sulfation (**2**) indicating that the reaction did not occur.

To investigate the hypothesis further, a simpler sulfated substituted benzyl alcohol, sodium 4-methylbenzyl sulfate (**171**) was selected to examine whether sodium 4-methylbenzyl sulfate could sulfate different benzyl alcohol derivatives adapting the previous optimised sulfation method to mimic the biological system.

First, sodium 4-methylbenzyl sulfate was synthesised using the optimised TBSAB sulfation methodology and characterised by ^1H and ^{13}C NMR spectroscopic data.^{46, 149} Next, sulfation reaction of 4-chlorobenzyl alcohol was conducted using sodium 4-methylbenzyl sulfate in 1:2 reaction ratio. This reaction mixture was dissolved in a 50:50 mixture of $\text{H}_2\text{O}/\text{MeCN}$ and heated at $37\text{ }^\circ\text{C}$ (**Scheme 75**).



Scheme 75: Attempted control experiment of sulfation of 4-chlorobenzyl alcohol with sodium 4-methylbenzyl sulfate.

A sample (0.6 mL) of the crude reaction mixture was prepared after 48 h and dissolved in deuterated DMSO- d_6 for ^1H NMR spectroscopy analysis. The ^1H NMR spectrum of the crude reaction mixture revealed two significant signals as follows; one signal was found at (d, 4.47 ppm) which corresponds to 4-chlorobenzyl alcohol (the starting material). The other signal was found at (4.71 ppm) as a singlet (s) that corresponds to the sulfate donor, sodium 4-methylbenzyl sulfate. As a result, it was concluded that this sulfation attempt did not occur under these conditions and more importantly the reported benzylic proton signal of sodium 4-chlorobenzyl sulfate (**157**) was not found at (4.75 ppm). Furthermore, no hydrolysis or degradation was observed during this attempt (**Figure 53**).⁴⁶

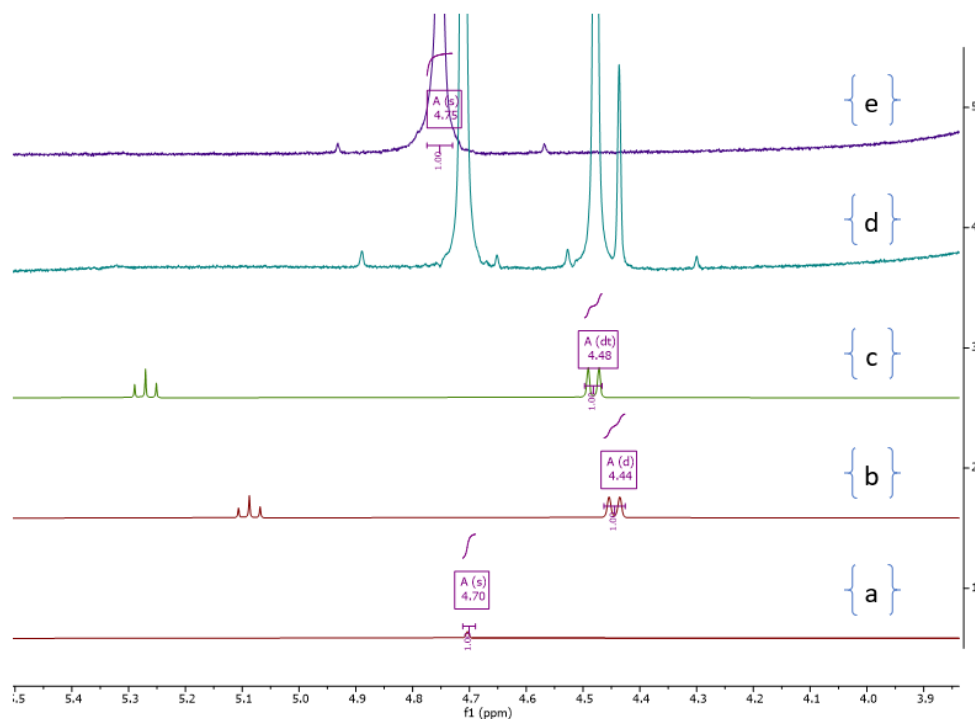
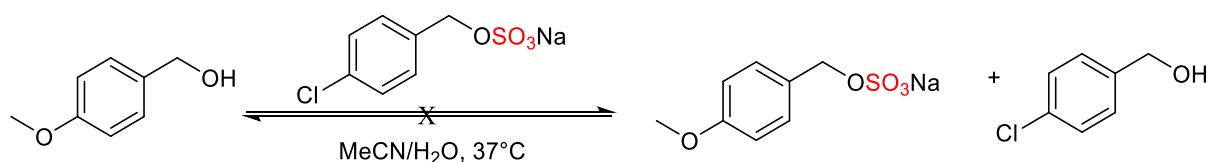


Figure 53: The stacked ^1H NMR spectra (400 MHz, $\text{DMSO-}d_6$) of (a) sodium 4-methylbenzyl sulfate, (b) 4-methylbenzyl alcohol, (c) 4-chlorobenzyl alcohol, (d) control experiment (the sulfation of 4-chlorobenzyl alcohol with sodium 4-methylbenzyl sulfate), and (e) sodium 4-chlorobenzyl sulfate.

Next, it was considered whether repeating this experiment using a different starting material of benzyl alcohol analogue, 4-methoxybenzyl alcohol may play a role in the sulfation reaction outcome. The methoxy group is an electron-donating via the mesomeric (+M) effects, increasing the electron density on the benzyl ring and at the benzylic position and making the benzylic hydroxyl group more nucleophilic and more reactive towards electrophiles such as SO_3 . 4-Methoxybenzyl alcohol was reacted with sodium 4-chlorobenzyl sulfate in 1:2 reaction ratio. The reaction mixture was dissolved in a 50:50 mixture of water/MeCN and heated at 37 °C. This was considered due to the benzylic proton signals differences between sodium 4-chlorobenzyl sulfate and sodium 4-methoxybenzyl sulfate, (5.04 ppm) vs (4.54 ppm), respectively which would enable detection (**Scheme 76**).



Scheme 76: The control experiment of sulfation of 4-methoxybenzyl alcohol with sodium 4-chlorobenzyl sulfate.

A sample (0.6 mL) of the crude reaction mixture was prepared and dissolved in deuterated DMSO- d_6 for ^1H NMR spectroscopy analysis. The ^1H NMR spectroscopic data showed that the benzylic proton signal for 4-methoxybenzyl alcohol was found at (4.41 ppm), whereas in the crude reaction mixture, two significant signals were also observed: one signal was found at (4.40 ppm) that corresponds to 4-methoxybenzyl alcohol and the other signal was found at (4.75 ppm) which corresponds to the sulfating agent, sodium 4-chlorobenzyl sulfate. More importantly, there was no evidence on the formation of the desired sulfated compound, sodium 4-methoxybenzyl sulfate due to the absence of the benzylic proton signals which would occur at (4.68 ppm) (**Figure 54**).⁴⁶

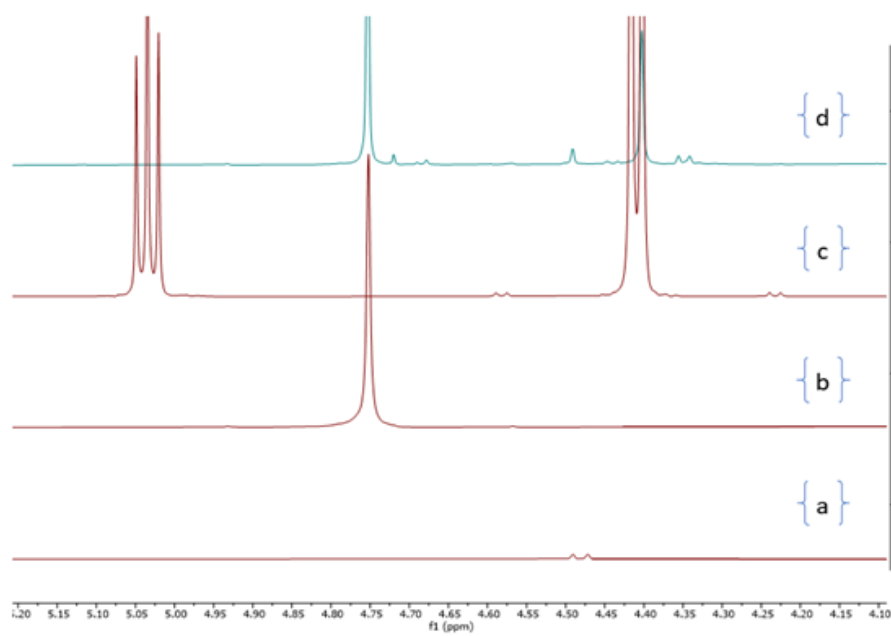


Figure 54: The stacked ^1H NMR spectra (400 MHz, DMSO- d_6) of (a) 4-chlorobenzyl alcohol, (b) sodium 4-chlorobenzyl sulfate, (c) 4-methoxybenzyl alcohol, (d) control experiment (the sulfation of 4-methoxybenzyl alcohol with sodium 4-chlorobenzyl sulfate).

As a result, despite the exploration of an electron-donating methoxy group which should hypothetically improve the reactivity of 4-methoxybenzyl alcohol and the extended reaction time, it was concluded that the sulfation reaction did not occur with different benzyl alcohol derivatives as the benzylic proton signal post-sulfation was not observed. This was attributed to several factors, including insufficient reactivity profile of the sulfating agents used to transfer a sulfate group to the acceptor molecule. Also, the structural complexity of the synthesised heparan sulfate-glycomimetics (*S-10*) was an additional challenge for exploring the sulfation chemistry.

6.3. Conclusion

In summary, the synthetic sulfated glycomimetic (*S-10*) was investigated as to whether it can act as a sulfating agent and transfer a sulfate group to other acceptor molecules within a biological system. This investigation was carried out by reacting glycomimetic (*S-10*) with benzyl alcohol under conditions that mimic a biological system. Unfortunately, this reaction did not occur as confirmed by ^1H NMR spectroscopy analysis. Next, several attempts were made to sulfate other benzyl alcohol analogues using synthesised sulfation sources such as sodium 4-methylbenzyl sulfate and sodium 4-chlorobenzyl sulfate. However, no evidence for the formation of the desired molecule was found, as confirmed by ^1H NMR spectroscopy analysis. Nevertheless, evidence for the first time of the stability of benzylic sulfates (a major issue with sulfation chemistry) as no hydrolysis was observed during this reaction over the time (up to 7 days) as determined by ^1H NMR spectroscopic analysis.

Chapter 7. Biological role of hydrogen sulfide and the synthesis and characterisation of cysteine trisulfide

Background

7.1. Hydrogen sulfide (H₂S)

Hydrogen sulfide (H₂S) is a colourless toxic gas, and an environmental hazard with a pungent smell of rotten eggs.²⁷⁷ The history of hydrogen sulfide begins in 1713 when the Italian physician Bernardino Ramazzini noted painful eye irritation and inflammation in sewer workers.²⁷⁸ This inflammation may lead to bacterial infections resulting in serious health complications such as blindness.²⁷⁸⁻²⁷⁹ Between 1785 and 1806, Parisians experienced some health complications including eye inflammation and severe asphyxia due to exposure to hydrogen sulfide gas.²⁸⁰ The biological effect of H₂S gas was also investigated in animals in 1803 by Francois Chaussier.²⁸¹ He demonstrated the toxic effect of H₂S gas when it was administered in a solution resulting in serious health issues, including respiratory inflammation, convulsive movements, and at high doses, asphyxia and death.²⁸¹ However, H₂S has also been known for its pharmacological applications including as a smooth muscle relaxant, neuromodulator, anti-inflammatory, blood pressure regulator, ion channel modulator, and anti-oxidant agent.^{277, 282-283} Moreover, H₂S acts as a neuroprotective by restoring neuronal functions and improving the defence mechanisms against oxidative stress.^{277, 284-286} Several studies have also revealed cytoprotective effects such as anti-apoptosis, anti-necrosis, and cell proliferation activities.²⁸⁷⁻²⁹¹ However, H₂S also has cytotoxicity activity, including stimulating apoptosis and cell death.²⁸⁷⁻²⁹¹

Abe and Kimura reported the important role of H₂S as an endogenous gasotransmitter in the mammalian tissues similar to nitric oxide and carbon monoxide.^{283, 292} Nitric oxide and carbon monoxide have several biological functions, including vasodilation, anti-inflammatory activity, and act as neuromodulator and neuroprotective agents.²⁹³ In mammalian tissues, the

production of H₂S is initially produced via enzymatic pathways involving cysteine and homocysteine amino acids (**Figure 55**).^{277, 283}

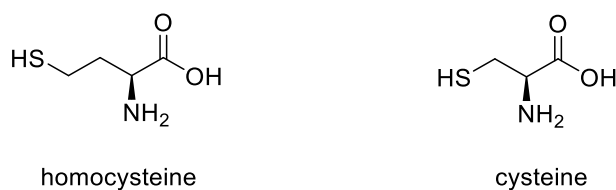
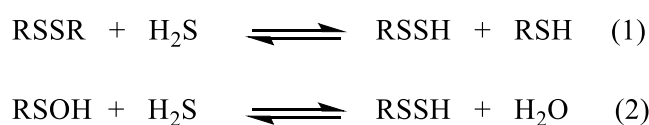


Figure 55: The structure of homocysteine and cysteine amino acids.

The enzymatic synthesis of H₂S is catalysed by pyridoxal-5'-phosphate (PLP)-dependent enzymes, including cystathionine β-synthase (CBS) and cystathionine γ-lyase (CSE).^{277, 283, 292, 294} The cystathionine β-synthase (CBS) enzyme catalyses the condensation reaction of homocysteine and serine to form cystathionine, resulting in the formation of cysteine, a key precursor to H₂S formation.²⁸² The cystathionine γ-lyase (CSE) enzyme catalyses the desulfhydration reaction leading to the formation of cysteine which is involved in the formation of H₂S (**Scheme 77**).^{283, 295-297}

SSH), glutathione persulfide (GSSH) and disulfane (HSSH).³⁰²⁻³⁰³ They have been recognised as cellular and tissue constituents which have biological applications including cellular protection, cellular redox signalling, and oxidative stress reduction.³⁰³

The formation of hydropersulfides occurs via the reaction of an oxidized cysteine residue (disulfide molecule) or sulfenic acid with hydrogen sulfide affording the corresponding hydropersulfide. This redox reaction involves a nucleophilic attack of H₂S to the disulfide substrate resulting in the cleavage of the disulfide bond and formation of thiolate anion (R-S⁻) which subsequently reacts with another H₂S affording the corresponding hydropersulfides and thiol. The reaction of sulfenic acid with H₂S occurs via a nucleophilic substitution reaction where the sulfur atom of H₂S attacks the sulfur atom of sulfenic acid affording the hydropersulfide molecule and water (**Scheme 78**).³⁰²



Scheme 78: The reaction of H₂S with disulfide (1) and sulfenic acid (2) affording hydropersulfides (RSSH).³⁰²

Endogenous cysteine persulfide also reduces lipid peroxidation and therefore may protect against myocardial ischaemia disease.³⁰³ Several studies have suggested that the exogenous cysteine persulfide donor, cysteine trisulfide (Cys-SSS-Cys) is involved in the protection of cardiac muscle against reperfusion injury by interfering with lipid peroxidation.³⁰³⁻³⁰⁴

7.2.1. Cysteine trisulfide (Cys-SSS-Cys)

Cysteine trisulfide (also known as thiocystine) is an exogenous cysteine persulfide donor which reacts with sulfide and other thiols forming the cysteine persulfide and related polysulfide molecules (**Figure 56**).³⁰⁵

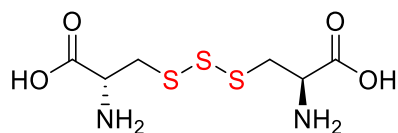


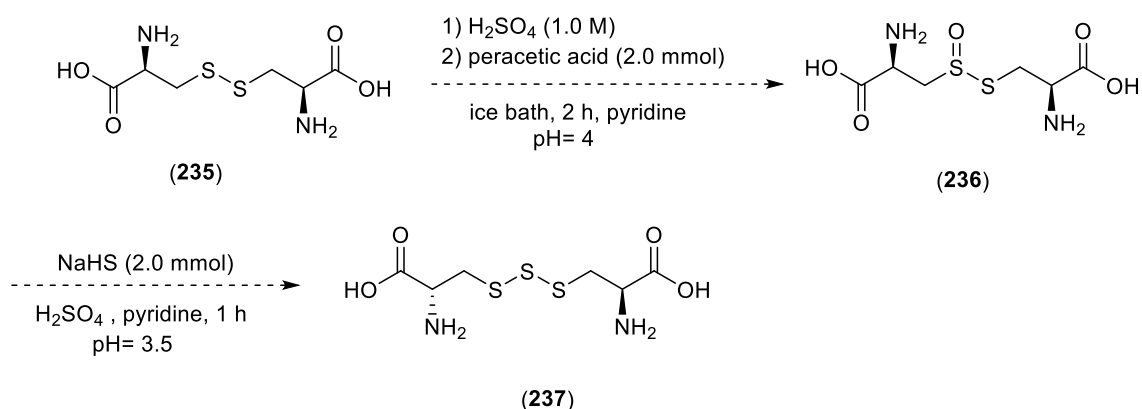
Figure 56: The structure of cysteine trisulfide (Cys-SSS-Cys).

Recent studies have reported the important role of cysteine trisulfide in various biological applications. For instance, cysteine trisulfide has been correlated with the protection of *Escherichia coli* bacterium from electrophile-induced cell death via the production of cysteine hydropersulfide.^{303, 305-306} Cysteine trisulfide is hypothesized to increase intracellular concentrations of cysteine hydropersulfide (Cys-SSH) within the body. This increase in Cys-SSH levels is expected to reduce lipid peroxidation, thereby reducing oxidative stress and enhancing cardiac functions by protecting against oxidative damage to cellular membranes.³⁰³ Lipid peroxidation is an oxidative degradation process where free radicals attack lipids containing carbon-carbon double bonds, particularly those in the cell membrane resulting in cell damage.³⁰⁷ A high concentration of cysteine hydropersulfides (Cys-SSH) reduces lipid peroxidation due to mainly the anti-oxidant properties of Cys-SSH which neutralises the free radical and therefore protects the cell.^{303, 307}

A recent report has discovered that cysteine trisulfide induces protein oxidation cell stress and provides evidence that trisulfide motifs have enhanced biological effects compared to disulfides such as cystine (Cys-SS-Cys).³⁰⁸

The first reported preparation of cysteine trisulfide dates back to 1964 by Savige and co-workers however, no isolated yield or characterisation data was reported.³⁰⁹ In 2018, Fukuto and co-workers reported the second preparation of cysteine trisulfide following the general method of Savige *et al.*³⁰⁶ This preparation was carried out by dissolving *L*-cystine in 1.0 M H₂SO₄ in an ice bath followed by the addition of peracetic acid. The reaction mixture was

stirred for an additional 2 h in an ice bath. After stirring, the pH was adjusted to 4 using pyridine to afford the cystine-S-monoxide intermediate which was used directly for the next step without purification. The cystine-S-monoxide intermediate was dissolved in 1.0 M H₂SO₄ and added to a separate flask which contains sodium hydrosulfide (NaHS). The flask was sealed and stirred at room temperature for 1 h. The pH was then adjusted to 3.5 using pyridine. A 50/50 mixture of ethanol/THF was then added to precipitate cysteine trisulfide. Cysteine trisulfide was filtered, washed again with 50/50 (ethanol/THF) and then dried affording the cysteine trisulfide in > 90% isolated yield.³⁰⁹ However, major impurities were detected including *L*-cystine from the starting material (**Scheme 79**).



Scheme 79: The proposed synthesis of cysteine trisulfide (Cys-SSS-Cys).

Fukuto and co-workers reported ^1H NMR spectroscopic data of Cys-SSS-Cys as follows: ^1H NMR (400 MHz, D_2O) δ 4.015 (dd, $J = 8.0, 4.0$ Hz, 1H), δ 3.42 (dd, $J = 15.2, 4.0$ Hz, 1H), δ 3.23 (dd, $J = 15.2, 8.0$ Hz, 1H) and did not assign resonances and did not include the correct integrals for the proposed structure. Furthermore, the mass spectrometry was also reported as: (ESI-MS) m/z $[\text{M}+\text{H}]^+$ calculated for $\text{C}_6\text{H}_{12}\text{N}_2\text{O}_4\text{S}_3$, 273.37 Da, found 272.98 Da. However, these data are incorrect due to the misinterpretation of ^1H NMR spectroscopic data where only three protons were reported which does not represent the final product, cysteine trisulfide, which contains 6 non-exchangeable and 6 exchangeable protons. Furthermore, there is inadequate literature evidence for the formation of cysteine trisulfide, including no ^{13}C NMR spectroscopy analysis. More importantly, there is a concern as to how cysteine trisulfide was purified considering the use of pyridine solvent which is biologically active and still be present and contaminate cysteine trisulfide. Only a portion (2.6-4.0 ppm) of the Cys-SSS-Cys ^1H NMR spectrum was revealed. All these errors and inadequate evidence, cast doubts over the reported biological activity reported with this synthesis of Cys-SSS-Cys (**Figure 57**, see **Scheme 79**).³⁰⁶

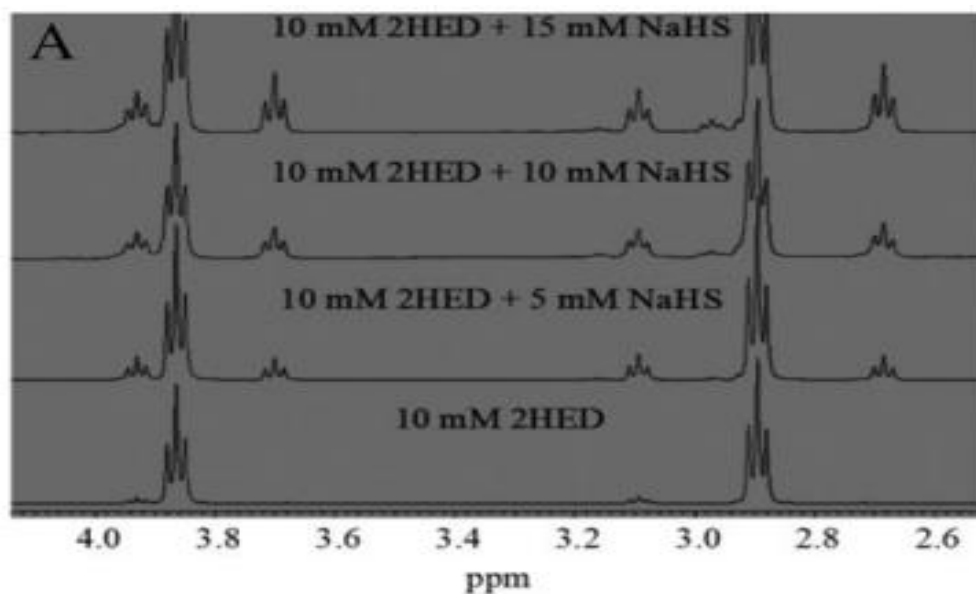


Figure 57: The selected region of the stacked ¹H NMR spectra of equilibrated samples (post 30 min) of 10 mM 2HED (2-hydroxyethyl disulfide, *L*-cystine like substrate) with increasing additions of NaHS (0, 5, 10 and 15 mM). the lower spectrum corresponds to 2HED (*L*-cystine like substrate), with two triplet signals ($\delta = 2.91\text{--}2.95$ and $3.85\text{--}3.90$ ppm). The addition of different concentrations of NaHS (sulfur donor) resulting in the formation of trisulfide substrates (2HET, 2-hydroxyethyl trisulfide). The top three spectra correspond to 2HET (trisulfide like substrate), 2 triplet signals ($\delta = 3.08\text{--}3.11$ and $3.91\text{--}3.94$ ppm). This spectrum was obtained directly from the original source.³⁰⁶

In this chapter, Cys-SSS-Cys will be synthesised for only the third time with improvements in purity and characterisation and will be screened by our biological collaborator; Dr Madhani (Institute of Cardiovascular Sciences, University of Birmingham, UK) for biological studies.

7.3. Results and Discussion

7.3.1. The synthesis of cysteine trisulfide (Cys-SSS-Cys)

This investigation was initiated with the attempted synthesis of Cys-SSS-Cys following Fukuto methodology (See the previous **Scheme 79**).³⁰⁹ After the completion of this reaction, a sample of the crude product was taken and dissolved in D₂O for ¹H NMR spectroscopy analysis (**Figure 58**). The cysteine trisulfide signals were detected despite the presence of *L*-cystine (**Figure 59**) as a major detectable impurity as well as pyridine contamination.

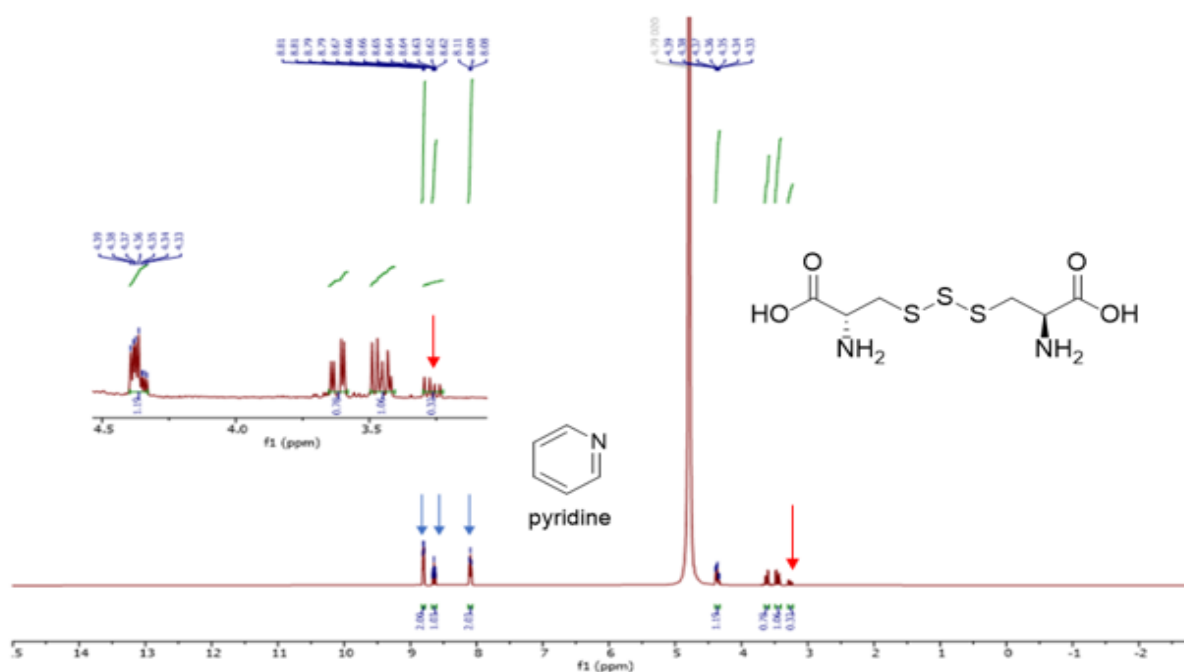


Figure 58: The ¹H NMR spectrum (400 MHz, D₂O) of Cys-SSS-Cys with major detectable impurities, *L*-cystine (red arrows) and pyridine (blue arrows).

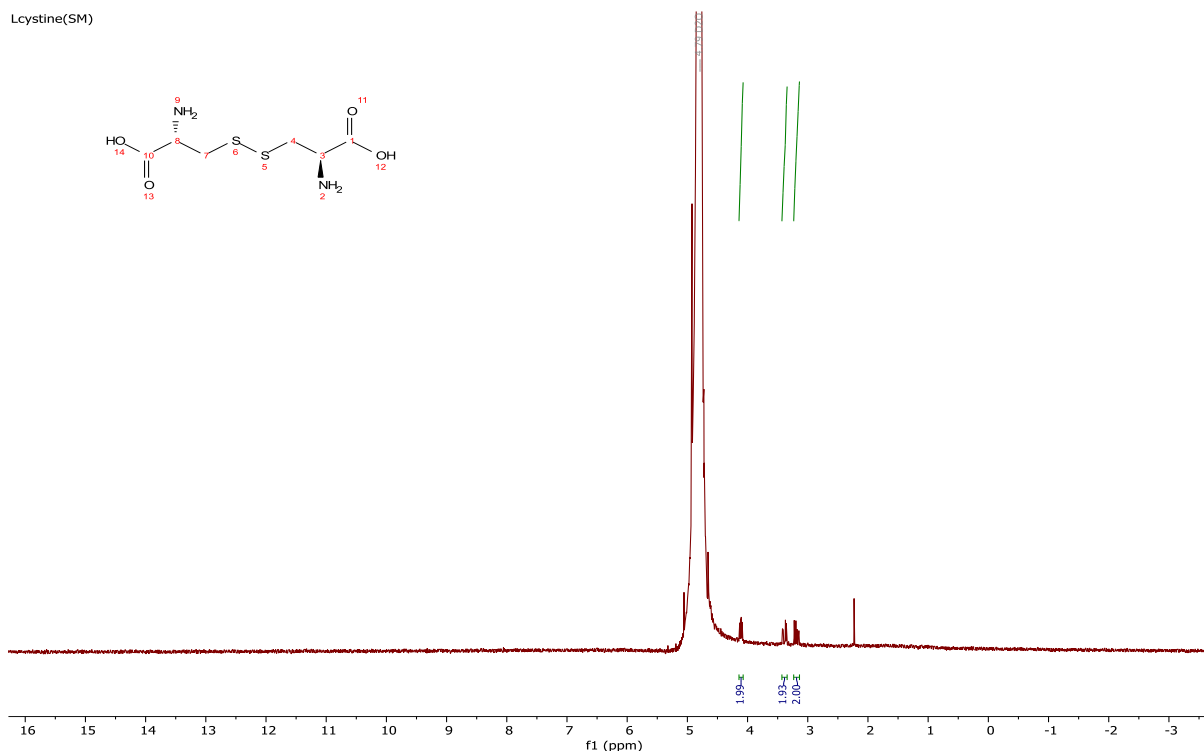
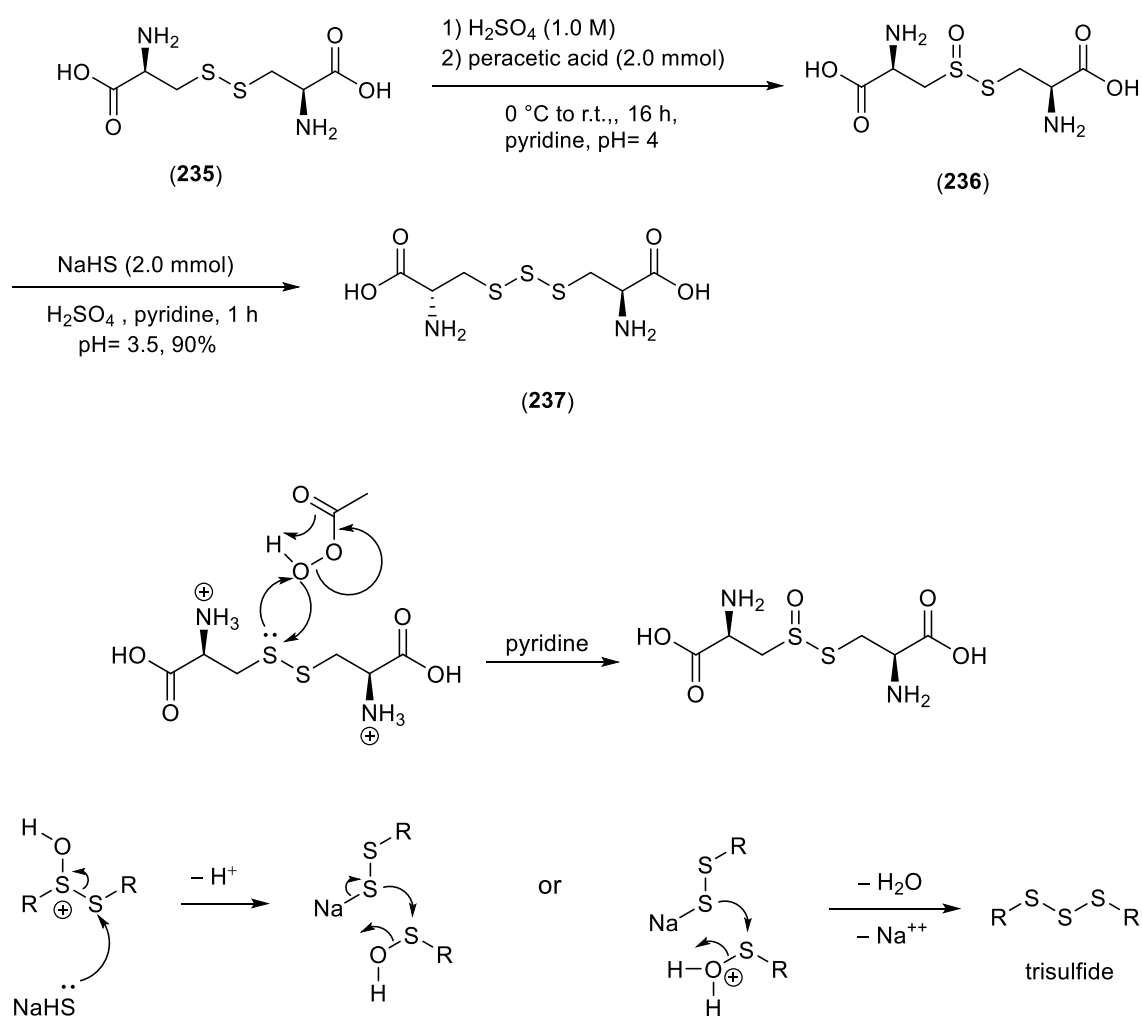


Figure 59: The ^1H NMR spectrum (400 MHz, D_2O) of the starting material, *L*-cystine.

Figure 58 showed several proton signals overlapped between 4.39–3.32 ppm region indicating that cysteine trisulfide was formed along with a major impurity, *L*-cystine further confirmed by mass spectrometric analysis (**Figure 59**). The signals between 4.39–3.32 ppm region correspond to the structure of cysteine trisulfide, including the diastereotopic protons representing two different signals (C1) and (C2) and the third signal which corresponds to the stereogenic centre (C3). The other signals between 8.08–8.81 ppm correspond to the pyridine solvent. As a result, optimisation studies and column chromatography were selected for further investigation.

Cysteine trisulfide (**237**, **Scheme 79**) was synthesised again following the published methodology with minor modifications.³¹⁰ First, cystine-*S*-monoxide (**236**) was dissolved in 1.0 M H_2SO_4 and reacted with peracetic acid (2.0 eq.). This reaction was stirred for 16 h at 0 °C to room temperature.³⁰⁶ Cystine-*S*-monoxide (**236**) was precipitated in ethanol and used directly for the next step without characterisation. Next, cystine-*S*-monoxide (**236**) was

dissolved in 1.0 M H₂SO₄, reacted with NaHS (2.0 eq.), and stirred for 1 h at room temperature affording the crude cysteine trisulfide. The crude compound was purified using reverse-phase column chromatography (SiO₂; water/MeCN, 95:5) and freeze-dried to afford the desired Cys-SSS-Cys as a white solid in 90% isolated yield. Potential diastereomers could also occur in this reaction due to the sulfoxide functional group but the cystine-*S*-monoxide (**236**) was directly used for the next step without further characterisation and purification (**Scheme 80**).



Scheme 80: Synthesis of Cys-SSS-Cys and the proposed mechanism (this scheme was based on the work of Roger and co-workers³¹¹).

A small quantity (10 mg) of Cys-SSS-Cys was dissolved in D₂O (0.6 mL) for ¹H NMR spectroscopy analysis. Due to the pH-dependant ionisation states of Cys-SSS-Cys, one drop of

HCl acid was added to the mixture of Cys-SSS-Cys and D₂O to help dissolve this sample and fix the ionisation state as cationic. Cys-SSS-Cys structure was confirmed by ¹H NMR spectroscopy analysis (**Figure 60**).

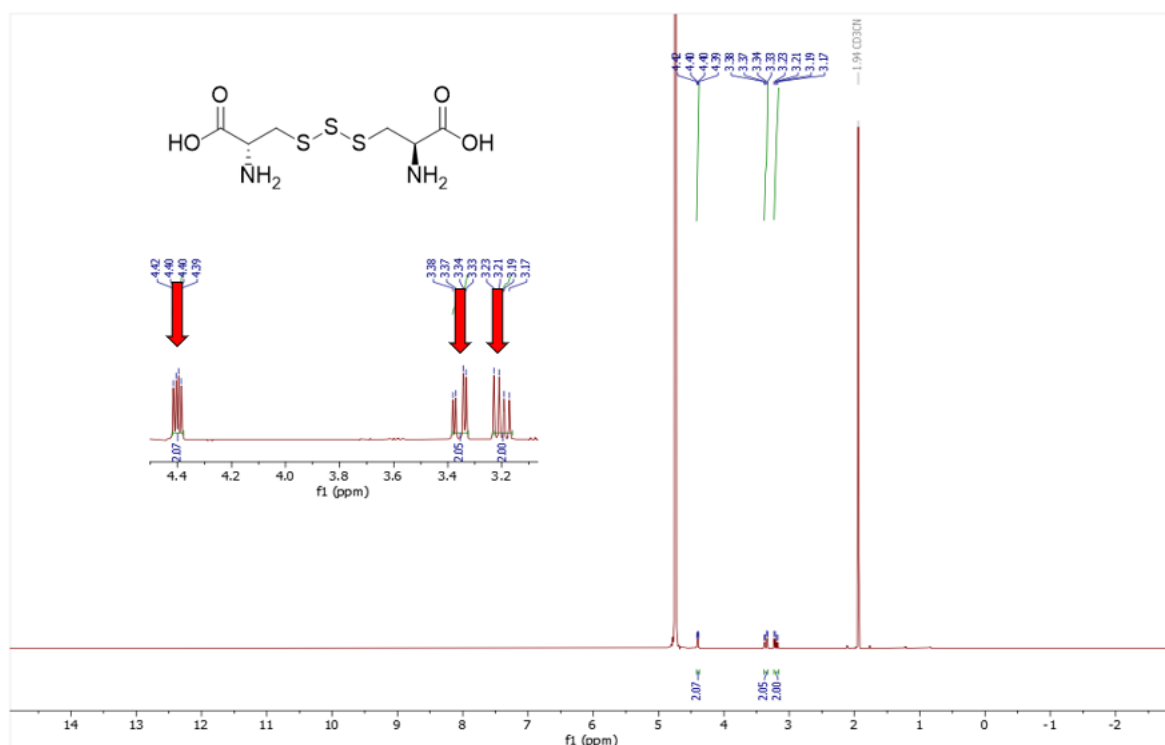


Figure 60: The ¹H NMR spectrum of Cys-SSS-Cys, (400 MHz, D₂O), MeCN was used as an internal reference: C1 (4.45 ppm, stereogenic centres). C2 (3.40 ppm) and C3 (3.25 ppm) are both diastereotopic protons.

The ¹H NMR spectroscopy data were reported as ¹H NMR (400 MHz, D₂O) δ 4.45 (dd, *J* = 7.8, 4.3 Hz, 2H), 3.40 (dd, *J* = 15.3, 4.3 Hz, 2H), 3.25 (dd, *J* = 15.2, 7.8 Hz, 2H), which represent both the diastereotopic protons and the protons on the stereogenic centres. The mass spectrometry analysis (ES+) *m/z* [M+H]⁺ was theoretically calculated for C₆H₁₂N₂O₄S₃, 273.0037, and found to be 273.0042 *m/z*. These results were compared with original Fukuto Cys-SSS-Cys sample obtained from our biological collaborator Dr Madhani. The ¹H NMR spectroscopy analysis of Fukuto's sample were reported with impurities, (most likely *L*-cystine) and obtained without the addition of HCl as follows; ¹H NMR (400 MHz, D₂O) δ 4.17

(dd, $J = 8.1, 4.2$ Hz, 1H), 3.58 (dd, $J = 14.9, 4.0$ Hz, 1H), 3.39 (dd, $J = 15.1, 8.1$ Hz, 1H) (**Figure 61**).

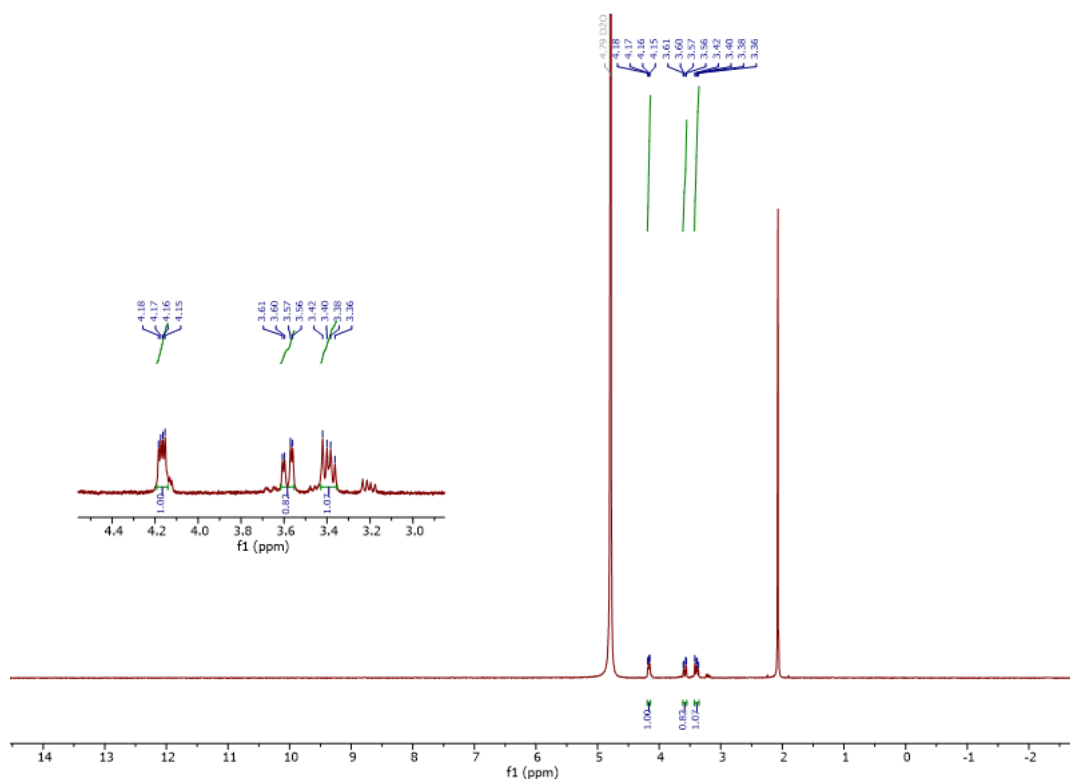
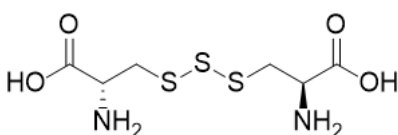


Figure 61: The ^1H NMR spectrum of Fukuto's sample, Cys-SSS-Cys (400 MHz, D_2O), MeCN was used as an internal reference (Provided by Dr Madhani).

However, after the addition of one drop of HCl to the Fukuto's sample, the ^1H NMR spectroscopy data changed presumably due to the ionisation state of Cys-SSS-Cys at the amine groups as follows; ^1H NMR (400 MHz, D_2O) δ 4.45 (dd, $J = 7.5, 4.4$ Hz, 2H), 3.55 (dd, $J = 15.3, 4.5$ Hz, 2H), 3.39 (dd, $J = 15.3, 7.5$ Hz, 2H). As a result of this investigation both sample (Fukuto's sample and this sample) are closely matched and in agreement with the proposed identity as confirmed by NMR spectroscopy and mass spectrometry analysis (**Table 11**).

Table 11: The ^1H and ^{13}C NMR spectroscopic data for cysteine trisulfide, Fukuto (original) sample vs this sample. Both are dissolved in D_2O , one drop of HCl was added (≈ 0.05 mL), and MeCN was used as internal reference.

The ^1H NMR data (400 MHz, D_2O)					The ^{13}C NMR data (400 MHz, D_2O) Post-HCl addition	
						
#	Fukuto (pre-HCl addition)	Fukuto (post-HCl addition)	This sample (pre-HCl addition)	This sample (post-HCl addition)	Fukuto	This sample
C1	4.04 (dd, $J = 8.1, 4.2$ Hz, 2H)	4.45 (dd, $J = 7.5, 4.4$ Hz, 2H)	4.13 (dd, $J = 7.7, 4.4$ Hz, 2H)	4.40 (dd, $J = 7.8, 4.3$ Hz, 2H)	169.5	169.4
C2	3.45 (dd, $J = 14.9, 4.0$ Hz, 2H)	3.55 (dd, $J = 15.3, 4.5$ Hz, 2H)	3.45 (dd, $J = 15.2, 4.4$ Hz, 2H)	3.36 (dd, $J = 15.3, 4.3$ Hz, 2H)	51.0	50.6
C3	3.26 (dd, $J = 15.1, 8.1$ Hz, 2H)	3.39 (dd, $J = 15.3, 7.5$ Hz, 2H)	3.20 (dd, $J = 15.3, 7.9$ Hz, 2H)	3.20 (dd, $J = 15.2, 7.8$ Hz, 2H)	36.3	35.1

Another attempt was made following our optimised conditions (extended reaction time) with the difference of using recrystallization purification technique rather than reverse-phase column chromatography. The crude compound was recrystallized in hot methanol, cooled to the room temperature, and filtered to afford Cys-SSS-Cys as a white solid. Both ^1H and ^{13}C NMR spectroscopy data matched our previous data confirming the formation of Cys-SSS-Cys. Finally, 1.0 g of cysteine trisulfide was delivered to our biological collaborator, Dr Madhani for further biological studies and investigation. The preliminary *unpublished* results indicated that this new Cys-SSS-Cys sample behaves analogously in the biological system compared to the original Fukuto's sample.

7.4. Conclusion

In summary, cysteine trisulfide was successfully synthesised and prepared for only the third time in a gram-scale following the adapted methodology by Fukuto and Savidge but for the first time fully characterised. The Cys-SSS-Cys structure was confirmed by ^1H and ^{13}C NMR spectroscopy and mass spectrometry analysis. Finally, 1 gram of Cys-SSS-Cys was obtained for future biological investigation.

7.5. Thesis conclusions and future work

Sulfation is a crucial modification that occurs in a diverse array of small biomolecules, such as polysaccharides, proteins, flavonoids, and steroids. Adding a sulfate group to a molecule typically enhances its hydrophilicity, which in turn facilitates its excretion from the body. Sulfation is catalysed by a group of enzymes known as sulfotransferases (SULTs). Sulfated biomolecules play key biological and pharmacological roles, including in cell signalling, immune modulation, inflammation regulation, anti-coagulation, anti-atherosclerosis, and anti-adhesion.

The aim of this research thesis was to design and develop novel sulfating reagents (and sulfur chemistry) and explore their application to a wide range of small molecules including alcohols, amines, carbohydrates, proteins, and steroids.

Chapter 2 describes the synthesis of a variety of novel sulfur trioxide-amine complexes, including those with bulky tertiary amines like tripropylamine and isopropyl-*N*-methyl-*tert*-butylamine. Moreover, hydrophilic *N*-substituted morpholine complexes were developed to sulfate water-soluble substrates such as α -amino acids. Additionally, a cinchonidine sulfur trioxide and isopropyl-*N*-methyl-*tert*-butylamine sulfur trioxide complexes were synthesized as potential chiral sulfating reagents. These reagents were tested and shown to be effective for sulfating simple benzyl alcohol and benzylamine substrates, paving the way for broader applications.

Chapter 3 describes the optimized conditions for the sulfation of selected α -amino acids using 4-methylmorpholine SO_3 and 4-ethylmorpholine SO_3 complexes. These methods employed a $\text{H}_2\text{O}/\text{MeCN}$ solvent system at lower temperatures, eliminating the need for column

chromatography and avoiding harsh conditions. This approach was particularly effective for protected aromatic amino acids, providing high yields of the sulfated products under mild conditions.

Chapter 4 presents a novel sulfation approach using $\text{Py}\cdot\text{SO}_3$ and $\text{Me}_3\text{N}\cdot\text{SO}_3$ complexes followed by a lipophilic exchange with tributylamine. This innovative method employs cost-effective and easily accessible reagents, yielding the desired sulfated compounds in good to excellent isolated yields. Although this method requires an additional operational step compared to the all-in-one TBSAB reagent, which can achieve similar transformations with higher yields, it is particularly advantageous for laboratories lacking the specialized equipment and techniques needed to prepare TBSAB. This method is effective for a range of substrates, including benzyl alcohols and benzylamines, providing high yields under mild conditions that are suitable for sensitive compounds.

Chapter 5 describes a robust and scalable approach for the selective sulfation of steroids using TBSAB. The methodology demonstrated high chemoselectivity for the sulfation of various steroids, including estrone, estradiol, cortisol, and pregnenolone, effectively producing biologically relevant sodium steroid sulfates without the need for complex ion-exchange chromatography. This method is versatile, allowing for the preparation of both mono- and disulfated steroidal structures, which are valuable in biological research and spectroscopic analysis. Additionally, this method extends to isotopically labelled derivatives, such as the sulfation of deuterated estrone (estrone- d_2), enhancing its application in biological studies.

Chapter 6 investigates whether heparan sulfate-glycomimetics could act as sulfate donors *in situ*. The experiment involved the reaction of glycomimetic (S-10) with benzyl alcohol under conditions designed to mimic the biological local environment. However, no reaction

occurred, as confirmed by ^1H NMR spectroscopy analysis. Furthermore, attempts to sulfate other benzyl alcohol derivatives using synthesized reagents such as sodium 4-methylbenzyl sulfate and sodium 4-chlorobenzyl sulfate also showed no significant formation of the desired products, based on ^1H NMR spectroscopic analysis. Despite these challenges, the study provided strong evidence for the stability of benzylic sulfates, as no hydrolysis was observed over a period of up to seven days, solving a pertained instability concern with sulfation chemistry.

Chapter 7 describes the synthesis and potential biological functions of cysteine trisulfide.

Future Work

- Confirm the structure of $\text{Pr}_3\text{N}\cdot\text{SO}_3$, 4-methylmorpholine SO_3 and 4-ethylmorpholine SO_3 complexes using X-ray crystallography and compare the findings with similar tertiary amine sulfur trioxide betaines, such as $\text{Et}_3\text{N}\cdot\text{SO}_3$ and TBSAB. This X-ray crystallography analysis will determine their complete molecular structures and confirm whether they exist as betaine forms or SO_3 complexes.
- Conduct additional studies on the use of the $\text{Pr}_3\text{N}\cdot\text{SO}_3$ as a novel sulfating reagent and as a low molecular weight compared to TBSAB and subsequently compare its results to the other tertiary amines SO_3 betaines, including TBSAB in reactions with a variety of small molecules, such as alcohols, phenols, carbohydrates, amino acids, and steroids.
- Further optimisation on the synthesis of the novel stereogenic sulfating agents; *isopropyl-N-methyl-N-tert-butylamine* SO_3 and cinchonidine SO_3 complexes, and evaluate their reactivity with a range of functional groups, such as alcohols and

phenols. These potential chiral reagents could be valuable in asymmetric synthesis or resolution.

- With α -amino acids substrates, additional optimisation efforts should include extending reaction times and utilizing column chromatography for purifying crude mixtures, particularly with more hydrophilic aliphatic amino acids such as *L*-serine, *L*-cysteine, and *L*-threonine. These optimised conditions should then be applied to a broader range of small molecules, including peptides.
- Further studies should be considered on the biological effects of cysteine trisulfide, to evaluate its therapeutic potential in protecting against oxidative stress and improving cardiovascular health.
- Future exploration should be also considered on the application of the novel sulfating reagents, including $\text{Pr}_3\text{N}\cdot\text{SO}_3$, 4-methylmorpholine SO_3 , and 4-ethylmorpholine SO_3 to a broader range of biologically relevant substrates, including more complex carbohydrates and glycomimetics, to enhance the scope and utility of the developed methods.

Chapter 8. Experimental and compound characterisation

General methods and experimental:

8.1. General Methods

All reactions involving moisture-sensitive reagents were carried out using standard Schlenk techniques, in a dry reaction vessel under argon. All solvents used under anhydrous conditions were decanted directly from an SPS dispensary or were stored over the activated 4 Å molecular sieves 24 h prior to use. The progress of reactions was monitored by thin layer chromatography (TLC) using Merck® silica gel 60 F254 plates, which were visualized with UV light and potassium permanganate.

Solvents used for workup procedures were of technical grade from Sigma-Aldrich, Honeywell, VWR or Fisher Scientific. Unless stated otherwise, solvents were removed by rotary evaporation under reduced pressure between 30-50 °C. All chemical reagents were used as received unless stated otherwise.

^1H , ^{13}C and ^{19}F NMR spectra were recorded on a Bruker Avance® III (300 MHz) and (400 MHz) spectrometer at 300, 400 (^1H), 101 (^{13}C), and 377 MHz (^{19}F). Chemical shift data are reported in parts per million (ppm, δ scale) downfield from tetramethylsilane (TMS: δ 0.0) and referenced internally to the residual proton in the solvent. The deuterated solvents used for NMR spectroscopy were: chloroform (CDCl_3 : δ_{H} 7.26, δ_{C} 77.16), dimethyl sulfoxide ($(\text{CD}_3)_2\text{SO}$: δ_{H} 2.50, δ_{C} 39.52), methanol (CD_3OD : δ_{H} 3.31, δ_{C} 49.00) and deuterium oxide (D_2O : δ_{H} 4.78). Coupling constants are given in Hertz (Hz). All individual signals were assigned using 2D NMR spectroscopy (^1H - ^1H -COSY, ^1H - ^{13}C -HSQC, and ^1H - ^{13}C -HMBC). The spectroscopic data are presented as follows: chemical shift, multiplicity (s = singlet, d = doublet, t = triplet, q = quartet, m = multiple, br = broad and combinations thereof), coupling constant, integration,

and structural assignment. Exchangeable protons such as in OH and NH groups are usually not observed in the NMR spectra when using deuterated solvents, including D₂O and CDCl₃.

Mass spectra were recorded on a Waters Xevo G2-XS TOF or SYNAPT G2-S mass spectrometer using Zspray, Electro-spray ionization in positive (ESI⁺), negative (ESI⁻), and ASAP⁺ ES modes.

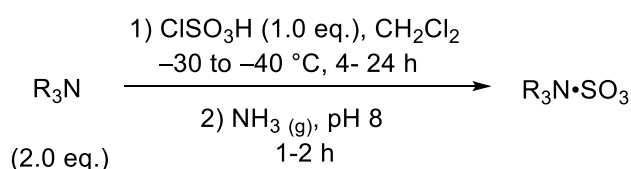
Infrared spectra were recorded on a Perkin Elmer Spectrum 100 FT-IR spectrometer and a Varian 660-IR FTIR spectrometer using Agilent Resolution Pro, with absorption maxima (ν_{\max}) reported in cm⁻¹.

Melting points were measured using a Gallenkamp melting point apparatus and are uncorrected.

Optical rotations were measured using a Bellingham and Stanley ADP450 Series-Peltier polarimeter at 25 °C using the sodium D line (589.3 nm) with the indicated concentration and solvent.

8.2. General Procedures

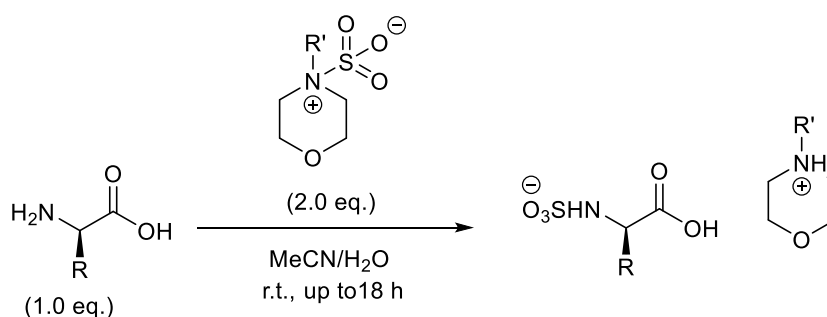
General procedure 1. Synthetic procedure for the preparation of tertiary amine sulfur trioxide complexes.



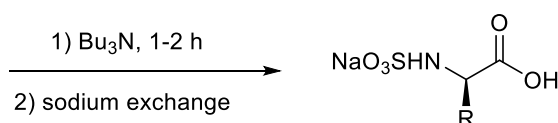
A three-necked round bottom flask was fitted with a temperature probe and a pressure-equalising dropping funnel. The flask under an atmosphere of argon was charged with a tertiary amine (2.0 eq.) (1 mL-60 mL) and anhydrous CH₂Cl₂ (7 mL-200 mL). The solution was

stirred vigorously and cooled to $-40\text{ }^{\circ}\text{C}$ (MeCN/CO₂). A solution of chlorosulfonic acid (1.0 eq.) (0.26 mL-16.75 mL) in anhydrous CH₂Cl₂ (7 mL-200 mL) was added dropwise at a rate ensuring the internal temperature did not exceed $-30\text{ }^{\circ}\text{C}$. After the full addition of the ClSO₃H solution, and stirring for a further 1 h, NH₃ (g) was gently bubbled through the reaction mixture until pH 7-8 was achieved. The precipitated solid was removed by vacuum filtration, washed with CH₂Cl₂ and the filtrate was collected. The solvent was removed under reduced pressure and the crude product was treated with cold H₂O. The precipitate was collected, washed with H₂O and freeze dried.

General procedure 2. Synthetic procedure for the sulfation of selective amino acids using 4-methyl and 4-ethylmorpholine sulfur trioxide complexes.



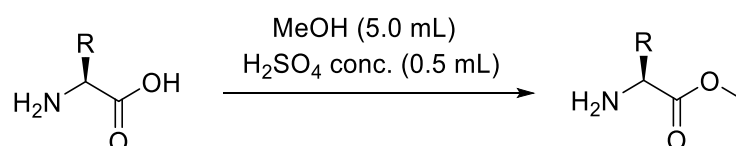
R' = Me or Et



A flask was charged with an amino acid (1.0 mmol) and 4-methylmorpholine SO₃ or 4-ethylmorpholine SO₃ (2.0 mmol) were dissolved in a 50:50 mixture of MeCN/H₂O (4 mL). The reaction mixture was stirred at room temperature and the reaction was monitored by TLC. After the completion of reaction, tributylamine (1.0 mmol) was added to the reaction mixture which was stirred for an additional 2 h. Then, the solvent was removed under reduced pressure and the intermediate was dissolved in MeCN (10 mL-20 mL) and the

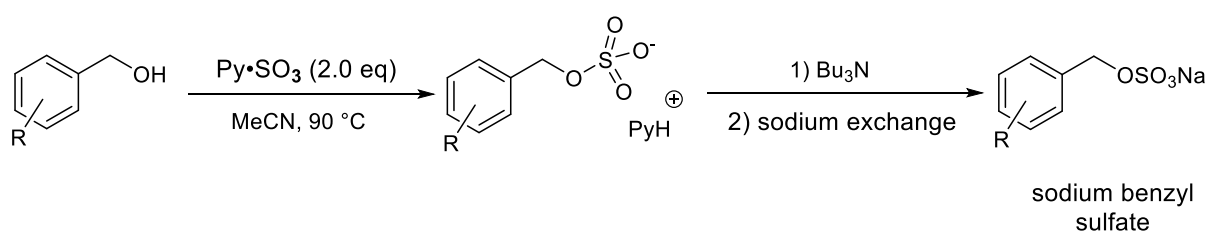
tributylammonium cation intermediate subsequently exchanged with NaI (2.5-5.0 eq.). The reaction mixture was stirred vigorously for an additional 1 h and the solid that formed was collected by filtration and dried under vacuum overnight affording the desired sulfamate compound.

General procedure 3. Preparation of amino acids methyl esters.



A flask was charged with amino acid (500 mg, 3.02 mmol) and dissolved in MeOH (5.0 mL). Concentrated H₂SO₄ (0.5 mL) was added dropwise over one minute and the reaction mixture was heated at reflux and monitored by TLC. After complete consumption of starting material was observed, solvent was removed under reduced pressure and the reaction was quenched with NaHCO₃ (aq.) (to pH 9-10). The aqueous mixture was extracted with ethyl acetate (4 x 40 mL). The combined organic extracts were washed with brine (10 mL), dried (MgSO₄) and filtered *in vacuo* to afford the methyl ester that was used directly in the next step without further purification.

General procedure 4. Synthetic procedure for the preparation of sodium benzyl sulfate esters using pyridine sulfur trioxide complex and tributylamine.



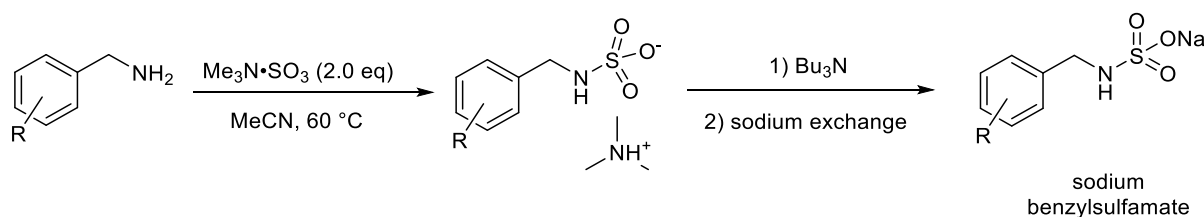
A flame-dried 100 mL round-bottom flask was charged with the appropriate alcohol (1.0 mmol) and sulfur trioxide pyridine complex (2.0 mmol) under argon. Anhydrous MeCN (2.0 mL) was added and the reaction mixture was heated at 90 °C (monitored by TLC). After 3 h, tributylamine (2.0 mmol) was added to the reaction mixture and the mixture was stirred for 30 min at 90 °C. The flask was cooled to room temperature and the solvent removed under reduced pressure to afford the desired sulfate ester as its tributylammonium salt.

Work-up procedure A: The flask containing the tributylammonium salt was charged with EtOH (30 mL) and sodium 2-ethylhexanoate (5.0 eq. per sulfate group). The reaction mixture was stirred vigorously for 1 h at room temperature. The precipitate was collected by filtration, washed with EtOH (3 × 20 mL) and dried to a constant weight to afford the desired sulfate ester as its sodium salt.

Work-up procedure B: The flask containing the tributylammonium salt was charged with ethyl acetate (30 mL) and sodium 2-ethylhexanoate (5.0 eq. per sulfate group). The reaction mixture was stirred vigorously for 1 h at room temperature. The precipitate was collected by filtration, washed with ethyl acetate (3 × 20 mL) and dried to a constant weight to afford the desired sulfate ester as its sodium salt.

Work-up procedure C: The flask containing the tributylammonium salt was charged with MeCN (25 mL) and sodium iodide (5.0 eq. per sulfate group). The reaction mixture was stirred vigorously for 1 h at room temperature. The precipitate was removed by filtration, washed with MeCN (3 × 20 mL) and dried to a constant weight to afford the desired sulfate ester as its sodium salt.

General procedure 5. Synthetic procedure for the preparation of sodium benzylsulfamates using trimethylamine sulfur trioxide and tributylamine.

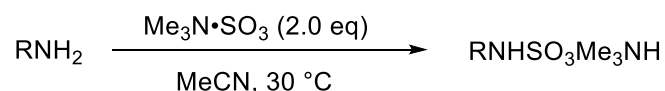


A flame-dried 100 mL round-bottom flask was charged with the appropriate amine (1.0 mmol) and sulfur trioxide trimethylamine complex (2.0 mmol) under argon. Anhydrous MeCN (2.0 mL) was added and the reaction mixture was heated at 60 °C (monitored by TLC). After 30 min, tributylamine (2.0 mmol) was added to the reaction mixture and the mixture was stirred for 30 min at 60 °C. The flask was cooled to room temperature and the solvent removed under reduced pressure to afford the desired sulfamate ester as its tributylammonium salt.

Work-up procedure A: The flask containing the tributylammonium salt was charged with EtOH (30 mL) and sodium 2-ethylhexanoate (1.5 eq. per sulfate group). The reaction mixture was stirred vigorously for 1 h at room temperature. The precipitate was removed by filtration, washed with EtOH (3 × 20 mL) and dried to a constant weight to afford the desired sulfamate ester as its sodium salt.

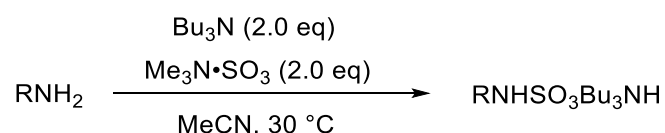
Work-up procedure B: The flask containing the tributylammonium salt was charged with MeCN (25 mL) and sodium iodide (1.5 eq. per sulfate group). The reaction mixture was stirred vigorously for 1 h at room temperature. The precipitate was removed by filtration, washed with MeCN (3 × 20 mL) and dried to a constant weight to afford the desired sulfamate ester as its sodium salt.

General procedure 6. Low-temperature preparation of trimethylammonium sulfamate salts using trimethylamine sulfur trioxide ($\text{Me}_3\text{N}\cdot\text{SO}_3$).



A 25 mL flask was charged with the appropriate amine (1.0 mmol) and $\text{Me}_3\text{N}\cdot\text{SO}_3$ complex (2.0 eq.) under argon. Anhydrous MeCN was added (giving a concentration of 0.50 mol dm^{-3} to the limiting reagent), the reaction mixture was heated at 30°C and monitored by TLC. After reaction completion, the flask was cooled to room temperature and the solvent removed under reduced pressure. The reaction was quenched with EtOH (10 mL) and filtered. The solution was evaporated and extracted with H_2O (10 mL) and ethyl acetate (4 x 40 mL). The organic layer was dried (MgSO_4), filtered, and the solvent was removed *in vacuo* giving the desired trimethylammonium salt as an oil.

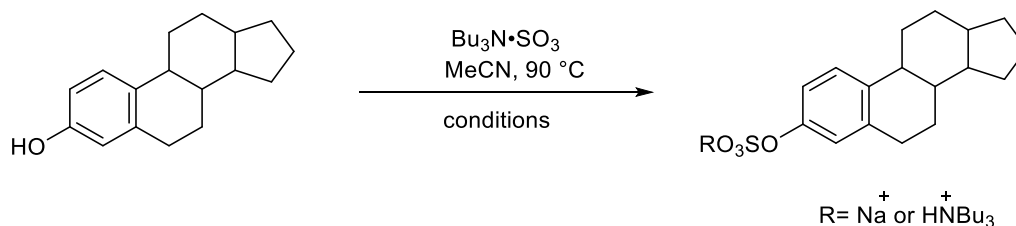
General procedure 7. *In situ* preparation of tributylammonium sulfamate salts using trimethylamine sulfur trioxide ($\text{Me}_3\text{N}\cdot\text{SO}_3$).



A 25 mL flask was charged with the appropriate amine (1.0 mmol) and tributylamine (2.0 eq.) dissolved in anhydrous MeCN (giving a concentration of 0.50 mol dm^{-3} to the limiting reagent) under argon. After addition of $\text{Me}_3\text{N}\cdot\text{SO}_3$ (2.0 eq.), the reaction mixture was heated at 30°C and monitored by TLC. After reaction completion, the flask was cooled to room temperature and the solvent removed under reduced pressure. The reaction was quenched with EtOH (10 mL) and filtered. The solution was evaporated and extracted with H_2O (10 mL) and ethyl

acetate (4 x 40 mL). The organic layer was dried (MgSO_4), filtered, and the solvent was removed *in vacuo* giving the desired tributylammonium salt as an oil.

General procedure 8. Synthetic procedure for preparation of sodium mono-sulfated steroids using tributylsulfonium betaine ($\text{Bu}_3\text{N}^+\cdot\text{SO}_3^-$, TBSAB).



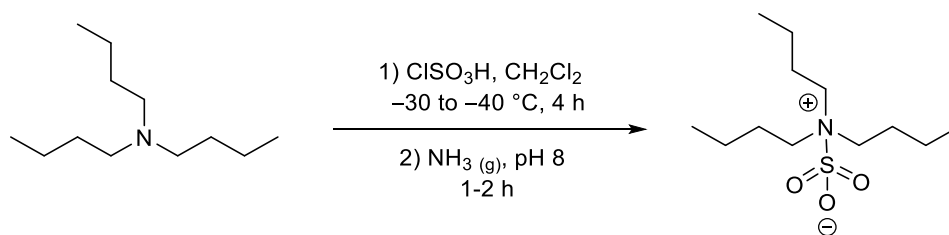
A flame-dried 100 mL round-bottom flask was charged with the appropriate steroid (1.0 mmol) and TBSAB (1.2-5.0 eq.) under argon. Anhydrous MeCN (1.5-4.0 mL per mmol of $\text{Bu}_3\text{N}^+\cdot\text{SO}_3^-$) was added to the flask and the reaction mixture was heated under reflux until the TLC indicated that the reaction mixture was complete (typically 2-7 h). Then, the flask was cooled to room temperature and the solvent was removed under reduced pressure to afford the desired sulfated steroid as its tributylammonium salt.

Work-up procedure A: The flask containing the tributylammonium salt was charged with EtOH (30 mL) and sodium 2-ethylhexanoate (5.0 eq.). The reaction mixture was stirred vigorously for 1 h at room temperature. The precipitate was removed by filtration, washed with EtOH (3 x 20 mL) and dried to a constant weight to afford the desired sulfated steroid as its sodium salt.

Work-up procedure B: The flask containing the tributylammonium salt was charged with MeCN (25 mL) and sodium iodide (5.0 eq.). The reaction mixture was stirred vigorously for 1 h at room temperature. The precipitate was removed by filtration, washed with MeCN (3 x 20 mL) and dried to a constant weight to afford the desired sulfated steroid as its sodium salt.

8.3. Compound characterisation

Preparation of TriButylSulfoAmmonium Betaine (TBSAB, Bu₃N•SO₃) (42)¹⁴⁹



A three-necked round-bottom flask was fitted with a temperature probe and a pressure equalising dropping funnel. The flask under an atmosphere of argon was charged with tributylamine (59.4 mL, 0.25 mol) and anhydrous CH₂Cl₂ (200 mL). The solution was stirred vigorously and cooled to -40 °C (MeCN/CO₂). A solution of chlorosulfonic acid (16.75 mL, 0.253 mol) in anhydrous CH₂Cl₂ (200 mL) was added dropwise over 2 h at a rate ensuring the internal temperature did not exceed -30 °C. After full addition of the ClSO₃H solution, and stirring for a further 1 h, NH₃ (g) was gently bubbled through the reaction mixture until pH 8 was achieved. The white solid was removed by vacuum filtration, washed with CH₂Cl₂ (100 mL) and the filtrate was collected. The solvent was removed under reduced pressure and the crude product was treated with H₂O (0 °C, 500 mL). The precipitate was collected, washed with H₂O (5 × 100 mL) and freeze dried. Recrystallization from CH₂Cl₂/hexane afforded Bu₃N•SO₃ (42) as a bright white solid (59.8 g, 90%).

M.P. 95-96 °C (Lit.¹⁵⁵ 94-96 °C).

IR ν_{\max} cm⁻¹ 2962 w, 2875 w, 1473 m, 1293 m (O-S).

¹H NMR (400 MHz, CDCl₃) 3.32 – 3.22 (m, 6H), 1.87 – 1.73 (m, 6H), 1.37 (dt, *J* = 7.4 Hz, 6H), 0.98 (t, *J* = 7.4 Hz, 9H).

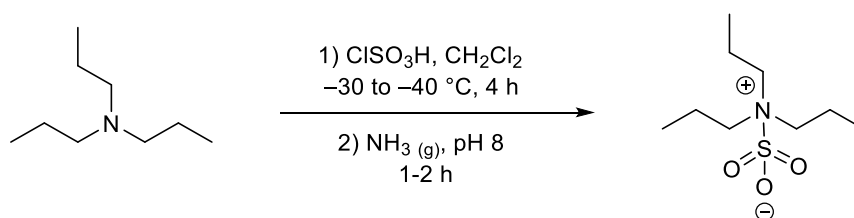
¹³C NMR (101 MHz, CDCl₃) 57.1, 25.6, 20.6, 13.7.

LRMS m/z (ESI⁻) 264.1 ([M-H]⁻, 100%).

HRMS m/z (ESI⁻) C₁₂H₂₆NO₃S [M-H]⁻ requires 264.1613, Found: 264.1612 ([M-H]⁻).

Data were consistent with those reported in the literature.¹⁴⁹

Preparation of tripropylamine sulfur trioxide complex (Pr₃N•SO₃) (**102**)



A three-necked round-bottom flask was fitted with a temperature probe and a pressure equalising dropping funnel. The flask under an atmosphere of argon was charged with tripropylamine (11.89 mL, 0.0625 mol) and anhydrous CH₂Cl₂ (50 mL). The solution was stirred vigorously and cooled to -40 °C (MeCN/CO₂). A solution of chlorosulfonic acid (4.16 mL, 0.0625 mol) in anhydrous CH₂Cl₂ (50 mL) was added dropwise over 1 h at a rate ensuring the internal temperature did not exceed -30 °C. After full addition of the ClSO₃H solution, and stirring for a further 1 h, NH₃ (g) was gently bubbled through the reaction mixture until pH 8 was achieved. The white solid was removed by vacuum filtration, washed with CH₂Cl₂ (25 mL) and the filtrate was collected. The solvent was removed under reduced pressure and the crude product was treated with H₂O (0 °C, 100 mL). The precipitate was collected, washed with H₂O (100 mL) and freeze dried. Recrystallization from CH₂Cl₂/hexane afforded Pr₃N•SO₃ (**102**) as a bright white solid (13.0 g, 89%).

M.P. 155-157 °C

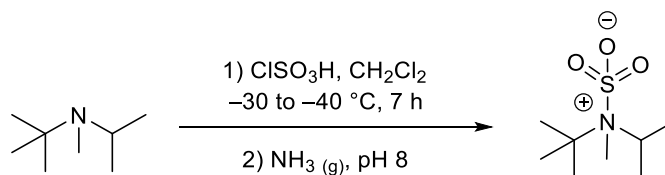
$^1\text{H NMR}$ (300 MHz, CDCl_3) δ 3.29 – 3.18 (m, 6H, NCH_2), 1.95 – 1.76 (m, 6H, CH_2), 0.97 (t, $J = 7.4$ Hz, 9H, CH_3).

$^{13}\text{C NMR}$ (101 MHz, CDCl_3) δ 58.8 (NCH_2), 17.2 (CH_2), 11.6 (CH_3).

LRMS m/z (ESI $^-$) 224.1 ($[\text{M}^{12}\text{C}+\text{H}]^-$, 100%), 225.1 ($[\text{M}^{13}\text{C}+\text{H}]^-$, 10%).

HRMS m/z (ESI $^-$) $\text{C}_9\text{H}_{21}\text{NO}_3\text{S}$ requires 224.1320, found 224.1307 $[\text{M}+\text{H}]^-$.

Preparation of *Isopropyl-N-methyl-tert-butylamine* sulfur trioxide complex (**112**)



A three-necked round-bottom flask was fitted with a temperature probe and a pressure equalising dropping funnel. The flask under an atmosphere of argon was charged with *Isopropyl-N-methyl-tert-butylamine* (1.35 mL, 0.008 mol) and anhydrous CH_2Cl_2 (7 mL). The solution was stirred vigorously and cooled to -40 °C (MeCN/CO_2). A solution of chlorosulfonic acid (0.53 mL, 0.008 mol) in anhydrous CH_2Cl_2 (7 mL) was added dropwise over 15 minutes at a rate ensuring the internal temperature did not exceed -30 °C. After full addition of the ClSO_3H solution, and stirring for a further 7 h, NH_3 (g) was gently bubbled through the reaction mixture until pH 7-8 was achieved. The white solid was removed by vacuum filtration, washed with CH_2Cl_2 (25 mL) and the filtrate was collected. The solvent was removed under reduced pressure and the crude product was treated with cold H_2O (100 mL). The precipitate was collected, washed with H_2O (100 mL) and freeze dried. Recrystallization from CH_2Cl_2 /hexane

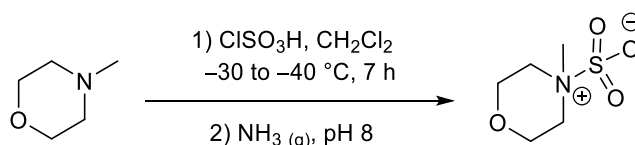
afforded *isopropyl-N-methyl-tert-butylamine* sulfur trioxide (**112**) as a brown solid (108.8, 7%).

$^1\text{H NMR}$ (300 MHz, CDCl_3) δ 3.92 – 3.77 (m, 1H), 2.60 (s, 3H), 1.49 (s, 9H), 1.40 – 1.34 (m, 6H).

$^{13}\text{C NMR}$ (101 MHz, CDCl_3) δ 64.0, 57.9, 56.8, 52.3, 48.4, 47.3, 29.6, 28.70, 26.8, 25.6, 23.1, 22.3. (additional signals; 56.8, 47.3, 26.8, 25.6, 22.3 were observed due to diastereomeric produced due to the potential stereogenic axis of this complex).

The product was directly used for *in situ* *N*-sulfamation reaction of benzylamine without further analysis.

Preparation of 4-methylmorpholine sulfur trioxide complex (**115**)



A three-necked round-bottom flask was fitted with a temperature probe and a pressure equalising dropping funnel. The flask under an atmosphere of argon was charged with 4-methylmorpholine (10 mL, 0.09 mol) and anhydrous CH_2Cl_2 (50 mL). The solution was stirred vigorously and cooled to -40 °C (MeCN/CO_2). A solution of chlorosulfonic acid (5.9 mL, 0.09 mol) in anhydrous CH_2Cl_2 (20 mL) was added dropwise over 1 h at a rate ensuring the internal temperature did not exceed -30 °C. After full addition of the chlorosulfonic acid solution, and stirring for a further 6 h, ammonia gas was gently bubbled through the reaction mixture until pH 8 was achieved. The white solid was removed by vacuum filtration, washed with CH_2Cl_2 (10 mL) and the filtrate was collected. The solvent was removed under reduced pressure affording 4-methylmorpholine sulfur trioxide complex (**115**) as an off-white solid (6.1 g, 37%).

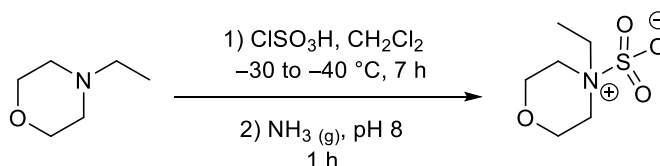
$^1\text{H NMR}$ (400 MHz, Methanol- d_4) δ 4.05 (dd, $J = 13.2, 3.7$ Hz, 2H), 3.80 (t, $J = 13.5, 11.8, 2.2$ Hz, 2H), 3.48 – 3.40 (m, 2H), 3.22 – 3.12 (m, 2H), 2.92 (s, 3H).

$^{13}\text{C NMR}$ (101 MHz, Methanol- d_4) δ 65.1, 54.6, 43.9.

LRMS m/z (ES+) 204.0 ($[\text{M}^{12}\text{C}+\text{Na}]^+$, 100%); 205.0 ($[\text{M}^{13}\text{C}+\text{Na}]^+$, 10%).

HRMS m/z (ES+) $\text{C}_5\text{H}_{11}\text{NO}_4\text{NaS}$ requires 204.0306, found 204.0311 ($[\text{M}+\text{Na}]^+$).

Preparation of 4-ethylmorpholine sulfur trioxide complex (**119**)



A three-necked round-bottom flask was fitted with a temperature probe and a pressure equalising dropping funnel. The flask under an atmosphere of argon was charged with 4-ethylmorpholine (10 mL, 0.079 mol) and anhydrous CH_2Cl_2 (60 mL). The solution was stirred vigorously and cooled to -40 °C (MeCN/ CO_2). A solution of chlorosulfonic acid (5.25 mL, 0.079 mol) in anhydrous CH_2Cl_2 (60 mL) was added dropwise over 1 h at a rate ensuring the internal temperature did not exceed -30 °C. After full addition of the chlorosulfonic acid solution, and stirring for a further 7 hours, ammonia gas was gently bubbled through the reaction mixture until pH 7 was achieved. The white solid was removed by filtration, washed with CH_2Cl_2 (30 mL) and the filtrate was collected. The solvent was removed under reduced pressure affording 4-ethylmorpholine sulfur trioxide complex (**119**) as a brown solid (7.4 g, 48%).

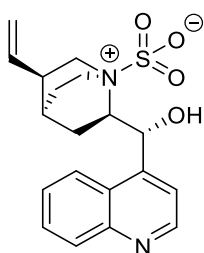
¹H NMR (400 MHz, Methanol-d₄) δ 4.05 (d, *J* = 13.1 Hz, 2H), 3.81 (t, *J* = 12.5 Hz, 2H), 3.54 – 3.42 (m, 2H), 3.23 (q, *J* = 7.4 Hz, 2H), 3.15 – 3.03 (m, 2H), 1.37 (t, *J* = 7.3 Hz, 3H).

¹³C NMR (101 MHz, Methanol-d₄) δ 65.1, 53.6, 52.6, 9.2.

LRMS *m/z* (ES⁻) 196.0 ([M]⁻, 100%), 197.0 ([M-H]⁻, 10%).

HRMS *m/z* (ES⁻) C₆H₁₄NO₄S requires 196.0644, found 196.0642 [M]⁻.

Preparation of cinchonidine sulfur trioxide complex (**122**)



A three-necked round-bottom flask was fitted with a temperature probe and a pressure equalising dropping funnel. The flask under an atmosphere of argon was charged with cinchonidine (500 mg, 1.69 mmol) and anhydrous CH₂Cl₂ (4 mL). The solution was stirred vigorously and cooled to -40 °C (MeCN/CO₂). A solution of chlorosulfonic acid (0.26 mL) in anhydrous CH₂Cl₂ (4 mL) was added dropwise over 15 minutes ensuring the internal temperature did not exceed -30 °C. After full addition of the chlorosulfonic acid solution, and stirring for a further 7 h, ammonia gas was gently bubbled through the reaction mixture until pH 7-8 was achieved. The white solid was removed by vacuum filtration, washed with CH₂Cl₂ (10 mL) and the filtrate was collected. The solvent was removed under reduced pressure and the crude product was treated with H₂O (0 °C, 10 mL). The precipitate was collected and

freeze dried to afford cinchonidine sulfur trioxide complex (**122**) as a white solid (349.0 mg, 55%).

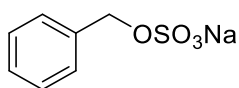
¹H NMR (300 MHz, CDCl₃) δ 8.86 (dd, *J* = 10.2, 4.5 Hz, 1H), 8.00 (dd, *J* = 8.5, 1.2 Hz, 1H), 7.84 – 7.72 (m, 2H), 7.68 – 7.57 (m, 1H), 7.56 – 7.47 (m, 1H), 5.84 (d, *J* = 2.6 Hz, 1H), 5.60 – 5.43 (m, 1H), 5.03 – 4.87 (m, 2H), 3.40 (t, *J* = 9.1 Hz, 1H), 3.18 (dd, *J* = 13.7, 10.7 Hz, 2H), 3.03 – 2.81 (m, 2H), 2.49 (d, *J* = 15.8 Hz, 1H), 2.11 – 1.81 (m, 3H), 1.74 – 1.56 (m, 2H), 1.36 – 1.19 (m, 1H).

¹³C NMR (101 MHz, CDCl₃) δ 150.0, 148.0, 146.8, 138.8, 130.1, 130.0, 129.2, 129.1, 127.0, 124.8, 122.4, 118.5, 116.4, 116.3, 68.8, 60.6, 60.0, 55.9, 55.6, 44.2, 43.8, 38.2, 38.0, 27.2, 26.9, 25.6, 19.7 (additional signals; 130.0, 129.1, 116.3, 60.0, 55.6, 43.8, 38.0, 26.9 were observed due to stereogenic centre formed suggesting a diastereomer produced).

LRMS *m/z* (ESI⁻) 373.1230 ([M¹²C-H]⁻, 100%), 374.1254 ([M¹²C-H]⁻, 20%).

HRMS *m/z* (ESI⁻) C₁₉H₂₂N₂O₄S requires 373.1230, found 373.1222 [M-H]⁻.

Preparation of sodium benzyl sulfate using Pr₃N•SO₃ (**105**)



A flame-dried 50 mL round-bottom flask was charged with benzyl alcohol (0.1 mL, 1.0 mmol) and Pr₃N•SO₃ complex (446.6 mg, 2.0 mmol) were dissolved in anhydrous MeCN (4.0 mL) and heated under reflux at 90 °C for 2 h. After the completion of reaction, the flask was cooled to room temperature and solvent removed under reduced pressure. The tripropylammonium intermediate was exchanged with sodium salt (NEH or NaI, 5.0 eq.) and dissolved in MeCN

(25 mL) or EtOH (25 mL). The reaction mixture was stirred vigorously for 1 h at room temperature. The solid was removed by filtration, washed with MeCN or EtOH (3 × 20 mL) and dried to a constant weight to afford sodium benzyl sulfamate (**105**) as a bright white solid (195.3 mg, 93%).

M.P. 193-195 °C (Lit. 208-210 °C)¹⁴⁹

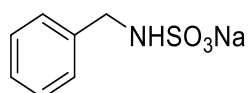
¹H NMR (400 MHz, D₂O) δ 7.54 – 7.43 (m, 5H), 5.11 (s, 2H).

¹³C NMR (101 MHz, D₂O) δ 135.1, 128.7 (CH, C), 128.4, 70.7.

LRMS m/z (ESI⁻) 187.0 ([M-Na]⁻, 100 %), 188.1 ([M¹³C-Na]⁻, 10 %).

Data were consistent with those reported in the literature.¹⁴⁹

Preparation of sodium benzyl sulfamate using Pr₃N•SO₃ (**108**)



A flame-dried 50 mL round-bottom flask was charged with benzylamine (0.1 mL, 1.0 mmol) and Pr₃N•SO₃ complex (446.6 mg, 2.0 mmol) were dissolved in anhydrous MeCN (4.0 mL). The reaction mixture was stirred at 30 °C for 2 h. After the completion of reaction, the solvent was removed under reduced pressure and the tripropylammonium cation intermediate was exchanged with NaI (5.0 eq.) and dissolved in MeCN (25 mL). The reaction mixture was stirred vigorously for 1 h at room temperature. The solid was removed by filtration, washed with MeCN (3 × 20 mL) and dried to a constant weight to afford sodium benzyl sulfamate (**108**) as a bright white solid (188.2 mg, 90%).

M.P. 238-240 °C (Lit. ^[2] >230 °C)

¹H NMR (400 MHz, D₂O) δ 7.43 – 7.30 (m, 5H), 4.12 (s, 2H).

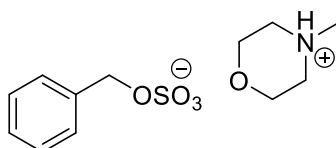
¹³C NMR (101 MHz, D₂O) δ 137.9, 128.6, 128.2, 127.5, 47.3.

LRMS *m/z* (ESI⁻) 186.0 ([M-Na]⁻, 100 %), 187.0 ([M¹³C-Na]⁻, 10 %).

HRMS *m/z* (ESI⁻) C₇H₈NO₃S requires 186.0225, found 186.0228 [M-Na]⁻.

Data were consistent with those reported in the literature.⁴⁷

Preparation of 4-methylmorpholinium benzyl sulfate using 4-methylmorpholine SO₃ (**116**)



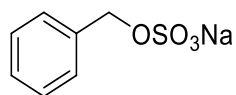
A flame-dried 50 mL round-bottom flask was charged with benzyl alcohol (0.05 mL, 0.5 mmol) and 4-methylmorpholine SO₃ complex (181.2 mg, 1.0 mmol) were dissolved in anhydrous MeCN (3.0 mL) and heated under reflux at 90 °C for 3 h. The flask was cooled, and the solvent removed under reduced pressure. The crude reaction product was purified by flash chromatography (SiO₂; CH₂Cl₂/MeOH, 9:1) to yield 4-methylmorpholinium benzyl sulfate using 4-methylmorpholine SO₃ (**116**) as a clear oil (100.0 mg, 69%).

¹H NMR (400 MHz, Methanol-*d*₄) δ 7.44 – 7.28 (m, 5H), 5.02 (s, 2H), 4.04 – 3.96 (m, 2H), 3.79 – 3.68 (m, 2H), 3.39 (d, *J* = 12.5 Hz, 2H), 3.17 – 3.06 (m, 2H), 2.87 (s, 3H).

¹³C NMR (101 MHz, Methanol-*d*₄) δ 137.6, 129.4, 129.2, 129.1, 70.8, 65.0, 54.5, 44.0.

Note: The product was directly used *in situ* for the next reaction, sodium salt exchange affording sodium benzyl sulfate (**105**) without further analysis.

Preparation of sodium benzyl sulfate (**105**) using 4-methylmorpholine SO₃ complex



A flame-dried 50 mL round-bottom flask was charged with benzyl alcohol (0.05 mL, 0.5 mmol) and 4-methylmorpholine SO₃ complex (181.2 mg, 1.0 mmol) were dissolved in anhydrous MeCN (3.0 mL). The mixture was heated under reflux at 90 °C for 3 h. The 4-methylmorpholinium cation intermediate was purified by flash chromatography (SiO₂; CH₂Cl₂/MeOH; 9:1) and subsequently exchanged with the lipophilic partner, tributylamine (0.23 mL, 1.0 mmol) and stirred for an additional 1 h at 90 °C. After the completion of reaction, the flask was cooled to room temperature and the solvent was removed under reduced pressure. The tributylammonium intermediate crude was treated with NEH (2.5 eq.) and dissolved in EtOH (10 mL) followed by stirring for an additional 1 h affording sodium benzyl sulfate (**105**) as a white solid (8.2 mg, 8%).

¹H NMR (400 MHz, DMSO-*d*₆) δ 7.37 – 7.24 (m, 5H), 4.77 (s, 2H).

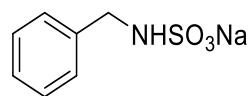
¹³C NMR (101 MHz, DMSO-*d*₆) δ 137.8, 128.1, 127.5, 127.3, 67.4.

LRMS *m/z* (ES⁻) 187.0 ([M-Na]⁻, 100%); 188.0 ([M¹³C-Na]⁻, 10%).

HRMS *m/z* (ES⁻) C₇H₇O₄S requires 187.0065, found 187.0069 ([M-Na]⁻).

Data were consistent with those reported in the literature.¹⁴⁹

Preparation of sodium benzyl sulfamate (**108**) using 4-methylmorpholine SO₃ complex



A flame-dried 50 mL round-bottom flask was charged with benzylamine (0.05 mL, 0.5 mmol) and 4-methylmorpholine SO₃ complex (181.2 mg, 1.0 mmol) were dissolved in anhydrous MeCN (3.0 mL) and stirred at room temperature for 4 h. The 4-methylmorpholinium cation intermediate was purified by flash chromatography (SiO₂; CH₂Cl₂/MeOH; 9:1) and subsequently exchanged with a lipophilic partner, tributylamine (0.23 mL, 1.0 mmol) and stirred for an additional 1 h at room temperature. After the completion of reaction, solvent was removed under reduced pressure and the tributylammonium intermediate crude was treated with NaI (2.5 eq.) and dissolved in MeCN (10 mL) followed by stirring for an additional 1 h afforded sodium benzyl sulfamate (**108**) as a white solid (58.3 mg, 56%).

¹H NMR (300 MHz, D₂O) δ 7.51 – 7.35 (m, 5H), 4.16 (s, 2H).

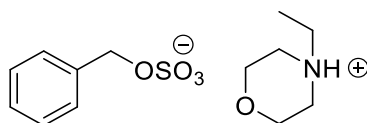
¹³C NMR (101 MHz, D₂O) δ 137.9, 128.6, 128.2, 127.5, 47.3.

LRMS *m/z* (ES⁻) 186.0 ([M–Na]⁻, 100%); 187.0 ([M¹³C–Na]⁻, 10%).

HRMS *m/z* (ES⁻) C₇H₈NO₃S requires 186.0225, found 186.0232 ([M–Na]⁻).

Data were consistent with those reported in the literature.⁴⁷

Preparation of 4-ethylmorpholinium benzyl sulfate (**120**) using 4-ethylmorpholine SO₃



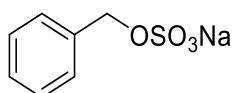
A flame-dried 50 mL round-bottom flask was charged with benzyl alcohol (0.1 mL, 1.0 mmol) and 4-ethylmorpholine SO₃ complex (390.4 mg, 2.0 mmol) were dissolved in anhydrous MeCN (3.0 mL) and heated under reflux at 90 °C for 4 h. The flask was cooled, and the solvent was removed under reduced pressure. The crude reaction product was purified by flash chromatography (SiO₂; CH₂Cl₂/MeOH, 9:1) to yield 4-ethylmorpholinium benzyl sulfate (**120**) as a clear oil (202.0 mg, 66%).

¹H NMR (400 MHz, DMSO-*d*₆) δ 9.33 (s, 1H), 7.39 – 7.23 (m, 5H), 4.78 (s, 2H), 4.04 – 3.89 (m, 2H), 3.62 (t, *J* = 12.5 Hz, 2H), 3.48 – 3.29 (m, 2H), 3.14 (q, *J* = 7.3 Hz, 2H), 3.02 (s, 2H), 1.20 (t, *J* = 7.3 Hz, 3H).

¹³C NMR (101 MHz, DMSO-*d*₆) δ 137.8, 128.1, 127.6, 127.3, 67.5, 63.4, 51.2, 50.6, 8.7.

4-ethylmorpholinium benzyl sulfate (**120**) was directly used for the next step without further analysis.

Preparation of sodium benzyl sulfate (**105**) using 4-ethylmorpholine SO₃ complex



A flame-dried 50 mL round-bottom flask was charged with benzyl alcohol (0.1 mL, 1.0 mmol) and 4-ethylmorpholine SO₃ complex (390.4 mg, 2.0 mmol) were dissolved in anhydrous MeCN

(3.0 mL) and heated under reflux at 90 °C for 4 h. The flask was cooled, and the solvent was removed under reduced pressure. The 4-ethylmorpholinium intermediate was purified by flash chromatography (SiO₂; CH₂Cl₂/MeOH; 9:1) and exchanged with NaI (5.0 eq.) and dissolved in MeCN (25 mL). This was followed by stirring the mixture for an additional 1 h at room temperature affording sodium benzyl sulfate (**105**) as a white solid (192.0 mg, 91%).

¹H NMR (400 MHz, DMSO-*d*₆) δ 7.37 – 7.24 (m, 5H), 4.77 (s, 2H).

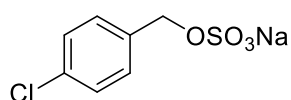
¹³C NMR (101 MHz, DMSO-*d*₆) δ 137.8, 128.1, 127.5, 127.3, 67.4.

LRMS *m/z* (ES⁻) 187.0 ([M-Na]⁻, 100%); 188.0 ([M¹³C-Na]⁻, 10%).

HRMS *m/z* (ES⁻) C₇H₇O₄S requires 187.0063, found 187.0065 ([M-Na]⁻).

Data were consistent with those reported in the literature.¹⁴⁹

Preparation of sodium 4-chlorobenzyl sulfate (**157**) using 4-ethylmorpholine SO₃ complex



A flame-dried 50 mL round-bottom flask was charged with 4-chlorobenzyl alcohol (71.2 mg, 0.5 mmol) and 4-ethylmorpholine SO₃ complex (195.2 mg, 1.0 mmol) were dissolved in anhydrous MeCN (2.0 mL) and the reaction mixture was heated under reflux at 90 °C for 4 h. The flask was cooled, and the solvent was removed under reduced pressure. The 4-ethylmorpholinium intermediate was purified by flash chromatography (SiO₂; CH₂Cl₂/MeOH; 9:1) and exchanged with NaI (2.5 eq.) and dissolved in MeCN (10 mL). This was followed by

stirring the mixture for an additional 1 h at room temperature affording sodium 4-chlorobenzyl sulfate (**157**) as a yellow solid (78.0 mg, 64%).

M.P. 227-229 °C (Lit.¹⁴⁹ 202- 204 °C)

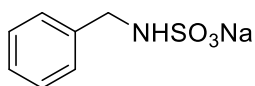
¹H NMR (400 MHz, DMSO-*d*₆) δ 7.43 – 7.30 (m, 4H), 4.76 (s, 2H).

¹³C NMR (101 MHz, DMSO-*d*₆) δ 137.0, 131.8, 129.3, 128.0, 66.5

LRMS *m/z* (ESI⁻) 220.9 ([M³⁵Cl–Na]⁻, 100 %), 222.9 ([M³⁷Cl–Na]⁻, 40 %).

HRMS *m/z* (ESI⁻) C₇H₆O₄SCl requires 220.9675, found 220.9681 [M³⁵Cl–Na]⁻.

Preparation of sodium benzyl sulfamate (**108**) using 4-ethylmorpholine SO₃ complex



A flame-dried 50 mL round-bottom flask was charged with benzylamine (0.05 mL, 0.5 mmol) and 4-methylmorpholine SO₃ complex (181.2 mg, 1.0 mmol) were dissolved in anhydrous MeCN (3.0 mL) and stirred at room temperature for 4 h. The 4-methylmorpholinium intermediate was purified by flash chromatography (SiO₂; CH₂Cl₂/MeOH; 9:1) and subsequently exchanged with tributylamine (0.23 mL, 1.0 mmol) and stirred at room temperature for an additional 1 h. After the completion of reaction, the solvent was removed under reduced pressure and the tributylammonium cation intermediate was treated with NaI (2.5 eq.) and MeCN (10 mL). The reaction mixture was stirred at room temperature for 1 h affording sodium benzyl sulfamate (**108**) as a white solid (58.3 mg, 56%).

$^1\text{H NMR}$ (400 MHz, D_2O) δ 7.43 – 7.30 (m, 5H), 4.12 (s, 2H).

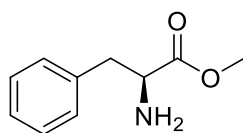
$^{13}\text{C NMR}$ (101 MHz, D_2O) δ 137.9, 128.6, 128.2, 127.5, 47.3.

LRMS m/z (ESI $^-$) 186.0 ($[\text{M}-\text{Na}]^-$, 100 %), 187.0 ($[\text{M}^{13}\text{C}-\text{Na}]^-$, 10 %).

HRMS m/z (ESI $^-$) $\text{C}_7\text{H}_8\text{NO}_3\text{S}$ requires 186.0225, found 186.0228 $[\text{M}-\text{Na}]^-$.

Data were consistent with those reported in the literature.⁴⁷

Preparation of *L*-phenylalanine methyl ester (**141**)



Following **general procedure 3**: A flask was charged with *L*-phenylalanine (500 mg, 3.02 mmol) which was dissolved in MeOH (5.0 mL). Concentrated H_2SO_4 (0.5 mL) was added dropwise over 1 minute and the reaction mixture was heated at reflux for 4 h. After the completion of reaction, the flask was cooled to room temperature and the solvent was removed under reduced pressure. The reaction mixture was quenched with NaHCO_3 (aq.) (to pH 9-10). The aqueous mixture was extracted with ethyl acetate (4 x 40 mL). The combined organic extracts were washed with brine (10 mL), dried (MgSO_4) and filtered affording *L*-phenylalanine methyl ester (**141**) as a clear oil (530.2 mg, 98%).

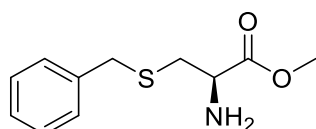
$^1\text{H NMR}$ (300 MHz, CDCl_3) δ 7.34 – 7.12 (m, 5H), 3.75 – 3.71 (m, 1H), 3.69 (s, 3H), 3.07 (dd, $J = 13.5, 5.2$ Hz, 1H), 2.84 (dd, $J = 13.5, 7.9$ Hz, 1H).

$^{13}\text{C NMR}$ (101 MHz, CDCl_3) δ 175.3, 137.2, 129.4, 128.7, 127.0, 55.8, 52.1, 41.0

The purified product (**141**) was used directly for the *N*-sulfamation reaction without further purification and analysis.

Data were consistent with those reported in the literature.³¹²

Preparation of *S*-benzyl-L-cysteine methyl ester (**144**)



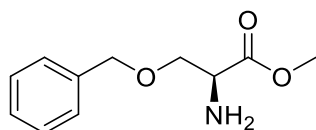
Following **general procedure 3**: A flask was charged with *S*-benzyl-L-cysteine (500 mg, 2.36 mmol) and dissolved in MeOH (5.0 mL). Concentrated H₂SO₄ (0.5 mL) was added dropwise over 1 minute and the reaction mixture was heated at reflux for 4 h. After the completion of reaction, the flask was cooled to room temperature and the solvent was removed under reduced pressure. The reaction mixture was quenched with NaHCO₃ (aq.) (to pH 9-10). The aqueous mixture was extracted with ethyl acetate (4 x 40 mL). The combined organic extracts were washed with brine (10 mL), dried (MgSO₄) and filtered affording *S*-benzyl-L-cysteine methyl ester (**144**) as a clear oil (420.0 mg, 79%).

¹H NMR (300 MHz, CDCl₃) δ 7.30 – 7.15 (m, 5H), 3.69 (s, 2H), 3.67 (s, 3H), 3.57 (dd, *J* = 7.4, 4.7 Hz, 1H), 2.79 (dd, *J* = 13.6, 4.8 Hz, 1H), 2.63 (dd, *J* = 13.5, 7.4 Hz, 1H), 1.93 (s, 2H).

Data were consistent with those reported in the literature.³¹³

The *S*-benzyl-L-cysteine methyl ester (**144**) was used directly for the next step without further purification and analysis.

Preparation of *O*-benzyl-*L*-serine methyl ester (**147**)



Following **general procedure 3**: A flask was charged with *O*-benzyl-*L*-serine (500 mg, 2.56 mmol) and dissolved in MeOH (5.0 mL). Concentrated H₂SO₄ (0.5 mL) was added dropwise over 1 minute and the reaction mixture was heated at reflux for 4 h. After the completion of reaction, the flask was cooled to room temperature and the solvent was removed under reduced pressure. The reaction mixture was quenched with NaHCO₃ (aq.) (to pH 9-10). The aqueous mixture was extracted with ethyl acetate (4 x 40 mL). The combined organic extracts were washed with brine (10 mL), dried (MgSO₄) and filtered affording *O*-benzyl-*L*-serine methyl ester (**147**) as a clear oil (462.0 mg, 86%).

¹H NMR (300 MHz, CDCl₃) δ 7.33 – 7.20 (m, 5H), 4.57 – 4.42 (m, 2H), 3.68 (s, 3H), 3.68 – 3.60 (m, 3H).

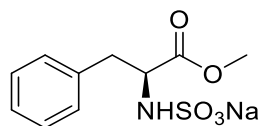
¹³C NMR (101 MHz, CDCl₃) δ 173.8, 137.8, 128.5, 127.9, 127.7, 73.4, 71.6, 54.8, 52.3.

LRMS *m/z* (ASAP⁺) 210.1138 ([M¹²C+H]⁺, 100%), 211.1166 ([M¹³C+H]⁺, 10%).

HRMS *m/z* (ASAP⁺) C₁₁H₁₅NO₃ requires 210.1130, found 210.1130 ([M¹²C+H]⁺).

Data were consistent with those reported in the literature.³¹⁴

Preparation of sodium *L*-phenylalanine methyl ester sulfamate (**143**)



Following **general procedure 2**: *L*-Phenylalanine methyl ester (89.6 mg, 0.5 mmol) and 4-methylmorpholine SO₃ (181.2 mg, 1.0 mmol) were dissolved in a mixture of MeCN/H₂O (2 mL). The reaction mixture was stirred at room temperature for 18 hours. Then tributylamine (0.24 mL) was added to the mixture and stirred for an additional 1 h. Then, the solvent was removed under reduced pressure and the tributylammonium cation intermediate was treated with NaI (2.5 eq.) and dissolved in MeCN (10 mL) and left to stir vigorously for 1 h. The solid was collected by filtration and dried under vacuum overnight affording sodium *L*-phenylalanine methyl ester sulfamate (**143**) as a yellow solid (73.8 mg, 53%).

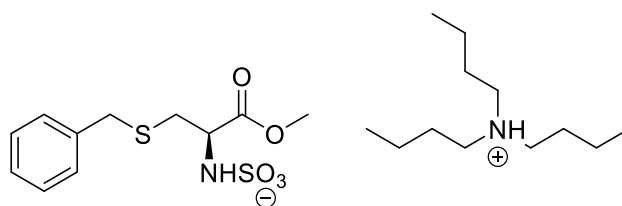
¹H NMR (400 MHz, DMSO-*d*₆) δ 7.31 – 7.06 (m, 5H), 4.38 (d, *J* = 9.1 Hz, 1H), 3.92 (t, *J* = 7.6 Hz, 1H), 3.47 (s, 3H), 2.92 (dd, *J* = 13.2, 5.9 Hz, 1H), 2.82 (dd, *J* = 13.4, 7.5 Hz, 1H).

¹³C NMR (101 MHz, DMSO-*d*₆) δ 173.8, 137.9, 129.1, 128.0, 126.2, 57.6, 51.1, 38.6.

LRMS *m/z* (ESI⁻) 258.0438 ([M-Na]⁻, 100 %), 259.0470 ([M¹³C-Na]⁻, 10 %).

Data were consistent with those reported in the literature.⁴⁷

Preparation of tributylammonium *S*-benzyl-*L*-cysteine methyl ester sulfamate (**145**)



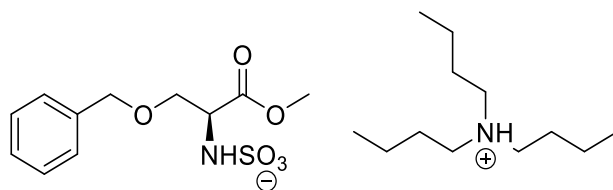
Following **general procedure 2**: *S*-Benzyl-*L*-cysteine methyl ester (385 mg, 1.7 mmol) and 4-methylmorpholine SO_3 (616 mg, 3.4 mmol) were dissolved in a mixture of MeCN/ H_2O (4 mL). The reaction mixture was stirred at room temperature for 18 hours. Tributylamine (3.4 mmol) was added to the mixture and stirred for an additional 1 h. Then, the solvent was removed under reduced pressure. The reaction was quenched with H_2O (10 mL) and filtered. The aqueous solution was extracted with ethyl acetate (4 x 30 mL). The organic layer was dried over (MgSO_4), filtered, and the solvent was removed under reduced pressure affording the desired tributylammonium *S*-benzyl-*L*-cysteine methyl ester sulfamate (**145**) as a clear oil (616.8 mg, 74%).

$^1\text{H NMR}$ (400 MHz, $\text{DMSO-}d_6$) δ 7.33 – 7.18 (m, 5H), 4.57 (d, $J = 8.3$ Hz, 1H), 3.98 – 3.88 (m, 1H), 3.79 – 3.67 (m, 2H), 3.60 (s, 3H), 2.98 (s, 6H), 2.77 – 2.62 (m, 2H), 1.60 – 1.51 (m, 6H), 1.38 – 1.24 (m, 6H), 0.90 (t, $J = 7.3$ Hz, 9H).

$^{13}\text{C NMR}$ (101 MHz, $\text{DMSO-}d_6$) δ 173.5, 138.9, 129.3, 128.8, 127.2, 56.8, 52.3, 52.1, 35.7, 33.6, 25.3, 19.8, 14.

The tributylammonium *S*-benzyl-*L*-cysteine methyl ester sulfamate (**145**) was used without further purification and analysis.

Preparation of tributylammonium *O*-benzyl-*L*-serine methyl ester sulfamate (**148**)



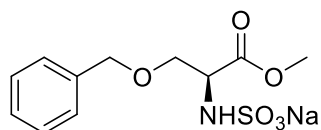
O-Benzyl-*L*-serine methyl ester (337 mg, 1.6 mmol) and TBSAB (848 mg, 3.2 mmol) were dissolved in a mixture of MeCN (3 mL). The reaction mixture was stirred at room temperature for 18 h. After the completion of the reaction, the crude compound was purified by flash chromatography (SiO₂; CH₂Cl₂/MeOH; 9:1) and the solvent was removed under reduced pressure and dried affording the desired tributylammonium *O*-benzyl-*L*-serine methyl ester sulfamate (**148**) as a clear oil (414.0 mg, 54%).

¹H NMR (400 MHz, DMSO-*d*₆) δ 8.87 (s, 1H), 7.39 – 7.23 (m, 5H), 4.45 (s, 2H), 3.89 (d, *J* = 6.2 Hz, 1H), 3.67 – 3.51 (m, 5H), 3.07 – 2.98 (m, 6H), 1.64 – 1.51 (m, 6H), 1.38 – 1.21 (m, 6H), 0.91 (t, *J* = 7.3 Hz, 9H).

¹³C NMR (101 MHz, DMSO-*d*₆) δ 172.9, 138.2, 128.2, 127.4, 127.3, 72.0, 70.6, 56.2, 51.8, 51.5, 25.1, 19.3, 13.5.

The tributylammonium *O*-benzyl-*L*-serine methyl ester sulfamate (**148**) was used for the next step without further purification and analysis.

Preparation of sodium *O*-benzyl-*L*-serine methyl ester sulfamate (**149**)



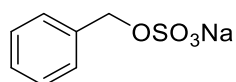
Following **general procedure 2**: *O*-Benzyl-*L*-serine methyl ester (337 mg, 1.6 mmol) and TBSAB (848 mg, 3.2 mmol) were dissolved in anhydrous MeCN (3 mL). The reaction mixture was stirred at room temperature for 18 hours. Then, the solvent was removed under reduced pressure and the tributylammonium cation intermediate was treated with NaI (5.0 eq.) and the mixture was dissolved in MeCN (20 mL) and the mixture was stirred vigorously for 1 h. The solid was collected by filtration and dried under vacuum overnight affording sodium *O*-benzyl-*L*-serine methyl ester sulfamate (**149**) as a yellow solid (302.0 mg, 61%).

¹H NMR (300 MHz, DMSO-*d*₆) δ 7.40 – 7.22 (m, 5H), 4.45 (s, 2H), 3.93 – 3.85 (m, 1H), 3.67 – 3.51 (m, 5H).

¹³C NMR (101 MHz, DMSO-*d*₆) δ 172.9, 138.2, 128.2, 127.4, 127.3, 72.0, 70.7, 56.2, 51.5.

LRMS *m/z* (ES⁻) 288.78 ([M¹²C-Na]⁻ 100%), 290.77 ([M¹³C-Na]⁻, 30%).

Preparation of sodium benzyl sulfate (**105**)¹⁴⁹



Following **general procedure 1**: Benzyl alcohol (0.1 mL, 1.0 mmol) and sulfur trioxide pyridine complex (318.3 mg, 2.0 mmol) were dissolved in anhydrous MeCN (2.0 mL) and heated under reflux at 90 °C for 3 h. Tributylamine (0.4 mL, 2.0 mmol) was added to the mixture and the mixture was stirred for 30 min. After the completion of reaction, the flask was cooled to room

temperature and the solvent was removed under reduced pressure. The crude product was purified by **work up procedure A** afforded sodium benzyl sulfate (**105**) as a bright white solid (196.2 mg, 93%).

M.P. 193-195 °C (Lit.¹⁴⁹ 208-210 °C)

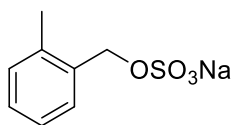
¹H NMR (300 MHz, D₂O) δ 7.57 – 7.33 (m, 5H), 5.09 (s, 2H).

¹³C NMR (101 MHz, D₂O) δ 135.1, 128.7 (CH and C), 128.4, 70.7.

LRMS *m/z* (ESI⁻) 187.0 ([M¹²C–Na]⁻, 100 %), 188.1 ([M¹³C–Na]⁻, 10 %).

Data were consistent with those reported in the literature.¹⁴⁹

Preparation of sodium 2-methylbenzyl sulfate (**169**)



Following **general procedure 1**: 2-Methylbenzyl alcohol (122.1 mg, 1.0 mmol) and sulfur trioxide pyridine complex (318.3 mg, 2.0 mmol) were dissolved in anhydrous MeCN (2.0 mL) and the mixture was heated under reflux at 90 °C for 3 h. Tributylamine (0.4 mL, 2.0 mmol) was added to the mixture and the mixture was stirred for 30 min. After the completion of the reaction, the flask was cooled to room temperature and the solvent was removed under reduced pressure. The crude product was purified by **work up procedure B** to yield sodium 2-methylbenzyl sulfate (**169**) as a bright white solid (215.5 mg, 96%).

M.P. 200-202 °C

IR. ν_{\max} cm⁻¹ 1475w, 1383w, 1247m, 1204s, 1108s, 1071s

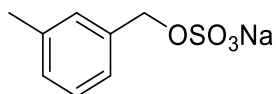
¹H NMR (400 MHz, D₂O) δ 7.41 – 7.23 (m, 4H), 5.09 (s, 2H), 2.36 (s, 3H).

^{13}C NMR (101 MHz, D_2O) δ 138.0, 132.9, 130.4, 129.8, 129.3, 126.1, 69.3, 17.7.

LRMS m/z (ESI $^-$) 201.0 ($[\text{M}^{12}\text{C}-\text{Na}]^-$, 100 %), 202.0 ($[\text{M}^{13}\text{C}-\text{Na}]^-$, 10 %).

HRMS m/z (ESI $^-$) $\text{C}_8\text{H}_9\text{O}_4\text{S}$ requires 201.0222, found 201.0225 $[\text{M}-\text{Na}]^-$.

Preparation of sodium 3-methylbenzyl sulfate (**170**)



Following **general procedure 1**: 3-Methylbenzyl alcohol (0.12 mL, 1.0 mmol) and sulfur trioxide pyridine complex (318.3 mg, 2.0 mmol) were dissolved in anhydrous MeCN (2.0 mL) and the mixture was heated under reflux at 90 °C for 3 h. Tributylamine (0.4 mL, 2.0 mmol) was added to the mixture and the mixture was stirred for 30 min. after the completion of the reaction, the flask was cooled to room temperature and the solvent was removed under reduced pressure. The crude product was purified by **work up procedure A** to yield sodium 3-methylbenzyl sulfate (**170**) as a bright white solid (190.7 mg, 85%).

M.P. 172- 174 °C

IR. ν_{max} cm^{-1} 2904w, 1469w, 1380w, 1248s, 1203s, 1130s

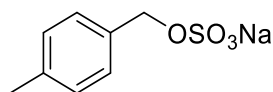
^1H NMR (400 MHz, D_2O) δ 7.50 – 7.08 (m, 4H), 5.03 (s, 2H), 2.34 (s, 3H).

^{13}C NMR (101 MHz, D_2O) δ 138.9, 135.1, 129.3, 129.0, 128.7, 125.3, 70.7, 20.3.

LRMS m/z (ESI $^-$) 201.0 ($[\text{M}^{12}\text{C}-\text{Na}]^-$, 100 %), 202.0 ($[\text{M}^{13}\text{C}-\text{Na}]^-$, 10 %).

HRMS m/z (ESI $^-$) $\text{C}_8\text{H}_9\text{O}_4\text{S}$ requires 201.0222, found 201.0228 $[\text{M}-\text{Na}]^-$.

Preparation of sodium 4-methylbenzyl sulfate (**171**)



Following **general procedure 1**: 4-Methylbenzyl alcohol (122.1 mg, 1.0 mmol) and sulfur trioxide pyridine complex (318.3 mg, 2.0 mmol) were dissolved in anhydrous MeCN (2.0 mL) and the mixture was heated under reflux at 90 °C for 3 h. Tributylamine (0.4 mL, 2.0 mmol) was added to the mixture and the mixture was stirred for 30 min. after the completion of the reaction, the flask was cooled to room temperature and the solvent was removed under reduced pressure. The crude product was purified by **work up procedure C** to yield sodium 4-methylbenzyl sulfate (**171**) as a bright white solid (212.2 mg, 94%).

M.P. 182- 184 °C

IR. ν_{\max} cm^{-1} 1615w, 1469w, 1380w, 1252s, 1202s, 1072s

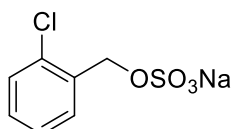
$^1\text{H NMR}$ (300 MHz, D_2O) δ 7.39 – 7.34 (m, 2H), 7.32 – 7.26 (m, 2H), 5.04 (s, 2H), 2.35 (s, 3H).

$^{13}\text{C NMR}$ (101 MHz, D_2O) δ 139.1, 132.0, 129.3, 128.6, 70.7, 20.2.

LRMS m/z (ESI $^-$) 201.0 ($[\text{M}^{12}\text{C}-\text{Na}]^-$, 100 %), 202.0 ($[\text{M}^{13}\text{C}-\text{Na}]^-$, 10 %).

HRMS m/z (ESI $^-$) $\text{C}_8\text{H}_9\text{O}_4\text{S}$ requires 201.0222, found 201.0222 $[\text{M}-\text{Na}]^-$.

Preparation of sodium 2-chlorobenzyl sulfate (**166**)¹⁴⁹



Following **general procedure 1**: 2-Chlorobenzyl alcohol (142.5 mg, 1.0 mmol) and sulfur trioxide pyridine complex (318.3 mg, 2.0 mmol) were dissolved in anhydrous MeCN (2.0 mL)

and the mixture was heated under reflux at 90 °C for 3 h. Tributylamine (0.4 mL, 2.0 mmol) was added to the mixture and the mixture was stirred for 30 min. after the completion of the reaction, the flask was cooled to room temperature and the solvent was removed under reduced pressure. The crude product was purified by **work up procedure C** to yield sodium 2-chlorobenzyl sulfate (**166**) as a yellow solid (179.7 mg, 73%).

M.P. 239- 241 °C (Lit.¹⁴⁹ 219-221°C)

¹H NMR (300 MHz, D₂O) δ 7.58 – 7.48 (m, 2H), 7.45 – 7.34 (m, 2H), 5.20 (s, 2H).

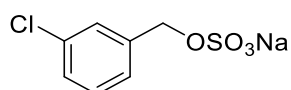
¹³C NMR (101 MHz, D₂O) δ 133.5, 132.4, 130.7, 130.4, 129.5, 127.2, 68.1.

LRMS *m/z* (ESI⁻) 220.9 ([M³⁵Cl-Na]⁻, 100 %), 222.9 ([M³⁷Cl-Na]⁻, 40 %).

HRMS *m/z* (ESI⁻) C₇H₆O₄SCl requires 220.9675, found 220.9680 [M³⁵Cl-Na]⁻.

Data were consistent with those reported in the literature.¹⁴⁹

Preparation of sodium 3-chlorobenzyl sulfate (**163**)



Following **general procedure 1**: 3-Chlorobenzyl alcohol (0.11 mL, 1.0 mmol) and sulfur trioxide pyridine complex (318.3 mg, 2.0 mmol) were dissolved in anhydrous MeCN (2.0 mL) and the mixture was heated under reflux at 90 °C for 3 h. Tributylamine (0.4 mL, 2.0 mmol) was added to the mixture and the mixture was stirred for 30 min. after the completion of the reaction, the flask was cooled to room temperature and the solvent was removed under

reduced pressure. The crude product was purified by **work up procedure A** to yield sodium 3-chlorobenzyl sulfate (**163**) as a bright white solid (216.4 mg, 88%).

M.P. 219- 221 °C

IR. ν_{\max} cm^{-1} 1573w, 1469w, 1378w, 1253m, 1205m, 1106s, 611s

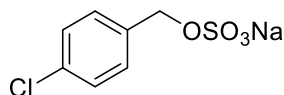
^1H NMR (400 MHz, D_2O) δ 7.59 – 7.23 (m, 4H), 5.04 (s, 2H).

^{13}C NMR (101 MHz, D_2O) δ 137.3, 133.7, 130.1, 128.5, 128.0, 126.4, 69.7.

LRMS m/z (ESI $^-$) 220.9 ($[\text{M}^{35}\text{Cl}-\text{Na}]^-$, 100 %), 222.9 ($[\text{M}^{37}\text{Cl}-\text{Na}]^-$, 40 %).

HRMS m/z (ESI $^-$) $\text{C}_7\text{H}_6\text{O}_4\text{SCL}$ requires 220.9675, found 220.9681 $[\text{M}^{35}\text{Cl}-\text{Na}]^-$.

Preparation of sodium 4-chlorobenzyl sulfate (**157**)¹⁴⁹



Following **general procedure 1**: 4-Chlorobenzyl alcohol (142.5 mg, 1.0 mmol) and sulfur trioxide pyridine complex (318.3 mg, 2.0 mmol) were dissolved in anhydrous MeCN (2.0 mL) and the mixture was heated under reflux at 90 °C for 3 h. Tributylamine (0.4 mL, 2.0 mmol) was added to the mixture and the mixture was stirred for 30 min. after the completion of the reaction, the flask was cooled to room temperature and the solvent was removed under reduced pressure. The crude product was purified by **work up procedure C** to yield sodium 4-chlorobenzyl sulfate (**157**) as a bright white solid (220.2 mg, 90%).

M.P. 227-229 °C (Lit.¹⁴⁹ 202-204 °C)

^1H NMR (400 MHz, $\text{DMSO}-d_6$) δ 7.43 – 7.30 (m, 4H), 4.76 (s, 2H).

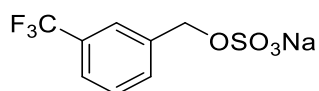
^{13}C NMR (101 MHz, DMSO- d_6) δ 137.0, 131.8, 129.3, 128.0, 66.5

LRMS m/z (ESI $^-$) 220.9 ($[\text{M}^{35}\text{Cl}-\text{Na}]^-$, 100 %), 222.9 ($[\text{M}^{37}\text{Cl}-\text{Na}]^-$, 40 %).

HRMS m/z (ESI $^-$) $\text{C}_7\text{H}_6\text{O}_4\text{S}$ requires 220.9675, found 220.9681 $[\text{M}^{35}\text{Cl}-\text{Na}]^-$.

Data were consistent with those reported in the literature.¹⁴⁹

Preparation of sodium 3-(trifluoromethyl) benzyl sulfate (**172**)



Following **general procedure 1**: 3-(Trifluoromethyl) benzyl alcohol (0.13 mL, 1.0 mmol) and sulfur trioxide pyridine complex (318.3 mg, 2.0 mmol) were dissolved in anhydrous MeCN (2.0 mL) and the mixture was heated under reflux at 90 °C for 3 h. Tributylamine (0.4 mL, 2.0 mmol) was added to the mixture and the mixture was stirred for 30 min. after the completion of the reaction, the flask was cooled to room temperature and the solvent was removed under reduced pressure. The crude product was purified by **work up procedure C** to yield sodium 3-(trifluoromethyl) benzyl sulfate (**172**) as a white solid (273.8 mg, 98%).

M.P. 224-226 °C

IR. ν_{max} cm^{-1} 3109w, 1470w, 1452w, 1329w, 1250w, 1203m, 1069m

^1H NMR (300 MHz, D_2O) δ 7.83 – 7.56 (m, 4H), 5.14 (s, 2H).

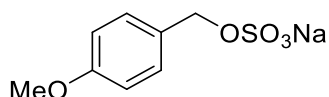
^{13}C NMR (101 MHz, D_2O) δ 136.2, 131.7, 130.1 (q, $^2J_{\text{C-F}} = 32.2$ Hz), 129.3, 125.3 (q, $^3J_{\text{C-F}} = 3.9$ Hz), 124.8 (q, $^3J_{\text{C-F}} = 4.1$ Hz), 123.5 (q, $^1J_{\text{C-F}} = 271.2$ Hz), 69.7.

^{19}F NMR (377 MHz, D_2O) δ -62.42.

LRMS m/z (ESI⁻) 254.9 ([M¹²C-Na]⁻, 100 %), 254.9 ([M¹³C-Na]⁻, 10 %).

HRMS m/z (ESI⁻) C₈H₆O₄F₃S requires 254.9939, found 254.9946 [M-Na]⁻.

Preparation of sodium 4-methoxybenzyl sulfate (**173**)



Following **general procedure 1**: 4-Methoxybenzyl alcohol (0.12 mL, 1.0 mmol) and sulfur trioxide pyridine complex (318.3 mg, 2.0 mmol) were dissolved in anhydrous MeCN (2.0 mL) and the mixture was heated under reflux at 90 °C for 3 h. Tributylamine (0.4 mL, 2.0 mmol) was added to the mixture and the mixture was stirred for 30 min. after the completion of the reaction, the flask was cooled to room temperature and the solvent was removed under reduced pressure. The crude product was purified by **work up procedure C** to yield sodium 4-methoxybenzyl sulfate (**173**) as a bright white solid (170.3 mg, 70%).

M.P. >235 °C (dec.)

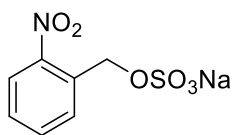
¹H NMR (400 MHz, D₂O) δ 7.41 – 7.23 (m, 2H), 6.98 (m, 2H), 4.54 (s, 2H), 3.80 (s, 3H).

¹³C NMR (101 MHz, D₂O) δ 158.3, 132.8, 129.2, 114.0, 63.4, 55.3.

LRMS m/z (ESI⁻) 217.0 ([M¹²C-Na]⁻, 100 %), 218.0 ([M¹³C-Na]⁻, 10 %).

HRMS m/z (ESI⁻) C₈H₉O₅S requires 217.0171, found 217.0177 [M-Na]⁻.

Preparation of sodium 2-nitrobenzyl sulfate (**174**)¹⁴⁹



Following **general procedure 1**: 2-Nitrobenzyl alcohol (153.1 mg, 1.0 mmol) and sulfur trioxide pyridine complex (318.3 mg, 2.0 mmol) were dissolved in anhydrous MeCN (2.0 mL) and the mixture was heated under reflux at 90 °C for 3 h. Tributylamine (0.4 mL, 2.0 mmol) was added to the mixture and the mixture was stirred for 30 min. after the completion of the reaction, the flask was cooled to room temperature and the solvent was removed under reduced pressure. The crude product was purified by **work up procedure C** to yield sodium 2-nitrobenzyl sulfate (**174**) as a yellow solid (166.4 mg, 65%).

M.P. 228-230 °C (Lit. not stated)

¹H NMR (300 MHz, D₂O) δ 8.14 (d, 1H), 7.83 – 7.70 (m, 2H), 7.59 (d, *J* = 9.0, 6.5, 2.6 Hz, 1H), 5.44 (s, 2H).

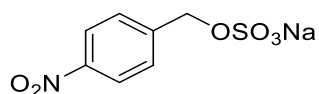
¹³C NMR (101 MHz, D₂O) δ 146.9, 134.4, 131.2, 129.4, 129.2, 124.9, 67.1.

LRMS *m/z* (ESI⁻) 231.9 ([M-Na]⁻, 100 %).

HRMS *m/z* (ESI⁻) C₇H₆NO₆S requires 231.9916, found 231.9918 [M-Na]⁻.

Data were consistent with those reported in the literature.¹⁴⁹

Preparation of sodium 4-nitrobenzyl sulfate (175)¹⁴⁹



Following **general procedure 1**: 4-Nitrobenzyl alcohol (153.1 mg, 1.0 mmol) and sulfur trioxide pyridine complex (318.3 mg, 2.0 mmol) were dissolved in anhydrous MeCN (2.0 mL) and the mixture was heated under reflux at 90 °C for 3 h. Tributylamine (0.4 mL, 2.0 mmol) was added to the mixture and the mixture was stirred for 30 min. after the completion of the reaction, the flask was cooled to room temperature and the solvent was removed under reduced pressure. The crude product was purified by **work up procedure C** to yield sodium 4-nitrobenzyl sulfate (**175**) as a white solid (167.3 mg, 66%).

M.P. 188-190 °C (Lit. not stated)

¹H NMR (300 MHz, D₂O) δ 8.39 – 8.13 (m, 2H), 7.76 – 7.53 (m, 2H), 5.19 (s, 2H).

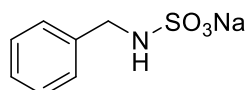
¹³C NMR (101 MHz, D₂O) δ 147.3, 143.1, 128.4, 123.7, 69.0.

LRMS *m/z* (ESI⁻) 231.9 ([M¹²C-Na]⁻, 100 %), 232.9 ([M¹³C-Na]⁻, 10 %).

HRMS *m/z* (ESI⁻) C₇H₆NO₆S requires 231.9916, found 231.9922 [M-Na]⁻.

Data were consistent with those reported in the literature.¹⁴⁹

Preparation of sodium benzyl sulfamate (108)⁴⁷



Following **general procedure 2**: Benzylamine (0.1 mL, 1.0 mmol) and sulfur trioxide trimethylamine complex (278.3 mg, 2.0 mmol) were dissolved in anhydrous MeCN (2.0 mL)

and the mixture was heated under reflux at 60 °C for 30 min. Tributylamine (0.4 mL, 2.0 mmol) was added to the mixture and the mixture was stirred for 30 min. After the completion of the reaction, the flask was cooled to room temperature and the solvent was removed under reduced pressure. The crude compound was purified by **work up procedure B** to yield sodium benzyl sulfamate (**108**) as a white solid (208.2 mg, 99%).

M.P. 238-240 °C (Lit.⁴⁷ >230 °C)

¹H NMR (400 MHz, D₂O) δ 7.43 – 7.30 (m, 5H), 4.12 (s, 2H).

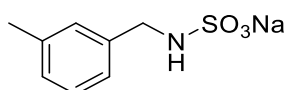
¹³C NMR (101 MHz, D₂O) δ 137.9, 128.6, 128.2, 127.5, 47.3.

LRMS *m/z* (ESI⁻) 186.0 ([M¹²C-Na]⁻, 100 %), 187.0 ([M¹³C-Na]⁻, 10 %).

HRMS *m/z* (ESI⁻) C₇H₈NO₃S requires 186.0225, found 186.0228 [M-Na]⁻.

Data were consistent with those reported in the literature.⁴⁷

Preparation of sodium (3-methylbenzyl) sulfamate (**178**)



Following **general procedure 2**: 3-Methylbenzylamine (0.12 mL, 1.0 mmol) and sulfur trioxide trimethylamine complex (278.3 mg, 2.0 mmol) were dissolved in anhydrous MeCN (2.0 mL) and the mixture was heated under reflux at 60 °C for 30 min. Tributylamine (0.4 mL, 2.0 mmol) was added to the mixture and the mixture was stirred for 30 min. After the completion of the reaction, the flask was cooled to room temperature and the solvent was removed under

reduced pressure. The crude compound was purified by **work up procedure A** to yield sodium (3-methylbenzyl) sulfamate (**178**) as a white solid (208.9 mg, 93%).

M.P. 224- 226 °C

IR. ν_{\max} cm^{-1} 3299w, 2907w, 1608w, 1400w, 1343w, 1166s

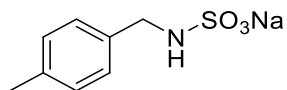
^1H NMR (300 MHz, D_2O) δ 7.37 – 7.14 (m, 4H), 4.10 (s, 2H), 2.35 (s, 3H).

^{13}C NMR (101 MHz, D_2O) δ 138.7, 138.0, 128.8, 128.6, 128.1, 125.1, 47.2, 20.3.

LRMS m/z (ESI $^-$) 200.0 ($[\text{M}^{12}\text{C}-\text{Na}]^-$, 100 %), 201.0 ($[\text{M}^{13}\text{C}-\text{Na}]^-$, 10 %).

HRMS m/z (ESI $^-$) $\text{C}_8\text{H}_{10}\text{NO}_3\text{S}$ requires 200.0381, found 200.0378 $[\text{M}-\text{Na}]^-$.

Preparation of sodium (4-methylbenzyl) sulfamate (**179**)



Following **general procedure 2**: 4-Methylbenzylamine (0.13 mL, 1.0 mmol) and sulfur trioxide trimethylamine complex (278.3 mg, 2.0 mmol) were dissolved in anhydrous MeCN (2.0 mL) and the mixture was heated under reflux at 60 °C for 30 min. Tributylamine (0.4 mL, 2.0 mmol) was added to the mixture and the mixture was stirred for 30 min. After the completion of the reaction, the flask was cooled to room temperature and the solvent was removed under reduced pressure. The crude compound was purified by **work up procedure A** to yield sodium (4-methylbenzyl) sulfamate (**179**) as a white solid (222.3 mg, 99%).

M.P. 234-236 °C

IR. ν_{\max} cm^{-1} 3300w, 1514w, 1403w, 1341w, 1167w, 1058m

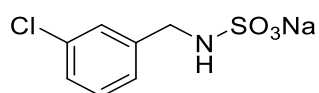
¹H NMR (300 MHz, D₂O) δ 7.35 – 7.22 (m, 4H), 4.10 (s, 2H), 2.33 (s, 3H).

¹³C NMR (101 MHz, D₂O) δ 137.6, 134.8, 129.2, 128.3, 47.0, 20.1.

LRMS *m/z* (ESI⁻) 200.0 ([M¹²C-Na]⁻, 100 %), 201.0 ([M¹³C-Na]⁻, 20 %).

HRMS *m/z* (ESI⁻) C₈H₁₀NO₃S requires 200.0381, found 200.0376 [M-Na]⁻.

Preparation of sodium (3-chlorobenzyl) sulfamate (**180**)⁴⁷



Following **general procedure 2**: 3-Chlorobenzylamine (0.12 mL, 1.0 mmol) and sulfur trioxide trimethylamine complex (278.3 mg, 2.0 mmol) were dissolved in anhydrous MeCN (2.0 mL) and the mixture was heated under reflux at 60 °C for 30 min. Tributylamine (0.4 mL, 2.0 mmol) was added to the mixture and the mixture was stirred for 30 min. After the completion of the reaction, the flask was cooled to room temperature and the solvent was removed under reduced pressure. The crude compound was purified by **work up procedure A** to yield sodium (3-chlorobenzyl) sulfamate (**180**) as a whit solid (220.1 mg, 90%).

M.P. 223-225 °C (Lit.⁴⁷ 223-225 °C)

¹H NMR (300 MHz, D₂O) δ 7.47 – 7.43 (m, 1H), 7.38 – 7.30 (m, 3H), 4.12 (s, 2H).

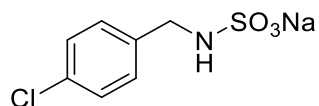
¹³C NMR (101 MHz, D₂O) δ 140.2, 133.5, 130.0, 127.9, 127.3, 126.4, 46.6.

LRMS *m/z* (ESI⁻) 219.98 ([M³⁵Cl-Na]⁻, 100 %), 221.98 ([M³⁷Cl-Na]⁻, 40 %).

HRMS *m/z* (ESI⁻) C₇H₇O₃NS Cl requires 219.9841, found 219.9835 [M³⁵Cl-Na]⁻.

Data were consistent with those reported in the literature.⁴⁷

Preparation of sodium (4-chlorobenzyl) sulfamate (**181**)⁴⁷



Following **general procedure 2**: 4-Chlorobenzylamine (0.12 mL, 1.0 mmol) and sulfur trioxide trimethylamine complex (278.3 mg, 2.0 mmol) were dissolved in anhydrous MeCN (2.0 mL) and the mixture was heated under reflux at 60 °C for 30 min. Tributylamine (0.4 mL, 2.0 mmol) was added to the mixture and the mixture was stirred for 30 min. After the completion of the reaction, the flask was cooled to room temperature and the solvent was removed under reduced pressure. The crude compound was purified by **work up procedure A** to yield sodium (4-chlorobenzyl) sulfamate (**181**) as a white solid (240.2 mg, 98%).

M.P. 234- 236 °C (Lit.⁴⁷ 202-203 °C)

¹H NMR (300 MHz, D₂O) δ 7.43 – 7.35 (m, 4H), 4.11 (s, 2H).

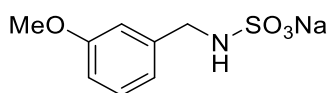
¹³C NMR (101 MHz, D₂O) δ 136.7, 132.5, 129.7, 128.4, 46.6.

LRMS *m/z* (ESI⁻) 219.9 ([M³⁵Cl-Na]⁻, 100 %), 221.9 ([M³⁷Cl-Na]⁻, 40 %), 220.9 ([C¹³M³⁵Cl-Na]⁻, 10%).

HRMS *m/z* (ESI⁻) C₇H₇O₃NS Cl requires 219.9839, found 219.9835 [M³⁵Cl-Na]⁻.

Data were consistent with those reported in the literature.⁴⁷

Preparation of sodium (3-methoxybenzyl) sulfamate (**182**)⁴⁷



Following **general procedure 2**: 3-Methoxybenzylamine (0.13 mL, 1.0 mmol) and sulfur trioxide trimethylamine complex (278.3 mg, 2.0 mmol) were dissolved in anhydrous MeCN (2.0 mL) and the mixture was heated under reflux at 60 °C for 30 min. Tributylamine (0.4 mL, 2.0 mmol) was added to the mixture and the mixture was stirred for 30 min. After the completion of the reaction, the flask was cooled to room temperature and the solvent was removed under reduced pressure. The crude compound was purified by **work up procedure A** to yield sodium (3-methoxybenzyl) sulfamate (**182**) as a white solid (224.2 mg, 93%).

M.P. 219-221 °C (Lit.⁴⁷ 218-220 °C)

¹H NMR (300 MHz, D₂O) δ 7.38 – 7.30 (m, 1H), 7.07 – 7.00 (m, 2H), 6.97 – 6.89 (m, 1H), 4.11 (s, 2H), 3.83 (s, 3H).

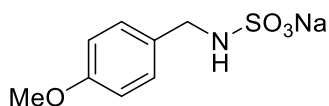
¹³C NMR (101 MHz, D₂O) δ 158.8, 139.9, 129.8, 120.9, 113.5, 113.1, 55.2, 47.1.

LRMS *m/z* (ESI⁻) 216.0 ([M¹²C-Na]⁻, 100 %), 217.0 ([M¹³C-Na]⁻, 10 %).

HRMS *m/z* (ESI⁻) C₈H₁₀NO₄S requires 216.0331, found 216.0327 [M-Na]⁻.

Data were consistent with those reported in the literature.⁴⁷

Preparation of sodium (4-methoxybenzyl) sulfamate (**183**)⁴⁷



Following **general procedure 2**: 4-Methoxybenzylamine (0.13 mL, 1.0 mmol) and sulfur trioxide trimethylamine complex (278.3 mg, 2.0 mmol) were dissolved in anhydrous MeCN (2.0 mL) and the mixture was heated under reflux at 60 °C for 30 min. Tributylamine (0.4 mL, 2.0 mmol) was added to the mixture and the mixture was stirred for 30 min. After the completion of the reaction, the flask was cooled to room temperature and the solvent was removed under reduced pressure. The crude compound was purified by **work up procedure A** to yield sodium (4-methoxybenzyl) sulfamate (**183**) as a white solid (238.2 mg, 99%).

M.P. 235-237 °C (Lit.⁴⁷ 232-237 °C)

¹H NMR (300 MHz, D₂O) δ 7.40 – 7.30 (m, 2H), 7.03 – 6.93 (m, 2H), 4.07 (s, 2H), 3.82 (s, 3H).

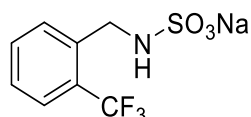
¹³C NMR (101 MHz, D₂O) δ 158.1, 130.5, 129.7, 114.0, 55.3, 46.7.

LRMS *m/z* (ESI⁻) 216.0 ([M¹²C-Na]⁻, 100 %), 217.0 ([M¹³C-Na]⁻, 10 %).

HRMS *m/z* (ESI⁻) C₈H₁₀NO₄S requires 216.0331, found 216.0329 [M-Na]⁻.

Data were consistent with those reported in the literature.⁴⁷

Preparation of sodium (2-trifluoromethylbenzyl) sulfamate (**184**)⁴⁷



Following **general procedure 2**: 2-(Trifluoromethyl) benzylamine (0.14 mL, 1.0 mmol) and sulfur trioxide trimethylamine complex (278.3 mg, 2.0 mmol) were dissolved in anhydrous MeCN (2.0 mL) and the mixture was heated under reflux at 60 °C for 30 min. Tributylamine

(0.4 mL, 2.0 mmol) was added to the mixture and the mixture was stirred for 30 min. After the completion of the reaction, the flask was cooled to room temperature and the solvent was removed under reduced pressure. The crude compound was purified by **work up procedure B** to yield sodium (2-trifluoromethylbenzyl) sulfamate (**184**) as a white solid (210.9 mg, 76%).

M.P. 210-212 °C (Lit.⁴⁷ 185-187 °C)

¹H NMR (300 MHz, DMSO-*d*₆) δ 7.86 (d, *J* = 7.7 Hz, 1H), 7.66 – 7.56 (m, 2H), 7.39 (t, *J* = 7.6 Hz, 1H), 5.03 (t, *J* = 7.3 Hz, 1H), 4.13 (d, *J* = 7.3 Hz, 2H).

¹³C NMR (101 MHz, DMSO-*d*₆) δ 139.7, 132.1, 129.5 (d, ²*J*_{C-F} = 32.2 Hz), 126.5, 126.0 (q, ³*J*_{C-F} = 3.9 Hz), 125.6, 125.0 (q, ¹*J*_{C-F} = 271.2 Hz), 43.1.

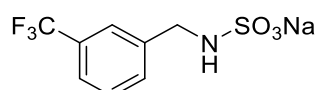
¹⁹F NMR (377 MHz, D₂O) δ -59.37.

LRMS *m/z* (ESI⁻) 254.0 ([M¹²C-Na]⁻, 100 %), 255.0 ([M¹³C-Na]⁻, 10 %).

HRMS *m/z* (ESI⁻) C₈H₇NO₃SF₃ requires 254.0099, found 254.0105 [M-Na]⁻.

Data were consistent with those reported in the literature.⁴⁷

Preparation of sodium (3-trifluoromethylbenzyl) sulfamate (**185**)



Following **general procedure 2**: 3-(Trifluoromethyl) benzylamine (0.14 mL, 1.0 mmol) and sulfur trioxide trimethylamine complex (278.3 mg, 2.0 mmol) were dissolved in anhydrous MeCN (2.0 mL) and the mixture was heated under reflux at 60 °C for 30 min. Tributylamine

(0.4 mL, 2.0 mmol) was added to the mixture and the mixture was stirred for 30 min. After the completion of the reaction, the flask was cooled to room temperature and the solvent was removed under reduced pressure. The crude compound was purified by **work up procedure B** to yield sodium (3-trifluoromethylbenzyl) sulfamate (**185**) as a white solid (270.7 mg, 97%).

M.P. 223- 225 °C

IR. ν_{\max} cm^{-1} 3300w, 1401w, 1327w, 1242w, 1164w, 1055w

^1H NMR (400 MHz, $\text{DMSO-}d_6$) δ 7.71 (m, $J = 1.8, 0.9$ Hz, 1H), 7.61 (m, $J = 7.0, 1.1$ Hz, 1H), 7.56 – 7.46 (m, 2H), 5.09 (s, 1H), 4.02 (s, 2H).

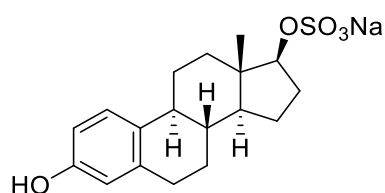
^{13}C NMR (101 MHz, $\text{DMSO-}d_6$) δ 142.7, 131.7, 128.6 (d, $^2J_{\text{C-F}} = 32.1$ Hz), 125.8, 124.1 (d, $^3J_{\text{C-F}} = 3.6$ Hz), 123.1, 122.8 (d, $^1J_{\text{C-F}} = 271.2$ Hz), 46.6.

^{19}F NMR (377 MHz, D_2O) δ –62.32.

LRMS m/z (ESI $^-$) 254.0 ($[\text{M}^{12}\text{C}-\text{Na}]^-$, 100 %), 255.0 ($[\text{M}^{13}\text{C}-\text{Na}]^-$, 10 %).

HRMS m/z (ESI $^-$) $\text{C}_8\text{H}_7\text{NO}_3\text{SF}_3$ requires 254.0099, found 254.0100 $[\text{M}-\text{Na}]^-$.

Preparation of sodium 17 β -estradiol sulfate or sodium (8*R*,9*S*,13*S*,14*S*,17*S*)-3-hydroxy-13-methyl-7,8,9,11,12,13,14,15,16,17-decahydro-6*H*-cyclopenta[*a*]phenanthren-17-yl sulfate (**207**)¹⁴⁹



Following **general procedure 6**: β -Estradiol (272.4 mg, 1.0 mmol) and TBSAB (398 mg, 1.5 mmol) were dissolved in anhydrous MeCN (4.0 mL) and the resulting mixture was heated under reflux for 3 h. After the completion of reaction, the flask was cooled to room temperature and the solvent was removed under reduced pressure. The contents were purified (SiO₂; CH₂Cl₂/MeOH, 9:1, R_f = 0.16) to yield an intermediate tributylammonium sulfate (**2**) as a clear oil which then was purified by **work up procedure B** to yield the title compound (**207**) as yellow powder (311.0 mg, 83%).

M.P. 157-159 °C (Lit.¹⁴⁹ 170 °C)

¹H NMR (300 MHz, DMSO-*d*₆) δ 9.20 – 8.80 (m, 1H), 7.19 – 6.83 (m, 1H), 6.56 – 6.36 (m, 2H), 4.04 (t, *J* = 8.3 Hz, 1H), 2.80 – 2.63 (m, 2H), 2.21 (d, *J* = 10.8 Hz, 1H), 2.05 (d, *J* = 11.5 Hz, 2H), 1.96 – 1.86 (m, 1H), 1.85 – 1.69 (m, 1H), 1.58 (q, *J* = 11.1, 10.6 Hz, 2H), 1.39 – 0.87 (m, 6H), 0.69 (s, 3H).

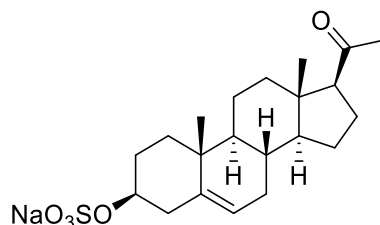
¹³C NMR (101 MHz, DMSO-*d*₆) δ 155.0, 137.3, 130.6, 126.3, 115.1, 112.9, 85.2, 49.3, 43.6, 42.6, 38.6, 36.7, 29.3, 28.3, 27.0, 26.1, 22.9, 11.8.

LRMS *m/z* (ESI⁻) 351.1 ([M¹²C-Na]⁻, 100 %), 352.1 ([M¹³C-Na]⁻, 20 %).

HRMS *m/z* (ESI⁻) C₁₈H₂₃O₅S requires 351.1276, found 351.1266 [M-Na]⁻.

Data were consistent with those reported in the literature.¹⁴⁹

Preparation of sodium-3-pregnenolone sulfate or sodium (3*S*,8*S*,9*S*,10*R*,13*S*,14*S*,17*S*)-17-acetyl-10,13-dimethyl-2,3,4,7,8,9,10,11,12,13,14,15,16,17-tetradecahydro-1H-cyclopenta[*a*]phenanthren-3-yl sulfate (212).



Following **general procedure 6**: Pregnenolone (100 mg, 0.3 mmol) and TBSAB (132.7 mg, 0.5 mmol) were dissolved in anhydrous MeCN (2.0 mL) and the resulting mixture was heated under reflux for 3 h. After the completion of reaction, the flask was cooled to room temperature and the solvent was removed under reduced pressure. The crude product was purified by **work up procedure B** to yield the title compound (**212**) as a white solid (194.0 mg, 98%).

M.P. 121-123 °C

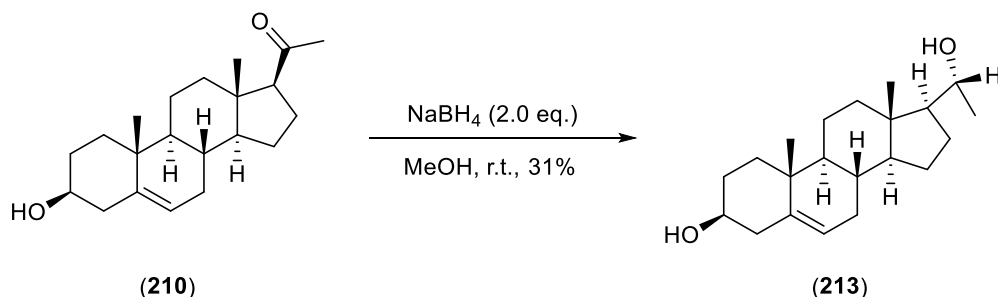
¹H NMR (400 MHz, DMSO-*d*₆) δ 5.29 (dt, *J* = 5.0, 2.1 Hz, 1H), 3.84 (tt, *J* = 11.5, 4.6 Hz, 1H), 2.57 (t, *J* = 8.9 Hz, 1H), 2.37 (ddd, *J* = 13.3, 4.9, 2.1 Hz, 1H), 2.19 – 2.10 (m, 1H), 2.06 (s, 3H), 2.04 – 1.97 (m, 2H), 1.97 – 1.84 (m, 2H), 1.81 (dt, *J* = 13.3, 3.5 Hz, 1H), 1.64 – 1.50 (m, 4H), 1.48 – 1.33 (m, 4H), 1.25 – 1.07 (m, 2H), 1.01 (dd, *J* = 13.8, 3.8 Hz, 1H), 0.94 (s, 3H), 0.53 (s, 3H).

¹³C NMR (101 MHz, DMSO-*d*₆) δ 208.5, 140.7, 121.0, 75.2, 62.5, 56.0, 49.4, 43.3, 37.9 (2C), 36.9, 36.1, 31.3, 31.3, 31.2, 28.8, 24.0, 22.2, 20.6, 19.0, 12.9.

LRMS *m/z* (ESI⁻) 395.1 ([M¹²C-Na]⁻, 100 %), 396.1 ([M¹³C-Na]⁻, 20%).

HRMS *m/z* (ESI⁻) C₂₁H₃₁O₅S requires 395.1892, found 395.1907[M-Na]⁻.

Preparation of pregnenolone or known as (3*S*,8*S*,9*S*,10*R*,13*S*,14*S*,17*S*)-17-((*R*)-1-hydroxyethyl)-10,13-dimethyl-2,3,4,7,8,9,10,11,12,13,14,15,16,17-tetradecahydro-1H-cyclopenta[*a*]phenanthren-3-ol (**213**) by the reduction reaction of pregnenolone using sodium borohydride (NaBH₄) and MeOH.



Pregnenolone (**210**) (1.0 g, 3.1 mol) and MeOH (20 mL) were added to a flame-dried round-bottom flask under inert environment. The sodium borohydride (240 mg, 6.3 mmol) was added slowly over the period of time to the flask. The reaction mixture was stirred for an additional 2 hours. After the completion of reaction, the white precipitate was collected by filtration and dried for overnight to afford the desired pregnenol (**213**) as a white solid (314.0 mg, 0.97 mol, 31%)

M.P. 174-176 °C (Lit.³¹⁵ 211-212°C)

¹H NMR (300 MHz, DMSO-*d*₆) δ 5.25 (d, *J* = 4.8, 2.7 Hz, 1H), 4.59 (d, *J* = 3.9 Hz, 1H), 4.09 (d, *J* = 5.3 Hz, 1H), 3.54 – 3.41 (m, 1H), 3.30 – 3.19 (m, 1H), 2.19 – 2.05 (m, 3H), 1.95 – 1.84 (m, 1H), 1.81 – 1.71 (m, 1H), 1.71 – 1.62 (m, 1H), 1.60 – 1.48 (m, 3H), 1.47 – 1.31 (m, 5H), 1.27 – 1.16 (m, 1H), 1.15 – 1.03 (m, 3H), 0.99 (d, *J* = 6.1 Hz, 3H), 0.94 (s, 3H), 0.92 – 0.79 (m, 2H), 0.68 (s, 3H).

¹³C NMR (101 MHz, DMSO-*d*₆) δ 141.3, 120.4, 70.0, 68.3, 57.6, 55.8, 49.8, 42.2, 41.8, 39.2, 36.9, 36.1, 31.5, 31.4, 31.4, 25.3, 24.2, 23.8, 20.4, 19.2, 11.9.

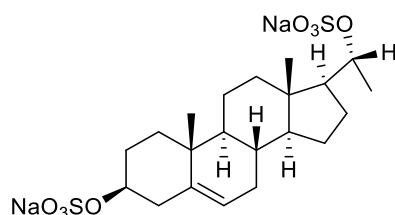
LRMS m/z (TOF MS APAP⁺) 283.2 ([M-2OH+H]⁺, 100%), 284.2 ([M¹³C-2OH+H]⁺, 100%), 301.2 ([M-OH]⁺, 70%), 302.2 ([M¹³C-OH]⁺, 20%).

HRMS m/z (TOF MS APAP⁺) C₂₁H₃₃O requires 301.2531, found 301.2541 [M-OH]⁺.

[α]_D^{26/589} = -17.3 (c 1.23, 95% ethanol)

Data were consistent with those reported in the literature.³¹⁵

Disodium-3,17-pregnendiol disulfate or sodium (3*S*,8*S*,9*S*,10*R*,13*S*,14*S*,17*S*)-10,13-dimethyl-17-((*R*)-1-(sulfonatooxy)ethyl)-2,3,4,7,8,9,10,11,12,13,14,15,16,17-tetradecahydro-1H-cyclopenta[*a*]phenanthren-3-yl sulfate (215)



Following **general procedure 6**: Pregnendiol (197 mg, 0.6 mmol) and TBSAB (530.8 mg, 2.0 mmol) were dissolved in anhydrous MeCN (4.0 mL) and the resulting mixture was heated under reflux for 5 h. After the completion of reaction, the flask was cooled to room temperature and the solvent was removed under reduced pressure. The crude product was purified by **work up procedure B** to yield the title compound (**215**) as a white solid (344.0 mg, 0.6 mmol, 40%).

M.P. 156-158 °C

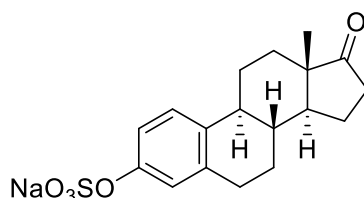
¹H NMR (400 MHz, DMSO-*d*₆) δ 5.30 – 5.25 (m, 1H), 4.16 – 3.97 (m, 1H), 3.92 – 3.70 (m, 1H), 2.41 – 2.32 (m, 1H), 2.22 (d, J = 12.9 Hz, 1H), 2.18 – 2.04 (m, 1H), 1.95 – 1.76 (m, 3H), 1.62 – 1.49 (m, 3H), 1.49 – 1.26 (m, 6H), 1.13 (d, J = 6.0 Hz, 4H), 1.04 – 0.80 (m, 7H), 0.72 (s, 3H).

^{13}C NMR (101 MHz, $\text{DMSO-}d_6$) δ 140.8, 121.1, 75.3, 74.4, 56.1, 55.6, 49.7, 41.7, 38.0, 36.9, 36.1, 31.5, 31.4 (2C), 28.8, 25.0, 23.9, 20.5, 20.4, 19.0, 11.3.

LRMS m/z (ES $^-$) 238.0 ($[\text{M}-2\text{Na}]^{2-}$, 100%), 239.0 ($[\text{M}^{13}\text{C}-2\text{Na}]^{2-}$, 100%), 477.1 ($[\text{M}-2\text{Na}]^-$, >1%), 478.1 ($[\text{M}^{13}\text{C}-2\text{Na}+\text{H}]^-$, <1%).

HRMS m/z (ES $^-$) $\text{C}_{21}\text{H}_{32}\text{O}_8\text{S}_2$ requires 476.1550, found 476.1538 $[\text{M}-2\text{Na}]^-$.

Preparation of sodium-3-sulfate estrone or sodium (8*R*,9*S*,13*S*,14*S*)-13-methyl-17-oxo-7,8,9,11,12,13,14,15,16,17-decahydro-6*H*-cyclopenta[*a*]phenanthren-3-yl sulfate (**221**)³¹⁶



Following **general procedure 6**: Estrone (270.4 mg, 1.0 mmol) and TBSAB (530.8 mg, 2.0 mmol) were dissolved in anhydrous MeCN (4.0 mL) and the resulting mixture was heated under reflux for 5 h. After the completion of reaction, the flask was cooled to room temperature and the solvent was removed under reduced pressure. The crude product was purified by **work up procedure B** to afford the title compound (**221**) as a white solid (269.0 mg, 72%).

M.P. 188-190 °C (dec.) (Lit.³¹⁶ 226-228 °C)

^1H NMR (300 MHz, CDCl_3) δ 7.15 (dd, $J = 8.4, 1.1$ Hz, 1H), 6.64 (dd, $J = 8.4, 2.8$ Hz, 1H), 6.59 (d, $J = 2.6$ Hz, 1H), 2.87 (dd, $J = 7.8, 3.3$ Hz, 2H), 2.51 (dd, $J = 18.4, 8.4$ Hz, 1H), 2.44 – 2.33 (m, 1H), 2.31 – 1.85 (m, 5H), 1.78 – 1.30 (m, 6H), 0.91 (s, 3H).

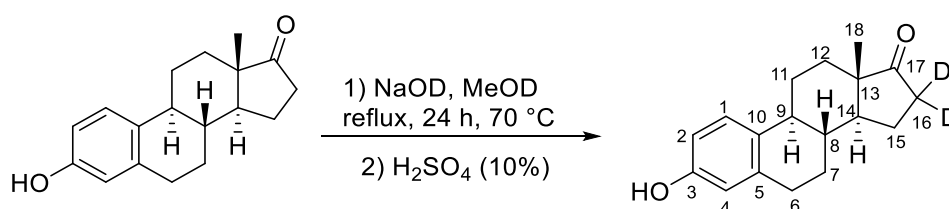
^{13}C NMR (101 MHz, CDCl_3) δ 221.3, 153.6, 138.2, 132.2, 126.6, 115.4, 112.9, 50.5, 48.1, 44.0, 38.4, 36.0, 31.7, 29.6, 26.6, 26.0, 21.7, 14.0.

LRMS m/z (ES^-) 349.1 ($[\text{M}^{12}\text{C}-\text{Na}]^-$, 100%), 350.1 ($[\text{M}^{13}\text{C}-\text{Na}]^-$, 10%).

HRMS m/z (ES^-) $\text{C}_{18}\text{H}_{21}\text{O}_5\text{S}$ requires 349.1110, found 349.1120 $[\text{M}-\text{Na}]^-$.

Data were consistent with those reported in the literature.³¹⁶

The preparation of deuterium-labelled of estrone (**222**) using sodium deuterioxide (NaOD) solution and CD_3OD solvent.



A round-bottom flask was charged with estrone (270.4 mg, 1.0 mmol), sodium deuterioxide (0.2 mL) and the mixture was dissolved in MeOD (8 mL) under an inert environment. The reaction mixture was heated under reflux for 24 h. After the completion of reaction, the flask was cooled to room temperature and 10% sulfuric acid was added dropwise to achieve pH 7. The white precipitate was collected by filtration, washed with distilled water (10 mL), and crystallized in ethanol (15 mL). The solvent was removed under reduced pressure to afford the desired deuterium-labelled of estrone (**222**) as a white solid (240.0 mg, 88%).

M.P. 201-203 °C

^1H NMR (400 MHz, $\text{DMSO}-d_6$) δ 9.01 (s, 1H, C3-OH), 7.08 – 7.01 (m, 1H, C1-H), 6.51 (dd, $J = 8.4, 2.7$ Hz, 1H, C2-H), 6.45 (d, $J = 2.6$ Hz, 1H, C4-H), 2.84 – 2.67 (m, 2H, C6-H₂), 2.34 – 2.26 (m, 1H, C11-H), 2.13 (s, 1H, C9-H), 1.94 (d, $J = 4.6$ Hz, 1H, C15-H), 1.89 (dd, $J = 7.3, 4.5$ Hz, 1H, C7-

H), 1.74 (dd, $J = 8.9, 2.6$ Hz, 1H, C12-H), 1.58 – 1.43 (m, 3H), 1.39 – 1.27 (m, 3H), 0.82 (s, 3H, C18-CH₃).

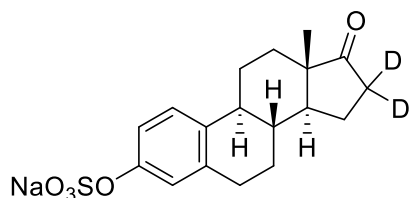
¹³C NMR (101 MHz, DMSO-*d*₆) δ 219.8 (C17), 155.0 (C3), 137.1(C5), 129.9 (C10), 126.0 (C1), 114.9 (C4), 112.8 (C2), 49.5 (C14), 47.3 (C13), 43.4 (C9), 37.9 (C8), 34.9 (C16), 31.3 (C12), 29.0 (C6), 26.1 (C7), 25.5 (C11), 20.9 (C15), 13.5 (C18).

LRMS m/z (TOF MS APAP⁺) 271.1 ([M-²H₂+¹H₃]⁺, 100%), 272.1 (M-¹³C²H₂+¹H₃]⁺, 80%), 273.1 ([M-²H₁+¹H₂]⁺, 20%).

HRMS m/z (TOF MS APAP⁺) C₁₈¹H₂₁²H₂O₂ requires 273.1824, found 273.1806 [M-²H₁+¹H₂]⁺,

It should be noted that a 72% level of ²H₂ deuterium incorporation was validated by ¹H NMR analysis due to the partial disappearance of C16 at 2.48–2.37 (m, 1H, C16-H) and 2.04 (dd, $J = 18.8, 8.9$ Hz, 1H, C16-H) signals indicating ²H₂ was present. Due to the exchangeability of the C16-²H₂ protons with ¹H a mixture of un-deuterated and partially deuterated estrone was observed.

Preparation of 16-d₂-sodium-3- β -estrone sulfate or sodium (8*R*,9*S*,13*S*,14*S*)-13-methyl-17-oxo-7,8,9,11,12,13,14,15,16,17-decahydro-6*H*-cyclopenta[*a*]phenanthren-3-yl-16,16-d₂ sulfate (224)



Following **general procedure 6**: Estrone-d₂ (136 mg, 0.5 mmol) and TBSAB (265 mg, 1.0 mmol) were dissolved in anhydrous MeCN (2.0 mL) and the resulting mixture was heated under

reflux for 7 h. After the completion of reaction, the flask was cooled to room temperature and the solvent was removed under reduced pressure. The crude product was purified by **work up procedure B** and washed with 10 mL of MeCN to afford the title compound (**224**) as a yellow solid (149.0 mg, 78%).

M.P. 210-212 °C

¹H NMR (400 MHz, DMSO-*d*₆) δ 7.16 (d, *J* = 8.3 Hz, 1H, C1-H), 6.91 – 6.86 (m, 2H, C2&C4-2H), 2.85 – 2.76 (m, 2H, C6-H₂), 2.39 – 2.32 (m, 1H, C11-H), 2.20 (q, *J* = 6.5, 3.8 Hz, 1H, C9-H), 1.99 – 1.89 (m, 2H, C15-H), 1.76 (dd, *J* = 8.7, 2.6 Hz, 1H, C12-H), 1.60 – 1.46 (m, 3H), 1.43 – 1.32 (m, 3H), 0.83 (s, 3H).

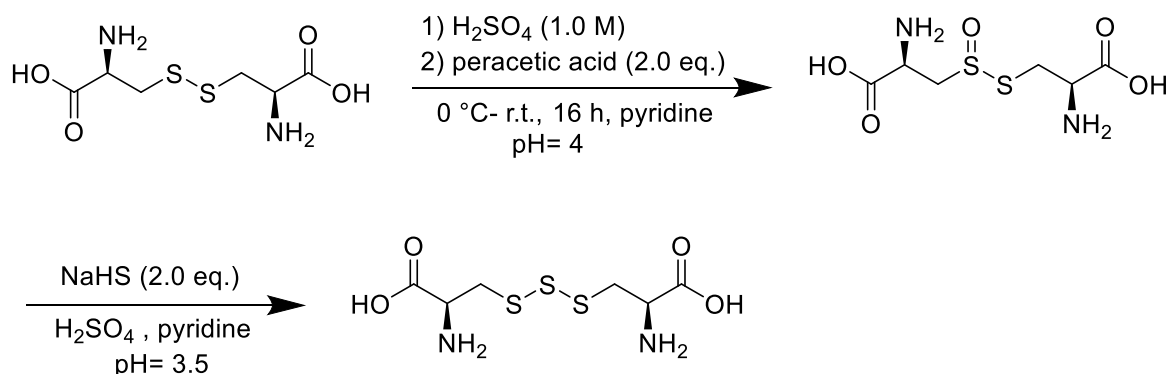
¹³C NMR (101 MHz, DMSO-*d*₆) δ 219.8 (C17), 151.29 (C3), 136.60 (C5), 134.31 (C10), 125.5 (C1), 120.5 (C4), 118.1 (C2), 49.5 (C14), 47.3 (C13), 43.6 (C9), 37.7 (C8), 35.4 (C16), 31.3 (C12), 29.0 (C6), 26.0 (C7), 25.5 (C11), 20.9 (C15), 13.4 (C18).

LRMS *m/z* (ESI⁻) 351.1 ([M-Na]⁻, 100%), 350.1 ([M-²H₁+¹H₁-Na]⁻, 50%), 352.1 ([M¹³C-Na]⁻, 20%), 353.1 (10%), 349.1 (10%).

HRMS *m/z* (ES⁻) C₁₈H₁₉²H₂O₅S requires 351.1235, found 351.1243 [M+²H₂]⁻.

¹H NMR analysis confirmed a 67% level of ²H₂ incorporation.

8.4. Preparation of cysteine trisulfide (**237**)³⁰⁶



Adapting Fukuto *et.al.* the procedure: Cystine-S-monoxide intermediate was synthesized by dissolving *L*-Cystine (1 g, 4.16 mmol) in 1M H₂SO₄ (10 mL) in an ice bath. Two equivalents of peracetic acid (0.13 mL) were then added slowly. The reaction mixture was stirred in an ice bath and then at room temperature for 16 hours. Then Pyridine (1.5 mL) was added to adjust the pH to 4. Cystine-S-monoxide was precipitated from the solution via the addition of ethanol (30 mL). The precipitate was filtered and dried and the resulting solution was neutralized with NaHSO₃ then disposed. The Cystine-S-monoxide intermediate was dissolved in 1M H₂SO₄ (10 mL). Sodium hydrosulfide hydrate (112.2 mg, 2.0 mmol) was transferred to a separate flask and the Cystine-S-monoxide solution was added to the NaHS. After this addition, the flask was sealed with a septum and stirred at room temperature for 1 h. The pH was then adjusted to 3.5 by adding pyridine (1.2 mL). A 50/50 mixture of ethanol/THF was then added (40 mL) to precipitate Cys-SSS-Cys. The precipitate was filtered, washed again with 50/50 ethanol/THF (30 mL), and dried. The desired product was purified by reverse phase chromatography (SiO₂, MeCN/H₂O 5%:95%) affording the title compound (**237**) as a white powder (980.0 mg, 86%).

M.P. > 230 (dec.)

¹H NMR (400 MHz, D₂O) δ 4.40 (dd, *J* = 7.8, 4.3 Hz, 2H), 3.36 (dd, *J* = 15.3, 4.3 Hz, 2H), 3.20 (dd, *J* = 15.2, 7.8 Hz, 2H).

^{13}C NMR (101 MHz, D_2O) δ 169.4, 50.6, 35.1.

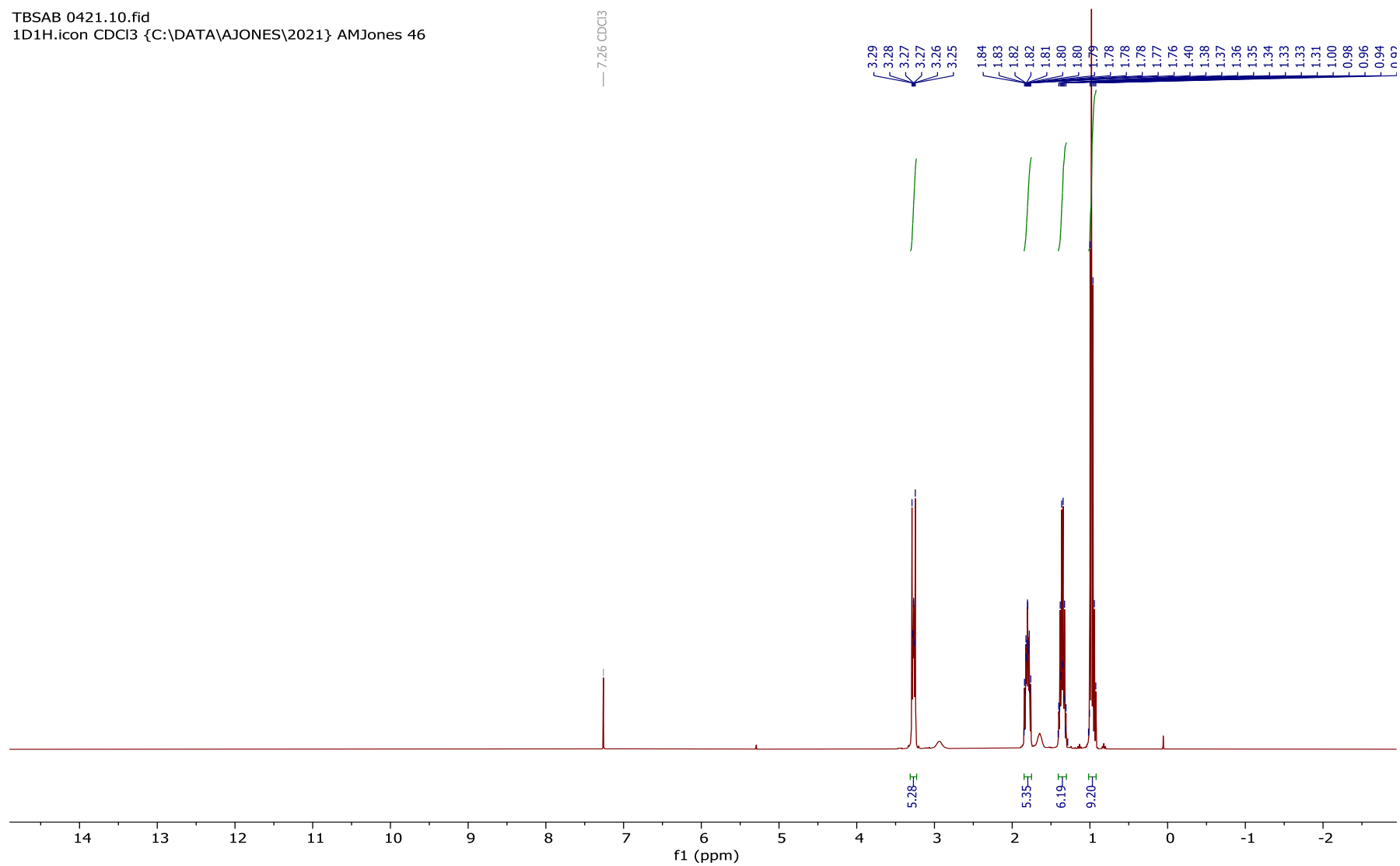
LRMS m/z (ES+) 273.0 ($[\text{M}^{12}\text{C}+\text{H}]^+$, 100%), 274.0 ($[\text{M}^{13}\text{C}+\text{H}]^+$, 10%).

HRMS m/z (ES+) $\text{C}_6\text{H}_{12}\text{N}_2\text{O}_4\text{S}_3$ requires 273.0037, found 273.0042 ($\text{M}+\text{H}^+$)

Copies of ^1H and ^{13}C NMR spectra

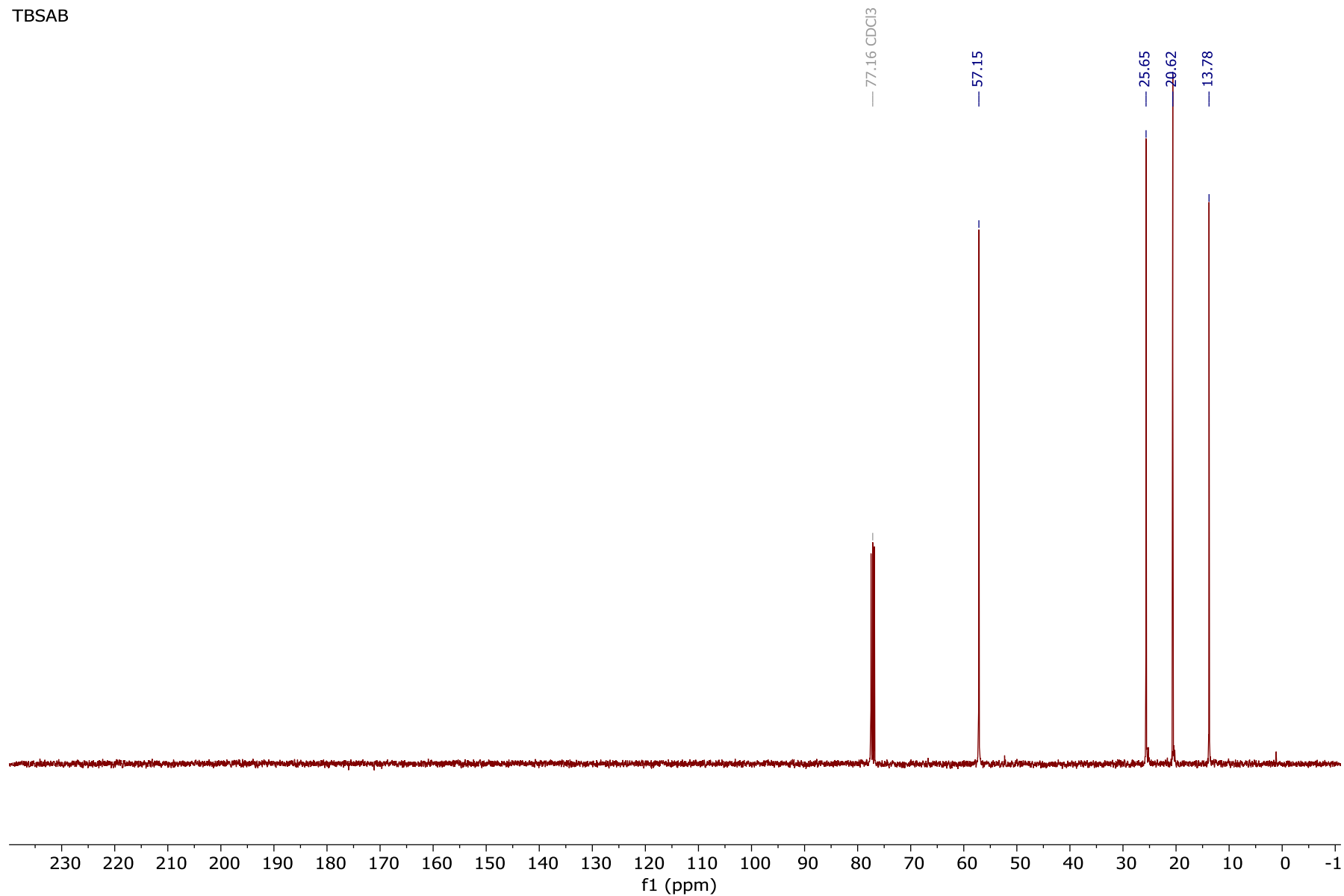
¹H NMR spectrum of **42** (300 MHz, CDCl₃)

TBSAB 0421.10.fid
1D1H.icon CDCl3 {C:\DATA\AJONES\2021} AMJones 46



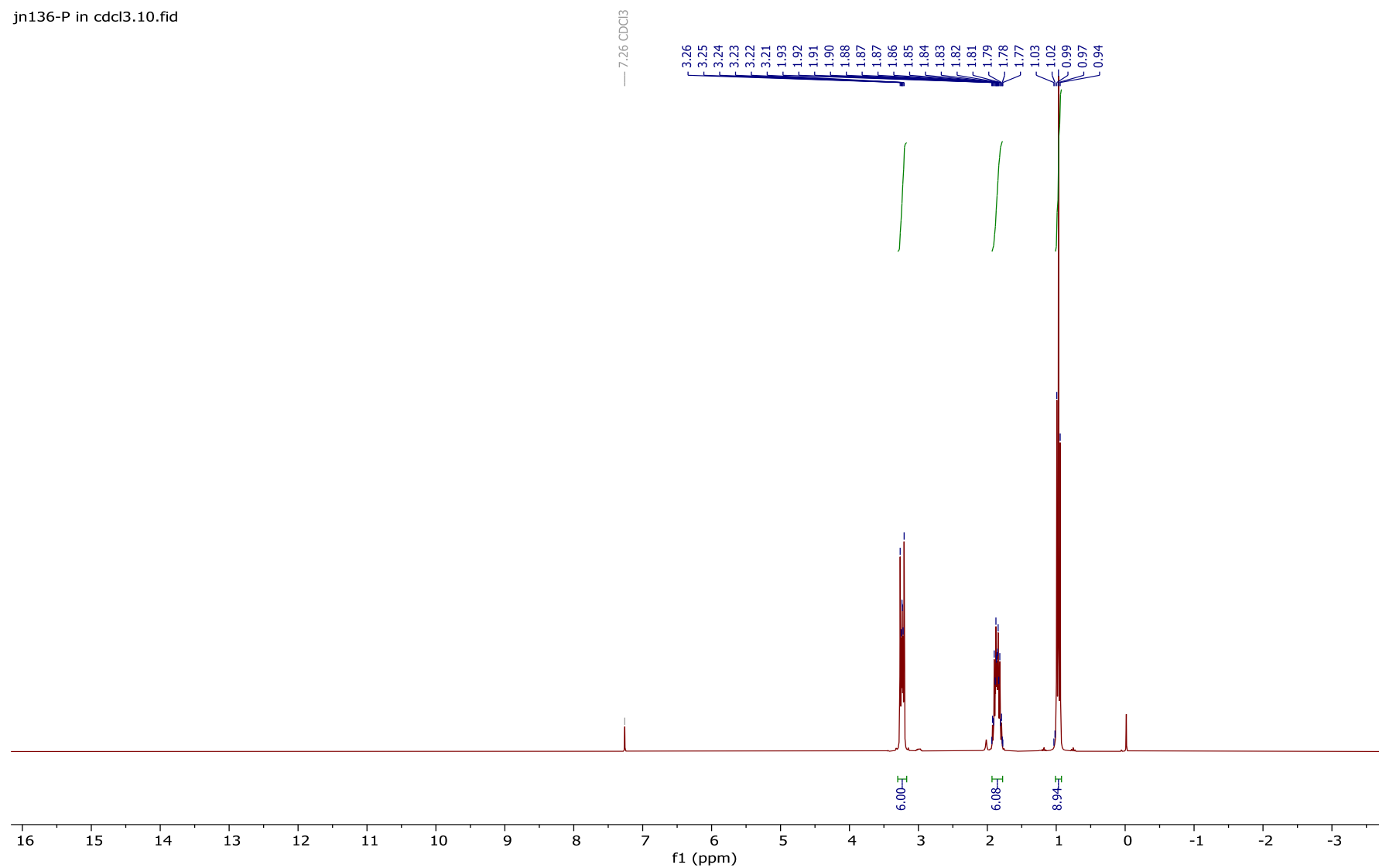
¹³C NMR spectrum of **42** (101 MHz, CDCl₃)

TBSAB



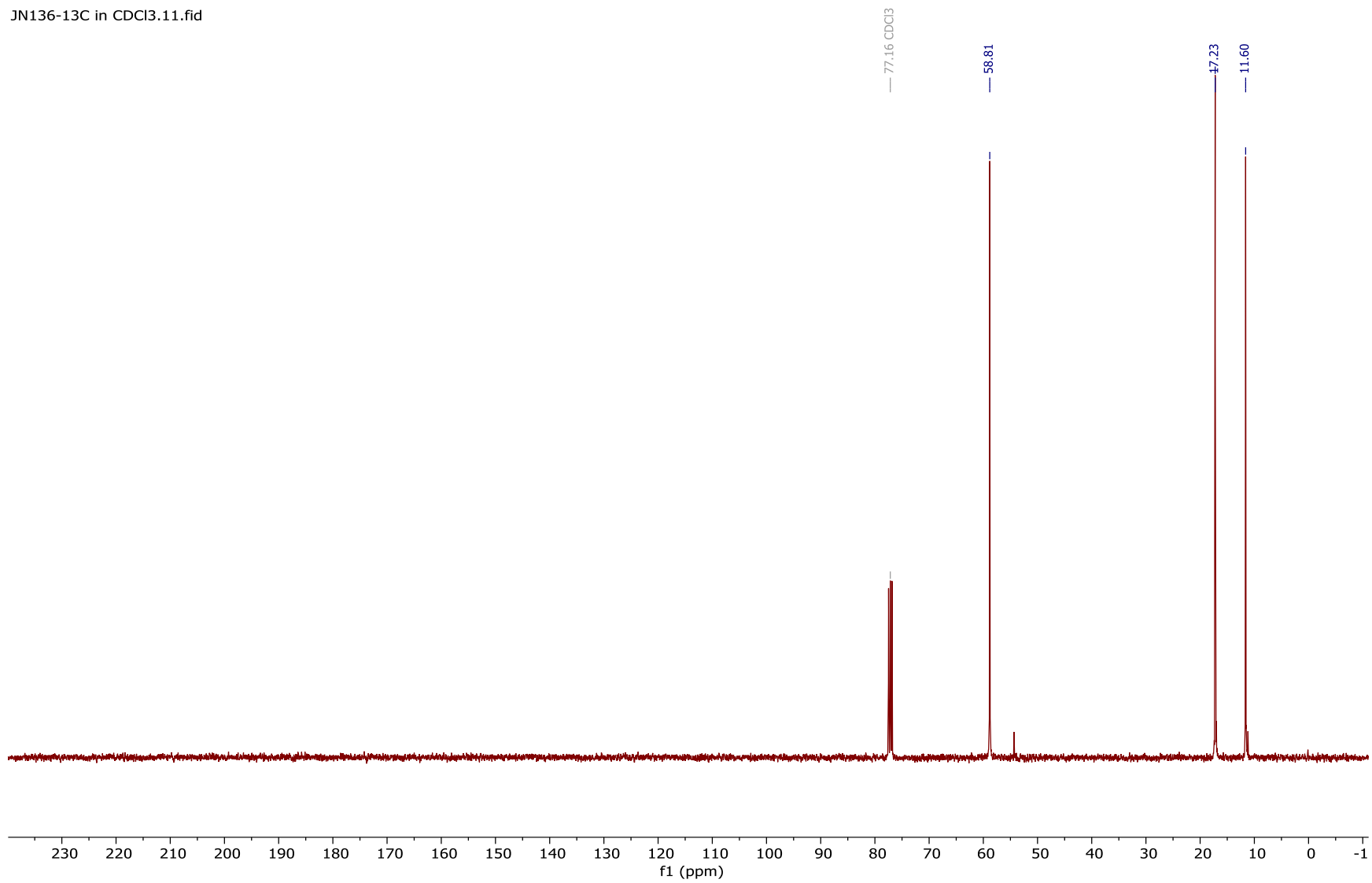
¹H NMR spectrum of **102** (300 MHz, CDCl₃)

jn136-P in cdcl3.10.fid



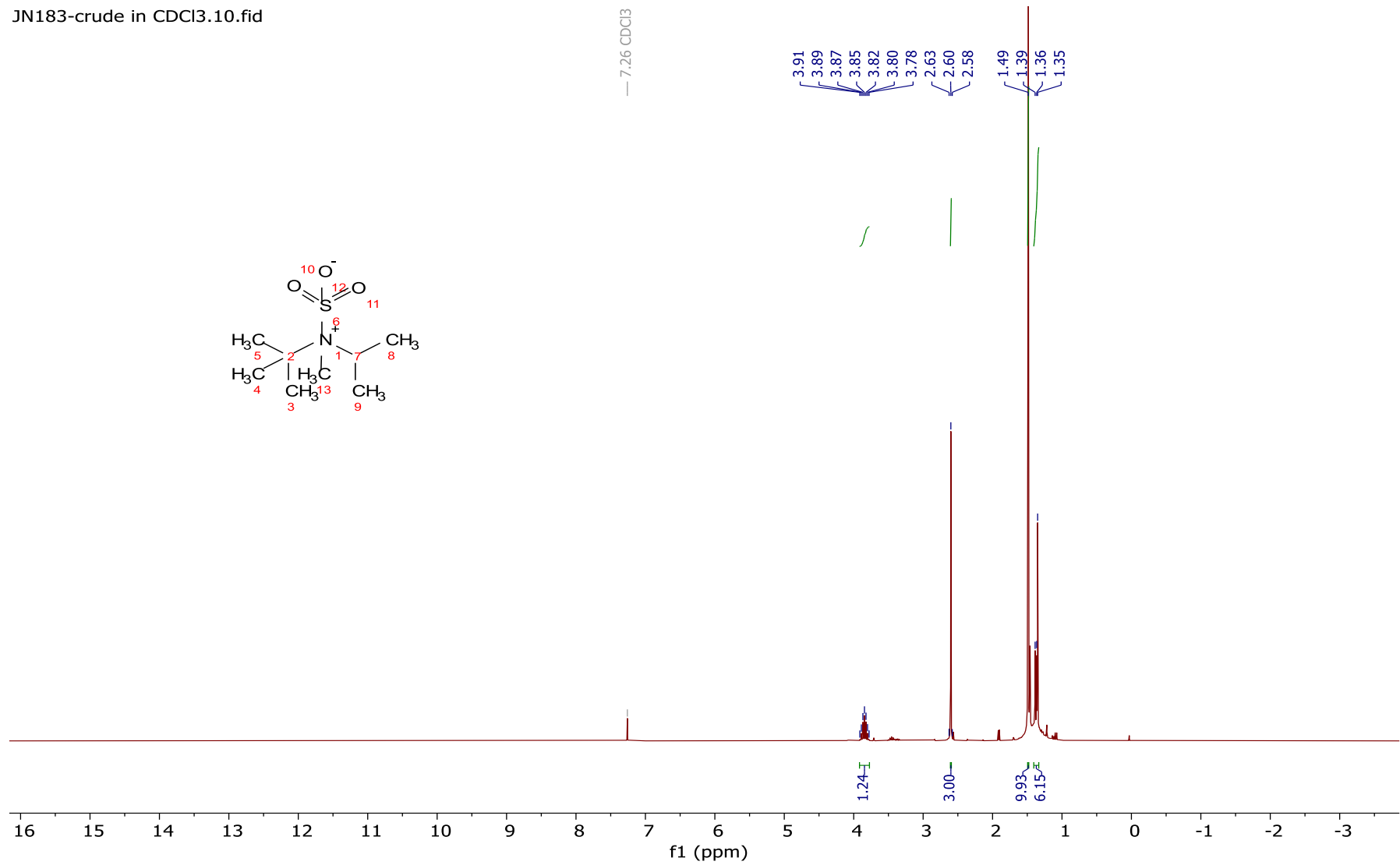
¹³C NMR spectrum of **102** (101 MHz, CDCl₃)

JN136-13C in CDCl₃.11.fid



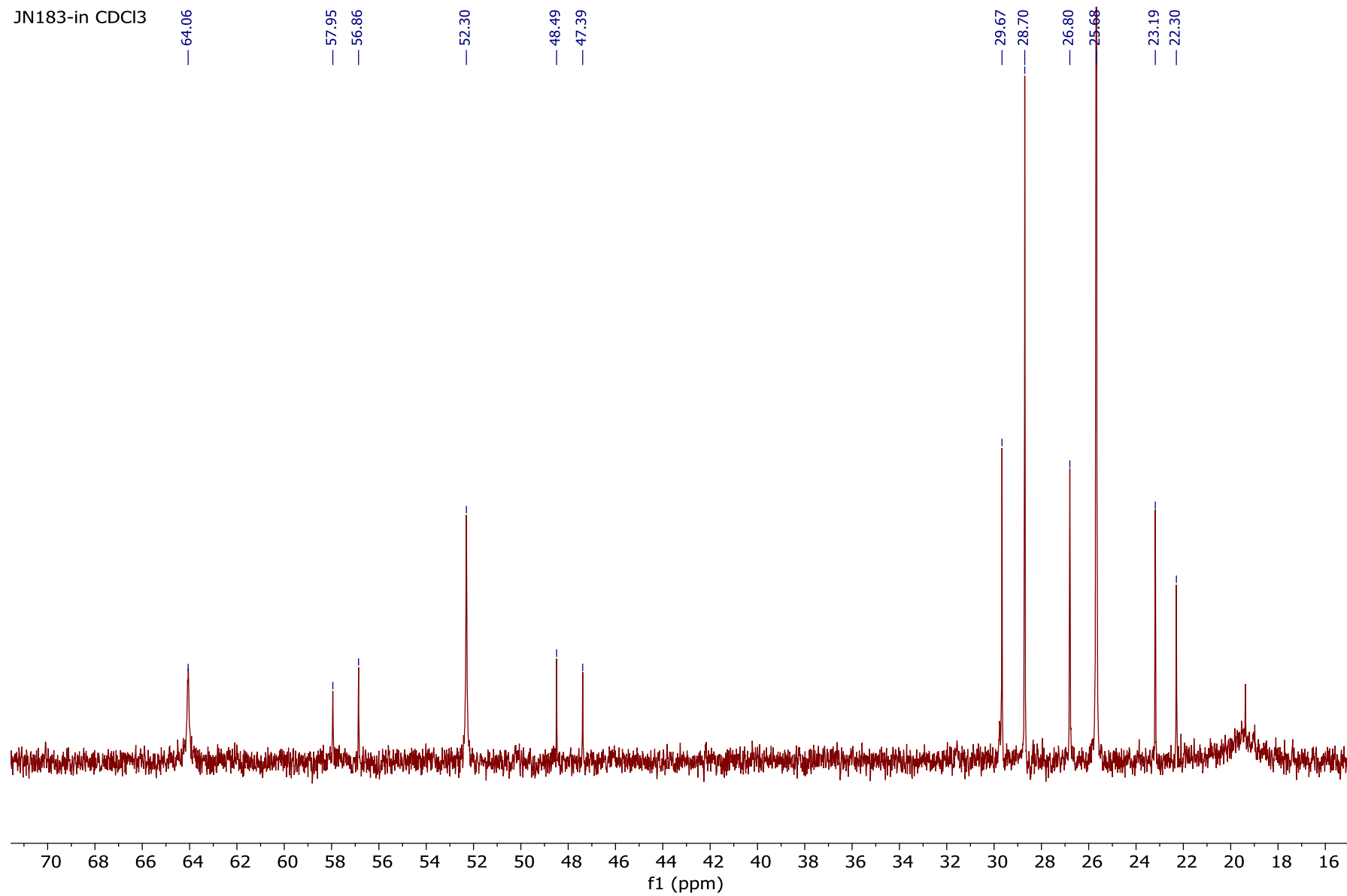
¹H NMR spectrum of **112** (300 MHz, CDCl₃)

JN183-crude in CDCl₃.10.fid



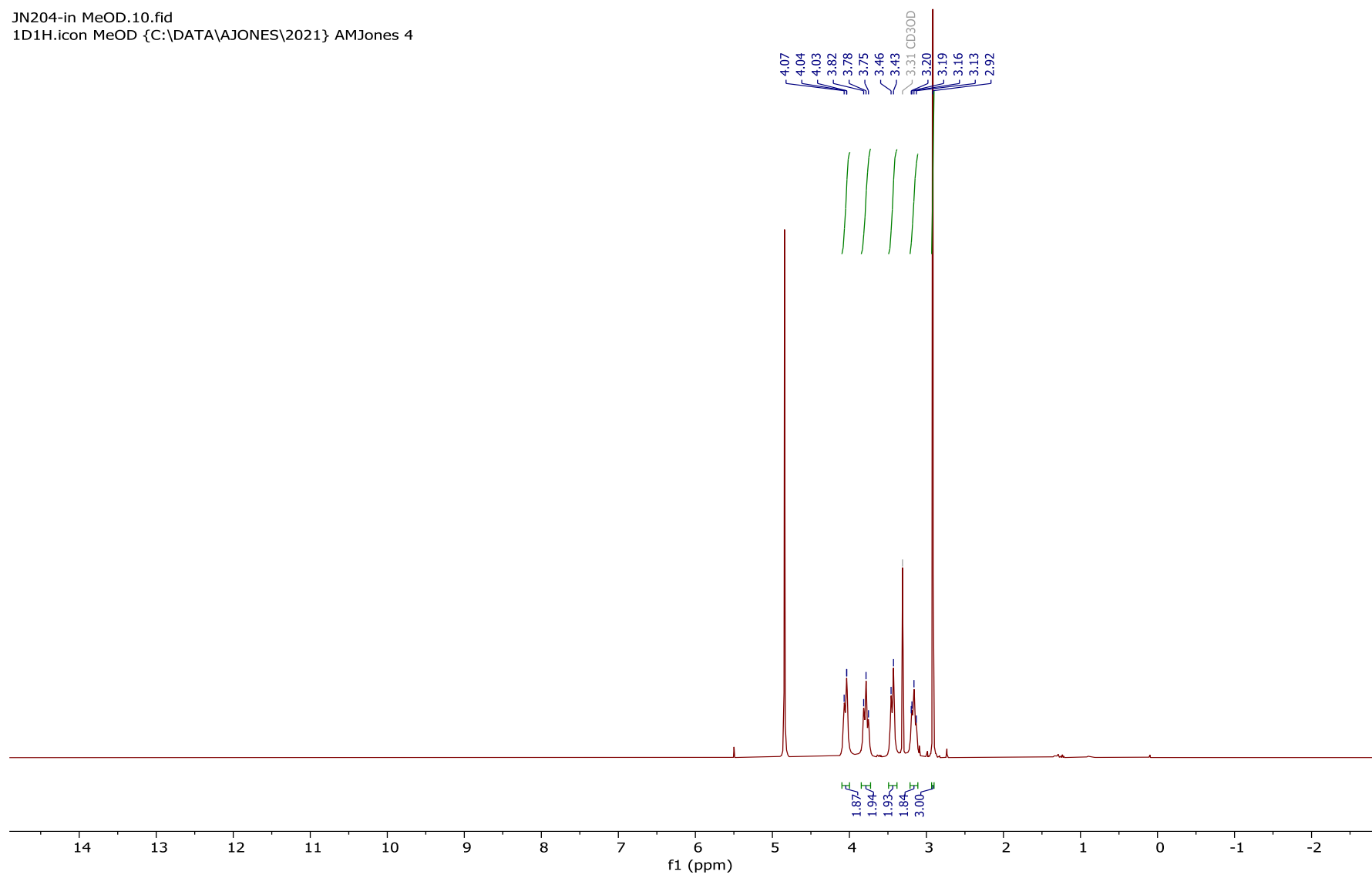
¹³C NMR spectrum of **112** (300 MHz, CDCl₃)

JN183-in CDCl3



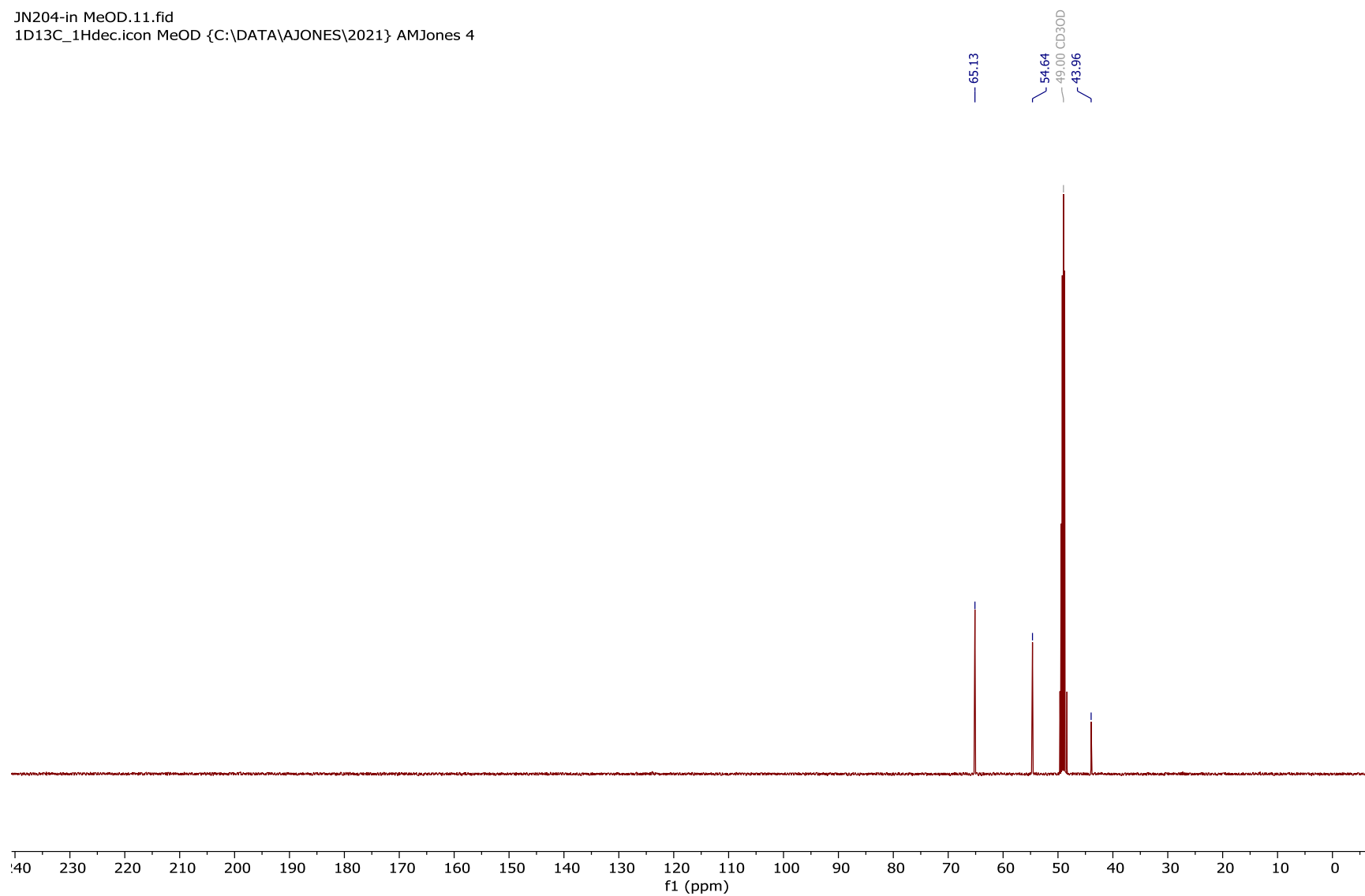
¹H NMR spectrum of **115** (300 MHz, MeOD)

JN204-in MeOD.10.fid
1D1H.icon MeOD {C:\DATA\AJONES\2021} AMJones 4



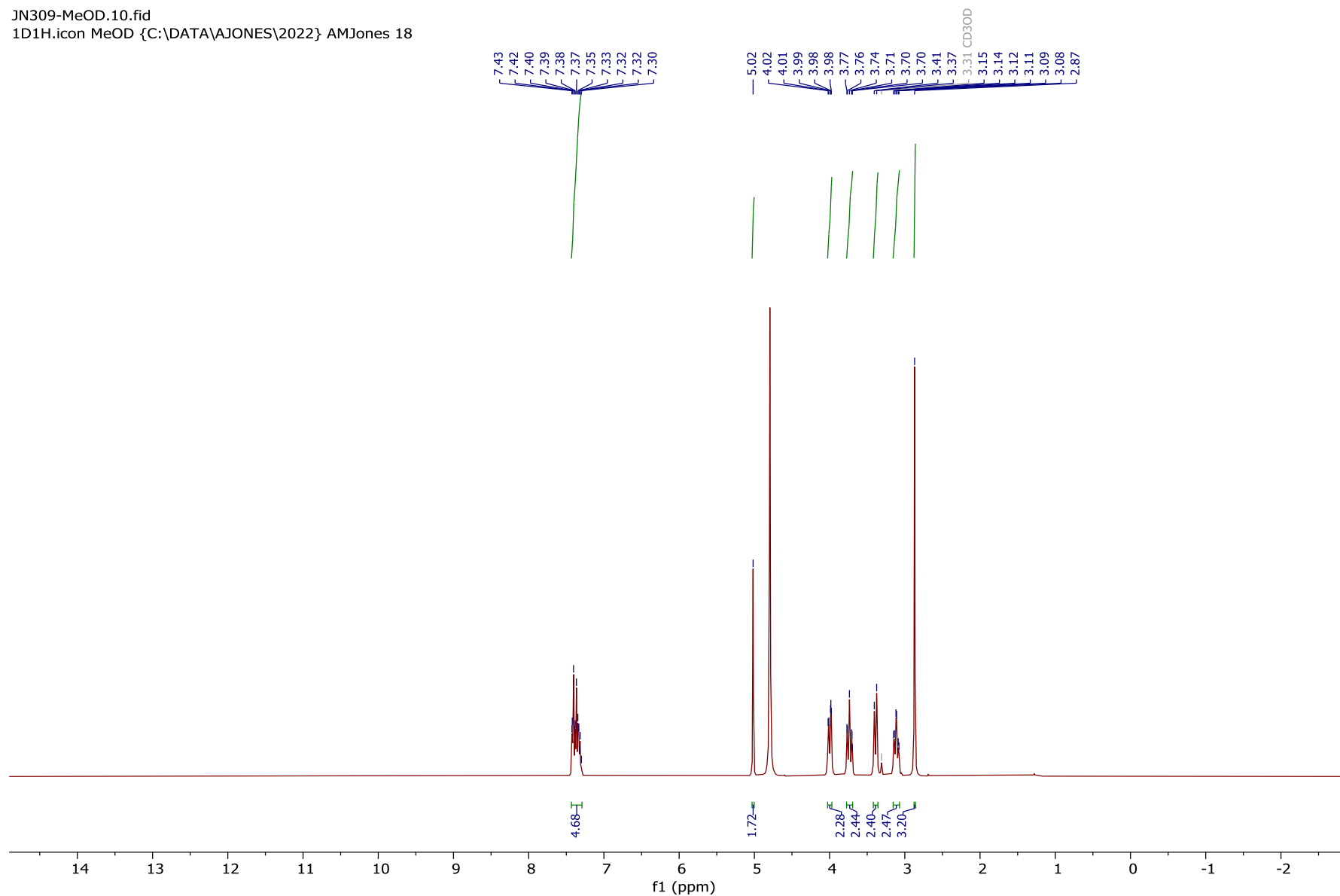
¹³C NMR spectrum of **115** (101 MHz, MeOD)

JN204-in MeOD.11.fid
1D13C_1Hdec.icon MeOD {C:\DATA\AJONES\2021} AMJones 4



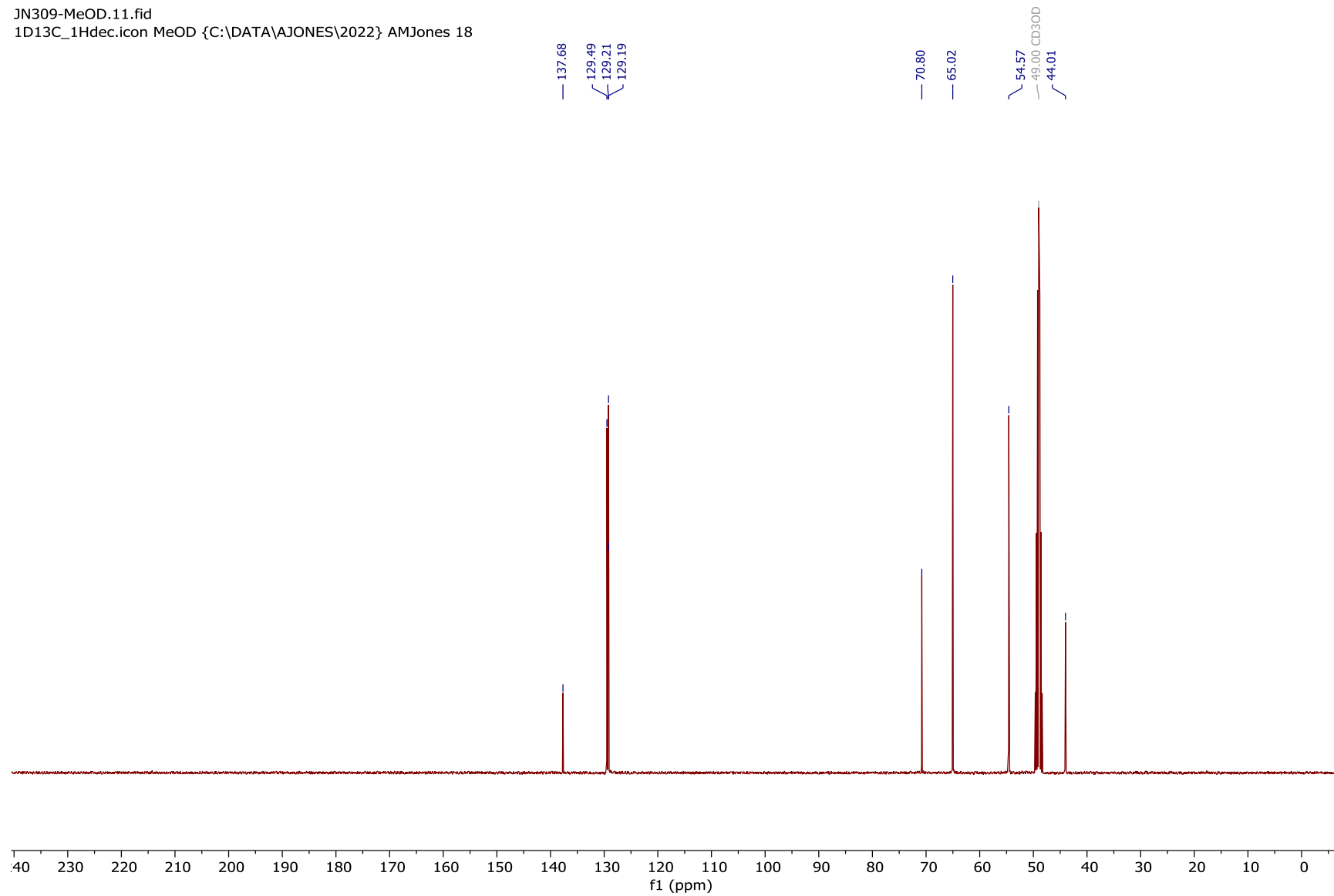
¹H NMR spectrum of **116** (300 MHz, MeOD)

JN309-MeOD.10.fid
1D1H.icon MeOD {C:\DATA\AJONES\2022} AMJones 18



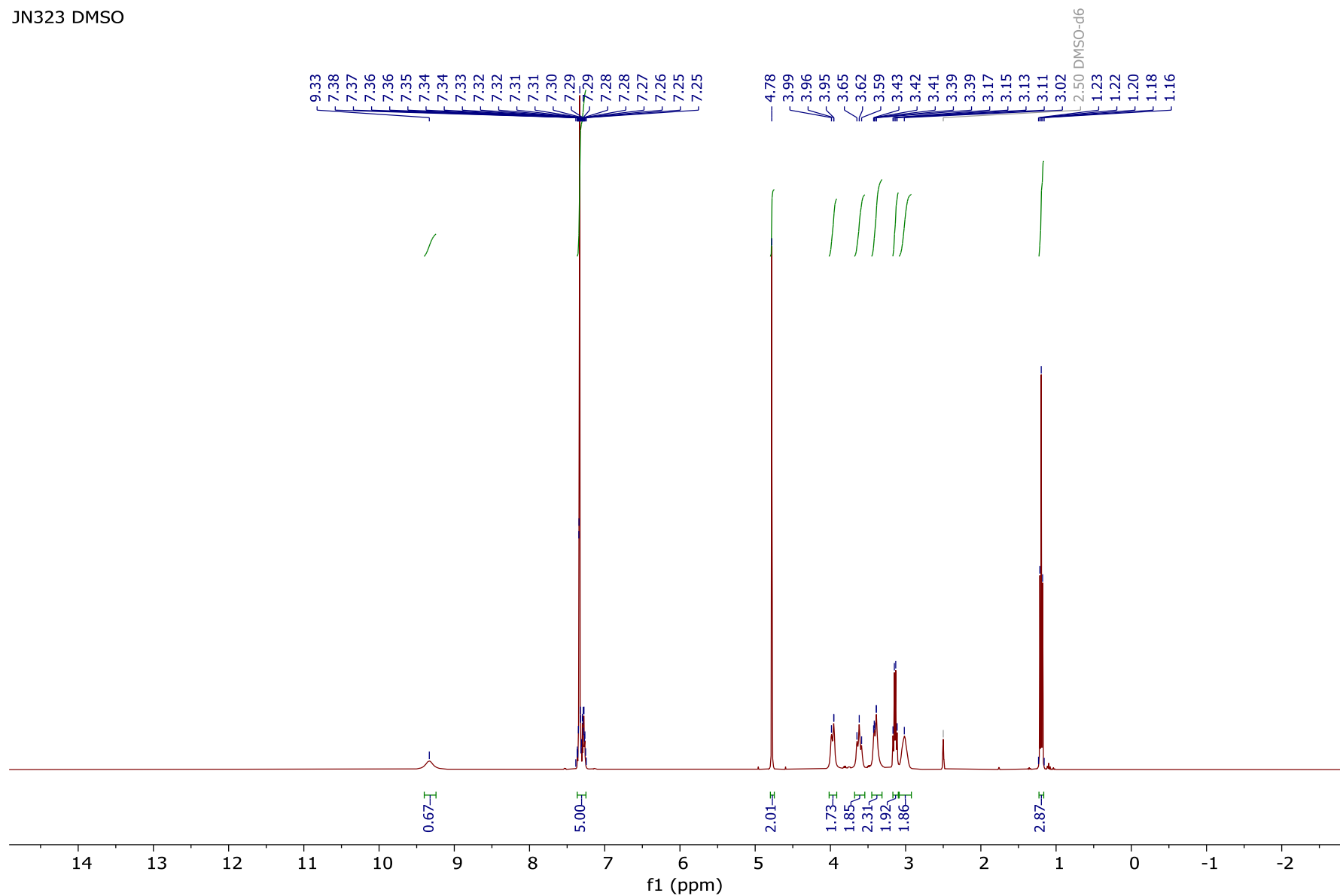
¹³C NMR spectrum of **116** (101 MHz, MeOD)

JN309-MeOD.11.fid
1D13C_1Hdec.icon MeOD {C:\DATA\AJONES\2022} AMJones 18

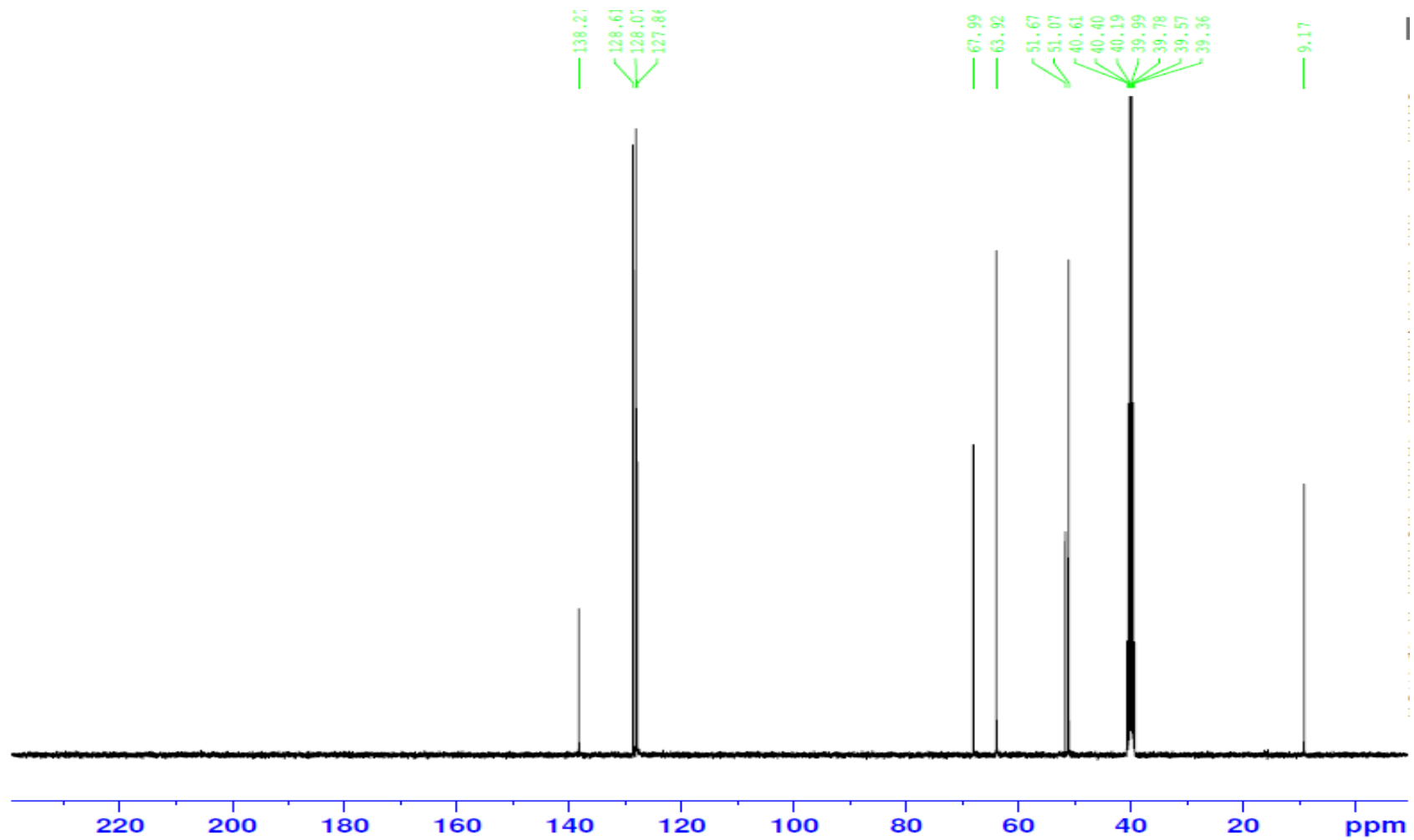


¹H NMR spectrum of **120** (400 MHz, DMSO-d₆)

JN323 DMSO

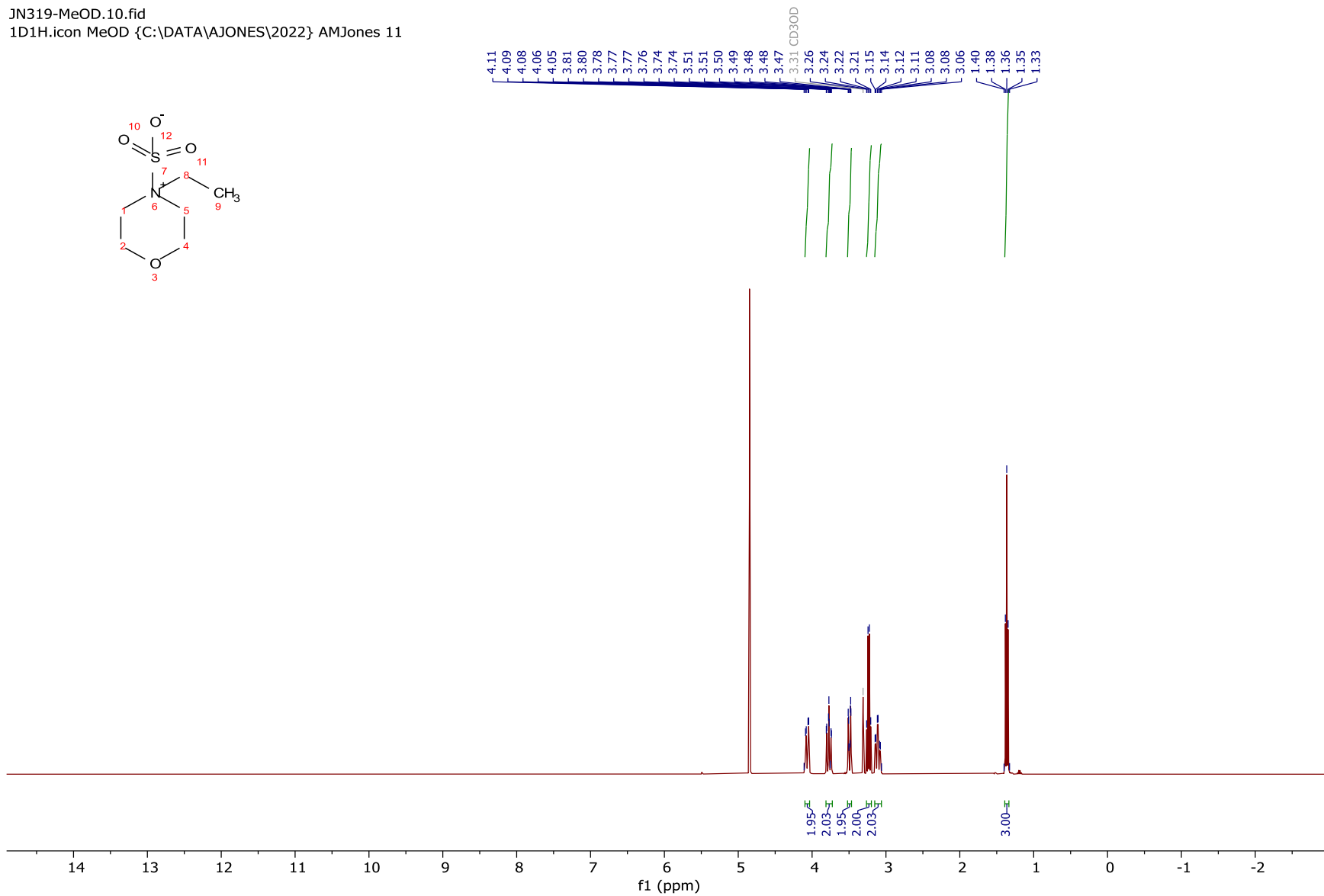
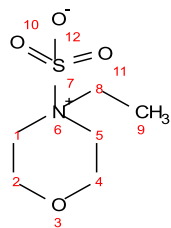


^{13}C NMR spectrum of **120** (101 MHz, $\text{DMSO-}d_6$)



¹H NMR spectrum of **119** (300 MHz, MeOD)

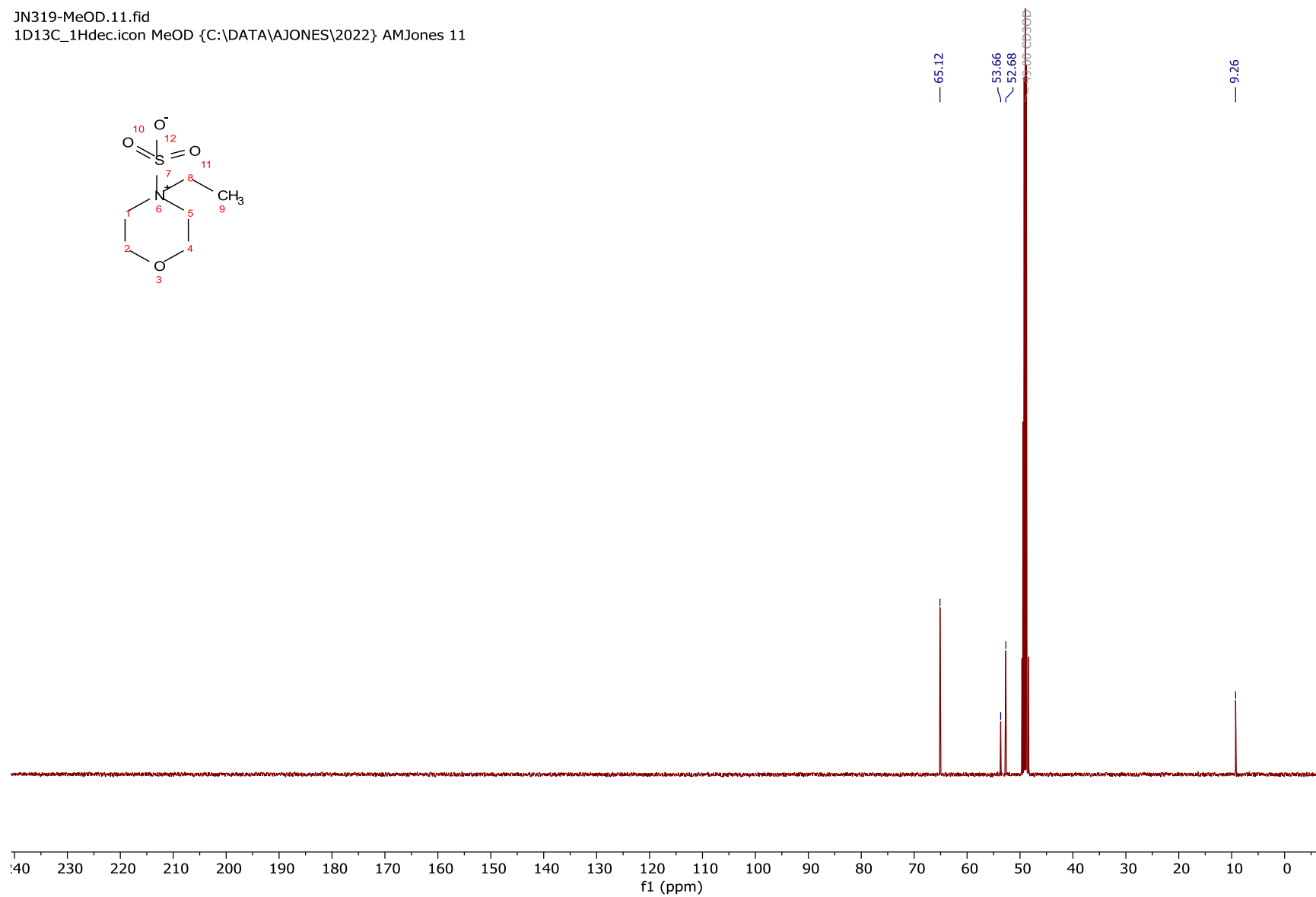
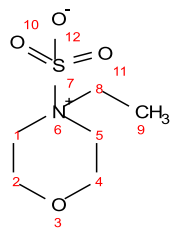
JN319-MeOD.10.fid
1D1H.icon MeOD {C:\DATA\AJONES\2022} AMJones 11



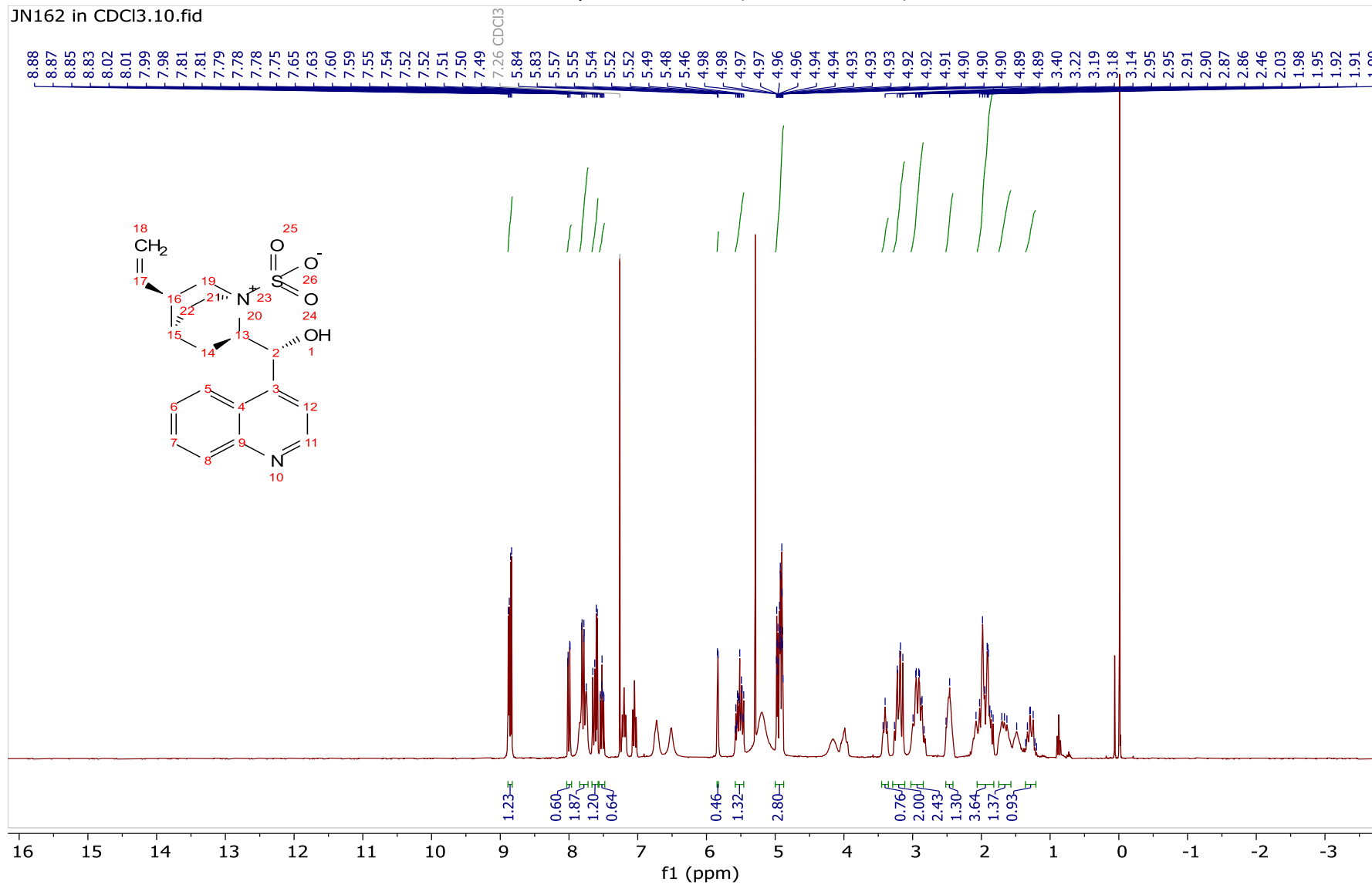
¹³C NMR spectrum of **119** (101 MHz, MeOD)

JN319-MeOD.11.fid

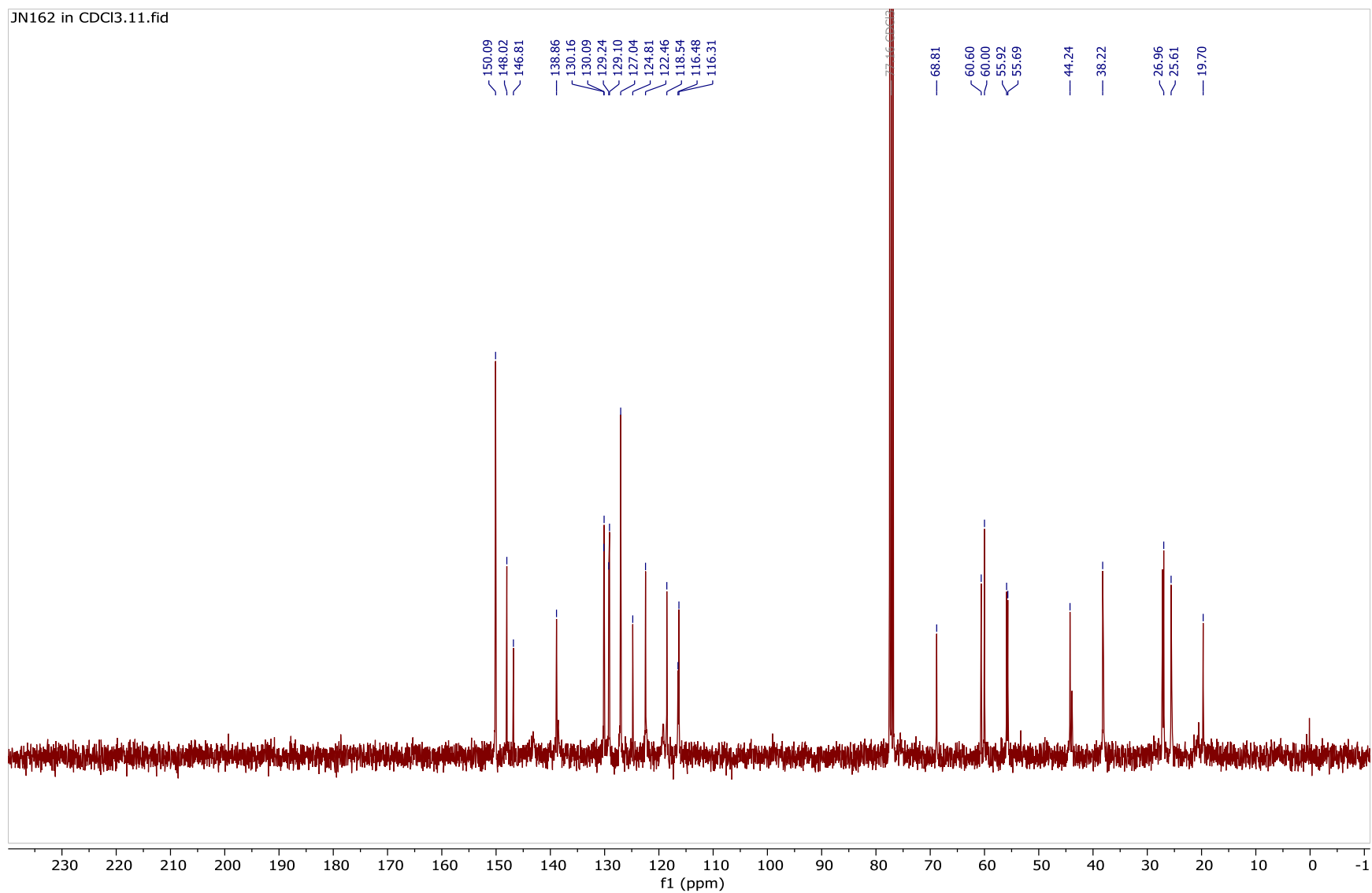
1D13C_1Hdec.icon MeOD {C:\DATA\AJONES\2022} AMJones 11



¹H NMR spectrum of **122** (300 MHz, CDCl₃)

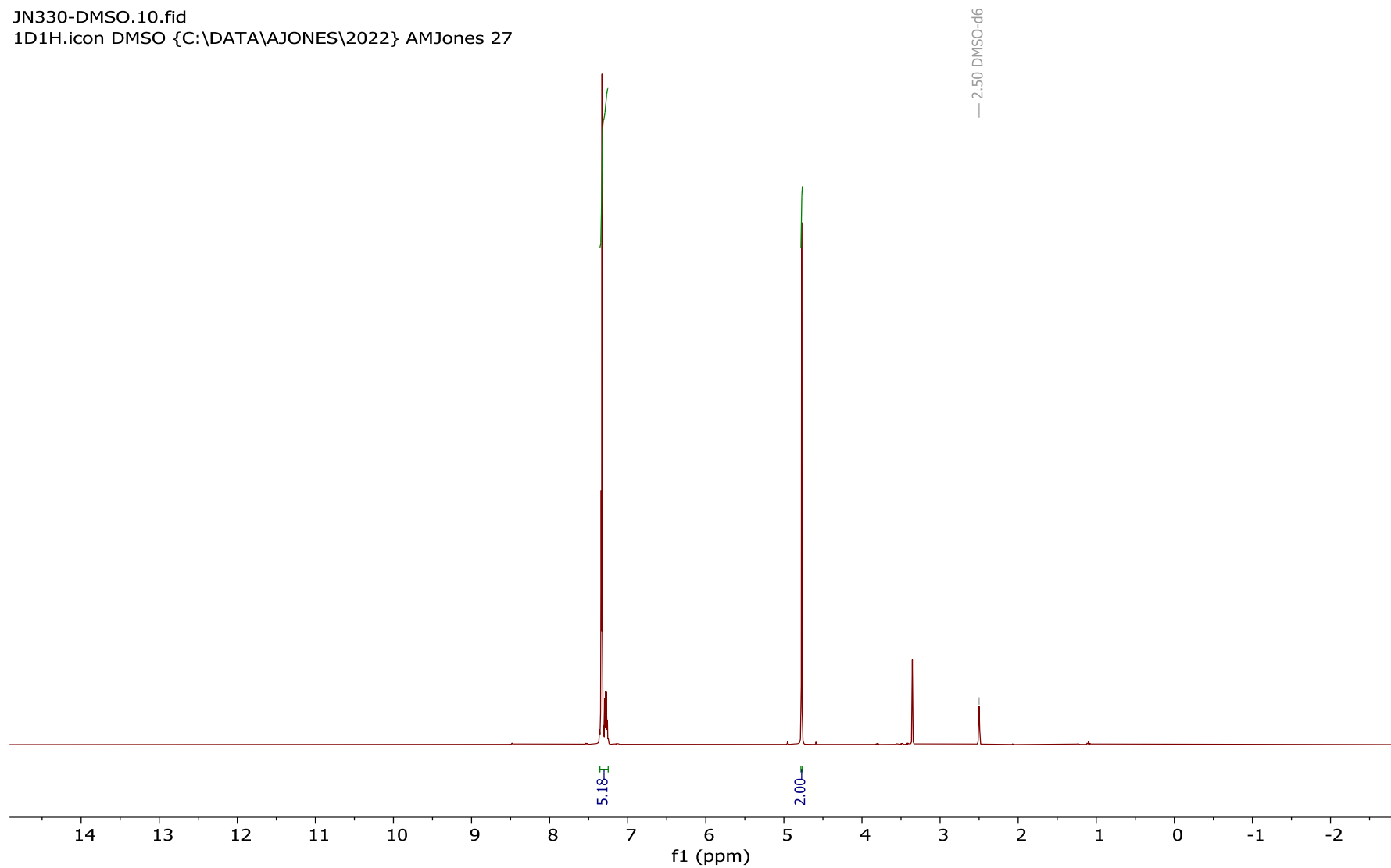


^{13}C NMR spectrum of **122** (101 MHz, CDCl_3)



¹H NMR spectrum of **105** (300 MHz, DMSO-*d*₆)

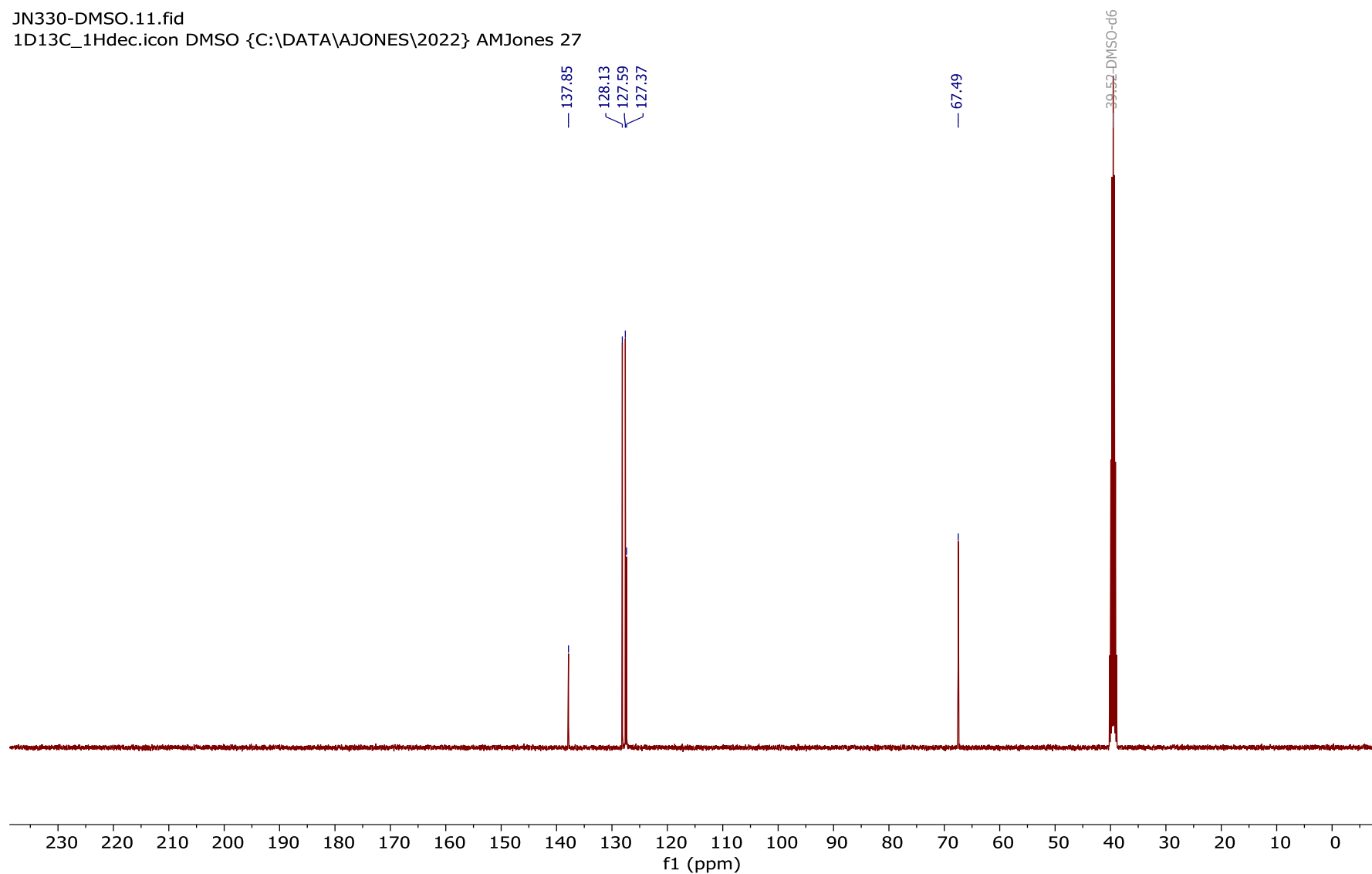
JN330-DMSO.10.fid
1D1H.icon DMSO {C:\DATA\AJONES\2022} AMJones 27



¹³C NMR spectrum of **105** (101 MHz, DMSO-*d*₆)

JN330-DMSO.11.fid

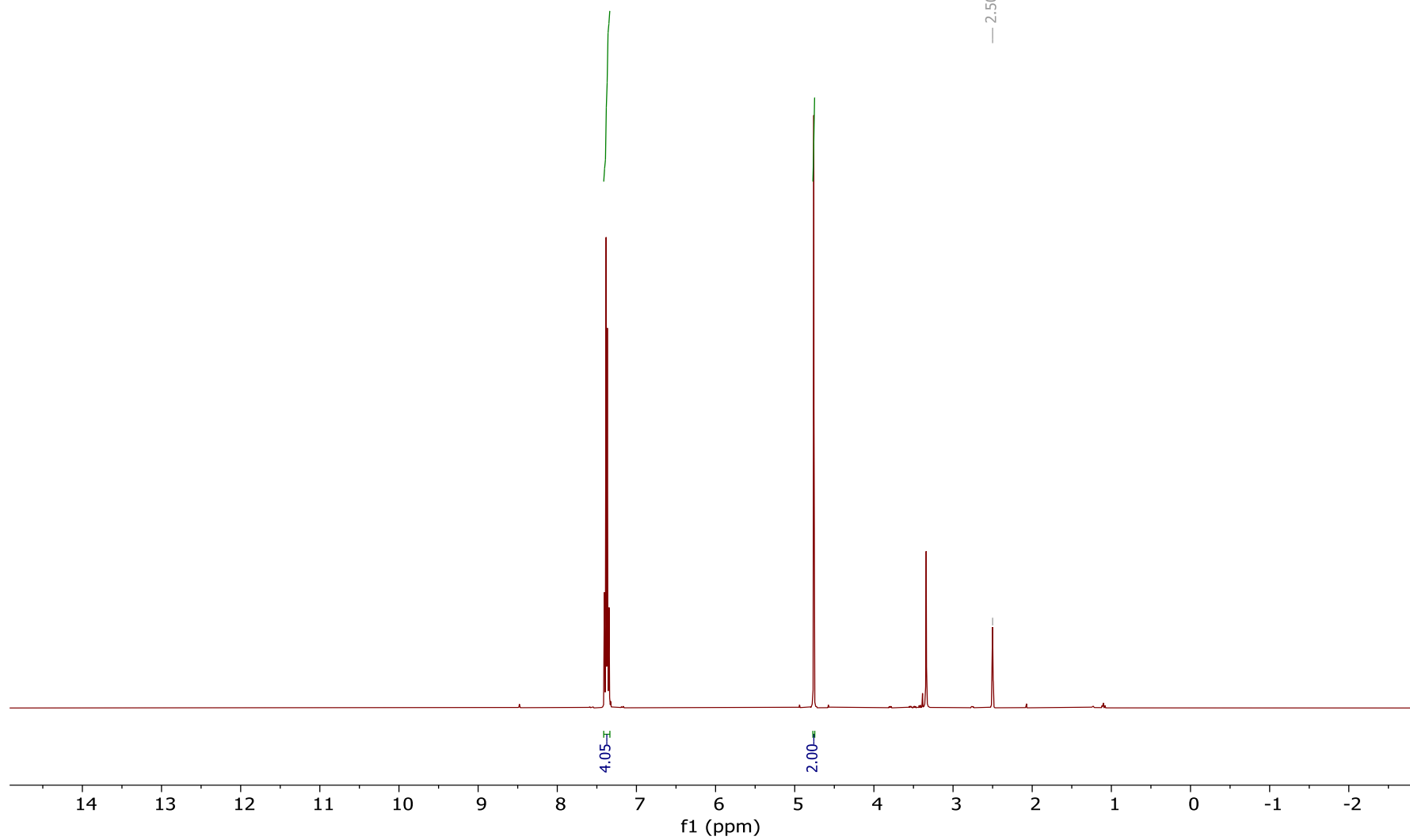
1D13C_1Hdec.icon DMSO {C:\DATA\AJONES\2022} AMJones 27



^1H NMR spectrum of **157** (300 MHz, $\text{DMSO-}d_6$)

JN331-crude-DMSO.10.fid

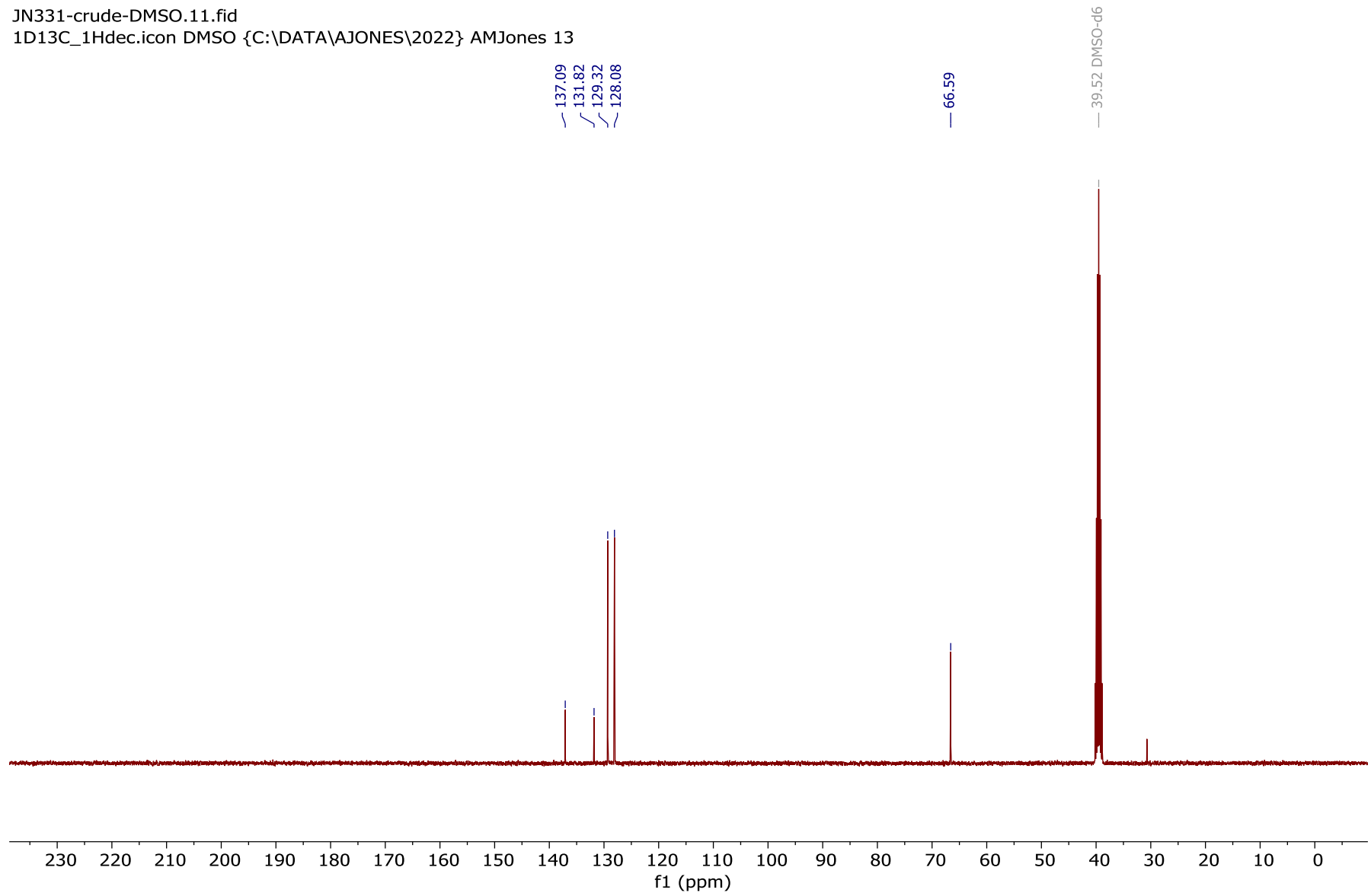
1D1H.icon DMSO {C:\DATA\AJONES\2022} AMJones 13



¹³C NMR spectrum of **157** (101 MHz, DMSO-*d*₆)

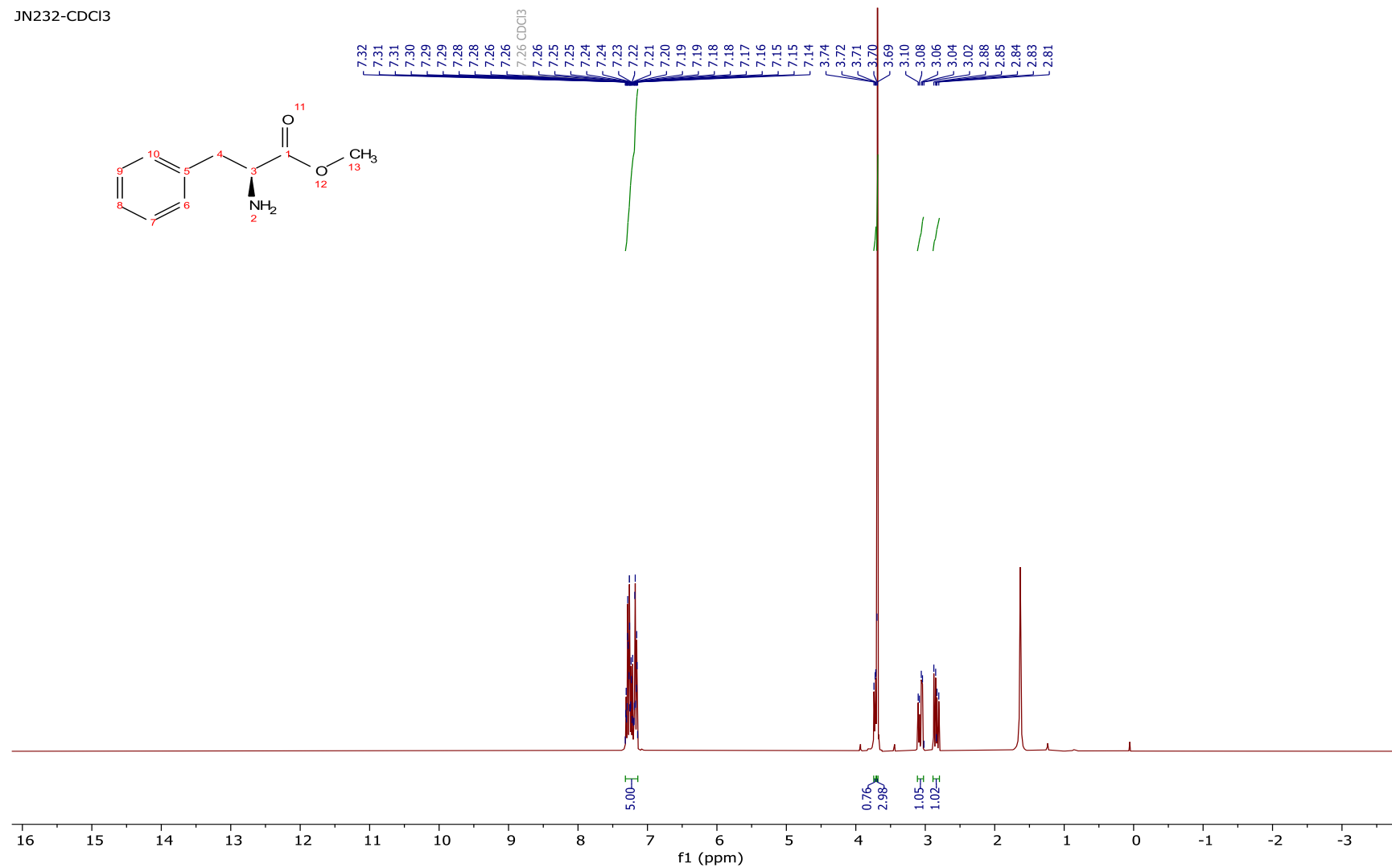
JN331-crude-DMSO.11.fid

1D13C_1Hdec.icon DMSO {C:\DATA\AJONES\2022} AMJones 13



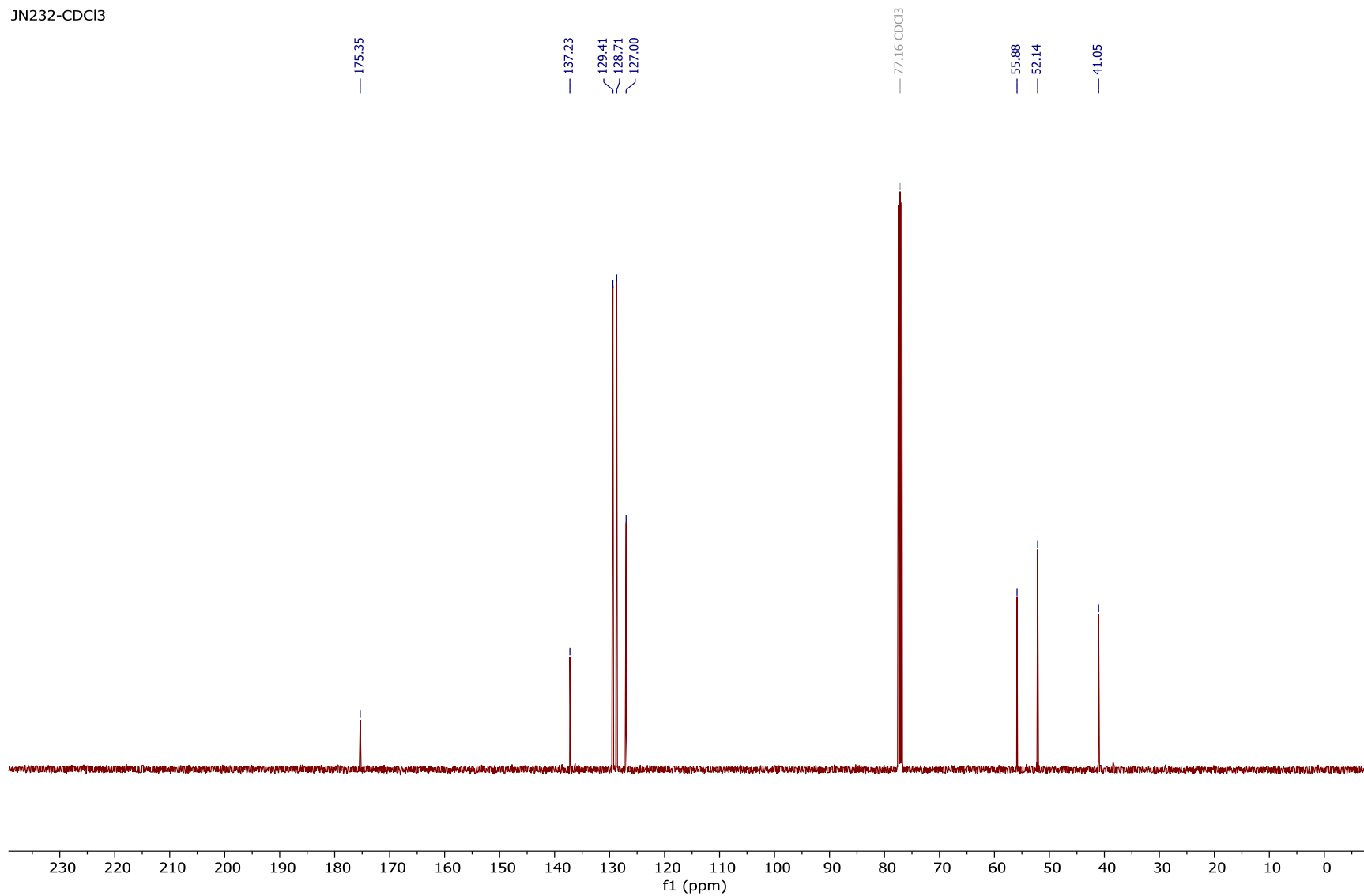
¹H NMR spectrum of **141** (300 MHz, CDCl₃)

JN232-CDCl₃



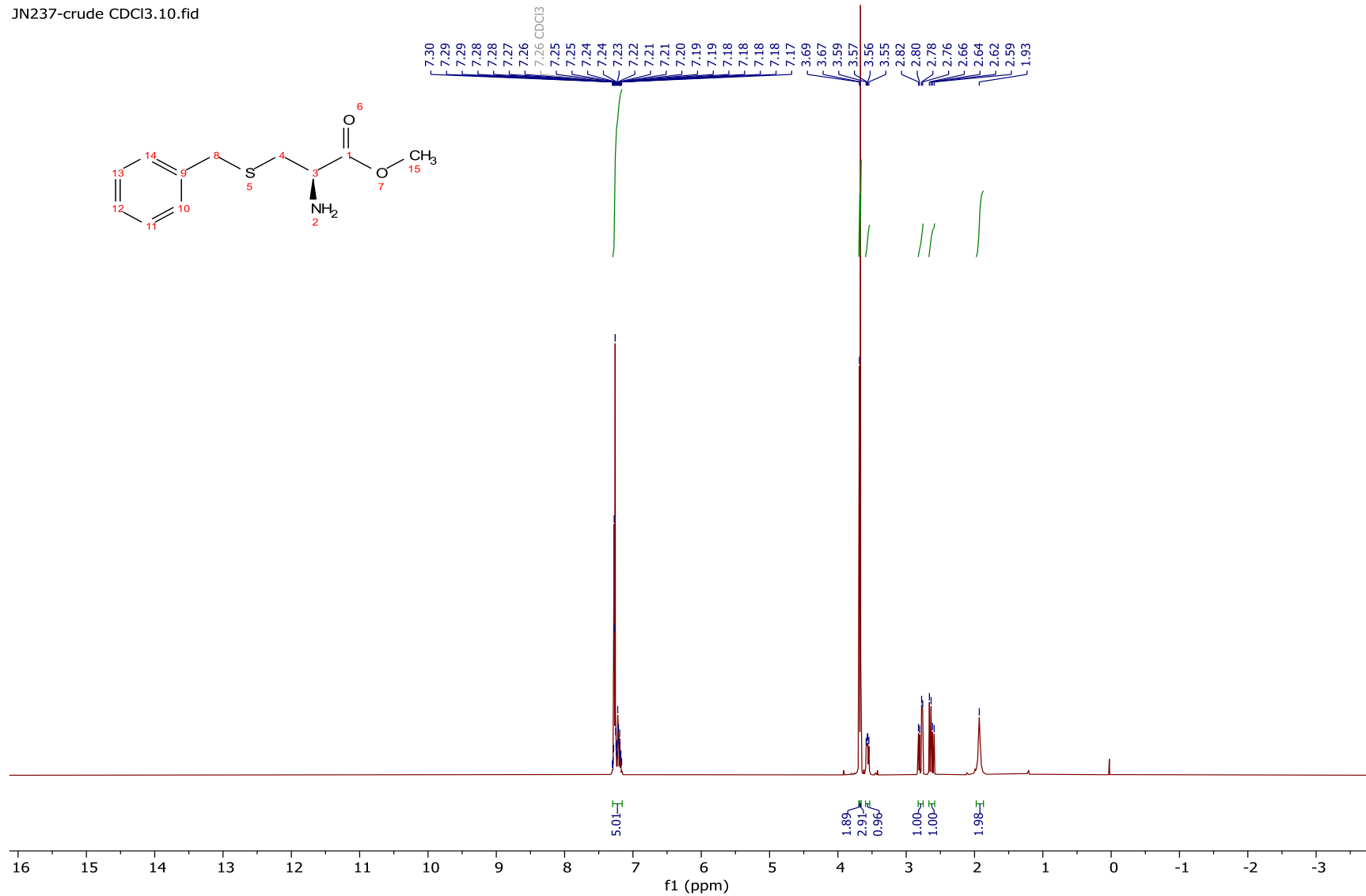
¹³C NMR spectrum of **141** (101 MHz, CDCl₃)

JN232-CDCl₃



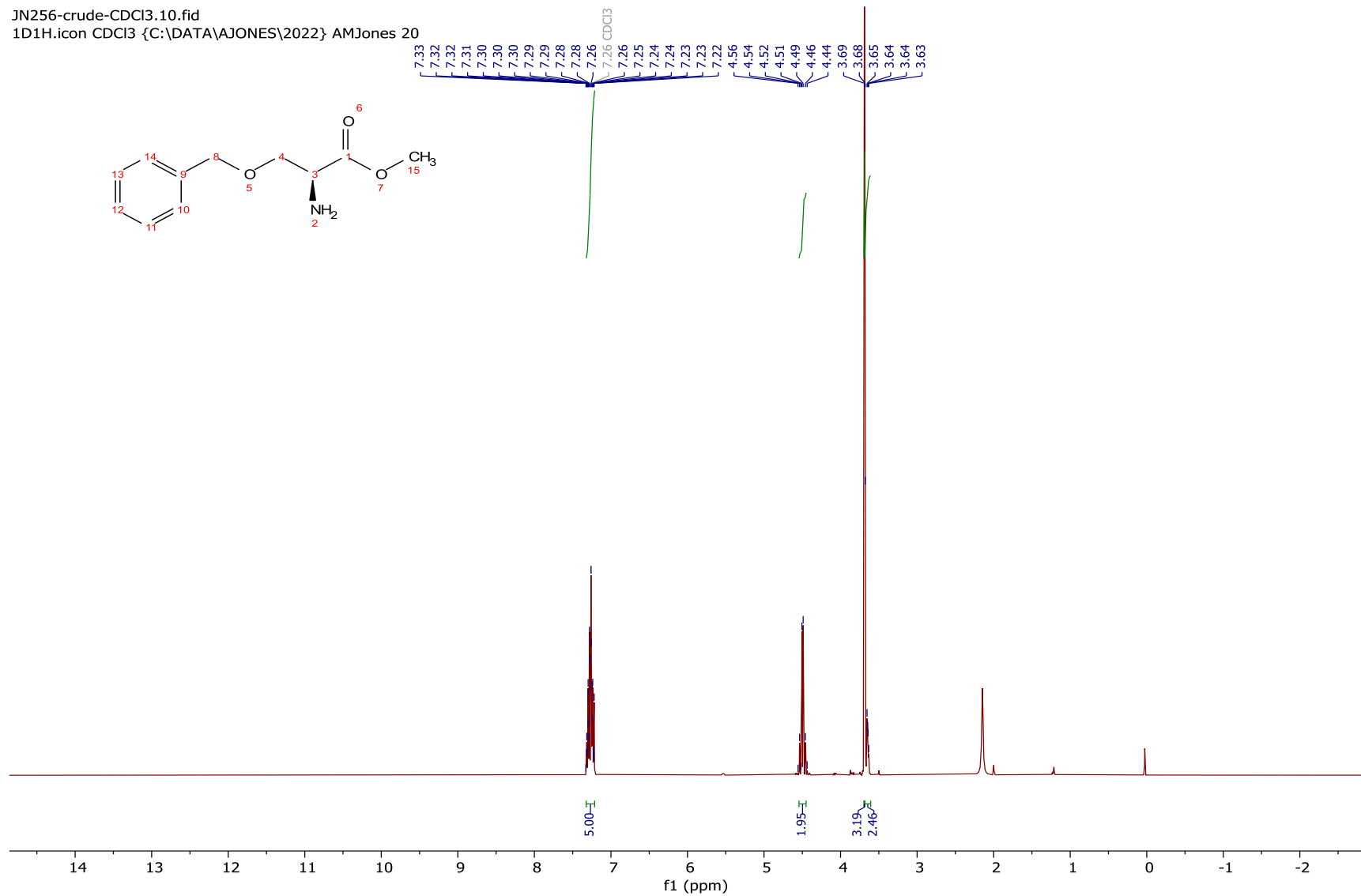
JN237-crude CDCl3.10.fid

¹H NMR spectrum of **144** (300 MHz, CDCl₃)



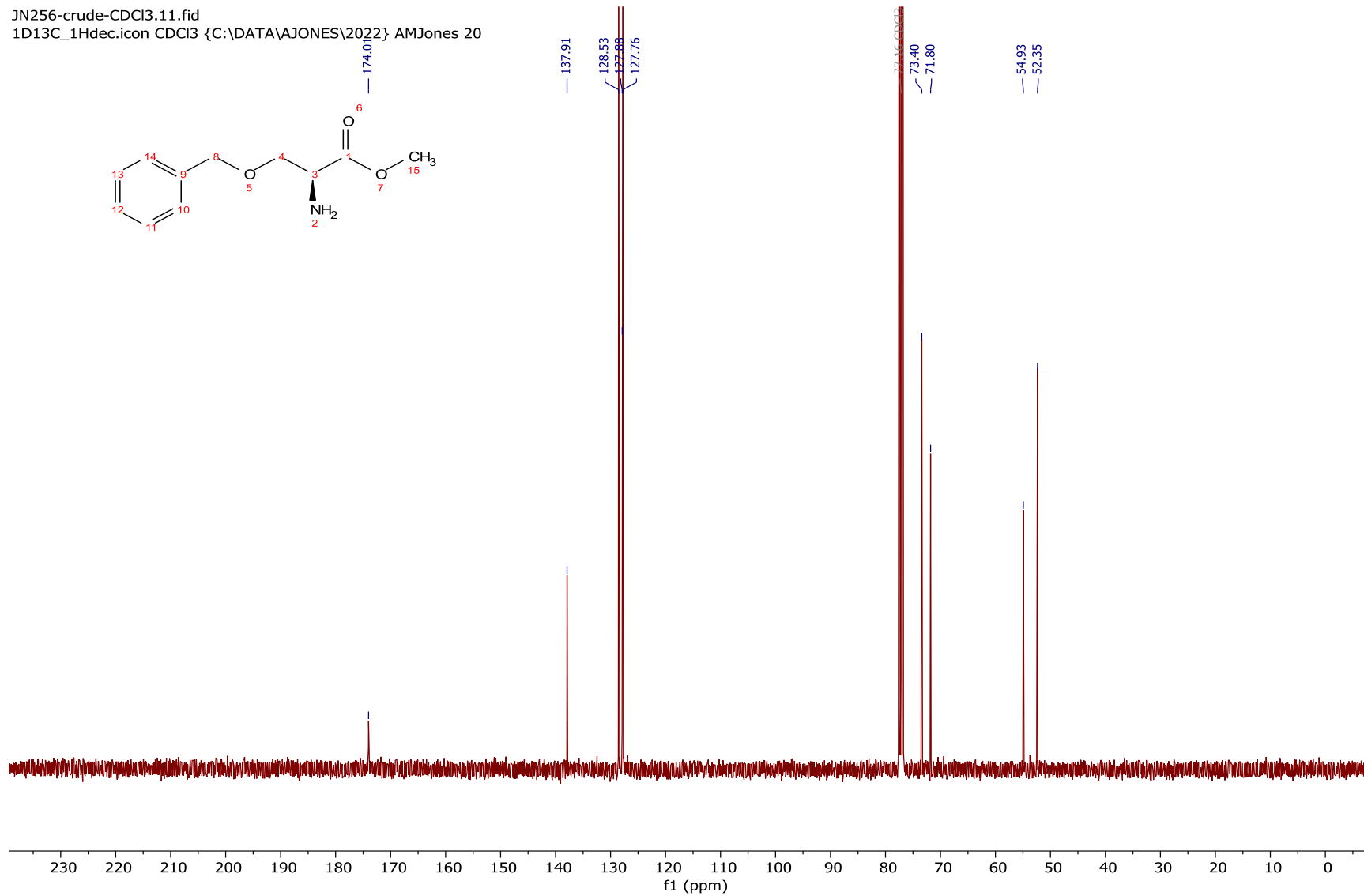
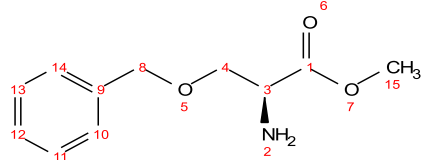
¹H NMR of **147** (300 MHz, CDCl₃)

JN256-crude-CDCl3.10.fid
1D1H.icon CDCl3 {C:\DATA\AJONES\2022} AMJones 20



¹³C NMR of **147** (101 MHz, CDCl₃)

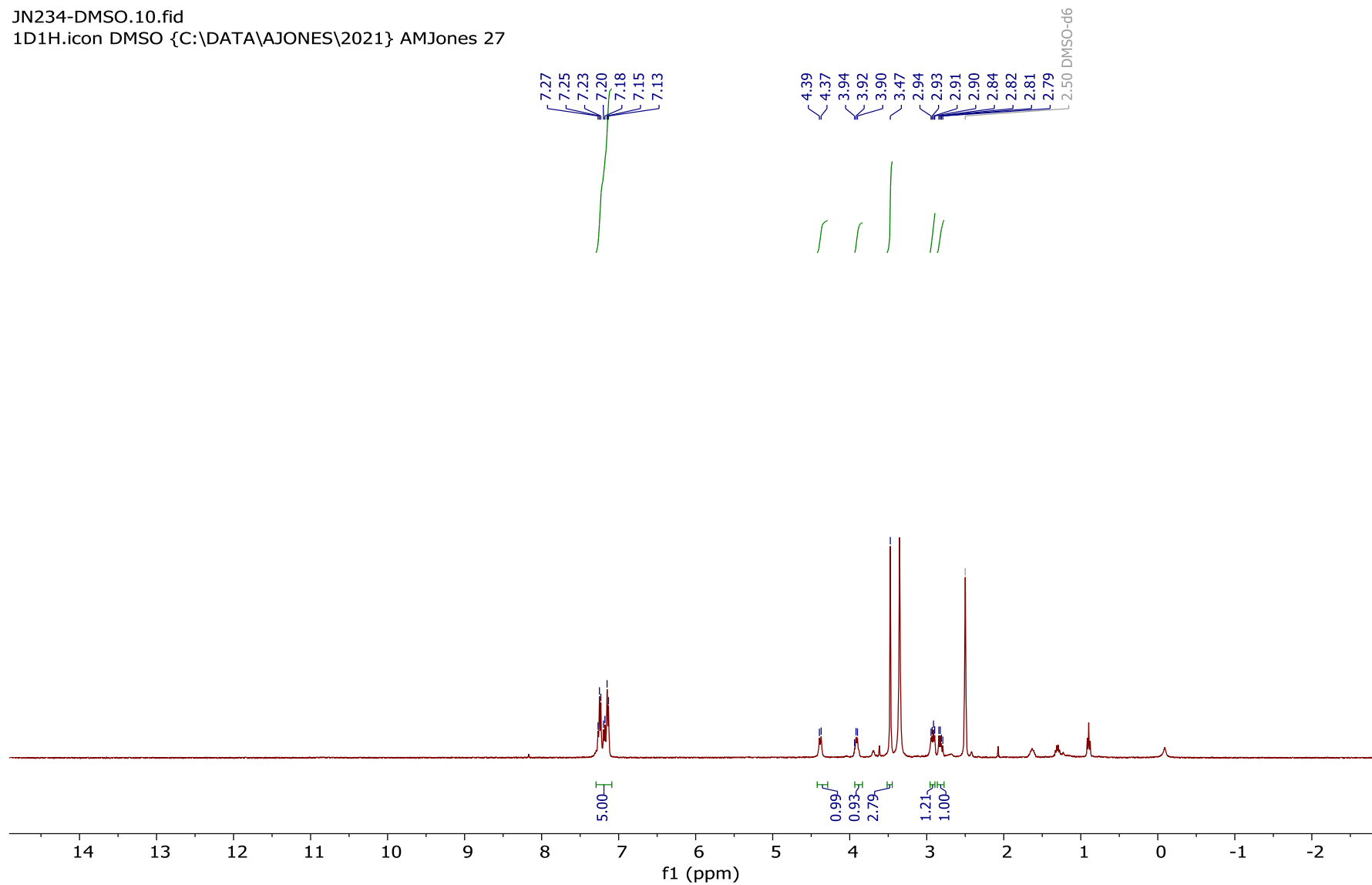
JN256-crude-CDCl3.11.fid
1D13C_1Hdec.icon CDCl3 {C:\DATA\AJONES\2022} AMJones 20



¹H NMR spectrum of **143** (400 MHz, DMSO-*d*₆)

JN234-DMSO.10.fid

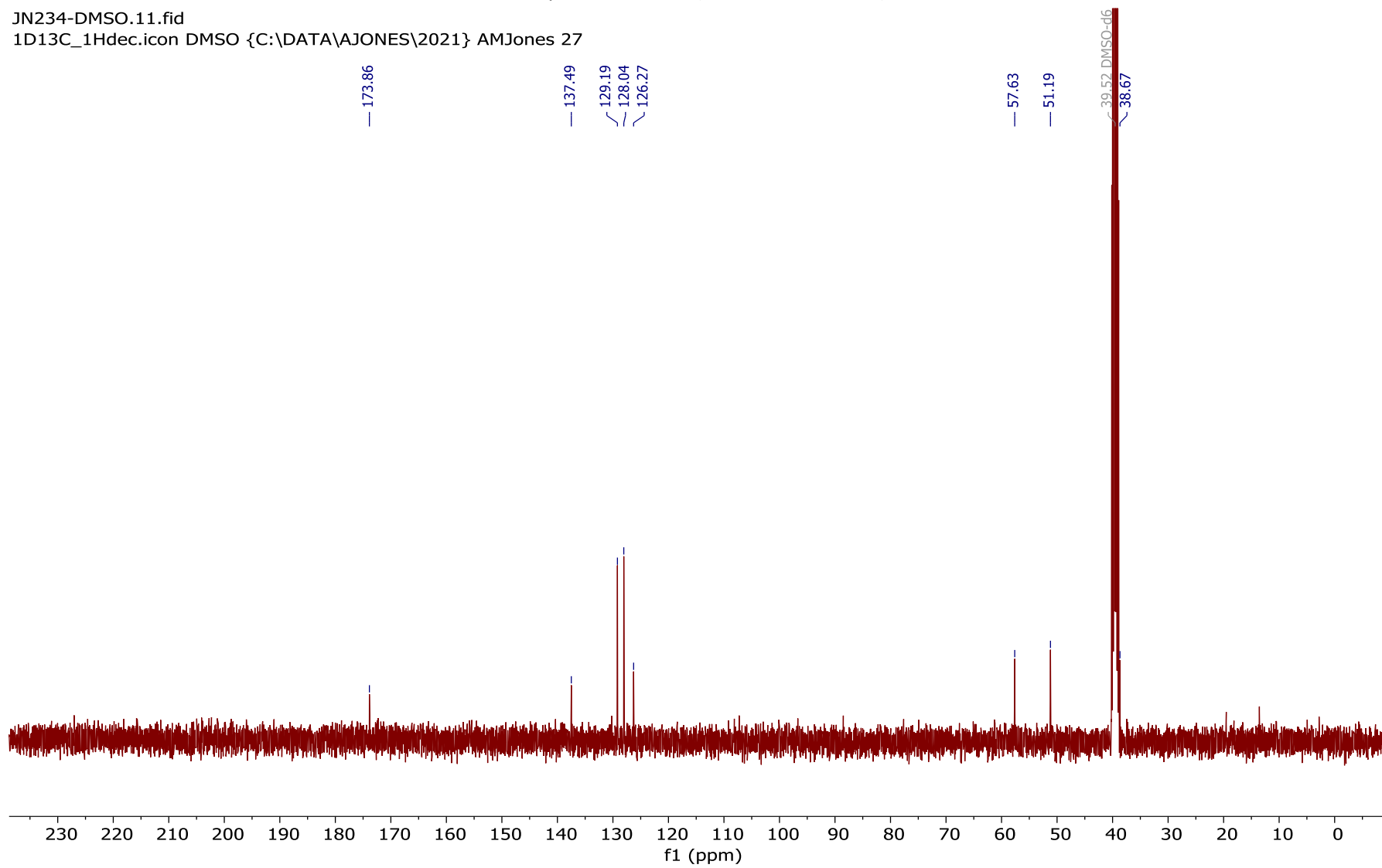
1D1H.icon DMSO {C:\DATA\AJONES\2021} AMJones 27



¹³C NMR spectrum of **143** (101 MHz, DMSO-*d*₆)

JN234-DMSO.11.fid

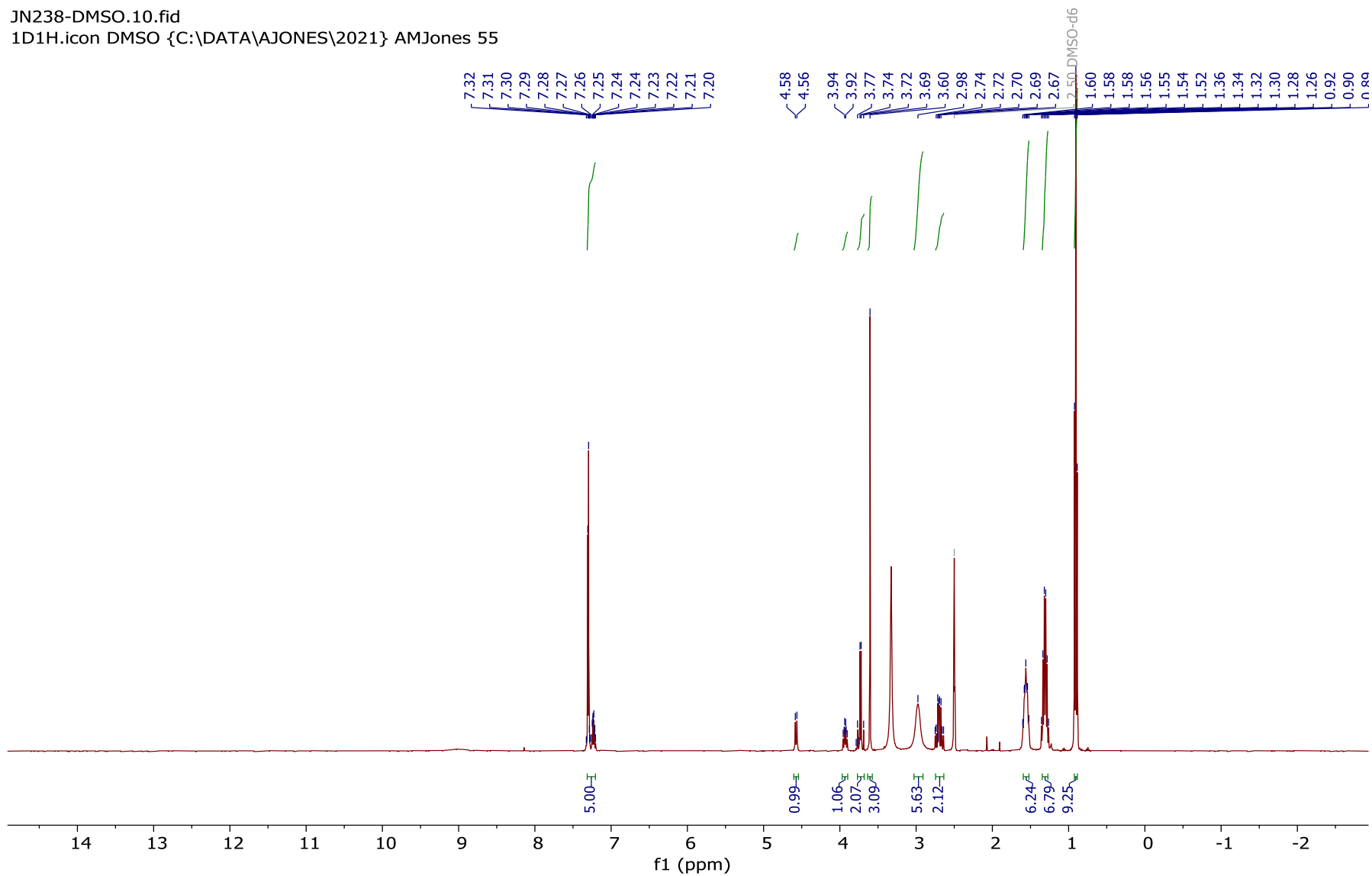
1D13C_1Hdec.icon DMSO {C:\DATA\AJONES\2021} AMJones 27



¹H NMR spectrum of **145** (400 MHz, DMSO-*d*₆)

JN238-DMSO.10.fid

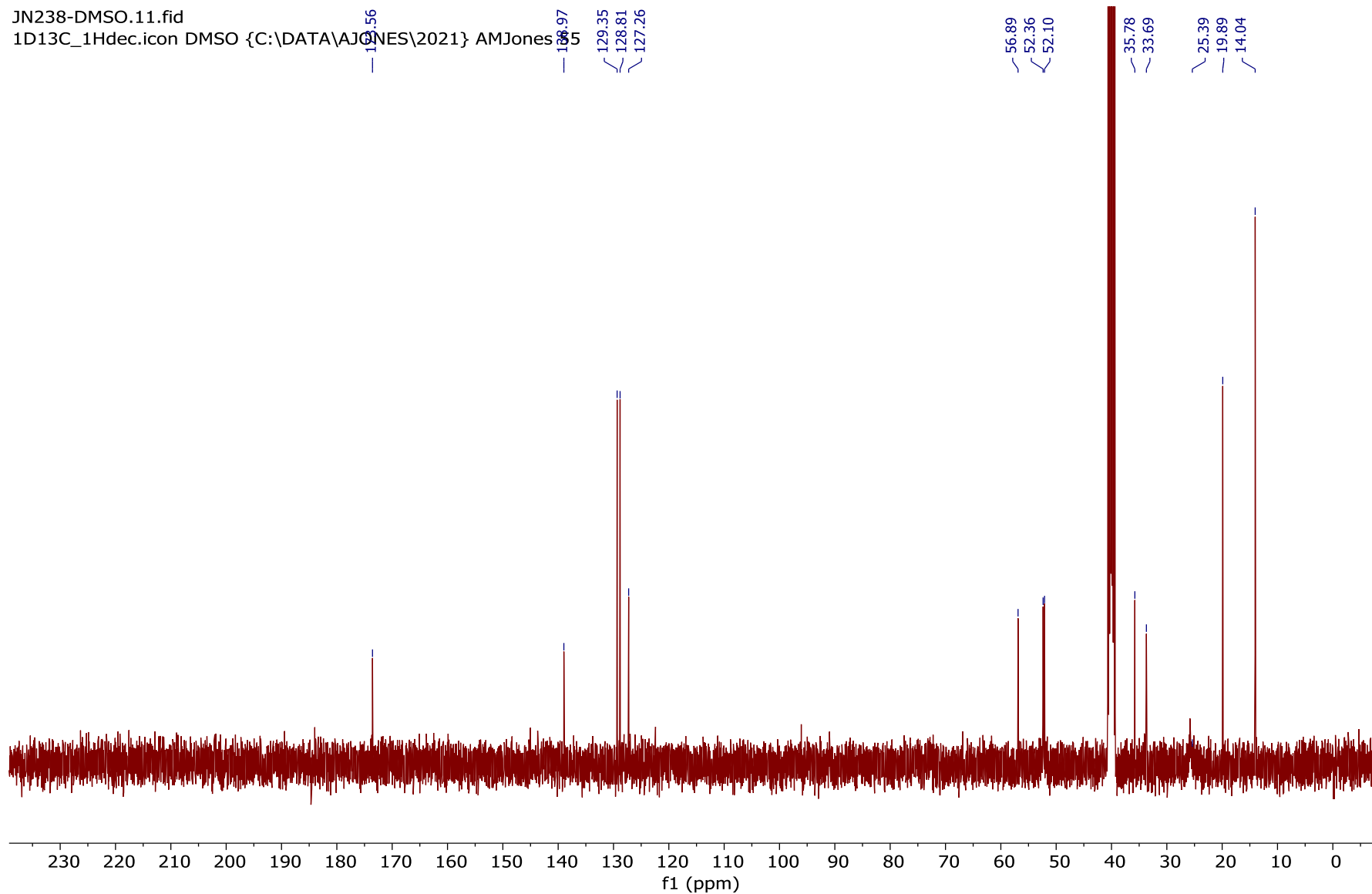
1D1H.icon DMSO {C:\DATA\AJONES\2021} AMJones 55



¹³C NMR spectrum of **145** (101 MHz, DMSO-*d*₆)

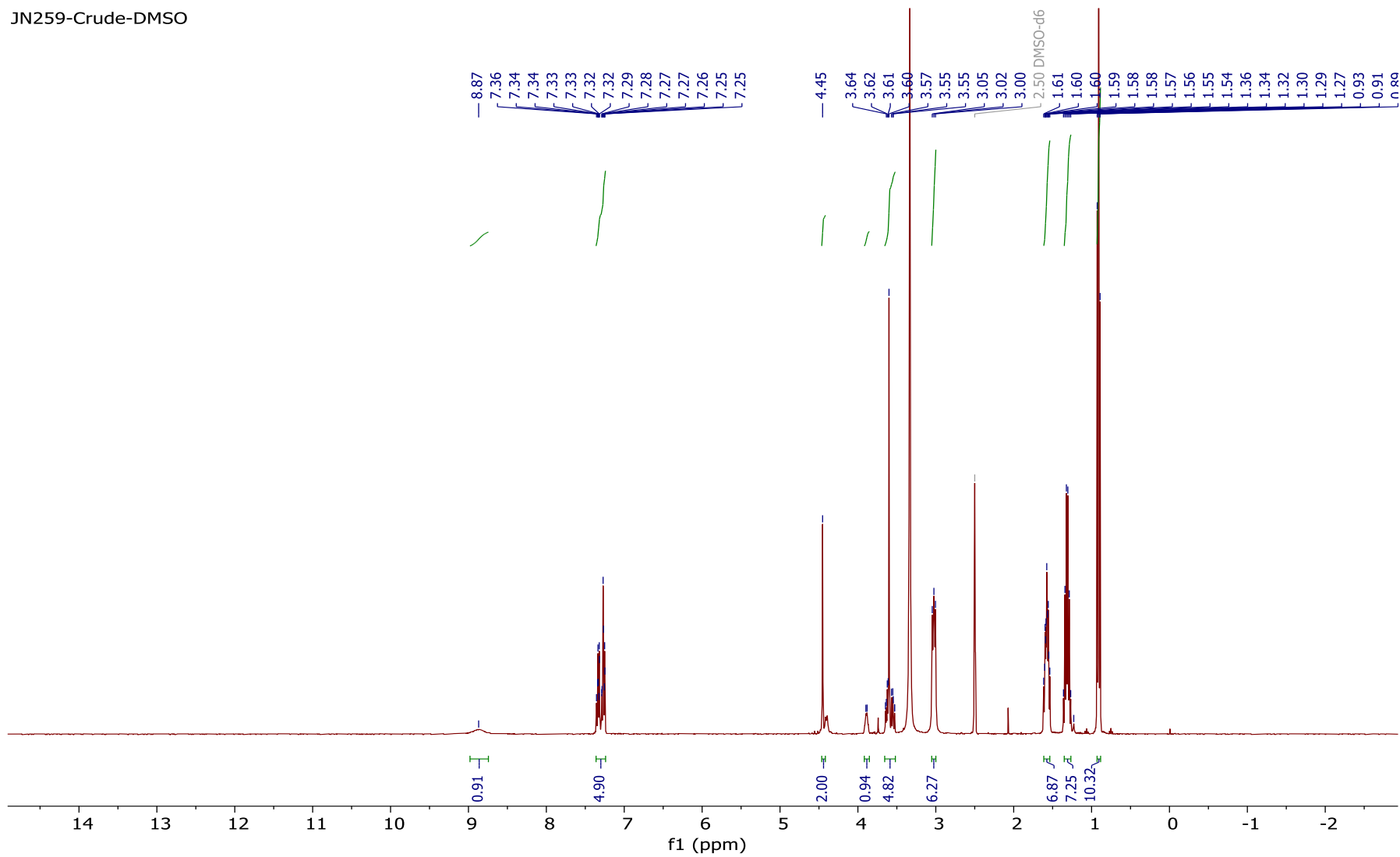
JN238-DMSO.11.fid

1D13C_1Hdec.icon DMSO {C:\DATA\AJONES\2021} AMJones



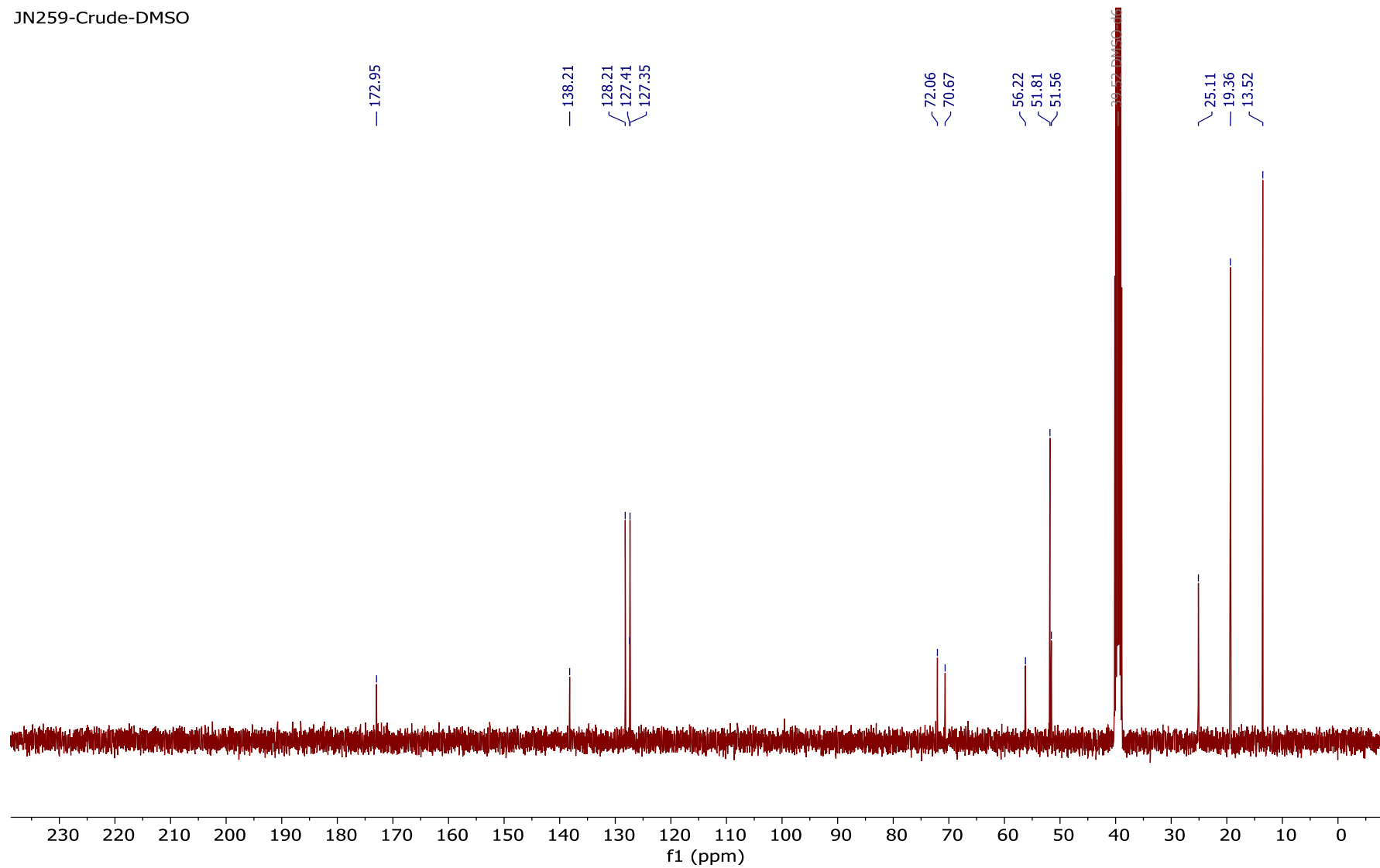
JN259-Crude-DMSO

¹H NMR spectrum of **148** (400 MHz, DMSO-d₆)



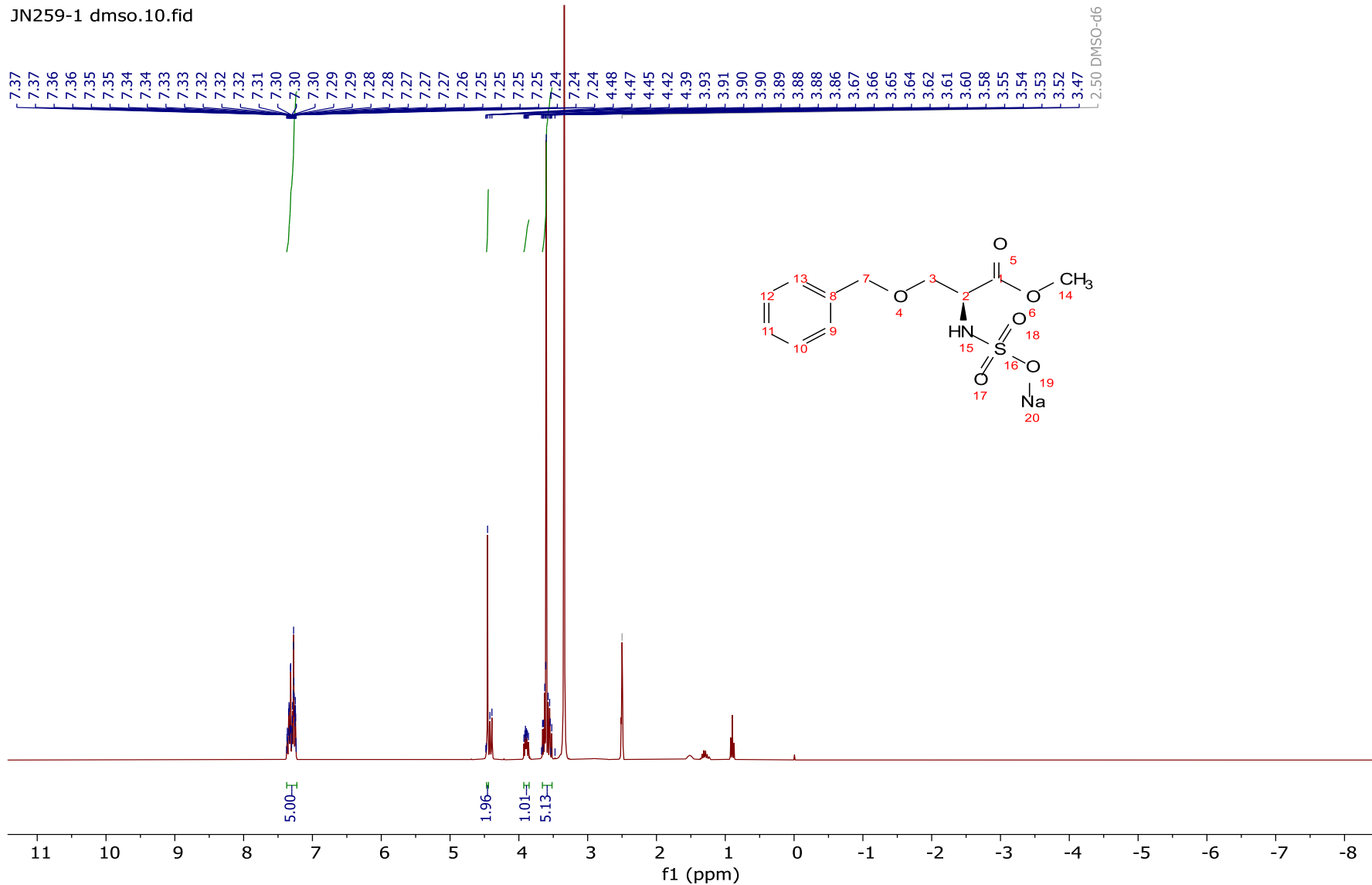
¹³C NMR spectrum of **148** (101 MHz, DMSO-*d*₆)

JN259-Crude-DMSO



¹H NMR spectrum of **149** (300 MHz, DMSO-d₆)

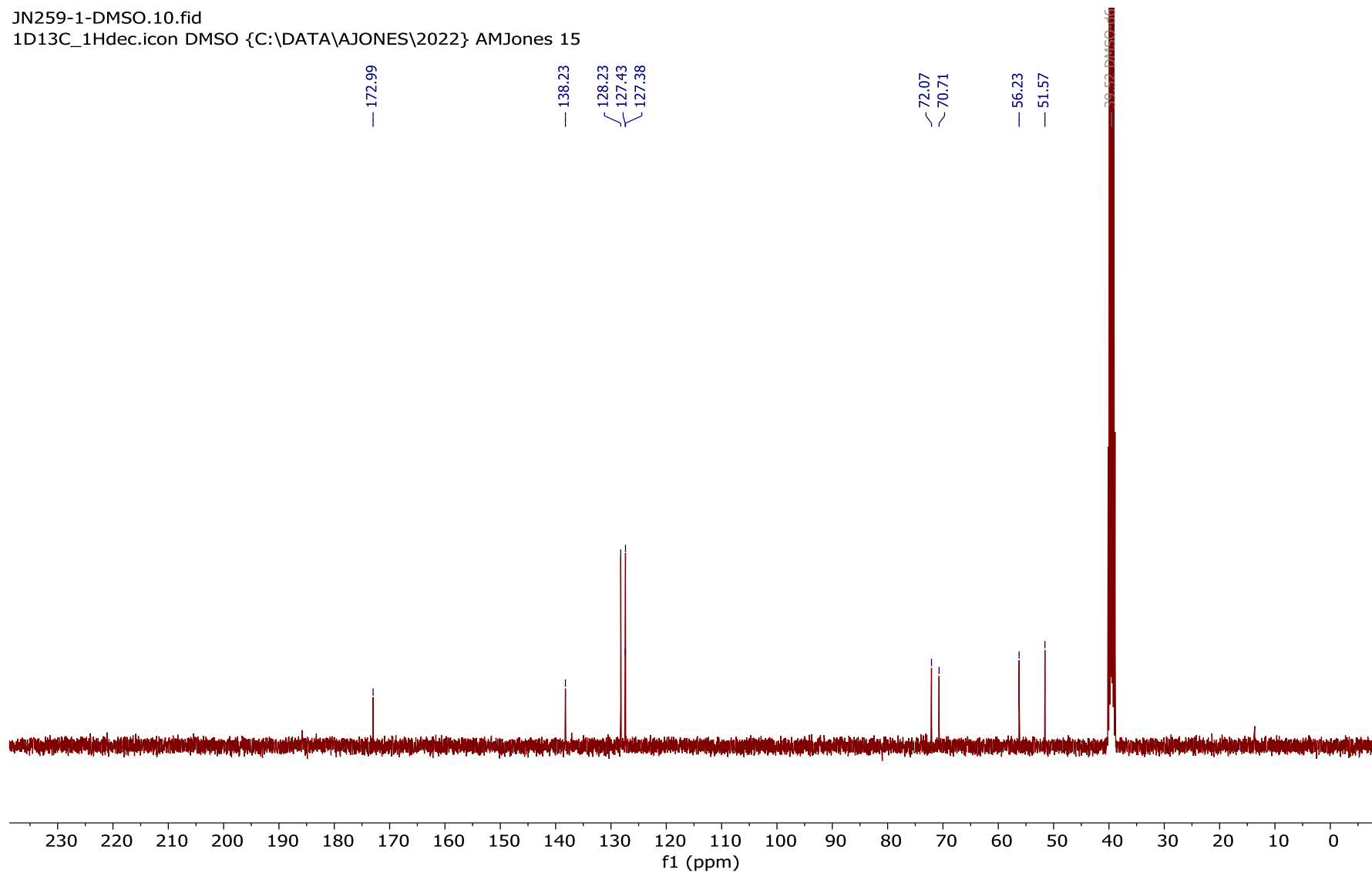
JN259-1 dmso.10.fid



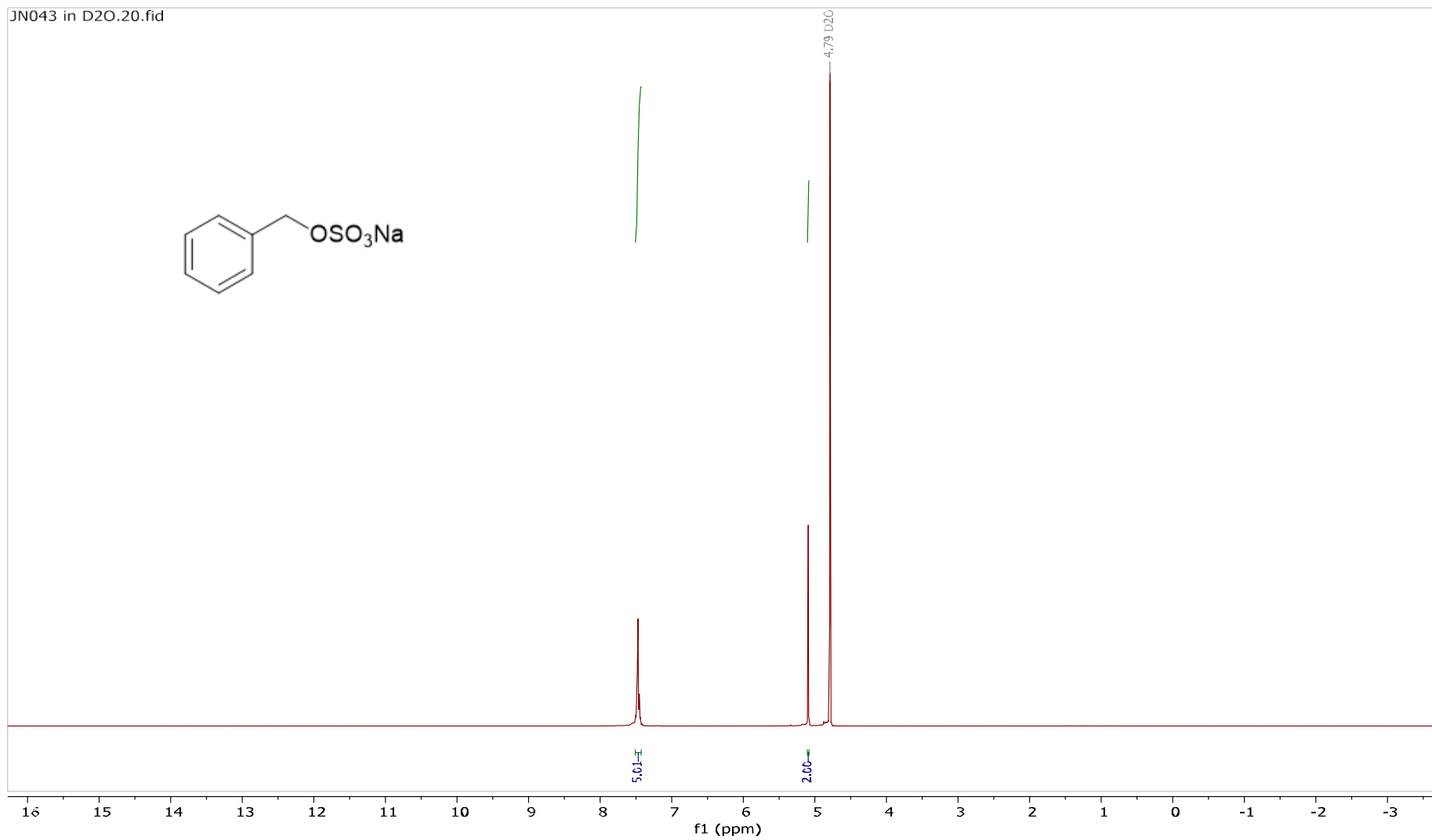
¹³C NMR spectrum of **149** (101 MHz, DMSO-*d*₆)

JN259-1-DMSO.10.fid

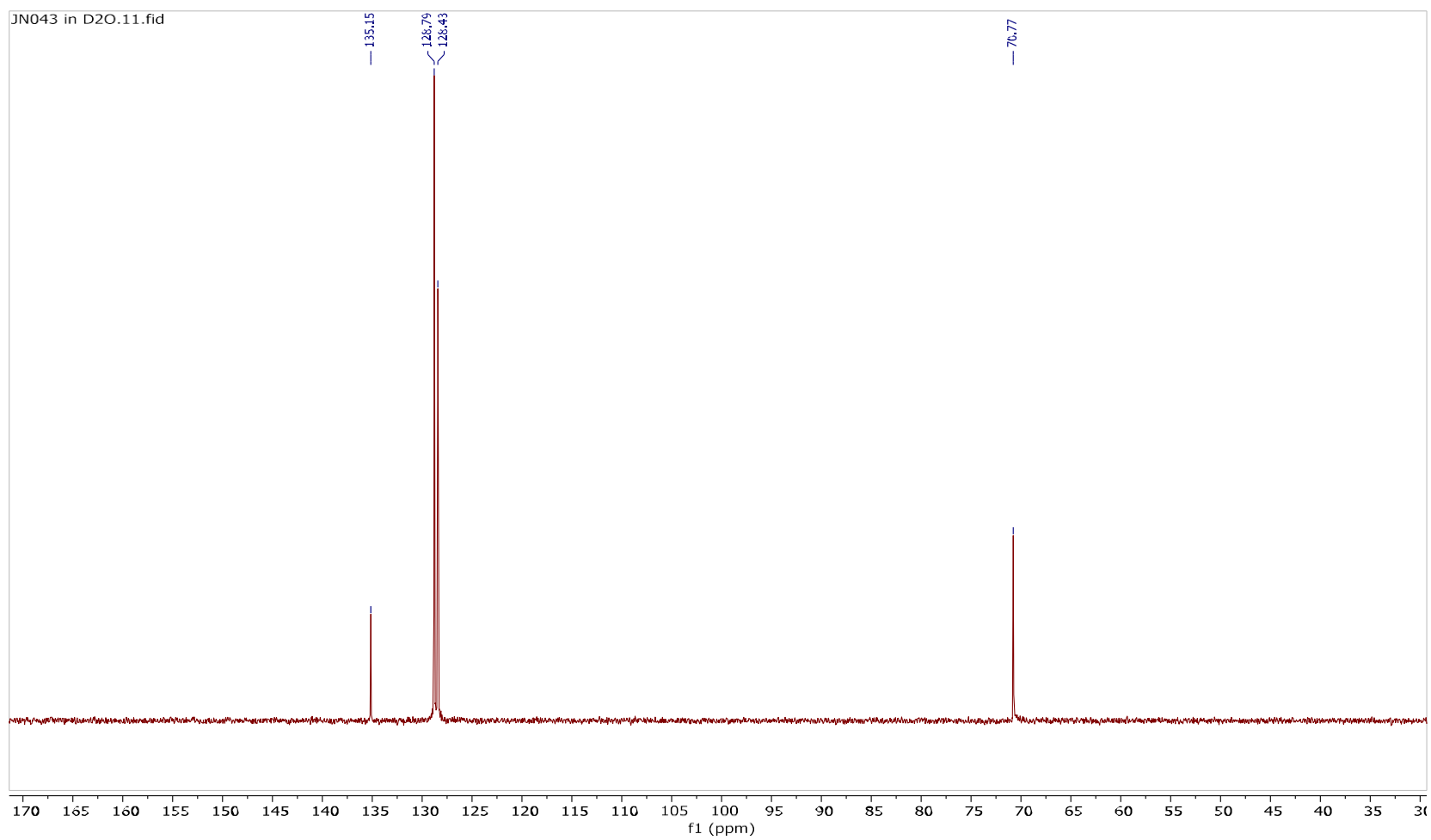
1D13C_1Hdec.icon DMSO {C:\DATA\AJONES\2022} AMJones 15



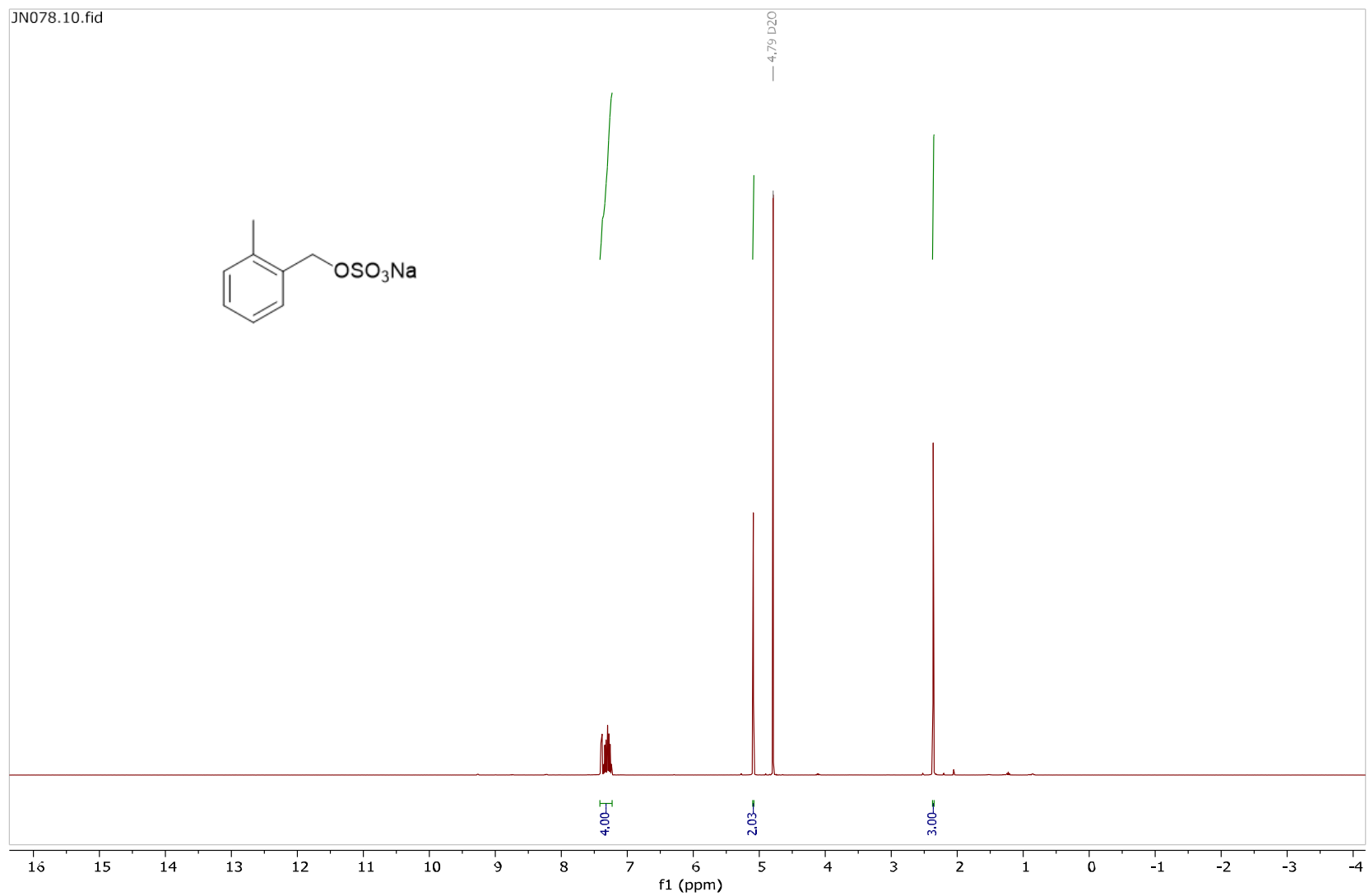
¹H NMR spectrum of **105** (300 MHz, D₂O)



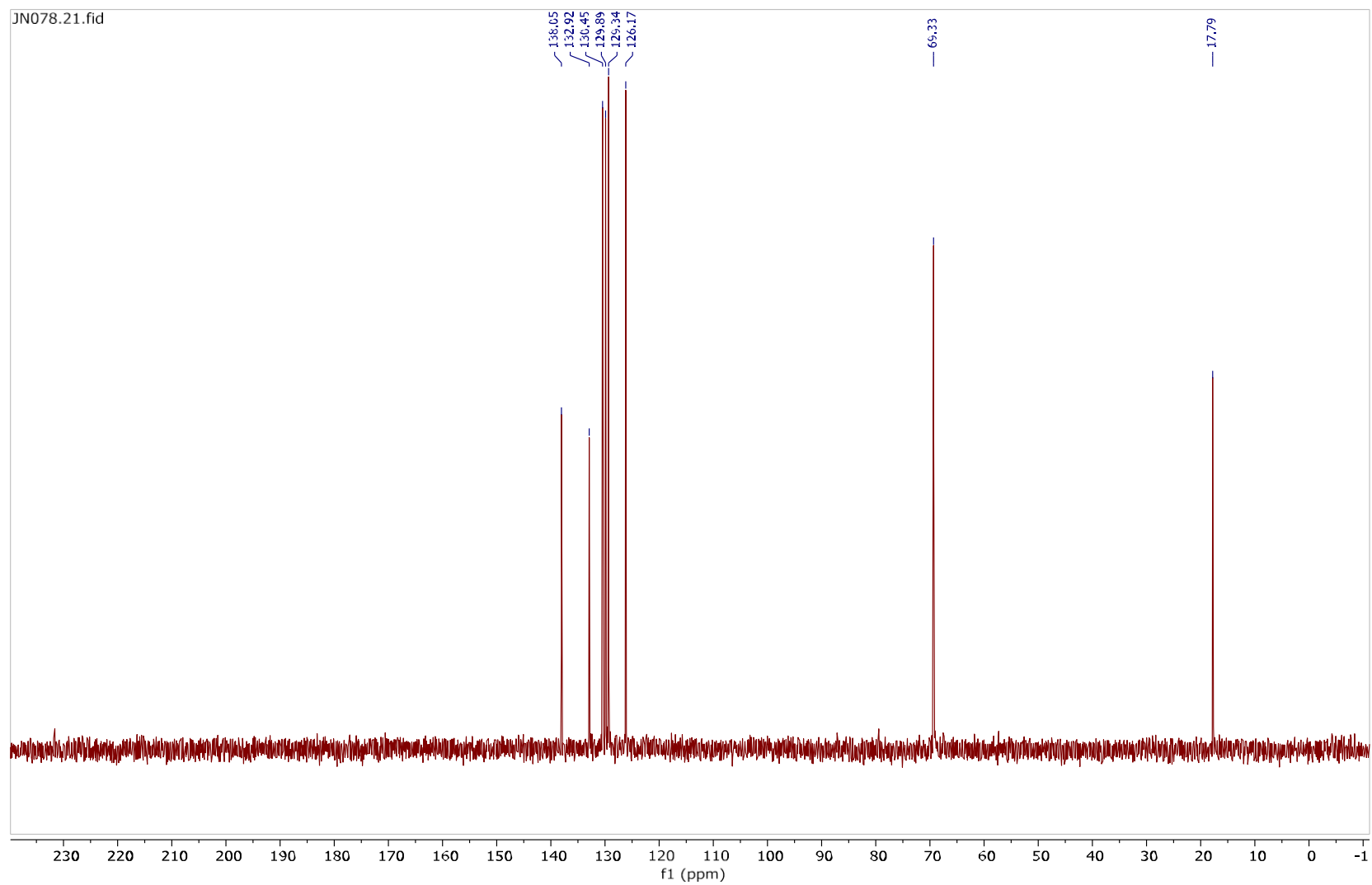
^{13}C NMR spectrum of **105** (400 MHz, D_2O)



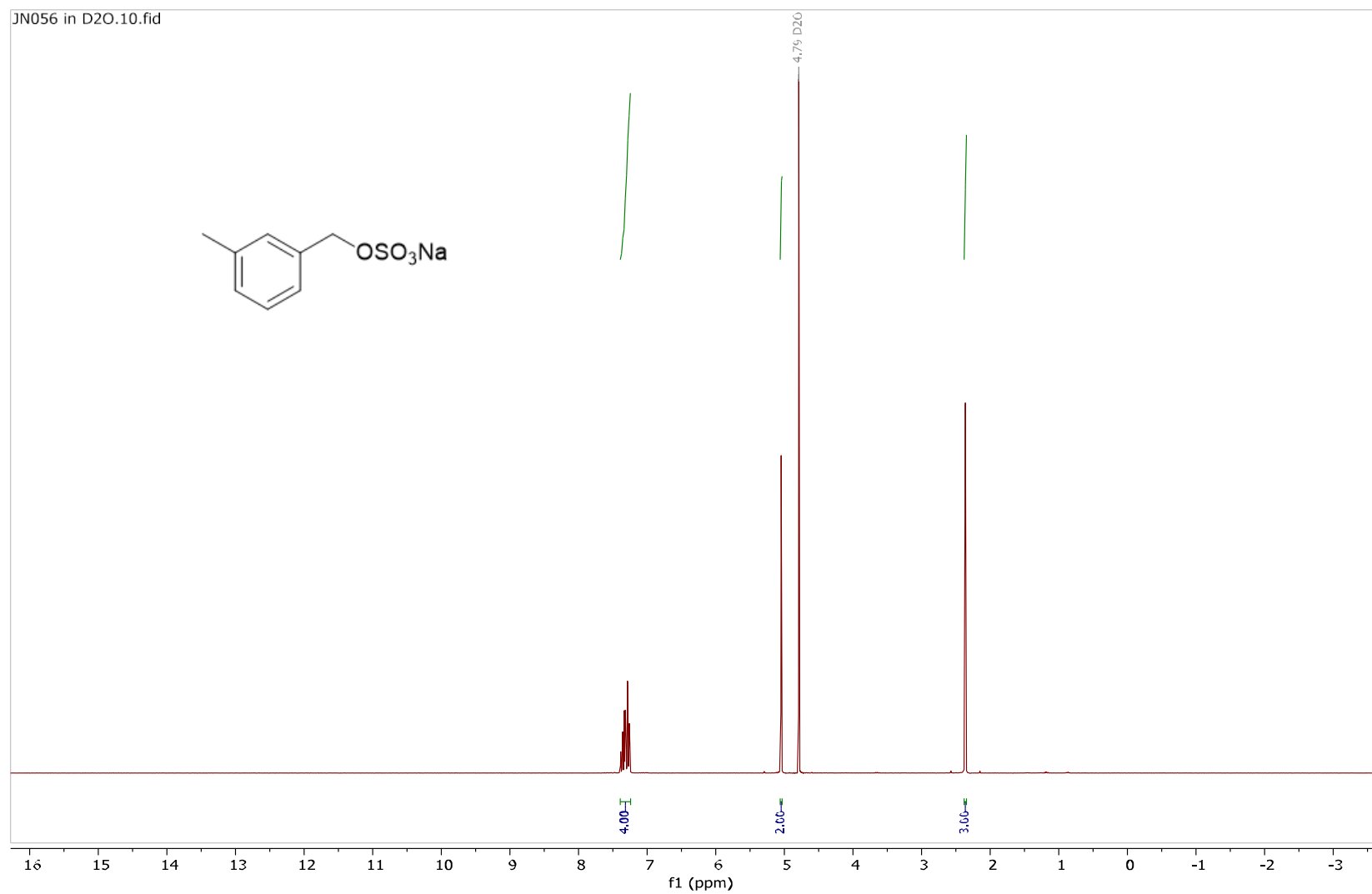
^1H NMR spectrum of **169** (300 MHz, D_2O)



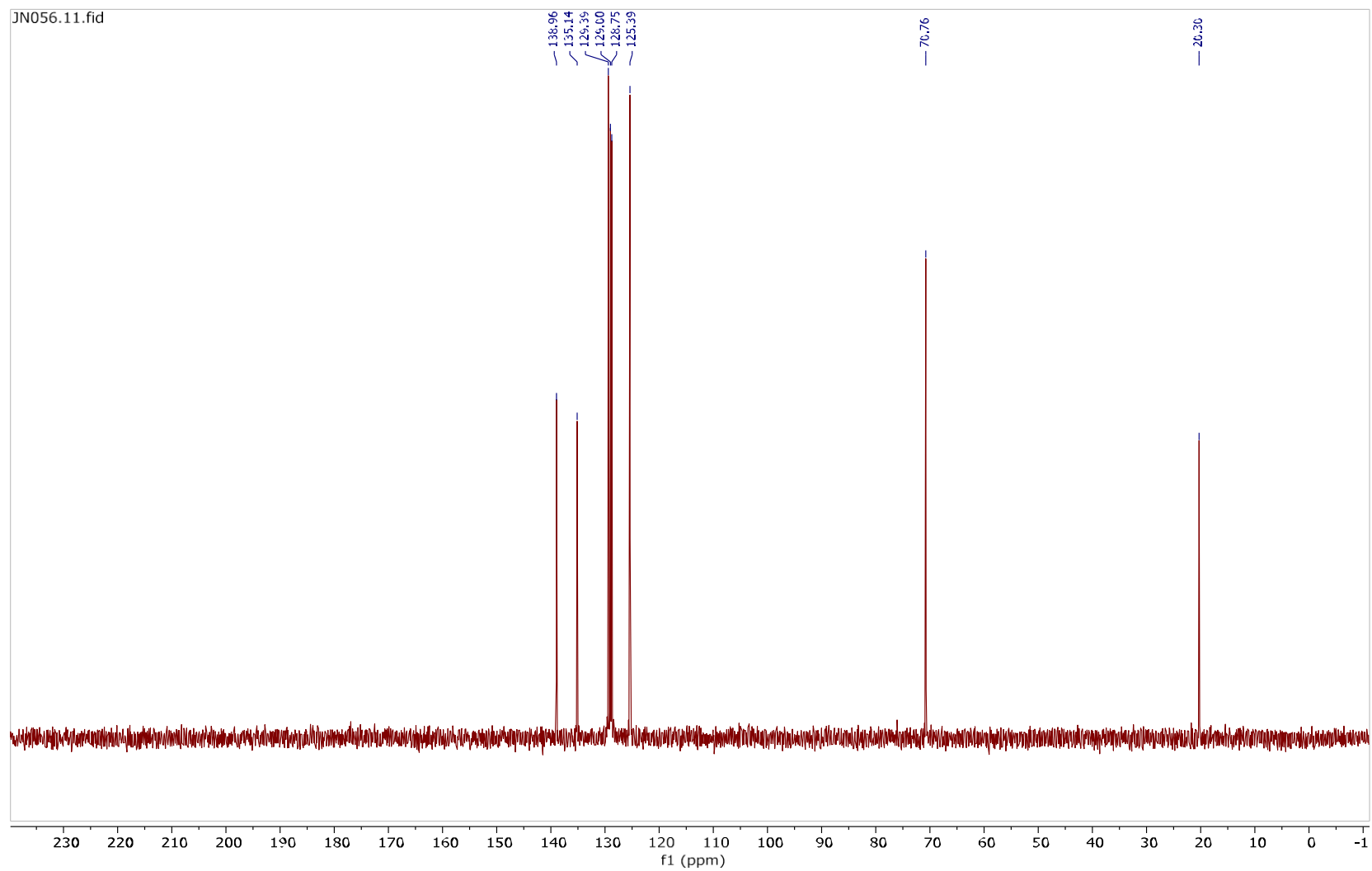
^{13}C NMR spectrum of **169** (101 MHz, D_2O)



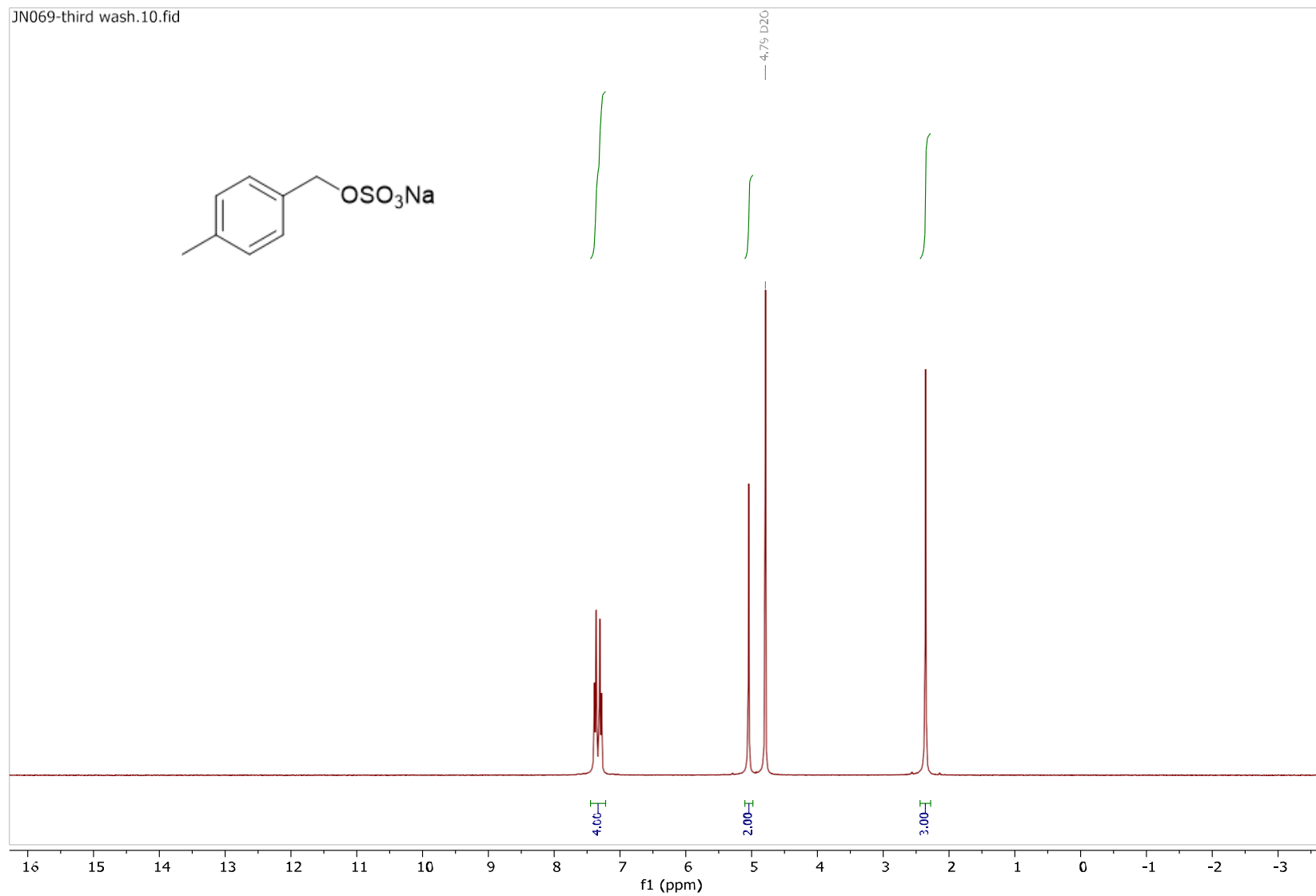
^1H NMR spectrum of **170** (300 MHz, D_2O)



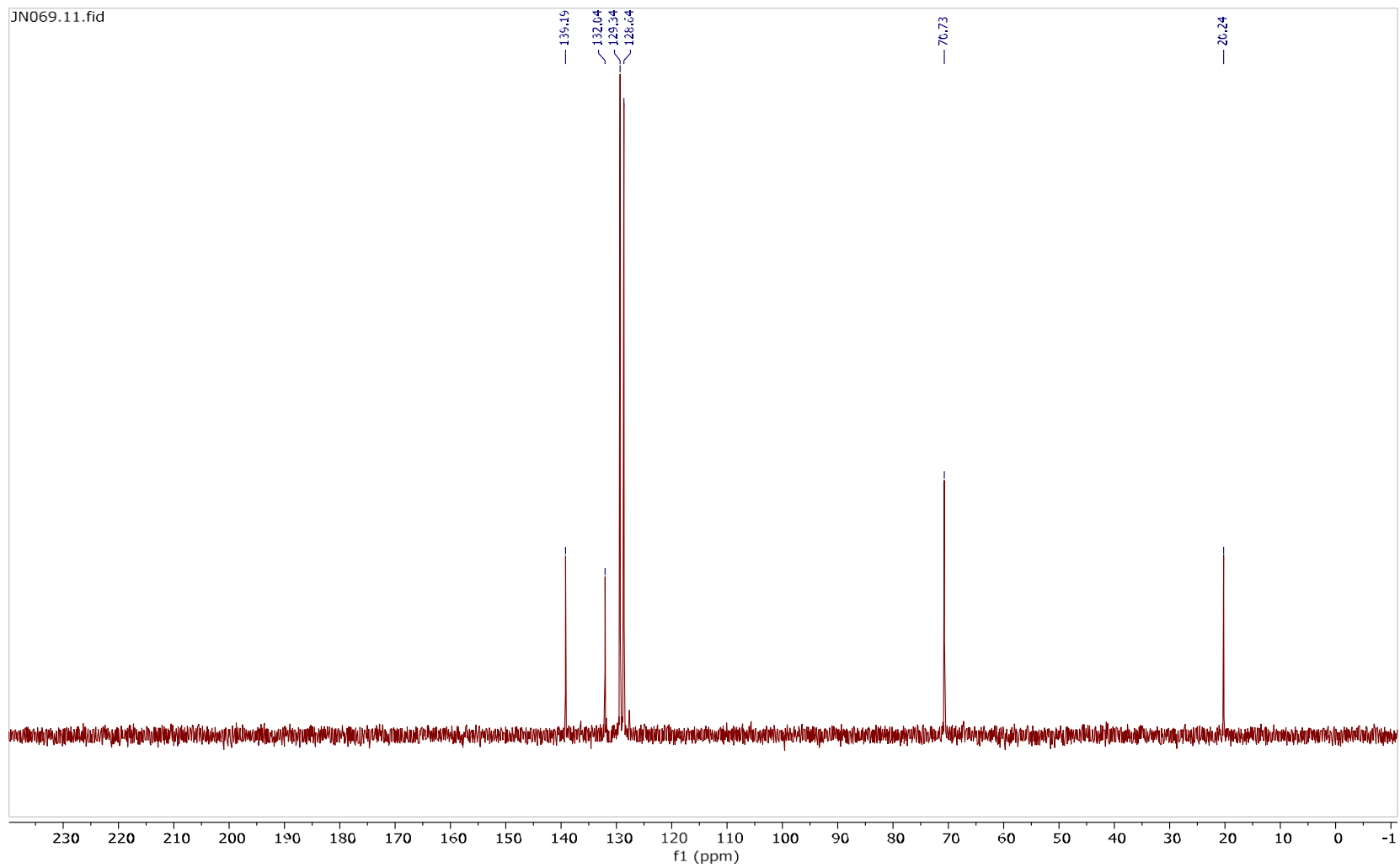
^{13}C NMR spectrum of **170** (101 MHz, D_2O)



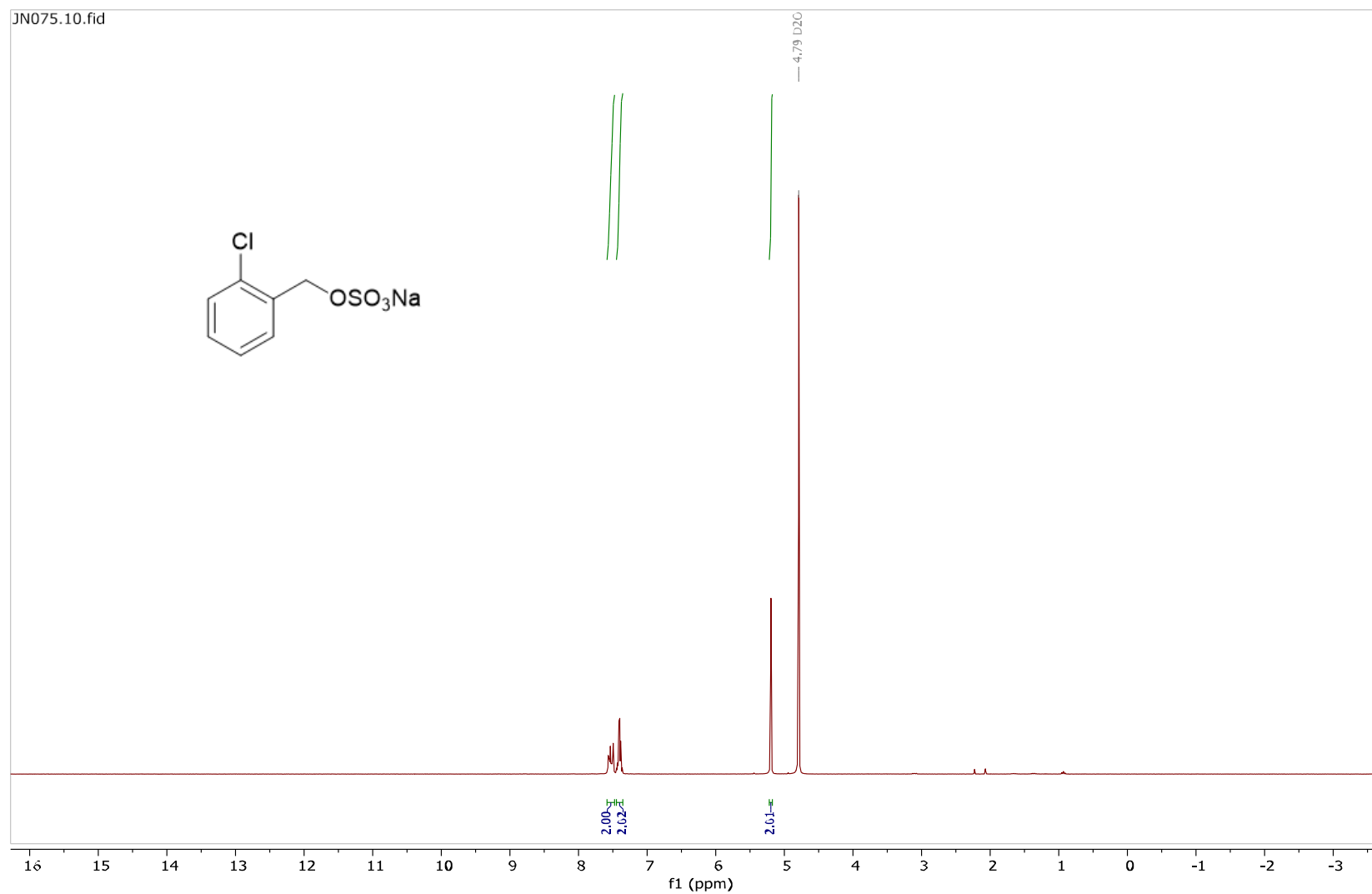
^1H NMR spectrum of **171** (300 MHz, D_2O)



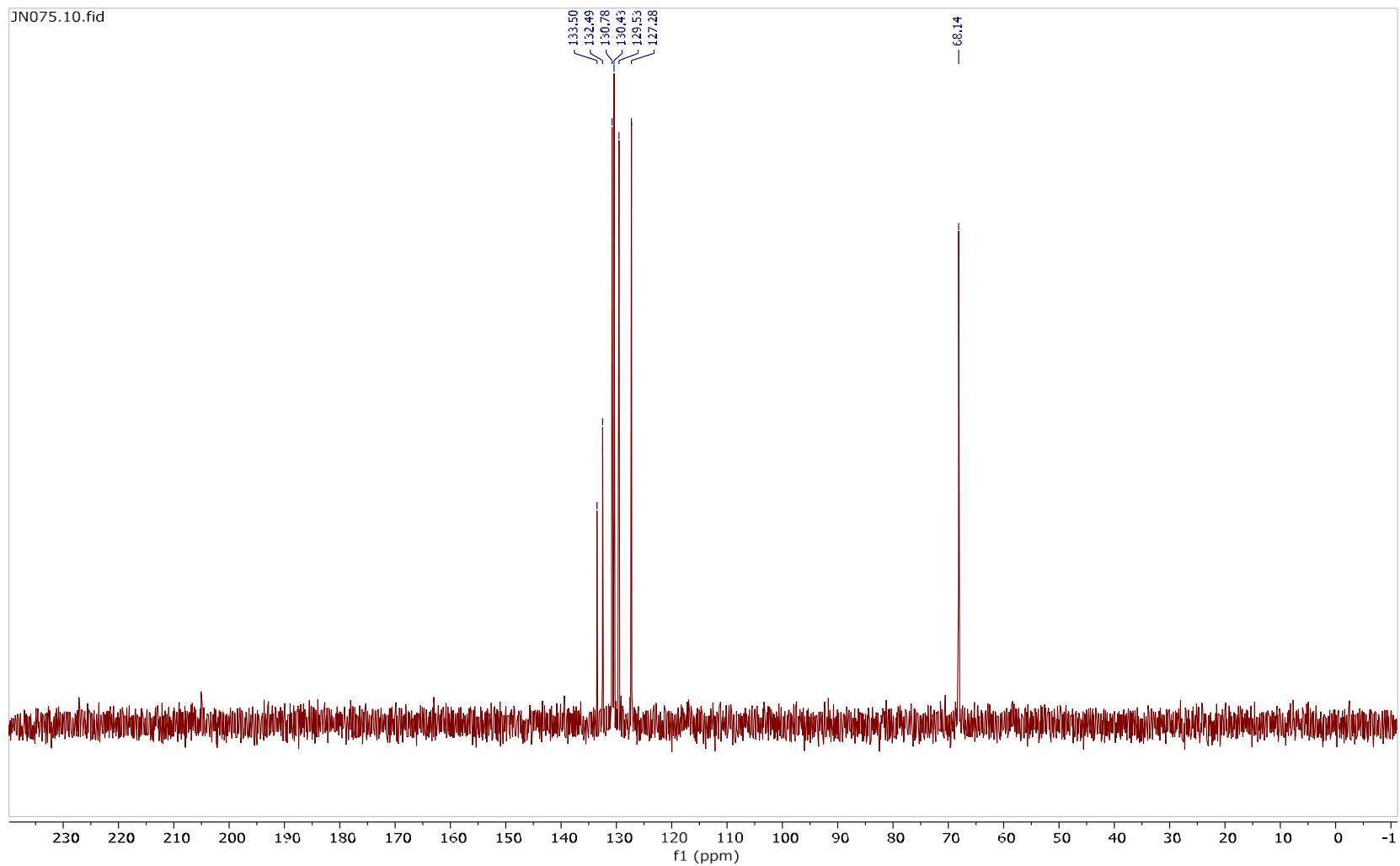
^{13}C NMR spectrum of **171** (101 MHz, D_2O)



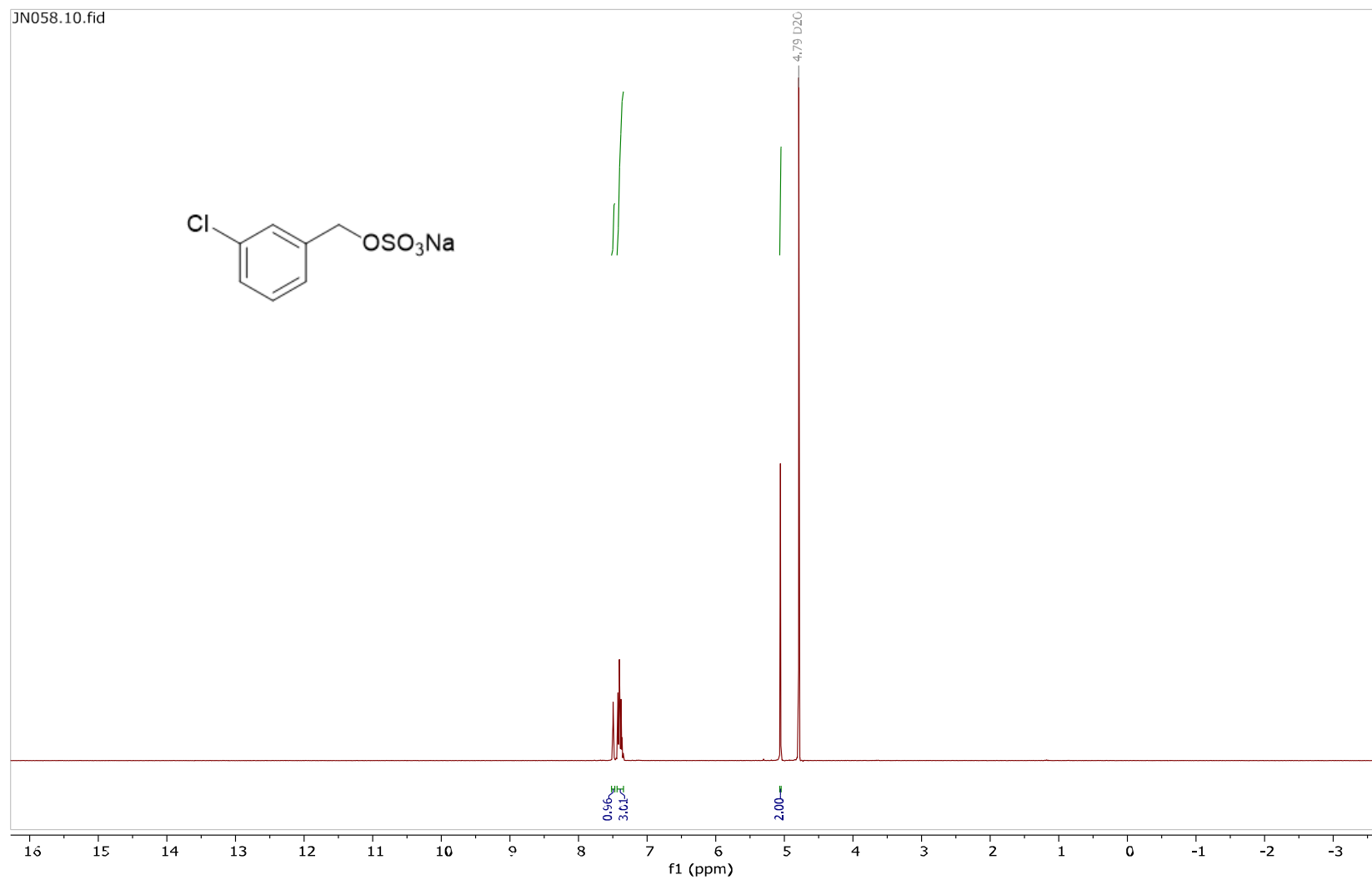
^1H NMR spectrum of **166** (300 MHz, D_2O)



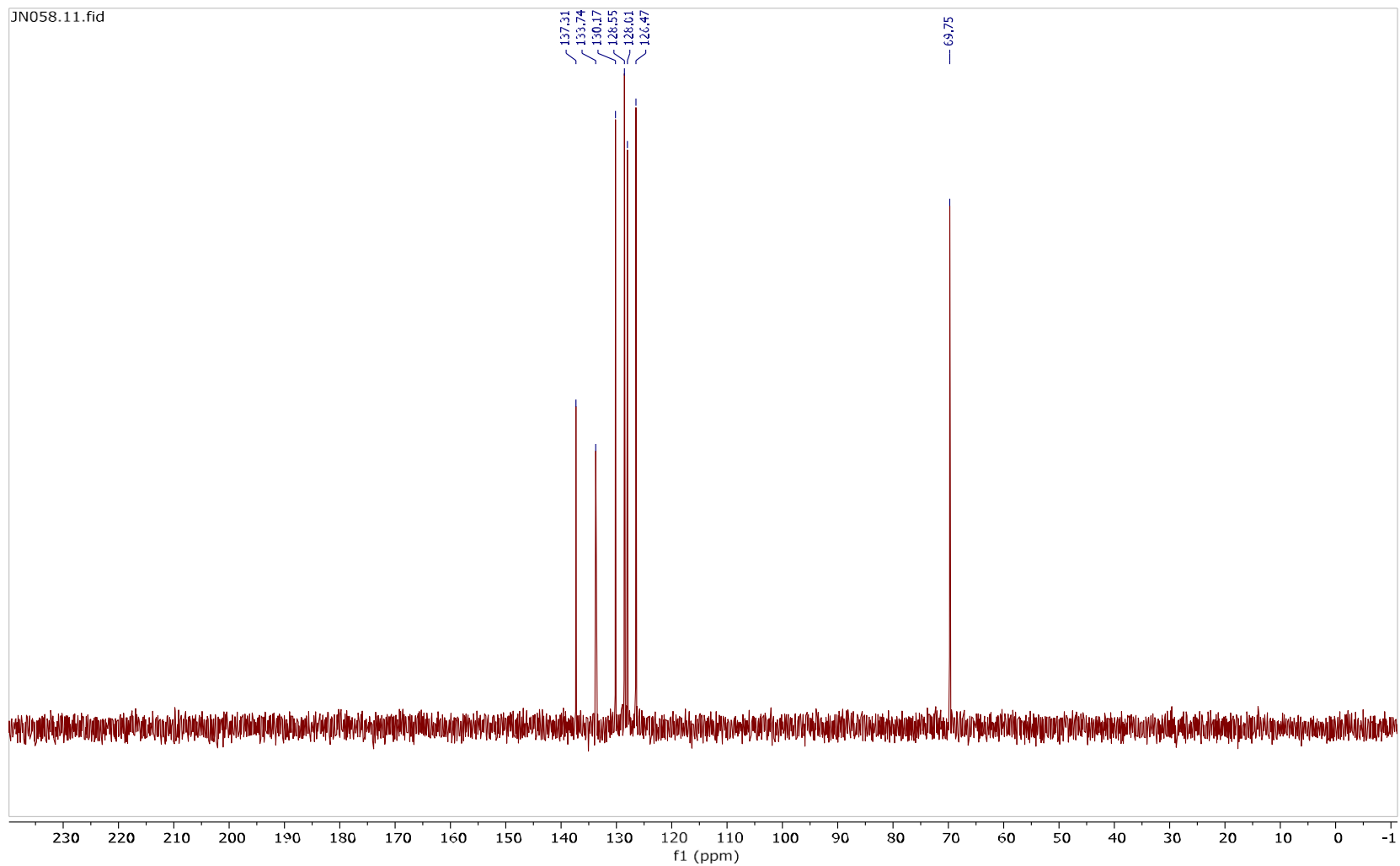
^{13}C NMR spectrum of **166** (101 MHz, D_2O)



^1H NMR spectrum of **163** (300 MHz, D_2O)

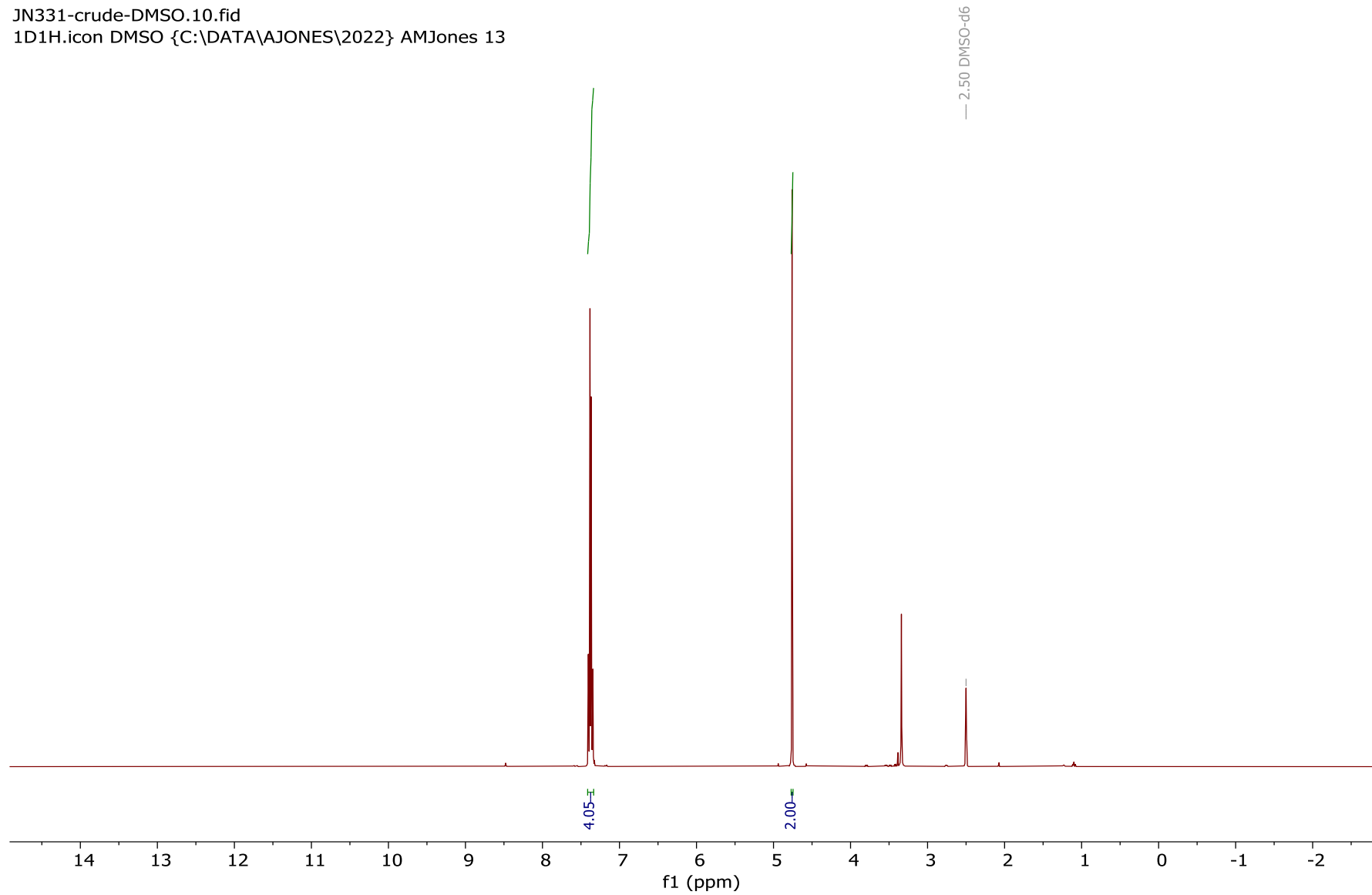


^{13}C NMR spectrum of **163** (101 MHz, D_2O)



^1H NMR spectrum of **157** (300 MHz, $\text{DMSO-}d_6$)

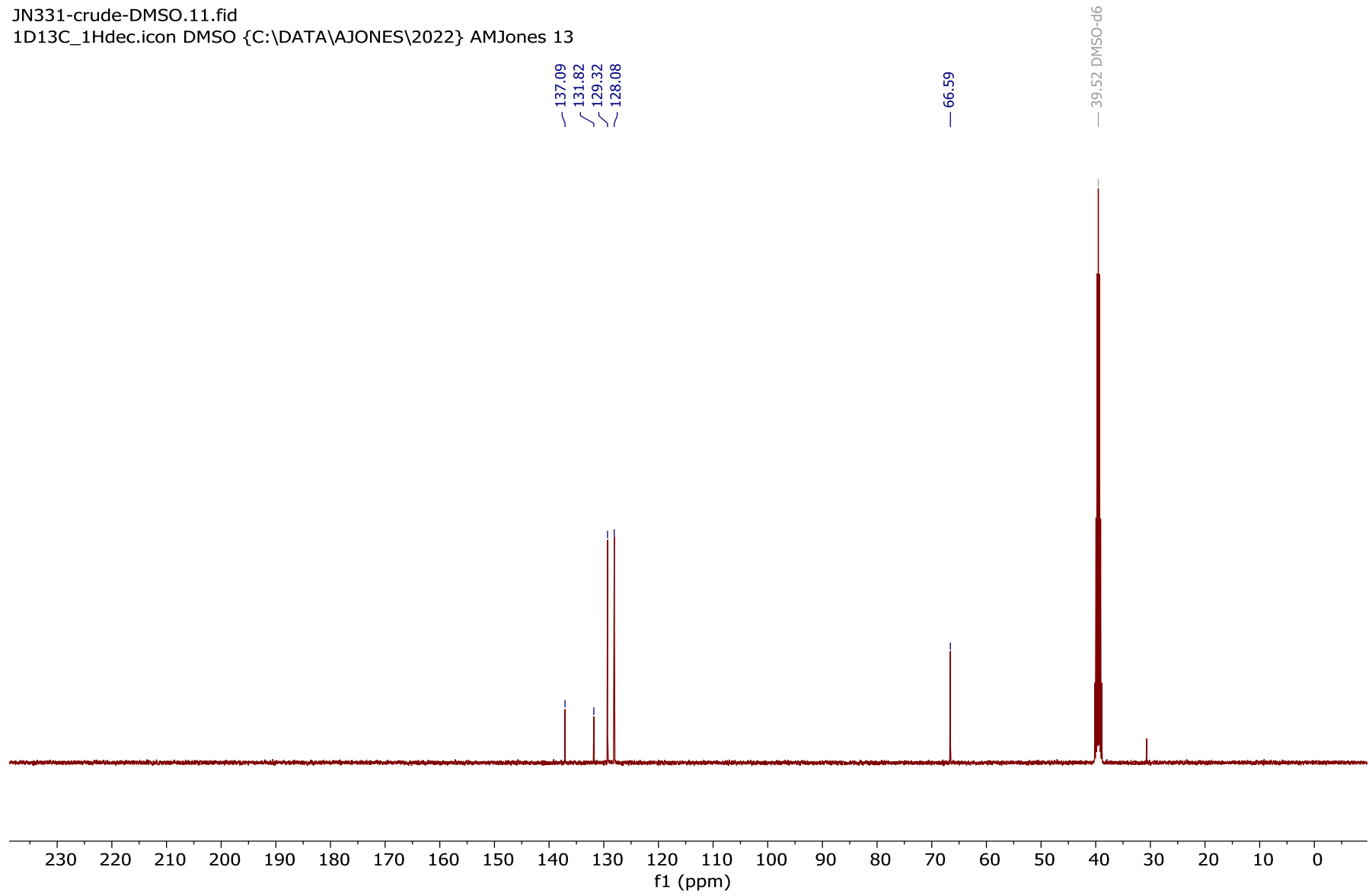
JN331-crude-DMSO.10.fid
1D1H.icon DMSO {C:\DATA\AJONES\2022} AMJones 13



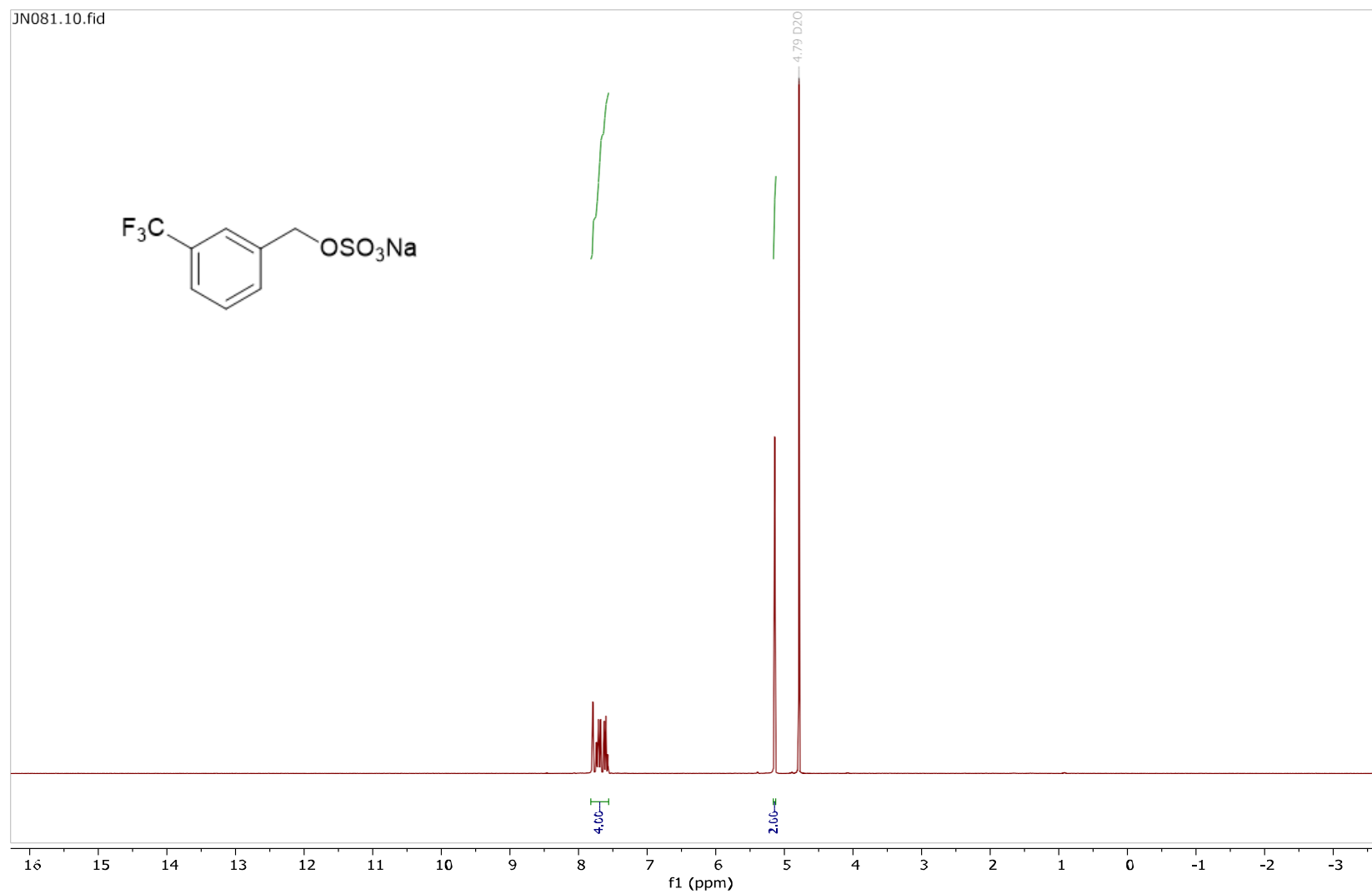
¹³C NMR spectrum of **157** (101 MHz, DMSO-*d*₆)

JN331-crude-DMSO.11.fid

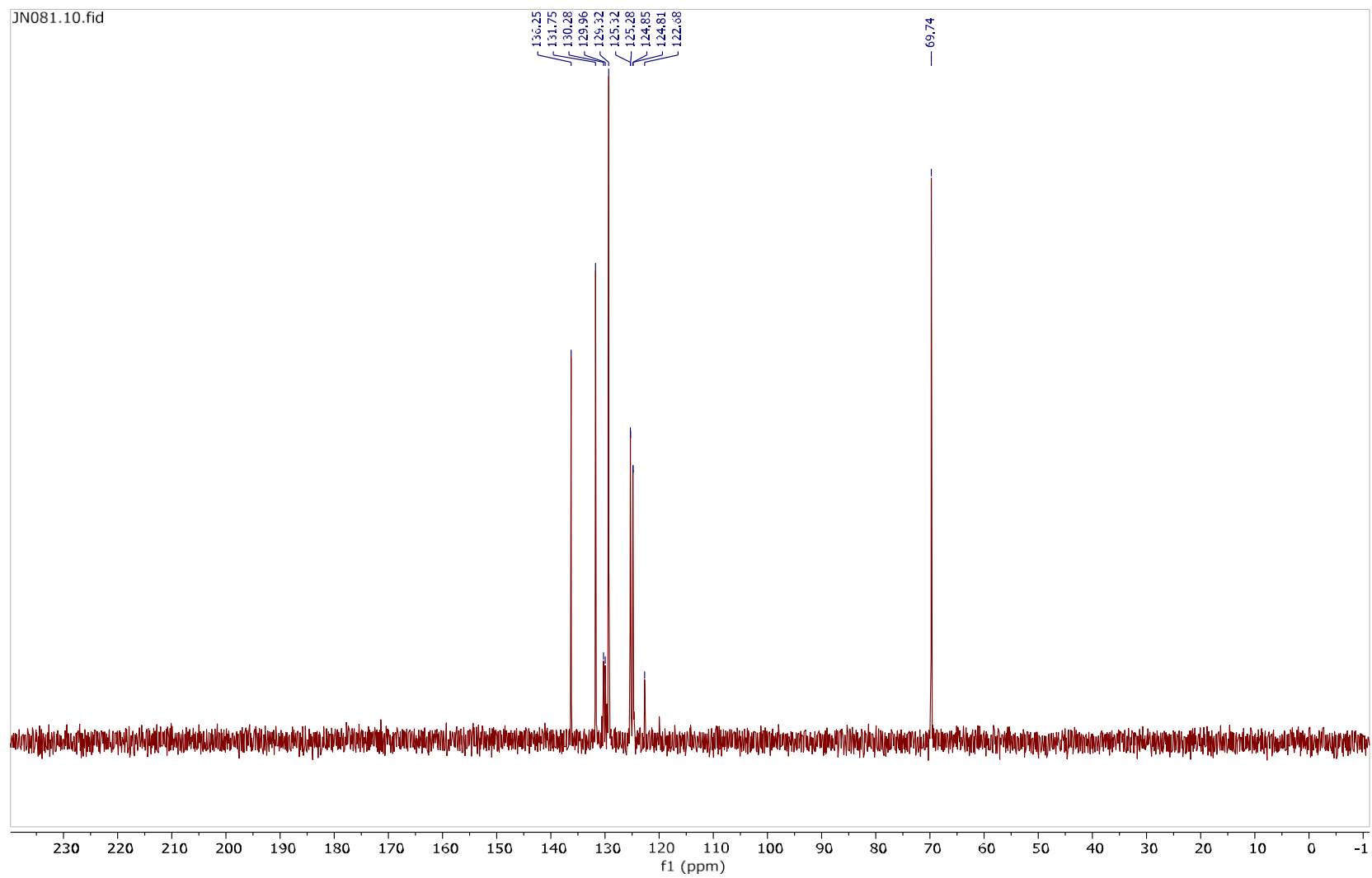
1D13C_1Hdec.icon DMSO {C:\DATA\AJONES\2022} AMJones 13



^1H NMR spectrum of **172** (300 MHz, D_2O)

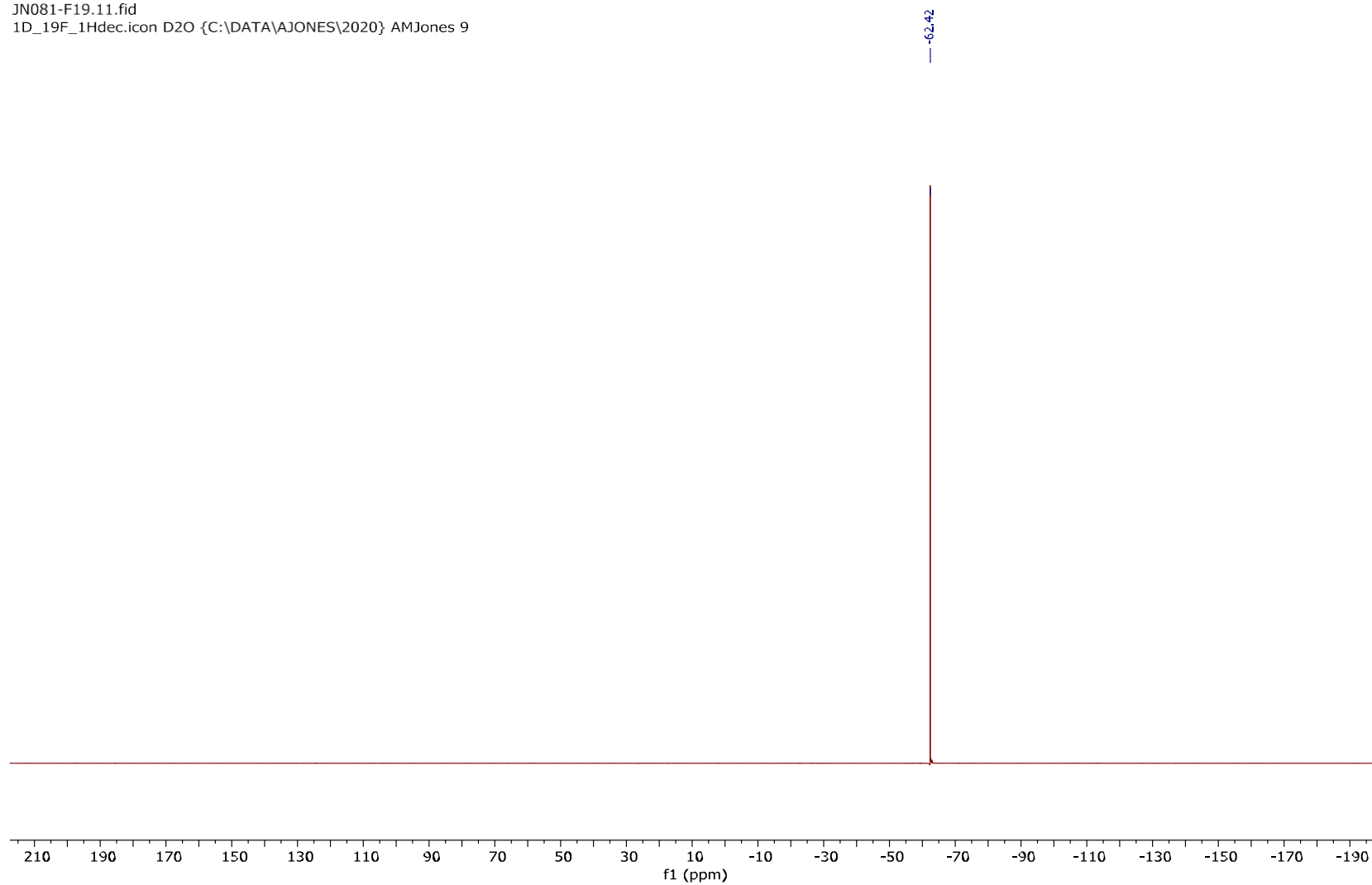


^{13}C NMR spectrum of **172** (101 MHz, D_2O)

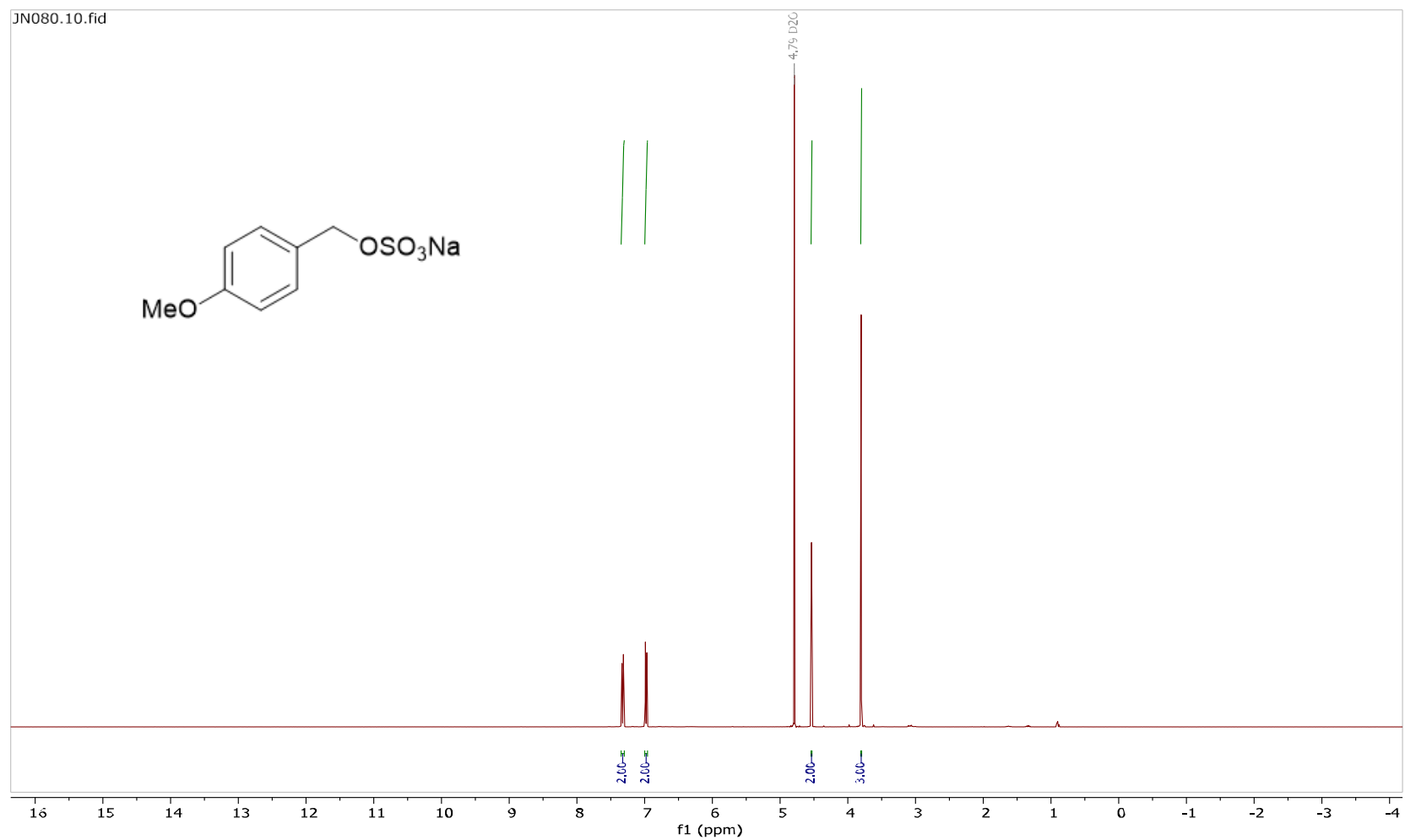


¹⁹F NMR spectrum of **172** (377 MHz, D₂O)

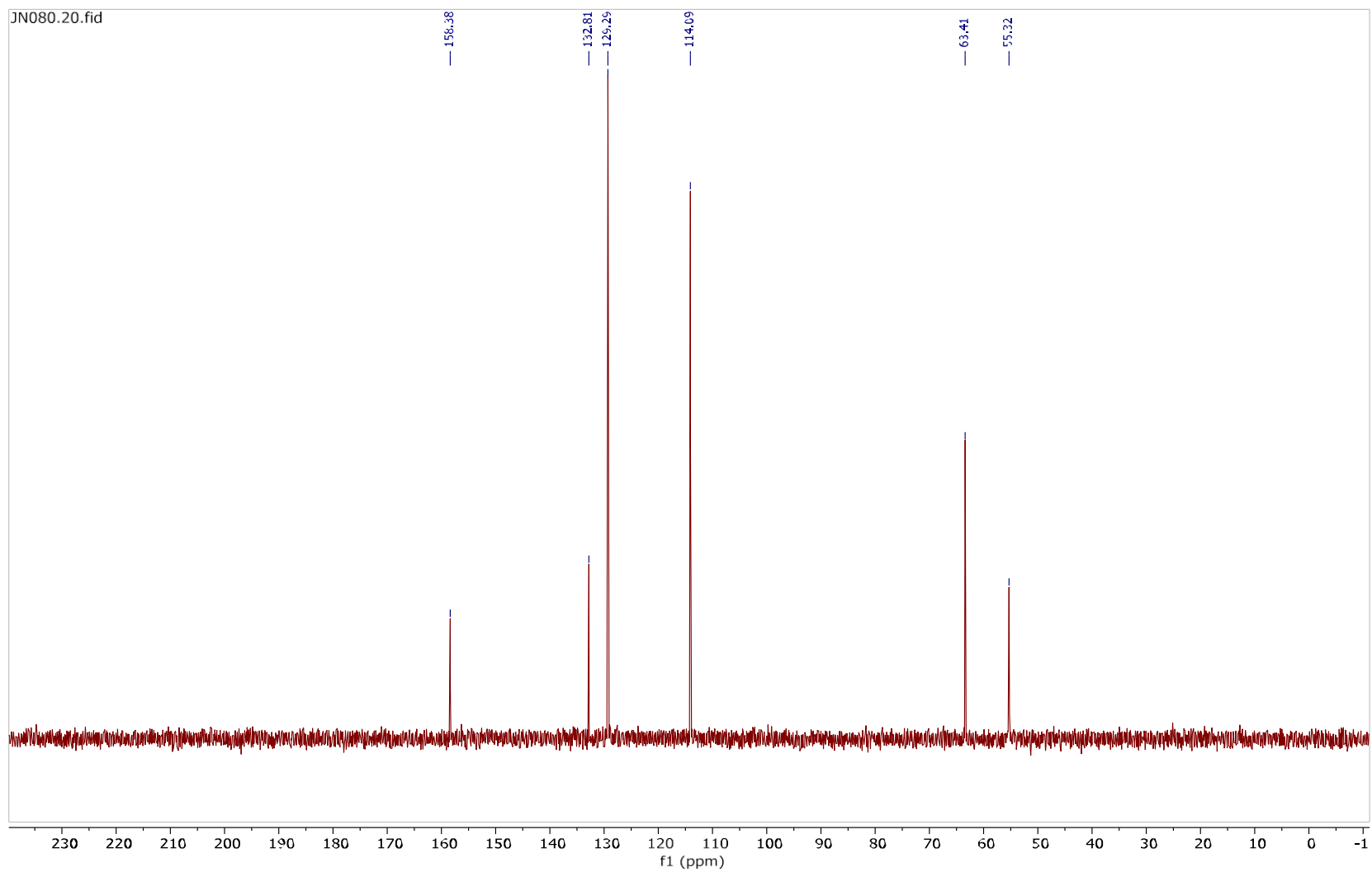
JN081-F19.11.fid
1D_19F_1Hdec.icon D2O {C:\DATA\AJONES\2020} AMJones 9



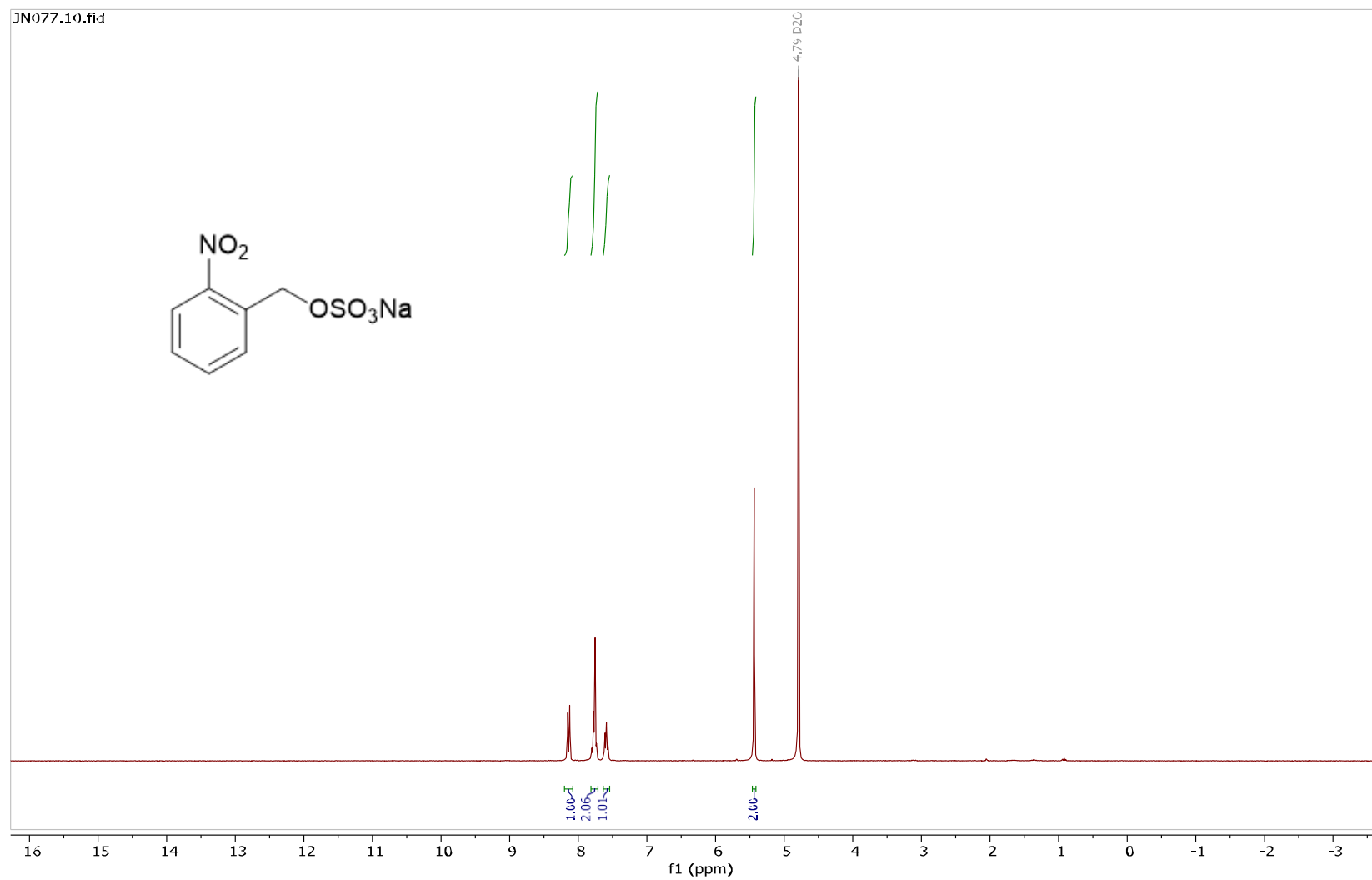
^1H NMR spectrum of **173** (300 MHz, D_2O)



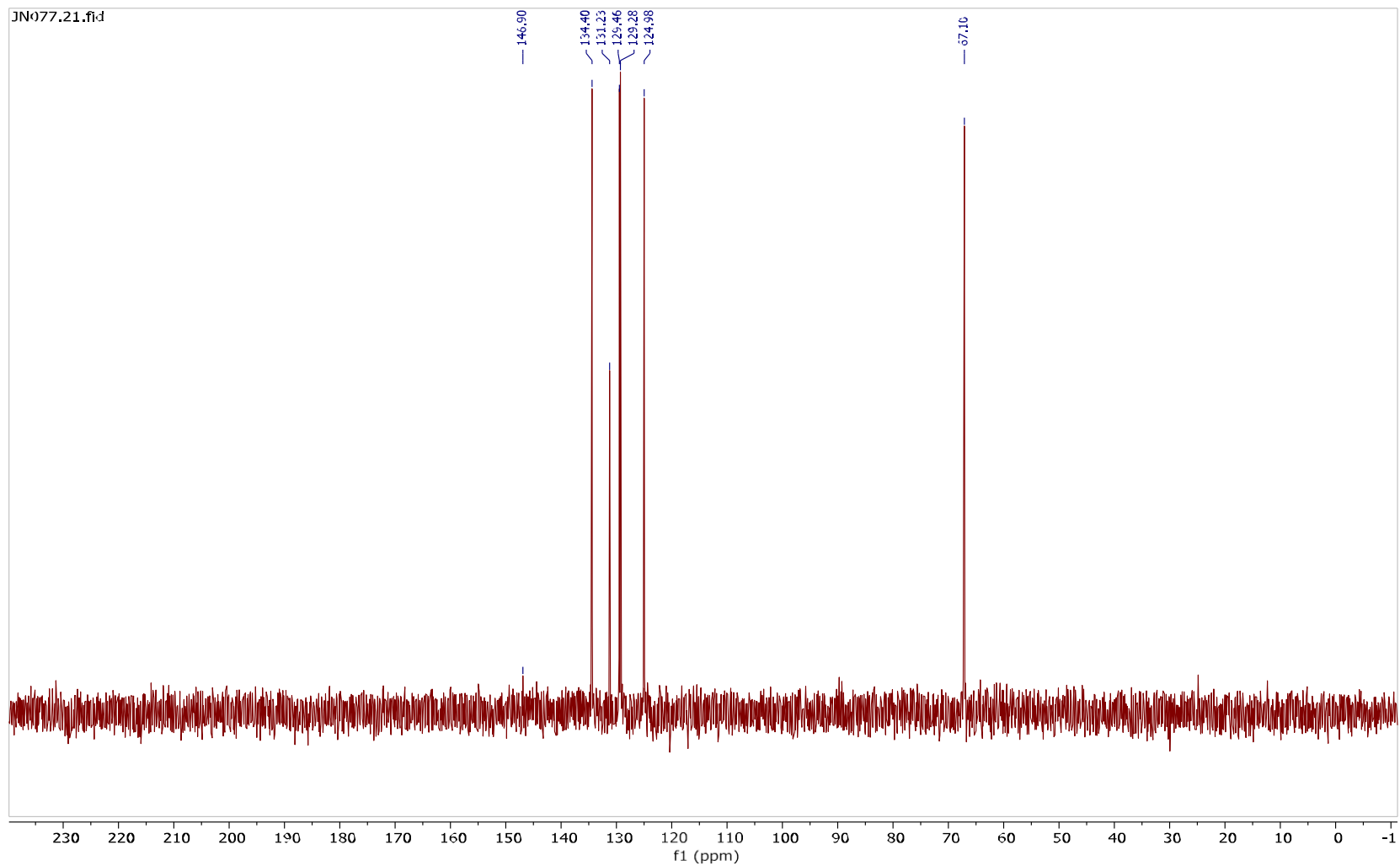
^{13}C NMR spectrum of **173** (101 MHz, D_2O)



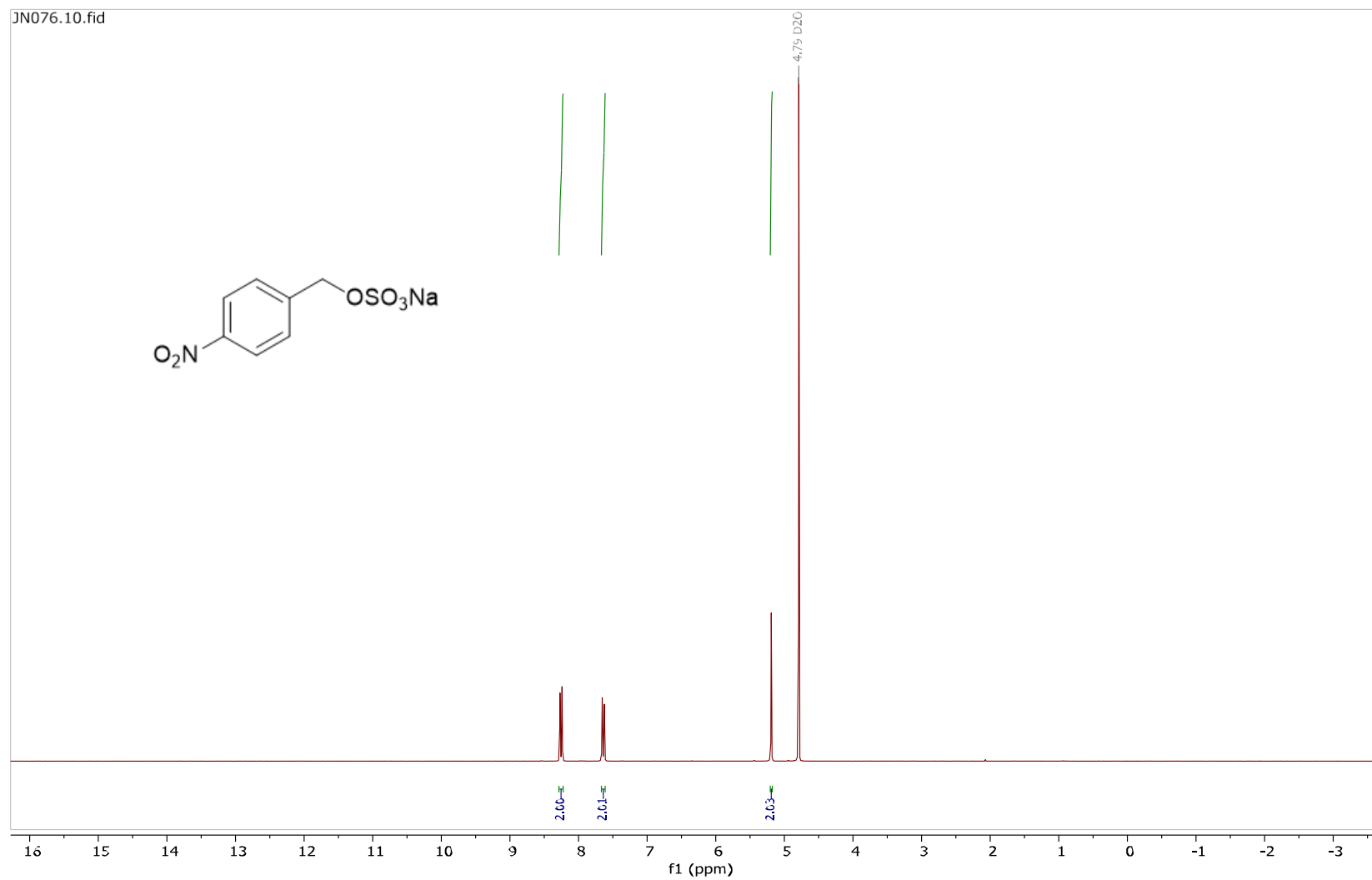
^1H NMR spectrum of **174** (300 MHz, D_2O)



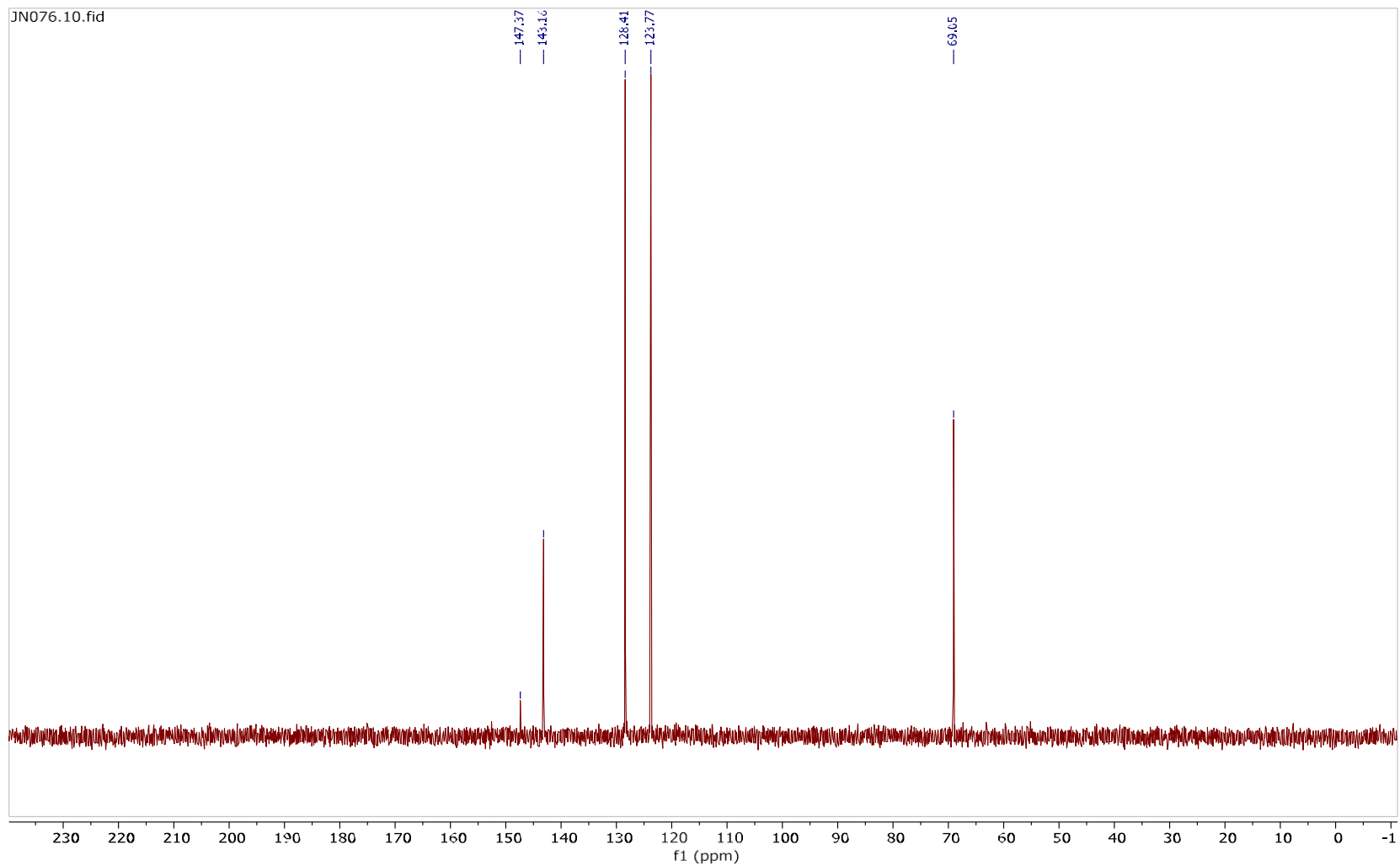
^{13}C NMR spectrum of **174** (101 MHz, D_2O)



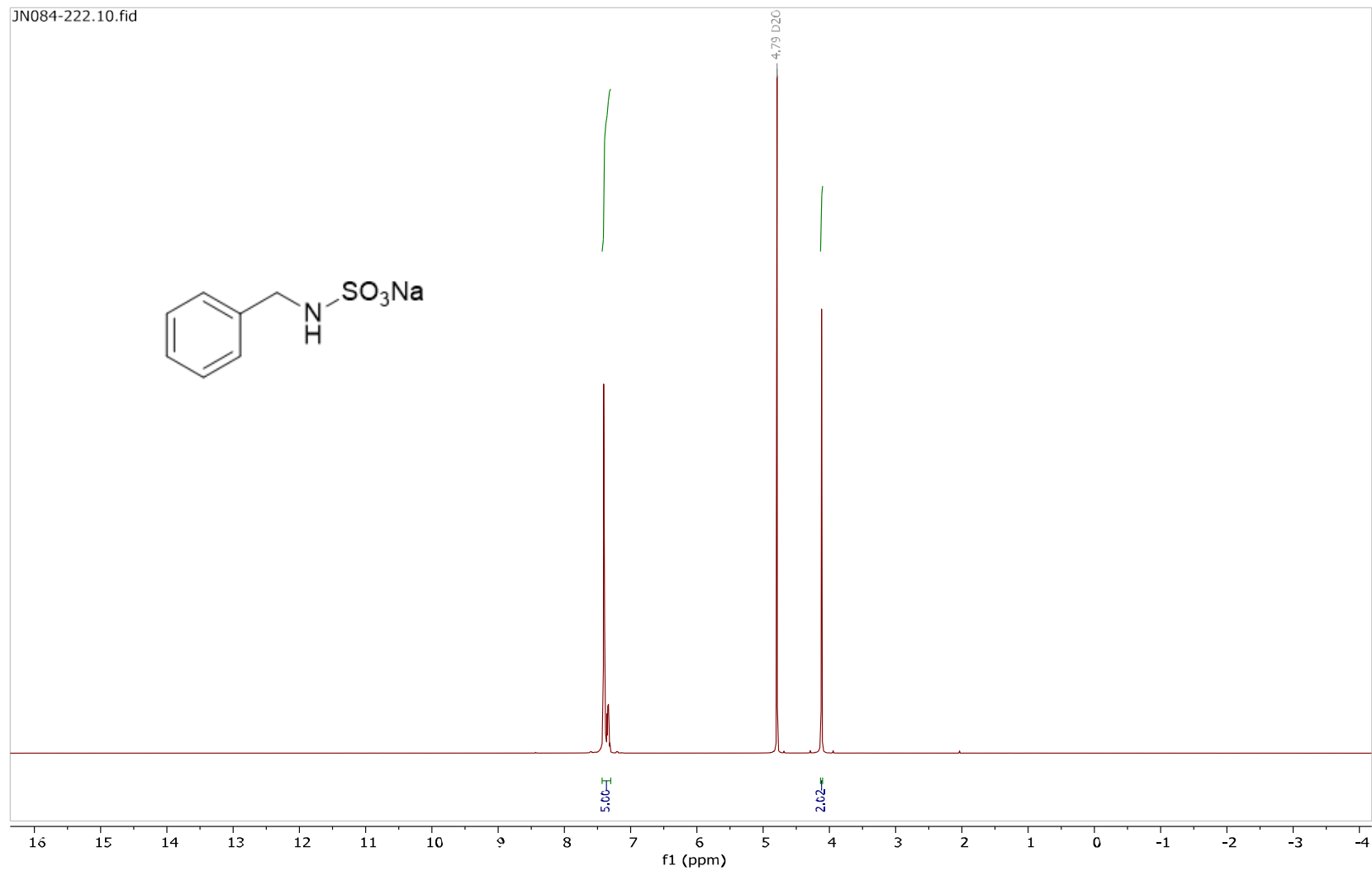
^1H NMR spectrum of **175** (300 MHz, D_2O)



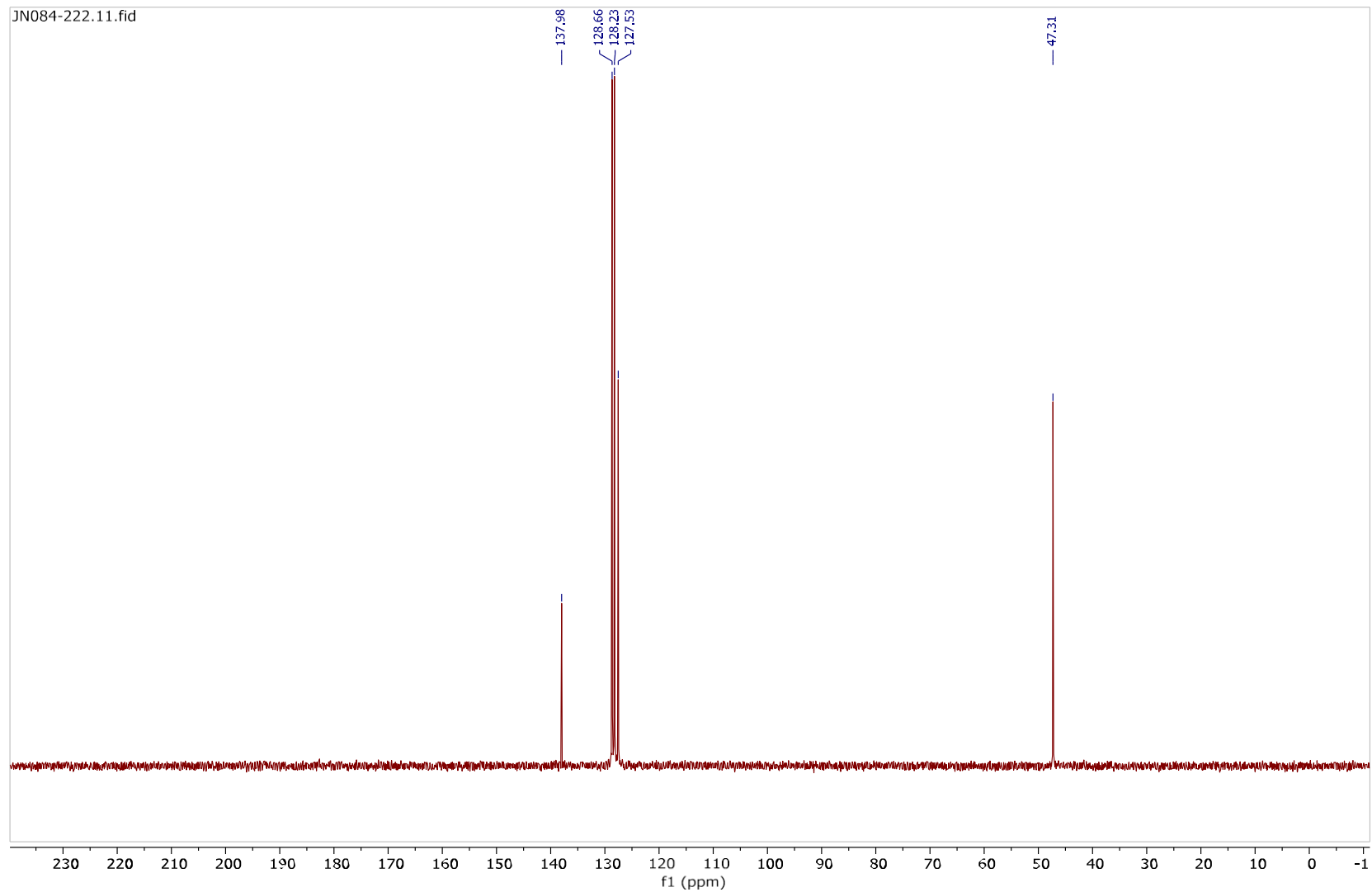
^{13}C NMR spectrum of **175** (101 MHz, D_2O)



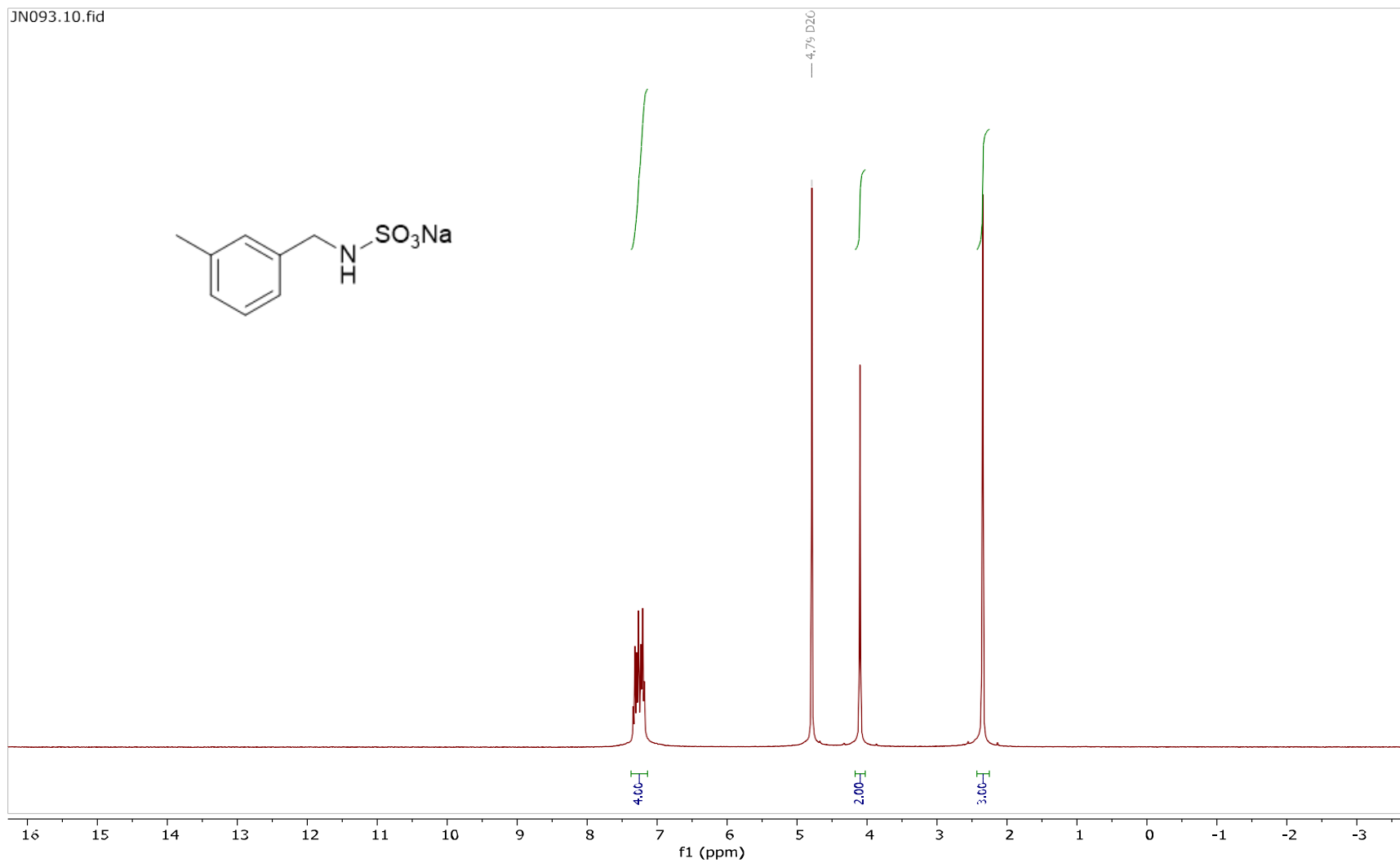
¹H NMR spectrum of **108** (300 MHz, D₂O)



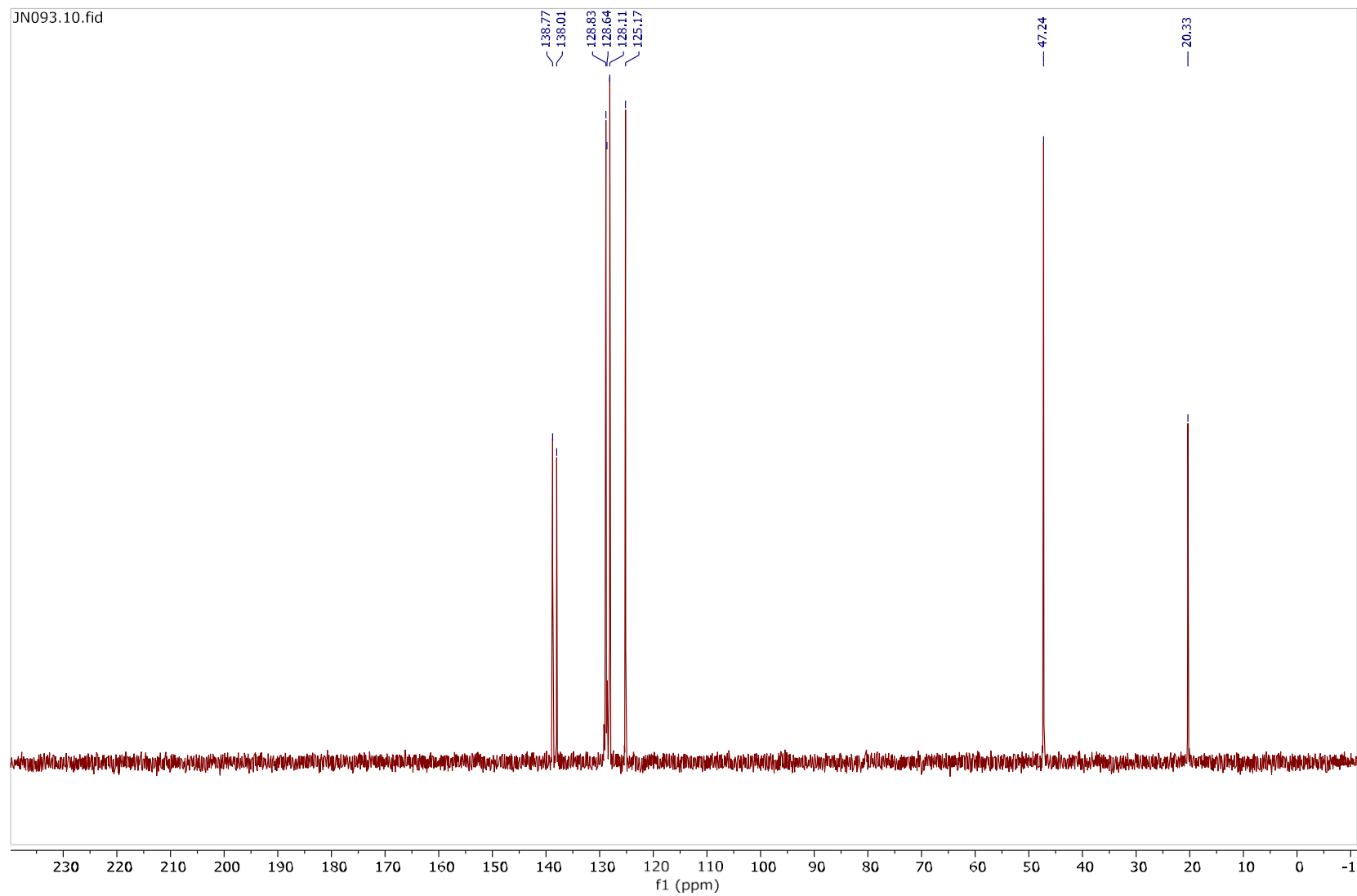
^{13}C NMR spectrum of **108** (101 MHz, D_2O)



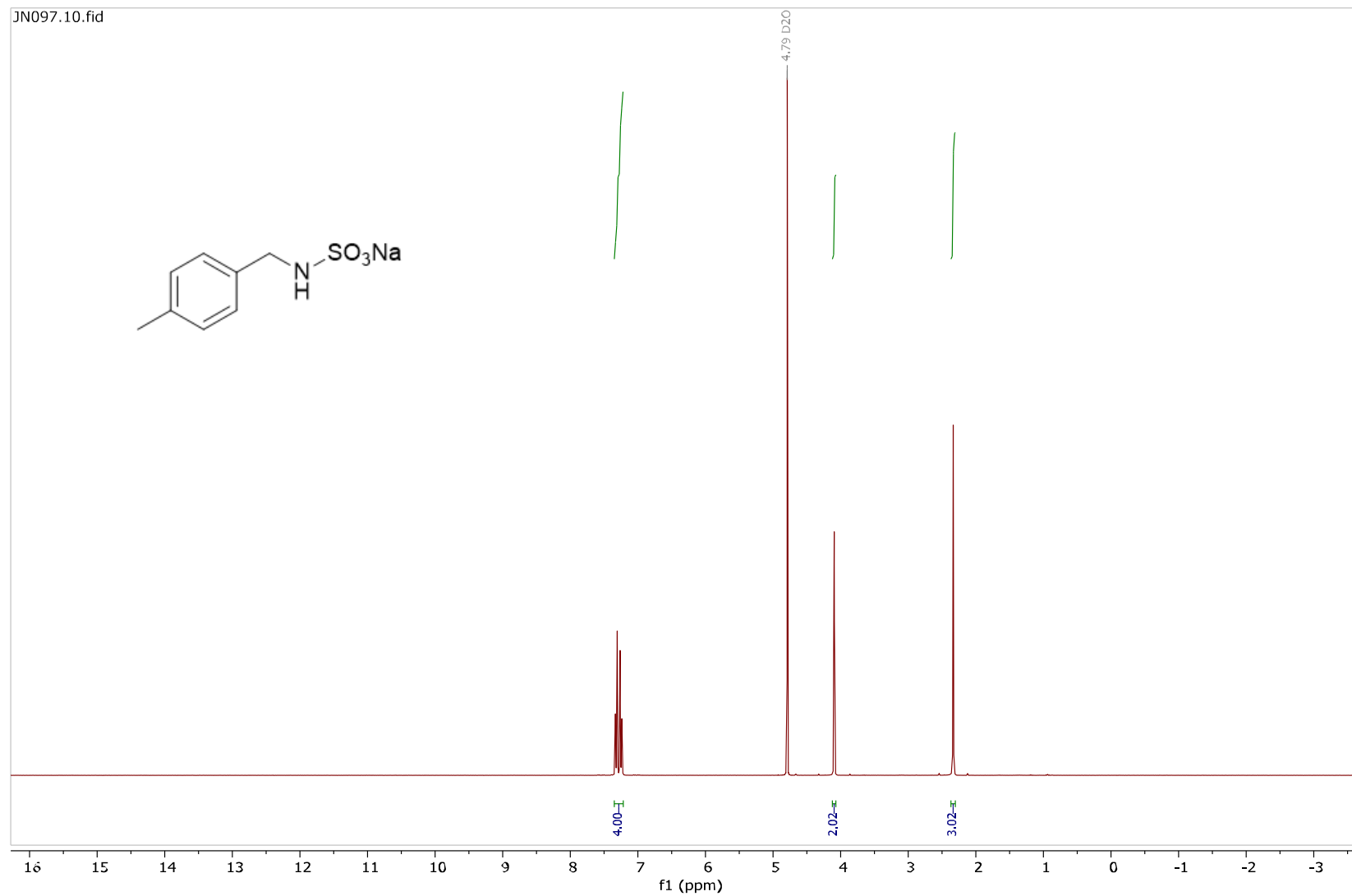
^1H NMR spectrum of **178** (300 MHz, D_2O)



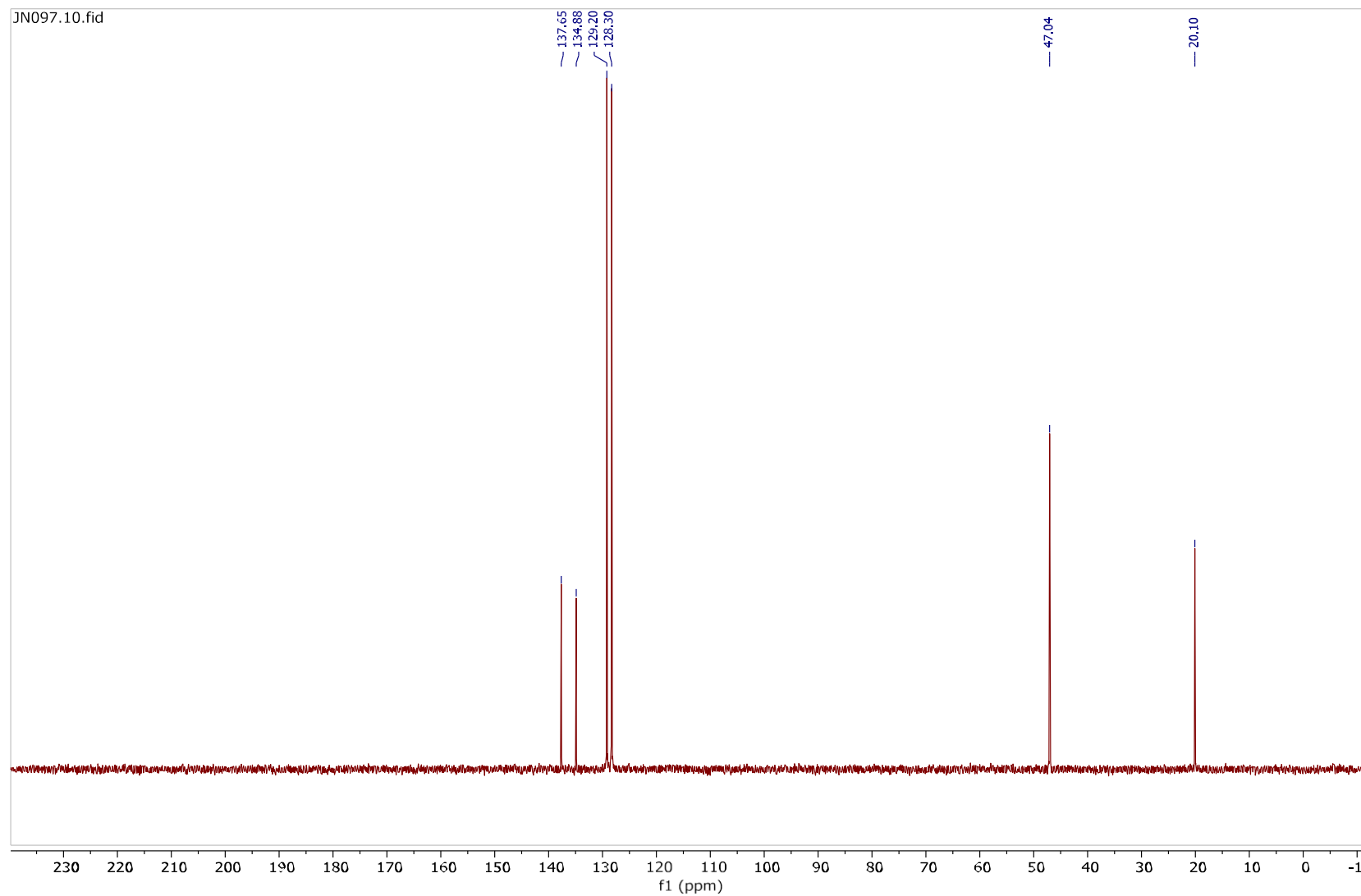
^{13}C NMR spectrum of **178** (101 MHz, D_2O)



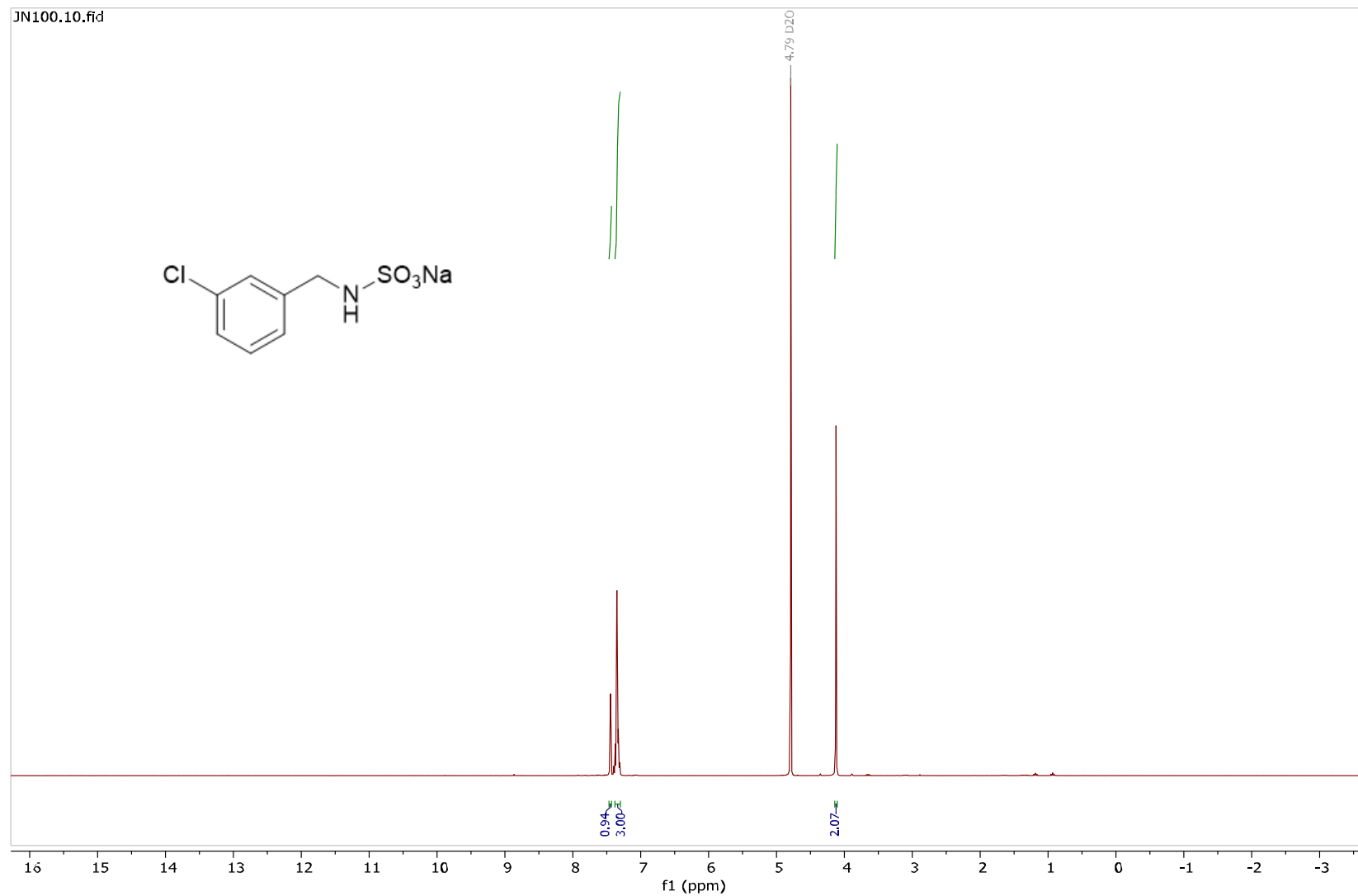
^1H NMR spectrum of **179** (300 MHz, D_2O)



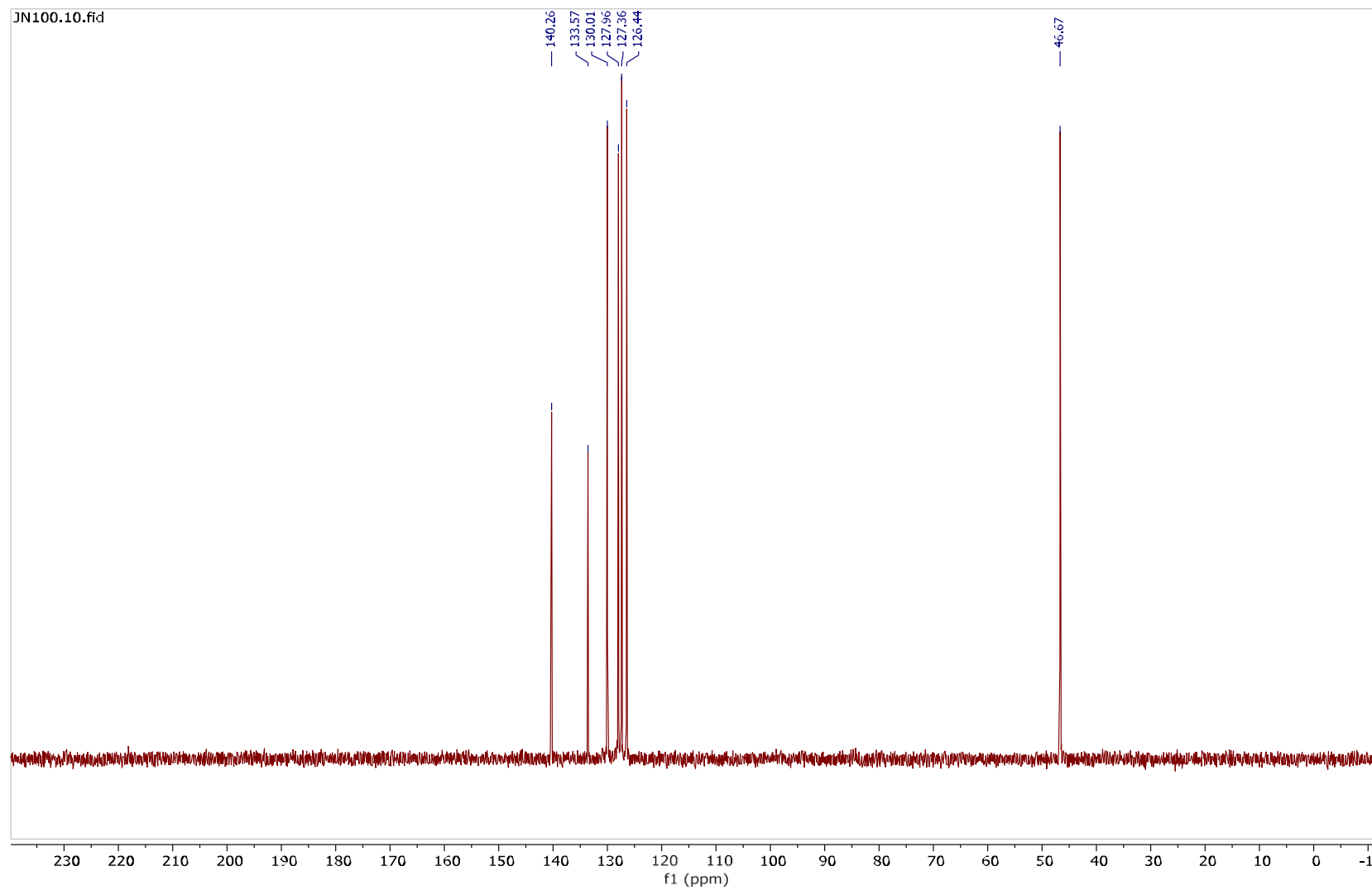
^{13}C NMR spectrum of **179** (101 MHz, D_2O)



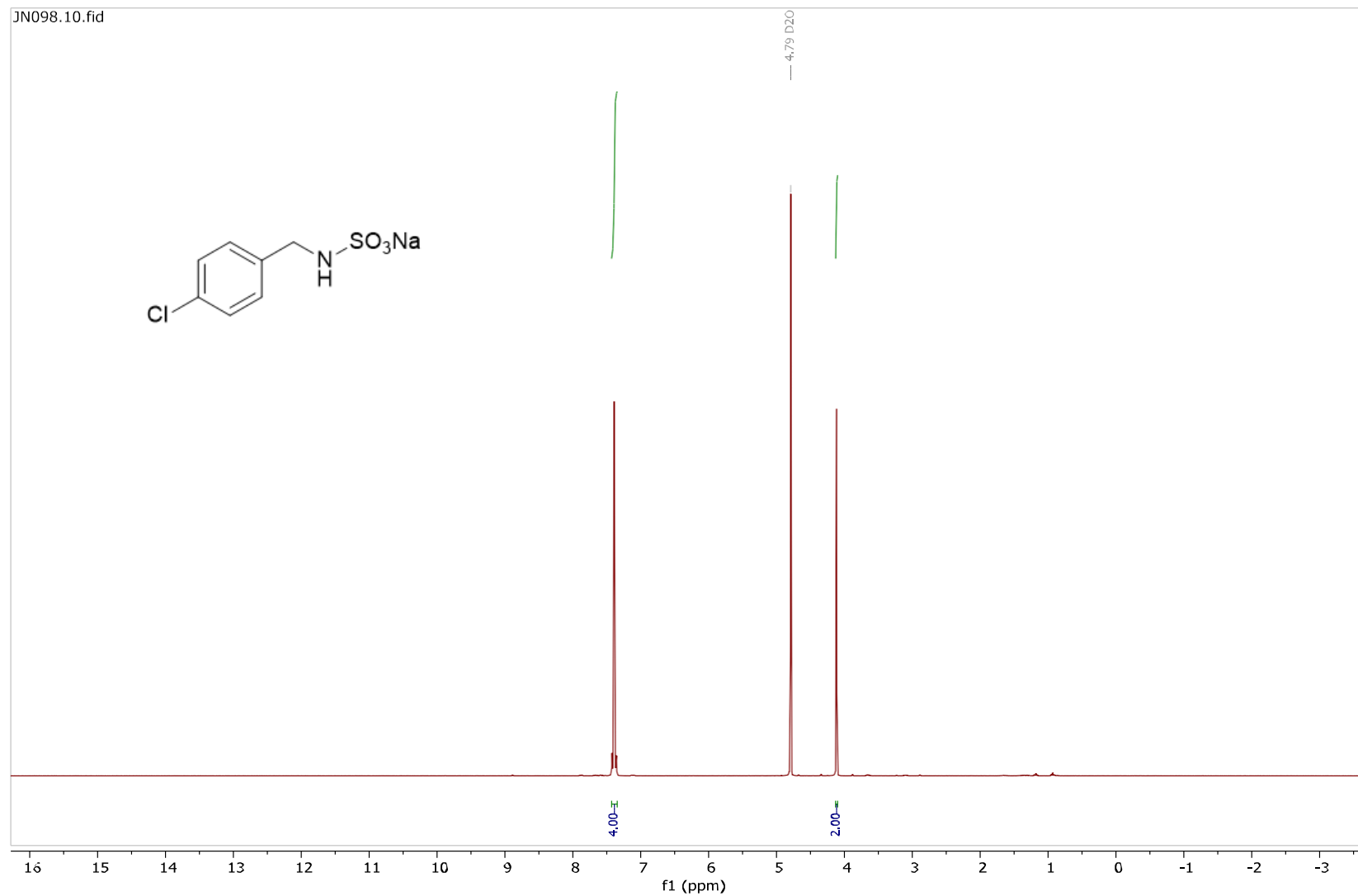
^1H NMR spectrum of **180** (300 MHz, D_2O)



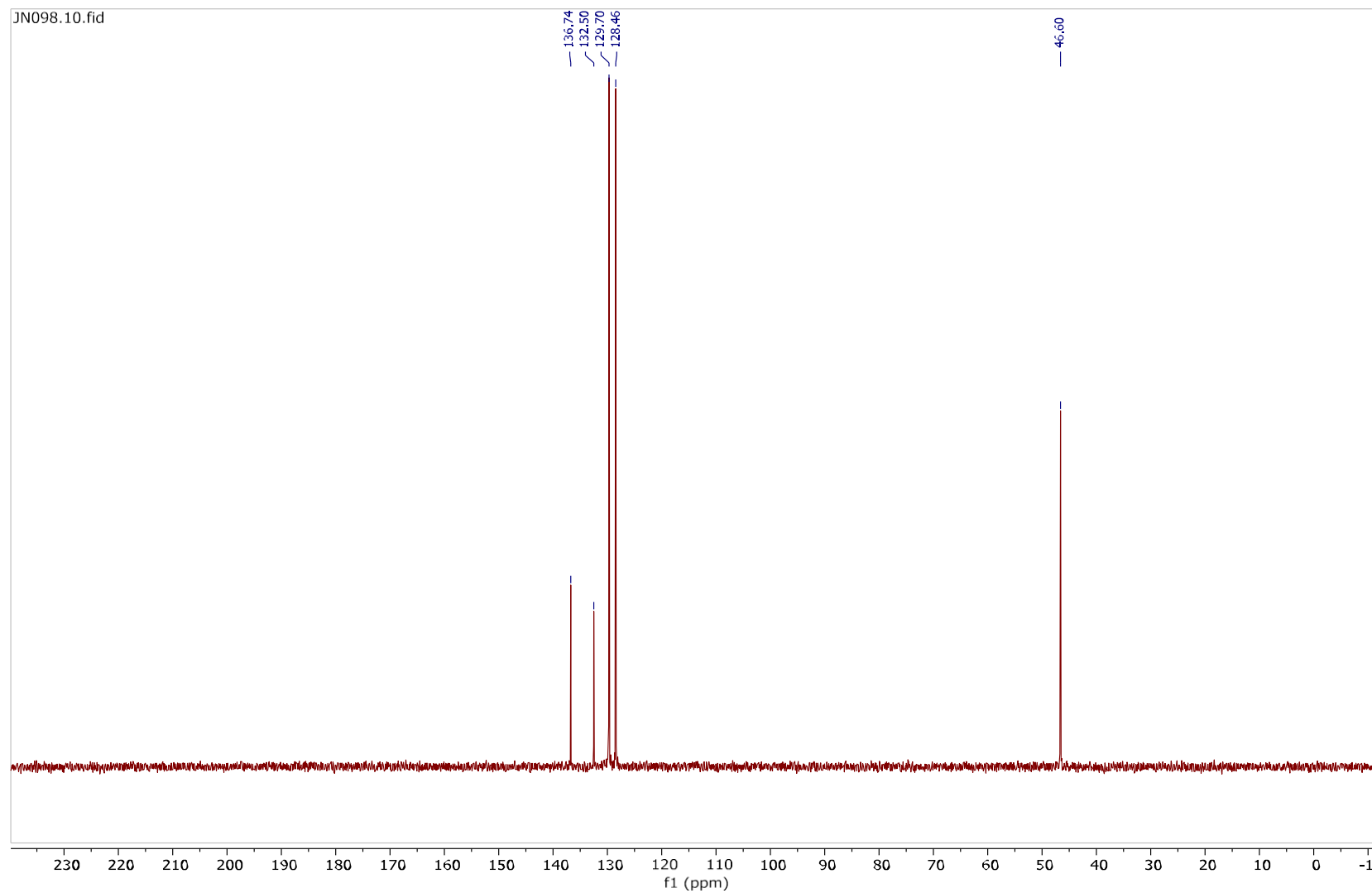
^{13}C NMR spectrum of **180** (101 MHz, D_2O)



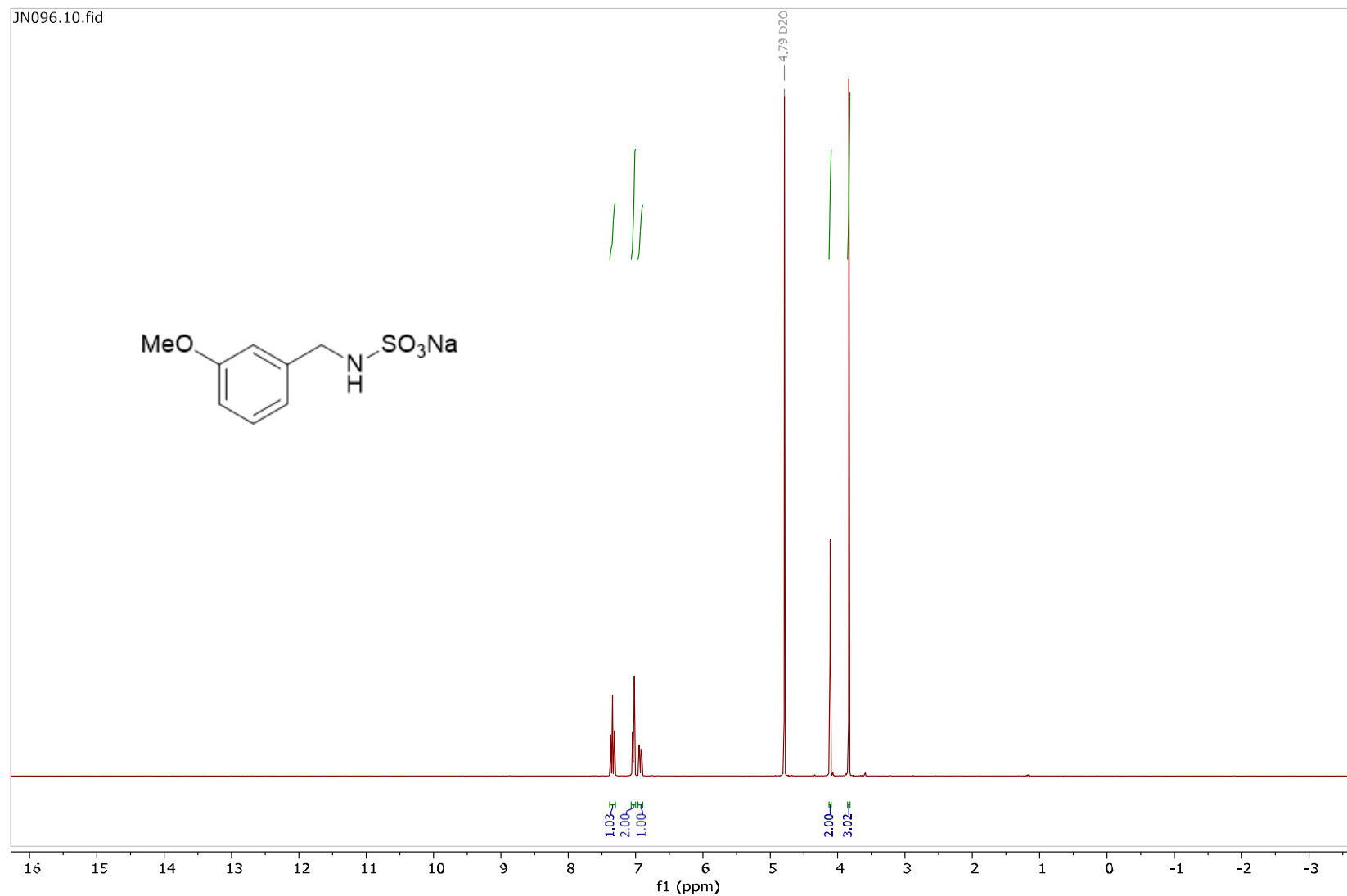
^1H NMR spectrum of **181** (300 MHz, D_2O)



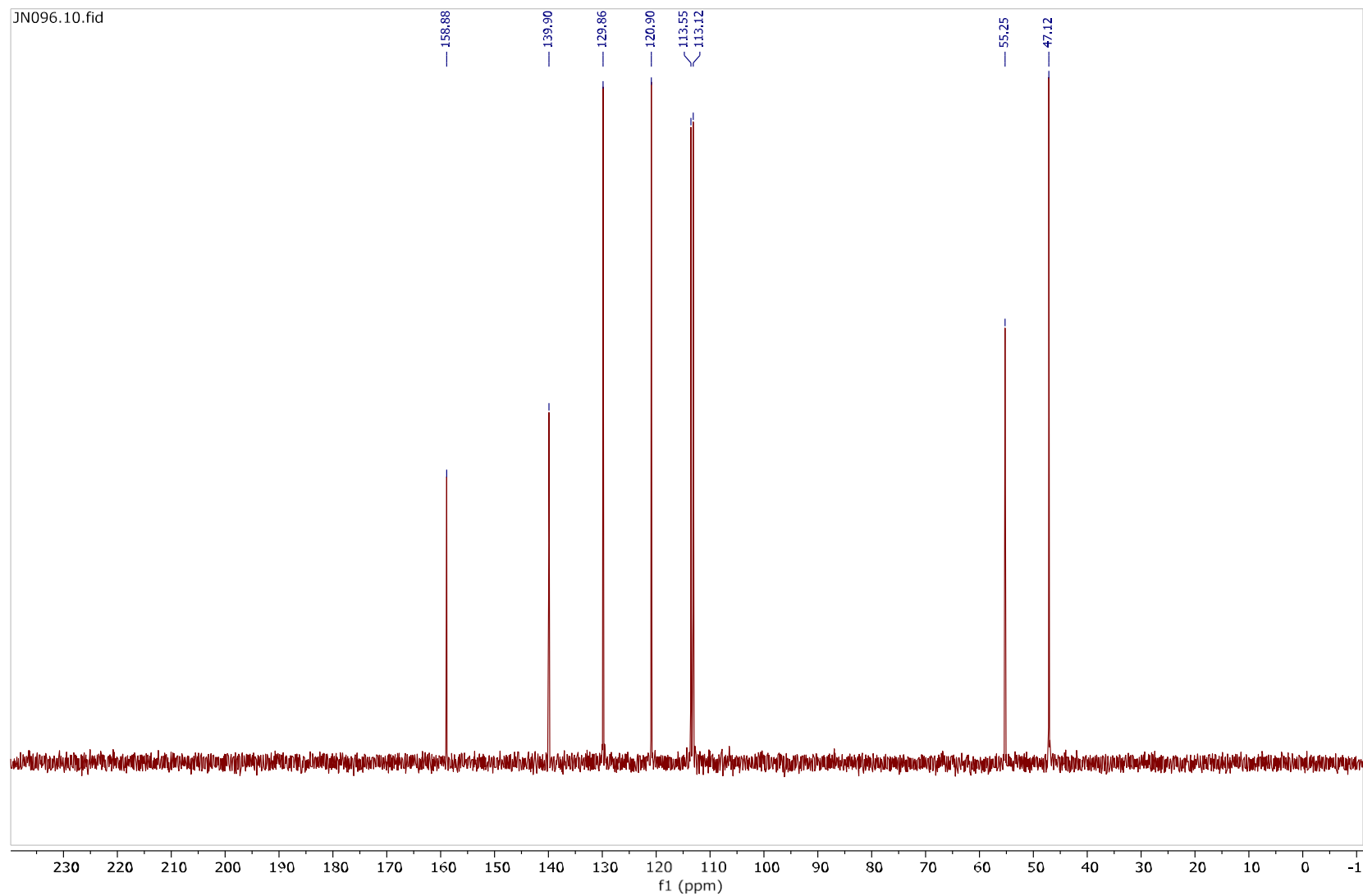
^{13}C NMR spectrum of **181** (101 MHz, D_2O)



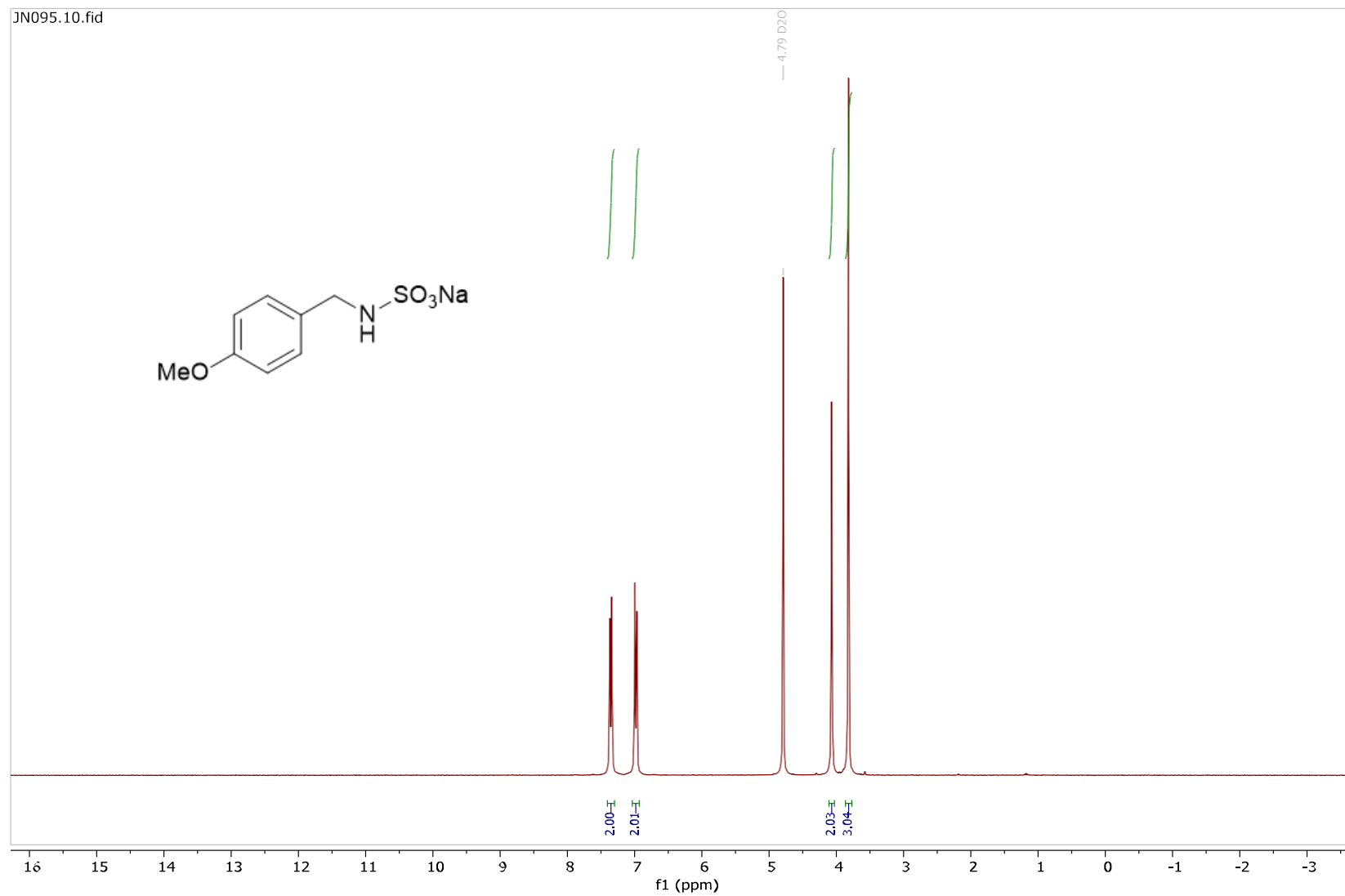
^1H NMR spectrum of **182** (300 MHz, D_2O)



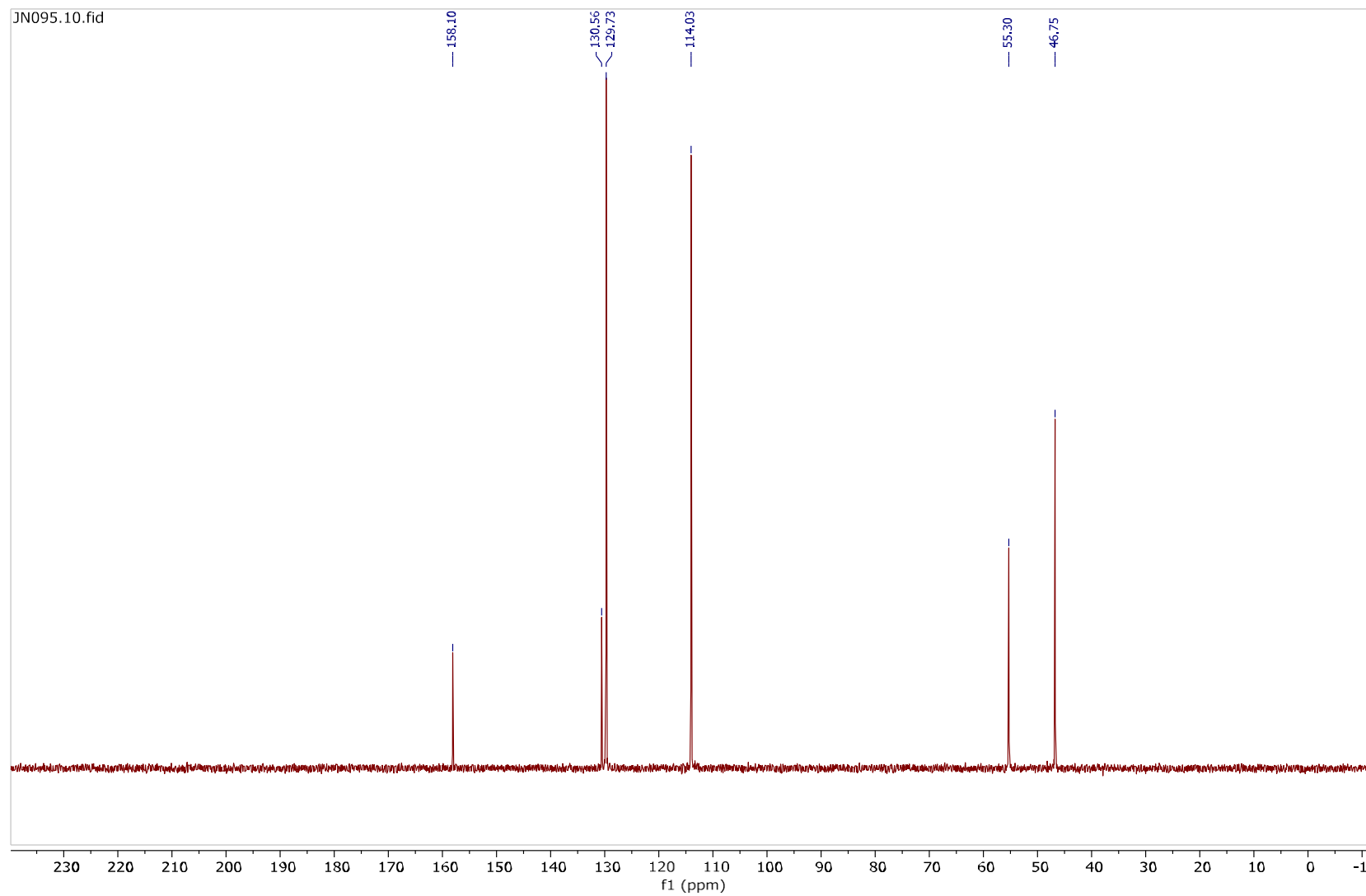
^{13}C NMR spectrum of **182** (101 MHz, D_2O)



^1H NMR spectrum of **183** (300 MHz, D_2O)

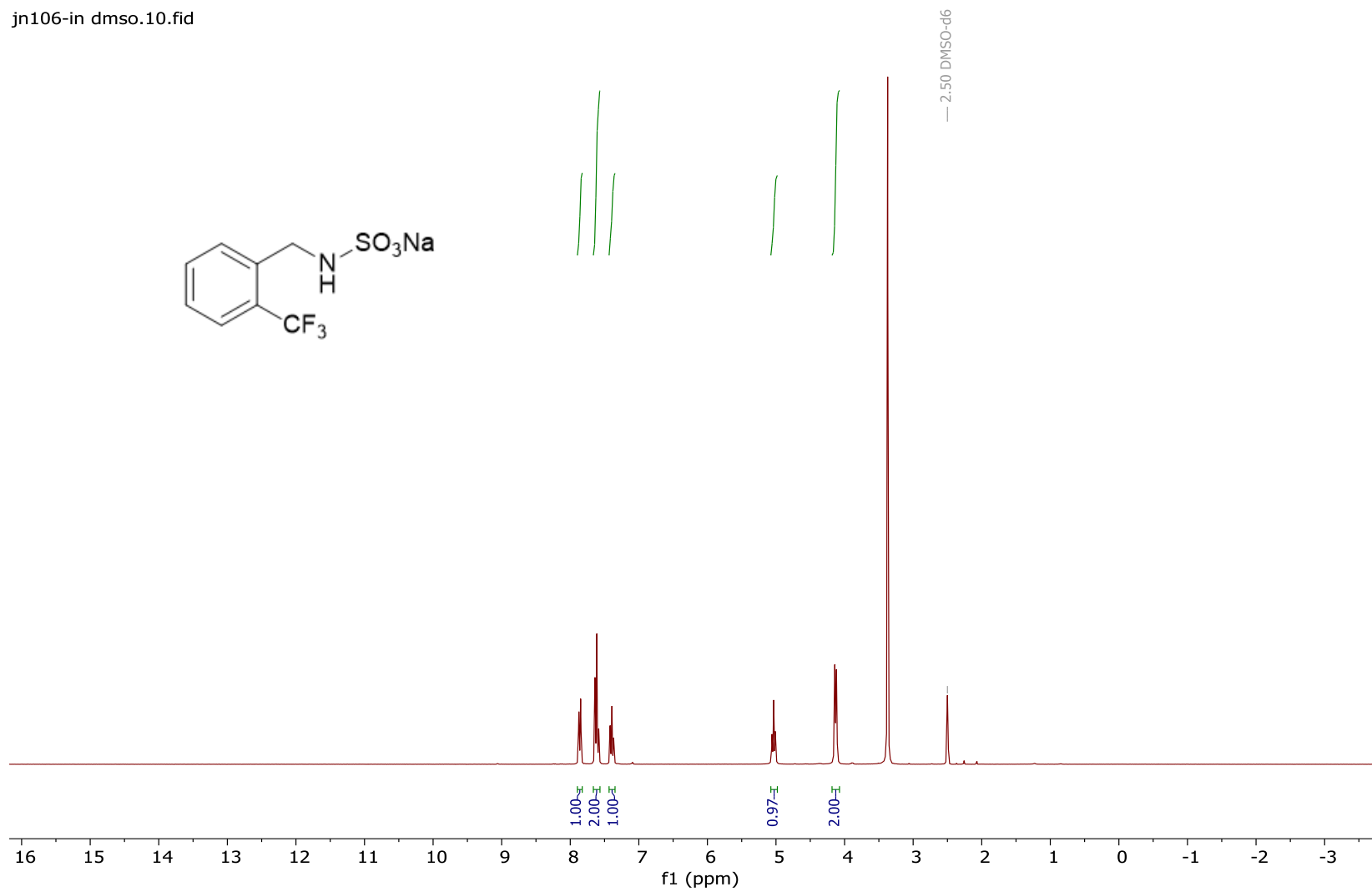


^{13}C NMR spectrum of **183** (101 MHz, D_2O)



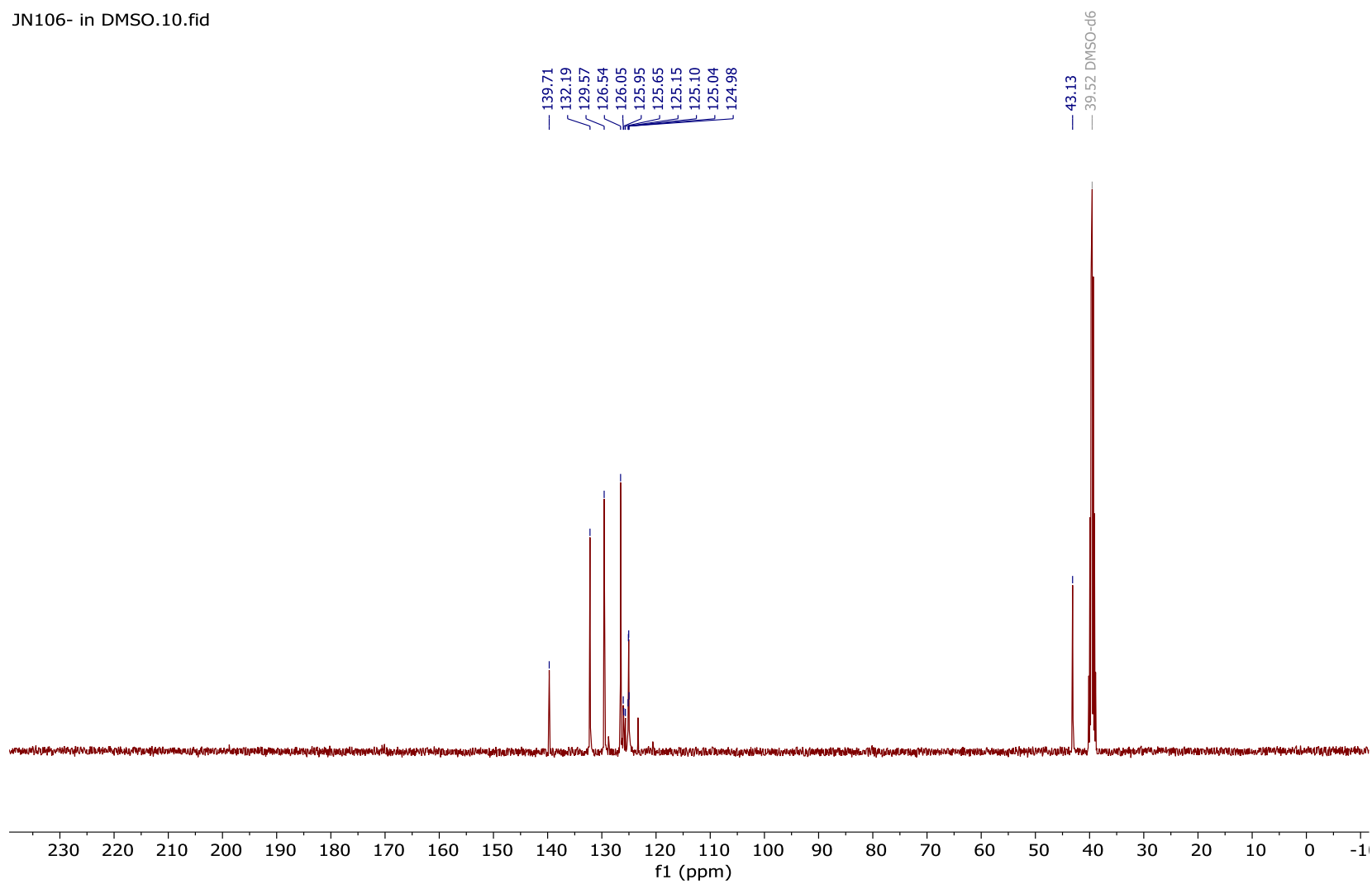
¹H NMR spectrum of **184** (300 MHz, DMSO-*d*₆)

jn106-in dms0.10.fid



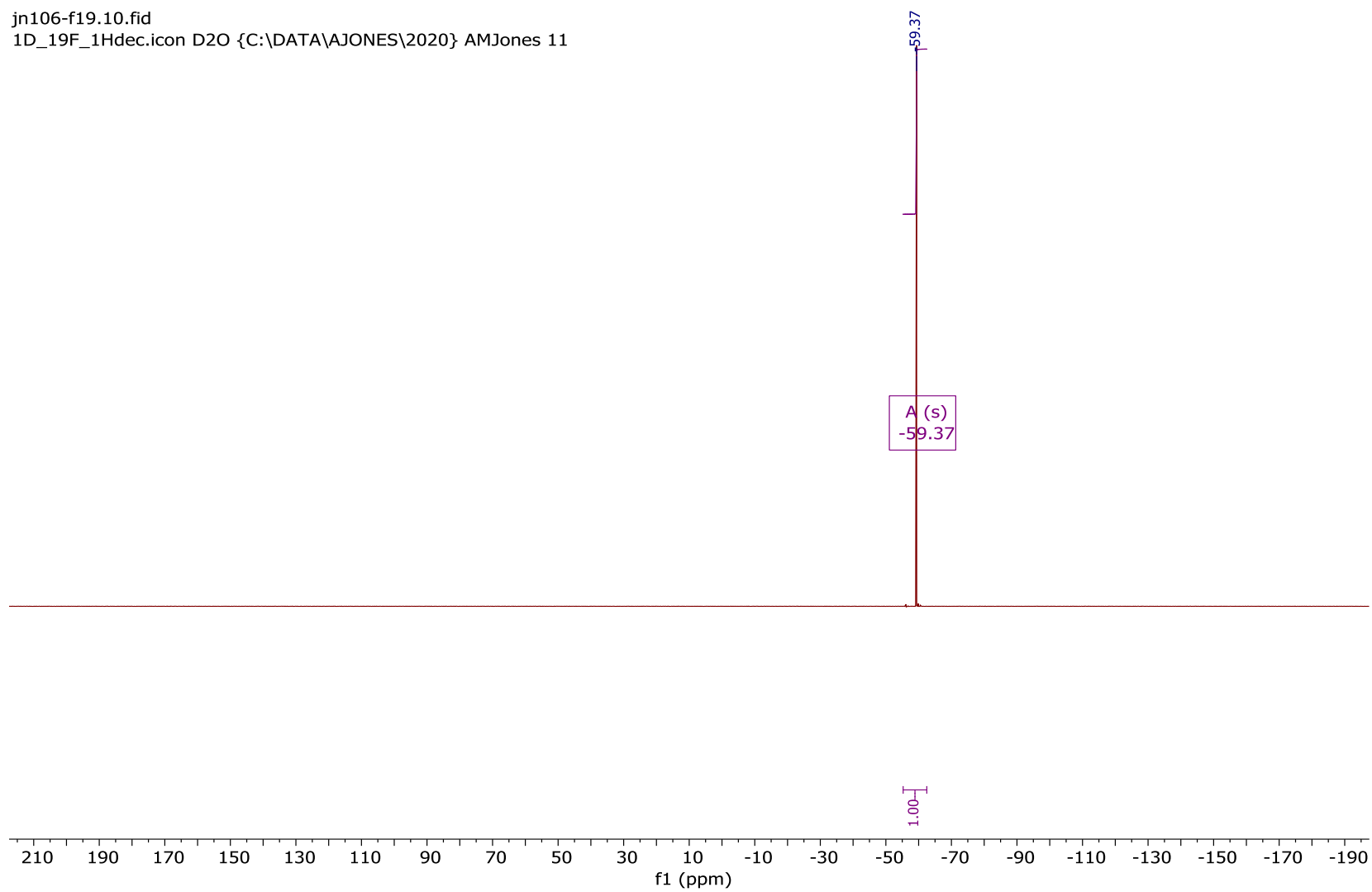
¹³C NMR spectrum of **184** (101 MHz, DMSO-*d*₆)

JN106- in DMSO.10.fid



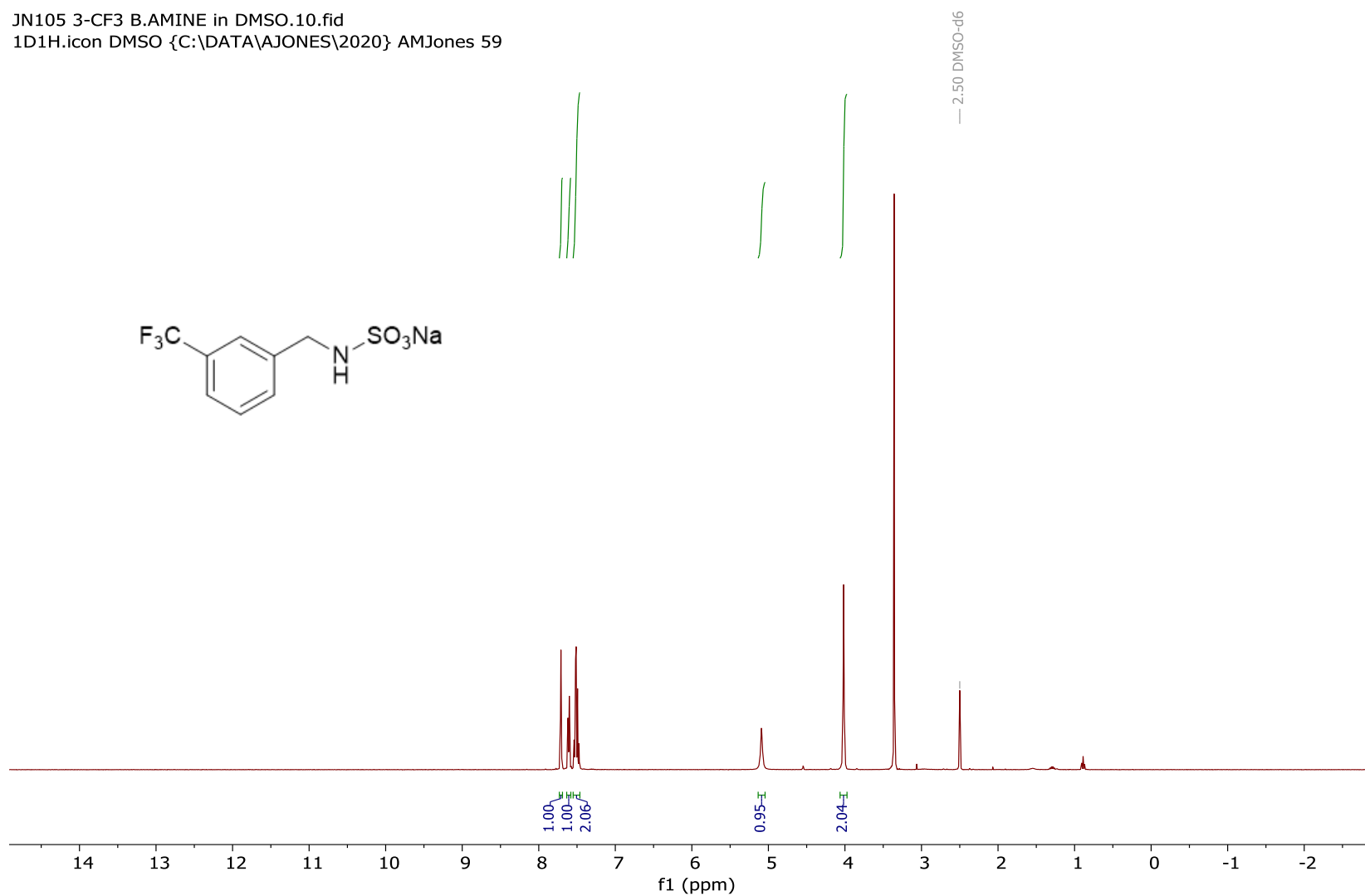
^{19}F NMR spectrum of **184** (377 MHz, D_2O)

jn106-f19.10.fid
1D_19F_1Hdec.icon D2O {C:\DATA\AJONES\2020} AMJones 11



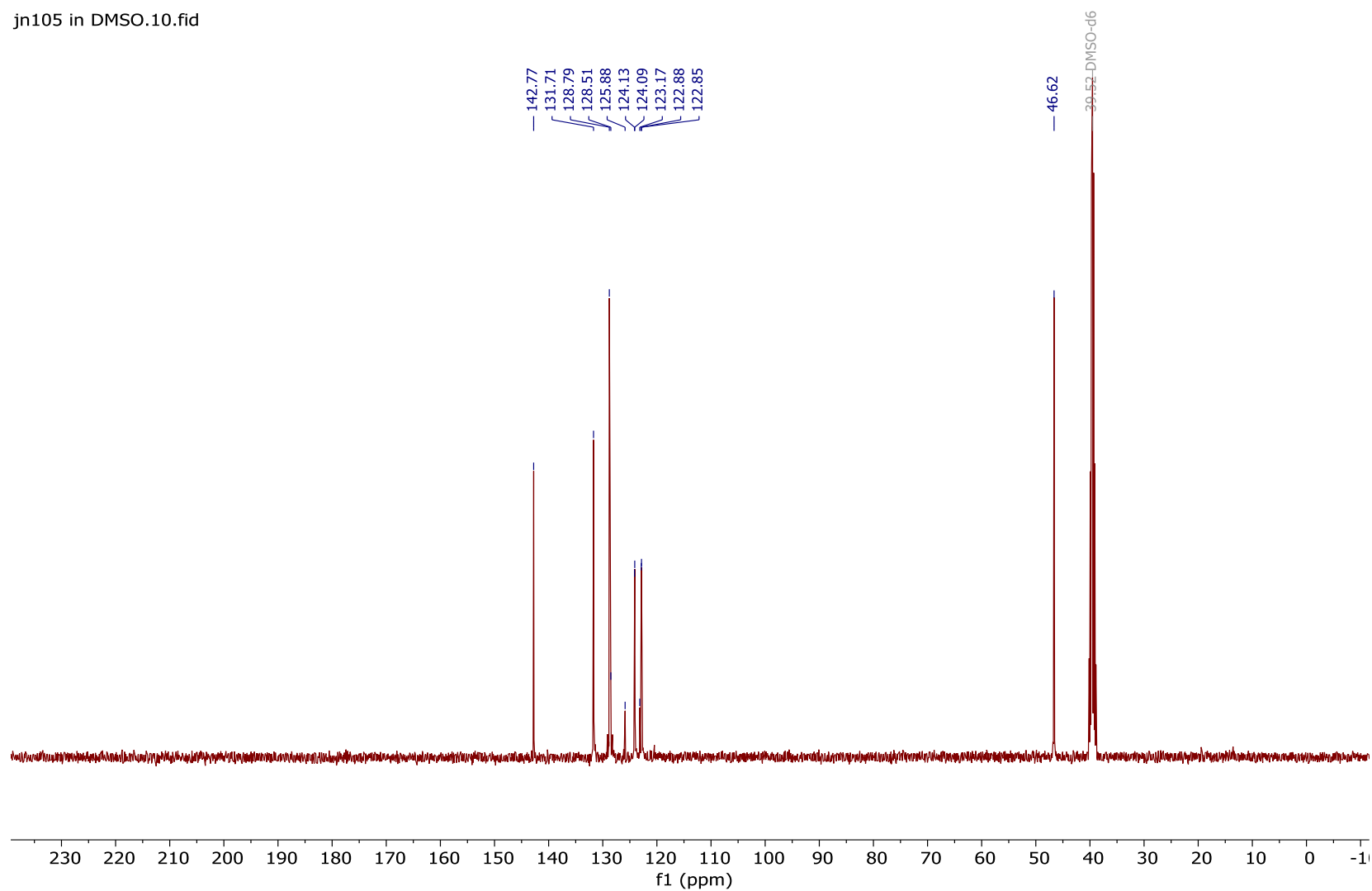
¹H NMR spectrum of **185** (300 MHz, DMSO-*d*₆)

JN105 3-CF3 B.AMINE in DMSO.10.fid
1D1H.icon DMSO {C:\DATA\AJONES\2020} AMJones 59



^{13}C NMR spectrum of **185** (101 MHz, $\text{DMSO-}d_6$)

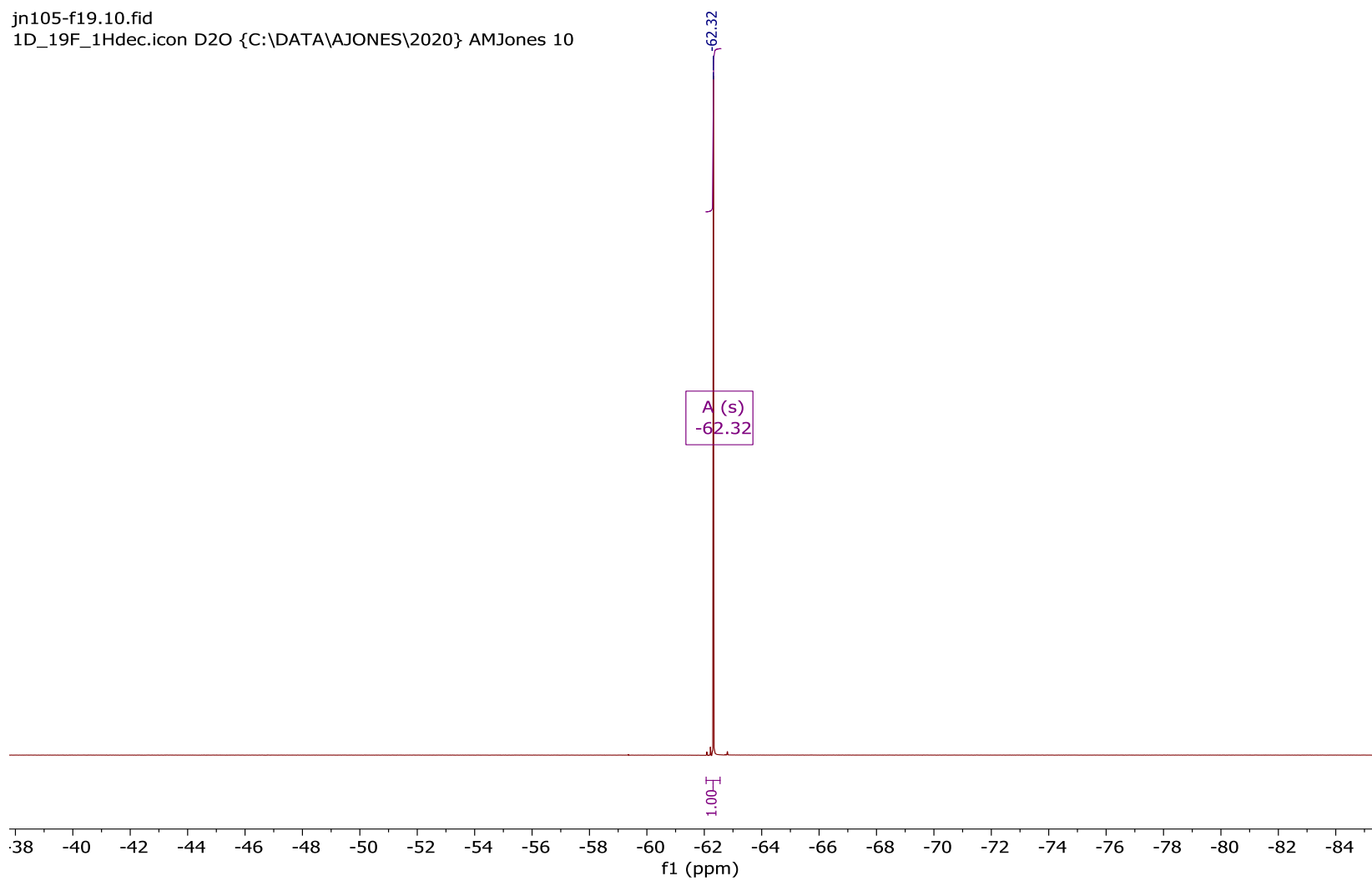
jn105 in DMSO.10.fid



¹⁹F NMR spectrum of **185** (377 MHz, D₂O)

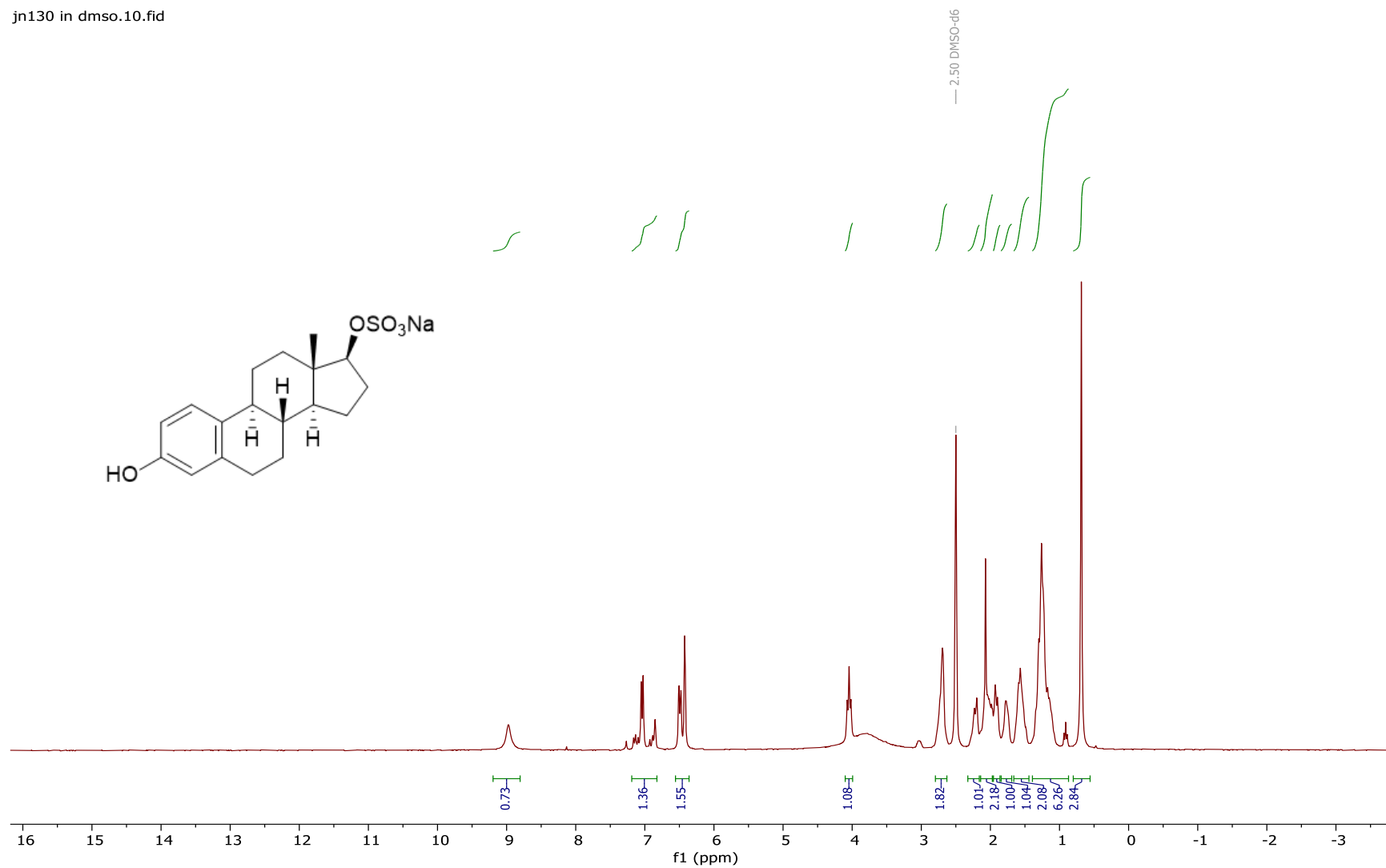
jn105-f19.10.fid

1D_19F_1Hdec.icon D2O {C:\DATA\AJONES\2020} AMJones 10



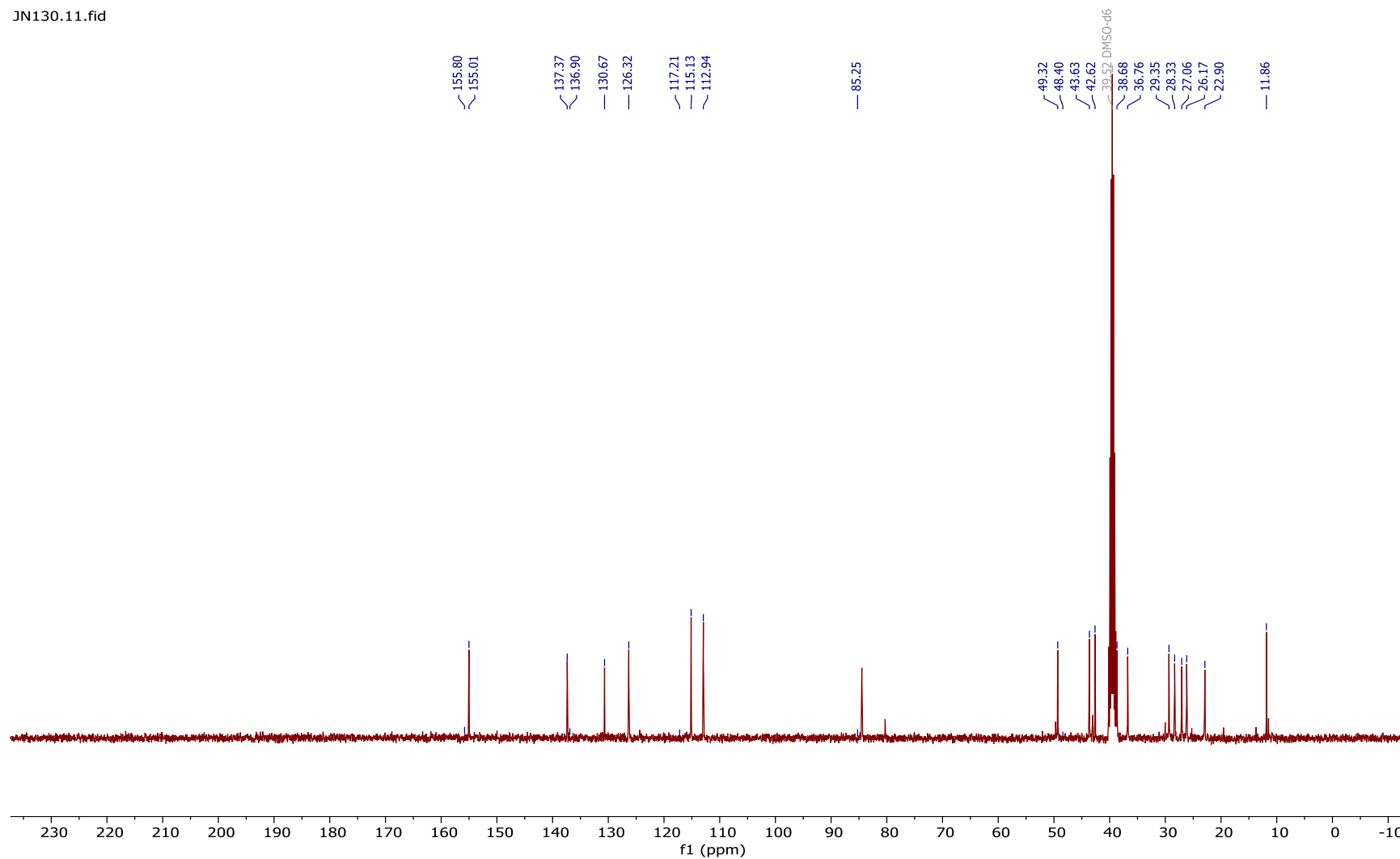
¹H NMR spectrum of **207** (400 MHz, DMSO-*d*₆)

jn130 in dms0.10.fid



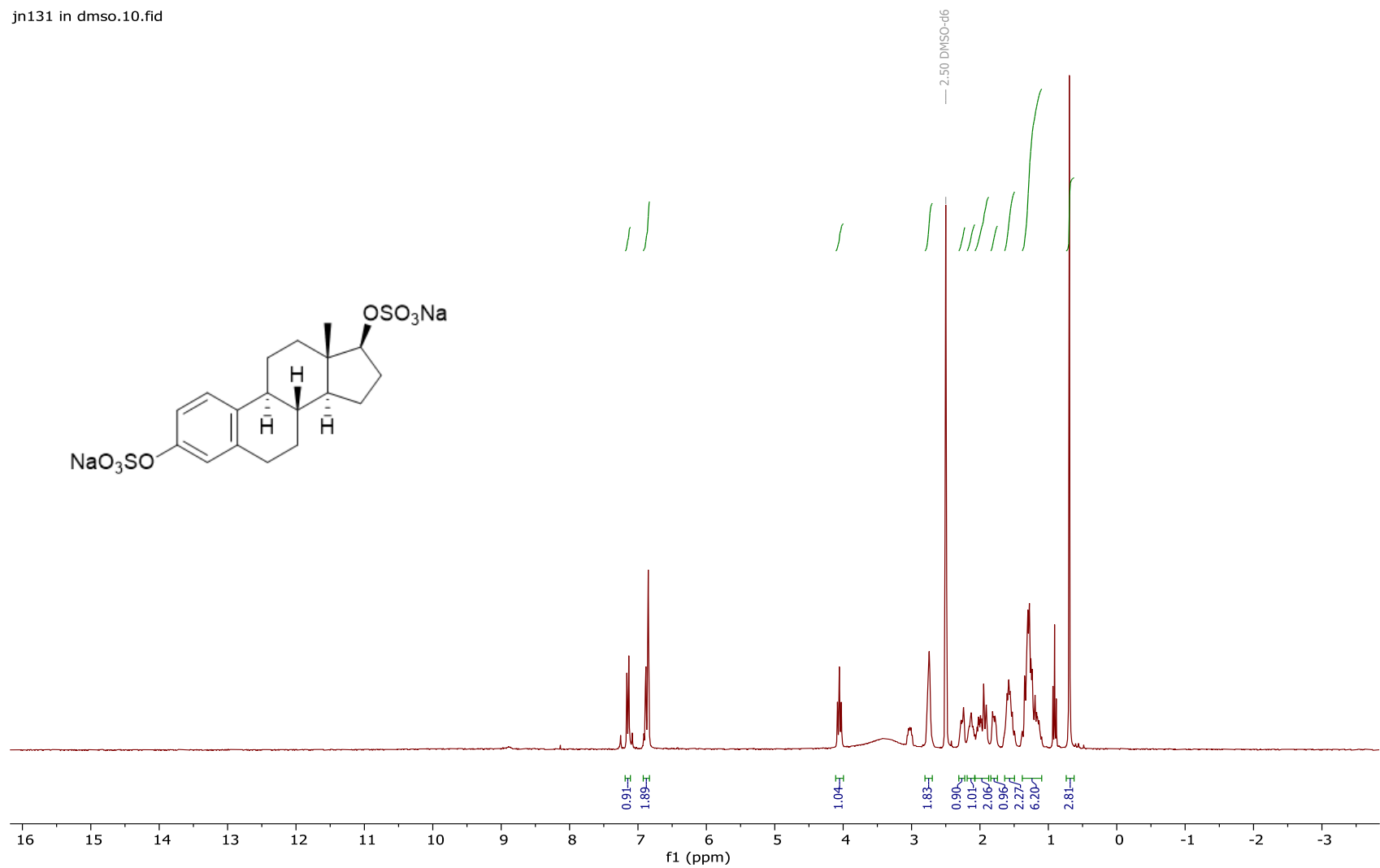
¹³C NMR spectrum of **207** (101 MHz, DMSO-*d*₆)

JN130.11.fid



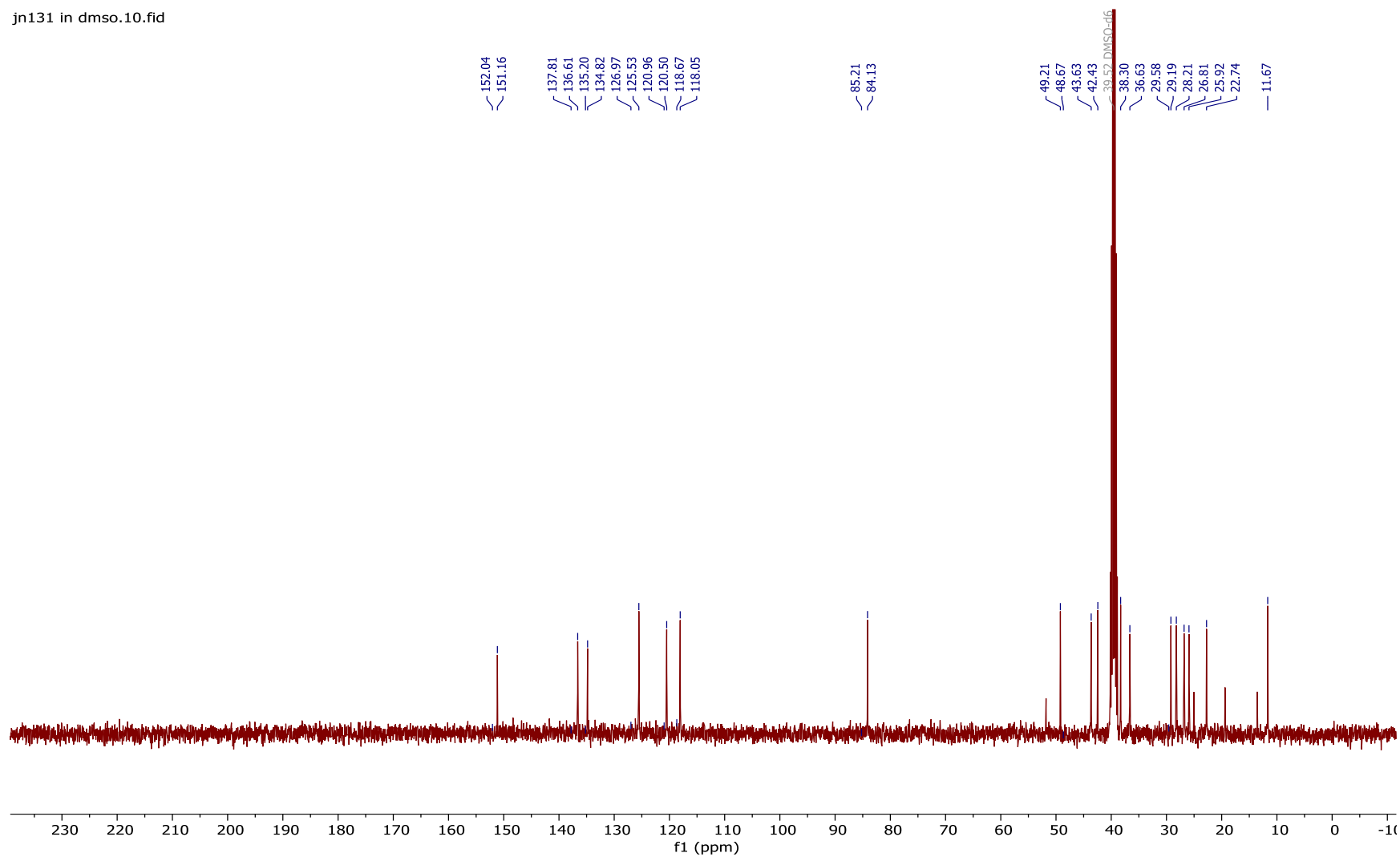
¹H NMR spectrum of **209** (400 MHz, DMSO-*d*₆)

jn131 in dms0.10.fid



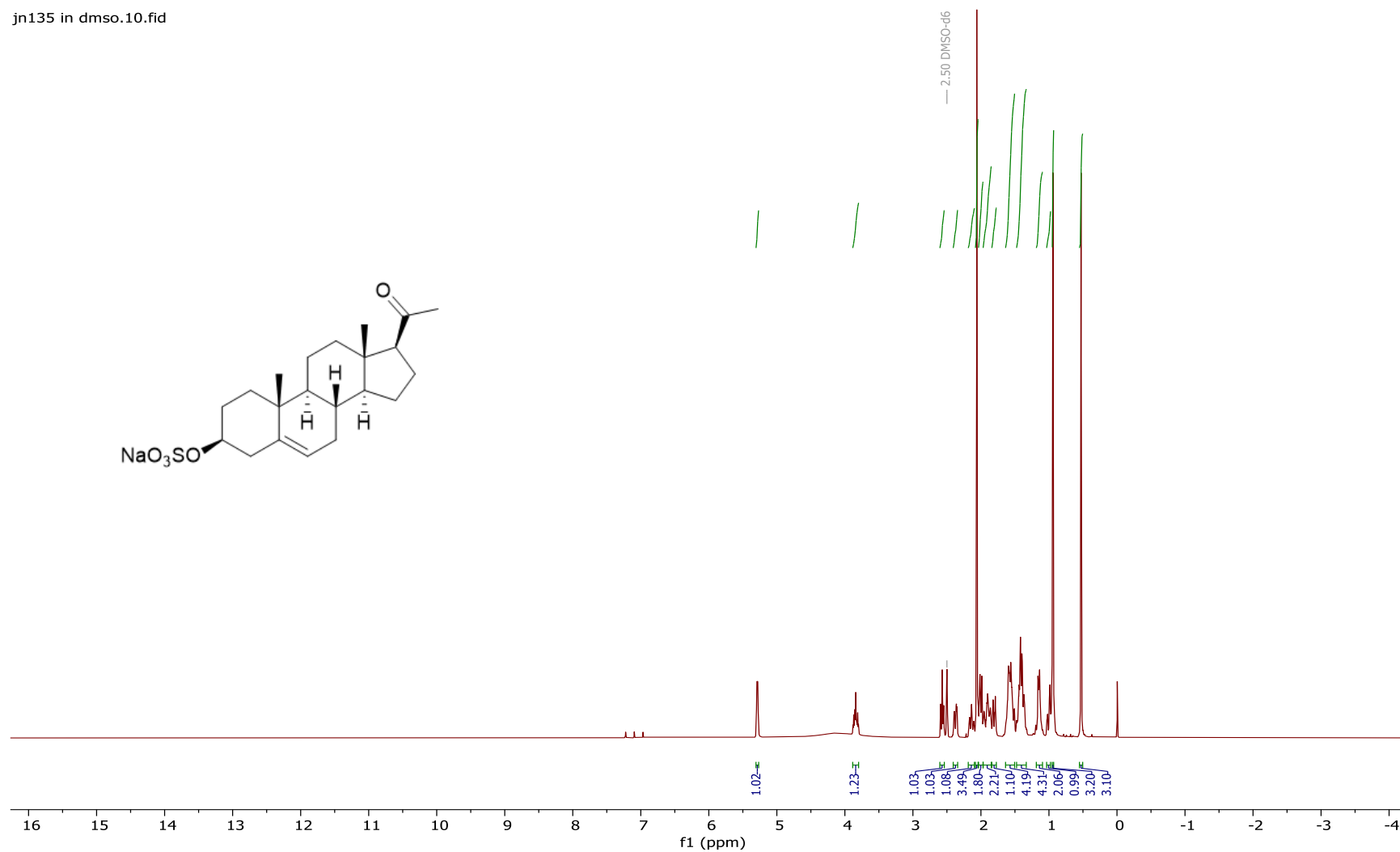
¹³C NMR spectrum of **209** (101 MHz, DMSO-*d*₆)

jn131 in dms0.10.fid



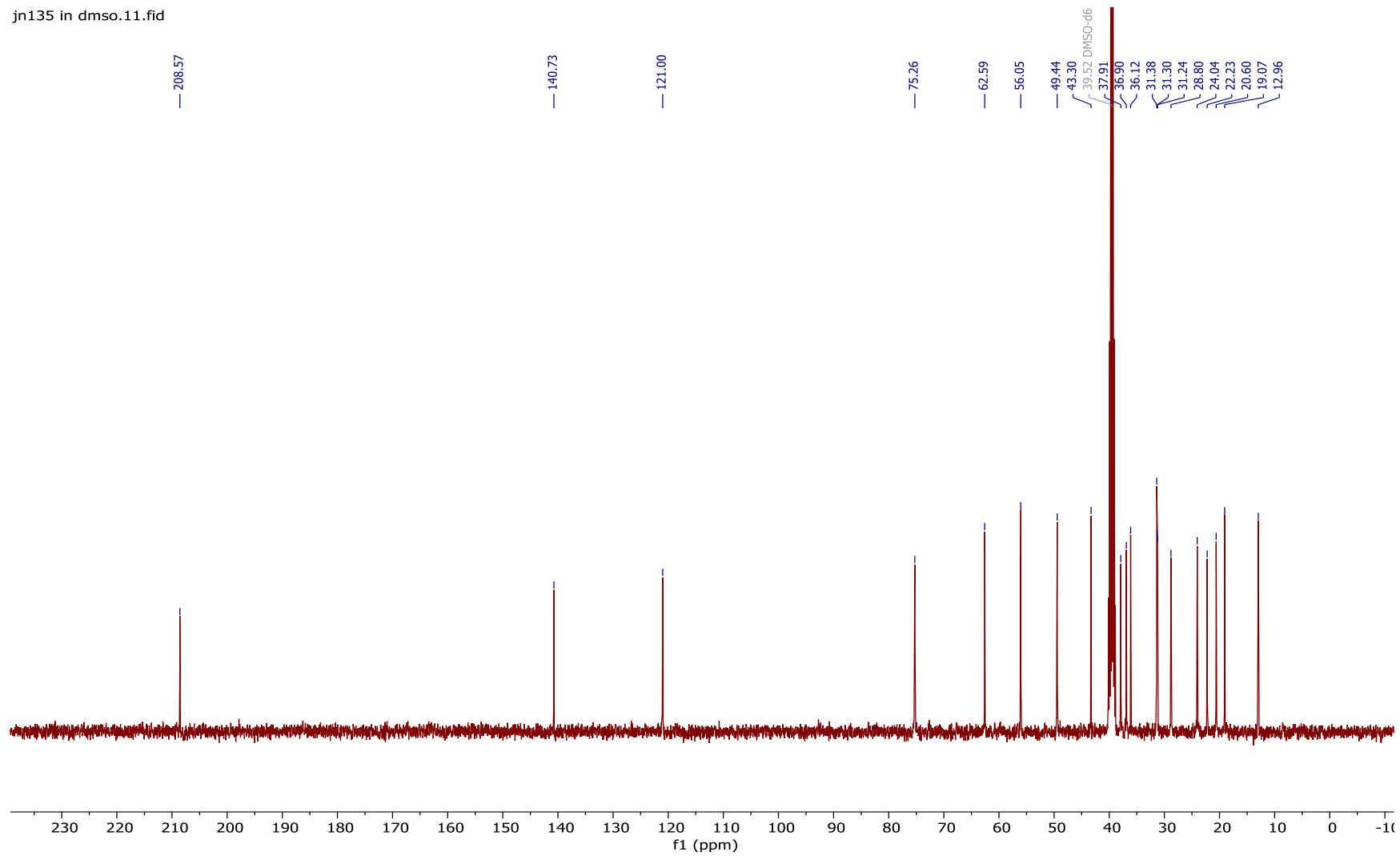
¹H NMR spectrum of **212** (400 MHz, DMSO-d₆)

jn135 in dms0.10.fid



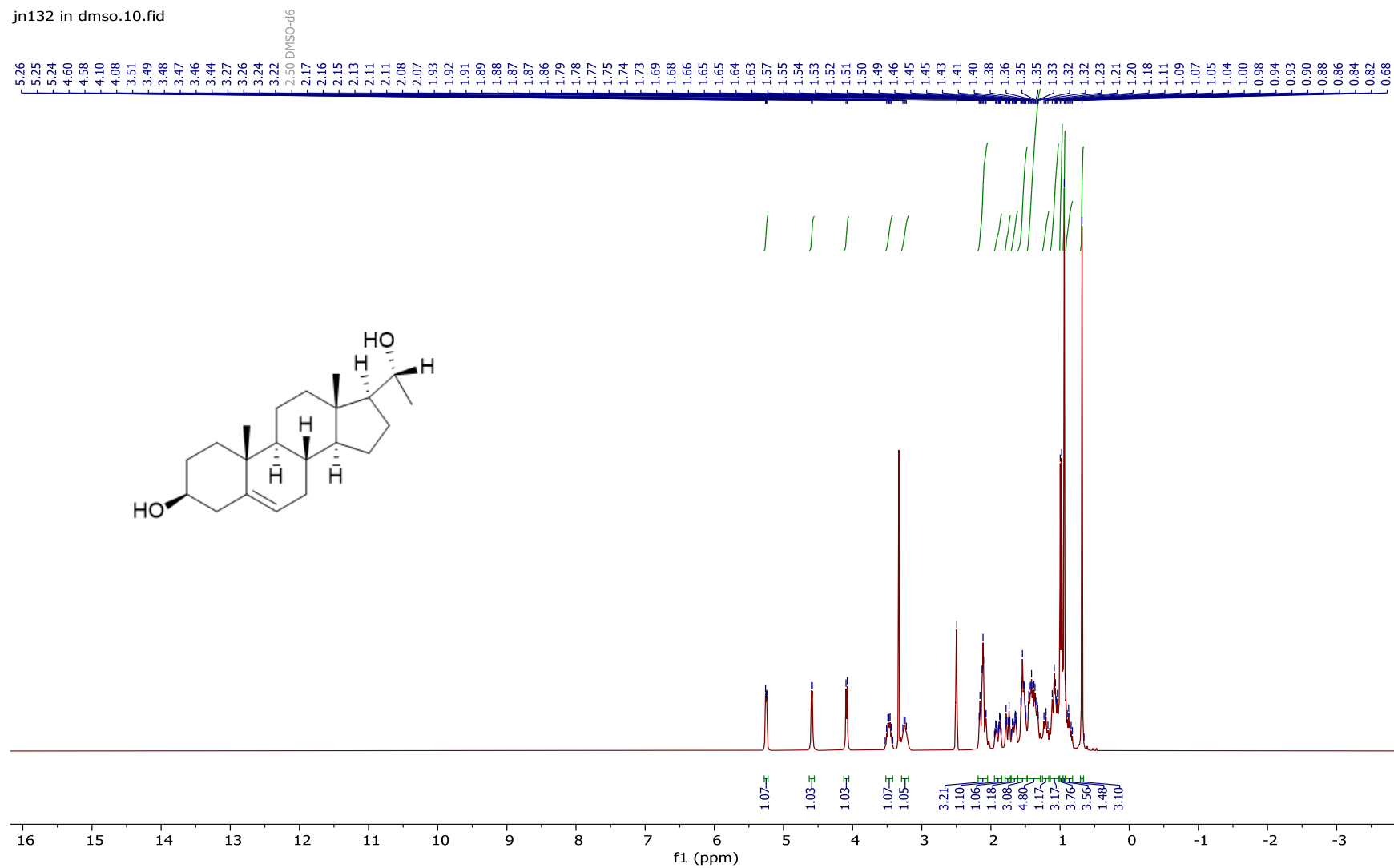
¹³C NMR spectrum of **212** (101 MHz, DMSO-*d*₆)

jn135 in dms0.11.fid



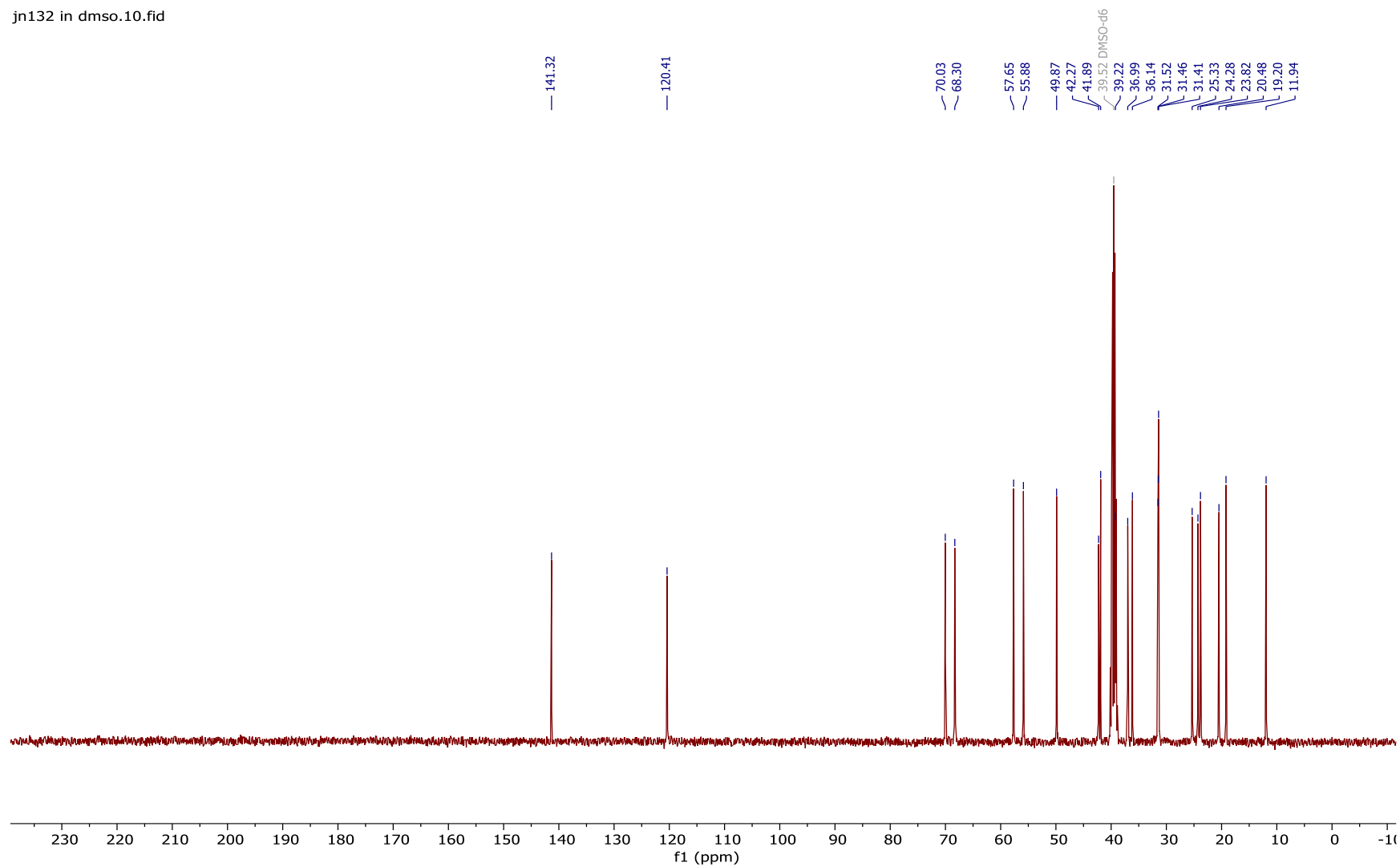
¹H NMR spectrum of **213** (400 MHz, DMSO-d₆)

jn132 in dms0.10.fid



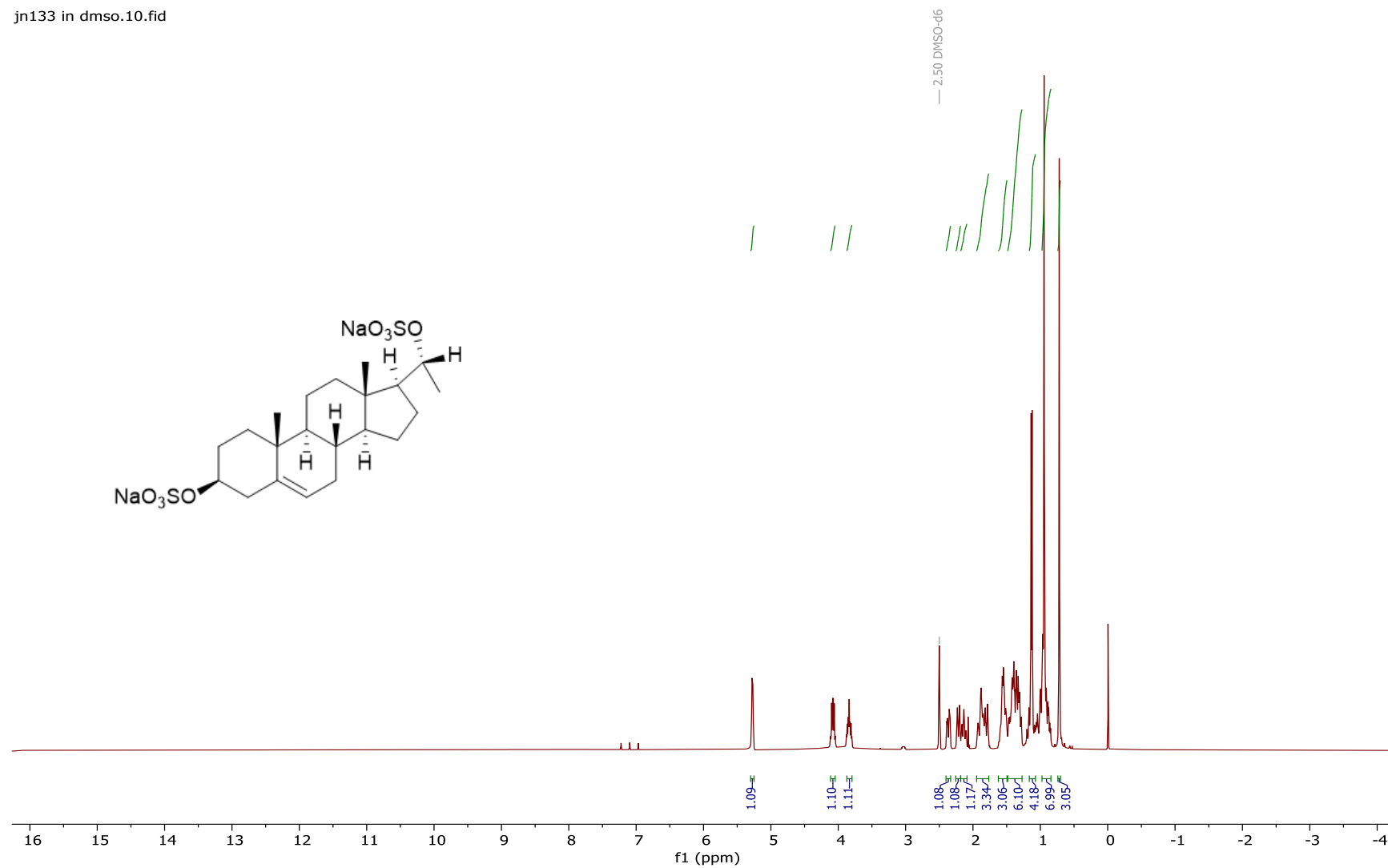
¹³C NMR spectrum of **213** (101 MHz, DMSO-d₆)

jn132 in dms0.10.fid



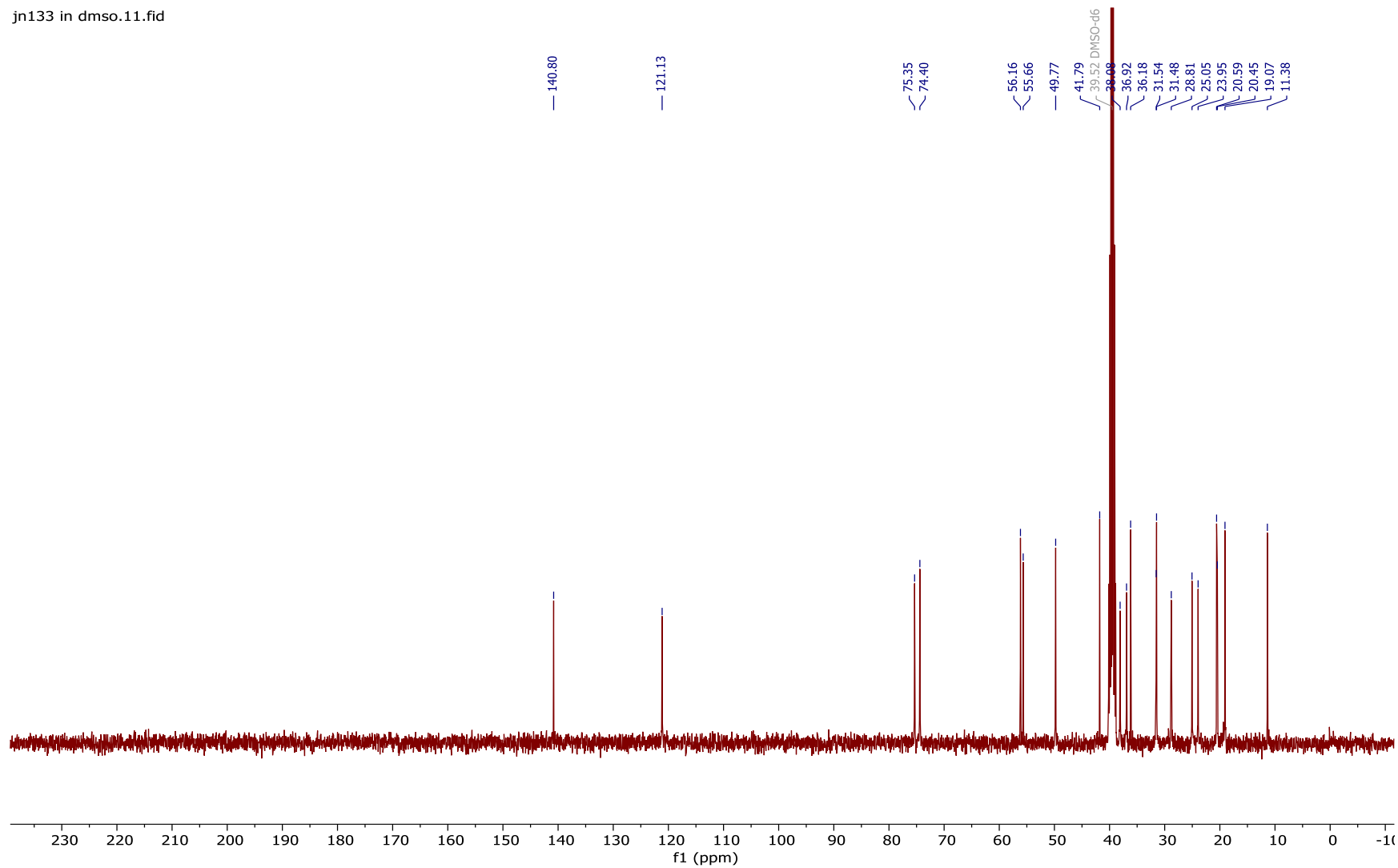
^1H NMR spectrum of **215** (400 MHz, $\text{DMSO-}d_6$)

jn133 in dms0.10.fid



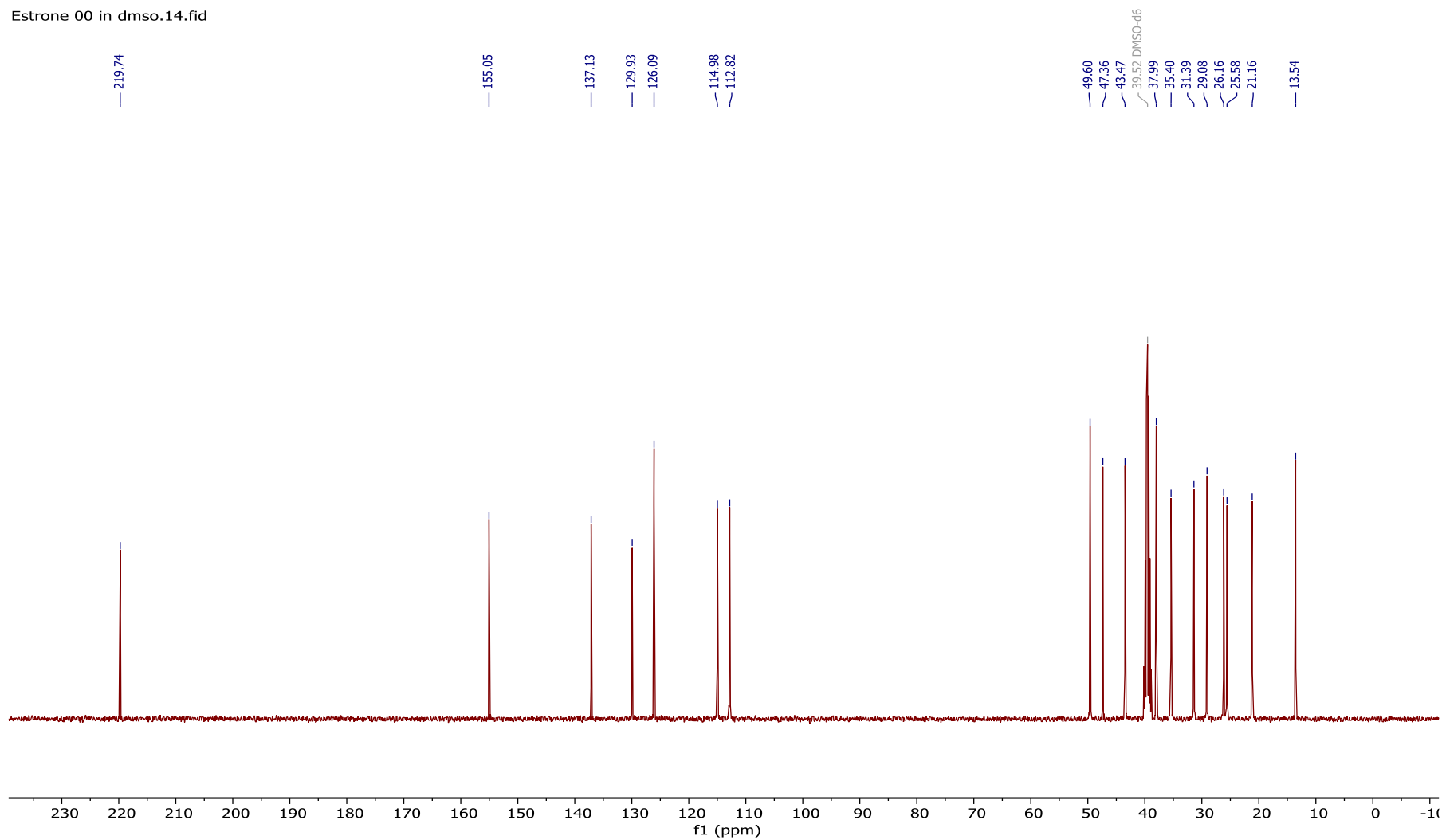
¹³C NMR spectrum of **215** (101 MHz, DMSO-d₆)

jn133 in dms0.11.fid



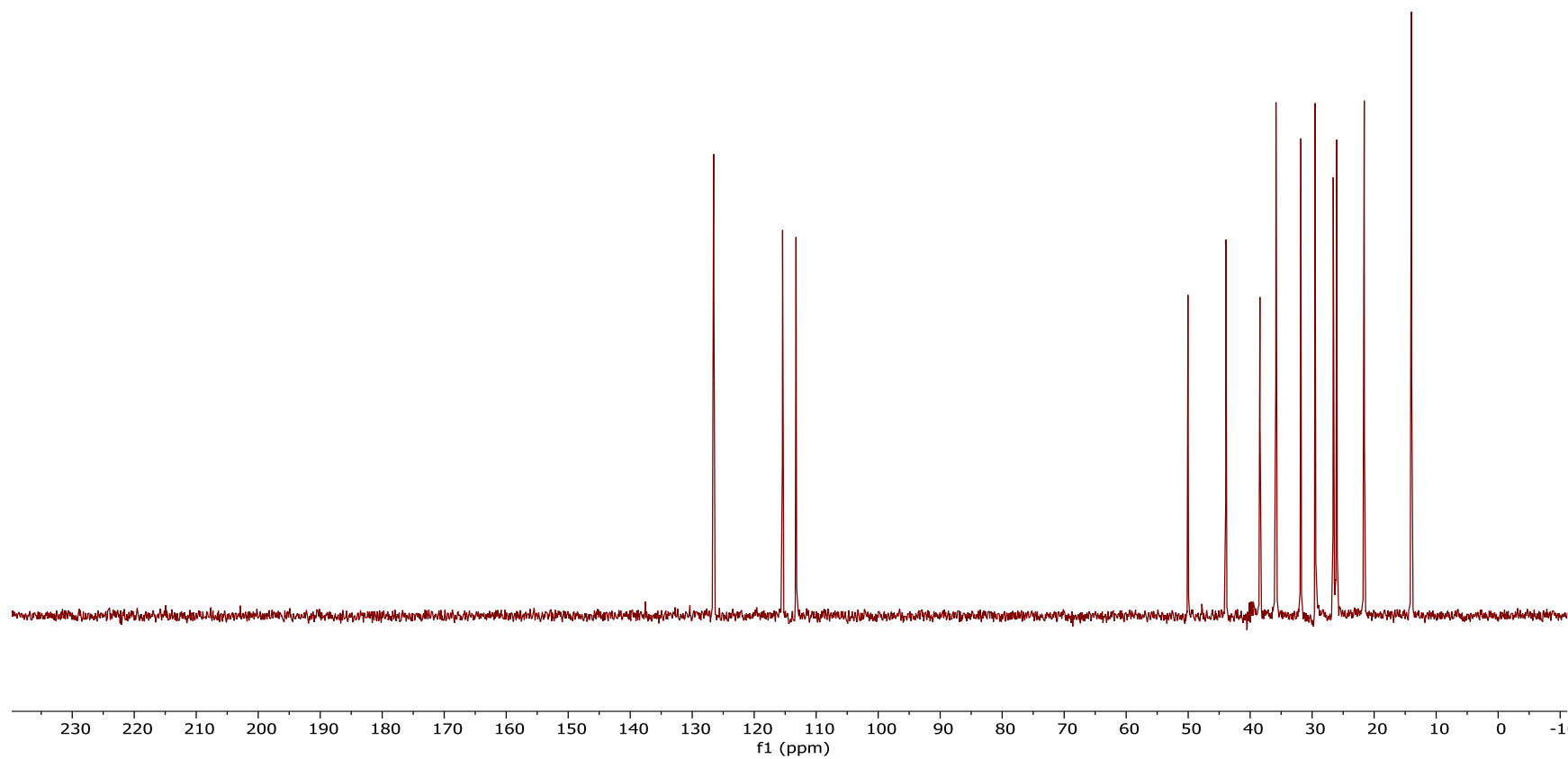
¹³C NMR spectrum of **219** (101 MHz, DMSO-d₆)

Estrone 00 in dms0.14.fid

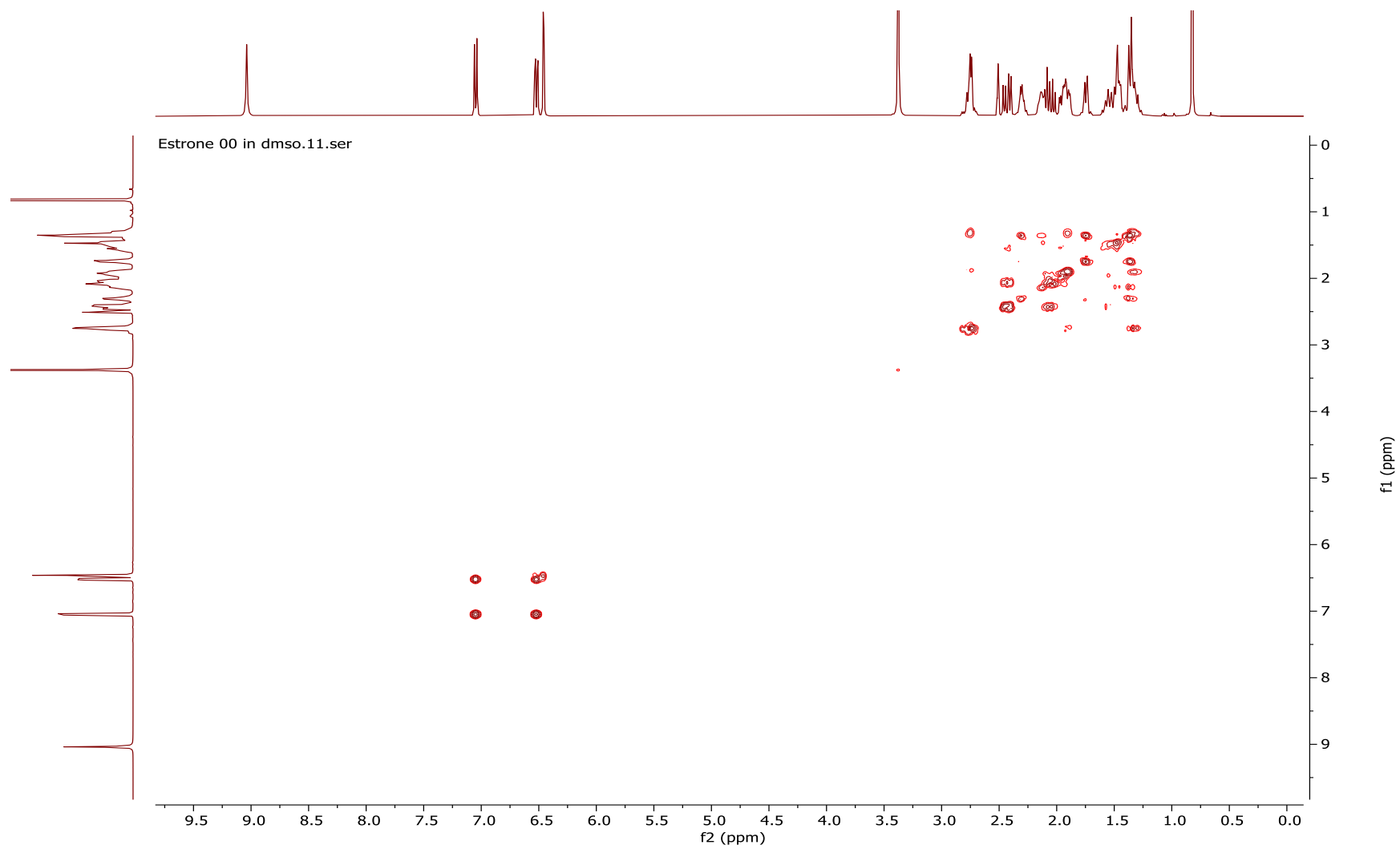


DEPT-45 spectrum of **219** (101 MHz, DMSO-*d*₆)

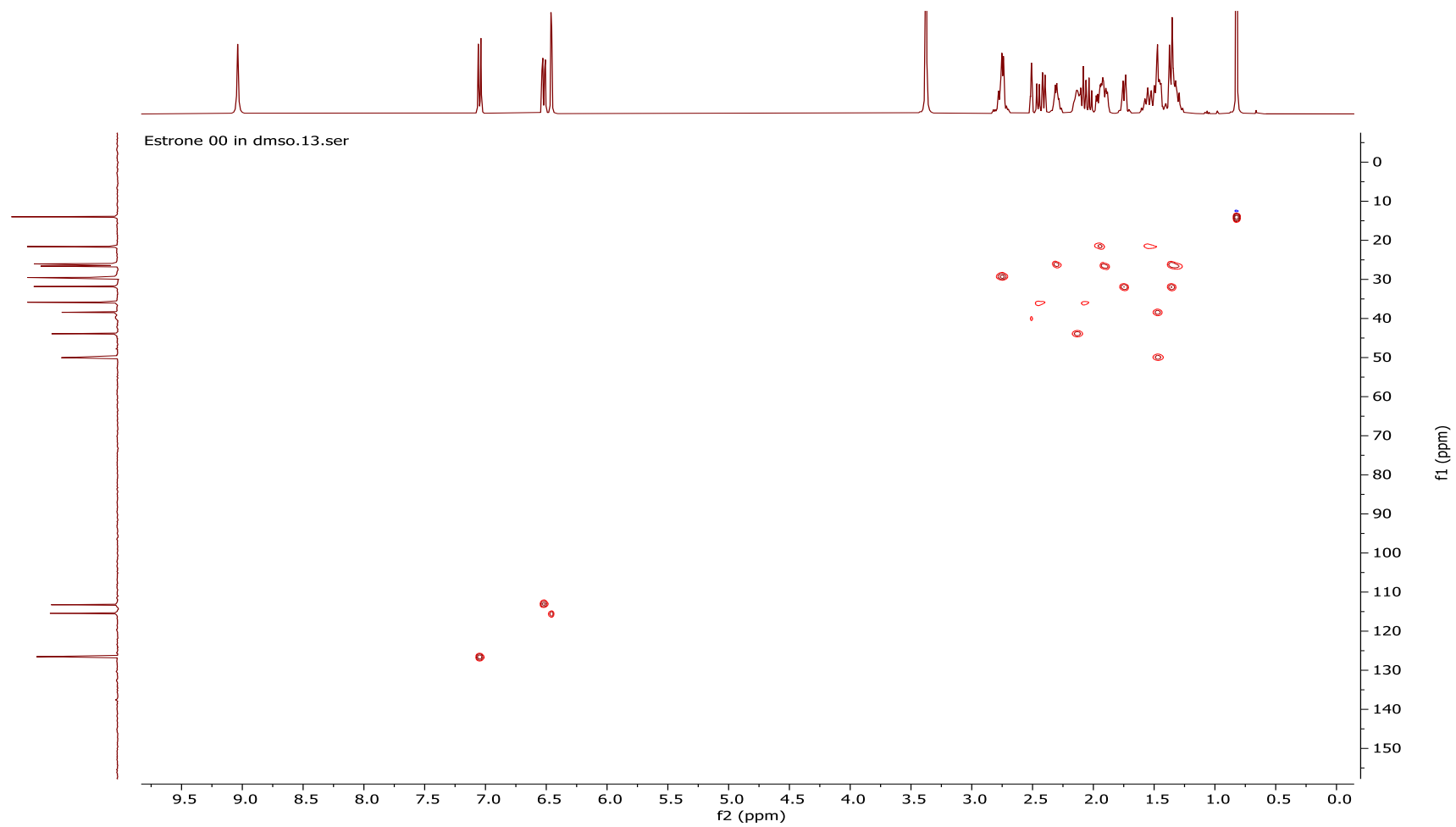
Estrone 00 in dms0.12.fid



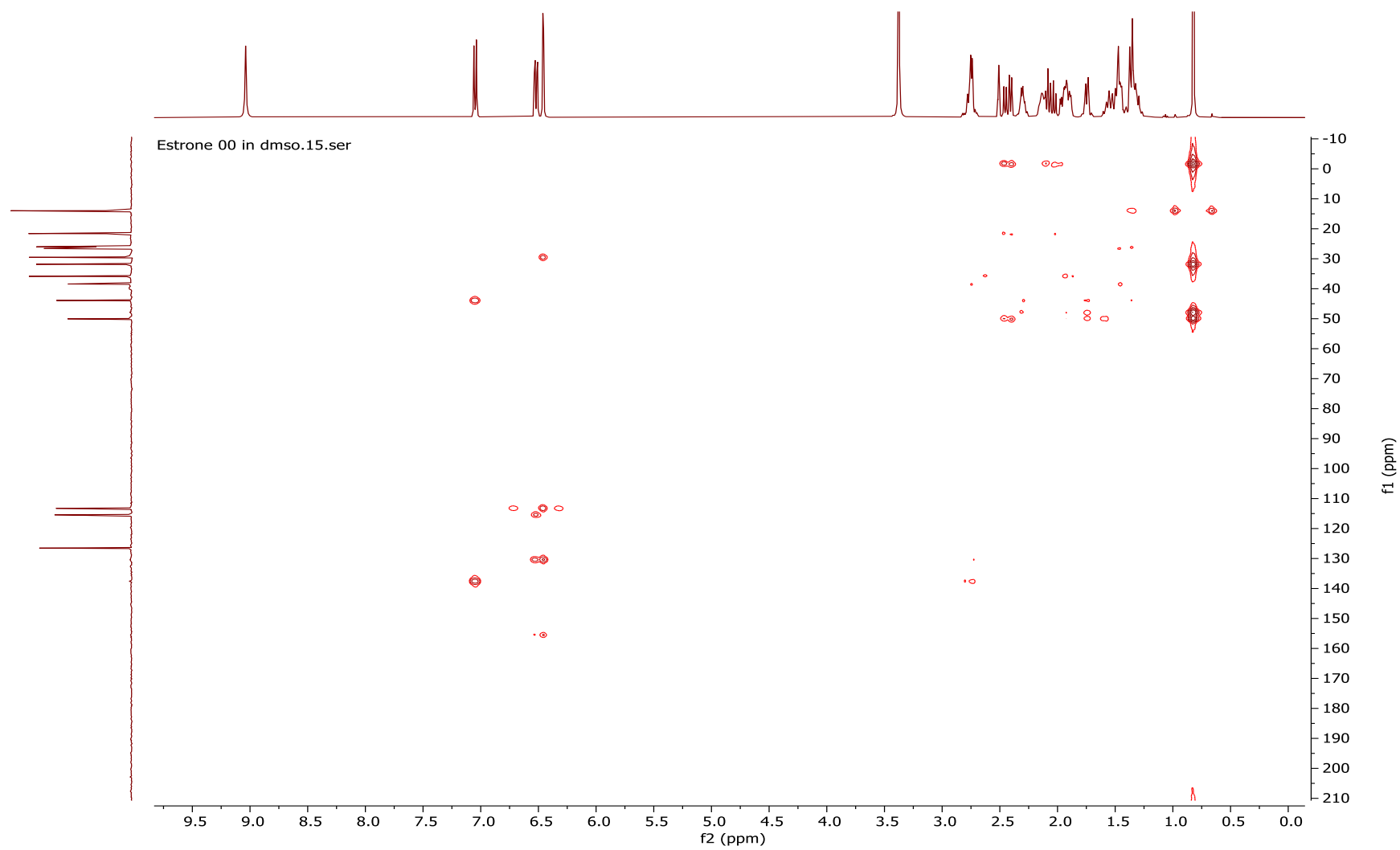
^1H - ^1H COSY spectrum of **219** (101 MHz, $\text{DMSO-}d_6$)



^1H - ^{13}C HSQC spectrum of **219** (101 MHz, $\text{DMSO-}d_6$)

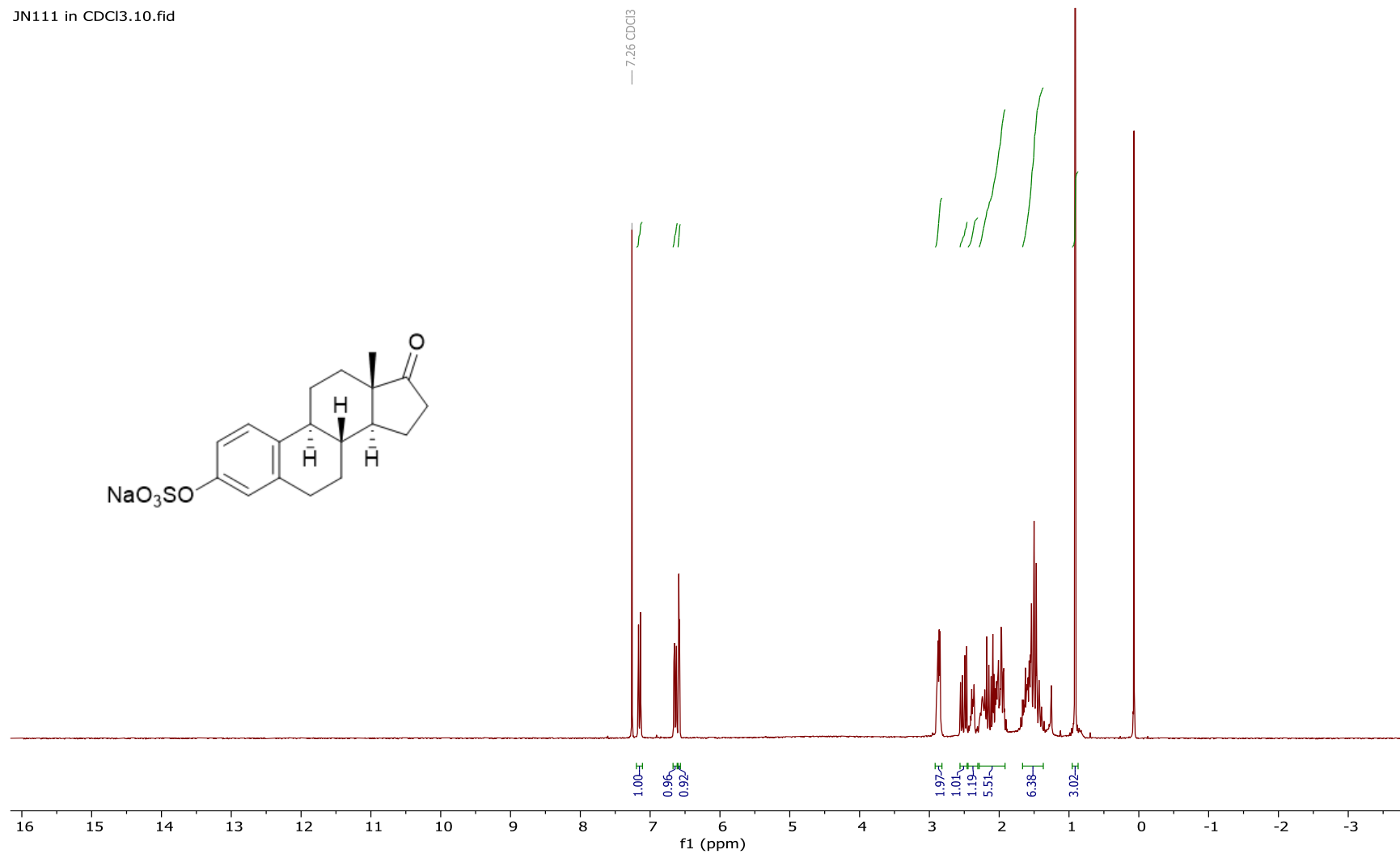
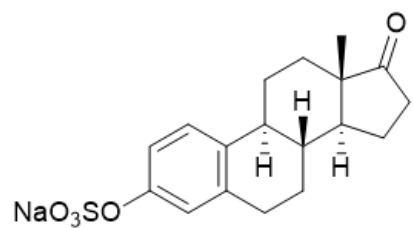


^1H - ^{13}C HMBC spectrum of **219** (101 MHz, $\text{DMSO-}d_6$)

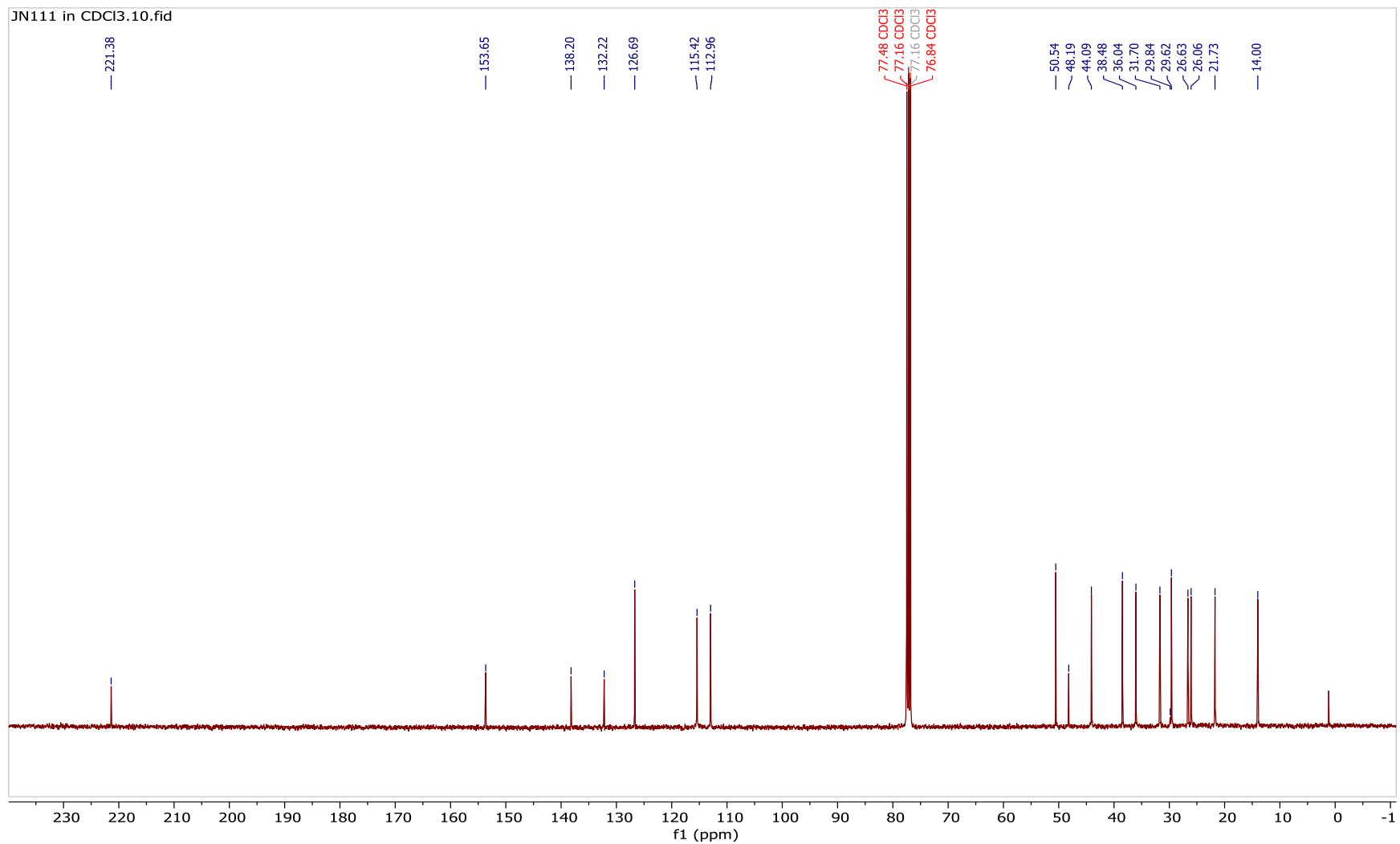


¹H NMR spectrum of **221** (300 MHz, CDCl₃)

JN111 in CDCl₃.10.fid

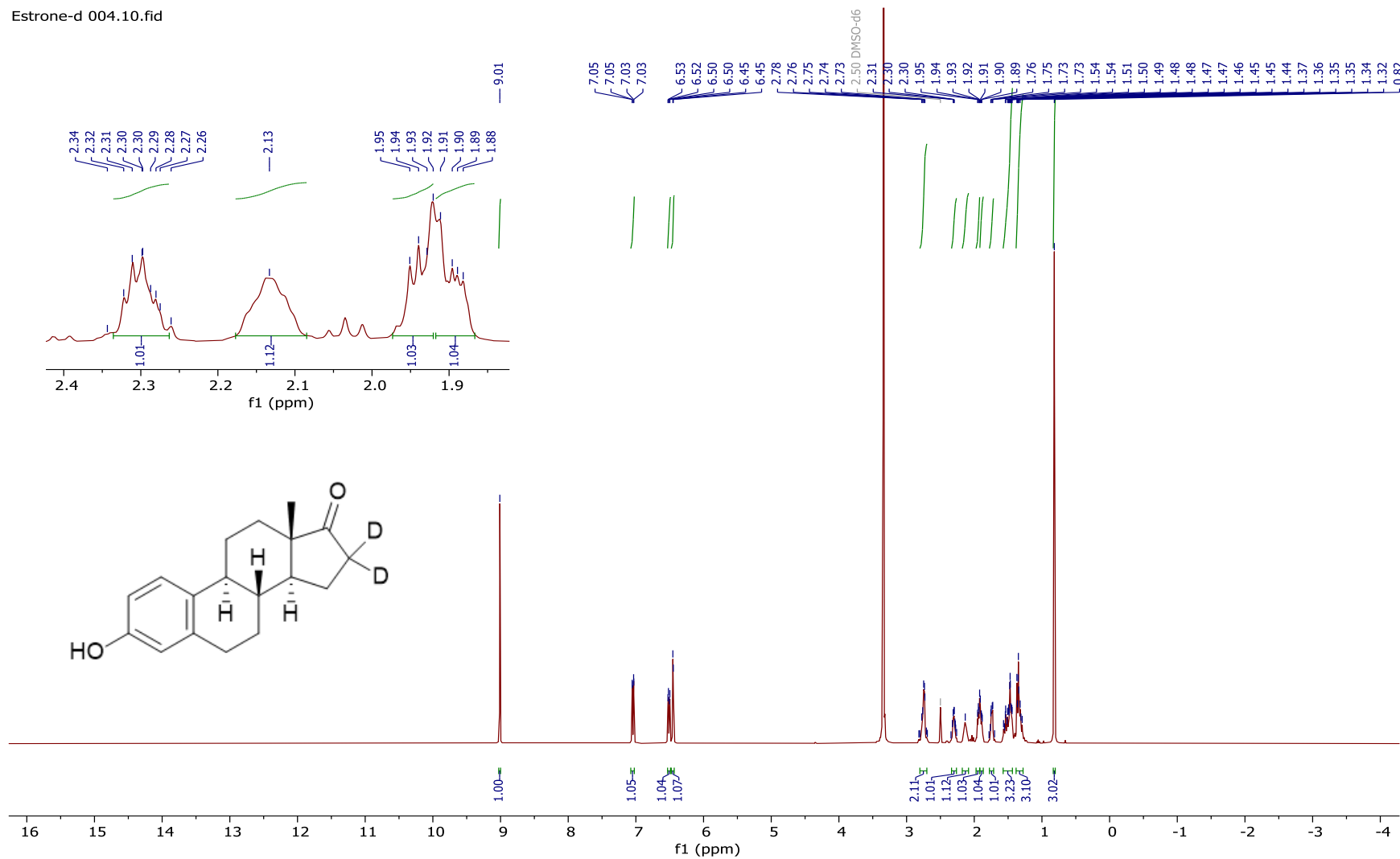


¹³C NMR spectrum of **221** (300 MHz, CDCl₃)



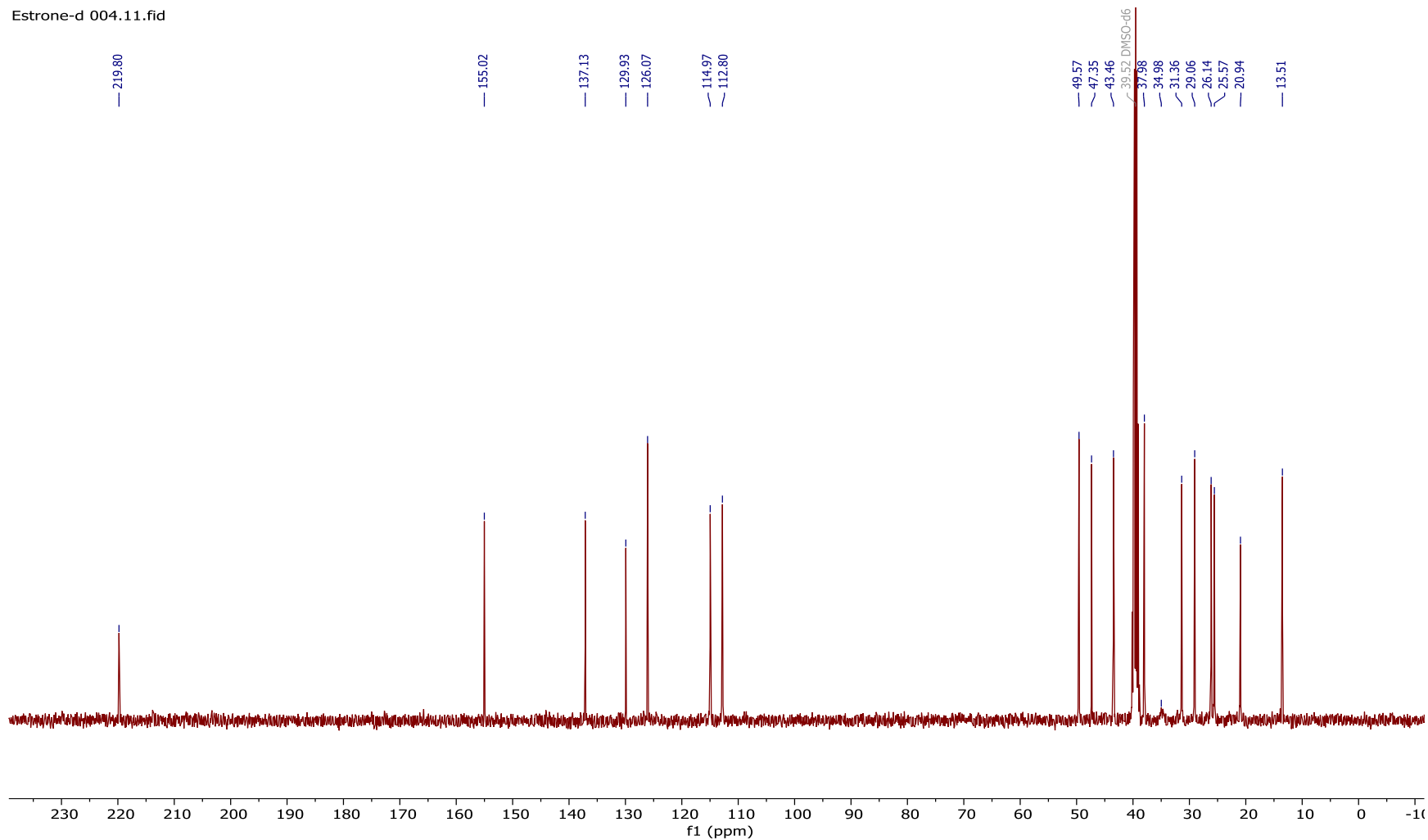
¹H NMR spectrum of **222** (400 MHz, DMSO-d₆)

Estrone-d 004.10.fid



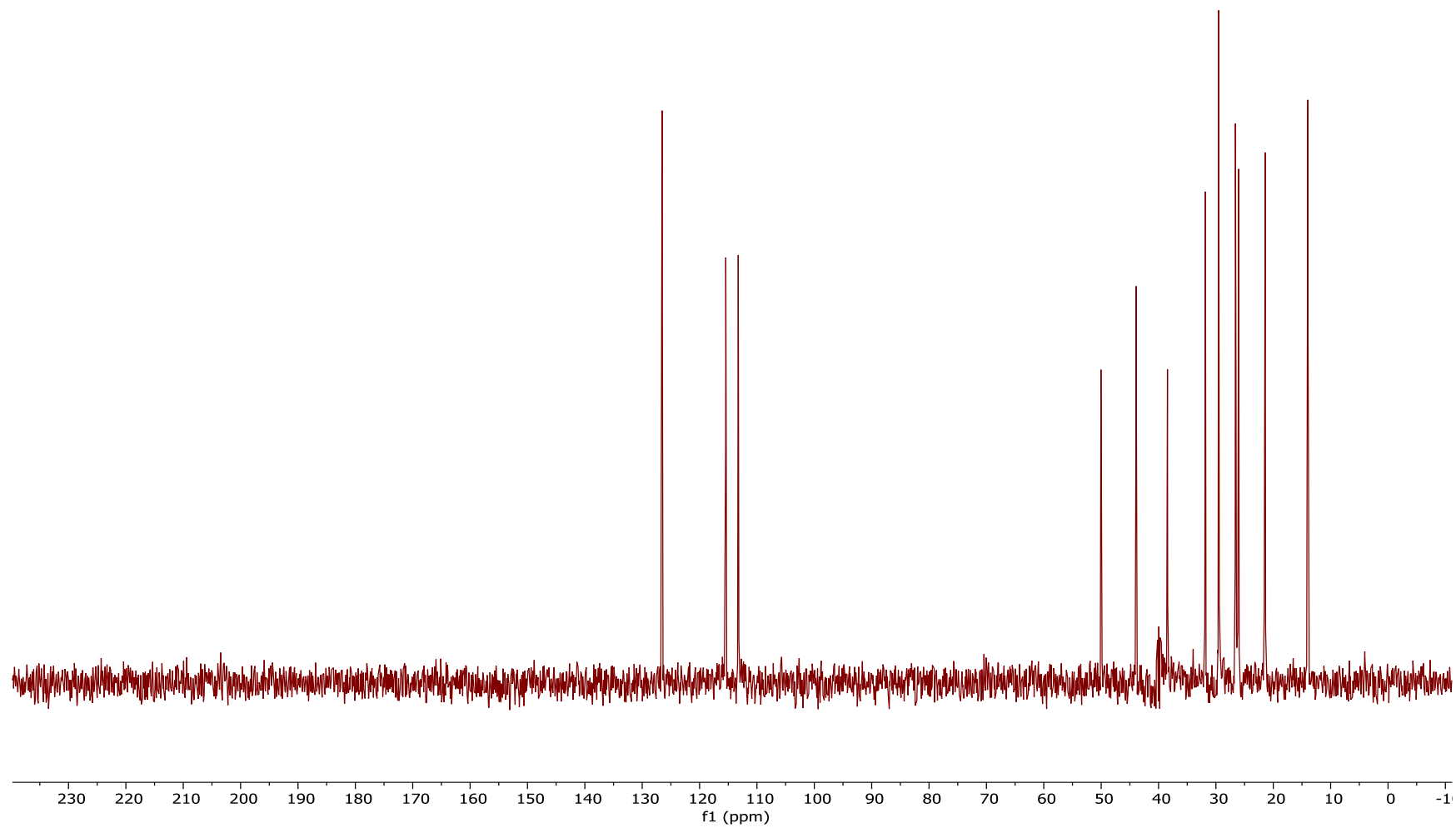
¹³C NMR spectrum of **222** (101 MHz, DMSO-d₆)

Estrone-d 004.11.fid

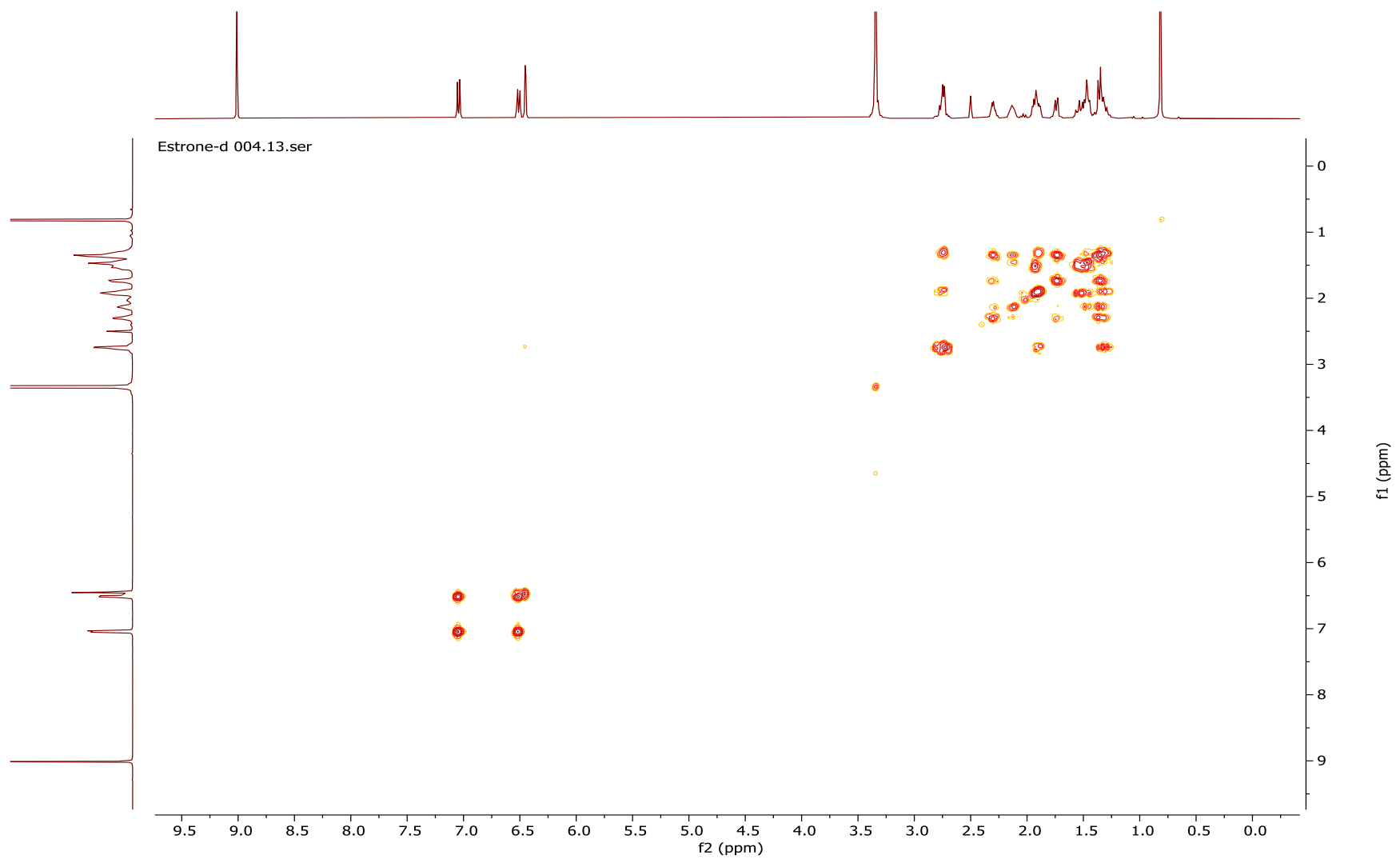


DEPT-45 spectrum of **222** (101 MHz, DMSO-*d*₆)

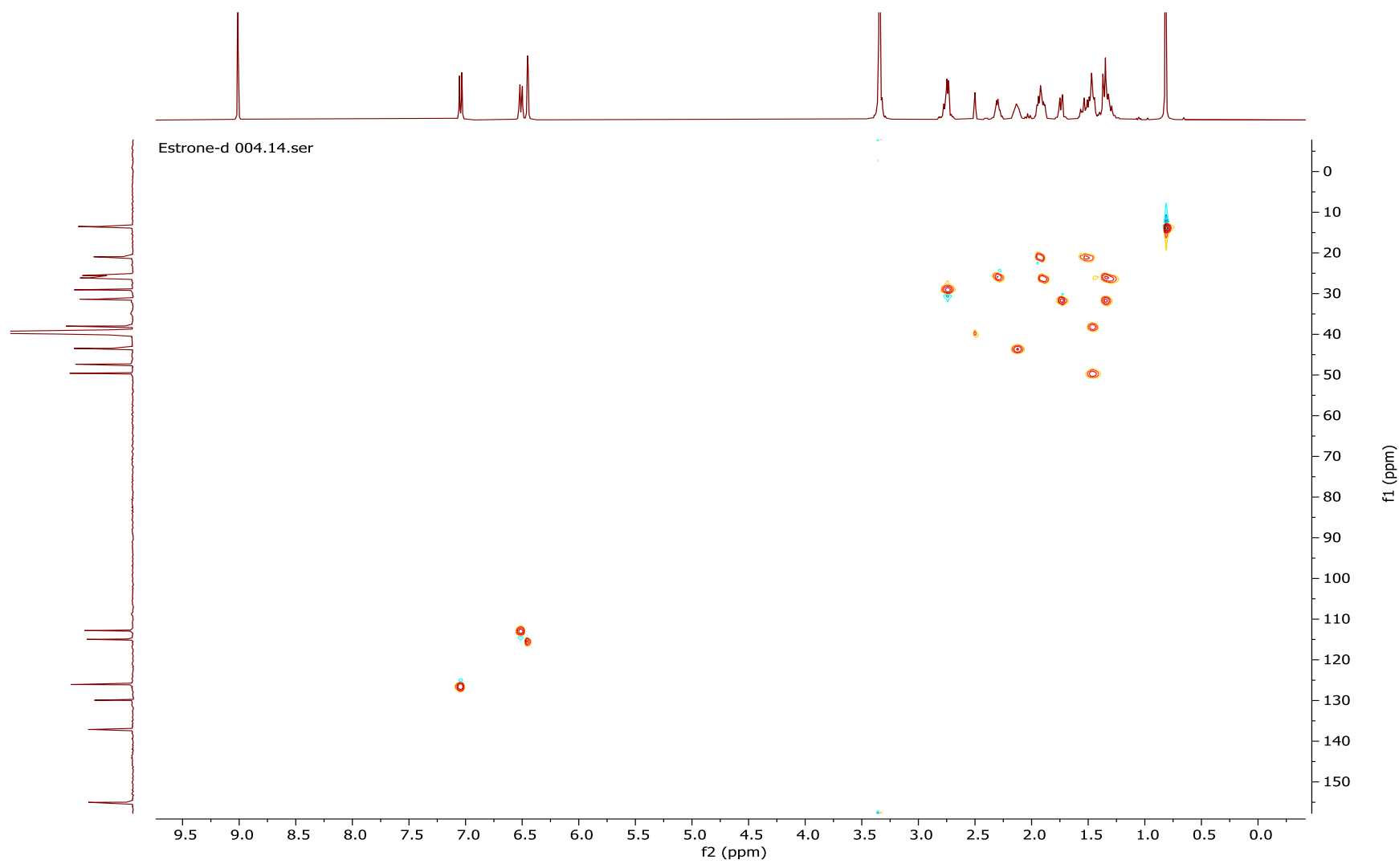
Estrone-d 004.12.fid



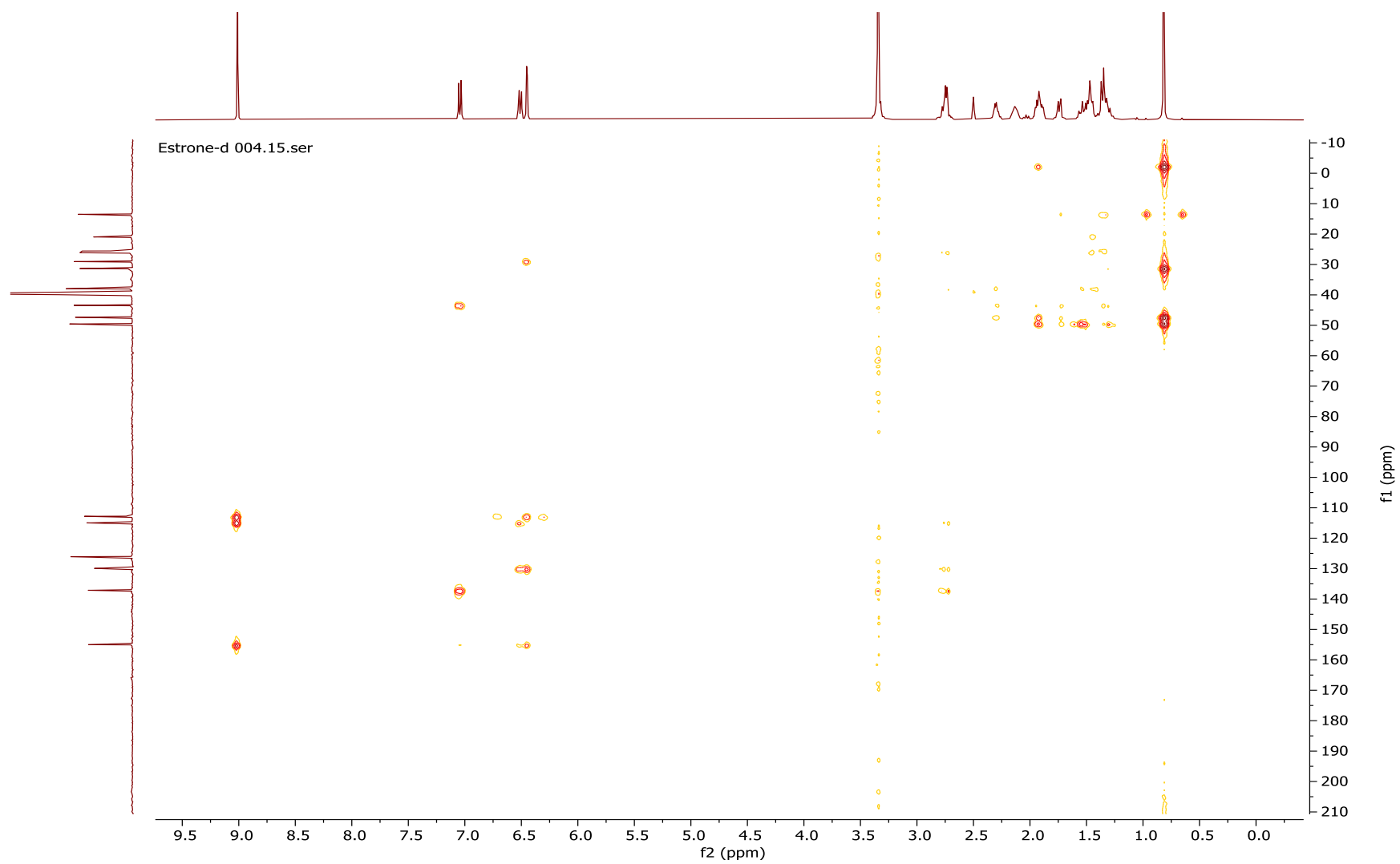
^1H - ^1H COSY spectrum of **222** (101 MHz, $\text{DMSO-}d_6$)



^1H - ^{13}C HSQC spectrum of **222** (101 MHz, $\text{DMSO-}d_6$)

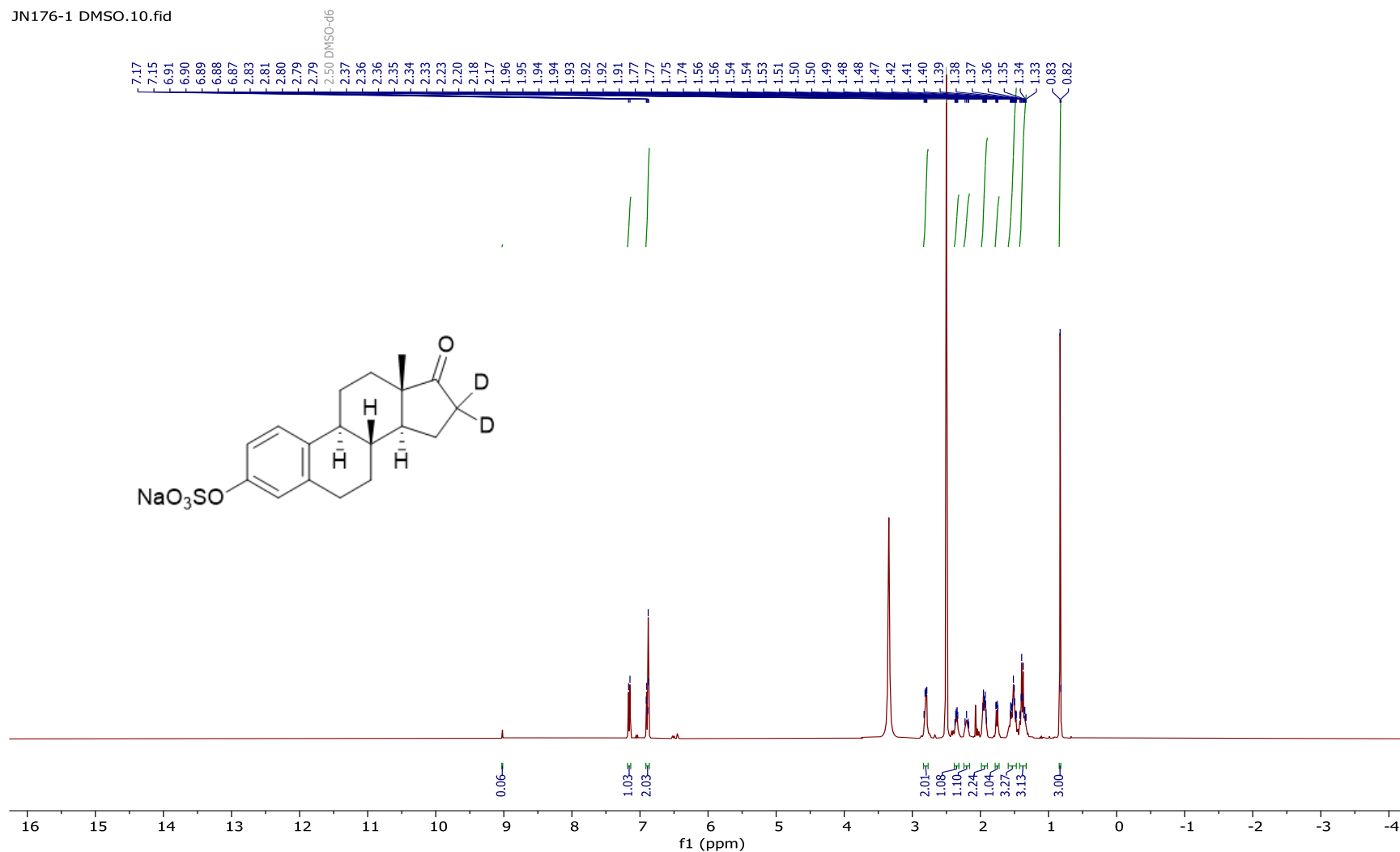


^1H - ^{13}C HMBC spectrum of **222** (101 MHz, $\text{DMSO-}d_6$)



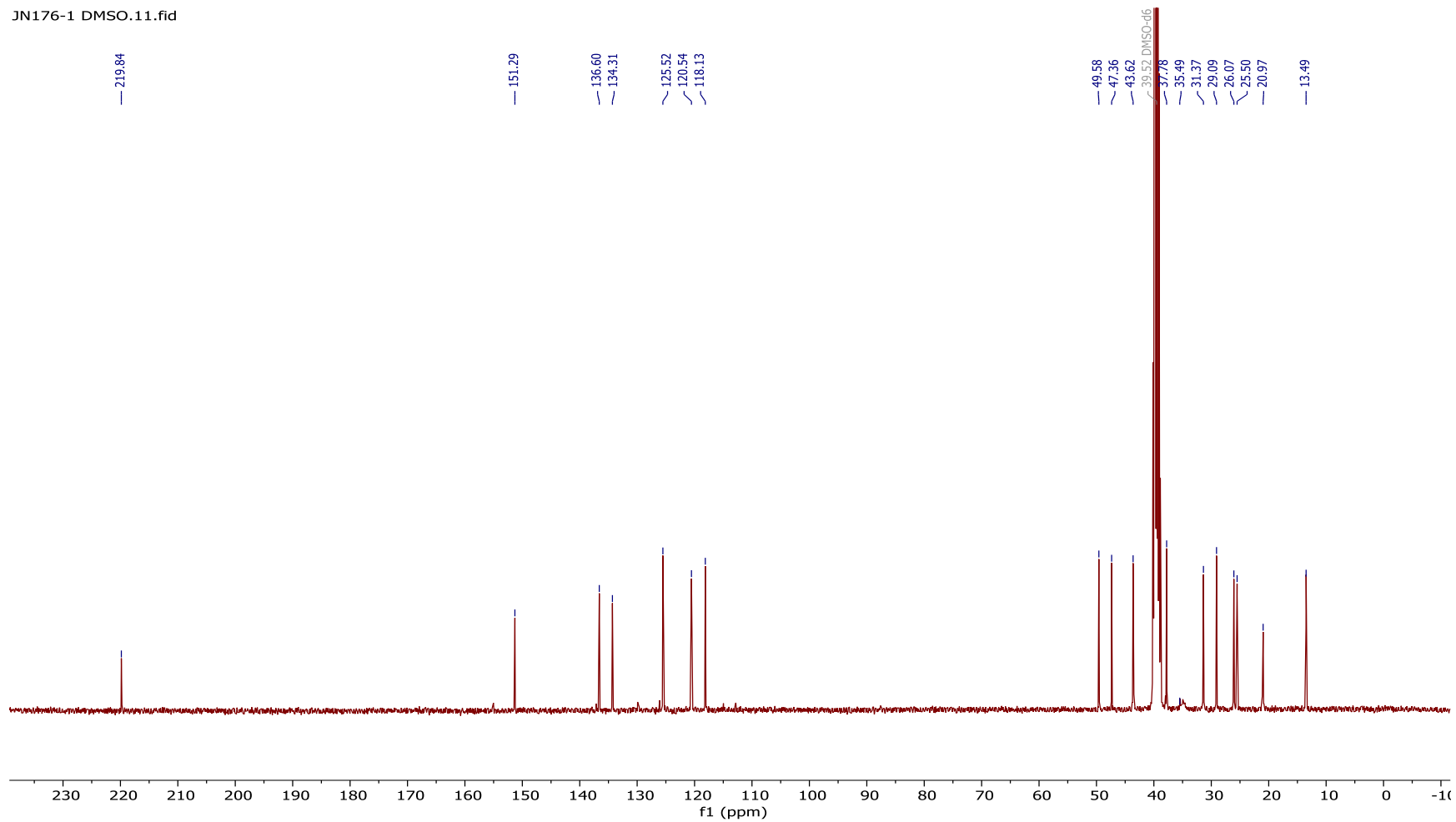
¹H NMR spectrum of **224** (400 MHz, DMSO-d₆)

JN176-1 DMSO.10.fid



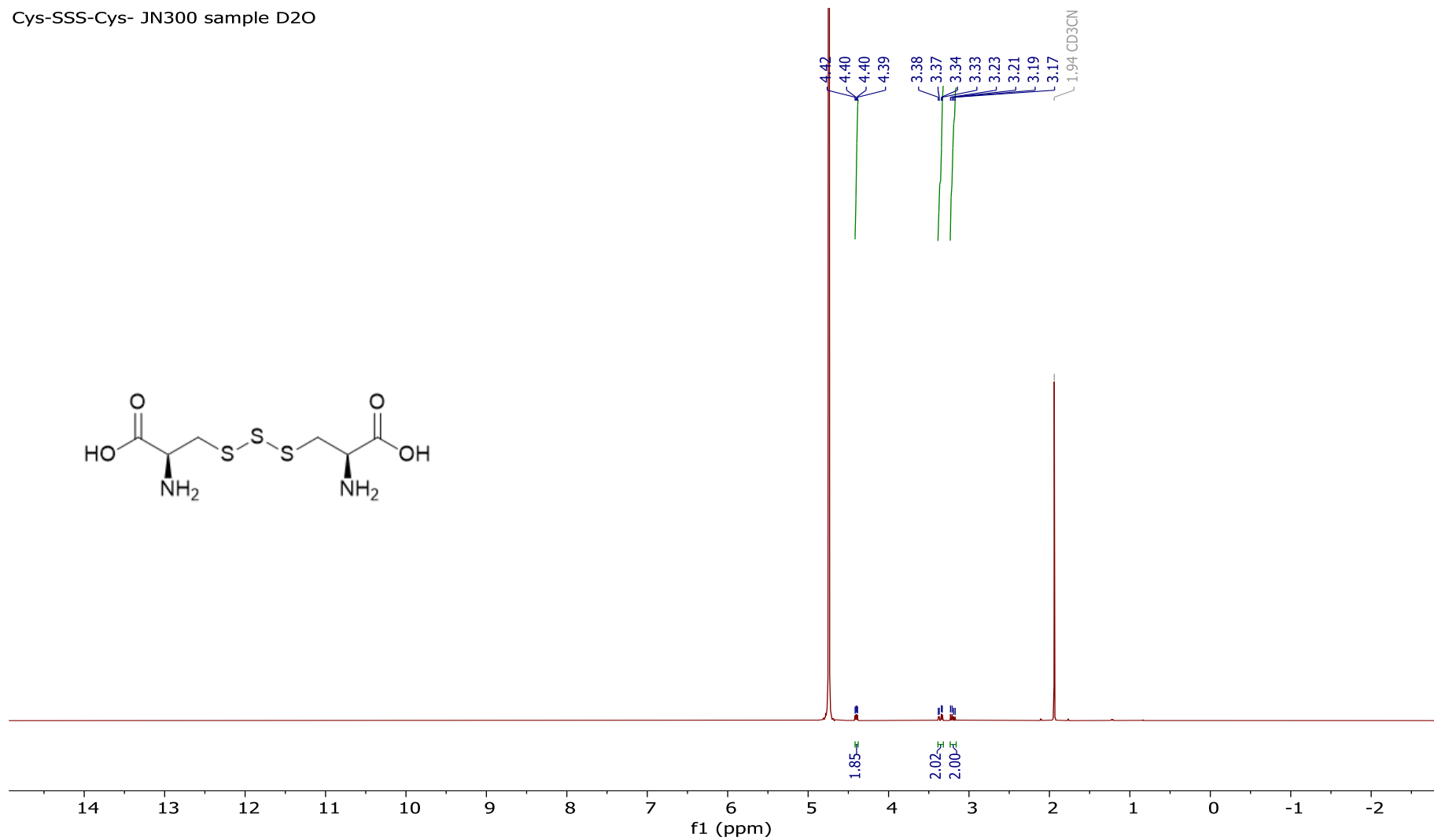
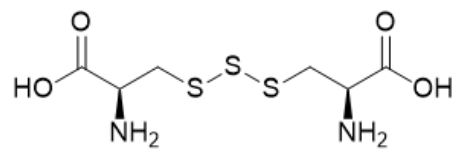
¹³C NMR spectrum of **224** (101 MHz, DMSO-*d*₆)

JN176-1 DMSO.11.fid



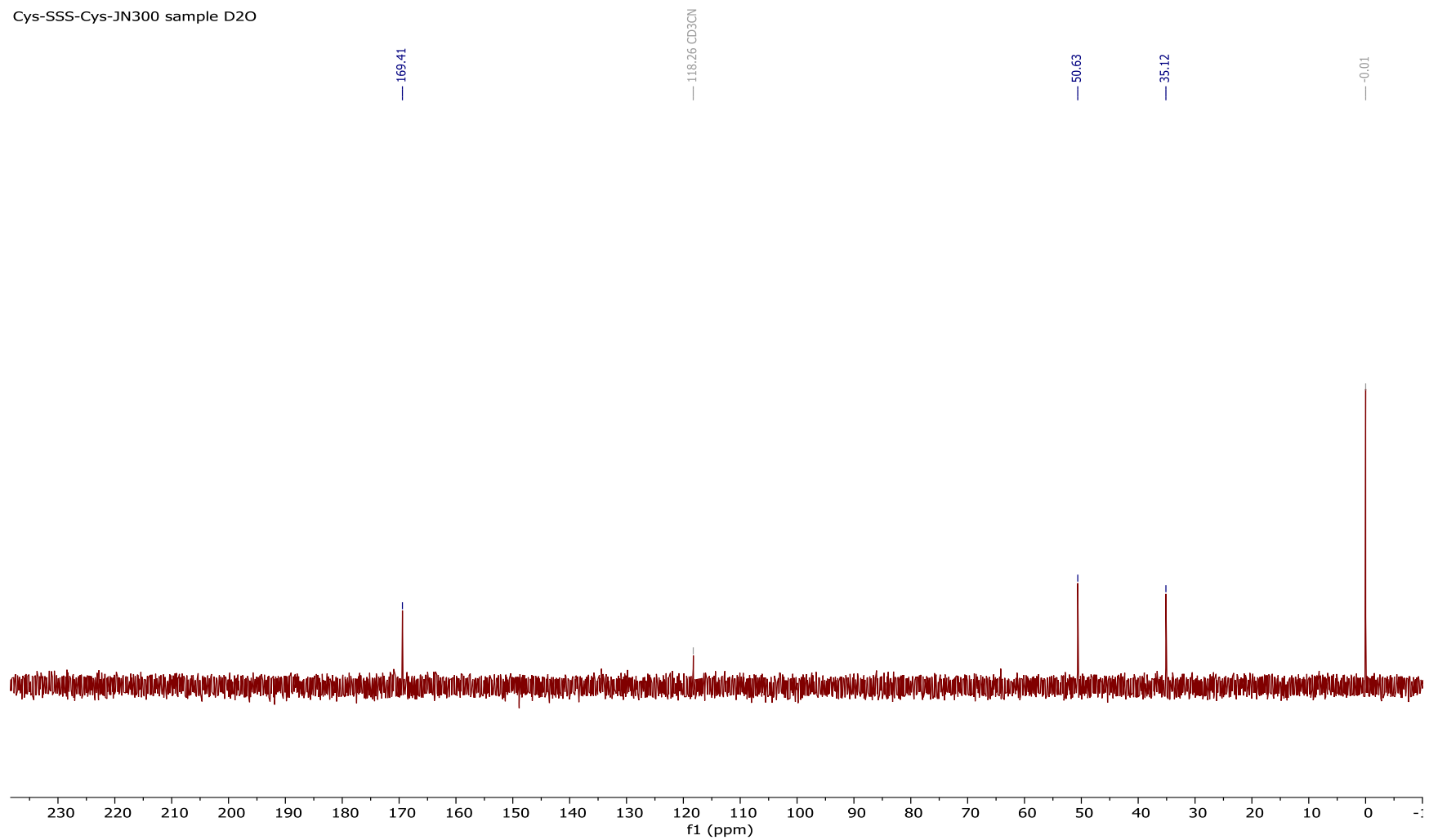
¹H NMR spectrum of **237** (400 MHz, D₂O)

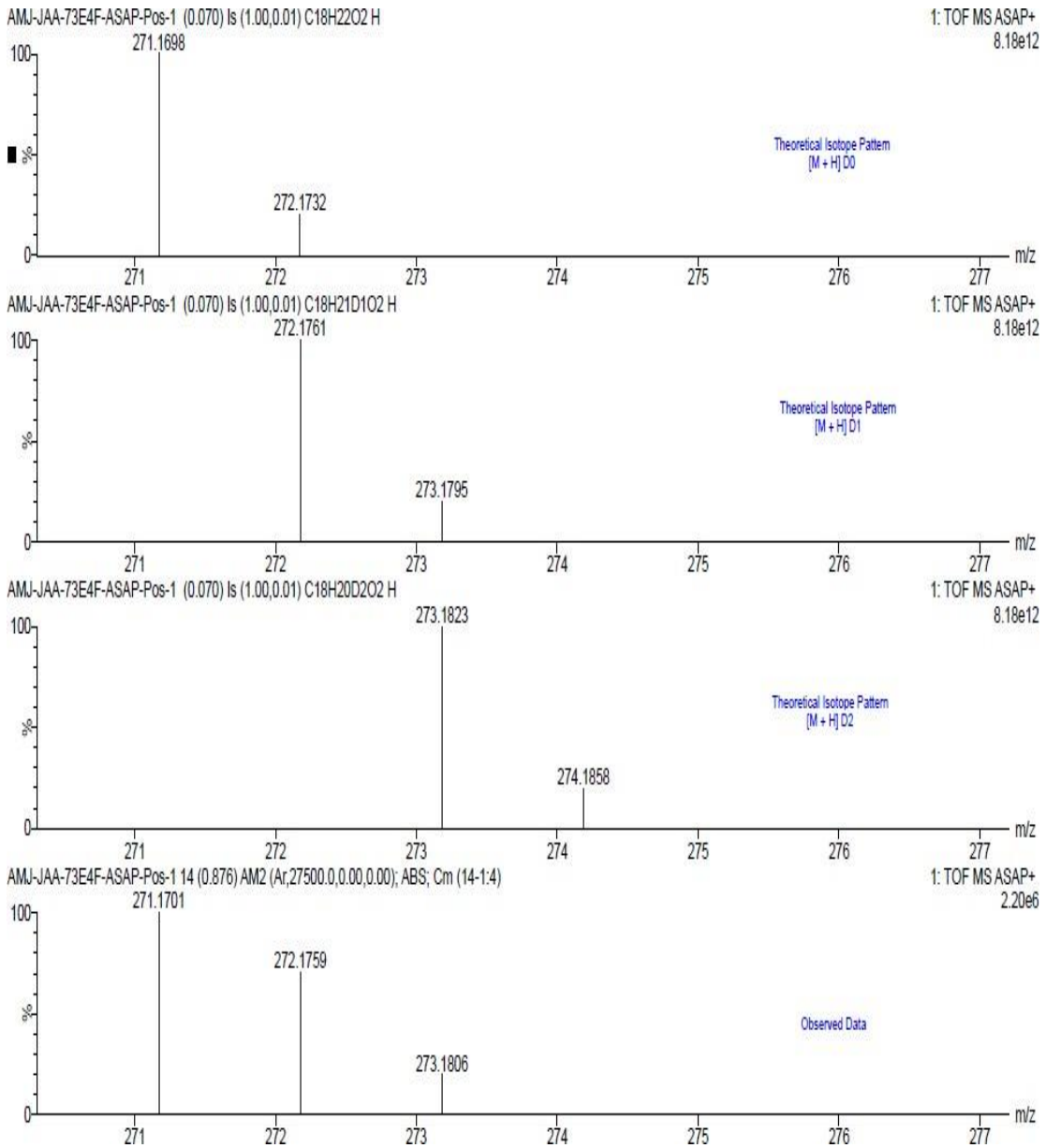
Cys-SSS-Cys- JN300 sample D2O



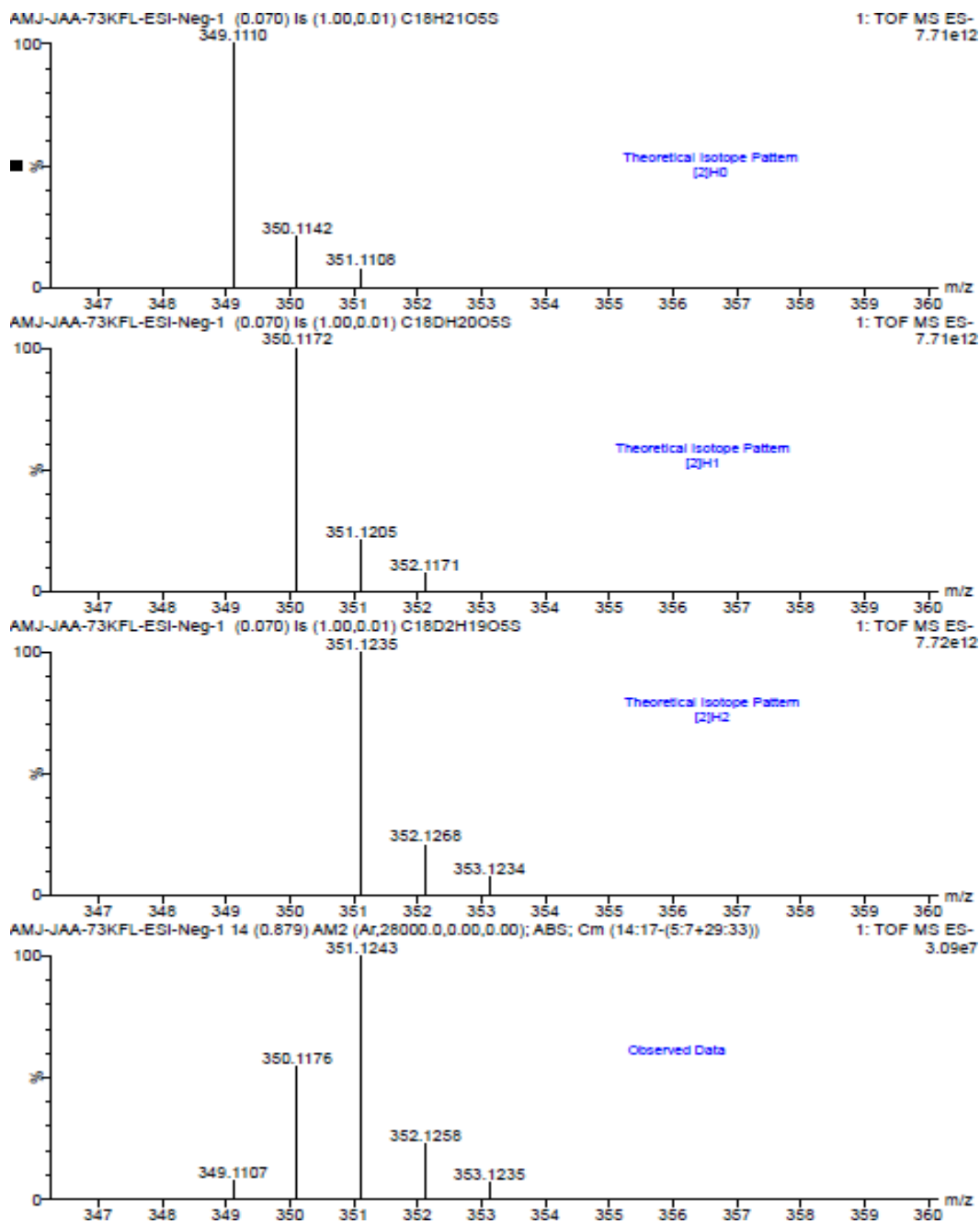
^{13}C NMR spectrum of **237** (101 MHz, D_2O)

Cys-SSS-Cys-JN300 sample D_2O



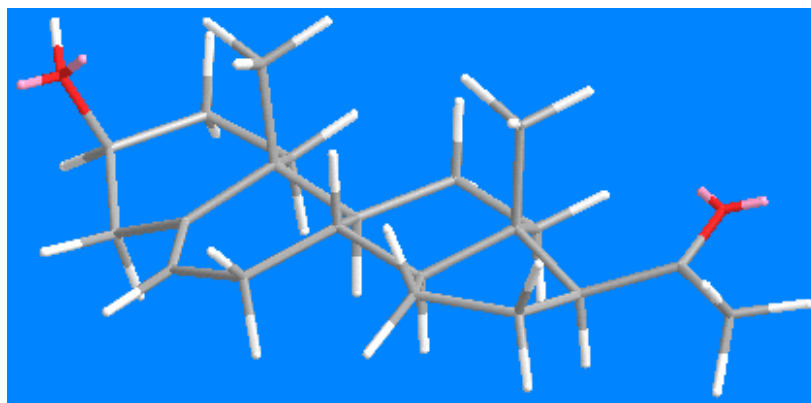
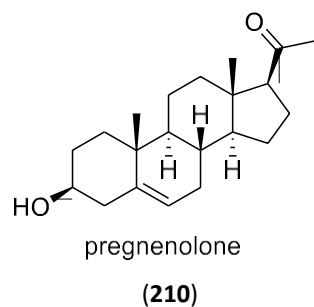


Mass spectroscopic theoretical versus observed deuteration levels for **estrone-d₂ (222)**.

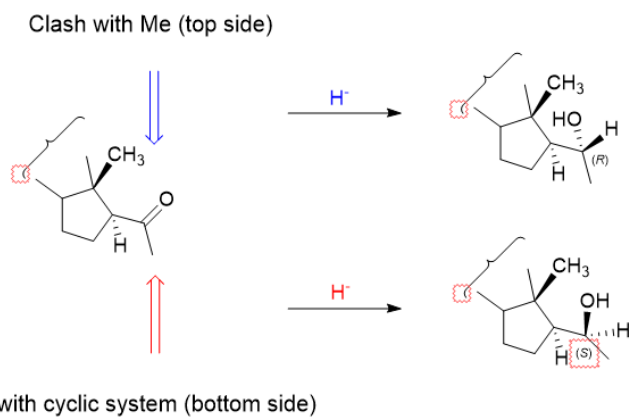


Mass spectroscopic theoretical versus observed deuteration levels for sodium estrone-d₂ sulfate (224)

(a)



(b)



Relative stereochemistry of bulk sample confirmed by X-ray crystallography

Figure S3. Explanation of observed diastereoselectivity in the ketone reduction of pregnenolone (**210**). (a) 3D depiction of pregnenolone and (b) X-ray confirmed outcome is *R*-C (20)-OH by relative orientation of stereocentres. This can be explained by the steric approaches of borohydride via the methyl group on the topface or the steroidal framework from the lower face.

X-ray crystallographic data for compound (*R*)-pregnendiol (**213**)

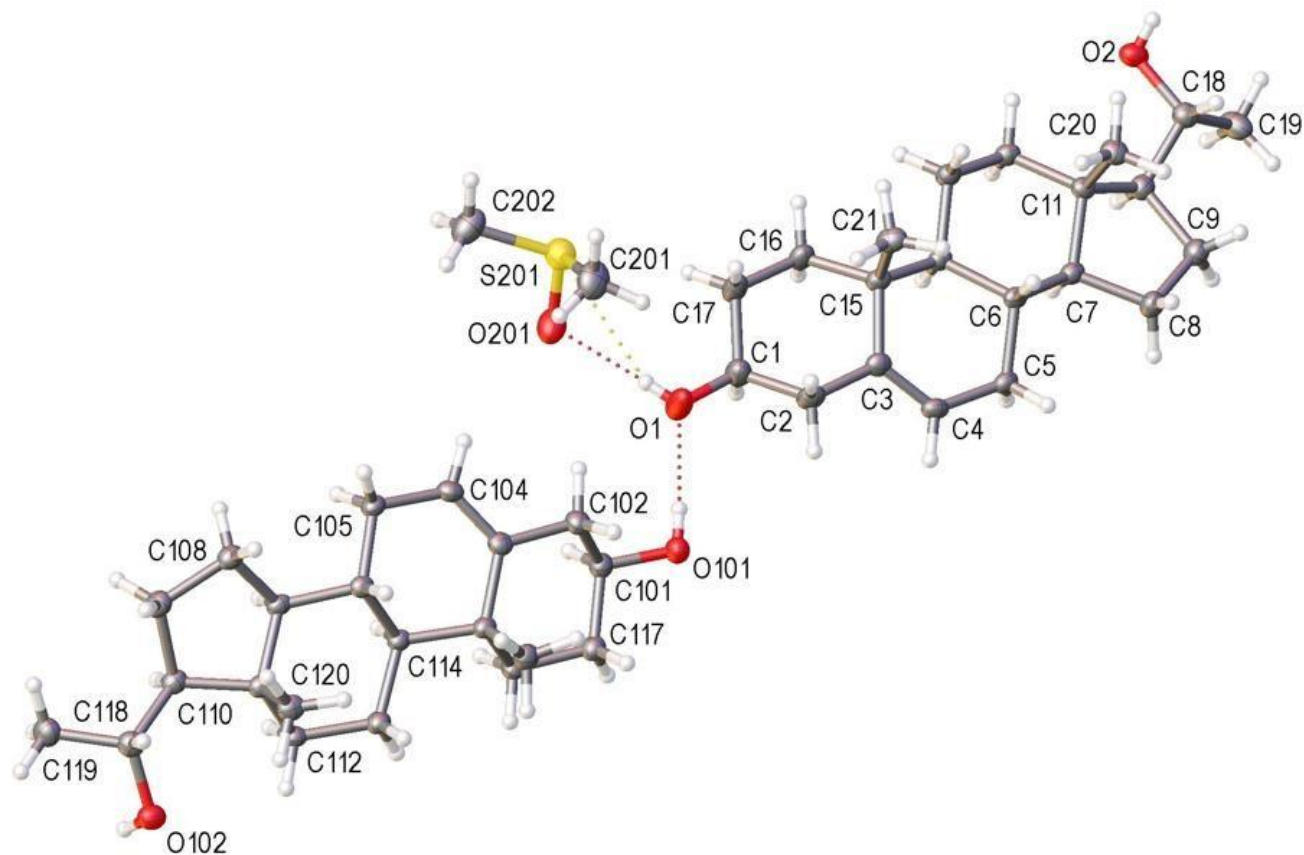


Figure S4 Crystal structure of compound (**213**) with ellipsoids drawn at the 50 % probability level. Hydrogenbonding within the asymmetric unit is shown using dotted lines.

Table S1: Crystal data and structure refinement for pregnendiol (213**)**

Identification code	213
Empirical formula	C ₂₂ H ₃₇ O _{2.5} S _{0.5}
Formula weight	357.54
Temperature/K	99.99(10)
Crystal system	monoclinic
Space group	P2 ₁
a/Å	9.70930(10)
b/Å	14.5298(2)
c/Å	14.3683(2)
α/°	90
β/°	97.7380(10)
γ/°	90
Volume/Å ³	2008.54(4)
Z	4
ρ _{calc} /cm ³	1.182

μ/mm^{-1}	1.045
F(000)	788.0
Crystal size/ mm^3	$0.262 \times 0.044 \times 0.015$
Radiation	Cu K α ($\lambda = 1.54184$)
2 θ range for data collection/ $^\circ$	6.208 to 155.712
Index ranges	$-11 \leq h \leq 12, -17 \leq k \leq 17, -17 \leq l \leq 18$
Reflections collected	44998
Independent reflections	7805 [$R_{\text{int}} = 0.0568, R_{\text{sigma}} = 0.0342$]
Data/restraints/parameters	7805/1/475
Goodness-of-fit on F^2	1.051
Final R indexes [$I \geq 2\sigma(I)$]	$R_1 = 0.0369, wR_2 = 0.0982$
Final R indexes [all data]	$R_1 = 0.0393, wR_2 = 0.0997$
Largest diff. peak/hole / $e \text{ \AA}^{-3}$	0.36/-0.32
Flack parameter	-0.015(9)

Crystal structure determination of **pregnendiol (213)**: $\text{C}_{22}\text{H}_{37}\text{O}_{2.5}\text{S}_{0.5}$ ($M = 357.54 \text{ g/mol}$): monoclinic, space group $P2_1$ (no. 4), $a = 9.70930(10) \text{ \AA}$, $b = 14.5298(2) \text{ \AA}$, $c = 14.3683(2) \text{ \AA}$, $\beta = 97.7380(10)^\circ$, $V = 2008.54(4) \text{ \AA}^3$, $Z = 4$, $T = 99.99(10) \text{ K}$, $\mu(\text{Cu K}\alpha) = 1.045 \text{ mm}^{-1}$, $D_{\text{calc}} = 1.182 \text{ g/cm}^3$, 44998 reflections measured ($6.208^\circ \leq 2\theta \leq 155.712^\circ$), 7805 unique ($R_{\text{int}} = 0.0568, R_{\text{sigma}} = 0.0342$) which were used in all calculations. The final R_1 was 0.0369 ($I > 2\sigma(I)$) and wR_2 was 0.0997 (all data). Flack: -0.015 (9).

The structure contains two crystallographically independent molecules and a molecule of DMSO. The structure occupies a chiral space group and has been confirmed from the diffraction data as being enantiometrically pure, with a Flack parameter of -0.015(9).

Thus C(1), C(6), C(7), C(10), C(11), C(14), C(101), C(106), C(107), C(110), C(111), C(114) are confirmed as *S* while C(15), C(18), C(115) and C(118) are *R*.

A suitable crystal was selected and a dataset for **(213)** was measured on an **XtaLAB Synergy, Dualflex** diffractometer using a HiPix detector. The data collection was driven and processed and an absorption correction was applied using CrysAlisPro.³¹⁷ The structure was solved using ShelXT³¹⁸ and was refined by a full-matrix least-squares procedure on F^2 in ShelXL.³¹⁹ Figures and reports were produced using OLEX2.³²⁰ All non-hydrogen atoms were refined with anisotropic displacement parameters. The hydrogen atoms bonded to O(1), O(2), O(101) and O(102) were located in the electron density and the positions refined. All remaining hydrogen atoms fixed as riding models and the isotropic thermal parameters (U_{iso}) of all hydrogen atoms were based on the U_{eq} of the parent atom.

CCDC 2120263 contains the supplementary crystallographic data for this paper. These data can be obtained free of charge from The Cambridge Crystallographic Data Centre via www.ccdc.cam.ac.uk/data_request/cif.

References

1. Mulder, G. J., *Sulfation of drugs and related compounds*. CRC Press Boca Raton, FL: 1981.
2. Al-Horani, R. A.; Desai, U. R., *Tetrahedron* **2010**, *66* (16), 2907-2918.
3. Baumann, E., *Ber Dtsch Chem Ges* **1876**, *9* (1), 54-58.
4. Testa, B.; Pedretti, A.; Vistoli, G., *Drug Discov Today* **2012**, *17* (11-12), 549-560.
5. Falany, C. N., *Fed Am Soc Exp Biol J* **1997**, *11* (4), 206-216.
6. Gamage, N.; Barnett, A.; Hempel, N.; Duggleby, R. G.; Windmill, K. F.; Martin, J. L.; McManus, M. E., *Toxicol Sci* **2006**, *90* (1), 5-22.
7. Chen, X.; Zhong, D.; Blume, H., *Eur J Pharm Sci* **2000**, *10* (1), 11-16.
8. Suiko, M.; Kurogi, K.; Hashiguchi, T.; Sakakibara, Y.; Liu, M.-C., *Biosci Biotechnol Biochem* **2017**, *81* (1), 63-72.
9. Gupta, A. K.; Talukder, M.; Venkataraman, M.; Bamimore, M. A., *J Dermatolog Treat* **2022**, *33* (4), 1896-1906.
10. Villani, A.; Fabbrocini, G.; Ocampo-Candiani, J.; Ruggiero, A.; Ocampo-Garza, S. S., *J Eur Acad Dermatol Venereol* **2021**, *35* (7), 1485-1492.
11. Kietzmann, M., Mulder, G.J. (Ed.), X+413 pp., London, New York, Philadelphia: Taylor and Francis (1990). Elsevier Ltd: 1991; Vol. 29, pp 396-396.
12. Weinshilboum, R. M.; Otterness, D. M.; Aksoy, I. A.; Wood, T. C.; Her, C.; Raftogianis, R. B., *Fed Am Soc Exp Biol* **1997**, *11* (1), 3-14.
13. Edenberg, H.; Bosron, W., *Biotransformation* **1997**, *3*, 119-131.
14. Lipmann, F., *American Association for the Advancement of Science* **1958**, *128*, 575-580.
15. Kauffman, F. C., *Drug Metab Rev* **2004**, *36* (3-4), 823-843.
16. Coughtrie, M. W. H., *Pharmacogenomics J* **2002**, *2* (5), 297-308.
17. Coughtrie, M. W. H.; Sharp, S.; Maxwell, K.; Innes, N. P., *Chem Biol Interact* **1998**, *109* (1), 3-27.
18. Nagata, K.; Yamazoe, Y., *Annu Rev Pharmacol Toxicol* **2000**, *40* (1), 159-176.
19. Kurogi, K.; Sakakibara, Y.; Hashiguchi, T.; Kakuta, Y.; Kanekiyo, M.; Teramoto, T.; Fukushima, T.; Bamba, T.; Matsumoto, J.; Fukusaki, E., *Proc Natl Acad Sci nexus* **2024**, *97*.
20. Niehrs, C.; Beißwanger, R.; Huttner, W. B., *Chem Biol Interact* **1994**, *92* (1), 257-271.
21. Thacker, B. E.; Xu, D.; Lawrence, R.; Esko, J. D., *Matrix Biol* **2014**, *35*, 60-72.
22. Scott, K. A.; Njardarson, J. T., *Top Curr Chem* **2018**, *376* (1).
23. Leustek, T., *The Arabidopsis Book/American Society of Plant Biologists* **2002**, *1*.
24. Wächtershäuser, G., *Science* **2000**, *289* (5483), 1307-1308.
25. Emmett, E. J.; Willis, M. C., *Asian J Org Chem* **2015**, *4* (7), 602-611.
26. Greenwood, N.; Earnshaw, A., *Chemistry of the Elements 2nd edition*. Butterworth-Heinemann: 1997.
27. Loerting, T.; Liedl, K. R., *Proc Natl Acad Sci U S A* **2000**, *97* (16), 8874-8878.
28. Gilbert, E. E., *Chem Rev* **1962**, *62* (6), 549-589.
29. Mustafa, M.; Winum, J.-Y., *Expert Opin Drug Discov.* **2022**, *17* (5), 501-512.
30. Ilardi, E. A.; Vitaku, E.; Njardarson, J. T., *J Med Chem* **2014**, *57* (7), 2832-2842.
31. Zaraei, S.-O.; Abduelkarem, A. R.; Anbar, H. S.; Kobeissi, S.; Mohammad, M.; Ossama, A.; El-Gamal, M. I., *Eur J Med Chem* **2019**, *179*, 257-271.
32. Mueller, J. W.; Gilligan, L. C.; Idkowiak, J.; Arlt, W.; Foster, P. A., *Endocr Rev* **2015**, *36* (5), 526-563.
33. Guglielmone, H. A.; Agnese, A. M.; Montoya, S. C. N.; Cabrera, J. L., *Thromb Res* **2002**, *105* (2), 183-188.
34. Lin, H.-W.; Sun, M.-X.; Wang, Y.-H.; Yang, L.-M.; Yang, Y.-R.; Huang, N.; Xuan, L.-J.; Xu, Y.-M.; Bai, D.-L.; Zheng, Y.-T., *Planta medica* **2010**, *76* (09), 889-892.
35. Arthan, D.; Svasti, J.; Kittakoop, P.; Pittayakhachonwut, D.; Tanticharoen, M.; Thebtaranonth, Y., *Phytochem* **2002**, *59* (4), 459-463.

36. Fang, S.-H.; Hou, Y.-C.; Chang, W.-C.; Hsiu, S.-L.; Chao, P.-D. L.; Chiang, B.-L., *Life Sci* **2003**, *74* (6), 743-756.
37. Arlov, Ø.; Rüttsche, D.; Asadi Korayem, M.; Öztürk, E.; Zenobi-Wong, M., *Adv Funct Mater* **2021**, *31* (19), 2010732.
38. Ernst, B.; Magnani, J., *Nat Rev Drug Discov* **2009**, *8*, 661-677.
39. Blakemore, D. C.; Castro, L.; Churcher, I.; Rees, D. C.; Thomas, A. W.; Wilson, D. M.; Wood, A., *Nat Chem* **2018**, *10* (4), 383-394.
40. Hemmerich, S.; Verdugo, D.; Rath, V. L., *Drug Discov Today* **2004**, *9* (22), 967-975.
41. Jandik, K. A.; Kruep, D.; Cartier, M.; Linhardt, R. J., *J Pharm Sci* **1996**, *85* (1), 45-51.
42. Liang, A.; Thakkar, J. N.; Desai, U. R., *J Pharm Sci* **2010**, *99* (3), 1207-1216.
43. Henry, B. L.; Thakkar, J. N.; Liang, A.; Desai, U. R., *Biochem Biophys Res Commun* **2012**, *417* (1), 382-386.
44. Raghuraman, A.; Riaz, M.; Hindle, M.; Desai, U. R., *Tetrahedron Lett* **2007**, *48* (38), 6754-6758.
45. Rawat, M.; Gama, C. I.; Matson, J. B.; Hsieh-Wilson, L. C., *J Am Chem Soc* **2008**, *130* (10), 2959-2961.
46. Alshehri, J. A.; Benedetti, A. M.; Jones, A. M., *Sci Rep* **2020**, *10* (1), 16559.
47. Benedetti, A. M.; Gill, D. M.; Tsang, C. W.; Jones, A. M., *Chembiochem* **2020**, *21* (7), 938-942.
48. Kolaříková, V.; Brodsky, K.; Petrásková, L.; Pelantová, H.; Cvačka, J.; Havlíček, L.; Křen, V.; Valentová, K., *Int J Mol Sci* **2022**, *23* (23), 15171.
49. Levdansky, A. V.; Vasilyeva, N. Y.; Malyar, Y. N.; Kondrasenko, A. A.; Fetisova, O. Y.; Kazachenko, A. S.; Levdansky, V. A.; Kuznetsov, B. N., *Molecules* **2022**, *27*, 6356.
50. Ball, M.; Boyd, A.; Ensor, G. J.; Evans, M.; Golden, M.; Linke, S. R.; Milne, D.; Murphy, R.; Telford, A.; Kalyan, Y.; Lawton, G. R.; Racha, S.; Ronsheim, M.; Zhou, S. H., *Org Process Res Dev* **2016**, *20* (10), 1799-1805.
51. Montero Bastidas, J. R.; Oleskey, T. J.; Miller, S. L.; Smith, M. R.; Maleczka, R. E., *J Am Chem Soc* **2019**, *141* (39), 15483-15487.
52. Mihai, M. T.; Williams, B. D.; Phipps, R. J., *J Am Chem Soc* **2019**, *141* (39), 15477-15482.
53. Kowalska, J.; Osowniak, A.; Zuberek, J.; Jemielity, J., *Bioorg Med Chem Lett* **2012**, *22* (11), 3661-3664.
54. Gill, D. M.; Povinelli, A. P. R.; Zazeri, G.; Shamir, S. A.; Mahmoud, A. M.; Wilkinson, F. L.; Alexander, M. Y.; Cornelio, M. L.; Jones, A. M., *RSC Med Chem* **2021**, *12* (5), 779-790.
55. Alshehri, J. A.; Gill, D. M.; Jones, A. M., *Front Mol Biosci* **2021**, *8*, 776900.
56. Alshehri, J. A.; Jones, A. M., *Essays Biochem* **2024**, EBC20240001.
57. Correia-da-Silva, M.; Sousa, E.; Pinto, M. M., *Med Res Rev* **2014**, *34* (2), 223-279.
58. Yi, Y.; Zhang, M.-W.; Liao, S.-T.; Zhang, R.-F.; Deng, Y.-Y.; Wei, Z.-C.; Tang, X.-J.; Zhang, Y., *Carbohydr Polym* **2012**, *87* (1), 636-643.
59. Zhu, Q.; Jiang, Y.; Lin, S.; Wen, L.; Wu, D.; Zhao, M.; Chen, F.; Jia, Y.; Yang, B., *Biomacromolecules* **2013**, *14* (6), 1999-2003.
60. Yang, B.; Zhao, M.; Shi, J.; Yang, N.; Jiang, Y., *Food Chem* **2008**, *106* (2), 685-690.
61. Levdanskii, V.; Levdanskii, A.; Kuznetsov, B., *Chem Nat Compd* **2014**, *50*, 1029-1031.
62. Tolstikov, G. A.; Flekhter, O. B.; Shultz, E.; Baltina, L.; Tolstikov, A., *Chem Sustain Develop* **2005**, *13* (1), 1-29.
63. Bureeva, S.; Andia-Pravdivy, J.; Symon, A.; Bichucher, A.; Moskaleva, V.; Popenko, V.; Shpak, A.; Shvets, V.; Kozlov, L.; Kaplun, A., *Bioorg Med Chem* **2007**, *15* (10), 3489-3498.
64. Patocka, J., *J Appl Biomed* **2003**, *1* (1), 7-12.
65. Wang, Z.; Xie, J.; Shen, M.; Nie, S.; Xie, M., *Trend Food Sci Tech* **2018**, *74*, 147-157.
66. Mumma, R. O., *Lipids* **1966**, *1* (3), 221-223.
67. Hoiberg, C. P.; Mumma, R. O., *J Am Chem Soc* **1969**, *91* (15), 4273-4278.
68. Morley, J. E., *Life Sci* **1982**, *30* (6), 479-493.

69. Rehfeld, J. F.; Friis-Hansen, L.; Goetze, J. P.; Hansen, T. V., *Curr Top Med Chem* **2007**, *7* (12), 1154-1165.
70. Maraganore, J. M.; Chao, B.; Joseph, M. L.; Jablonski, J.; Ramachandran, K., *J Biol Chem* **1989**, *264* (15), 8692-8698.
71. Todd, J. S.; Zimmerman, R. C.; Crews, P.; Alberte, R. S., *Phytochem* **1993**, *34* (2), 401-404.
72. Soidinsalo, O.; Wähälä, K., *Steroids* **2007**, *72* (13), 851-854.
73. Jie, Y.; Zhang, L.; Chen, P.; Mao, X.; Tang, S., *Journal of Wuhan University of Technology-Mater Sci Ed* **2012**, *27*, 110-114.
74. Qian, X.-P.; Zha, X.-Q.; Xiao, J.-J.; Zhang, H.-L.; Pan, L.-H.; Luo, J.-P., *Carbohydr Polym* **2014**, *101*, 982-989.
75. Gao, L.; Wang, F.; Hou, T.; Geng, C.; Xu, T.; Han, B.; Liu, D., *Front Pharmacol* **2022**, *13*, 920823-920823.
76. Lee, P. L.; Chen, J. T., *Acta Physiol Plant* **2014**, *36*, 2619-2625.
77. Zhang, C.-C.; Gao, Z.; Luo, L.-N.; Liang, H.-H.; Xiang, Z.-X., *China Journal of Chinese Materia Medica* **2020**, *45* (23), 5669-5676.
78. Zhu, Y.; Kong, Y.; Hong, Y.; Zhang, L.; Li, S.; Hou, S.; Chen, X.; Xie, T.; Hu, Y.; Wang, X., *Front Chem* **2022**, *9*, 807508.
79. Stachyra, T.; Lévassieur, P.; Péchereau, M.-C.; Girard, A.-M.; Claudon, M.; Miossec, C.; Black, M. T., *J Antimicrob Chemother* **2009**, *64* (2), 326-329.
80. Zhanel, G. G.; Lawson, C. D.; Adam, H.; Schweizer, F.; Zelenitsky, S.; Lagacé-Wiens, P. R. S.; Denisuk, A.; Rubinstein, E.; Gin, A. S.; Hoban, D. J.; Lynch, J. P.; Karlowsky, J. A., *Drugs* **2013**, *73* (2), 159-177.
81. Gorelik, D.; Lin, Y. C.; Briceno-Strocchia, A. I.; Taylor, M. S., *J Org Chem* **2019**, *84* (2), 900-908.
82. Pawliczek, M.; Hashimoto, T.; Maruoka, K., *Chem Sci* **2018**, *9* (5), 1231-1235.
83. D'Angelo, K. A.; Taylor, M. S., *J Am Chem Soc* **2016**, *138* (34), 11058-11066.
84. Reihill, M.; Ma, H.; Bengtsson, D.; Oscarson, S., *Beilstein J Org Chem* **2024**, *20* (1), 173-180.
85. Ju, T.; Otto, V. I.; Cummings, R. D., *Angew Chem Int Ed* **2011**, *50* (8), 1770-1791.
86. Yu, L.-G., *Glycoconj J* **2007**, *24*, 411-420.
87. Vokhmyanina, O. A.; Rapoport, E. M.; André, S.; Severov, V. V.; Ryzhov, I.; Pazynina, G. V.; Korchagina, E.; Gabius, H.-J.; Bovin, N. V., *Glycobiol* **2012**, *22* (9), 1207-1217.
88. Raghuraman, A.; Riaz, M.; Hindle, M.; Desai, U. R., *Tetrahedron Lett* **2007**, *48* (38), 6754-6758.
89. Hoshino, J.; Park, E.-J.; Kondratyuk, T. P.; Marler, L.; Pezzuto, J. M.; van Breemen, R. B.; Mo, S.; Li, Y.; Cushman, M., *J Med Chem* **2010**, *53* (13), 5033-5043.
90. Gutierrez-Zetina, S. M.; Gonzalez-Manzano, S.; Perez-Alonso, J. J.; Gonzalez-Paramas, A. M.; Santos-Buelga, C., *Molecules* **2019**, *24* (2), 307.
91. Dueñas, M.; González-Manzano, S.; Surco-Laos, F.; González-Paramas, A.; Santos-Buelga, C., *J Agric Food Chem* **2012**, *60* (14), 3592-3598.
92. Kakkar, S.; Bais, S., *Int Sch Res Notices* **2014**, *2014*.
93. Khan, A. K.; Rashid, R.; Fatima, N.; Mahmood, S.; Mir, S.; Khan, S.; Jabeen, N.; Murtaza, G., *Acta Pol Pharm* **2015**, *72* (4), 643-650.
94. Amin, H. P.; Czank, C.; Raheem, S.; Zhang, Q.; Botting, N. P.; Cassidy, A.; Kay, C. D., *Mol Nutr Food Res* **2015**, *59* (6), 1095-1106.
95. Gonzalez-Manzano, S.; Gonzalez-Paramas, A.; Santos-Buelga, C.; Duenas, M., *J Agric Food Chem* **2009**, *57* (4), 1231-1238.
96. Boots, A. W.; Haenen, G. R.; Bast, A., *Eur J Pharmacol* **2008**, *585* (2-3), 325-337.
97. Perez-Vizcaino, F.; Duarte, J., *Mol Asp Med* **2010**, *31* (6), 478-494.
98. Cooper, K. A.; Donovan, J. L.; Waterhouse, A. L.; Williamson, G., *Br J Nutr* **2008**, *99* (1), 1-11.
99. Correia-da-Silva, M.; Sousa, E.; Duarte, B.; Marques, F.; Cunha-Ribeiro, L. M.; Pinto, M. M., *Eur J Med Chem* **2011**, *46* (6), 2347-2358.
100. Viles-Gonzalez, J. F.; Fuster, V.; Badimon, J. J., *Eur Heart J* **2004**, *25* (14), 1197-1207.

101. Kappe, C. O.; Dallinger, D., *Nat Rev Drug Discov* **2006**, *5* (1), 51-63.
102. Caputo, H. E.; Straub, J. E.; Grinstaff, M. W., *Chem Soc Rev* **2019**, *48* (8), 2338-2365.
103. Krylov, V. B.; Ustyuzhanina, N. E.; Grachev, A. A.; Nifantiev, N. E., *Tetrahedron Lett* **2008**, *49* (41), 5877-5879.
104. Krylov, V.; Ushakova, N.; Ustyuzhanina, N.; Preobrazhenskaya, M.; Yashunsky, D.; Menshov, V.; Tsvetkov, D.; Sharma, G.; Radha Krishna, P.; Nifantiev, N., *Russ Chem Bull* **2010**, *59*, 232-235.
105. Gill, D. M.; Male, L.; Jones, A. M., *ChemComm* **2019**, *55* (30), 4319-4322.
106. Scalbert, A.; Williamson, G., *J Nutr* **2000**, *130* (8), 2073S-2085S.
107. Zhou, C. L.; Liu, W.; Kong, Q.; Song, Y.; Ni, Y. Y.; Li, Q. H.; O'Riordan, D., *Int J Food Sci Technol* **2014**, *49* (2), 508-514.
108. Quanhong, L.; Caili, F.; Yukui, R.; Guanghui, H.; Tongyi, C., *Plant Foods Hum Nutr* **2005**, *60*, 13-16.
109. Song, Y.; Li, J.; Hu, X.; Ni, Y.; Li, Q., *Macromol Res* **2011**, *19*, 1172-1178.
110. Song, Y.; Zhang, Y.; Zhou, T.; Zhang, H.; Hu, X.; Li, Q., *Int J Food Sci Technol* **2012**, *47* (2), 357-361.
111. Neurath, A. R., *N Engl J Med* **2008**, *359* (19), 2066-7; author reply 2067.
112. Aggarwal, N.; Altgårde, N.; Svedhem, S.; Zhang, K.; Fischer, S.; Groth, T., *Langmuir* **2013**, *29* (45), 13853-13864.
113. Wang, T.; Lacík, I.; Brissová, M.; Anilkumar, A. V.; Prokop, A.; Hunkeler, D.; Green, R.; Shahrokhi, K.; Powers, A. C., *Nat Biotechnol* **1997**, *15* (4), 358-362.
114. Heinze, T.; Daus, S.; Gericke, M.; Liebert, T., *Nova Science Publishers* **2010**, 213-259.
115. Heinze, T.; Genco, T.; Petzold-Welcke, K.; Wondraczek, H., *Cellulose* **2012**, *19*, 1305-1313.
116. Chen, G.; Zhang, B.; Zhao, J.; Chen, H., *Carbohydr Polym* **2013**, *95* (1), 332-337.
117. Richter, A.; Klemm, D., *Cellulose* **2003**, *10*, 133-138.
118. Sun, L.; Chopra, P.; Boons, G.-J., *J Org Chem* **2020**, *85* (24), 16082-16098.
119. Cassidy, A.; O'Reilly, É. J.; Kay, C.; Sampson, L.; Franz, M.; Forman, J.; Curhan, G.; Rimm, E. B., *Am J Clin Nutr* **2011**, *93* (2), 338-347.
120. Hooper, L.; Kroon, P. A.; Rimm, E. B.; Cohn, J. S.; Harvey, I.; Le Cornu, K. A.; Ryder, J. J.; Hall, W. L.; Cassidy, A., *Am J Clin Nutr* **2008**, *88* (1), 38-50.
121. Mink, P. J.; Scrafford, C. G.; Barraji, L. M.; Harnack, L.; Hong, C.-P.; Nettleton, J. A.; Jacobs Jr, D. R., *Am J Clin Nutr* **2007**, *85* (3), 895-909.
122. McCullough, M. L.; Peterson, J. J.; Patel, R.; Jacques, P. F.; Shah, R.; Dwyer, J. T., *Am J Clin Nutr* **2012**, *95* (2), 454-464.
123. Milenkovic, D.; Jude, B.; Morand, C., *Free Radical Biol Med* **2013**, *64*, 40-51.
124. Mladěnka, P.; Zatloukalová, L.; Filipický, T.; Hrdina, R., *Free Radic Biol Med* **2010**, *49* (6), 963-975.
125. Del Rio, D.; Rodriguez-Mateos, A.; Spencer, J. P.; Tognolini, M.; Borges, G.; Crozier, A., *Antioxid Redox Signal* **2013**, *18* (14), 1818-1892.
126. Almeida, A. F.; Borge, G. I. A.; Piskula, M.; Tudose, A.; Tudoreanu, L.; Valentová, K.; Williamson, G.; Santos, C. N., *Compr Rev Food Sci Food Saf* **2018**, *17* (3), 714-731.
127. Almeida, A. F.; Santos, C. N.; Ventura, M. R., *J Agric Food Chem* **2017**, *65* (31), 6460-6466.
128. Hartmann, A.; Ganzera, M.; Karsten, U.; Skhirtladze, A.; Stuppner, H., *Molecules* **2018**, *23* (11), 2735.
129. Vo, Y.; Schwartz, B. D.; Onagi, H.; Ward, J. S.; Gardiner, M. G.; Banwell, M. G.; Nelms, K.; Malins, L. R., *Chem Eur J* **2021**, *27* (38), 9830-9838.
130. Alekseeva, A.; Raman, R.; Eisele, G.; Clark, T.; Fisher, A.; Lee, S. L.; Jiang, X.; Torri, G.; Sasisekharan, R.; Bertini, S., *Carbohydr Polym* **2020**, *234*, 115913.
131. Gabriel, L.; Günther, W.; Pielenz, F.; Heinze, T., *Macromol Chem Phys* **2020**, *221* (1), 1900327.
132. Buncel, E., *Chem Rev* **1970**, *70* (3), 323-337.
133. Binkley, W.; Degering, E. F., *J Am Chem Soc* **1938**, *60* (11), 2810-2811.

134. Yue, S.; Ding, G.; Zheng, Y.; Song, C.; Xu, P.; Yu, B.; Li, J., *Nat Commun* **2024**, *15* (1), 1861.
135. Liu, C.; Yang, C.; Hwang, S.; Ferraro, S. L.; Flynn, J. P.; Niu, J., *Angew Chem Int Ed* **2020**, *59* (42), 18435-18441.
136. Penney, C. L.; Perlin, A. S., *Carbohydr Res* **1981**, *93* (2), 241-246.
137. Dong, J.; Sharpless, K. B.; Kwisnek, L.; Oakdale, J. S.; Fokin, V. V., *Angew Chem Int Ed* **2014**, *53* (36), 9466-9470.
138. Dong, J.; Krasnova, L.; Finn, M.; Sharpless, K. B., *Angew Chem Int Ed* **2014**, *53* (36), 9430-9448.
139. Lee, C.; Cook, A. J.; Elisabeth, J. E.; Friede, N. C.; Sammis, G. M.; Ball, N. D., *ACS Catal* **2021**, *11* (11), 6578-6589.
140. Liu, Y.; Lien, I.-F. F.; Ruttgaizer, S.; Dove, P.; Taylor, S. D., *Org Lett* **2004**, *6* (2), 209-212.
141. Ingram, L. J.; Taylor, S. D., *Angew Chem* **2006**, *118* (21), 3583-3586.
142. Simpson, L. S.; Widlanski, T. S., *J Am Chem Soc* **2006**, *128* (5), 1605-1610.
143. Feng, M.; Tang, B.; H Liang, S.; Jiang, X., *Curr Top Med Chem* **2016**, *16* (11), 1200-1216.
144. Hai, Y.; Wei, M.-Y.; Wang, C.-Y.; Gu, Y.-C.; Shao, C.-L., *Mar Life Sci Technol* **2021**, *3* (4), 488-518.
145. Gillespie, R.; Robinson, E., *Can J Chem* **1961**, *39* (11), 2189-2200.
146. Dado, G. P.; Knaggs, E. A.; Nepras, M. J., *Kirk-Othmer Encycl Chem Technol* **2000**.
147. Lohr, J. W. Sulfur trioxide sulfation and sulfonation. U.S. Patent 3232976A, 1966.
148. Kelly, D., *Synlett* **2003**, *2003* (14), 2263-2264.
149. Gill, D. M.; Male, L.; Jones, A. M., *Chemcomm* **2019**, *55* (30), 4319-4322.
150. Lecher, H.; Hardy, W., *J Am Chem Soc* **1948**, *70* (11), 3789-3792.
151. Guberovic, Z.; Hohnjec, M.; Kufcinec, J.; Oklobzija, M. Method of producing tertiary amine-sulphur-trioxide-complexes. U.S. Patent 5336775A, 1994.
152. Xie, J.; Male, L.; Jones, A. M., *Results Chem* **2024**, *9*, 101650.
153. Hardy, W. B.; Scalera, M., *J Am Chem Soc* **1952**, *74* (20), 5212-5214.
154. El-hiti, G. A., *Sulfur Rep* **2001**, *22* (3), 217-250.
155. Moede, J. A.; Curran, C., *J Am Chem Soc* **1949**, *71* (3), 852-858.
156. Passet, B.; Parshikov, V., *Org React* **1976**, *13* (4), 555-560.
157. Gill, D. New methods towards the synthesis, characterisation and analysis of small molecule glycomimetics. University of Birmingham, 2020.
158. Gill, D. M.; Povinelli, A. P. R.; Zazeri, G.; Shamir, S. A.; Mahmoud, A. M.; Wilkinson, F. L.; Alexander, M. Y.; Cornelio, M. L.; Jones, A. M., *RSC Med Chem* **2021**, *12* (5), 779-790.
159. Manahan, S. E., *Green Chemistry and the Ten Commandments of Sustainability*. Carbon: 2006; Vol. 100, p 12-011.
160. Datta, S.; Limpanuparb, T., *RSC Adv* **2021**, *11* (34), 20691-20700.
161. Hall Jr, H., *J Phys Chem* **1956**, *60* (1), 63-70.
162. Hall, N. F.; Sprinkle, M. R., *J Am Chem Soc* **1932**, *54* (9), 3469-3485.
163. Baptist, H. W. Process for preparing sulfur trioxide compounds of 4-alkyl morpholines. US2502839A, 1950.
164. Kacprzak, K. M., *Nat Prod* **2013**, *1*, 605-641.
165. Hu, B.; Bezpalko, M. W.; Fei, C.; Dickie, D. A.; Foxman, B. M.; Deng, L., *J Am Chem Soc* **2018**, *140* (42), 13913-13920.
166. Fanourakis, A.; Docherty, P. J.; Chuentragool, P.; Phipps, R. J., *ACS Catal* **2020**, *10* (18), 10672-10714.
167. Bischoff, R.; Schlüter, H., *J Proteomics* **2012**, *75* (8), 2275-2296.
168. Bakker, B. H.; Cerfontain, H., *Tetrahedron Lett* **1989**, *30* (40), 5451-5454.
169. Feliciello, A.; Gottesman, M. E.; Avvedimento, E. V., *J Mol Biol* **2001**, *308* (2), 99-114.
170. Michel, K., *Role of Protein-Protein Interactions in Metabolism: Genetics, Structure, Function*. Frontiers Media SA: 2018.

171. Petsko, G. A., Protein structure and function / Gregory A. Petsko, Dagmar Ringe. Ringe, D., Ed. London, 2004.
172. Xie, H.; Vucetic, S.; Iakoucheva, L. M.; Oldfield, C. J.; Dunker, A. K.; Uversky, V. N.; Obradovic, Z., *J. Proteome Res* **2007**, *6* (5), 1882-1898.
173. Naowarajna, N.; Cheng, R.; Lopez, J.; Wong, C.; Qiao, L.; Liu, P., *Synth Syst Biotechnol* **2021**, *6* (1), 32-49.
174. Monigatti, F.; Hekking, B.; Steen, H., *Biochim Biophys Acta* **2006**, *1764* (12), 1904-13.
175. Suter, C. M.; Evans, P. B.; Kiefer, J. M., *J Am Chem Soc* **1938**, *60* (3), 538-540.
176. Bettelheim, F. R., *J Am Chem Soc* **1954**, *76* (10), 2838-2839.
177. Huttner, W. B., *Nature* **1982**, *299* (5880), 273-276.
178. Lee, R. W.; Huttner, W. B., *J Biol Chem* **1983**, *258* (18), 11326-11334.
179. Stone, M. J.; Chuang, S.; Hou, X.; Shoham, M.; Zhu, J. Z., *N Biotechnol* **2009**, *25* (5), 299-317.
180. Nakahara, T.; Waki, M.; Uchimura, H.; Hirano, M.; Kim, J. S.; Matsumoto, T.; Nakamura, K.; Ishibashi, K.; Hirano, H.; Shiraiishi, A., *Anal Biochem* **1986**, *154* (1), 194-199.
181. Vázquez Campos, S.; Miranda, L. P.; Meldal, M., *J Chem Soc* **2002**, (5), 682-686.
182. Rogers, H.; Humphrey, G.; Chiu, A.; Pei, T., *Synthesis* **2008**, (14), pp.2298-2302.
183. Ingold, C., *Chem Soc* **1957**, *11* (1), 1-14.
184. Dusza, J. P.; Joseph, J. P.; Bernstein, S., *Steroids* **1985**, *45* (3), 303-315.
185. Kakiyama, G.; Muto, A.; Shimada, M.; Mano, N.; Goto, J.; Hofmann, A. F.; Iida, T., *Steroids* **2009**, *74* (9), 766-772.
186. Dusza, J. P.; Joseph, J. P.; Bernstein, S., *Steroids* **1968**, *12* (1), 49-61.
187. Érdi, P.; Tóth, J., *Mathematical models of chemical reactions: theory and applications of deterministic and stochastic models*. Manchester University Press: 1989.
188. Reitz, H. C.; Ferrel, R. E.; Olcott, H. S.; Fraenkel-Conrat, H., *J Am Chem Soc* **1946**, *68* (6), 1031-1035.
189. Donova, M. V.; Egorova, O. V., *Appl Microbiol Biotechnol* **2012**, *94* (6), 1423-1447.
190. Hannich, J. T.; Umabayashi, K.; Riezman, H., *Cold Spring Harb Perspect Biol* **2011**, *3* (5), 1-14.
191. Starling, E. H., In *Scientific and Medical Knowledge Production, 1796-1918*, Routledge: 2023; pp 185-216.
192. Tata, J. R., *EMBO Rep* **2005**, *6* (6), 490-496.
193. Manna, P. R.; Stetson, C. L.; Slominski, A. T.; Pruitt, K., *Endocr* **2016**, *51*, 7-21.
194. Baksi, S.; Pradhan, A., *Biol Sex Differ* **2021**, *12* (1), 1-13.
195. Chen, C.; Gong, X.; Yang, X.; Shang, X.; Du, Q.; Liao, Q.; Xie, R.; Chen, Y.; Xu, J., *Oncol Lett* **2019**, *18* (6), 5673-5680.
196. Cerqueira, N. M.; Oliveira, E. F.; Gesto, D. S.; Santos-Martins, D.; Moreira, C.; Moorthy, H. N.; Ramos, M. J.; Fernandes, P., *Biochem* **2016**, *55* (39), 5483-5506.
197. Gordon, D. J.; Probstfield, J. L.; Garrison, R. J.; Neaton, J. D.; Castelli, W. P.; Knoke, J. D.; Jacobs Jr, D. R.; Bangdiwala, S.; Tyroler, H. A., *Circ* **1989**, *79* (1), 8-15.
198. Maser, E.; Rižner, T. L., *Steroids and microorganisms*. Elsevier: 2012; Vol. 129, pp 1-3.
199. Banerjee, M.; Robbins, D.; Chen, T., *Molecules* **2013**, *18* (7), 7389-7406.
200. Fragkaki, A. G.; Angelis, Y. S.; Koupparis, M.; Tsantili-Kakoulidou, A.; Kokotos, G.; Georgakopoulos, C., *Steroids* **2009**, *74* (2), 172-197.
201. Funder, J. W., *Endocrinol* **2010**, *151* (11), 5098-5102.
202. Mensah-Nyagan, A. G.; Meyer, L.; Schaeffer, V.; Kibaly, C.; Patte-Mensah, C., *Psychoneuroendocrinology* **2009**, *34* (1), S169-S177.
203. Hogg, J. A., *Steroids* **1992**, *57* (12), 593-616.
204. Fernandes, P.; Cruz, A.; Angelova, B.; Pinheiro, H. M.; Cabral, J. M. S., *Enzyme Microb Technol* **2003**, *32* (6), 688-705.
205. Staels, B.; Fonseca, V. A., *Diabetes care* **2009**, *32* (Suppl 2), S237.
206. Ziff, O. J. M. B.; Kotecha, D. M. P. M. F. F., *Trends Cardiovasc Med* **2016**, *26* (7), 585-595.
207. Ko, D.-H.; Heiman, A. S.; Chen, M.; Lee, H. J., *Steroids* **2000**, *65* (4), 210-218.

208. Tuba, Z.; Bardin, C. W.; Dancsi, A.; Francsics–Czinege, E.; Molnár, C.; Csörgei, J.; Falkay, G.; Koide, S. S.; Kumar, N.; Sundaram, K.; Dukát–Abrók, V.; Balogh, G., *Steroids* **2000**, *65* (5), 266-274.
209. Siemes, C.; Visser, L. E.; de Jong, F. H.; Coebergh, J.-W. W.; Uitterlinden, A. G.; Hofman, A.; Stricker, B. H. C.; van Schaik, R. H. N., *Steroids* **2010**, *75* (12), 1024-1032.
210. Nicolás Díaz-Chico, B.; Germán Rodríguez, F.; González, A.; Ramírez, R.; Bilbao, C.; Cabrera de León, A.; Aguirre Jaime, A.; Chirino, R.; Navarro, D.; Díaz-Chico, J. C., *J Steroid Biochem Mol Biol* **2007**, *105* (1), 1-15.
211. Schiffer, L.; Barnard, L.; Baranowski, E. S.; Gilligan, L. C.; Taylor, A. E.; Arlt, W.; Shackleton, C. H.; Storbeck, K.-H., *J Steroid Biochem Mol Biol* **2019**, *194*, 105439.
212. Pozo, O. J.; Marcos, J.; Khymenets, O.; Pranata, A.; Fitzgerald, C. C.; McLeod, M. D.; Shackleton, C., *J Mol Endocrinol* **2018**, *61* (2), M1-M12.
213. Pranata, A.; Fitzgerald, C. C.; Khymenets, O.; Westley, E.; Anderson, N. J.; Ma, P.; Pozo, O. J.; McLeod, M. D., *Steroids* **2019**, *143*, 25-40.
214. Mortola, J. F.; Yen, S. S. C., *Maturitas* **1991**, *13* (2), 170-171.
215. Gomes, R. L.; Meredith, W.; Snape, C. E.; Sephton, M. A., *J Pharm Biomed Anal* **2009**, *49* (5), 1133-1140.
216. Mueller, J. W.; Vogg, N.; Lightning, T. A.; Weigand, I.; Ronchi, C.; Foster, P.; Kroiss, M., **2021**.
217. Strott, C. A., *Endocr Rev* **2002**, *23* (5), 703-732.
218. Carvalhal, F.; Correia-da-Silva, M.; Sousa, E.; Pinto, M.; Kijjoo, A., *J Mol Endocrinol* **2018**, *61* (2), T211-T231.
219. Fusetani, N.; Matsunaga, S.; Konosu, S., *Tetrahedron Lett* **1981**, *22* (21), 1985-1988.
220. Hobkirk, R., *Trends Endocrinol Metab* **1993**, *4* (2), 69-74.
221. Liu, Y.; Lien, I. F. F.; Ruttgaizer, S.; Dove, P.; Taylor, S. D., *Org Lett* **2004**, *6* (2), 209-212.
222. Young, T.; Kiessling, L. L., *Angew Chem Int Ed* **2002**, *41* (18), 3449-3451.
223. Liu, C.; Yang, C.; Hwang, S.; Ferraro, S. L.; Flynn, J. P.; Niu, J., *Angew Chem Int Ed* **2020**, *59* (42), 18435-18441.
224. Waller, C. C.; McLeod, M. D., *Steroids* **2014**, *92*, 74-80.
225. Hungerford, N. L.; McKinney, A. R.; Stenhouse, A. M.; McLeod, M. D., *Org Biomol Chem* **2006**, *4* (21), 3951-3959.
226. Langston, S.; Bernet, B.; Vasella, A., *Helv Chim Acta* **1994**, *77* (8), 2341-2353.
227. Zhou, Y.; Jones, A. M., *Molecules* **2024**, *29*(7), P.1445.
228. Gill, D. M.; Male, L.; Jones, A. M., *Eur J Org Chem* **2019**, (46), 7568-7577.
229. Mahmoud, A. M.; Jones, A. M.; Sidgwick, G. P.; Arafat, A. M.; Alexander, M. Y.; Wilkinson, F. L., *Cell Physiol Biochem* **2019**, *53* (2), 323-336.
230. Langford-Smith, A. W. W.; Hasan, A.; Weston, R.; Edwards, N.; Jones, A. M.; Boulton, A. J. M.; Bowling, F. L.; Rashid, S. T.; Wilkinson, F. L.; Alexander, M. Y., *Sci Rep* **2019**, *9* (1), 2309-2309.
231. Mahmoud, A. M.; Wilkinson, F. L.; Jones, A. M.; Wilkinson, J. A.; Romero, M.; Duarte, J.; Alexander, M. Y., *Biochim Biophys Acta Gen Subj* **2017**, *1861* (1), 3311-3322.
232. Dawson, P. A., *Steroids—from physiology to clinical medicine* **2012**, 45-64.
233. Wang, L.-Q.; James, M. O., *J Steroid Biochem Mol Biol* **2005**, *96* (5), 367-374.
234. Loriaux, D.; Ruder, H.; Knab, D.; Lipsett, M., *J Clin Endocrinol Metab* **1972**, *35* (6), 887-891.
235. Wood, C. E.; Gridley, K. E.; Keller-Wood, M., *Endocrinol* **2003**, *144* (2), 599-604.
236. Lambert, G.; Brichant, J.-F.; Hartstein, G.; Bonhomme, V.; Dewandre, P.-Y., *Acta Anaesthesiol Belg* **2014**, *65* (4), 137-49.
237. Eiland, E.; Nzerue, C.; Faulkner, M., *J Pregnancy* **2012**, 2012.
238. Pasqualini, J.; Gelly, C.; Nguyen, B.-L.; Vella, C., *J Steroid Biochem* **1989**, *34* (1-6), 155-163.
239. Pasqualini, J. R.; Chetrite, G. S., *J Steroid Biochem Mol Biol* **2005**, *93* (2-5), 221-236.
240. Vignon, F.; Terqui, M.; Westley, B.; Derocq, D.; Rochefort, H., *Endocrinol* **1980**, *106* (4), 1079-1086.
241. Harteneck, C., *Molecules* **2013**, *18* (10), 12012-12028.
242. Jewett, B. E.; Thapa, B., *Physiology, NMDA receptor*. StatPearls Publishing: 2022.

243. Vallée, M.; Mayo, W.; Le Moal, M., *Brain Res Rev* **2001**, *37* (1-3), 301-312.
244. Naylor, J. C.; Kilts, J. D.; Hulette, C. M.; Steffens, D. C.; Blazer, D. G.; Ervin, J. F.; Strauss, J. L.; Allen, T. B.; Massing, M. W.; Payne, V. M., *Biochim Biophys Acta Mol Cell Biol Lipids* **2010**, *1801* (8), 951-959.
245. Daugherty, D. J.; Selvaraj, V.; Chechneva, O. V.; Liu, X. B.; Pleasure, D. E.; Deng, W., *EMBO Mol Med* **2013**, *5* (6), 891-903.
246. Vallée, M., *J Steroid Biochem Mol Biol* **2016**, *160*, 78-87.
247. Lis, A.; Lambert, S.; Straub, I.; Mannebach, S.; Flockerzi, V.; Philipp, S. E.; Wagner, T. F. J.; Mathar, I.; Düfer, M.; Oberwinkler, J.; Loch, S., *Nat Cell Biol* **2008**, *10* (12), 1421-1430.
248. Fitzgerald, C. C.; McLeod, M. D., *Org Biomol Chem* **2022**, *20* (16), 3311-3322.
249. Rudqvist, U., *J Labelled Compd Radiopharm* **1983**, *20* (10), 1159-1170.
250. Potter, B. V. L. 16-and 17-deuterated estrogen-3-sulfamates as estrogenic agents. U.S. Patent 20160039866A1, 2016.
251. Wudy, S. A., *Steroids* **1990**, *55* (10), 463-471.
252. Rowlands, D.; Sugahara, K.; Kwok, J. C. F., *Molecules* **2015**, *20* (3), 3527-3548.
253. Meanwell, M.; Fehr, G.; Ren, W.; Adluri, B.; Rose, V.; Lehmann, J.; Silverman, S. M.; Rowshanpour, R.; Adamson, C.; Bergeron-Brlek, M.; Foy, H.; Challa, V. R.; Campeau, L.-C.; Dudding, T.; Britton, R., *Commun Chem* **2021**, *4* (1), 96-96.
254. Leusmann, S.; Ménová, P.; Shanin, E.; Titz, A.; Rademacher, C., *Chem Soc Rev* **2023**, *52* (11), 3663-374.
255. Hevey, R., *Pharmaceuticals (Basel)* **2019**, *12* (2), 55.
256. Ernst, B.; Magnani, J. L., *Nat Rev Drug Discov* **2009**, *8* (8), 661-677.
257. Zhang, Y.; Wang, F., *Drug Discov Ther* **2015**, *9* (2), 79-87.
258. Tamburrini, A.; Colombo, C.; Bernardi, A., *Med Res Rev* **2020**, *40* (2), 495-531.
259. Arjona, O.; Gómez, A. M.; López, J. C.; Plumet, J., *Chem Rev* **2007**, *107* (5), 1919-2036.
260. Krämer, K., *Angew Chem* **2008**, *120*, 9518-9519.
261. Meanwell, N. A., *J Med Chem* **2018**, *61* (14), 5822-5880.
262. Lew, W.; Chen, X.; Kim, C. U., *Curr Med Chem* **2000**, *7* (6), 663-672.
263. Kinch, M. S.; Merkel, J., *Drug Discov Today* **2015**, *20* (8), 920-923.
264. Bauer, K. A.; Hawkins, D. W.; Peters, P. C.; Petitou, M.; Herbert, J. M.; Boeckel, v. C. A. A.; Meuleman, D. G., *Cardiovasc Drug Rev* **2002**, *20* (1), 37-52.
265. Rajendran, P.; Rengarajan, T.; Thangavel, J.; Nishigaki, Y.; Sakthisekaran, D.; Sethi, G.; Nishigaki, I., *Int J Biol Sci* **2013**, *9* (10), 1057-1069.
266. Bonetti, P. O.; Lerman, L. O.; Lerman, A., *Arterioscler Thromb Vasc Biol* **2003**, *23* (2), 168-175.
267. Paravicini, T. M.; Touyz, R. M., *Diabetes Care* **2008**, *31* (2), S170-S180.
268. Versari, D.; Daghini, E.; Viridis, A.; Ghiadoni, L.; Taddei, S., *Diabetes Care* **2009**, *32* (suppl 2), S314-S321.
269. Birukova, A. A.; Wu, T.; Tian, Y.; Meliton, A.; Sarich, N.; Tian, X.; Alan, L.; Birukov, K. G., *Eur Respir J* **2013**, *41* (1), 165-176.
270. Chen, L. W.; Tsai, M. C.; Chern, C. Y.; Tsao, T. P.; Lin, F. Y.; Chen, S. J.; Tsui, P. F.; Liu, Y. W.; Lu, H. J.; Wu, W. L.; Lin, W. S.; Tsai, C. S.; Lin, C. S., *Br J Pharmacol* **2020**, *177* (23), 5375-5392.
271. Raiber, E.-A.; Wilkinson, J. A.; Manetti, F.; Botta, M.; Deakin, J.; Gallagher, J.; Lyon, M.; Ducki, S. W., *Bioorg Med Chem Lett* **2007**, *17* (22), 6321-6325.
272. Liu, Y.; Wang, T.; Yan, J.; Jiagbogu, N.; Heideman, D. A.; Canfield, A. E.; Alexander, M. Y., *Atherosclerosis* **2011**, *219* (2), 440-447.
273. Gallo, S.; Sala, V.; Gatti, S.; Crepaldi, T., *Clin Sci* **2015**, *129* (12), 1173-1193.
274. Mahmoud, A. M.; Jones, A. M.; Sidgwick, G. P.; Arafat, A. M.; Alexander, Y. M.; Wilkinson, F. L., *Cell Physiol Biochem Press GmbH & Co KG* **2019**, *53* (2), 323-336.
275. Komosińska-Vassev, K. B.; Winsz-Szczotka, K.; Kuznik-Trocha, K.; Olczyk, P.; Olczyk, K., *Clin Chem Lab Med* **2008**, *46* (2), 219-224.
276. Oh, J. H.; Kim, Y. K.; Jung, J. Y.; Shin, J. e.; Chung, J. H., *Exp Dermatol* **2011**, *20* (5), 454-456.

277. Wu, D.; Hu, Q.; Zhu, Y., *Front Med* **2016**, *10* (1), 18-27.
278. Smith, R. P., *American Scientist* **2010**, *98* (1), 6-9.
279. Szabo, C., *Biochem Pharmacol* **2018**, *149*, 5-19.
280. Dupuytoren, M., *J de Med* **1806**, *9*, 187-213.
281. Chaussier, F., *J Gen Med Chir Pharm* **1908**, *15*, 19-39.
282. Chen, X.; Jhee, K.-H.; Kruger, W. D., *J Biol Chem* **2004**, *279* (50), 52082-52086.
283. Abe, K.; Kimura, H., *J Neurosci* **1996**, *16* (3), 1066-1071.
284. Kulkarni-Chitnis, M.; Mitchell-Bush, L.; Belford, R.; Robinson, J.; Opere, C. A.; Ohia, S. E.; Mbye, Y. F. N., *AIMS Neurosci* **2019**, *6* (3), 104-115.
285. Kwiatkoski, M.; Soriano, R. N.; Araujo, R. M.; Azevedo, L. U.; Batalhao, M. E.; Francescato, H. D. C.; Coimbra, T. M.; Carnio, E. C.; Branco, L. G. S., *Exp Neurol* **2013**, *240* (1), 88-95.
286. Szabo, C.; Papapetropoulos, A., *Pharmacol Rev* **2017**, *69* (4), 497-564.
287. Szabo, C., *Nat Rev Drug Discov* **2007**, *6* (11), 917-935.
288. Hackfort, B. T.; Mishra, P. K., *Am J Physiol Heart Circ Physiol* **2016**, *310* (7), H802-H812.
289. Meng, G.; Ma, Y.; Xie, L.; Ferro, A.; Ji, Y., *Br J Pharmacol* **2015**, *172* (23), 5501-5511.
290. Szabo, C., *Biomolecules* **2022**, *12* (10), 1372.
291. Takeuchi, H.; Setoguchi, T.; MacHigashira, M.; Kanbara, K.; Izumi, Y., *J Periodontal Res* **2008**, *43* (1), 90-95.
292. Li, Q.; Lancaster, J. R., *Nitric Oxide* **2013**, *35*, 21-34.
293. Snyder, S. H.; Jaffrey, S. R.; Zakhary, R., *Brain Res Rev* **1998**, *26* (2-3), 167-175.
294. Zhao, W.; Zhang, J.; Lu, Y.; Wang, R., *EMBO J* **2001**, *20* (21), 6008.
295. Kimura, H., *Amino Acids* **2011**, *41* (1), 113-121.
296. Diwakar, L.; Ravindranath, V., *Neurochem Int* **2007**, *50* (2), 418-426.
297. Vitvitsky, V.; Thomas, M.; Ghorpade, A.; Gendelman, H. E.; Banerjee, R., *J Biol Chem* **2006**, *281* (47), 35785-35793.
298. Ida, T.; Sawa, T.; Ihara, H.; Tsuchiya, Y.; Watanabe, Y.; Kumagai, Y.; Suematsu, M.; Motohashi, H.; Fujii, S.; Matsunaga, T.; Yamamoto, M.; Ono, K.; Devarie-Baez, N. O.; Xian, M.; Fukuto, J. M.; Akaike, T., *Proc Natl Acad Sci U S A* **2014**, *111* (21), 7606-7611.
299. Ono, K.; Akaike, T.; Sawa, T.; Kumagai, Y.; Wink, D. A.; Tantillo, D. J.; Hobbs, A. J.; Nagy, P.; Xian, M.; Lin, J.; Fukuto, J. M., *Free Radic Biol Med* **2014**, *77*, 82-94.
300. Paul, B. D.; Snyder, S. H., *Nat Rev Mol Cell Biol* **2012**, *13* (8), 499-507.
301. Filipovic, M. R.; Zivanovic, J.; Alvarez, B.; Banerjee, R., *Chem Rev* **2018**, *118* (3), 1253-1337.
302. Fukuto, J. M.; Ignarro, L. J.; Nagy, P.; Wink, D. A.; Kevil, C. G.; Feelisch, M.; Cortese-Krott, M. M.; Bianco, C. L.; Kumagai, Y.; Hobbs, A. J.; Lin, J.; Ida, T.; Akaike, T., *FEBS Lett* **2018**, *592* (12), 2140-2152.
303. Griffiths, K.; Ida, T.; Morita, M.; Lamb, R. J.; Lee, J. J.; Frenneaux, M. P.; Fukuto, J. M.; Akaike, T.; Feelisch, M.; Madhani, M., *Redox Biol* **2023**.
304. Switzer, C. H.; Guttzeit, S.; Eykyn, T. R.; Eaton, P., *Redox Biol* **2021**, *47*, 102155.
305. Henderson, C. F.; Bica, I.; Long, F. T.; Irwin, D. D.; Stull, C. H.; Baker, B. W.; Suarez Vega, V.; Taugher, Z. M.; Fletes, E. D.; Bartleson, J. M.; Humphrey, M. L.; Álvarez, L. a.; Akiyama, M.; Kumagai, Y.; Fukuto, J. M.; Lin, J., *Chem Res Toxicol* **2020**, *33* (2), 678-686.
306. Bianco, C. L.; Akaike, T.; Ida, T.; Nagy, P.; Bogdandi, V.; Toscano, J. P.; Kumagai, Y.; Henderson, C. F.; Goddu, R. N.; Lin, J.; Fukuto, J. M., *Br J Pharmacol* **2019**, *176* (4), 671-683.
307. Halliwell, B.; Chirico, S., *Am J Clin Nutr* **1993**, *57* (5), 715S-725S.
308. Akaike, T.; Ida, T.; Wei, F.-Y.; Nishida, M.; Kumagai, Y.; Alam, M. M.; Ihara, H.; Sawa, T.; Matsunaga, T.; Kasamatsu, S.; Nishimura, A.; Morita, M.; Tomizawa, K.; Nishimura, A.; Watanabe, S.; Inaba, K.; Shima, H.; Tanuma, N.; Jung, M.; Fujii, S.; Watanabe, Y.; Ohmuraya, M.; Nagy, P.; Feelisch, M.; Fukuto, J. M.; Motohashi, H., *Nat Commun* **2017**, *8* (1), 1177-15.
309. Savige, W. E.; Eager, J.; Maclaren, J. A.; Roxburgh, C. M., *Tetrahedron Lett* **1964**, *5* (44), 3289-3293.
310. Nagy, P.; Ashby, M. T., *Chem Res Toxicol* **2005**, *18* (6), 919-923.

311. Kaschula, C. H.; Hunter, R., *Stud Nat Prod Chem* **2016**, *50*, 1-43.
312. Da, C.-s.; Ni, M.; Han, Z.-j.; Yang, F.; Wang, R., *J Mol Catal A Chem* **2006**, *245* (1-2), 1-7.
313. Jia, Y.; Dong, X.; Zhou, P.; Liu, X.; Pan, L.; Xin, H.; Zhu, Y. Z.; Wang, Y., *Eur J Med Chem* **2012**, *55*, 176-187.
314. Islam, M. A.; Zhang, Y.; Wang, Y.; McAlpine, S. R., *MedChemComm* **2015**, *6* (2), 300-305.
315. Wang, Y.; Wang, J.; Lin, Y.; Si-Ma, L.-F.; Wang, D.-h.; Chen, L.-G.; Liu, D.-K., *Bioorg Med Chem Lett* **2011**, *21* (19), 6019-6019.
316. Foucher, V.; Guizzardi, B.; Groen, M. B.; Light, M.; Linclau, B., *Org Lett* **2010**, *12* (4), 680-683.
317. Le Magueres, P.; DelCampo, M.; Saito, K.; Ferrara, J. D.; Wojciechowski, J.; Jones, A.; Kucharczyk, D.; Meyer, M., *Acta Cryst* **2019**, *75*, a163.
318. Sheldrick, G. M., *Acta Crystallogr* **2015**, *A71* (1), 3-8.
319. Sheldrick, G. M., *Acta Crystallogr* **2015**, *C71* (1), 3-8.
320. Bourhis, L.; Dolomanov, O.; Gildea, R.; Howard, J.; Puschmann, H., *J Appl Cryst* **2009**, *42*, 339-341.